THE EVOLVING LANDSCAPE, CLINICAL IMPLICATIONS AND FUTURE PERSPECTIVE OF BIOMARKERS IN GASTROINTESTINAL CANCERS

EDITED BY: Jaw-Yuan Wang and Kenneth K. W. To
PUBLISHED IN: Frontiers in Oncology

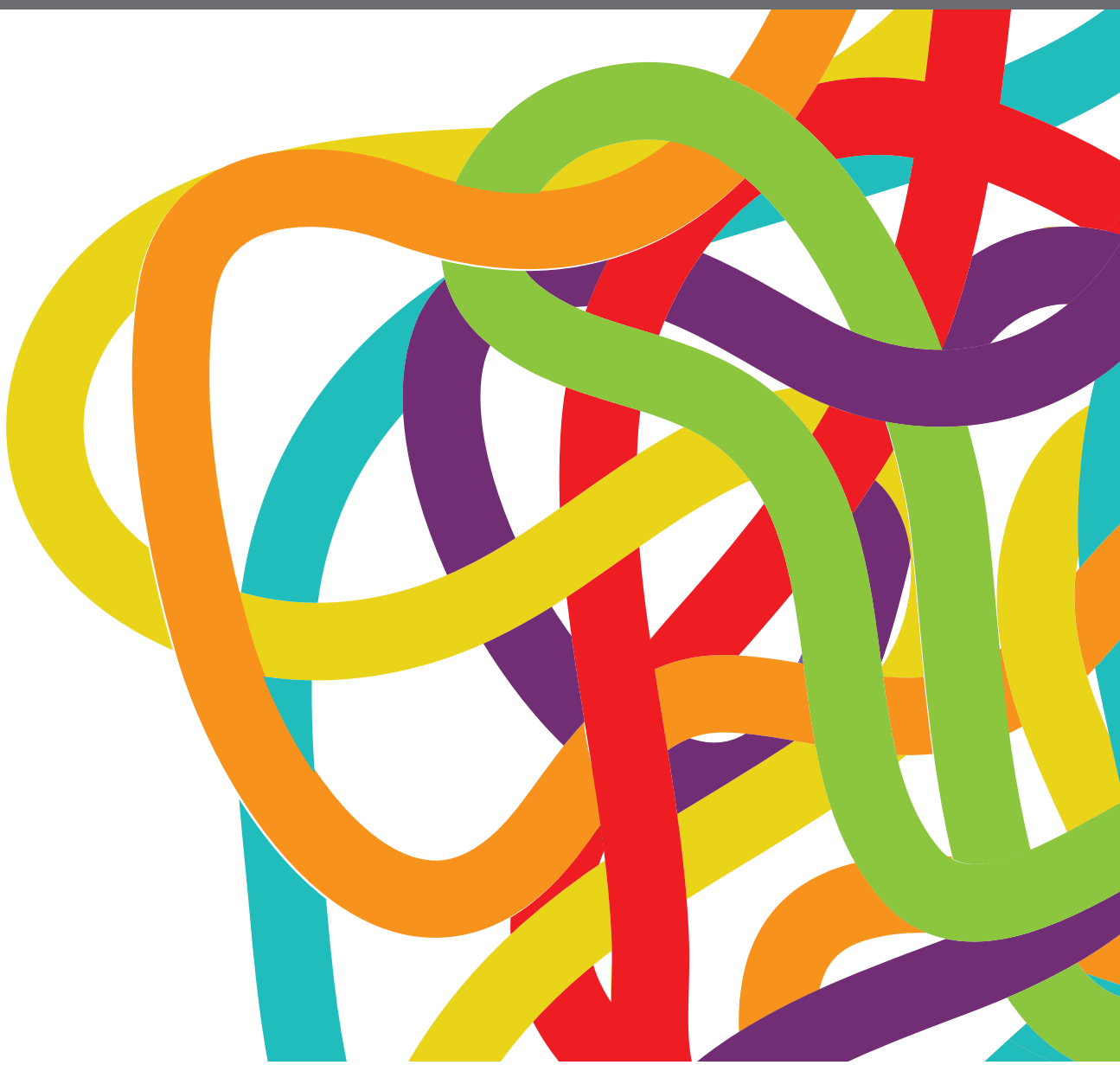

frontiers Research Topics

frontiers

ISSN 1664-8714
ISBN 978-2-88974-859-4
DOI 10.3389/978-2-88974-859-4

About Frontiers

Frontiers is more than just an open-access publisher of scholarly articles: it is a pioneering approach to the world of academia, radically improving the way scholarly research is managed. The grand vision of Frontiers is a world where all people have an equal opportunity to seek, share and generate knowledge. Frontiers provides immediate and permanent online open access to all its publications, but this alone is not enough to realize our grand goals.

Frontiers Journal Series

The Frontiers Journal Series is a multi-tier and interdisciplinary set of open-access, online journals, promising a paradigm shift from the current review, selection and dissemination processes in academic publishing. All Frontiers journals are driven by researchers for researchers; therefore, they constitute a service to the scholarly community. At the same time, the Frontiers Journal Series operates on a revolutionary invention, the tiered publishing system, initially addressing specific communities of scholars, and gradually climbing up to broader public understanding, thus serving the interests of the lay society, too.

Dedication to Quality

Each Frontiers article is a landmark of the highest quality, thanks to genuinely collaborative interactions between authors and review editors, who include some of the world's best academicians. Research must be certified by peers before entering a stream of knowledge that may eventually reach the public - and shape society; therefore, Frontiers only applies the most rigorous and unbiased reviews.
Frontiers revolutionizes research publishing by freely delivering the most outstanding research, evaluated with no bias from both the academic and social point of view. By applying the most advanced information technologies, Frontiers is catapulting scholarly publishing into a new generation.

What are Frontiers Research Topics?

Frontiers Research Topics are very popular trademarks of the Frontiers Journals Series: they are collections of at least ten articles, all centered on a particular subject. With their unique mix of varied contributions from Original Research to Review Articles, Frontiers Research Topics unify the most influential researchers, the latest key findings and historical advances in a hot research area! Find out more on how to host your own Frontiers Research Topic or contribute to one as an author by contacting the Frontiers Editorial Office: frontiersin.org/about/contact

THE EVOLVING LANDSCAPE, CLINICAL IMPLICATIONS AND FUTURE PERSPECTIVE OF BIOMARKERS IN GASTROINTESTINAL CANCERS

Topic Editors:
Jaw-Yuan Wang, Kaohsiung Medical University Hospital, Taiwan
Kenneth K. W. To, The Chinese University of Hong Kong, China

Citation: Wang, J.-Y., To, K. K. W., eds. (2022). The Evolving Landscape, Clinical Implications and Future Perspective of Biomarkers in Gastrointestinal Cancers. Lausanne: Frontiers Media SA. doi: 10.3389/978-2-88974-859-4

Table of Contents

frontiers | Frontiers in Oncology

EDITORIAL
published: 03 May 2022
doi: 10.3389/fonc.2022.895231

Editorial: The Evolving Landscape, Clinical Implications, and Future Perspective of Biomarkers in Gastrointestinal Cancers

Hsiang-Lin Tsai[1,2], *Yen-Cheng Chen*[1,3], *Kenneth KW To*[4*] and *Jaw-Yuan Wang*[1,2,3,5,6,7,8*]

[1] Division of Colorectal Surgery, Department of Surgery, Kaohsiung Medical University Hospital, Kaohsiung Medical University, Kaohsiung, Taiwan, [2] Department of Surgery, Faculty of Medicine, College of Medicine, Kaohsiung Medical University, Kaohsiung, Taiwan, [3] Graduate Institute of Clinical Medicine, College of Medicine, Kaohsiung Medical University, Kaohsiung, Taiwan, [4] School of Pharmacy, Faculty of Medicine, The Chinese University of Hong Kong, Hong Kong, Hong Kong SAR, China, [5] Graduate Institute of Medicine, College of Medicine, Kaohsiung Medical University, Kaohsiung, Taiwan, [6] Center for Cancer Research, Kaohsiung Medical University, Kaohsiung, Taiwan, [7] Center for Liquid Biopsy and Cohort Research, Kaohsiung Medical University, Kaohsiung, Taiwan, [8] Pingtung Hospital, Ministry of Health and Welfare, Pingtung, Taiwan

Keywords: gastrointestinal cancers, biomarkers, evolving landscape, early detection, postoperative surveillance

OPEN ACCESS

Edited and reviewed by:
Liang Qiao,
Westmead Institute for Medical Research, Australia

***Correspondence:**
Jaw-Yuan Wang
cy614112@ms14.hinet.net;
jawyuanwang@gmail.com
Kenneth KW To
kennethto@cuhk.edu.hk

Specialty section:
This article was submitted to Gastrointestinal Cancers: Gastric & Esophageal Cancers, a section of the journal Frontiers in Oncology

Received: *13 March 2022*
Accepted: *04 April 2022*
Published: *03 May 2022*

Citation:
Tsai H-L, Chen Y-C, To KKW and Wang J-Y (2022) Editorial: The Evolving Landscape, Clinical Implications, and Future Perspective of Biomarkers in Gastrointestinal Cancers. Front. Oncol. 12:895231. doi: 10.3389/fonc.2022.895231

Editorial on the Research Topic

The Evolving Landscape, Clinical Implications and Future Perspective of Biomarkers in Gastrointestinal Cancers

Gastrointestinal (GI) cancer is a major public health problem worldwide. Early GI cancer detection, pretherapeutic responsiveness prediction, and postoperative micrometastasis monitoring are the hallmarks for successful GI cancer treatment. The approval of novel prognostic models and therapies for metastatic GI cancer (mGIC) has led to important improvements in patient outcomes.

Histocompatibility leukocyte antigen complex P5 (HCP5) is a momentous long non-coding RNA (lncRNA) and is involved in many autoimmune diseases and malignant tumors. Qin et al. demonstrated that the increase of serum HCP5 could significantly distinguish between patients with primary gastric cancer (GC) and healthy subjects, and the combined diagnosis of HCP5, CEA, and CA199 had high diagnostic efficiency.

Identification of a simplified prediction model for lymph node metastasis (LNM) for patients with early colorectal cancer (CRC) is urgently needed to determine treatment and follow-up strategies. CRC patients with tumor larger than 3 cm, who were identified as high-risk through the model, may require careful attention. Early CRC could be detected through the development of a novel prognostic model for predicting lymph node metastasis (Ahn et al.). Likewise, Log odds of positive lymph node scheme (LODDS) is an innovative N staging system and has been recently introduced as a new prognostic index in CRCs, which could powerfully stratify patients into different risk groups even when dissected lymph nodes were insufficient. Zhu et al. presented that a novel prognostic model incorporating common TBs (CA 199, CA125, and CEA) and LODDS displayed better predictive performance than both single factor and the TNM classification.

Systematic inflammatory factors, such as lymphocytes, monocytes, neutrophils, and blood biochemical indicators related to nutritional status, such as C-reactive protein (CRP) levels and albumin (ALB) levels, are valuable prognostic indicators for cancers including CRC. The prognostic

value of new index (LANR) composed of pre-operative lymphocytes, albumin, and neutrophils has been demonstrated to be an important prognostic indicator for patients with resectable CRC (Liang et al.). Immunotherapy and induction of ferroptosis are both considered to be of great significance in clinical management of CRC. A ferroptosis-related genes model consisted of five genes: AKR1C1, ALOX12, CARS1, FDFT1, and ATP5MC3. This was built as a prognosis model for ferroptosis and might provide clues for further therapy in CRC (Nie et al.).

Various studies have suggested that the pathogenesis of CRC is influenced not only by genetic factors but also by altered gut microbial composition. Gut microbes can produce extracellular vesicles (EVs), also called nanovesicles, and are upregulated during cell activation and growth during cancer development. Profiling of microbe-derived EVs may offer a novel biomarker for detecting and predicting CRC prognosis (Park et al.).

Liquid biopsies allowing for individualized risk stratification of cancer patients have become of high significance in individualized cancer diagnostics and treatment. Ottaiano et al. contribute to a biological basis approach of *KRAS* testing with a more dynamic attitude (liquid biopsy) giving both new prognostic and therapeutic chances. Furthermore, they demonstrated that an association between *KRAS* regressive trajectory and the oligo-metastatic status was found and regressive and progressive mutational trajectories emerged as independent prognostic factors for survival. Hendricks et al. showed a novel immunofluorescence-based and a molecular detection approach for enumeration and detection of circulating tumor cells (CTCs). They enlighten the kinetics of CTC in CRC patients and support that the significance of CTC as a prognostic biomarker in a more in-depth longitudinal analysis of CTC over the course of the disease. Chen et al. reported that emerging technologies (liquid biopsy and exosomes media) may help early diagnosis of peritoneal metastasis by screening exosome miRNAs and exosomes-based treatment by transferring anti-tumor drugs and restricting exosomes homing in peritoneal metastasis.

Immune checkpoint blockade (ICB) shows remarkable clinical effects in patients with metastatic microsatellite-unstable (MSI) cancer. Busch et al. demonstrates that beta-2-microglobulin mutations are linked to a distant metastatic pattern and a favorable outcome in MSI stage IV GI cancers.

This editorial describes the novel biomarkers relevant to GI cancers. There is currently great focus on the discovery and validation of further biomarkers, with many new potential prognostic and predictive markers being identified alongside developments in molecular profiling technologies. Furthermore, the future perspective of emerging biomarkers' development for the unmet medical need for GI cancer patients is mandatory.

AUTHOR CONTRIBUTIONS

H-LT and Y-CC contributed to the draft and writing; J-YW and KT reviewed the final version of this manuscript. All authors contributed to the article and approved the submitted version.

Conflict of Interest: The authors declare that the research was conducted in the absence of any commercial or financial relationships that could be construed as a potential conflict of interest.

frontiers in Oncology

ORIGINAL RESEARCH
published: 18 February 2021
doi: 10.3389/fonc.2020.616440

Detection of Circulating Tumor Cells in Resectable Pancreatic Ductal Adenocarcinoma: A Prospective Evaluation as a Prognostic Marker

Byeong Geun Song[1†], Wooil Kwon[2†], Hyemin Kim[1,3†], Eun Mi Lee[1], Young Min Han[2], Hongbeom Kim[2], Yoonhyeong Byun[2], Kyung Bun Lee[4], Kwang Hyuck Lee[1,5], Kyu Taek Lee[1], Jong Kyun Lee[1], Jin-Young Jang[2] and Joo Kyung Park[1,5*]*

[1] Department of Medicine, Samsung Medical Center, Sungkyunkwan University School of Medicine, Seoul, South Korea, [2] Departments of Surgery, Seoul National University College of Medicine, Seoul, South Korea, [3] Medical Research Institute, Sungkyunkwan University School of Medicine, Seoul, South Korea, [4] Departments of Pathology, Seoul National University College of Medicine, Seoul, South Korea, [5] Department of Health Sciences and Technology, SAIHST, Sungkyunkwan University, Seoul, South Korea

Circulating tumor cells (CTCs) are useful biomarkers of many solid tumors, but are infrequently detected in early stage pancreatic ductal adenocarcinomas (PDACs). The first drainage of pancreatic venous blood flow come to portal vein and pass through the liver, and they finally go out for peripheral blood. We thought that comparing CTCs from portal vein and peripheral blood could enable us to understand the clinical meaning of CTCs from each different site in PDACs. Therefore, we aimed to determine 1) whether CTCs could be reliably identified in early stages (operable) of PDACs, 2) if there are any differences in the detected number of CTC in portal vein blood and peripheral blood, and 3) whether CTCs can be sensitive biomarkers for the prognosis of resectable PDAC patients. Newly diagnosed PDAC patients who underwent operation with curative intention between 2013 and 2015 were prospectively enrolled. Blood draws from portal and peripheral vein ran through the microfabricated porous filter, and anti-epithelial cell adhesion molecule (EpCAM) and anti-Plectin-1 antibodies were used for CTC identification. Baseline clinical characteristics, tumor characteristics, treatment, and clinical outcomes were assessed. The clinical stages of the 32 enrolled patients were as follows: IA/IB 1 (3.1%); IIA 9 (28.1%); IIB 17 (53.1%); III 5 (15.6%). Twenty-seven patients (84.4%) received R0 resection, while five patients (15.6%) received R1 resection. EpCAM+ CTCs were detected in 20 portal blood (62.5%) and 22 peripheral blood (68.8%). Plectin-1+ CTCs were identified in 14 portal blood (43.8%) and 16 peripheral blood (50%). Plectin-1-expressing CTCs were picked from CTC platform (microfabricated porous filter) and we could find out all KRAS mutation. Patients with detectable EpCAM+ CTC less than one in peripheral blood showed longer overall survival (OS) compared to

OPEN ACCESS

Edited by:
Jaw-Yuan Wang, Medical University, Taiwan

Reviewed by:
Yi-Chia Wu, Kaohsiung Medical University, Taiwan
Wen-Tsan Chang, Kaohsiung Medical University Hospital, Taiwan
Yan-Shen Shan, National Cheng Kung University, Taiwan

***Correspondence:**
Joo Kyung Park
mdsophie@gmail.com
Jin-Young Jang
jangjy4@snu.ac.kr

[†]These authors have contributed equally to this work

Specialty section:
This article was submitted to Gastrointestinal Cancers, a section of the journal Frontiers in Oncology

Received: *12 October 2020*
Accepted: *30 December 2020*
Published: *18 February 2021*

Citation:
Song BG, Kwon W, Kim H, Lee EM, Han YM, Kim H, Byun Y, Lee KB, Lee KH, Lee KT, Lee JK, Jang J-Y and Park JK (2021) Detection of Circulating Tumor Cells in Resectable Pancreatic Ductal Adenocarcinoma: A Prospective Evaluation as a Prognostic Marker. Front. Oncol. 10:616440. doi: 10.3389/fonc.2020.616440

patients with detectable CTCs more than one (35.5 months vs. 16.0 months). EpCAM and Plectin-1 successfully identified CTCs at the early stage of PDACs. Also, the number of CTCs could be a prognostic marker for survival in resectable PDACs.

Keywords: circulating tumor cell, plectin-1, epithelial cell adhesion molecule, pancreatic ductal adenocarcinoma, overall survival

INTRODUCTION

Pancreatic ductal adenocarcinoma (PDAC) is associated with poor prognosis due to early metastatic spread. The 5-year survival rate for metastatic PDAC is approximately 2% (1). Only 20% of patients have resectable PDAC at diagnosis, and only 20% of them survive for more than 5 years (2). Nonetheless, early diagnosis and curative resection is the only means to improve prognosis of PDAC patients. However, there are no useful biomarkers for early diagnosis, and predicting prognosis and treatment response. Among several novel biomarker candidates, circulating tumor cell (CTC) is one of the most promising candidates. Capturing, isolating, and characterizing CTCs have been developed, which revealed that CTCs usually circulate in the blood of patients with various cancers such as breast, lung, prostate and colorectal cancers (3–10). Several studies have been reported the prognostic and predictive value of CTCs in cancer patients (11–14). It is easy to detect CTCs in the peripheral circulation of cancer patients where tumor drainages are into the peripheral circulation. However, the first venous drainage of PDAC is into the portal circulation, leading some difficulties to capture CTCs in peripheral circulation. Thus, portal vein could be a more promising location for the detection of CTCs in PDAC. The investigation of CTCs in portal vs. peripheral blood may give us insights into the importance of tumor drainage pattern in CTC detection.

Antibodies against epithelial cell adhesion molecule (EpCAM) have been known to provide the specificity for CTC capture from blood because EpCAM is often overexpressed by epithelial tumors including breast, prostate, colon, and lung cancers (15). Plectin-1 is a cytolinker protein and was recently suggested as a biomarker for PDAC (16). As it was identified not only in primary and metastatic PDAC but also in pre-invasive Pancreatic Intraepithelial Neoplasia (PanIN) III lesions, Plectin-1 may be detected in early stage PDAC. It can also distinguish malignant pancreatic disease from chronic pancreatitis (16). In conclusion, Plectin-1 might be an ideal biomarker for PDAC. However, till date, it has not been studied to verify the usefulness of CTC detected by Plectin-1.

This study is the first to explore several aspects of CTCs in resectable PDACs. Firstly, the reliability of a microfabricated porous filter in identifying CTCs in patients with resectable PDACs was tested. Secondly, the feasibility of Plectin-1 as PDAC-specific identifier was examined. Thirdly, the clinical significance of CTCs captured from the portal vein was compared with that of CTCs captured from peripheral circulation. Lastly, the prognostic significance of number of CTCs was evaluated in terms of overall survival (OS).

PATIENTS AND METHODS

Study Design and Blood Draws

Thirty-two newly diagnosed PDAC patients who underwent surgery with curative intention between 2013 and 2015 at Seoul National University Hospital were prospectively enrolled. The study patients were followed up until February of 2020 (5 years after the last study patient). Intraoperatively, 10 ml of blood was drawn from the portal vein from the surgical field just before complete resection and extraction of specimen. Simultaneous, 10 ml of blood was drawn from the cephalic vein. The blood samples were collected in Ethylenediaminetetraacetic acid (EDTA) tubes and processed within 4 h. Clinical variables collected included: age at diagnosis, sex, stages defined by the eighth edition American Joint Committee on Cancer (AJCC), date of surgery, date and site of recurrence, date of death and laboratory data. This study was conducted under the principles of the Declaration of Helsinki. The institutional review board (IRB) of Seoul National University Hospital approved the study protocol. All patients provided written informed consent, and all specimens were collected according to IRB regulations and approval (IRB No. 1305-573-489).

Flow Cytometry Analysis and Immunofluorescent Staining

Pancreatic cancer cell lines were grown as a confluent monolayer in various culture media including Dulbecco's Modified Eagle's Medium for PANC1, SW1990, MIA-PaCa2, PaTu8902 and CFPAC-1 cells, RPMI-1640 Medium for COLO357, AsPC-1, KP-1NL, MPanc-96, BxPC3, PaTu8988, and CAPAN-2 cells, Iscove's Modified Dulbecco's Medium for CAPAN-1 cells, and Eagle's Minimum Essential Medium for HPAFII at 37°C in a humidified atmosphere containing 5% CO2. All culture media were supplemented with 10% fetal bovine serum (FBS) and 1% Antibiotic Antimicotic, and they were purchased from Thermo Fisher Scientific (Waltham, MA, USA). After detaching with 0.25% Typsin/EDTA solution and washing with phosphate buffered saline (PBS), harvested cells were resuspended in ice cold flow cytometry staining buffer (PBS with 1% bovine serum albumin (BSA) and 0.1% sodium azide) to a concentration of $1x10^7$ cells/ml. Primary EpCAM or Plectin-1 antibody (Cell Signaling Technology (CST), Danvers, MA, USA) was added into polystyrene round bottom tube containing cells ($1x10^6$ cells/0.1 ml/tube) and cells were incubated for 60 min in dark on ice with gentle shaking. After washing three times, cells were incubated with fluorochrome (APC for EpCAM, Alexa 594 for Plectin-1)-conjugated secondary antibody (CTS) for 30 min. Followed by rinsing cells, resuspended cells were analyzed on

FACS Calibur flow cytometry system (BD Biosciences, San Jose, CA, USA). For immunofluorescent (IF) staining, pancreatic cancer cell lines were seeded on coated glasses, and they were stained with Alexa488-conjugated EpCAM, Plectin-1 (CST) and Alexa594-conjugated CD45 (eBioscience, San Diego, CA, USA) for 2 h at room temperature. After additional staining with Alexa488-conjugated anti-rabbit IgG (CST) for Plectin-1, all nuclei were counterstained with 4'6-diamidino-2-phenylindole (DAPI). Stained cells were observed under the Eclipse Ti2 inverted microscope (Nikon, Tokyo, Japan) with 10x and 20x objectives.

Microfabricated Filter-Based CTC Enrichment

CTCs were enriched from 10 ml whole blood samples using a microfabricated porous filter according to the manufacturer's instruction (Cytogen Inc., Seoul, Korea) (17). The Buffy coat was separated by Ficoll-Hypaque density gradient centrifugation, and passed through the nickel electroformed membrane filter designed with the size of the square pores to 6.5×6.5 μm and gap size of 6 μm. The resulting CTCs were recovered and processed for IF staining.

CTC Immunostaining and Enumeration

For CTC enumeration, recovered cells were fixed with 4% formaldehyde for 10 min at room temperature and permeabilized for 15 min with 0.2% Triton X-100 in PBS. After blocking with 1% BSA in PBS for 30 min, they were incubated with primary antibodies against EpCAM, Plectin-1 (CST), and CD45 (eBioscience). This was followed by matched fluorochrome (Alexa 488 for EpCAM, Alexa 647 for Plectin-1, Alexa 594 for CD45)-conjugated secondary antibody incubation. Nuclei were counterstained with DAPI. CTCs were identified on the basis of cell size, morphology, and fluorescence staining based on EpCAM or Plectin-1 expression. Total cells were counted by DAPI staining, white blood cells (WBCs) were identified by CD45 staining. Captured cells were determined to be CTC if they were CD45 negative and EpCAM or Plectin-1 positive. Then number of CTCs/ml was determined by comprehensive image analysis. A count of one or more CTCs per ml of blood was defined as positive.

Single Cell Isolation and KRAS Mutation Analysis

After CTC enrichment from the blood of PDAC patients, CTCs were stained with Plectin-1 antibody and DAPI. Two Plectin-1^+ CTCs were isolated in a tube using CellCelector (ALS Automated Lab Solutions GmbH, Jena, Germany), and whole genome amplification (WGA) was carried out by using REPLI-g single cell kit (Qiagen, Venlo, Netherlands). Droplet Digital polymerase chain reaction (ddPCR) was performed using 2X ddPCR Supermix (Bio-Rad, Hercules, CA, USA) for KRAS probes (KRAS wild-type (WT) 5'-HEX-AGTTGGAGCTGGTGG CGTA-BHQ1-3'; KRAS mutant G12D 5'-FAM-AGTTGGAGC TGATGGCGTAG-BHQ1-3'; KRAS mutant G12V 5'-FAM-AGTTGGAGCTGTTGGCGTAG-BHQ1-3') by QX200 Droplet Digital PCR System (Bio-Rad). After Plectin-1^+ cell isolation, remaining cells captured on the filter membrane were also processed to WGA and ddPCR for KRAS WT and G12D mutant. Data analyses were performed as recommended by the manufacturer using the QuantaSoft Software version 1.7.4. (Bio-Rad).

Statistical Analysis

Statistical significance of difference among continuous variables and categorical variables was examined using Student's t-test (or Mann-Whitney's test, as appropriate) and Chi-square test (or Fisher's exact test, as appropriate), respectively. OS was calculated and plotted using Kaplan-Meier's method and compared by log-rank test. We compared for the number of CTCs between-patients and within-patients for portal vein vs. peripheral vein, p-value<0.05 was considered statistically significant. Statistical analysis was performed using SPSS version 23.0 (SPSS Inc., Chicago, IL) and GraphPad Prism8.0 (GraphPad Software Inc., LA Jolla, CA).

RESULTS

Evaluation of EpCAM and Plectin-1 Expression in PDAC Cells

To evaluate the feasibility of EpCAM and Plectin-1 antibodies in verifying CTCs of PDAC patients, the expressions of EpCAM and Plectin-1 were examined in human PDAC cell lines by flow cytometry. Most cells expressed EpCAMs in PDAC cells including PANC-1, CFPAC-1, AsPC-1, CAPAN-1, CAPAN-2, HPAFII, SW1990, KP-1NL, PaTu8902, PaTu8988, and MPanc-96 (**Figures 1A, C**), which was compatible with other cancer cell lines such as prostate cancer cells (PC3) and non-small cell lung cancer cells (H1650). In addition, IF staining showed that most CAPAN-1 cells intensely expressed EpCAM (**Figure 1E**). The expression of Plectin-1 was also abundant in PDAC cells such as PANC-1, COLO357, KP-1NL, PaTu8902, PaTu8988, MiaPaCa2, BxPC3, and SW1990 (**Figures 1B, D**). Otherwise, WBCs that could be contaminated during CTC preparation rarely expressed EpCAM or Plectin-1 on their surfaces (<1%). In addition, Plectin-1 was extensively expressed in MIA-PaCa2 cells (**Figure 1F**), but not in WBCs (**Figure 1G**). Therefore, it seems that EpCAM and Plectin-1 are suitable for identifying CTCs in PDACs.

Detection of KRAS Mutation in Plectin-1-Expressing CTCs

To prove circulating cells expressing Plectin-1 in the blood sample from PDAC patients were CTCs of PDAC, we performed singe cell isolation and ddPCR for KRAS mutations. After CTC enrichment with microfabricated porous filter, CTCs on the filter membrane were stained with Plectin-1 and DAPI (**Figure 2A**). Then, Plectin-1^+ CTC was picked under fluorescent microscopy, and a small amount of DNA was amplified to process to the ddPCR for KRAS wild-type (WT) and KRAS mutant (G12D). As a result, the Plectin-1^+ CTC had KRAS G12D

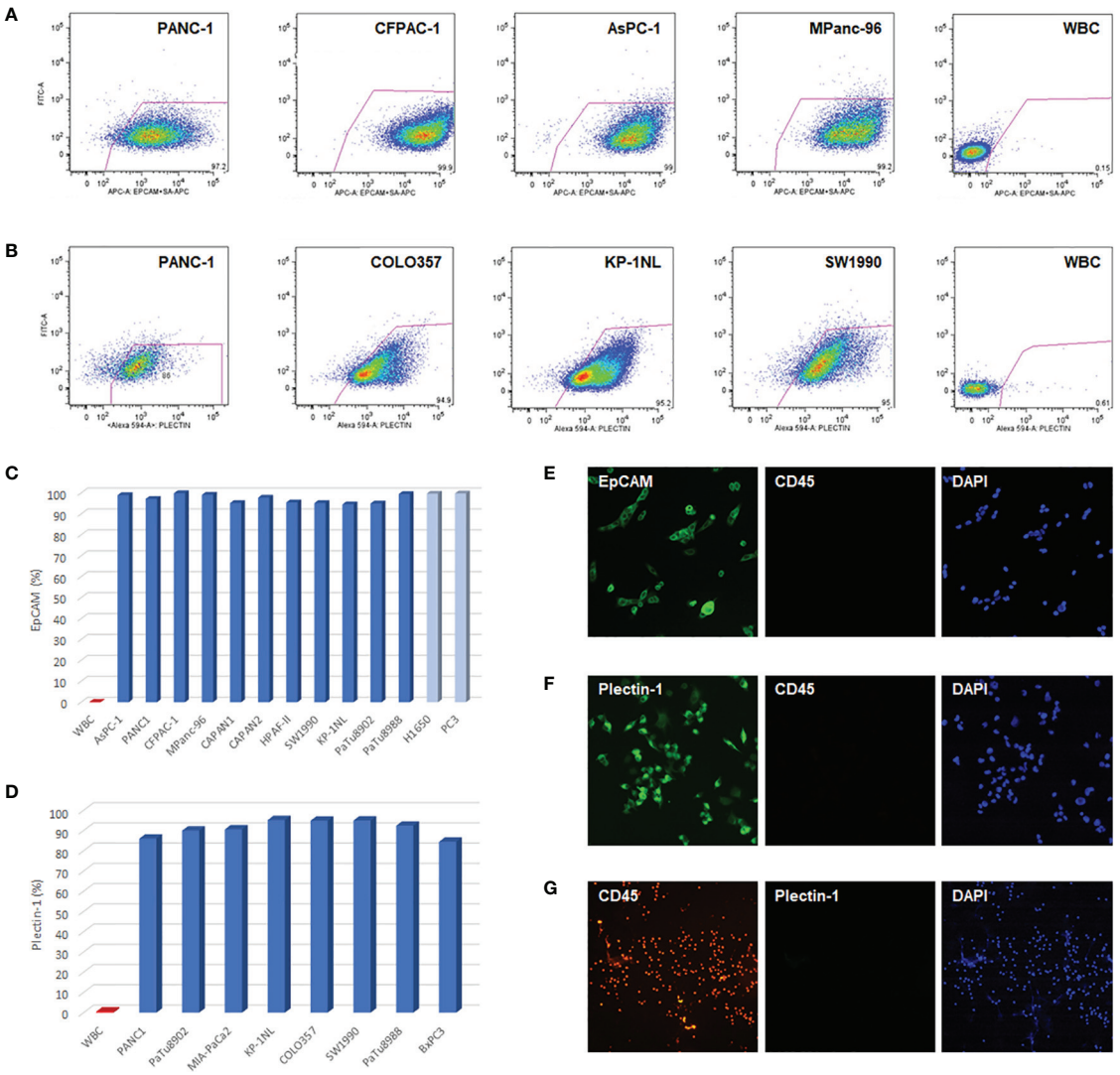

FIGURE 1 | EpCAM and Plectin-1 expression in PDAC cells. To evaluate the anti-EpCAM and anti-Plectin-1 antibodies for detecting CTCs, the expression of EpCAM and Plectin-1 antigen was examined in PDAC cell lines by flow cytometry. **(A)** The surface expression of EpCAM in PDAC cell lines (PANC-1, CFPAC-1, AsPC-1, MPanc-96). **(B)** The expression of Plectin-1 in PDAC cell lines (PANC-1, COLO357, KP-1NL, SW1990). The expression of **(C)** EpCAM and **(D)** Plectin-1 in various PDAC cell lines were represented as percentages. WBCs were used as negative controls. To examine the expression of EpCAM and Plectin-1, **(E)** CAPAN-1 cells were stained with EpCAM (green) and CD45 (red), **(F)** MIA-PaCa2 cells were stained with Plectin-1 (green) and CD45 (red), and **(G)** WBCs were stained with CD45 (red) and Plectin-1 (green). All nucleated cells were stained with DAPI (blue).

mutation (**Figure 2B**), and KRAS G12D mutation was also detected in bulk captured cells on the membrane (**Figure 2C**). It indicates that circulating Plectin-1$^+$ cells in the blood of PDAC patient are circulating tumor cells of PDAC.

Optimization and Validation of Plectin-1 Identification Antibody in Healthy Controls

We examined the circulating Plectin-1$^+$ cells in healthy controls to validate the specificity of Plectin-1 antibody. Peripheral blood was collected from 18 healthy volunteers, CTCs were enriched and processed for immunostaining with anti-Plectin-1 and anti-CD45 antibodies. Five samples showed some of positive staining of Plectin-1 antibody and the number of Plectin-1+ CTC was only 0.3–0.4 per 1 ml blood sample of healthy controls (Mean ± SD, 0.09 ± 0.16 CTCs/ml; Median 0.00 CTCs/ml). The rest of 13 samples showed no positive staining of Plectin-1 antibody (**Figure 3**). We have defined one or more CTCs per 1 ml of blood is positive for CTC capturing and therefore, there was no positive CTCs with Plectin-1 antibody in healthy volunteers.

Identification of CTCs in PDAC Patients

The identification of CTCs in PDACs was based on immunostaining with anti-EpCAM and anti-Plectin-1

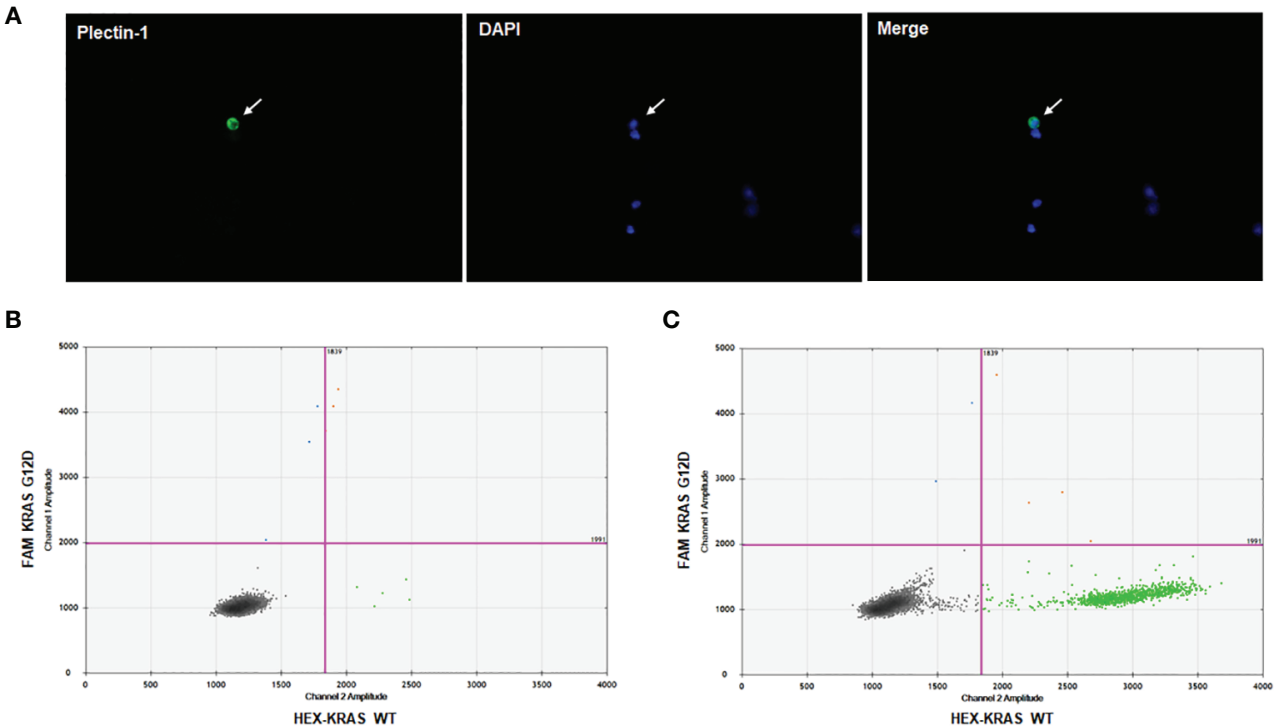

FIGURE 2 | Plectin-1$^+$ cell isolation and KRAS mutation analysis. To clarify Plectin-1-expressing cells in the blood, immunofluorescence staining was carried out to isolate Plectin-1-expressing cells, and ddPCR for KRAS wildtype (WT) and mutant (G12D) was performed. **(A)** A representative image of the circulating tumor cell (CTC) stained with Plectin-1 antibody (green) and 4'6-diamidino-2-phenylindole (DAPI) (blue). Arrow indicates the Plectin-1$^+$ CTC. The detection of KRAS G12D mutation in **(B)** Plectin-1$^+$ CTCs and **(C)** all capture cells on the microfabricated porous filter in the same patient.

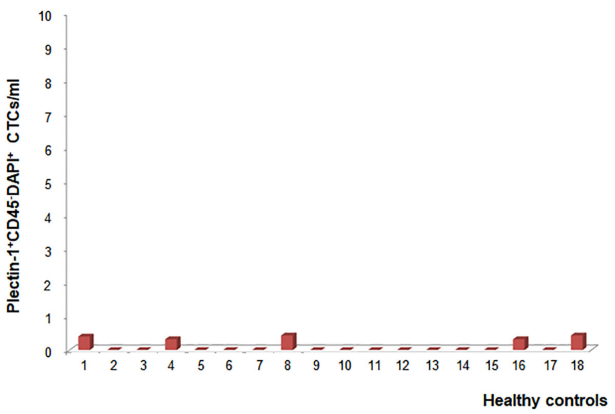

FIGURE 3 | Optimization and validation of Plectin-1 in healthy controls. To validate the specificity of Plectin-1 antigen in detecting circulating tumor cells (CTCs), the number of CTCs was counted in peripheral blood samples of eighteen healthy volunteers after immunostaining with anti-Plectin-1 and anti-CD45 antibody. Plectin-1$^+$CD45$^-$DAPI$^+$ CTC counts per 1 ml blood were calculated individually.

antibodies. All nucleated cells were verified with DAPI staining, and WBCs were excluded with CD45 staining. We defined DAPI$^+$CD45$^-$EpCAM$^+$ (**Figure 4A**) or DAPI$^+$CD45$^-$ Plectin-1$^+$ cells (**Figure 4B**) as PDAC CTCs. It indicated that CTCs are reliably identified in the blood at the early stage of PDACs.

Baseline Characteristics and Clinical Course of Study Patients

Baseline characteristics of 32 study patients are summarized in **Table 1**. Twenty-one male and eleven female patients aged 44–81 years (median 62 years). Distribution of stage was as follows: stage IA/IB 1 (3.1%); stage IIA 9 (28.1%); stage IIB 17 (53.1%); stage III 5 (15.6%). Of all the patients, 22 (68.8%) received pancreaticoduodenectomy, nine (28.1%) received distal pancreatectomy, and one (3.1%) received total pancreatectomy. Twenty-seven patients (84.4%) received R0 resection, while five patients (15.6%) received R1 resection. Twenty-six patients (81.3%) received adjuvant treatment, and five patients (15.6%) received neoadjuvant treatment. Median (range) of total bilirubin, Carbohydrate Antigen (CA) 19-9, and Carcinoembryonic Antigen (CEA) were 1.0 mg/dl (0.2–19.2), 156.6 IU/ml (2.0–12,000), and 2.4 ng/ml (0.7–51.2), respectively.

The study patients were followed up until February of 2020 (5 years after the last study patient). The median follow-up period of 32 patients was 19 months (range: 4 – 70). The median progression free and overall survivals were 11 (range: 0 – 68) and 19 months (range: 4–70), respectively. Recurrence was found in 27 patients (84.4%), of which only two were locoregional and

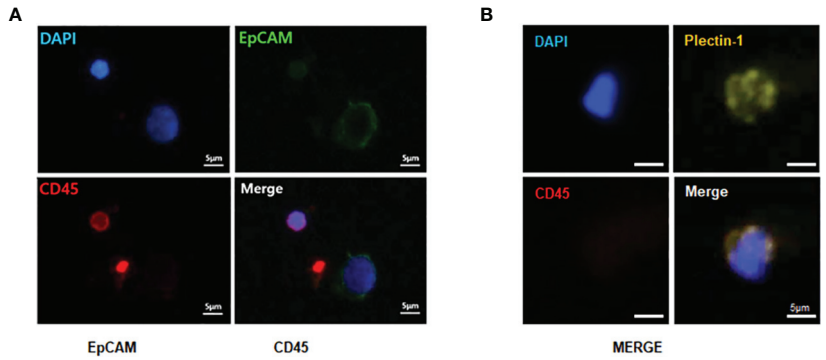

FIGURE 4 | Immunofluorescence staining of captured circulating tumor cells (CTCs) from patients with resectable pancreatic ductal adenocarcinomas (PDACs). To identify CTCs, captured CTCs from PDAC patients were immunostained with anti-epithelial cell adhesion molecule (EpCAM) (green), anti-Plectin-1 (gold) and anti-CD45 (red) antibodies. Nuclei were counterstained with DAPI (blue). CTCs are **(A)** $EpCAM^+$ or **(B)** $Plectin\text{-}1^+$ among $CD45^-DAPI^+$ cells. Scale bar, 5 μm.

TABLE 1 | Patient characteristics (n = 32).

Characteristics	n = 32
Age, median (range)	62 (44–81)
Sex, n (%)	
Male	21 (65.6)
Female	11 (34.4)
Stage (pAJCC)*, n (%)	
IA, IB	1 (3.1)
IIA	9 (28.1)
IIB	17 (53.1)
III	5 (15.6)
Name of Operation, n (%)	
Pancreatoduodenectomy	22 (68.8)
Distal pancreatectomy	9 (28.1)
Total pancreatectomy	1 (3.1)
Resection margin, n (%)	
R0	25 (78.1)
R1	7 (21.9)
Adjuvant treatment, n (%)	28 (87.5)
Neoadjuvant treatment, n (%)	6 (18.8)
Total bilirubin, median (range)	1.0 (0.2–19.2)
CA 19-9 (IU/ml), median (range)	156.6 (2.0–12,000)
CEA (ng/ml), median (range)	2.4 (0.7–51.2)

CA 19-9, carbohydrate antigen 19-9; CEA, carcinoembryonic antigen.
**pathological stage according to the AJCC.*

25 involved systemic recurrence (six local and systemic, and 19 systemic). The most common site of distant metastasis was the liver (n=10) followed by peritoneal seeding (n=6) and lung (n=5). Twenty-seven patients were dead at last follow-ups. Among five survivors, four were free of disease and one was alive with lung metastasis.

Comparison of the Number of CTCs Detected in Portal Draws and Peripheral Blood

CTCs were enriched and enumerated from both portal draws and peripheral blood of 32 resectable PDAC patients. As a result, $EpCAM^+$ CTCs were detected in 20 (62.5%) portal blood and 22 (68.8%) peripheral blood samples, ranged from 0 to 100 in portal blood and peripheral blood (**Figure 5A**). There was no significance in the number of $EpCAM^+$ CTCs between portal and peripheral bloods (p=0.426) (**Figure 5B**). $Plectin\text{-}1^+$ CTCs were identified in 14 (43.8%) portal and 16 (50.0%) peripheral blood samples. Captured CTCs with anti-Plectin-1 antibody ranged from 0 to 100 in portal vein and in peripheral vein (**Figure 5C**). There was also no significant difference in the number of CTCs detected with Plectin-1 antibody between peripheral vein and portal vein (p=0.607) (**Figure 5D**). In addition, there was no significant difference of CTC numbers between patients with R0 resection and patients with R1 resection (p = 0.387) (**Supplementary Table 1**).

CTC Enumeration for Staging

The number of captured CTCs using EpCAM and Plectin-1 was analyzed according to the 8^{th} AJCC staging system. There was no significant difference in the number of CTCs detected across stages with EpCAM from peripheral vein, p=0.841; EpCAM from portal vein, p=0.729; Plectin-1 from peripheral vein, p=0.586; Plectin-1 from portal vein, p=0.480 (**Figure 6).** It seems that the number of CTCs is not a predictive marker for staging in resectable PDAC patients.

Survival Analysis According to the Number of CTCs

It was examined that the prognostic value of CTCs from portal vein and peripheral blood. We compared patients with one or more CTCs vs. less than one CTC. When we detected CTCs using EpCAM in peripheral blood, OS for patients with one or more CTCs and patients with CTC under one were 16.0 and 35.5 months, respectively (p=0.048). PDAC patients having $EpCAM^+$ CTCs in peripheral circulation showed significantly worse prognosis (**Figure 7A**). For detection of $EpCAM^+$ CTCs in portal vein, OS for patients with one or more CTCs and CTC under one were 17.0 and 40.0 months, respectively (p=0.176) (**Figure 7B**). In addition, OS for patients with more than one CTCs using Plectin-1 in peripheral blood and OS for patients less than one CTC were 20.0 and 17.5 months, respectively (p=0.155)

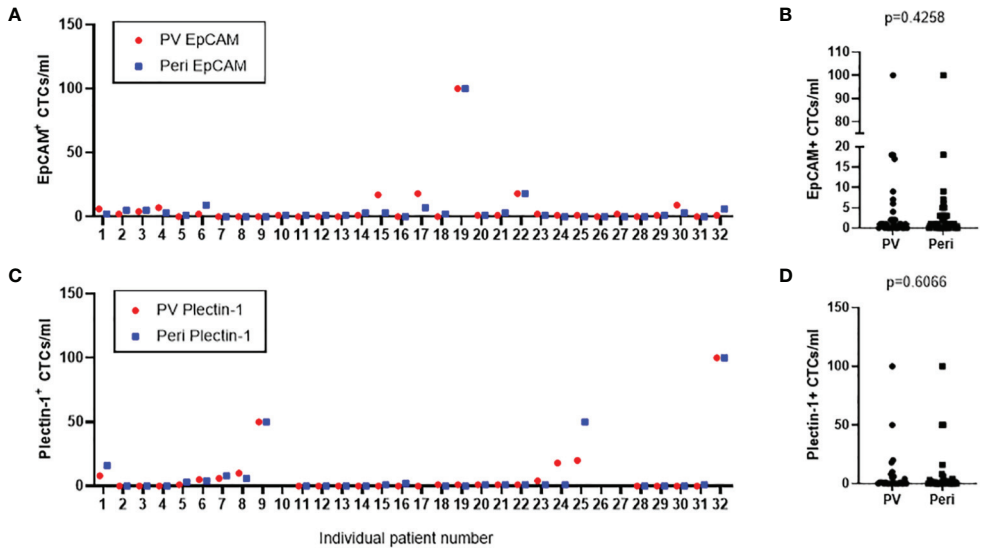

FIGURE 5 | Number of circulating tumor cells (CTCs) detected from the study patients in both portal vein and peripheral blood draws. CTCs were isolated from portal vein (PV) and peripheral vein (Peri) of 32 PDAC patients. **(A)** EpCAM$^+$ CTCs in PV and Peri blood were enumerated from each patient. **(C)** Plectin-1$^+$ CTCs in PV and Peri blood were counted from each patient. **(B)** CTCs positive to epithelial cell adhesion molecule (EpCAM) or **(D)** CTCs positive to Plectin-1 were compared in PV and Peri blood samples.

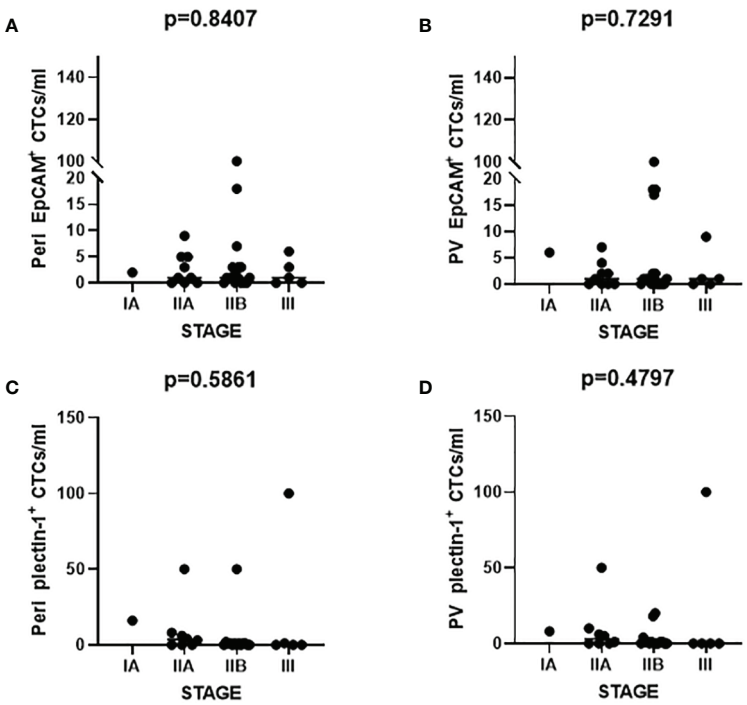

FIGURE 6 | Number of circulating tumor cells (CTCs) according to the American Joint Committee on Cancer (AJCC) staging. The number of CTCs identified with epithelial cell adhesion molecule (EpCAM) from **(A)** peripheral vein (Peri) and **(B)** portal vein (PV) was enumerated. CTCs detected from **(C)** Peri and **(D)** PV were counted after Plectin-1 immunostaining. Each count was evaluated according to the AJCC staging.

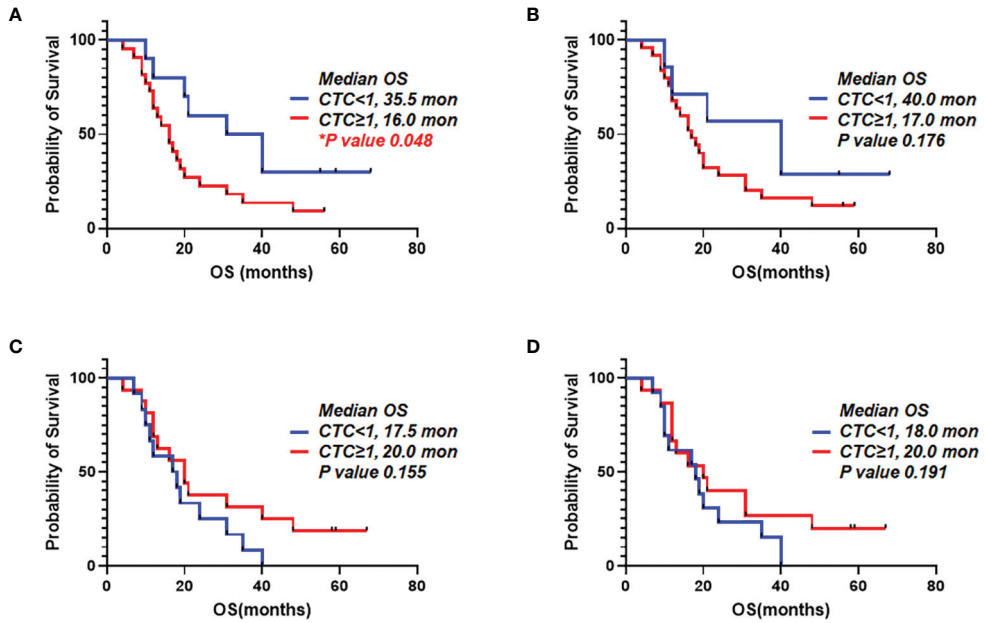

FIGURE 7 | Overall survival correlated to number of circulating tumor cells (CTCs) detected using epithelial cell adhesion molecule (EpCAM) and Plectin-1 in peripheral blood and portal blood. CTC counts based on EpCAM and Plectin-1 expression were evaluated with Overall survival (OS) of 32 PDAC patients. Patients were divided into two groups depending on detectable EpCAM$^+$ CTCs in **(A)** Peripheral vein and **(B)** Portal vein. Patients were divided into two groups depending on detectable Plectin-1$^+$ CTCs in **(C)** Peripheral vein and **(D)** Portal vein. OS was analyzed with the number of CTCs using Kaplan-Meier estimator.

(**Figure 7C**). For detection of CTCs in the portal blood using Plectin-1, OS for patients with more than one CTCs and less than one CTC were 20.0 and 18.0 months, respectively (p=0.191) (**Figure 7D**). For both portal and peripheral bloods, CTC enumeration based on Plectin-1 expression could not predict the survival of PDAC. However, peripheral EpCAM$^+$ CTCs could be a prognostic marker for resectable PDACs.

DISCUSSION

In this study, CTCs were reliably captured by a microfabricated porous filter from resectable patients at the early stage of PDAC. We verified Plectin-1 as a practical PDAC CTC identifier. CTCs from peripheral circulation and portal drainage had no remarkable differences in the number, and only EpCAM$^+$ CTCs in peripheral blood was a factor associated with prognosis whereas others were not.

PDAC is fatal because of its early metastasis (18, 19). Thus, early findings of subclinical metastasis are clinically significant in diagnosis. In this regard, CTCs are good candidates for detection of early metastasis. However, the association between prognosis and CTCs in resectable PDAC patients had not been studied elaborately. Moreover, there are no practical methods to identify PDAC-specific CTCs.

Mehmet et al. first developed a unique microfluidic platform (CTC-chip) capable of efficient and selective separation of viable CTCs from peripheral whole bloods. It was mediated by the interaction of target CTCs with EpCAM antibody-coated microspots under precisely controlled laminar flow conditions, without requisite pre-labeling or processing of samples (20). Although the method of using EpCAM as a capture antibody is now widely used, EpCAM-based enrichment systems are associated with the problem that EpCAM expression of CTCs might be down-regulated during the epithelial mesenchymal transition. CTC isolation dependent on epithelial markers such as EpCAM and cytokeratin might miss mesenchymal type CTCs. Label-independent enrichment methods including size-based selection, inertial focusing-based selection, dielectric field-based selection, and density-based approaches were also developed. Additionally, a combination of different enrichment strategies has been practically used (21, 22). We utilized a size-based microfabricated porous filter platform and label-dependent detection for CTCs. Moreover, several studies have tried to detect heterogenous CTCs by using additional markers, for example, mesenchymal markers including vimentin, N-cadherin, and twist1, and stemness markers such as CD133, CD44, and ALDH1 (23). There have been efforts to find a better marker for identifying CTCs specifically for PDAC. Recently, Plectin-1 was suggested as a biomarker for PDAC, and broadly expressed from pre-invasive lesions to metastatic PDACs (16). Also, it was verified that circulating cells expressing Plectin-1 in the blood of patients with PDACs had KRAS G12D mutation (**Figure 2B**). A very high rate of activating mutations in KRAS (>90%) is included in PDAC (24), and KRAS G12D is the most dominant one (25). In this sense, Plectin-1 is a fascinating target for CTC platform development. This study is the first report to examine the feasibility of Plectin-1 as a new detection marker for

PDAC CTCs, and showed that Plectin-1 can be reliably used to detect CTCs in resectable PDAC patients. Plectin-1^+ CTC counts were not significantly different from $EpCAM^+$ CTC counts in both portal vein and peripheral vein (**Figure 5**). Further investigations are needed to clarify whether Plectin-1 was co-expressed in $EpCAM^+$ CTCs and whether captured CTCs expressed one of two.

The number and detection rate of CTCs were higher in portal vein compared to peripheral blood in pancreatobiliary cancer and colorectal cancer (26, 27). However, the count and frequency of $EpCAM^+$ or Plectin-1+ CTCs were not statically significant between portal and peripheral vein (**Figure 5**). Furthermore, CTC counts utilizing microfluidic NanoVelcro CTC chips were correlated with PDAC stage (28), which was contradictory to our result that numbers of $EpCAM^+$ and Plectin-1^+ CTCs were not dependent on the AJCC staging in resectable PDAC patients (**Figure 6**). CTC-positivity was not associated with tumor characteristics, lymph node metastasis, resectability, or advanced TNM stage (29), and the percentage of CTC detection was not related to the TNM stage or distant metastasis (30, 31). It should be considered that we utilized a size-based filter platform instead of an immunomagnetic platform, and the enrolled patients had resectable PDACs with prominently stage II but not advanced or metastatic PDAC.

The role of CTC is still controversial but many reports have shown promising results of CTCs as a tool for refining prognosis and identifying personalized treatment to patients in various gastrointestinal cancers including colorectal cancer and gastric cancer (32–34). Some studies have shown that CTCs can predict the survival rate, diagnosis, and stage of PDAC. CTC presence evaluated by using the CellSearch platform was an independent prognostic factor with respect to OS of advanced PDAC patients (35). Another study used size-based ScreenCell Cyto filtration device and hematoxylin-eosin-safran staining to detect CTCs, reported no differences in survival between patients with positive and negative results for CTC (36). Khoja et al. isolated CTCs by size and identified them solely by morphological characters such as nuclear to cytoplasmic ratio, diameter, hyperchromatic nuclei and cellular shape. They detected CTCs in 93% of pancreatic cancer patients, but did not find any significant difference in either regular survival or progression-free survival (37). The debatable conclusion seems to be associated with varied detection and identification methods.

To date, there are only few studies investigating the prognostic relevance of CTCs in both PV and peripheral blood in PDAC. There were some studies reporting that CTC from portal vein predicts liver metastasis in resectable PDAC patients (38, 39), but no reports have explicitly investigated the correlation between survival rate and CTCs in portal draws as well as peripheral blood of patients with resectable PDAC. We enrolled PDAC patients from 2013 to 2015 prospectively, and followed up till the February of 2020 to collect the complete survival data. In **Figure 7**, $EpCAM^+$ CTC counts in peripheral blood was adversely associated with OS, and more than one $EpCAM^+$ CTCs in portal vein was not significantly related to OS. The enumeration of Plectin-1^+ CTCs in both peripheral blood and portal vein showed none of significant association with OS. In addition, overall recurrence did not differ between the patients without portal vein $EpCAM^+$ CTCs and those with portal vein $EpCAM^+$ CTCs (83.3% vs. 85.0%, $p > 0.999$). Also, we did not find statistically significant difference between the patients without portal vein $EpCAM^+$ CTCs and those with portal vein $EpCAM^+$ CTCs (**Supplementary Table 2**).

We need more investigation of $EpCAM^+$ and Plectin-1^+ CTCs with larger groups of PDAC patients. Further insights into the character and genetic signature of CTCs compared to the parent tumor in surgical patients may allow us to detect or predict recurrence patterns, location and time of relapse.

Here, we would like to address the practicability of Plectin-1 to detect CTCs and the prognostic value of CTCs positive for EpCAM and Plectin-1 from both peripheral and portal venous blood of resectable PDAC patients. In conclusion, Plectin-1 is reliable in identifying CTCs captured by microfabricated filter, and the enumeration of $EpCAM^+$ CTCs in peripheral blood might be associated with poor prognosis in resectable PDAC patients.

DATA AVAILABILITY STATEMENT

The raw data supporting the conclusions of this article will be made available by the authors, without undue reservation.

ETHICS STATEMENT

Ethical approval was obtained from the institutional review board of Seoul National University Hospital (IRB no. 1305-573-489). The patients/participants provided their written informed consent to participate in this study.

AUTHOR CONTRIBUTIONS

BGS, WK, HK: study concept, study design, data acquisition, data analysis, data interpretation, and drafting of the manuscript; EML, YMH, HK, YB: data acquisition; KBL: data interpretation; KHL, JKL, KTL: data acquisition and critical revision of the manuscript for important intellectual content; J-YJ and JKP: study concept, study design, data acquisition, and study supervision. All authors contributed to the article and approved the submitted version.

FUNDING

This project was supported by intramural fund, Seoul National University Hospital Research Fund (grant 04-2013-0990) and Korean Gastroenterology Fund for Future Development. This material is based on the work supported by the Ministry of

Trade, Industry & Energy (MOTIE, Korea) under Industrial Technology Innovation Program (grant10047614, Development of digital cell imaging system). This work was supported by a grant from SK Chemical Research Fund of the Korean Society of Gastroenterology (grant 800-20130378).

SUPPLEMENTARY MATERIAL

The Supplementary Material for this article can be found online at: https://www.frontiersin.org/articles/10.3389/fonc.2020.616440/full#supplementary-material

REFERENCES

1. Sohal DPS, Kennedy EB, Khorana A, Copur MS, Crane CH, Garrido-Laguna I, et al. Metastatic Pancreatic Cancer: ASCO Clinical Practice Guideline Update. *J Clin Oncol* (2018) 36:2545–56. doi: 10.1200/jco.2018.78.9636
2. Yeo CJ, Cameron JL, Lillemoe KD, Sitzmann JV, Hruban RH, Goodman SN, et al. Pancreaticoduodenectomy for cancer of the head of the pancreas. 201 patients. *Ann Surg* (1995) 221:721–31; discussion 31-3. doi: 10.1097/00000658-199506000-00011
3. Allard WJ, Matera J, Miller MC, Repollet M, Connelly MC, Rao C, et al. Tumor cells circulate in the peripheral blood of all major carcinomas but not in healthy subjects or patients with nonmalignant diseases. *Clin Cancer Res* (2004) 10:6897–904. doi: 10.1158/1078-0432.Ccr-04-0378
4. Bockmann B, Grill HJ, Giesing M. Molecular characterization of minimal residual cancer cells in patients with solid tumors. *Biomol Eng* (2001) 17:95–111. doi: 10.1016/S1389-0344(00)00073-3
5. Fetsch PA, Cowan KH, Weng DE, Freifield A, Filie AC, Abati A. Detection of circulating tumor cells and micrometastases in stage II, III, and IV breast cancer patients utilizing cytology and immunocytochemistry. *Diagn Cytopathol* (2000) 22:323–8. doi: 10.1002/(SICI)1097-0339(200005)22:5<323::AID-DC13>3.0.CO;2-L
6. Loberg RD, Fridman Y, Pienta BA, Keller ET, McCauley LK, Taichman RS, et al. Detection and isolation of circulating tumor cells in urologic cancers: a review. *Neoplasia* (2004) 6:302–9. doi: 10.1593/neo.03484
7. Kapeleris J, Kulasinghe A, Warkiani ME, Vela I, Kenny L, O'Byrne K, et al. The Prognostic Role of Circulating Tumor Cells (CTCs) in Lung Cancer. *Front Oncol* (2018) 8:311 doi: :10.3389/fonc.2018.00311
8. Molnar B, Sipos F, Galamb O, Tulassay Z. Molecular detection of circulating cancer cells. Role in diagnosis, prognosis and follow-up of colon cancer patients. *Dig Dis* (2003) 21:320–5. doi: 10.1159/000075355
9. Pelkey TJ, Frierson HFJr., Bruns DE. Molecular and immunological detection of circulating tumor cells and micrometastases from solid tumors. *Clin Chem* (1996) 42:1369–81. doi: 10.1093/clinchem/42.9.1369
10. Zippelius A, Pantel K. RT-PCR-based detection of occult disseminated tumor cells in peripheral blood and bone marrow of patients with solid tumors. An overview. *Ann N Y Acad Sci* (2000) 906:110–23. doi: 10.1111/j.1749-6632.2000.tb06600.x
11. Zhang L, Riethdorf S, Wu G, Wang T, Yang K, Peng G, et al. Meta-analysis of the prognostic value of circulating tumor cells in breast cancer. *Clin Cancer Res* (2012) 18:5701–10. doi: 10.1158/1078-0432.Ccr-12-1587
12. Cristofanilli M, Budd GT, Ellis MJ, Stopeck A, Matera J, Miller MC, et al. Circulating tumor cells, disease progression, and survival in metastatic breast cancer. *N Engl J Med* (2004) 351:781–91. doi: 10.1056/NEJMoa040766
13. Groot Koerkamp B, Rahbari NN, Buchler MW, Koch M, Weitz J. Circulating tumor cells and prognosis of patients with resectable colorectal liver metastases or widespread metastatic colorectal cancer: a meta-analysis. *Ann Surg Oncol* (2013) 20:2156–65. doi: 10.1245/s10434-013-2907-8
14. Maheswaran S, Sequist LV, Nagrath S, Ulkus L, Brannigan B, Collura CV, et al. Detection of mutations in EGFR in circulating lung-cancer cells. *N Engl J Med* (2008) 359:366–77. doi: 10.1056/NEJMoa0800668
15. Micalizzi DS, Maheswaran S, Haber DA. A conduit to metastasis: circulating tumor cell biology. *Genes Dev* (2017) 31:1827–40. doi: 10.1101/gad.305805.117
16. Bausch D, Thomas S, Mino-Kenudson M, Fernandez-del CC, Bauer TW, Williams M, et al. Plectin-1 as a novel biomarker for pancreatic cancer. *Clin Cancer Res* (2011) 17:302–9. doi: 10.1158/1078-0432.Ccr-10-0999
17. Kim EH, Lee JK, Kim BC, Rhim SH, Kim JW, Kim KH, et al. Enrichment of cancer cells from whole blood using a microfabricated porous filter. *Anal Biochem* (2013) 440:114–6. doi: 10.1016/j.ab.2013.05.016
18. Ying H, Dey P, Yao W, Kimmelman AC, Draetta GF, Maitra A, et al. Genetics and biology of pancreatic ductal adenocarcinoma. *Genes Dev* (2016) 30:355–85. doi: 10.1101/gad.275776.115
19. Makohon-Moore A, Iacobuzio-Donahue CA. Pancreatic cancer biology and genetics from an evolutionary perspective. *Nat Rev Cancer* (2016) 16:553–65. doi: 10.1038/nrc.2016.66
20. Sequist LV, Nagrath S, Toner M, Haber DA, Lynch TJ. The CTC-chip: an exciting new tool to detect circulating tumor cells in lung cancer patients. *J Thorac Oncol* (2009) 4:281–3. doi: 10.1097/JTO.0b013e3181989565
21. Joosse SA, Gorges TM, Pantel K. Biology, detection, and clinical implications of circulating tumor cells. *EMBO Mol Med* (2015) 7:1–11. doi: 10.15252/emmm.201303698
22. DiPardo BJ, Winograd P, Court CM, Tomlinson JS. Pancreatic cancer circulating tumor cells: applications for personalized oncology. *Expert Rev Mol Diagn* (2018) 18:809–20. doi: 10.1080/14737159.2018.1511429
23. Barriere G, Fici P, Gallerani G, Fabbri F, Zoli W, Rigaud M. Circulating tumor cells and epithelial, mesenchymal and stemness markers: characterization of cell subpopulations. *Ann Transl Med* (2014) 2:109. doi: 10.3978/j.issn.2305-5839.2014.10.04
24. Ryan DP, Hong TS, Bardeesy N. Pancreatic adenocarcinoma. *N Engl J Med* (2014) 371:1039–49. doi: 10.1056/NEJMra1404198
25. Bryant KL, Mancias JD, Kimmelman AC, Der CJ. KRAS: feeding pancreatic cancer proliferation. *Trends Biochem Sci* (2014) 39:91–100. doi: 10.1016/j.tibs.2013.12.004
26. Catenacci DV, Chapman CG, Xu P, Koons A, Konda VJ, Siddiqui UD, et al. Acquisition of Portal Venous Circulating Tumor Cells From Patients With Pancreaticobiliary Cancers by Endoscopic Ultrasound. *Gastroenterology* (2015) 149:1794–803. doi: 10.1053/j.gastro.2015.08.050
27. Jiao LR, Apostolopoulos C, Jacob J, Szydlo R, Johnson N, Tsim N, et al. Unique localization of circulating tumor cells in patients with hepatic metastases. *J Clin Oncol* (2009) 27:6160–5. doi: 10.1200/jco.2009.24.5837
28. Ankeny JS, Court CM, Hou S, Li Q, Song M, Wu D, et al. Circulating tumour cells as a biomarker for diagnosis and staging in pancreatic cancer. *Br J Cancer* (2016) 114:1367–75. doi: 10.1038/bjc.2016.121
29. Cauley CE, Pitman MB, Zhou J, Perkins J, Kuleman B, Liss AS, et al. Circulating Epithelial Cells in Patients with Pancreatic Lesions: Clinical and Pathologic Findings. *J Am Coll Surg* (2015) 221:699–707. doi: 10.1016/j.jamcollsurg.2015.05.014
30. Bobek V, Gurlich R, Eliasova P, Kolostova K. Circulating tumor cells in pancreatic cancer patients: enrichment and cultivation. *World J Gastroenterol* (2014) 20:17163–70. doi: 10.3748/wjg.v20.i45.17163
31. Kulemann B, Pitman MB, Liss AS, Valsangkar N, Fernandez-Del Castillo C, Lillemoe KD, et al. Circulating tumor cells found in patients with localized and advanced pancreatic cancer. *Pancreas* (2015) 44:547–50. doi: 10.1097/mpa.0000000000000324
32. Huang MY, Tsai HL, Huang JJ, Wang JY. Clinical Implications and Future Perspectives of Circulating Tumor Cells and Biomarkers in Clinical Outcomes of Colorectal Cancer. *Transl Oncol* (2016) 9:340–7. doi: 10.1016/j.tranon.2016.06.006
33. Yang C, Chen F, Wang S, Xiong B. Circulating Tumor Cells in Gastrointestinal Cancers: Current Status and Future Perspectives. *Front Oncol* (2019) 9:1427:1427. doi: 10.3389/fonc.2019.01427
34. Kang HM, Kim GH, Jeon HK, Kim DH, Jeon TY, Park DY, et al. Circulating tumor cells detected by lab-on-a-disc: Role in early diagnosis of gastric cancer. *PloS One* (2017) 12:e0180251. doi: 10.1371/journal.pone.0180251
35. Okubo K, Uenosono Y, Arigami T, Mataki Y, Matsushita D, Yanagita S, et al. Clinical impact of circulating tumor cells and therapy response in pancreatic cancer. *Eur J Surg Oncol* (2017) 43:1050–5. doi: 10.1016/j.ejso.2017.01.241
36. Sefrioui D, Blanchard F, Toure E, Basile P, Beaussire L, Dolfus C, et al. Diagnostic value of CA19.9, circulating tumour DNA and circulating tumour cells in patients with solid pancreatic tumours. *Br J Cancer* (2017) 117:1017–25. doi: 10.1038/bjc.2017.250

37. Khoja L, Backen A, Sloane R, Menasce L, Ryder D, Krebs M, et al. A pilot study to explore circulating tumour cells in pancreatic cancer as a novel biomarker. *Br J Cancer* (2012) 106:508–16. doi: 10.1038/bjc.2011.545
38. Bissolati M, Sandri MT, Burtulo G, Zorzino L, Balzano G, Braga M. Portal vein-circulating tumor cells predict liver metastases in patients with resectable pancreatic cancer. *Tumour Biol* (2015) 36:991–6. doi: 10.1007/s13277-014-2716-0
39. Tien YW, Kuo HC, Ho BI, Chang MC, Chang YT, Cheng MF, et al. A High Circulating Tumor Cell Count in Portal Vein Predicts Liver Metastasis From Periampullary or Pancreatic Cancer: A High Portal Venous CTC Count Predicts Liver Metastases. *Med (Baltimore)* (2016) 95:e3407. doi: 10.1097/md.0000000000003407

Conflict of Interest: The authors declare that the research was conducted in the absence of any commercial or financial relationships that could be construed as a potential conflict of interest.

frontiers in Oncology

ORIGINAL RESEARCH
published: 25 March 2021
doi: 10.3389/fonc.2021.614398

Development of a Novel Prognostic Model for Predicting Lymph Node Metastasis in Early Colorectal Cancer: Analysis Based on the Surveillance, Epidemiology, and End Results Database

Ji Hyun Ahn, Min Seob Kwak, Hun Hee Lee, Jae Myung Cha, Hyun Phil Shin, Jung Won Jeon and Jin Young Yoon*

Department of Internal Medicine, Kyung Hee University Hospital at Gangdong, Kyung Hee University College of Medicine, Seoul, South Korea

OPEN ACCESS

Edited by:
Jaw-Yuan Wang, Kaohsiung Medical University Hospital, Taiwan

Reviewed by:
Zhangya Pu, Central South University, China
Katsuro Ichimasa, Showa University Yokohama Northern Hospital, Japan

***Correspondence:**
Min Seob Kwak
kwac63@khu.ac.kr

Specialty section:
This article was submitted to Gastrointestinal Cancers, a section of the journal Frontiers in Oncology

Received: *06 October 2020*
Accepted: *11 March 2021*
Published: *25 March 2021*

Citation:
Ahn JH, Kwak MS, Lee HH, Cha JM, Shin HP, Jeon JW and Yoon JY (2021) Development of a Novel Prognostic Model for Predicting Lymph Node Metastasis in Early Colorectal Cancer: Analysis Based on the Surveillance, Epidemiology, and End Results Database. Front. Oncol. 11:614398. doi: 10.3389/fonc.2021.614398

Background: Identification of a simplified prediction model for lymph node metastasis (LNM) for patients with early colorectal cancer (CRC) is urgently needed to determine treatment and follow-up strategies. Therefore, in this study, we aimed to develop an accurate predictive model for LNM in early CRC.

Methods: We analyzed data from the 2004-2016 Surveillance Epidemiology and End Results database to develop and validate prediction models for LNM. Seven models, namely, logistic regression, XGBoost, k-nearest neighbors, classification and regression trees model, support vector machines, neural network, and random forest (RF) models, were used.

Results: A total of 26,733 patients with a diagnosis of early CRC (T1) were analyzed. The models included 8 independent prognostic variables; age at diagnosis, sex, race, primary site, histologic type, tumor grade, and, tumor size. LNM was significantly more frequent in patients with larger tumors, women, younger patients, and patients with more poorly differentiated tumor. The RF model showed the best predictive performance in comparison to the other method, achieving an accuracy of 96.0%, a sensitivity of 99.7%, a specificity of 92.9%, and an area under the curve of 0.991. Tumor size is the most important features in predicting LNM in early CRC.

Conclusion: We established a simplified reproducible predictive model for LNM in early CRC that could be used to guide treatment decisions. These findings warrant further confirmation in large prospective clinical trials.

Keywords: machine learning, colorectal cancer, prediction, metastasis, model

INTRODUCTION

Colorectal cancer (CRC) is a major cause of morbidity and mortality worldwide, its importance is expected to continue increasing over time (1, 2). In recent years, increased awareness and the introduction of population-based surveillance and screening programs have led to achieving higher rates of precancerous dysplastic lesions or early CRC detection (3, 4).

Early CRC is a tumor that is confined to the mucosa and/or submucosa regardless of the presence of regional lymph node metastasis (LNM). In certain cases of early CRC, endoscopic resection is a less invasive and cost-effective treatment compared to surgery (5–7). However, the CRC patients with LNM or distant metastasis cannot be adequately cured by local endoscopic treatment alone, and therefore subsequently require surgical resection for achieving a curative treatment.

LNM is found in approximately 6–16% of the patients with submucosal invasive CRC (8–10), however, the number might be underestimated, as clinicians make important treatment decisions based on limited examinations, such as computed tomography (CT) and ultrasonography.

Thus, an accurate and fast assessment of locoregional and/or distant metastases in patients with early CRC is essential to determine whether these patients should undergo additional surgical resections or be needed surveillance regularly. Currently, no universally accepted indications and criteria exist for additional surgical resection after endoscopic resection, even though a fast and accurate assessment of the risk of locoregional LNM after local endoscopic treatment of patients with early CRC is necessary.

Therefore, the aim of present study was to develop a novel prediction model for LNM by using simple histopathological and clinical parameters with high reliability, that can be used to improve patient risk stratification in early CRC.

MATERIALS AND METHODS

Data Source

This study used the Surveillance, Epidemiology, and End Results (SEER) Program database from the National Cancer Institute, which is publicly available U.S. cancer registries. The registry collects and publishes cancer incidence, mortality, and survival data from 17 population-based cancer registries, covering approximately 34.6% of the U.S. population (Iowa, Los Angeles, Connecticut, Utah, Greater California, Idaho, Georgia Center for Cancer Statistics, San Francisco-Oakland, San Jose-Monterey, Louisiana, Hawaii, Massachusetts, Alaska Native tumor registry, Kentucky, New Mexico, New York, Seattle-Puget Sound) (11). The database is roughly represent the U.S. population and includes information on over 9 million cancer cases with over 550,000 new cases added to the database annually. It offers a powerful resource for researchers focused on understanding the natural history of CRC and improving quality healthcare for the patients (11, 12). This retrospective cohort study was evaluated and approved by the Institutional Review Board of the Kyung Hee University Hospital at Gangdong (KHNMC IRB 2020-01-015).

Study Population

The SEER registry collects data including age at diagnosis, sex, race, primary site, histologic type, tumor grade, tumor size, and tumor depth. Using the SEER 1975–2016 database (released 4/15/2019), we analyzed data from all patients diagnosed with T1 CRC for the years 2004-2016. T1 CRC was defined as infiltration of the tumor into the submucosa. We extracted clinical demographic data, including age at diagnosis, sex, race and tumor information including location, size, grade, histologic type, and American Joint Committee on Cancer 7th TNM stages by using SEER disease codes. Tumor location was determined by using the following codes: C18.0 (cecum); C18.1 (appendix); C18.2 (ascending colon); C18.3 (hepatic flexure); C18.4 (transverse colon); C18.5 (splenic flexure); C18.6 (descending colon); C18.7 (sigmoid colon); C18.8 (overlapping lesion of colon); C18.9 (colon); rectosigmoid (C19.9); and rectum (C20.9). The morphology of cancer was categorized according to the ICD-0-3 histology and behavior codes: 8010/3, (carcinoma, NOS); 8020/3, (carcinoma, undifferentiated, NOS); 8140/3, (adenocarcinoma, NOS); 8144/3, (adenocarcinoma, intestinal type); 8210/3, (adenocarcinoma in adenomatous polyp); 8211/3, (tubular adenocarcinoma); 8255/3, (adenocarcinoma with mixed subtypes); 8261/3, (adenocarcinoma in villous adenoma); 8262/3, (villous adenocarcinoma); 8263/3, (adenocarcinoma in tubulovillous adenoma); 8440/3, (cystadenocarcinoma, NOS); 8470/3, (mucinous cystadenocarcinoma, NOS); 8480/3, (mucinous adenocarcinoma); 8481/3, (mucin-producing adenocarcinoma); 8490/3, (signet ring cell carcinoma); and8221/3, (adenocarcinoma in multiple adenomatous polyps). For tumor differentiation grading, we used a four tier classification including well differentiated, moderately differentiated, poorly differentiated, undifferentiated, which is proposed by WHO grading system (13). In order to exclude potentially confounding factor, the patients who received preoperative radiation treatment were excluded. The overall scheme of the workflow is illustrated in **Figure 1**.

Establishment of the Predictive Model

In this study, we used seven machine-learning (ML) models that are commonly used to predict LNM in patients with early CRC. For the linear model, the logistic regression model (LR) was selected (14). The neural network model (NN), which is one of the important classes of nonlinear prediction models and has been reported in a previous study was used (15). For the kernel-based model, we applied the support vector machine (SVM), which is adopted in many clinical applications (16). For the decision tree approach, the classification and regression trees model (CART), XGBoost (XGB) model and random forest (RF) model, which have also been used in clinical research were included (17–19). Finally, for the basic prediction technique, k-nearest neighbor algorithm (kNN) was selected (20).

We used random oversampling method to improve the classifier performance for the minority classes in our imbalanced classes (21). First, the patients were randomly assigned to a training set (90%) and a test set (10%), where the two class (LNM group vs. non-LNM group) proportions in each

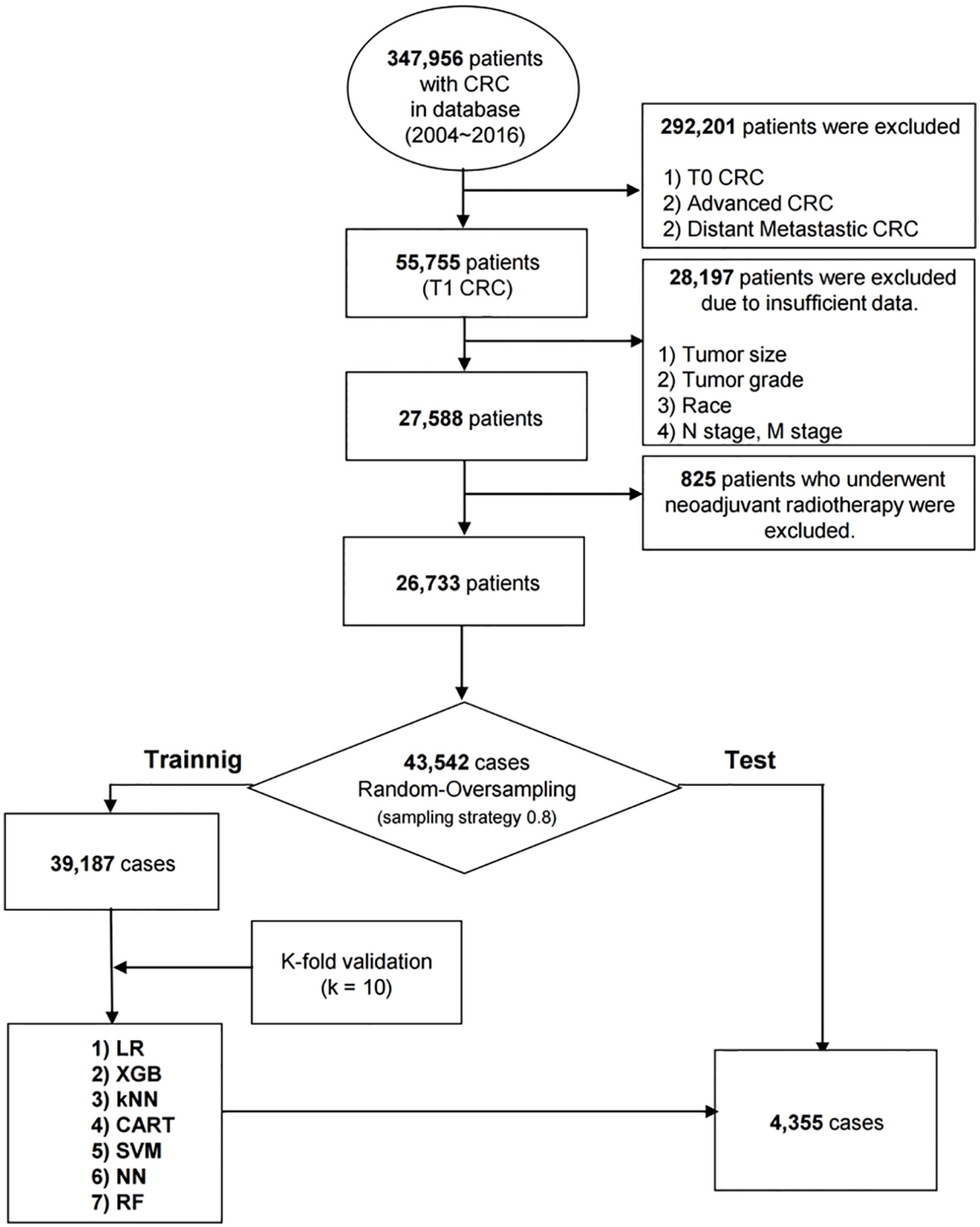

FIGURE 1 | The Workflow of the development process.

set were the same. In the training set, we performed k-fold cross-validation (k = 10), and grid search was used to find the best parameter combinations. For each set of parameters, we fitted the model in turn with 9/10 of data and used 1/10 of data for validation.

Assessment of Prediction Models

To ensure a fair comparison of the models, we used the confusion matrix, area under the curve (AUC), sensitivity (recall), specificity, accuracy, average precision (AP), false positive rate, and precision as performance indicators. We used

the AU-ROC as the performance index and the AP value as the criterion for the precision-recall (PR) curve (22). The average value of the parameter was finally executed on the test set.

Statistical Analysis

All data were obtained using the SEER*Stat software (8.3.6 version; Surveillance Research Program, National Cancer Institute). All analyses were performed with Python (version 3.6.9) and R statistical software (version 3.6.0). Demographic differences between the two groups were tested using the Student's t-test and Pearson chi-square test. To better evaluate the performance of the models, we used a paired t test to compare the AU-ROC further in each resampling calculation. A two-sided $P \leq 0.05$ was considered statistically significant.

RESULTS

Baseline Characteristics

A total of 347,956 patients with CRC between 2004 and 2016 were collected, of which about 292,201 patients were excluded from the study because they were diagnosed with T0 or advanced CRC with or without distant metastasis. After excluding 28,197 patients with insufficient data and 825 patients treated with preoperative radiation therapy, 26,733 patients with a diagnosis of early CRC (T1) were analyzed. The model included eight independent prognostic variables, including age at diagnosis, sex, race, primary site, histologic type, tumor grade, and, tumor size. The analyzed patients were divided into the LNM (2,543 patients, 9.5%) and non-LNM groups (24,190 patients, 90.5%). The younger people (< 60 years) tended to have more LNM at diagnosis compared with the older group ($P < 0.001$). Significantly higher LNM in women compared with men was observed in the patients with early CRC ($P < 0.001$). The proportion of LNM in the distal colon included the descending colon, sigmoid colon, and the rectosigmoid junction, was significantly higher than that in the colon proximal to the splenic flexure ($P < 0.001$). The overall racial and/or ethnic distribution was 69.7% non-Hispanic whites, 11.9% non-Hispanic blacks, 9.0% Hispanics, 8.9% non-Hispanic Asians or Pacific Islander, and 0.5% others (non-Hispanic American, Indian, Alaska natives). Among all patients evaluated, 20.8% (n=5,572) had well differentiated tumor; 71.2% (n=19,026), moderately differentiated; 7.1% (n=1,902), poorly differentiated; 0.9% (n=233), undifferentiated cancer. The mean tumor size was significantly larger in the early CRC patients with LNM than in those of without LNM (22.8mm vs. 20.6 mm) ($P < 0.001$). **Table 1** shows the overall distribution of baseline characteristics of the study population.

Tuning of Parameters

We trained the SVM a combination of a C value of 1.0 and a kernel smoothing parameter σ of 0.001. For kNN, a relatively large number of k = 14 was optimal. XGB was performed using the parameters with a maximum depth of 6 and a minimum child weight of 1. For NN, the hyper-parameters were changed during training to obtain the optimal model based on the validation set. The final selected hyper-parameters were a learning rate of 0.001, epoch of 300, hidden layer of 3, dropout rate of 0.3, and batch size of 128. For RF, a relatively large number of randomly selected 61 subtrees provided the best performance.

Performance of Developed Models

The average ROC curves and PR curves during the training are shown in **Figure 2**. Most models had AUC values above 0.81, but the values of LR, XGB, and SVM were lower. The confusion matrix was also calculated for the seven models (**Table 2**). As shown in **Table 2**, LR, XGB, and SVM generated a large number of FNs, and kNN and CART models had a large number of FPs during the prediction process. The RF model produced the minimum number of FN (= 5) and FP (= 171). **Table 3** shows the AUC, sensitivity, specificity, precision, negative predictive value (NPV), false discovery rate (FDR), accuracy, AP, F1, and Matthews correlation coefficient of each model. The linear model LR showed the worst performance; its accuracy rate was up to 0.60, whereas the accuracy of RF was up to 0.96.

The accuracy of the other models was less than 0.90. RF achieved the highest AUC value of 0.991, and CART had an AU-ROC value of 0.944. LR had the lowest AUC value of 0.623. The RF model showed the best sensitivity and specificity, as well as the best precision, NPV, FDR, accuracy, AP score, F1 score and Matthews correlation coefficient value.

Feature Importance Comparisons between Algorithms

We quantified the variable importance using the coefficients of permutation importance for LNM in each model (**Figure 3**). For most of the models, the variables including tumor grade, depth of tumor, and age had important influences on the predictability for LNM in early CRC. Based on our quantification, tumor size showed the highest frequency for the top predictors in four of the six models.

DISCUSSION

In this study, we established a novel predictive model by combining eight clinicopathologic parameters to predict LNM in early CRC using seven ML models. To the best of our knowledge, this is the first large-scale study to develop a predictive model for LNM by combining easily available simple clinical and pathological data in patients with early CRC. Clinicians are often confronted with the difficulty of selecting candidates who will benefit from surgery after local endoscopic resection.

Currently, in clinical practice, risk stratification in these patients is usually performed by histopathologists carefully analyzing the specimen to determine the risk of LNM, caused by the limited capacity of CT to accurately identify LNM (23).

In previous studies, the pathological factors that showed the strongest independent predictive value for LNM in early CRC are tumor type, poor histological differentiation, and the depth of submucosal invasion (24–27). However, the high interobserver variability in the pathological assessment limits their clinical usefulness and should therefore be interpreted with caution as a univariate marker when deciding whether to proceed with surgery (28, 29). Therefore, the multivariable risk model combining the

TABLE 1 | Baseline characteristics.

Variables	LNM (-)	LNM (+)	
	N = 24190	N = 2543	*P*-value
Age at diagnosis, n (%)			<0.001
0-9	0 (0.0)	1 (0.0)	
10-19	5 (0.0)	1 (0.0)	
20-29	73 (0.3)	10 (0.4)	
30-39	339 (1.4)	61 (2.4)	
40-49	1511 (6.3)	241 (9.5)	
50-59	5684 (23.5)	730 (28.7)	
60-69	6775 (28.0)	683 (26.9)	
70-79	5952 (24.6)	544 (21.4)	
80-89	3410 (14.1)	245 (9.6)	
90-99	441 (1.8)	27 (1.1)	
Sex, n (%)			<0.001
M	12864 (53.2)	1254 (49.3)	
F	11326 (46.8)	1289 (50.7)	
Primary site, n (%)			<0.001
Cecum	3355 (13.9)	381 (15.0)	
Appendix	119 (0.5)	4 (0.2)	
Ascending colon	3493 (14.4)	300 (11.8)	
Hepatic flexure of colon	665 (2.7)	61 (2.4)	
Transverse colon	1545 (6.4)	119 (4.7)	
Splenic flexure of colon	381 (1.6)	39 (1.5)	
Descending colon	1009 (4.2)	97 (3.8)	
Sigmoid colon	6193 (25.6)	773 (30.4)	
Overlapping lesion of colon	78 (0.3)	5 (0.2)	
Colon, NOS	111 (0.5)	7 (0.3)	
Rectosigmoid junction	1737 (7.2)	268 (10.5)	
Rectum, NOS	5504 (22.7)	489 (19.2)	
Tumor grade, n (%)			<0.001
Well differentiated	5284 (21.8)	288 (11.3)	
Moderately differentiated	17173 (71.0)	1853 (72.9)	
Poorly differentiated	1538 (6.4)	364 (14.3)	
Undifferentiated	195 (0.8)	38 (1.5)	
Race, n (%)			<0.001
Hispanic	2186 (9.1)	228 (9.0)	
Non-Hispanic American Indian/Alaska Native	129 (0.5)	10 (0.4)	
Non-Hispanic Asian or Pacific Islander	2099 (8.7)	270 (10.6)	
Non-Hispanic Black	2837 (11.7)	354 (13.9)	
Non-Hispanic White	16939 (70.0)	1681 (66.1)	
Tumor type, n (%)			<0.001
Carcinoma, NOS	40 (0.2)	6 (0.2)	
Carcinoma, undifferentiated, NOS	1 (0.0)	1 (0.0)	
Adenocarcinoma, NOS	9657 (39.9)	1148 (45.1)	
Adenocarcinoma, intestinal type	2 (0.0)	2 (0.1)	
Adenocarcinoma in adenomatous polyp	5943 (24.6)	513 (20.2)	
Tubular adenocarcinoma	47 (0.2)	2 (0.1)	
Adenocarcinoma with mixed subtypes	20 (0.1)	4 (0.2)	
Adenocarcinoma in villous adenoma	1378 (5.7)	130 (5.1)	
Villous adenocarcinoma	27 (0.1)	1 (0.0)	
Adenocarcinoma in tubulovillous adenoma	6420 (26.5)	614 (24.2)	
Cystadenocarcinoma, NOS	1 (0.0)	0 (0.0)	
Mucinous cystadenocarcinoma, NOS	11 (0.1)	0 (0.0)	
Mucinous adenocarcinoma	487 (2.0)	82 (3.2)	
Mucin-producing adenocarcinoma	107 (0.4)	20 (0.8)	
Signet ring cell carcinoma	49 (0.2)	20 (0.8)	
Tumor size, mm, mean (SD)	20.6 (25.4)	22.8 (20.9)	<0.001

SD, standard deviation.

histopathological data with clinical data can reduce the inaccuracies associated with relying on individual subjective markers and to better define the optimal treatment strategy for early CRC.

With the recent rapid development of computer-aided technology, the application of ML model in cancer diagnosis has an important role; it is being widely used in the medical field with growing trend toward predictive medicine (30–32). We hereby developed an ML model by using the simple clinicopathological parameters in large data, which provided high predictive ability of LNM for patients with early CRC.

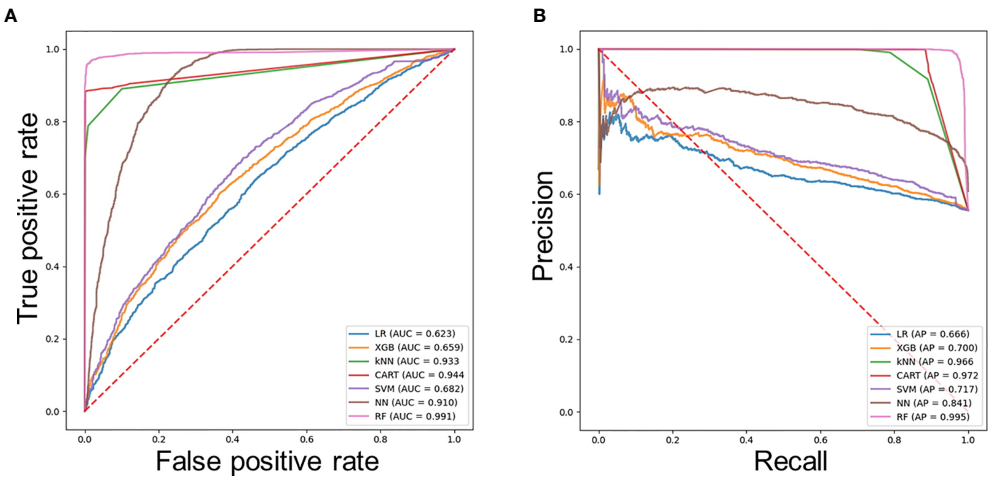

FIGURE 2 | Evaluation of the predictive models. **(A)** Average ROC curves of seven models. **(B)** Average PR curves, indicating the tradeoff between precision and recall.

TABLE 2 | Confusion matrices of developed models.

Confusion matrix	Actual	Prediction	
		LNM (-)	LNM (+)
LR	LNM (-)	1903	516
	LNM (+)	1240	696
XGB	LNM (-)	2163	256
	LNM (+)	1468	468
kNN	LNM (-)	1907	512
	LNM (+)	18	1918
CART	LNM (-)	1907	512
	LNM (+)	18	1918
SVM	LNM (-)	1898	521
	LNM (+)	1053	883
NN	LNM (-)	1995	424
	LNM (+)	304	1632
RF	LNM (-)	2248	171
	LNM (+)	5	1931

LR, logistic regression; XGB, XGBoost, kNN, k-nearest neighbor; CART, classification and regression trees model; SVM, support vector machine; NN, neural network; RF, random forest.

To date, a few ML models for prediction of metastasis in patients with early CRC have been developed and evaluated for prognosis and prediction in patients with early CRC (33–36). Ichimasa et al. developed the SVM model with 45 clinicopathologic factors for prediction of LNM in patients with early CRC. They reported that artificial intelligence significantly reduces unnecessary extra surgery after endoscopic resection of T1 CRC without LNM positive in comparison to the current guidelines (33). Another Japanese study showed a deep learning model for predicting LNM from pathology images with cytokeratin immunohistochemistry in early CRC (34). However, these studies were retrospective in nature with single center or small numbers of patients. Due to the low rate of metastasis in early CRC, only a limited number of events exist, leading to limited data. Furthermore, inadequate data could not provide sufficient satisfactory performance under ML algorithms and may have led to lower predictive performance ranging from 0.821 to 0.913, which is less than the result from our RF model. A recent Chinese study also presented a predicting model for LNM that incorporates both the radiomics signature, which combine multiple individual CT imaging features, and several clinical factors using the multivariable logistic regression analysis (35). Although this might be an interesting attempt, the model validity is not guaranteed considering the heterogeneity in the quality of CT image between facilities and its accuracy of approximately 78%, which is lower than the performance of the predictive model we constructed. Lastly, Kudo et al. also employed deep-learning-based modeling to predict LNM in

TABLE 3 | Performance of developed models.

Models	AUC	Sensitivity	Specificity	Precision	NPV	FDR	Accuracy	AP	F1 Score	Matthews correlation coefficient
LR	0.623	0.360	0.787	0.574	0.606	0.426	0.597	0.666	0.442	0.162
XGB	0.659	0.242	0.894	0.646	0.596	0.354	0.604	0.700	0.352	0.181
kNN	0.933	0.991	0.788	0.789	0.991	0.211	0.878	0.966	0.879	0.780
CART	0.944	0.991	0.788	0.789	0.991	0.211	0.878	0.972	0.879	0.780
SVM	0.682	0.456	0.785	0.629	0.643	0.371	0.639	0.717	0.529	0.256
NN	0.910	0.843	0.825	0.794	0.868	0.206	0.833	0.841	0.818	0.665
RF	0.991	0.997	0.929	0.919	0.998	0.081	0.960	0.995	0.956	0.922

AUC, area under curve; NPV, negative predictive value; FDR, false discovery rate; AP, average precision; LR, logistic regression; XGB, XGBoost, kNN, k-nearest neighbor; CART, classification and regression trees model; SVM, support vector machine; NN, neural network; RF, random forest.

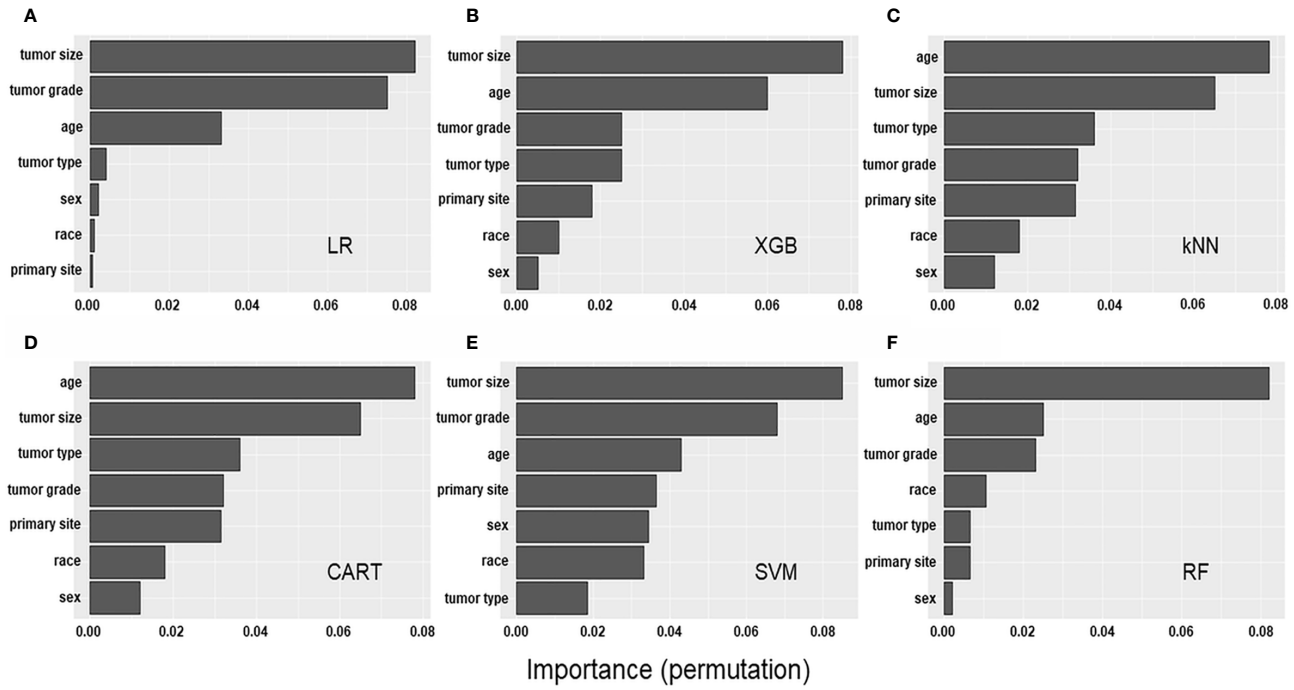

FIGURE 3 | Factor importance of the developed models. The **(A–F)** Bar graphs describe the proportion of importance of the different predictors in the model.

T1 CRC (36). However, they only used NN model for nonlinear dynamic system with smaller sample size than our study and assessed LNM using only CT imaging in the cases treated by endoscopic resection, because pathologic confirmation was not available.

Meanwhile, the reason why the RF model outperforms the other ML algorithms is not easily explained. It might be attributed to that the RF models generally demonstrate the most substantial improvement over linear methods and, might be outperform kernel-based model and neural network model in many categorical variables and some outliers from the nature of large retrospective cohort data. However, to build robust prognostic models for LNM in early CRC, other variables, such as gene expression and histologic image data beyond clinical-pathological variables, should be needed.

In our study, we investigated the variable importance of the predictive models developed, as it could be useful for decision-making by clinicians. Our findings indicated that tumor size was the most important factor for predicting the presence of LNM in early CRC. The prognostic value of tumor size in CRC has long been studied, but no consensus has been reached. Zhang et al. and Kornprat et al. demonstrated a significant association between tumor size and metastasis in CRC (37, 38), whereas Miller et al. indicated no prognostic significance of tumor size in CRC (39). Furthermore, its potential prognostic role in patients with early CRC has not been well investigated. This is the first largest study to identify the prognostic value of tumor size for early CRC and provide statistical evidence for further prospective study. Despite the aforementioned, the current study has several limitations. First, since the SEER database is a nationwide program, several diagnostic criteria, such as histological grades and verification of tumor locations might be subjective, which could cause potential systematic bias. Second, detailed histopathological data, such as lymphovascular invasion, tumor budding, and precise depth of tumor invasion that have been associated with metastasis are insufficient. These data require further assessment to improve the performance of our ML algorithms. Third, our study comprised predominately of white patients; thus, the findings may not be generalized to other racial populations. Finally, the data have a class imbalance problem between the patients with and those without LNM, which means that the rate of LNM is low in early CRC. Therefore, during the tuning process, the parameters had to be further optimizing to avoid overfitting. To further improve the accuracy of the established model, it is necessary to collect more clinical data and further optimizing the parameters are necessary in subsequent studies.

In conclusion, we established and compared seven models to predict metastasis in early CRC by using easily available clinical and histopathological features in real practice. The RF model, a simplified reproducible predictive model, showed the highest predictive power compared with the other models. Tumor size the most important predictor of LNM in early CRC. Therefore, the patients with tumor larger than 3 cm, who were identified as high-risk through the model, may requires careful attention to selection and additional surgical treatment in early CRC. However, because of the limitations inherent in studies based on observational data, these findings should be confirmed in prospective clinical trials.

DATA AVAILABILITY STATEMENT

Publicly available datasets were analyzed in this study. This data can be found here: https://seer.cancer.gov.

AUTHOR CONTRIBUTIONS

MK designed the study. JA, JC and HS analyzed and interpreted the data and wrote the manuscript. JJ and JY supervised the project and revised the paper. All authors contributed to the article and approved the submitted version.

FUNDING

This research was supported by the Basic Science Research Program of the National Research Foundation of Korea (NRF), which is funded by the Korean Ministry of Science, ICT and Future Planning [grant number NRF- 2019R1C1C1003524].

REFERENCES

1. Bray F, Ferlay J, Soerjomataram I, Siegel RL, Torre LA, Jemal A. Global cancer statistics 2018: GLOBOCAN estimates of incidence and mortality worldwide for 36 cancers in 185 countries. *CA Cancer J Clin* (2018) 68:394–424. doi: 10.3322/caac.21492
2. Ferlay J, Shin HR, Bray F, Forman D, Mathers C, Parkin DM. Estimates of worldwide burden of cancer in 2008: GLOBOCAN 2008. *Int J Cancer* (2010) 127:2893–917. doi: 10.1002/ijc.25516
3. Logan RF, Patnick J, Nickerson C, Coleman L, Rutter MD, Von Wagner C, et al. Outcomes of the Bowel Cancer Screening Programme (BCSP) in England after the first 1 million tests. *Gut* (2012) 61:1439–46. doi: 10.1136/gutjnl-2011-300843
4. Inadomi JM. Screening for Colorectal Neoplasia. *N Engl J Med* (2017) 376:149–56. doi: 10.1056/NEJMcp1512286
5. Seitz U, Bohnacker S, Seewald S, Thonke F, Brand B, Braiutigam T, et al. Is endoscopic polypectomy an adequate therapy for malignant colorectal adenomas? Presentation of 114 patients and review of the literature. *Dis Colon Rectum* (2004) 47:1789–96; discussion 1796–87. doi: 10.1007/s10350-004-0680-2
6. Kawamura YJ, Sugamata Y, Yoshino K, Abo Y, Nara S, Sumita T, et al. Endoscopic resection for submucosally invasive colorectal cancer: is it feasible? *Surg Endosc* (1999) 13:224–7. doi: 10.1007/s004649900949
7. Kashida H, Kudo SE. Early colorectal cancer: concept, diagnosis, and management. *Int J Clin Oncol* (2006) 11:1–8. doi: 10.1007/s10147-005-0550-5
8. Ricciardi R, Madoff RD, Rothenberger DA, Baxter NN. Population-based analyses of lymph node metastases in colorectal cancer. *Clin Gastroenterol Hepatol* (2006) 4:1522–7. doi: 10.1016/j.cgh.2006.07.016
9. Tominaga K, Nakanishi Y, Nimura S, Yoshimura K, Sakai Y, Shimoda T. Predictive histopathologic factors for lymph node metastasis in patients with nonpedunculated submucosal invasive colorectal carcinoma. *Dis Colon Rectum* (2005) 48:92–100. doi: 10.1007/s10350-004-0751-4
10. Bayar S, Saxena R, Emir B, Salem RR. Venous invasion may predict lymph node metastasis in early rectal cancer. *Eur J Surg Oncol* (2002) 28:413–7. doi: 10.1053/ejso.2002.1254
11. Daly MC, Paquette IM. Surveillance, Epidemiology, and End Results (SEER) and SEER-Medicare Databases: Use in Clinical Research for Improving Colorectal Cancer Outcomes. *Clin Colon Rectal Surg* (2019) 32:61–8. doi: 10.1055/s-0038-1673355
12. Weiss JM, Pfau PR, O'connor ES, King J, Loconte N, Kennedy G, et al. Mortality by stage for right- versus left-sided colon cancer: analysis of surveillance, epidemiology, and end results–Medicare data. *J Clin Oncol* (2011) 29:4401–9. doi: 10.1200/JCO.2011.36.4414
13. Nagtegaal ID, Odze RD, Klimstra D, Paradis V, Rugge M, Schirmacher P, et al. The 2019 WHO classification of tumours of the digestive system. *Histopathology* (2020) 76:182–8. doi: 10.1111/his.13975
14. Menard S. *Applied logistic regression analysis*. SAGE Publications (2002). doi: 10.4135/9781412983433
15. Nigrin A. *Neural networks for pattern recognition*. MIT press ACM SIGART Bulletin (1993). doi: 10.1145/182053.1064827
16. Cortes C, Vapnik V. Support-vector networks. *Mach Learn* (1995) 20:273–97. doi: 10.1007/BF00994018
17. Breiman L. Random forests. *Mach Learn* (2001) 45:5–32. doi: 10.1023/A:1010933404324
18. Zhang H, Guo H, Wang J. Research on type 2 diabetes mellitus precise prediction models based on XGBoost algorithm. *Chin J Lab Diagn* (2018) 22:408–12. doi: 10.3969/j.issn.1007-4287.2018.03.008
19. Marshall RJ. The use of classification and regression trees in clinical epidemiology. *J Clin Epidemiol* (2001) 54:603–9. doi: 10.1016/S0895-4356(00)00344-9
20. Altman NS. An introduction to kernel and nearest-neighbor nonparametric regression. *Am Stat* (1992) 46:175–85. doi: 10.1080/00031305.1992.10475879
21. Lemaître G, Nogueira F, Aridas CK. Imbalanced-learn: A python toolbox to tackle the curse of imbalanced datasets in machine learning. *J Mach Learn Res* (2017) 18:559–63. doi: arXiv:1609.06570
22. Bewick V, Cheek L, Ball J. Statistics review 13: receiver operating characteristic curves. *Crit Care* (2004) 8:508. doi: 10.1186/cc3000
23. Dighe S, Purkayastha S, Swift I, Tekkis PP, Darzi A, A'hern R, et al. Diagnostic precision of CT in local staging of colon cancers: a meta-analysis. *Clin Radiol* (2010) 65:708–19. doi: 10.1016/j.crad.2010.01.024
24. Xu F, Xu J, Lou Z, Di M, Wang F, Hu H, et al. Micropapillary component in colorectal carcinoma is associated with lymph node metastasis in T1 and T2 Stages and decreased survival time in TNM stages I and II. *Am J Surg Pathol* (2009) 33:1287–92. doi: 10.1097/PAS.0b013e3181a5387b
25. Bosch SL, Teerenstra S, De Wilt JH, Cunningham C, Nagtegaal ID. Predicting lymph node metastasis in pT1 colorectal cancer: a systematic review of risk factors providing rationale for therapy decisions. *Endoscopy* (2013) 45:827–41. doi: 10.1055/s-0033-1344238
26. Glasgow SC, Bleier JI, Burgart LJ, Finne CO, Lowry AC. Meta-analysis of histopathological features of primary colorectal cancers that predict lymph node metastases. *J Gastrointestinal Surg* (2012) 16:1019–28. doi: 10.1007/s11605-012-1827-4
27. Sun Z-Q, Ma S, Zhou Q-B, Yang S-X, Chang Y, Zeng X-Y, et al. Prognostic value of lymph node metastasis in patients with T1-stage colorectal cancer from multiple centers in China. *World J Gastroenterol* (2017) 23:8582. doi: 10.3748/wjg.v23.i48.8582
28. Brockmoeller SF, West NP. Predicting systemic spread in early colorectal cancer: Can we do better? *World J Gastroenterol* (2019) 25:2887–97. doi: 10.3748/wjg.v25.i23.2887
29. Harris EI, Lewin DN, Wang HL, Lauwers GY, Srivastava A, Shyr Y, et al. Lymphovascular invasion in colorectal cancer: an interobserver variability study. *Am J Surg Pathol* (2008) 32:1816. doi: 10.1097/PAS.0b013e3181816083
30. Kourou K, Exarchos TP, Exarchos KP, Karamouzis MV, Fotiadis DI. Machine learning applications in cancer prognosis and prediction. *Comput Struct Biotechnol J* (2015) 13:8–17. doi: 10.1016/j.csbj.2014.11.005
31. Statnikov A, Wang L, Aliferis CF. A comprehensive comparison of random forests and support vector machines for microarray-based cancer classification. *BMC Bioinf* (2008) 9:319. doi: 10.1186/1471-2105-9-319
32. Xiao Y, Wu J, Lin Z, Zhao X. A deep learning-based multi-model ensemble method for cancer prediction. *Comput Methods Programs Biomed* (2018) 153:1–9. doi: 10.1016/j.cmpb.2017.09.005
33. Ichimasa K, Kudo S-E, Mori Y, Misawa M, Matsudaira S, Kouyama Y, et al. Artificial intelligence may help in predicting the need for additional surgery

after endoscopic resection of T1 colorectal cancer. *Endoscopy* (2018) 50:230–40. doi: 10.1055/s-0043-122385
34. Takamatsu M, Yamamoto N, Kawachi H, Chino A, Saito S, Ueno M, et al. Prediction of early colorectal cancer metastasis by machine learning using digital slide images. *Comput Methods Programs Biomed* (2019) 178:155–61. doi: 10.1016/j.cmpb.2019.06.022
35. Huang YQ, Liang CH, He L, Tian J, Liang CS, Chen X, et al. Development and Validation of a Radiomics Nomogram for Preoperative Prediction of Lymph Node Metastasis in Colorectal Cancer. *J Clin Oncol* (2016) 34:2157–64. doi: 10.1200/JCO.2015.65.9128
36. Kudo SE, Ichimasa K, Villard B, Mori Y, Misawa M, Saito S, et al. Artificial Intelligence System to Determine Risk of T1 Colorectal Cancer Metastasis to Lymph Node. *Gastroenterology* (2020) 160:1075–84. doi: 10.1053/j.gastro.2020.09.027
37. Zhang H, Chen C-S, Cong J-C, Qiao L, Hasegawa T, Takashima S. Clinicopathological characteristics of advanced colorectal cancer 30 mm or smaller in diameter. *Chin Med Sci J Chung-kuo i hsueh k'o hsueh tsa chih* (2007) 22:98–103.
38. Kornprat P, Pollheimer MJ, Lindtner RA, Schlemmer A, Rehak P, Langner C. Value of tumor size as a prognostic variable in colorectal cancer: a critical reappraisal. *Am J Clin Oncol* (2011) 34:43–9. doi: 10.1097/COC.0b013e3181cae8dd
39. Miller W, Ota D, Giacco G, Guinee V, Irimura T, Nicolson G, et al. Absence of a relationship of size of primary colon carcinoma with metastasis and survival. *Clin Exp Metastasis* (1985) 3:189–96. doi: 10.1007/BF01786762

Conflict of Interest: The authors declare that the research was conducted in the absence of any commercial or financial relationships that could be construed as a potential conflict of interest.

frontiers in Oncology

ORIGINAL RESEARCH
published: 29 March 2021
doi: 10.3389/fonc.2021.632962

KRAS Mutational Regression Is Associated With Oligo-Metastatic Status and Good Prognosis in Metastatic Colorectal Cancer

Alessandro Ottaiano[1†], Guglielmo Nasti[1†], Mariachiara Santorsola[1], Vincenzo Altieri[2], Giuseppina Di Fruscio[2], Luisa Circelli[3], Amalia Luce[4,5], Alessia Maria Cossu[4,5], Giosuè Scognamiglio[1], Francesco Perri[1], Marco Correra[1], Andrea Belli[1], Paolo Delrio[1], Gerardo Botti[1‡] and Michele Caraglia[4,5‡]*

[1] Istituto Nazionale Tumori di Napoli, IRCCS "G. Pascale", Naples, Italy, [2] INNOVALAB, Centro Direzionale Isola A2, Naples, Italy, [3] Department of Precision Oncology, AMES-Centro Polidiagnostico Strumentale, Casalnuovo di Napoli, Italy, [4] Department of Precision Medicine, University of Campania "L. Vanvitelli", Naples, Italy, [5] Biogem Scarl, Institute of Genetic Research, Laboratory of Precision and Molecular Oncology, Ariano Irpino, Italy

OPEN ACCESS

Edited by:
Jaw-Yuan Wang,
Kaohsiung Medical University Hospital, Taiwan

Reviewed by:
Giovanni Li Volti,
University of Catania, Italy
Alessandra Rosati,
University of Salerno, Italy

***Correspondence:**
Alessandro Ottaiano
a.ottaiano@istitutotumori.na.it

[†]These authors share first authorship

[‡]These authors share last authorship

Specialty section:
This article was submitted to Gastrointestinal Cancers, a section of the journal Frontiers in Oncology

Received: 24 November 2020
Accepted: 10 March 2021
Published: 29 March 2021

Citation:
Ottaiano A, Nasti G, Santorsola M, Altieri V, Di Fruscio G, Circelli L, Luce A, Cossu AM, Scognamiglio G, Perri F, Correra M, Belli A, Delrio P, Botti G and Caraglia M (2021) KRAS Mutational Regression Is Associated With Oligo-Metastatic Status and Good Prognosis in Metastatic Colorectal Cancer. Front. Oncol. 11:632962. doi: 10.3389/fonc.2021.632962

Background: We previously reported that loss of *KRAS* mutations ("regressive" mutational trajectories) from primary tumors to metastases associated with the oligo-metastatic status in colorectal cancer (CRC). The present study was undertaken in order to analyze the mutational trajectories of *KRAS* in a well-characterized cohort of CRC patients who developed poly- or oligo-metastatic disease.

Material and Methods: Patients were treated and followed-up according to European Society of Medical Oncology guidelines. Primary CRC FFPE tissue and metastatic circulating-free DNA were extracted using the QIAamp DNA specific kits (Qiagen, Hilden, Germany). Samples were sequenced with the Oncomine Solid Tumour DNA kit (Thermo Fisher Scientific, Waltham, MA, USA). Plasma collection for liquid biopsy was done from 1 to 14 days before starting first-line chemotherapy. Analysis of the prognostic power of *KRAS* evolutionary trajectories was done with uni- and multivariate analyses.

Results: One-hundred-fourteen patients were enrolled. Sixty-three patients presented with mutated *KRAS* (mut*KRAS*) and 51 with wild-type *KRAS* (wt*KRAS*). *KRAS* mutational concordance was high (70.1%).Two divergent subsets were identified: mut*KRAS* in primary tumors and wt*KRAS* in metastatic ones (regressive: mut*KRAS* → wt*KRAS* in 8.8% of patients), and *vice versa* (progressive: wt*KRAS* → mut*KRAS* in 21.1% of patients). An association between *KRAS* regressive trajectory and the oligo-metastatic status (P <0.0001) was found. At multivariate analysis, regressive and progressive mutational trajectories emerged as independent prognostic factors for survival, with Hazard Ratios of 0.22 (CI 95%: 0.08–0.61; median survival: not reached) and 2.70 (CI 95%: 1.11–6.56, median survival: 12.1 months), respectively.

Conclusions: Our data provide evidence that the evolutionary trajectories of *KRAS* can have a strong clinical prognostic role and that they can be involved in discriminating between poly-metastatic aggressive *vs* oligo-metastatic indolent CRC.

Keywords: *KRAS*, metastatic colorectal cancer, DNA, liquid biopsy, prognosis

INTRODUCTION

Colorectal cancer (CRC) is the third cause of cancer-related death worldwide (1). About 30% of patients present at diagnosis with metastatic disease, and half of them will develop metastases after surgical resection of the primary tumor (2). The survival of metastatic colorectal cancer (mCRC) patients significantly improved in the last 20 years with the introduction of target-oriented drugs [anti-EGFR (Epidermal Growth Factor Receptor) and anti-angiogenic agents] associated with chemotherapy (fluoropirimidines, oxaliplatin and irinotecan); however, it still very rarely encompasses 30 months (3). The selection of patients on a genetic basis allowed the selection of those more prone to respond to specific treatments. In fact, it is now clear that mCRC patients bearing specific *KRAS* (Kirsten RAt Sarcoma viral oncogene homolog) mutations do not benefit from anti-EGFR treatment because mutated and constitutively hyper-activated *KRAS* determine a ligand-independent activation of EGFR (4). We previously reported that loss of *KRAS* mutations ("regressive" mutational trajectories) from primary tumors to metastases on FFPE (Formalin-Fixed Paraffin Embedded) resected tissues was associated with long-term survivals and the oligo-metastatic status in mCRC (5, 6). However, the evaluation of circulating tumor DNA (ctDNA) sequences, also called "liquid biopsy", has provided a great opportunity to study the mutational evolution of cancers with a non-invasive, real-time and repeatable approach. On these bases, Misale et al. (7) demonstrated that the occurrence of *KRAS* point mutations preceded the resistance to anti-EGFR monoclonal antibodies in mCRC patients who experienced an initial response. Furthermore, Siravegna et al. (8) showed that in mCRC patients, during anti-EGFR treatment withdrawals, *KRAS* mutated mCRC cells regain drug-sensitivity due to decay in frequency of *KRAS* mutations which, in some cases, become undetectable. Altogether, these data indicate that mCRC genetics is dynamic and that the evaluation of the tumor mutational status in a single moment could not be representative of the cancer mutational evolution.

The present study was undertaken in order to analyze the mutational trajectories of *KRAS* in a well-characterized cohort of mCRC patients and to correlate those trajectories with the prognosis and the extent of the disease (oligo- *versus* poly-metastatic status).

MATERIAL AND METHODS

Patients' Selection and Management

This was a retrospective, non-interventional and biomarkers study officially approved by the Scientific Directorate on November 11, 2020. The source of data was the electronic database reporting clinical records of CRC patients who underwent to radical excision of primary tumor from 2015 to 2018 and characterization of *KRAS* mutational status. Thereafter, they developed metastatic and unresectable disease and were enrolled into the study upon signature of an informed consent to perform a liquid biopsy for *KRAS* reassessment just before starting the first-line chemotherapy. The treatments were administered at the SSD (*Struttura Semplice Dipartimentale*) Innovative Therapies for Abdominal Metastases of the *Istituto Nazionale Tumori di Napoli, IRCCS "G. Pascale*. Oligo-metastatic patients were intended as those having one to three lesions per organ with a maximum tumor diameter smaller than 70 mm and no lesions encompassing 25 mm diameter. To avoid clear negative prognostic influences, some clinical criteria for patients' inclusion were established *a priori* and consisted on: Performance Status ECOG (Eastern Cooperative Oncology Group) 0 or 1, age <80 years and life expectancy of at least three months. According to these criteria, 114 patients were selected: 63 had *KRAS* mutations (mutated *KRAS*: mut*KRAS*), 51 were *KRAS* wild-type (wt*KRAS*) (see DNA sequencing). Treatments were chosen according to ESMO (European Society of Medical Oncology) guidelines (9). All patients signed a written informed consent before treatment administration and molecular assessments. The primary outcome of this study was the analysis of the prognostic power of different *KRAS* evolutionary trajectories between the mutational status in primary tumor and that in liquid biopsy at metastases occurrence in both wild-type (wt*KRAS* → wt*KRAS* and wt*KRAS* → mut*KRAS*) and mutated (mut*KRAS* → mut*KRAS* and mut*KRAS* → wt*KRAS*) CRCs. Patients harboring double mutations of *KRAS* or *NRAS* or *BRAF* (v-raf murine sarcoma viral oncogene homolog B) mutations were not included in this study.

Patients Follow-Up

Total body Computed Tomography (tbCT) scan and CEA (CarcinoEmbryonic Antigen) monitoring were not centralized and were done every three months. The response to chemotherapy was evaluated by RECIST (Response Evaluation Criteria In Solid Tumours v1.1) (10). Complete response (CR) was defined as complete disappearance of all detectable evidence of disease on tbCT. Partial response (PR) was defined as at least a 30% decrease in the sum of diameters of target lesions. Stable disease (SD) was defined as everything between 30% decrease and 20% growth of tumour size. Progressive disease (PD) was defined as at least a 20% increase in the sum of diameters of target lesions. Disease Control (DC) was the sum of CR + PR + SD.

Plasma Collection

Six mL of whole blood was collected through sting of a peripheral vein, using Vacutainer® with EDTA as anticoagulant (K2EDTA, purple cap, Becton Dickinson). Plasma was separated by two sequential centrifugation steps (the first at room temperature for 10 min at 1,500×*g* and the second at 2,000×*g* for the same time and temperature). Plasma was stored at −80°C until analysis (see beyond).

Plasma Circulating-Free and Formalin-Fixed Paraffin-Embedded (FFPE) Tissue DNA Extraction

Circulating-free (cf)-DNA was extracted from 1-ml samples of plasma with a commercial kit (QIAamp Circulating Nucleic Acid Kit; QIAGEN GmbH, Hilden, Germany) according to the manufacturer instructions. Cf-DNA samples were then stored at −20°C. FFPE tissue DNA was extracted from three 10 μm FFPE sections using the QIAamp DNA FFPE Tissue kit (Qiagen, Hilden, Germany) and the QIAcube apparatus (Qiagen). The DNA quantity was evaluated with the dsDNA HS assay kit using the Qubit 2.0 Fluorometer (Invitrogen, Monza, Italy).

DNA Sequencing

Tumour samples were sequenced with the Oncomine Solid Tumour DNA kit (Thermo Fisher Scientific, Waltham, MA, USA) covering hotspot variants and actionable mutations of 22 genes involved in colon cancer. However, our analysis focused on *KRAS*-related genetic results. Ten nanograms of genomic DNA (gDNA) were used to prepare libraries according to the manufacturer's instructions.

The amplified libraries were sequenced on the Ion Torrent PGM semiconductor (https://www.thermofisher.com/it/en/home/life-science/sequencing/next-generation-sequencing/ion-torrent-next-generation-sequencingworkflow.html) and the data were analyzed using the torrent suite software v5.0 (Thermo Fisher Scientific) and the obtained variants confirmed by the integrative genome viewer (IGV) from the Broad Institute. The limit of mutations detection (LOD) of tissue NGS approach is 2% allelic frequency. Reference sequence for *KRAS* was NM_004958.4. Mutations were also checked according to ClinVar identifier numbers (https://www.ncbi.nlm.nih.gov/clinvar/intro/).

Statistical Analyses, Study Design, and Data Presentation

Associations between *KRAS* mutations and clinical and pathologic variables were evaluated by χ^2 test. P <0.05 was considered statistically significant. The primary outcome measure was the Overall Survival (OS), measured from the start of the first-line chemotherapy until death from any cause. The Kaplan–Meier product limit method was applied to graph OS. The study was exploratory considering the scarcity of data about the prognostic power of different mutational evolutions of *KRAS* oncogene in primary *vs* metastatic lesions and, thus, it does not have a pre-specified study design. All patients registered in an observational database (STORIA database) (11) between 2015 and 2018 and who accepted to perform liquid biopsy before starting first-line chemotherapy were enrolled. We chose do not prolong the enrolment period to avoid any prognostic interferences related to therapeutic and methodologic changes occurring in clinical practice. With an estimated survival difference between patients with *KRAS* mutational regression (defined as an expected rare group, mut*KRAS* → wt*KRAS*) *vs* patients with stably mutated *KRAS* (mut*KRAS* → mut*KRAS*) higher than 50% at 12 months, an estimated ratio mut*KRAS* → wt*KRAS*:mut*KRAS* → mut*KRAS* of about 1:10, a sample size of at least 60 patients was required to generate a significant hypothesis (P <0.005) on survival time differences at Log-Rank Test.

Univariate analysis was performed with the Log-Rank test. Multivariate analysis was performed through the Cox proportional-hazards regression in order to analyze the effect of several risk factors (co-variates) on OS. The HR is the estimate of the end-point probability and it can be interpreted as the instantaneous relative risk of an event (death), at any time, for an individual with the risk factor present compared with an individual with the risk factor absent, given both individuals are the same on all other covariates. Covariates were selected after consensus discussion between authors and were dichotomized: age <65 *vs* age ≥65, male *vs* female, left sided *vs* right sided, one involved organ *vs* two or more, response to first-line chemotherapy (Disease Control *vs* No Disease Control), *KRAS* mutational evolution in mutated KRAS (mut*KRAS* → mut*KRAS vs* mut*KRAS* → wt*KRAS*) and in wild-type KRAS (wt*KRAS* → wt*KRAS vs* wt*KRAS* → mut*KRAS*). 95% confidence intervals (CI) of HR are also reported. Statistical analysis was performed using the MedCalc® 9.3.7.0 and Excel software.

RESULTS

Clinico-Pathological and Treatment Characteristics According to the Initial Mutational Status of KRAS

One-hundred-fourteen patients who received surgical removal and *KRAS* oncogene evaluation of a primary CRC between 2015 and 2018 accepted to reassess *KRAS* mutational status through liquid biopsy before starting the first-line chemotherapy for the occurrence of distant and non-resectable metastases. However, first-line and subsequent chemotherapies were established according to the *KRAS* assessed on the primary FFPE tumoral tissue as established by National Regulatory Authorities (a detailed description is reported in **Table S1**). **Table 1** shows the clinic-pathologic characteristics of patients according to the *KRAS* mutational status in primary tumors. Overall, 63 patients presented with mut*KRAS* and 51 with wt*KRAS*. The three most frequent mutations were p.G12D (19 patients), p.G13D (nine patients) and p.G12V (seven patients). There were no statistically significant associations at χ^2 test between the mutational status of *KRAS* on primary tumors and age (<65 *vs* ≥65 years), gender (male *vs* female), grading (G1/G2 *vs* G3), side of primary tumor (left *vs* right), pT (pT1/pT2 *vs* pT3 *vs* pT4), and lymphnodes involvement (pN: 0 *vs* 1–3 *vs* >3). According to Oncology Societies' guidelines and National Pharmaceutical Authorities' regulations, patients bearing mut*KRAS* in primary tumors did

TABLE 1 | Clinico-pathological characteristics according to KRAS status at diagnosis.

KRAS status in primary tumor	Total	Age		Gender		Grading		Side of primary tumor		pT*			Lymph nodes involvement (pN)*		
		<65	≥65	M	F	G1/G2	G3	Left	Right	T1/T2	T3	T4	0	1–3	>3
p.G12D	**63**	7	12	11	8	5	14	8	11	3	9	7	2	5	12
p.G13D		5	4	3	6	1	8	4	5	1	7	1	1	7	1
p.G12V		3	4	3	4	1	6	2	5	1	5	1	0	5	2
p.G12A		3	3	3	3	1	5	2	4	1	4	1	0	3	3
p.G12C		4	2	3	3	0	6	1	5	2	3	1	1	3	2
p.A146T		3	2	3	2	1	4	2	3	0	3	2	0	2	3
p.G12S		1	3	2	2	0	4	0	4	1	2	1	1	3	0
p.A146V		1	1	1	1	0	2	0	2	1	1	0	0	2	0
p.G13R		0	2	0	2	0	2	1	1	2	0	0	1	0	1
p.G13C		0	1	1	0	1	0	1	0	0	1	1	0	1	1
p.K117N		1	0	0	1	0	1	0	1	0	0	1	1	0	0
p.G12F		1	0	1	0	0	1	1	0	1	0	0	1	0	0
Wild-type	**51**	18	23	20	21	9	32	28	23	11	21	9	15	19	17

*pT, pathological staging of primary tumor according to AJCC; pN, pathological staging of loco-regional lymph-nodes involvement. *According to AJCC. There were no significant associations between KRAS mutations and clinical and pathologic variables at χ^2 test.*

Sequence change is described at protein level with "p." followed by the amino acid abbreviation, followed by the position of the amino acid sequence, followed by the new amino acid which replaces the former.

not receive anti-EGFR-based treatments (**Table 2**). In this patients' setting, the use of chemotherapy (CT) and bevacizumab was predominant (56/63 patients, 88.8%); conversely, in wt*KRAS* patients the 76.4% of them was treated with CT plus an anti-EGFR agent (39/51 patients). Interestingly, wt*KRAS* patients received more CT lines (43.3% *vs* 20.6% in mut*KRAS* patients) and had a longer cumulative median time-on-therapy (20.5 *vs* 16.9 months in mut*KRAS* patients). This was indirectly related to the detrimental prognostic effect on survival of mut*KRAS* (11).

Genetic Evolution of KRAS

KRAS mutational concordance (mut*KRAS* or wt*KRAS* in both primary and liquid biopsy at metastases occurrence: mut*KRAS* → mut*KRAS* and wt*KRAS* → wt*KRAS*) was high (70.1%). However, two divergent subsets were identified: 1. mut*KRAS* in primary tumors and wt*KRAS* in metastatic ones (mut*KRAS* → wt*KRAS* in 8.8% of patients), and *vice versa* (wt*KRAS* → mut*KRAS* in 21.1% of patients) (**Table 3**). These subsets are particularly interesting because they represent a dynamic aspect of cancer heterogeneity. **Table 3** shows some clinical characteristics that could have influenced the genetic evolution of *KRAS*. There were statistically significant associations: 1. adjuvant chemotherapy based on capecitabine and oxaliplatin more frequently preceded the evolution towards mut*KRAS* from wt*KRAS* (wt*KRAS* → mut*KRAS*) (P = 0.001), 2. There was a strong association between *KRAS* regressive trajectory (mut*KRAS* → wt*KRAS*) and the oligometastatic status (P <0.0001) (see *Material and Methods* for the definition of oligo-metastatic disease), 3. Regression of mut*KRAS* (mut*KRAS*

TABLE 2 | Treatment characteristics according to KRAS status at diagnosis.

KRAS status in primary tumor	Total	Type of first-line CT			No. of CT lines			Time on therapy*(months)
		CT	CT/Beva	CT/anti-EGFR	1	2	>2	Median (Range)
p.G12D	**63**	2	17	0	7	8	4	15.9 (12.3–21.5)**
p.G13D		1	8	0	3	4	2	
p.G12V		1	6	0	1	2	4	
p.G12A		0	6	0	1	5	0	
p.G12C		1	5	0	4	2	0	
p.A146T		0	5	0	1	4	0	
p.G12S		0	4	0	2	1	1	
p.A146V		1	1	0	0	1	1	
p.G13R		0	2	0	0	2	0	
p.G13C		0	1	0	0	0	1	
p.K117N		0	1	0	0	1	0	
p.G12F		1	0	0	0	1	0	
Wild-type	**51**	8	4	39	8	20	23	20.6 (16.2–27.6)

anti-EGFR, Anti-Epidermal Growth Factor Receptor antibodies; Beva, Bevacizumab; CT, ChemoTherapy.

**Cumulative time spent on therapy (including also "maintenance therapy").*

***Time-on-therapy for all mutated patients.*

Sequence change is described at protein level with "p." followed by the amino acid abbreviation, followed by the position of the amino acid sequence, followed by the new amino acid which replaces the former.

TABLE 3 | Tumor burden, adjuvant chemotherapy and response to first-line CT according to KRAS evolution.

KRAS evolution		Adjuvant CT		P*	Sites of first recurrence				P*	Oligo-metastases		P*	Best response tofirst-line CT			P*
		Yes (52)	No (62)		Liver	Lungs	Lymph-nodes	More thanone site		Yes	No		CR, PR or SD	PD	NA	
Mut in PT → Mut in MT	53	24	29		16	8	7	22		2	51		31	19	3	
Mut in PT → WT in MT	10	3	7		5	4	0	1		9	1		10	0	0	
WT in PT → WT in MT	27	7	20		8	8	4	7		4	23		19	5	1	
WT in PT → Mut in MT	24	19	5	*0.001*	5	3	2	14	*0.058*	1	23	*<0.0001*	11	10	2	*0.026*

*CR, Complete Response; CT, ChemoTherapy; MT, Metastatic Tumors; Mut, KRAS mutated; NA, Not Assessable; PD, Progressive Disease; PR, Partial Response; PT, Primary Tumors; SD, Stable Disease; WT, Wild-Type. *Chi-square test.*

→ wt*KRAS*) before starting first-line chemotherapy was associated with response to CT alone or CT plus bevacizumab (P = 0.026) (**Table 3**).

Prognostic Significance of KRAS Mutations Evolution

Given the opportunity to distinguish four *KRAS* evolutionary subsets, we studied the prognostic impact of these subsets on survival, the most reliable and synthetic outcome. Time-to-progression was not evaluated considering the potential prognostic biases related to different first-line chemotherapies and/or different therapeutic sequences. **Table 4** and **Figure 1** show respectively, univariate analysis of overall survival (OS) and Kaplan Meyer curves depicting the survival of patients according to different evolutionary subsets. After a median follow-up for the whole series of 25.0 months, median OS (mOS) of *KRAS* genetically concordant patients was 9.6 for mut*KRAS* → mut *KRAS* and 27.5 months for wt*KRAS* → wt*KRAS*. Median OS (mOS) for mut*KRAS* → wt*KRAS* ("regressive trajectory") was not reached (NR), while median mOS in patients developing *KRAS* mutations in metastatic tumors from wt*KRAS* in primary lesions (wt*KRAS* → mut*KRAS*) was 12.1 months (P = 0.0001 at Long Rank test).

A multivariate analysis was performed including as dichotomized co-variates, age (<65 *vs* ≥65 years), gender (male *vs* female), side (left *vs* right), extent of metastatic involvement (one *vs* multiple sites), response to first-line CT [CR/PR/SD (DC, Disease Control) *vs* PD (no DC)], genetic concordance in mut*KRAS vs* regressive trajectory (mut*KRAS* → wt*KRAS*), and genetic concordance in wt*KRAS vs* progressive trajectory (wt*KRAS* → mut*KRAS*). Interestingly, the following conclusions from the statistical analysis can be derived: i. metastatic involvement (one *vs* multiple sites; mOS: 30.6 *vs* 11.0 months; HR: 4.16, CI 1.25–13.7), ii. response to first-line CT (DC *vs* no DC; mOS: 28.3 *vs* 9.6.0 months; HR: 2.11, CI 1.78–4.26), and *KRAS* evolutionary iii. regressive (mut*KRAS* → mut*KRAS vs* mut*KRAS* → wt*KRAS*; mOS: 9.6 months *vs* NR; HR: 0.22, CI 0.08–0.61) and iv. progressive trajectories (wt*KRAS* → wt*KRAS vs* wt*KRAS* → mut*KRAS*; mOS: 27.5 *vs* 12.1 months; HR: 2.70, CI 1.11–6.56) emerged as independent prognostic factors for OS (**Table 5**).

TABLE 4 | Univariate analysis of KRAS mutations' evolution prognostic power.

KRAS evolution	No. ofevents/ patients	Median survival	95% CI	P at Log Rank test
Mut in PT → Mut in MT	20/53	9.6	6.7–16.4	
Mut in PT → WT in MT	4/10	NR	21.1–33.6	
WT in PT → WT in MT	15/27	27.5	22.8–29.8	
WT in PT → Mut in MT	11/24	12.1	9.6–15.9	*0.0001*

CI, Confidence Interval; MT, Metastatic Tumors; Mut, KRAS mutated; NR, Not Reached; PT, Primary Tumors; WT, Wild-Type.

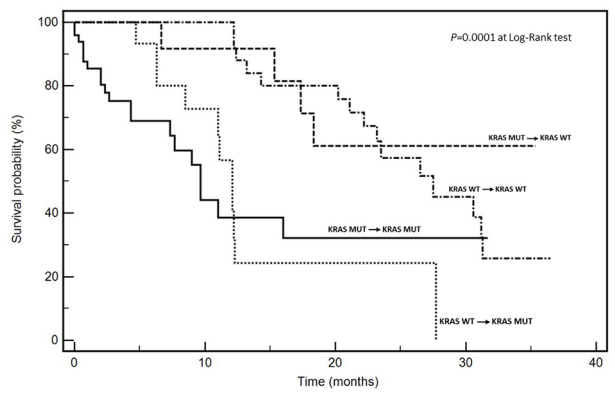

FIGURE 1 | Kaplan-Meier survival curves according to KRAS mutational trajectories.

DISCUSSION

In this work, we found that the genetic dynamics of mCRC is clinically relevant since patients bearing divergent mutational evolution have a prognosis consistent with the results of liquid biopsy: in fact, patients bearing mut*KRAS* at liquid biopsy from a wt*KRAS* in primary tumor have both poorer survival and responsiveness to chemotherapy similar to *KRAS* mutated CRCs. This subset could represent a particularly aggressive phenotype on an evolutionary point of view ("progressive" genetic trajectory). By contrast, in 8.8% of cases we observed a "regressive" mutational trajectory that was associated to the best prognosis and high responsiveness to chemotherapy independently from the lack of anti-EGFR treatment administration. The last data are particularly surprising and could indicate that additional unexplored anti-tumoral mechanisms could work to downsize the neoplastic

TABLE 5 | Multivariate analysis of RAS mutations' evolution prognostic power.

Co-variate	Dicothomization	Median survivals	No. ofevents/patients	*P* at univariate	HR	95% CI	*P* at multivariate
Age	<65 y *vs* ≥65 y	15.3 vs 18.3	12/47 vs 13/57	0.90	0.69	0.24–1.96	0.49
Gender	M *vs* F	15.3 vs 17.3	13/51 vs 12/53	0.92	1.05	0.37–2.97	0.91
Side	L *vs* R	17.5 vs 16.0	21/50 vs 29/64	0.63	1.57	0.48–5.12	0.44
Metastatic involvment	1 site *vs* >1	30.6 vs 11.0	33/70 vs 17/44	0.0006	4.16	1.25–13.7	0.001
Response to firs-line CT	DC *vs* no DC	28.3 vs 9.6	22/71 vs 28/43	0.002	2.11	1.78–4.26	0.03
KRAS evolution	Mut in PT → Mut in MT vs Mut in PT → WT in MT	9.6 vs NR	20/53 vs 4/10	<0.0001	0.22	0.08–0.61	0.0001
	WT in PT → WT in MT vs WT in PT → Mut in MT	27.5 vs 12.1	15/27 vs 11/24	0.0001	2.70	1.11–6.56	0.002

CI, Confidence Interval; DC, Disease Control; F, Female; HR, Hazard Ratio; L, Left; M, Male; MT, Metastatic Tumors; PT, Primary Tumors; mut, KRAS mutated; NR, Not Reached; R, Right; WT, Wild-Type.

population. Multivariate analysis showed that both mutational trajectories had an independent and significant prognostic power. As in our previous studies (5, 6), we cannot definitively demonstrate if this effect depends on a negative immunologic selection (12) or on a spontaneous genetic devolution. Our translational studies are in progress to identify and isolate, from oligo-metastatic CRC patients, eventual T-cells responsible of mut*KRAS* clones' elimination.

Surprisingly, we found that "progressive" genetic trajectories (wt*KRAS* → mut*KRAS*) were much more frequent in patients treated with adjuvant chemotherapy (**Table 3**). These findings were consistent with two previous studies performed in well-defined models of oligo-metastatic CRC (5, 6). We hypothesized that chemotherapy would induce a genetic remodelling. The existence of this selection mechanisms was supported by our findings on much more divergent mutational signatures and events between primary and matched metastases when the resection of metachronous metastases was preceded by adjuvant chemotherapy (mutational sharing: >90% in non-chemotherapy-pre-treated lesions *vs* <15% in chemotherapy-pre-treated lesions). In other words, *RAS* wild-type CRC patients progressing after oxaliplatin/capecitabine-based adjuvant chemotherapy developed more *RAS* mutations and resistance to anti-EGFR treatments than metastatic patients who did not receive adjuvant treatment. Therefore, chemotherapy could induce both genetic remodelling and evolutionary pushing. The neoplastic progeny of chemotherapy pre-treated CRC patients could have much more extensive intra-tumour mutation heterogeneity including some clones evolved towards mut*KRAS*. In our opinion, a similar effectwas observed in a very recent study by Wu et al. (13) reporting a trial on the use of osimertinib in completely resected EGFR mutated non-small cell lung cancers (NSCLC). Osimertinib adjuvant administration was less effective on disease-free survival when preceded by chemotherapy. Importantly, we are describing our scientific observations and not deploring adjuvant chemotherapy that is a standard of care in high-risk resected CRC and NSCLC. A useful suggestion rising from our work would be to reassess the mutational status of *KRAS*, particularly in patients underwent to adjuvant chemotherapies, in order to predict the major risk to develop a chemotherapy-induced genetic remodelling requiring both more aggressive treatment strategies and more careful follow-up.

Some limitations of the present study deserve to be discussed. The sample size is limited to 114 patients. In fact, about half of patients did not accept to reassess *KRAS* with liquid biopsy in order to modulate the planningof the therapeutic approach that remained based on the first FFPE tissue *RAS* evaluation. Furthermore, only 10 patients showed a regressive trajectory of *KRAS* (mut*KRAS* → wt*KRAS*) and this was related to the lower incidence of this effect if compared to the progressive trajectory (wt*KRAS* → mut*KRAS*) which represents an advantageous gain for cancer cells. First-line treatments were physiologically heterogeneous according to clinical and genetic assessments; however, the mono-institutional and exploratory nature of this study, along with the uniformity of technical approaches, makes our results precious and informative. Moreover, we did not evaluate *KRAS* status at different time-points because of budget limitations. This is a limit and a missed opportunity to observe the complete *KRAS* cancer cells "plasticity" during the time. Finally, we did not investigate if wt*KRAS* patients on liquid biopsy were again responsive to anti-EGFR treatments. The latter is a crucial question, which deserves to be explored in large prospective trials. At this stage, we can observe that our patients bearing a regressive trajectory (mut*KRAS* → wt*KRAS*) were responsive to treatments and had a good OS regardless of whether they did not receive anti-EGFR agents in first or second lines of treatments.

This work may have a strong practice-changing power in our context since results of liquid biopsy are considered not standard and the National Sanitary System does not reimburse the relative costs. Our results strongly suggest that a single *KRAS* mutational status determination at the diagnosis is nor correct neither useful because cancer clonal heterogeneity can determine a change of the mutational status over the space (in different sites of disease localization) and time, as already suggested by other researchers (4, 7, 8). In our opinion, our work could contribute to provide a biological basis to approach *KRAS* testing with a more dynamic attitude (liquid biopsy) giving both new prognostic and therapeutic chances. The identification of regressive genetic trajectories (mut*KRAS* → wt*KRAS*) in specific mCRC patients could open unexpected therapeutic scenarios. In fact, in this subset, treatment with anti-EGFR-based drugs (cetuximab or panitumumab) could regain relevance and it deserves to be further explored in clinical trials. Furthermore, our data

provides an additional direct evidence that studies of the evolutionary trajectories of *KRAS* can have a strong clinical and prognostic impact also in discriminating between poly-metastatic aggressive *vs* oligo-metastatic indolent CRC subsets.

DATA AVAILABILITY STATEMENT

The original contributions presented in the study are included in the article/**Supplementary Material**. Further inquiries can be directed to the corresponding author.

ETHICS STATEMENT

Ethical review and approval was not required for the study on human participants in accordance with the local legislation and institutional requirements. The patients/participants provided their written informed consent to participate in this study.

AUTHOR CONTRIBUTIONS

Conceptualization, AO, GN, and MS. Methodology, VA, GD, and LC. Software, FP and AB. Validation, GB, GN, and GS. Formal analysis, AO, MaC, and PD. Investigation, AO, GN, AL, and MiC. Resources, GN. Data curation, AO and MiC. Writing/original draft preparation, AO, MS, and MiC. Writing/review and editing, GN, GB, and GS. Supervision, MiC. All authors contributed to the article and approved the submitted version.

FUNDING

This work was funded by Mrs. Antonietta Nacca.

ACKNOWLEDGMENTS

We acknowledge the LILT (Lega Italiana per la Lotta contro i Tumori—sezione di Napoli) for the precious collaboration.

SUPPLEMENTARY MATERIAL

The Supplementary Material for this article can be found online at: https://www.frontiersin.org/articles/10.3389/fonc.2021.632962/full#supplementary-material

REFERENCES

1. Ferlay J, Colombet M, Soerjomataram I, Mathers C, Parkin DM, Piñeros M, et al. Estimating the global cancer incidence and mortality in 2018: GLOBOCAN sources and methods. *Int J Cancer* (2019) 144:1941–53. doi: 10.1002/ijc.31937
2. Hadden WJ, de Reuver PR, Brown K, Mittal A, Samra JS, Hugh TJ. Resection of colorectal liver metastases and extra-hepatic disease: a systematic review and proportional meta-analysis of survival outcomes. *HPB (Oxford)* (2016) 18:209–20. doi: 10.1016/j.hpb.2015.12.004
3. Nappi A, Berretta M, Romano C, Tafuto S, Cassata A, Casaretti R, et al. Metastatic Colorectal Cancer: Role of Target Therapies and Future Perspectives. *Curr Cancer Drug Targets* (2018) 18:421–9. doi: 10.2174/1568009617666170209095143
4. Serna-Blasco R, Sanz-Álvarez M, Aguilera Ó, García-Foncillas J. Targeting the RAS-dependent chemoresistance: The Warburg connection. *Semin Cancer Biol* (2019) 54:80–90. doi: 10.1016/j.semcancer.2018.01.016
5. Ottaiano A, Caraglia M, Di Mauro A, Botti G, Lombardi A, Galon J, et al. Evolution of Mutational Landscape and Tumor Immune-Microenvironment in Liver Oligo-Metastatic Colorectal Cancer. *Cancers (Basel)* (2020) 12:3073. doi: 10.3390/cancers12103073
6. Ottaiano A, Circelli L, Lombardi A, Scala S, Martucci N, Galon J, et al. Genetic trajectory and immune microenvironment of lung-specific oligometastatic colorectal cancer. *Cell Death Dis* (2020) 11:275. doi: 10.1038/s41419-020-2480-6
7. Misale S, Yaeger R, Hobor S, Scala E, Janakiraman M, Liska D, et al. Emergence of KRAS mutations and acquired resistance to anti-EGFR therapy in colorectal cancer. *Nature* (2012) 486:532–6. doi: 10.1038/nature11156
8. Siravegna G, Mussolin B, Buscarino M, Corti G, Cassingena A, Crisafulli G, et al. Clonal evolution and resistance to EGFR blockade in the blood of colorectal cancer patients. *Nat Med* (2015) 21:795–801. doi: 10.1038/nm.3870
9. Van Cutsem E, Cervantes A, Adam R, Sobrero A, Van Krieken JH, Aderka D, et al. ESMO consensus guidelines for the management of patients with metastatic colorectal cancer. *Ann Oncol* (2016) 27:1386–422. doi: 10.1093/annonc/mdw235
10. Eisenhauer EA, Therasse P, Bogaerts J, Schwartz LH, Sargent D, Ford R, et al. New response evaluation criteria in solid tumours: revised RECIST guideline (version 1.1). *Eur J Cancer* (2009) 45:228–47. doi: 10.1016/j.ejca.2008.10.026
11. Ottaiano A, Normanno N, Facchini S, Cassata A, Nappi A, Romano C, et al. Study of Ras Mutations' Prognostic Value in Metastatic Colorectal Cancer: STORIA Analysis. *Cancers (Basel)* (2020) 12:1919. doi: 10.3390/cancers12071919
12. Tran E, Robbins PF, Lu YC, Prickett TD, Gartner JJ, Jia L, et al. T-Cell Transfer Therapy Targeting Mutant KRAS in Cancer. *N Engl J Med* (2016) 375:2255–62. doi: 10.1056/NEJMoa1609279
13. Wu YL, Tsuboi M, He J, John T, Grohe C, Majem M, et al. Osimertinib in Resected EGFR-Mutated Non-Small-Cell Lung Cancer. *N Engl J Med* (2020) 383:1711–23. doi: 10.1056/NEJMoa2027071

Conflict of Interest: The authors declare that the research was conducted in the absence of any commercial or financial relationships that could be construed as a potential conflict of interest.

frontiers in Oncology

ORIGINAL RESEARCH
published: 16 April 2021
doi: 10.3389/fonc.2021.661040

A Novel Prognostic Model and Practical Nomogram for Predicting the Outcomes of Colorectal Cancer: Based on Tumor Biomarkers and Log Odds of Positive Lymph Node Scheme

Jun Zhu[1†], Jun Hao[2†], Qian Ma[3†], Tingyu Shi[4], Shuai Wang[1], Jingchuan Yan[5], Rujie Chen[1], Dong Xu[2], Yu Jiang[2], Jian Zhang[6] and Jipeng Li[1*]*

[1] State Key Laboratory of Cancer Biology, Institute of Digestive Diseases, Xijing Hospital, The Fourth Military Medical University, Xi'an, China, [2] Department of Experiment Surgery, Xijing Hospital, Fourth Military Medical University, Xi'an, China, [3] School of Clinical Medicine, Xi'an Medical University, Xi'an, China, [4] Health Company, Airborne Special Operations Brigade Support Battalion, Xiaogan, China, [5] Department of Basic Medicine, The Fourth Military Medical University, Xi'an, China, [6] State Key Laboratory of Cancer Biology, Department of Biochemistry and Molecular Biology, The Fourth Military Medical University, Xi'an, China

Background: Emerging evidence shows that serum tumor biomarkers (TBs) and log odds of positive lymph node scheme (LODDS) are closely associated with the prognosis of colorectal cancer (CRC) patients. The aim of our study is to validate the predictive value of TBs and LODDS clinically and to develop a robust prognostic model to predict the overall survival (OS) of patients with CRC.

Methods: CRC patients who underwent radical resection and with no preoperative chemotherapy were enrolled in the study. The eligible population were randomized into training (70%) and test (30%) cohorts for the comprehensive evaluation of the prognostic model. Clinical implications of serum biomarkers and LODDS were identified by univariate and multivariate Cox proportion regression analysis. The predictive ability and discriminative performance were evaluated by Kaplan–Meier (K–M) curves and receiver operating characteristic (ROC) curves. Clinical applicability of the prognostic model was assessed by decision curve analysis (DCA), and the corresponding nomogram was constructed based on the above factors.

Results: A total of 1,202 eligible CRC patients were incorporated into our study. Multivariable COX analysis demonstrated that CA199 (HR = 1.304), CA125 (HR = 1.429), CEA (HR = 1.307), and LODDS (HR = 1.488) were independent risk factors for OS (all $P < 0.0001$). K–M curves showed that the high-risk group possessed a shorter OS than the low-risk counterparts. The area under curves (AUCs) of the model for 1-, 3- and 5-year OS were 86.04, 78.70, and 76.66% respectively for the train cohort (80.35, 77.59, and 74.26% for test cohort). Logistic DCA and survival DCA confirmed that the prognostic

OPEN ACCESS

Edited by:
Kenneth K.W. To, The Chinese University of Hong Kong, China

Reviewed by:
Peng Xia, The First Affiliated Hospital of Xi'an Jiaotong University, China
Shui-xiang He, The First Affiliated Hospital of Xi'an Jiaotong University, China

***Correspondence:**
Jian Zhang
biozhangj@fmmu.edu.cn
Jipeng Li
jipengli1974@aliyun.com

[†]These authors have contributed equally to this work

Specialty section:
This article was submitted to Gastrointestinal Cancers, a section of the journal Frontiers in Oncology

Received: *30 January 2021*
Accepted: *22 March 2021*
Published: *16 April 2021*

Citation:
Zhu J, Hao J, Ma Q, Shi T, Wang S, Yan J, Chen R, Xu D, Jiang Y, Zhang J and Li J (2021) A Novel Prognostic Model and Practical Nomogram for Predicting the Outcomes of Colorectal Cancer: Based on Tumor Biomarkers and Log Odds of Positive Lymph Node Scheme. Front. Oncol. 11:661040. doi: 10.3389/fonc.2021.661040

model displayed more clinical benefits than the conventional AJCC 8th TNM stage and CEA model. The nomograms were built accordingly, and the calibration plot for the probability of survival at 3- or 5-years after surgery showed an optimal agreement between prediction and actual observation.

Conclusions: Preoperative serum TBs and LODDS have significant clinical implications for CRC patients. A novel prognostic model incorporating common TBs (CA199, CA125, and CEA) and LODDS displayed better predictive performance than both single factor and the TNM classification. A novel nomogram incorporating TBs and LODDS could individually predict OS in patients with CRC.

Keywords: colorectal cancer, CA199, CA125, CEA, log odds of positive lymph node scheme, prognostic model, nomogram

INTRODUCTION

Colorectal cancer (CRC) is one of the most common malignancies globally and causes 900,000 deaths annually (1). Although the slow progression of CRC and increasing use of screening have led to favorable clinical outcomes when patients are diagnosed at an early stage (2), about 40% of the patients still die within five years after diagnosis (3). The newly accurate prognostic assessment of CRC patients is essential for adopting personalized therapeutics and improving patients' life-quality.

Tumor biomarkers (TBs) are associated with prognosis of patients (4) and may serve as complements of TNM staging (5). Carcinoembryonic antigen (CEA) is the most critical serum tumor marker during the assessment of both prognosis and therapeutic effect of CRC (6–8). Recent researchers have found that CEA and carbohydrate antigen199 (CA199) were independent predictors of cancer recurrence and prognostic factors of overall survival (OS). Combined detection of them could assist evaluating the prognosis of patients with stage II–III CRC (9, 10). Similarly, patients with upregulated serum carbohydrate antigen125 (CA125) tend to have poor survival status (11). Nevertheless, these serum biomarkers exclusively reflex the substance released by tumor cells and cannot comprehensively represent the microenvironment of primary tumor or post-surgical residue foci.

Despite the strong dependency of CRC patients' prognosis on conventional TNM (tumor–node–metastasis) staging system (12), the TNM stage could not behave favorably in predicting the outcomes of patients, especially those in the same stage (13). Accurate personalized prognostic assessments for CRC patients are an essential step for surgeons to better determine therapeutic strategies. Log odds of positive lymph node scheme (LODDS) is an innovative N staging system and has been recently introduced as a new prognostic index in CRCs (14–18), which could powerfully stratify patients into different risk groups (17) even when dissected lymph nodes were insufficient. Besides, LODDS is determined to have a better predictive priority than other N staging systems, such as lymph node ratio (LNR) and AJCC/UICC N staging (14, 15). Therefore, LODDS could be reckoned as an additional indicator for supplementing pN scheme. Given that serum TBs are reflection of the circulatory substance released by tumor cells and LODDS is representation of the local lymph metastasis capacity, it is reasonable and feasible to combine these factors to enhance the predictive ability for the outcomes of CRC patients

In the present study, the overriding aim is to establish a handy and personalized predictive model based on the TBs and LODDS, which could meet surgeons' demand to predict prognosis of CRC patients. A novel prognostic model was constructed by multivariable Cox regression analysis and optimized by a "step-and-forward" algorithm. The area under the receiver operating characteristic curve (AUC, ROC) analysis demonstrated both highly discriminative ability and outstanding specificity. According to logistic DCA and survival DCA, we concluded that the prognostic model displayed more net clinical benefits than the conventional AJCC 8th TNM stage and CEA model. Ultimately, we presented a novel nomogram that incorporated the serum CA125, CA199, CEA, and LODDS, which could be conveniently applied to facilitate the preoperative individualized OS prediction in patients with CRC.

METHODS

CRC Patients and Study Design

A retrospective study was investigated based on a primary cohort of CRC patients who underwent radical resection between February 2014 and December 2016 in the Air Force Military Medical University first affiliation Xijing digestive hospital (Shaanxi, China). The inclusion criteria were as follows: 1) CRC was the only primary carcinoma. 2) CRC patients had complete following-up and multiple baseline clinical information. 3) Patients underwent radical resection. 4) Serum CEA, CA19-9, CA125, and other TBs were detected before surgery. 5) Patients had available post-surgical information including positive lymph nodes (LNs), dissected LNs, and 7th or 8th editions of the AJCC/UICC TNM stage. Patients were excluded if radiotherapy or

chemotherapy is received before surgery, both of which could influence the level of TBs and the outcomes of patients.

The study was censored on September 20, 2020 and was approved by the institutional ethics committee of Xijing Hospital. Informed consent for patients was obtained before surgery. Harvested LNs are the retrieved LNs for pathological examination after surgeon and positive LNs (pLNs) are defined as the metastatic lymph node counts determined by postoperative pathology. To calculate the LODDS value, negative LNs (nLNs) representing non-metastatic lymph nodes should be derived by subtracting pLNs from the harvested LNs. Afterwards, LODDS was determined as the following formula: LODDS = In ([pLNs + 0.5]/[nLNs + 0.5]) (5, 15).

Peripheral venous blood was obtained every morning at six from CRC patients who received no treatment. The serum levels of CEA, CA125, and CA19-9 were determined by a Cobas 8000 Analyzer (Roche Diagnostics, Mannheim, Germany). Other clinical parameters such as age, gender, height, weight, nationality, marriage state, Body Mass Index (BMI), Blood type, and FVC (Forced Vital Capacity) were also collected from electronic medical records in the Xijing digestive hospital database.

Follow-Up

CRC patients were contacted once every three months in the first two years after surgery and then every six months after that. A detailed history and a complete physical examination were carried out. The primary endpoint of our study is OS, which was calculated from the time of diagnosis to the date of death, whatever the cause is.

Statistical Analysis

All statistical analysis was conducted in R software (version:3.63, https://www.r-project.org/). The numeric data were expressed as the mean ± SE, and Student's t test or One-way analysis of variance (ANOVA) was used to compare the difference. Qualitative data between two groups were compared using the X^2 test or Fisher's exact test. The eligible patients were separated into train cohort (70%) and test cohort (30%) by random algorithm by R software. Univariable and multivariable COX proportional hazards regression analyses were performed to screen and identify the key clinical factors in the risk model, which was used to predict outcomes of CRC patients. The final risk model with the smallest AIC was determined by a backward and stepdown process. The Kaplan–Meier curves (corrected by log-rank test) and ROC curves were utilized to assess the performance of the risk model.

Via exploring the package of '*rms*', a nomogram was established according to the results of multivariate analysis. The nomogram was measured by concordance index (C-index). The larger the C-index was, the more accurate the prediction of the prognostic risk model was. Calibration curves (3- and 5-year prediction) were plotted to validate the nomogram's predictive value. Related packages used in the study of R software was shown as follows: 'rms', 'survival', 'survminer', 'timeROC', 'rmda', 'MASS', 'dplyr', 'tableone'. P <0.05 was considered as significantly important.

RESULTS

Clinical Characteristics of CRC Patients

From 2014 to 2016, the number of collected CRC patients who underwent radical resection was 1,486. Those patients were informed to participate in the retrospective study. Eight patients had no survival time, while 92 cases missed the following-up information due to alternation of cell phone number. Meanwhile, 184 patients had incomplete clinical information, including none CEA (94 cases), CA199 (85 cases), and CA125 (106 cases). Finally, 1,202 eligible patients were identified in this study. According to the indicated ratio of 7:3, patients were divided into train and test cohorts randomly. Afterward, we constructed a robust prognostic model in the train cohort by multivariate Cox analysis. Predictive performance of the prognostic model was validated in the train and test cohorts by K–M and ROC curves. To further confirm the clinical value of this model, DCA analysis was adopted and nomogram was built based on the whole cohort. Subgroup analysis was performed to validate the predictive efficiency of the model in different subgroups (**Figure 1**).

852 CRC patients were included in the train cohort, while 350 patients were recruited to the test cohort of our study. The primary serum TBs contain CEA, CA199, and CA125. To better fit the prognostic model and avoid the zero value, we transformed these TBs by log2 (values + 1). The LODDS of every patient was calculated as mentioned above. The average survival time of the train and test cohorts was 4.01 and 4.12 years, respectively. There were no significant differences about other baseline characteristics between the two cohorts (all P > 0.05; **Table 1**). The detailed clinical features of train and test cohorts were shown in **Table 1**.

Prognostic Impact of Routine Clinical Investigations

The median follow-up time of the train cohort was 4.47 years, and the survival rate of 1-, 3-and 5-year was 91.8, 77.3, and 67.8%, respectively. The median follow-up time of the test cohort was 4.36 years, and the survival rate of 1-, 3-and 5-year was 91.7, 76.3, and 63.4%, respectively. The results of the univariate Cox analysis in the train cohort were listed in **Table 2**. The outcomes indicated that pLNs (HR =1.536, P < 0.0001) and LODDS were risky factors (HR = 1.488, P < 0.0001) while nLNs (HR = 0.919, P < 0.0001) and total harvested LNs (HR = 0.953, P= 0.0001) were protective factors in predicting OS of CRC patients. When it comes to the serum TBs, all these three common markers [CA199 (HR = 1.304), CA125 (HR = 1.429), CEA (HR = 1.307)] contribute to the unfavorable outcomes of CRC patients (all P < 0.0001). Results of TNM staging system were consistent [T stage (HR=2.956), N stage (HR=3.638), M stage (HR=5.079), all P < 0.0001] with the previous literature (12).

Due to the predictive priority of LODDS than other lymph node index (such as pLNs, nLNs, and LNR) (15–17), we incorporated the LODDS in the prognostic model. Multivariable Cox analysis also demonstrated that CA199,

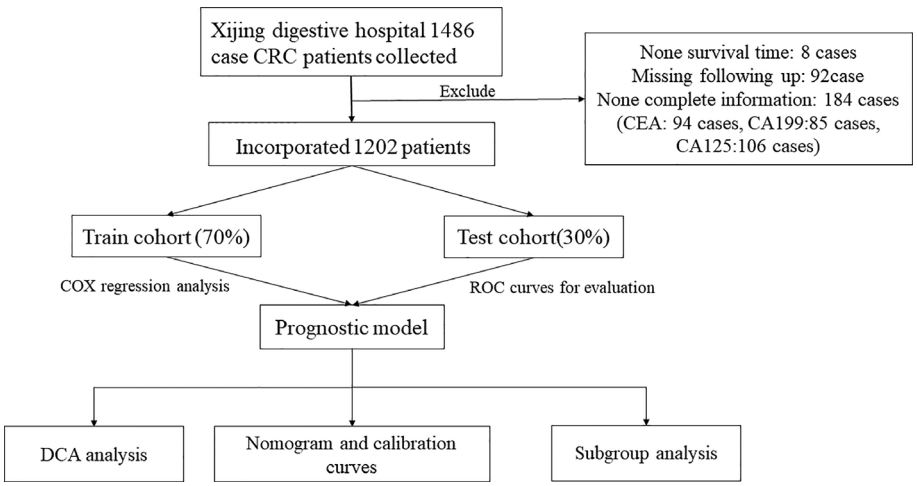

FIGURE 1 | Selection criteria and workflow of the study.

CA125, CEA, and LODDS were independent risk factors for OS (**Table 3**). Therefore, the four independent factors were used to construct a prognostic model based on a step-and-forward algorithm with the least AIC.

TABLE 1 | Basic clinical features in train and test cohorts.

Characteristics	Train cohort	Test cohort	P value
No. of case	852 (70.9)	350 (29.1)	
Survival status (%)			0.339
Dead	271 (31.8)	122 (34.9)	
Alive	581 (68.2)	228 (65.1)	
Survival time (year)	4.01 (1.71)	4.12 (1.72)	0.287
Age (year)	59.8 (12.4)	60.3 (12.5)	0.593
Sex (%)			0.740
Male	478 (56.1)	192 (54.9)	
Female	374 (43.9)	158 (45.1)	
Weight (kg)	63.7 (15.9)	62.8 (11.5)	0.336
Hight (cm)	165 (8.18)	164 (9.48)	0.094
BMI (kg/m^2)	23.8 (7.74)	23.0 (3.30)	0.063
CA125	3.67 (1.12)	3.63 (1.07)	0.599
CA199	3.71 (1.97)	3.82 (2.06)	0.379
CEA	2.07 (1.89)	2.31 (2.05)	0.060
PLNs	2.16 (3.90)	1.74 (3.03)	0.070
DLNs	15.7 (5.02)	15.5 (5.03)	0.608
LODDS	−2.38 (1.43)	−2.24 (1.63)	0.165
T stage (%)			0.140
1	30 (3.52)	14 (4.0)	
2	162 (19.0)	47 (13.4)	
3	549 (64.4)	242 (69.1)	
4	111 (13.0)	47 (13.4)	
M stage (%)			0.599
0	837 (98.2)	346 (98.9)	
1	15 (1.8)	4 (1.1)	
N stage (%)			0.882
0	443 (52.0)	177 (50.6)	
1	264 (31.0)	110 (31.4)	
2	145 (17.0)	63 (18.0)	

BMI, body mass index; PLNs, positive lymph nodes; DLNs, dissected lymph nodes; LODDS, log odds of positive lymph nodes scheme.

Construction of Prognostic Model of CRC

By multivariable Cox analysis and least AIC value (3319.37), the prognostic model based on the train cohort was easily calculated as follows: RiskScore = 0.1129 * CA199 + 0.1246 * CEA + 0.3207 * CA125 + 0.3365 * LODDS.

As shown in **Table 3**, the hazard ratio (HR) of CA125 and LODDS were significantly larger than other factors, which indicated that they contributed overwhelmingly in the predicting model.

Assessment of the Prognostic Model and DCA Analysis

To validate the predictive value of the prognostic model, we stratified the train cohort and test cohort into two groups according to the cut-off value determined by R survminer package. The optimal cut-off threshold for train and test cohort were 1.100 and 1.070, respectively. Kaplan–Meier (K–M) curves displayed that low-risk patients in both groups had a significantly longer OS than those with high-risk ($P < 0.001$, **Figures 2A, B**).

ROC curve was conducted to predict short- and long-term prognosis of this risk model. As is vividly demonstrated in **Figure 3A**, the AUCs of the risk model for the train cohort of 1-, 3- and 5-year were 85.0, 78.5, and 76.8%. Likewise, the AUCs for the test cohort were 80.6, 77.3, and 77.0%, respectively (**Figure 3B**). More importantly, the AUC of the predictive model was significantly higher than the TNM stage and the alone indicator (**Figure S1**), which suggested that the predictive model showed better discriminative ability and model-fitting performance than the conventional TNM staging.

Moreover, DCA analysis was performed to verify clinical implications and guidance of the risk model. Two methods of DCA were designed: logistic DCA and survival DCA. Both confirmed that the risk model (also called complex model) displayed more clinical benefits than either CEA model (**Figures 3C, D**) or TNM stage model (**Figure S2**).

To validate whether the risk model could be an independent prognostic factor, we adopted univariate and multivariate COX

TABLE 2 | Univariable Cox regression analysis for CRC train cohort.

Variables	β	HR	95% CI	P value
PLNs	0.42909	1.5359	1.4006–1.6841	<0.0001
DLNs	–0.04805	0.9531	0.9303–0.9765	0.0001
NLNs	–0.08403	0.9194	0.8992–0.9400	<0.0001
LODDS	0.39723	1.4877	1.3881–1.5945	<0.0001
Sex	0.08991	1.0941	0.8591–1.3934	0.4662
Age	0.01137	1.0114	1.0011–1.0218	0.0292
Height	–0.02199	0.9782	0.9639–0.9928	0.0036
BMI	–0.02042	0.9798	0.9441–1.0169	0.2815
CEA	0.26796	1.3073	1.2369–1.3817	<0.0001
CA199	0.26568	1.3043	1.2295–1.3837	<0.0001
CA125	0.35689	1.4289	1.3074–1.5617	<0.0001
FVC	-0.00639	0.9936	0.9875–0.9998	0.0437
T (T3-4 vs T1-2)	1.08382	2.9559	2.0095–4.3481	<0.0001
N (N1-2 vs N0)	1.29147	3.6381	2.7804–4.7605	<0.0001
M (M1 vs M0)	1.62511	5.0790	2.955–8.7296	<0.0001

CRC, colorectal cancer; β is calculated by univariable Cox regression analysis; PLNs, Positive lymph nodes; DLNs, dissected lymph nodes, NLNs, Negative lymph nodes; LODDS, log odds of positive lymph nodes scheme; BMI, body mass index; FVC (forced vital capacity), a common indicator for respiratory function.

TABLE 3 | Multivariable Cox regression analysis for CRC training cohort.

Variables	Coefficient	HR	95% CI	P value
CA199	0.1129	1.1195	1.055–1.187	0.0002
CEA	0.1246	1.1327	1.065–1.205	<0.0001
CA125	0.3207	1.3780	1.252–1.517	<0.0001
LODDS	0.3365	1.4000	1.305–1.502	<0.0001

CRC, colorectal cancer; HR, hazard ration; CI, confidential internal; LODDS, log odds of positive lymph nodes scheme.

analyses (**Table 4**). We found that the model was an independent risky factor of the TNM stage (HR = 1.045, P < 0.0001).

Taken together, these results suggested that the risk model (including CEA, CA125, CA199, and LODDS) in this study displayed a better predictive performance and had a higher sensitivity and specificity for predicting outcomes of CRC patients.

Nomogram for CRC Patients and Clinical Use

The prognostic nomogram that integrated significant independent factors (CEA, CA199, CA125, and LODDS) for OS in the whole cohort (including train and test cohorts) is shown in **Figure 4A**. The concordance index (C index) for the nomogram was 0.7431. The calibration plot for the probability of survival at 3- or 5-year after surgery demonstrated an optimal consensus between the prediction *via* nomogram and actual observation (**Figures 4B, C**).

Subgroup Analysis in Rectal and Colon Cancer Patients

To further explore the discriminative performance and predictive of the prognostic model, we divided patients into colon and rectal cancer groups according to the tumor site. The number of colon cancer patients and rectal cancer patients was 408 and 532 in the study. Based on the indicated optimal cut-off value, patients were stratified into high- or low-risk groups. K–M curves revealed that low-risk group had a longer OS than the high-risk group (P < 0.0001), wherever the tumor is (rectal or colon cancer; **Figures S3A, B**). Simultaneously, ROC curves showed outstanding accuracy and sensitivity in rectal and colon groups. The AUC values of the colon cancer group (**Figure S3C**) were 90.36, 82.84, and 78.4% in predicting 1-, 3-, and 5-year OS, respectively. Likewise, the AUC values of the rectal cancer group were 83.13, 76.67, and 77.07% in our study (**Figure S3D**).

DISCUSSION

Despite noteworthy advances in chemotherapy and targeted therapy, the 5-year OS and life-quality of CRC patients are far from satisfactory, especially patients in stage IV. To enhance patients' life-quality, it is necessary to accurately estimate their prognosis and adopt personalized therapeutics. An increasing number of literatures had confirmed the crucial roles of TBs, pLNs, and dissected LNs in the management of advanced diseases (19) and in the prognosis of CRC patients (4, 6, 9–11). Meanwhile, a novel LN-related index LODDS has gained more and more attention due to its robustness and accuracy. Here, we estimated the association of preoperative serum TBs, LODDS, and 5-year OS of CRC patients. We further developed an innovative risk model based on CA125, CA199, CEA, and LODDS. ROC curves demonstrated favorably accurate concordance of the model, and DCA analysis validated more net benefits of the prognostic model than CEA model and even conventional TNM staging. Ultimately, a novel nomogram was constructed based on these independent clinical factors and had a great potential to be widely applied in clinical practice.

Serum CEA and CA199 were universally acknowledged as classical tumor markers in CRC patients. A multitude of studies have demonstrated that preoperative serum CEA was an independent prognostic factor which plays a vital role in predicting outcomes of cancer patients (20).

Postoperative level of serum CEA is the most sensitive detector for liver metastases. Upregulated postoperative level of serum CEA was intimately associated with local recurrence of tumor and necessitated immediate evaluation for metastatic disease (21). CA199 is another vital biological marker for CRC (19, 22). Increment of serum CA199 indicates significantly high frequency of cancer metastasis and considerably low survival rate of patients, which makes it a poor prognostic factor for CRC patients. CA125 is extensively used in tumor detection (23) and associated with outcomes of CRC patients (11). A recent research suggested the combination of CXCL7, CEA, CA125, and CA199 may facilitate diagnosis of CRC with high sensitivity and specificity (23). However, few researches focused on the prognostic value of the above combined panel in CRC patients. Unlike the previous report, we for the first time developed a new

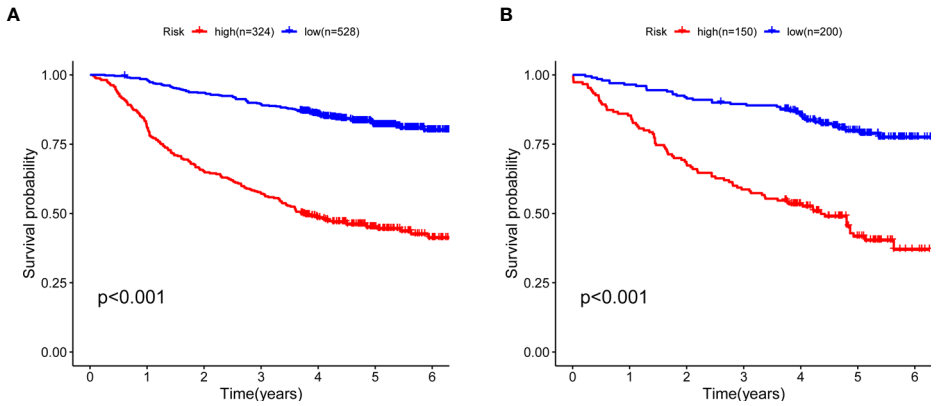

FIGURE 2 | Kaplan–Meier curves for five-year OS between high- and low-risk CRC patients. **(A)** Survival curves in the train cohort and the cut-off value is 1.1001 **(B)** Survival curves in test cohort and the cut-off value 1.070. OS, overall survival; CRC, colorectal cancer.

TBs panel according to their continuous value rather than the binary results of "negative" or "positive".

Emerging evidence indicated that pLNs have a strong association with poor OS and can serve as a robust risk factor for advanced CRC, which may determine subsequent adjuvant therapies and surveillance strategies (24, 25). Additionally, in order to achieve accurate N staging of CRC, the widely accepted minimum of recommendations was 12 (26–29). Nevertheless, nearly half of patients had an inadequate examination of lymph nodes partly due to tumor size, depth of invasion and complexity of tumor microenvironments (30). LODDS is a novel staging system that describes the LN status and has great potential to further improve. accuracy of LN staging for predicting prognosis. Moreover, increasing evidence indicates similar conclusions that LODDS is more accurate than LNR in assessing survival time of colon cancer patients (16, 31). Consistent with previous reports, we also found that LODDS played a critical role in progression and development of CRC patients. Besides, AUCs of LODDS alone in 1-, 3- and 5-year were 0.7242, 0.694, and 0.6969, which displayed that LODDS had robust predictive ability of CRC and could act as an excellent indicator for CRC patients. In addition, the coefficient of LODDS was the biggest weight (0.3365) in the model, which demonstrated its irreplaceable contribution in predicting OS of patients.

According to the results of univariate Cox regression analysis, it was manifested that harvested LNs had protective effect on the prognosis of CRC, which was consistent with previous studies (29, 32, 33). FVC is a common indicator of respiratory function and our results revealed its protective role in predicting OS of CRC patients. There were few investigations concerning the role of preoperative spirometry in postoperative complications and outcomes of CRC patients. Researchers have concluded that FVC/predicted VC may be a predictor of postoperative complications in CRC surgery, especially pneumonia (34).

With rapid advancement of genetic testing and bioinformatic technologies, abundant researchers have focused on developing the onco-RNA signatures and constructing the corresponding nomograms by a series of bioinformatic methods, to accurately predict the 1-, 3- and 5-year OS of CRC patients. Z. Zhou et al. indicated that an autophagy-related gene signature could effectively divide CRC patients into low- and high- risk groups and predict their postoperative survival (35). Likewise, a recent research has suggested that a CXCR5-based nomogram may also assist surgeons in devising personalized treatments (36). However, these literatures commonly centered on the RNA expression in the cancerous tissues of CRC patients and had not been validated by prospective clinical studies. Besides, these identified signatures might exacerbate the financial burden of patients and remain far from application in clinical practice (13). In recent clinical investigations, quite a few researchers started to focus on predicting OS of cancer patients based on handy clinical features. Daniel Boakye et al. constructed a clinical nomogram incorporating comorbidities and functional status, which could substantially enhance prediction of CRC prognosis (37). Likewise, a novel nomogram incorporating preoperative inflammatory and nutritional markers, built by Zhang Nannan et al. (5), could individually predict both OS and disease-free survival (DFS) of patients with CRC. Here, the aim of our study was to construct a convenient and clinically available prognostic model to better predict outcomes of CRC patients.

General characteristics and innovation points of our research are illustrated as follows. Firstly, the study was strictly conducted based on the real-world population, conclusions of which were consistent with some investigations from the publicly available database (16, 17, 38). Secondly, the four independent factors incorporated in our predictive model are easily available in clinical practice, and the model could accurately predict the postsurgical OS of CRC patients. Thirdly, the combination of serum TBs and LODDS was first adopted to construct a novel

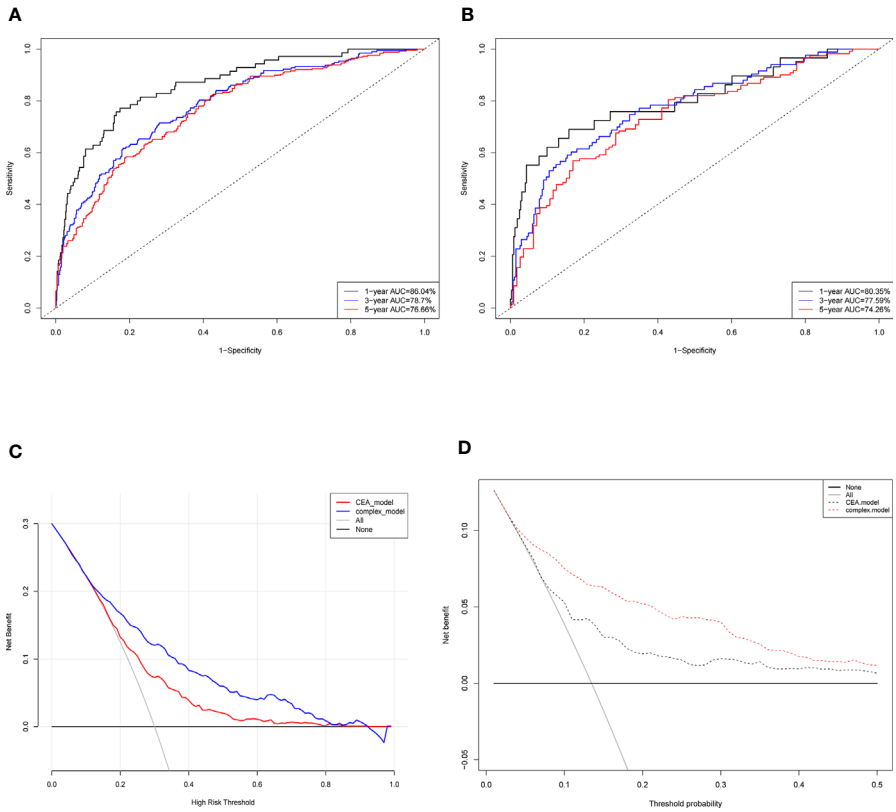

FIGURE 3 | Evaluation of the predictive model and DCA analysis. ROC curves of the predictive model in the train cohort **(A)** and test cohort **(B)**. **(C)** Logistic DCA analysis for two models in the whole cohort. Red line (CEA model) represents the traditional model only based on CEA value, and blue line (complex model) means the prognostic model in our study. **(D)** Survival DCA analysis for two models. Red dotted line represents the prognostic model in the study and grey line means the CEA model. Whole cohort is the combination of the train cohort and test cohort. ROC, receiver operating characteristic; DCA, decision curve analysis; CEA, carcinoembryonic antigen.

TABLE 4 | Univariate and multivariate COX analysis for clinical factors.

Factors	Univariate COX analysis			Multivariate COX analysis		
	HR	95%CI	P value	HR	95%CI	P value
Age	1.008	0.999–1.016	0.0560	1.012	1.004–1.021	0.0046
Sex (Female *vs* male)	1.074	0.880–1.309	0.4839	0.9519	0.778–1.165	0.6328
T stage (T3–4 *vs* T1–2)	2.541	1.851–3.489	<0.0001	1.964	1.425–2.705	<0.0001
N stage (N1–2 *vs* N0)	3.764	3.011–4.705	<0.0001	3.155	2.512–3.963	<0.0001
M stage (M1 *vs* M0)	4.781	2.974–7.688	<0.0001	3.070	1.887–4.994	<0.0001
Prognostic model	1.053	1.044–1.062	<0.0001	1.045	1.035–1.055	<0.0001

nomogram with stable clinical utilities. Nonetheless, there exist several limitations in our study. In light that this is a retrospective study based on single-center researches, there will inevitably be some selection bias, and the prognostic model should be validated by other hospitals. Moreover, our clinical research combined some common and non-innovative TBs with LODDS. But these common TBs could be more easily applied into clinical practice, compared with those complex and expensive gene sequencing. Hopefully, above-mentioned shortcomings could be solved in multicenter studies with larger population in the future.

CONCLUSIONS

In conclusion, we confirmed the clinical implications of CA199, CA125, CEA, and LODDS in predicting OS of CRC patients. A new prognostic model incorporating these factors was identified by multivariate Cox analysis. ROC curves demonstrated the

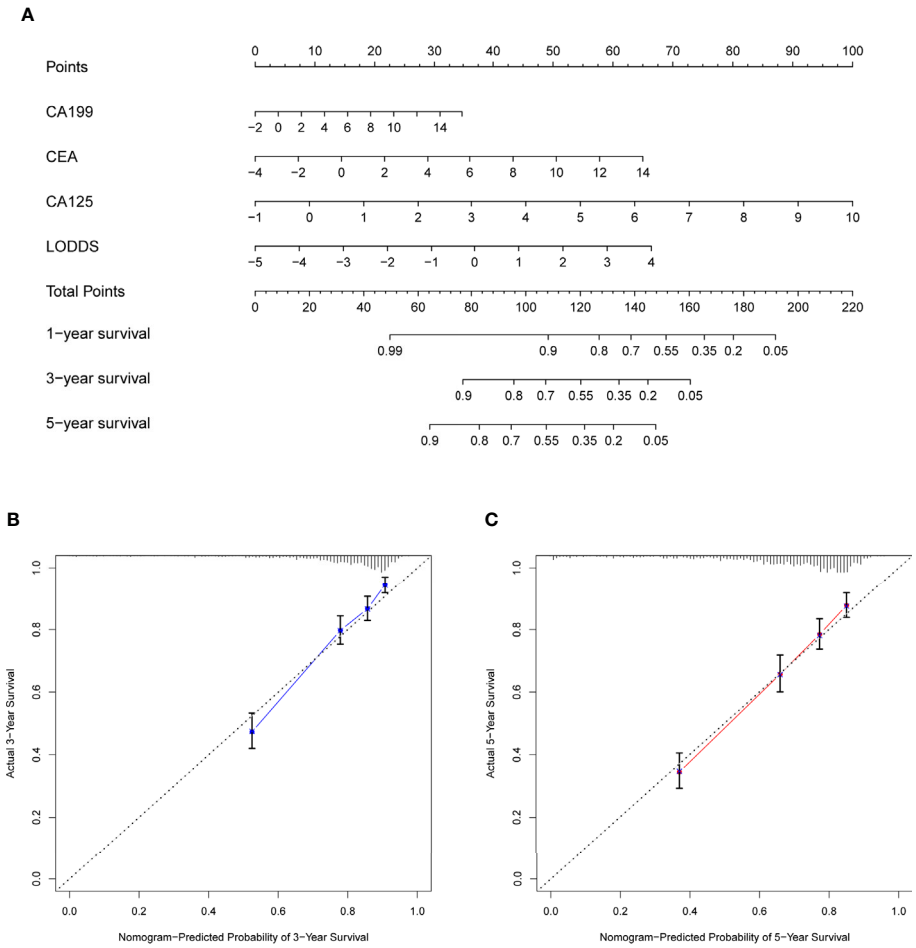

FIGURE 4 | Construction of nomogram and calibration diagram. **(A)** Nomogram incorporating CEA, CA199, CA125, and LODDS for predicting the OS of CRC patients. **(B, C)** Three-year calibration and five-year calibration diagram for assessment of the nomogram. In the nomogram, total points were obtained by summing up individual points from the respective variables, and higher points indicate poorer survival. In the calibration diagram, the nearer distance of red or blue dots to the diagonal line, the more accurate is the prediction of the nomogram. CEA, carcinoembryonic antigen; CA199, carbohydrate antigen199; CA125, carbohydrate antigen125; LODDS, log odds of positive lymph nodes scheme; OS, overall survival; CRC, colorectal cancer.

relatively high sensitivity and specificity of the model. A novel nomogram was further constructed which possessed great potential to be applied in clinical practice.

DATA AVAILABILITY STATEMENT

The raw data supporting the conclusions of this article will be made available by the authors, without undue reservation.

ETHICS STATEMENT

The studies involving human participants were reviewed and approved by the Medical Ethics Committee of the First Affiliated Hospital of the Air Force Medical University. Written informed consent to participate in this study was provided by the participants' legal guardian/next of kin.

AUTHOR CONTRIBUTIONS

JL designed the study. JuZ, JH, and QM contributed to the conception of the study and completed the manuscript together. TS, JY, and SW contributed significantly to statistical analysis and manuscript preparation. RC, DX, and YJ completed the following-up information. JL and JiZ helped perform the analysis with constructive discussions. All authors contributed to the article and approved the submitted version.

FUNDING

The work was financed in part by grants from the National Natural Science Foundation of China (81672751) and the Key Research and Development Program of Shaanxi (2019SF-010).

SUPPLEMENTARY MATERIAL

The Supplementary Material for this article can be found online at: https://www.frontiersin.org/articles/10.3389/fonc.2021.661040/full#supplementary-material

Supplementary Figure 1 | ROC curves of included variables and TNM staging system. ROC curves for **(A)** CEA, **(B)** CA199, **(C)** CA125, **(D)** LODDS and **(E)** TNM stage. CEA, Carcinoembryonic antigen; CA199, carbohydrate antigen199, CA125, carbohydrate antigen125; LODDS, log odds of positive lymph nodes scheme; TNM stage: AJCC/UICC 8th edition TNM staging system.

Supplementary Figure 2 | DCA curves between the prognostic model and TNM staging system. **(A)** Logistic DCA curve and **(B)** survival DCA analysis between the prognostic model and TNM stage. DCA, decision curve analysis; TNM stage, AJCC/UICC 8th edition TNM staging system.

Supplementary Figure 3 | Predictive value of the model in colon and rectal cancer. Kaplan–Meier curves for the model in colon cancer **(A)** and rectal cancer **(B)**. ROC curves for predicting 1-, 3-, and 5-year OS of patients in colon cancer **(C)** and rectal cancer **(D)**. ROC, receiver operating characteristic; OS, overall survival.

REFERENCES

1. Bray F, Ferlay J, Soerjomataram I, Siegel RL, Torre LA, Jemal A. Global cancer statistics 2018: GLOBOCAN estimates of incidence and mortality worldwide for 36 cancers in 185 countries. *CA Cancer J Clin* (2018) 68:394–424. doi: 10.3322/caac.21492
2. Zhu J, Lv Y, Hao J, Shi T, Wang S, Wang K, et al. N-myc downstream-regulated gene 2 promotes the protein stability of estrogen receptor beta via inhibition of ubiquitin-protein ligase E3A to suppress colorectal cancer. *J Gastrointest Oncol* (2020) 11:1200–13. doi: 10.21037/jgo-20-557
3. Siegel RL, Miller KD, Fedewa SA, Ahnen DJ, Meester RGS, Barzi A, et al. Colorectal cancer statistics, 2017. *CA Cancer J Clin* (2017) 67:177–93. doi: 10.3322/caac.21395
4. Holch JW, Ricard I, Stintzing S, Fischer von Weikersthal L, Decker T, Kiani A, et al. Relevance of baseline carcinoembryonic antigen for first-line treatment against metastatic colorectal cancer with FOLFIRI plus cetuximab or bevacizumab (FIRE-3 trial). *Eur J Cancer* (2019) 106:115–25. doi: 10.1016/j.ejca.2018.10.001
5. Zhang N, Ning F, Guo R, Pei J, Qiao Y, Fan J, et al. Prognostic Values of Preoperative Inflammatory and Nutritional Markers for Colorectal Cancer. *Front Oncol* (2020) 10:585083. doi: 10.3389/fonc.2020.585083
6. Van Cutsem E, Cervantes A, Adam R, Sobrero A, Van Krieken JH, Aderka D, et al. ESMO consensus guidelines for the management of patients with metastatic colorectal cancer. *Ann Oncol* (2016) 27:1386–422. doi: 10.1093/annonc/mdw235
7. You W, Yan L, Cai Z, Xie L, Sheng N, Wang G, et al. Clinical Significances of Positive Postoperative Serum CEA and Post-preoperative CEA Increment in Stage II and III Colorectal Cancer: A Multicenter Retrospective Study. *Front Oncol* (2020) 10:671. doi: 10.3389/fonc.2020.00671
8. Duffy MJ, Lamerz R, Haglund C, Nicolini A, Kalousová M, Holubec L, et al. Tumor markers in colorectal cancer, gastric cancer and gastrointestinal stromal cancers: European group on tumor markers 2014 guidelines update. *Int J Cancer* (2014) 134:2513–22. doi: 10.1002/ijc.28384
9. Chen L, Jiang B, Di J, Zhang C, Wang Z, Zhang N, et al. [Predictive value of preoperative detection of CEA and CA199 for prognosis in patients with stage II-III colorectal cancer]. *Zhonghua Wei Chang Wai Ke Za Zhi* (2015) 18:914–9.
10. Huang L, Fang J, Wu J, Zhou X, Wei H. [Prognostic value of combining preoperative serum tumor markers and peripheral blood routine indexes in patients with colorectal cancer]. *Zhonghua Wei Chang Wai Ke Za Zhi* (2018) 21:1421–6.
11. You W, Sheng N, Yan L, Chen H, Gong J, He Z, et al. The difference in prognosis of stage II and III colorectal cancer based on preoperative serum tumor markers. *J Cancer* (2019) 10:3757–66. doi: 10.7150/jca.31660
12. Edge SB, Compton CC. The American Joint Committee on Cancer: the 7th edition of the AJCC cancer staging manual and the future of TNM. *Ann Surg Oncol* (2010) 17:1471–4. doi: 10.1245/s10434-010-0985-4
13. Mo S, Zhou Z, Li Y, Hu X, Ma X, Zhang L, et al. Establishment and validation of a novel nomogram incorporating clinicopathological parameters into the TNM staging system to predict prognosis for stage II colorectal cancer. *Cancer Cell Int* (2020) 20:285. doi: 10.1186/s12935-020-01382-w
14. Persiani R, Cananzi FC, Biondi A, Paliani G, Tufo A, Ferrara F, et al. Log odds of positive lymph nodes in colon cancer: a meaningful ratio-based lymph node classification system. *World J Surg* (2012) 36:667–74. doi: 10.1007/s00268-011-1415-x
15. Wang J, Hassett JM, Dayton MT, Kulaylat MN. The prognostic superiority of log odds of positive lymph nodes in stage III colon cancer. *J Gastrointest Surg* (2008) 12:1790–6. doi: 10.1007/s11605-008-0651-3
16. Pei JP, Zhang CD, Fan YC, Dai DQ. Comparison of Different Lymph Node Staging Systems in Patients With Resectable Colorectal Cancer. *Front Oncol* (2018) 8:671. doi: 10.3389/fonc.2018.00671
17. Zhang QW, Zhang CH, Pan YB, Biondi A, Fico V, Persiani R, et al. Prognosis of colorectal cancer patients is associated with the novel log odds of positive lymph nodes scheme: derivation and external validation. *J Cancer* (2020) 11:1702–11. doi: 10.7150/jca.38180
18. Arslan NC, Sokmen S, Canda AE, Terzi C, Sarioglu S. The prognostic impact of the log odds of positive lymph nodes in colon cancer. *Colorectal Dis* (2014) 16:O386–92. doi: 10.1111/codi.12702
19. Berretta M, Alessandrini L, De Divitiis C, Nasti G, Lleshi A, Di Francia R, et al. Serum and tissue markers in colorectal cancer: State of art. *Crit Rev Oncol Hematol* (2017) 111:103–16. doi: 10.1016/j.critrevonc.2017.01.007
20. Park YJ, Park KJ, Park JG, Lee KU, Choe KJ, Kim JP. Prognostic factors in 2230 Korean colorectal cancer patients: analysis of consecutively operated cases. *World J Surg* (1999) 23:721–6. doi: 10.1007/PL00012376
21. Locker GY, Hamilton S, Harris J, Jessup JM, Kemeny N, Macdonald JS, et al. ASCO 2006 update of recommendations for the use of tumor markers in gastrointestinal cancer. *J Clin Oncol* (2006) 24:5313–27. doi: 10.1200/JCO.2006.08.2644
22. Park YJ, Youk EG, Choi HS, Han SU, Park KJ, Lee KU, et al. Experience of 1446 rectal cancer patients in Korea and analysis of prognostic factors. *Int J Colorectal Dis* (1999) 14:101–6. doi: 10.1007/s003840050193
23. Li L, Zhang L, Tian Y, Zhang T, Duan G, Liu Y, et al. Serum Chemokine CXCL7 as a Diagnostic Biomarker for Colorectal Cancer. *Front Oncol* (2019) 9:921. doi: 10.3389/fonc.2019.00921
24. Muro K. [Systemic chemotherapy for metastatic colorectal cancer -Japanese Society for Cancer of the Colon and Rectum (JSCCR) Guidelines 2016 for treatment of colorectal cancer]. *Nihon Shokakibyo Gakkai Zasshi* (2017) 114:1217–23. doi: 10.11405/nisshoshi.114.1217
25. Kahi CJ, Boland CR, Dominitz JA, Giardiello FM, Johnson DA, Kaltenbach T, et al. Colonoscopy Surveillance After Colorectal Cancer Resection: Recommendations of the US Multi-Society Task Force on Colorectal Cancer. *Gastroenterology* (2016) 150:758–68.e11. doi: 10.1053/j.gastro.2016.01.001
26. Chang GJ, Rodriguez-Bigas MA, Skibber JM, Moyer VA. Lymph node evaluation and survival after curative resection of colon cancer: systematic review. *J Natl Cancer Inst* (2007) 99:433–41. doi: 10.1093/jnci/djk092
27. Benson ,AB3, Venook AP, Cederquist L, Chan E, Chen YJ, Cooper HS, et al. Colon Cancer, Version 1.2017, NCCN Clinical Practice Guidelines in Oncology. *J Natl Compr Canc Netw* (2017) 15:370–98. doi: 10.6004/jnccn.2017.0036
28. Feinstein AR, Sosin DM, Wells CK. The Will Rogers phenomenon. Stage migration and new diagnostic techniques as a source of misleading statistics for survival in cancer. *N Engl J Med* (1985) 312:1604–8. doi: 10.1056/NEJM198506203122504

29. Dillman RO, Aaron K, Heinemann FS, McClure SE. Identification of 12 or more lymph nodes in resected colon cancer specimens as an indicator of quality performance. *Cancer* (2009) 115:1840–8. doi: 10.1002/cncr.24185
30. Altintas S, Bayrak M. Assessment of Factors Influencing Lymph Node Count in Colorectal Cancer. *J Coll Physicians Surg Pak* (2019) 29:1173–8. doi: 10.29271/jcpsp.2019.12.1173
31. Scarinci A, Di Cesare T, Cavaniglia D, Neri T, Colletti M, Cosenza G, et al. The impact of log odds of positive lymph nodes (LODDS) in colon and rectal cancer patient stratification: a single-center analysis of 323 patients. *Updates Surg* (2018) 70:23–31. doi: 10.1007/s13304-018-0519-3
32. Sarli L, Bader G, Iusco D, Salvemini C, Mauro DD, Mazzeo A, et al. Number of lymph nodes examined and prognosis of TNM stage II colorectal cancer. *Eur J Cancer (Oxford Engl 1990)* (2005) 41:272–9. doi: 10.1016/j.ejca.2004.10.010
33. Ning FL, Pei JP, Zhang NN, Wang J, Quan HG, Mei ZB, et al. Harvest of at least 18 lymph nodes is associated with improved survival in patients with pN0 colon cancer: a retrospective cohort study. *J Cancer Res Clin Oncol* (2020) 146:2117–33. doi: 10.1007/s00432-020-03212-y
34. Tajima Y, Tsuruta M, Yahagi M, Hasegawa H, Okabayashi K, Shigeta K, et al. Is preoperative spirometry a predictive marker for postoperative complications after colorectal cancer surgery? *Japanese J Clin Oncol* (2017) 47:815–9. doi: 10.1093/jjco/hyx082
35. Zhou Z, Mo S, Dai W, Ying Z, Zhang L, Xiang W, et al. Development and Validation of an Autophagy Score Signature for the Prediction of Post-operative Survival in Colorectal Cancer. *Front Oncol* (2019) 9:878. doi: 10.3389/fonc.2019.00878
36. Song W, Fu T. Circular RNA-Associated Competing Endogenous RNA Network and Prognostic Nomogram for Patients With Colorectal Cancer. *Front Oncol* (2019) 9:1181. doi: 10.3389/fonc.2019.01181
37. Boakye D, Jansen L, Schneider M, Chang-Claude J, Hoffmeister M, Brenner H. Personalizing the Prediction of Colorectal Cancer Prognosis by Incorporating Comorbidities and Functional Status into Prognostic Nomograms. *Cancers (Basel)* (2019) 11(10). doi: 10.3390/cancers11101435
38. Huang B, Chen C, Ni M, Mo S, Cai G, Cai S. Log odds of positive lymph nodes is a superior prognostic indicator in stage III rectal cancer patients: A retrospective analysis of 17,632 patients in the SEER database. *Int J Surg* (2016) 32:24–30. doi: 10.1016/j.ijsu.2016.06.002

Conflict of Interest: The authors declare that the research was conducted in the absence of any commercial or financial relationships that could be construed as a potential conflict of interest.

frontiers in Oncology

ORIGINAL RESEARCH
published: 16 April 2021
doi: 10.3389/fonc.2021.620361

Significance of Kynurenine 3-Monooxygenase Expression in Colorectal Cancer

*Chun-Yu Liu[1,2,3,4], Tzu-Ting Huang[3], Ji-Lin Chen[3], Pei-Yi Chu[5,6], Chia-Han Lee[3], Hsin-Chen Lee[7], Yu-Hsuan Lee[3], Yuan-Ya Chang[3], Shung-Haur Yang[1,4,8,9], Jeng-Kai Jiang[1,4,8], Wei-Shone Chen[1,4,8], Yee Chao[1,3,4] and Hao-Wei Teng[1,3,4]**

[1] School of Medicine, National Yang-Ming University, Taipei, Taiwan, [2] Division of Transfusion Medicine, Department of Medicine, Taipei Veterans General Hospital, Taipei, Taiwan, [3] Division of Medical Oncology, Department of Oncology, Center for Immuno-Oncology, Taipei Veterans General Hospital, Taipei, Taiwan, [4] School of Medicine, National Yang Ming Chiao Tung University, Hsinchu, Taiwan, [5] Department of Pathology, Show Chwan Memorial Hospital, Changhua City, Taiwan, [6] School of Medicine, Fu Jen Catholic University, New Taipei City, Taiwan, [7] School of Medicine, Institute of Pharmacology, National Yang-Ming Chiao Tung University, New Taipei City, Taiwan, [8] Division of Colon and Rectum Surgery, Department of Surgery, Taipei Veterans General Hospital, Taipei, Taiwan, [9] Department of Surgery, National Yang Ming Chiao Tung University Hospital, Yilan, Taiwan

Colorectal cancer (CRC) is a leading cause of cancer-related deaths. Because of the lack of reliable prognostic and predictive biomarkers for CRC, most patients are often diagnosed at a late stage. The tryptophan–kynurenine pathway plays a crucial role in promoting cancer progression. Kynurenine is considered an oncometabolite in colon cancer, and its downstream metabolites are also associated with CRC. Kynurenine 3-monooxygenase (KMO), a pivotal enzyme that catalyzes kynurenine metabolism, is essential for several cellular processes. In the current study, we explored the role of KMO in CRC. Immunohistochemical results showed that KMO was upregulated in CRC tissues relative to paired healthy tissue and polyps. Moreover, CRC patients with higher KMO expression were associated with higher metastasis and poorer survival rates. Knockdown of KMO decreased the expression of cancer stem cell markers, as well as the sphere-forming, migration, and invasion abilities of CRC cells. Additionally, blockade of the enzymatic activity of KMO using an inhibitor suppressed sphere formation and cell motility in CRC cells. These findings suggest the clinical relevance of KMO in CRC tumorigenesis and aggressiveness.

Keywords: kynurenine 3-monooxygenase, colorectal cancer, overall survival, metastasis, stemness

OPEN ACCESS

Edited by:
Kenneth K. W. To, The Chinese University of Hong Kong, China

Reviewed by:
Matthew Ciorba, Washington University in St. Louis, United States
Chen-Si Lin, National Taiwan University, Taiwan

***Correspondence:**
Hao-Wei Teng
hwteng1971@gmail.com

Specialty section:
This article was submitted to Gastrointestinal Cancers, a section of the journal Frontiers in Oncology

Received: *22 October 2020*
Accepted: *18 February 2021*
Published: *16 April 2021*

Citation:
Liu C-Y, Huang T-T, Chen J-L, Chu P-Y, Lee C-H, Lee H-C, Lee Y-H, Chang Y-Y, Yang S-H, Jiang J-K, Chen W-S, Chao Y and Teng H-W (2021) Significance of Kynurenine 3-Monooxygenase Expression in Colorectal Cancer. Front. Oncol. 11:620361. doi: 10.3389/fonc.2021.620361

INTRODUCTION

Colorectal cancer (CRC) ranks as the third-highest cause of cancer-related deaths and has increasing incidence in Taiwan (1). Different molecular subtypes of CRC exhibit distinct genetic signatures and clinical outcomes. Mutations, including *RAS*, *BRAF*, *PIK3CA*, *APC*, *TP53* mutations, and loss of *PTEN* expression, are usually present in metastatic CRC, and some of these genes have been suggested as promising predictive markers, and some act as predictive markers (2, 3). Tumor metastasis, relapse, and drug resistance lead to poor prognosis in CRC, despite advances in CRC treatments, such as radiotherapy, surgery, and chemotherapy (4, 5). Considering the high morbidity and modest effectiveness of CRC treatment, identifying reliable biomarkers of prognosis and therapeutic targets for patients with CRC is of paramount importance.

Almost 95% of dietary tryptophan, an essential amino acid, is metabolized along the kynurenine pathway. The tryptophan–kynurenine pathway is a crucial mechanism in the control of epithelial–mesenchymal transition (EMT) and helps cancers escape immune surveillance (6–8). Tryptophan-2,3-dioxygenase (TDO) and indoleamine-2,3-dioxygenases (IDOs), the enzymes responsible for the first and rate-limiting steps of tryptophan catabolism to kynurenine, are crucial in limiting adaptive immune responses and are expressed in many malignant and inflammatory diseases (9). In the kynurenine pathway, kynurenine 3-monooxygenase (KMO), a flavoprotein hydroxylase located on the outer membrane of mitochondria, catalyzes the conversion of kynurenine to 3-hydroxykynurenine (3-HK) and is broadly expressed in various tissues and cell types (10). The metabolites of kynurenine play a crucial role in infection, inflammation, and maintenance of the immunosuppressive microenvironment in many types of cancers. Kynurenine metabolites promote CRC cell proliferation and inhibit cell apoptosis by activating the PI3K–Akt pathway (11). A higher 3-HK to 8-hydroxykynurenic acid ratio is associated with increased CRC risk (12). KMO serves as a therapeutic target in multiple-organ failure, systemic inflammatory response, Huntington's disease, and immune adaptive response (13, 14). Recently, upregulation of KMO in hepatocellular carcinoma and triple-negative breast cancer tissues has been reported (15, 16). These studies suggest that KMO participates in cancer progression, whereas the role of KMO in CRC tumorigenesis and aggressiveness has not yet been demonstrated. In this study, we characterized KMO as an oncogene and link it to poor outcomes in CRC.

MATERIALS AND METHODS

Patient Specimens

A total of 242 medical samples from patients with CRC were obtained from the in-house Biobank of Taipei Veterans General Hospital (VGHTPE). This study was approved by the Institutional Review Board of Taipei Veterans General Hospital (IRB-TPEVGH) and conducted in compliance with the Helsinki Declaration. IRB-TPEVGH waived the requirement for informed consent. The clinicopathological stage was assessed based on the American Joint Committee on Cancer staging system, 7th edition. The clinical course was determined by searching a computer database containing detailed information. The experiments were performed in accordance with the approved guidelines and regulations.

Immunohistochemical Staining and Histochemical Score Determination

The paraffin-embedded CRC tissue sections were deparaffinized with xylene for 5 min, followed by two changes of xylene; the slides were then rehydrated. Peroxidase activity was blocked using 3% H_2O_2 for 10 min. The slides were incubated with blocking solution (2% FBS and 1% bovine serum albumin) for 1 h at room temperature. Primary antibodies against KMO (Abcam, Cambridge, MA, USA) were used at 1:100 dilution for overnight incubation at 4°C. The slides were counterstained with hematoxylin stain solution followed by detection with an EnVision Detection Systems Peroxidase/DAB, Rabbit/Mouse kit (Agilent, Santa Clara, CA, USA) according to the manufacturer's instructions. MSI status was identified by mismatch repair protein expressions. Antibodies against MLH1 (clone M1), PMS2 (clone EPR3947), MSH2 (clone G219–1129), and MSH6 (clone 44) were used for immunohistochemical staining with a BenchMark ULTRA system (Ventana, Indianapolis, IN, USA) according to the manufacturers' recommendations. The protein levels were determined with a semiquantitative method represented as H-scores. The assessment of the H-scores was performed by a single medical oncologist (Dr. HW Teng) who was blinded to clinical information. The H-score (0–300) was determined using semiquantitative assessment and was calculated by multiplying the percentage of positively stained cells (0–100) by the staining intensity (0 to 3+, **Supplementary Figure 1**) (17).

The Cancer Genome Atlas Database

The expression data of the KMO transcript, RNA-Seq by Expectation–Maximization (RSEM), was downloaded from the Broad GDAC Firehose data portal (https://gdac.broadinstitute.org/). KMO alterations and clinical data from patients with CRC were downloaded from the cbioportal (18, 19).

Cell Culture

SW480, Caco-2, HT-29, HCT-116 HCT-15, and Lovo cell lines were obtained from the American Type Culture Collection (Manassas, VA). SW480, Caco-2, and Lovo cells were maintained in Dulbecco's Modified Eagle Medium (Gibco); HT-29, HCT116, and HCT15 cells were maintained in the RPMI 1640 medium. All culture media were supplemented with 10% FBS, 0.1-mM nonessential amino acids, 2-mM L-glutamine, and 100 U/mL penicillin–streptomycin. Cells were maintained in a 5% CO_2 atmosphere at 37°C. The KMO inhibitor, UPF 648, was purchased from Axon Medchem (Reston, VA, USA) and dissolved in dimethyl sulfoxide (DMSO).

Lentiviral Production and Infection

To knock down endogenous KMO, plasmids containing siRNA against KMO (siKMO) and vector were obtained from the National RNAi Core Facility Platform (Academia Sinica, Taiwan). The target sequence of KMO (5′-CCACAGGCTGTTGAAATGTAA-3′) located within the KMO CDS region was constructed into the vector. To make lentivirus, briefly, 293T cells were seeded and co-transfected with pCMVdR8.91, pMD.G, and siKMO, or control (siCtrl) plasmids using Lipofectamine 3000 (Thermo Fisher Scientific, Waltham, MA, USA) following the manufacturer's instructions. After 24–48 h of transfection, viral supernatants were harvested and stored at −80°C. Cells were infected in medium containing 8 μg/mL polybrene with lentivirus expressing siKMO or siCtrl for 24 h.

Western Blot Analysis

Cells were trypsinized and harvested for further protein extraction; cell lysates were separated using SDS-PAGE

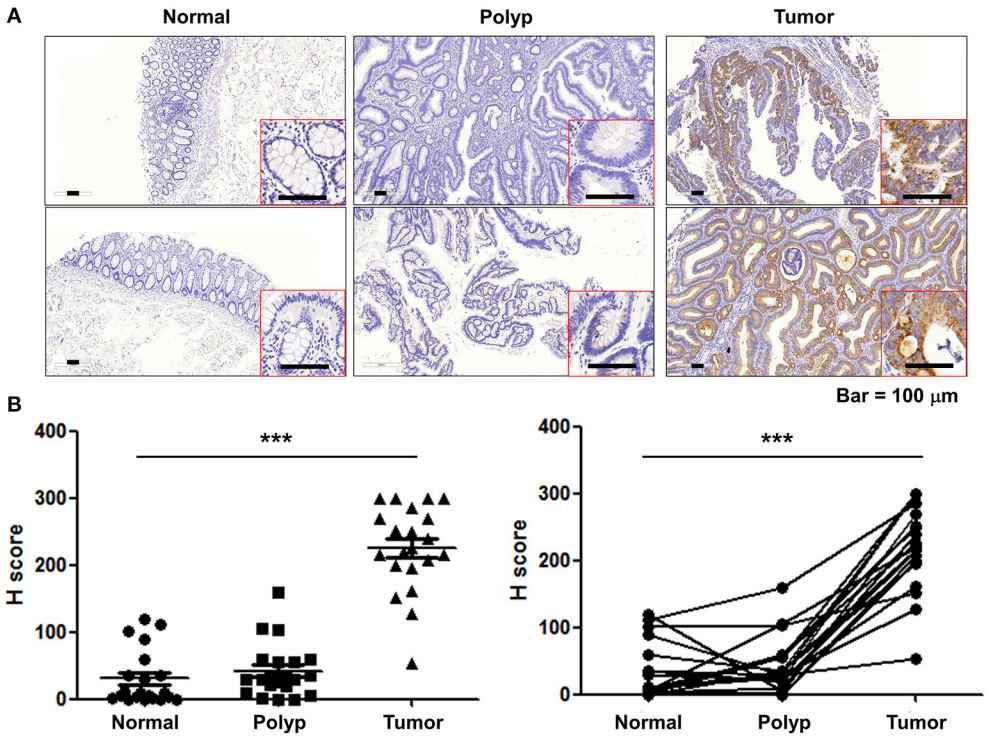

FIGURE 1 | KMO are upregulated in CRC tumor tissues. **(A)** Representative images for KMO expressions in CRC tumor, paired polyps, and paired normal counterparts' specimens were detected by immunohistochemistry. Scar bar, 100 μm. **(B)** Scatter dot plots for H-score of KMO staining ($N = 21$). Student's *t*-test, $^{***}P < 0.001$.

electrophoresis as described previously (20). Antibodies against KMO (Abcam, Cambridge, MA, USA), Nanog, CD44, and β-actin (Cell Signaling, Danvers, MA, USA) were used. Protein levels were quantified using ImageJ software.

Migration and Invasion Assays

As described previously (21), the migration and invasion assays were performed in 24-well-plates. SW480 (1×10^5), Caco-2 (1.5×10^5), or HT-29 cells (2×10^5) in 200 μL of serum-free medium were seeded onto apical transwells with 8-μm pores (Greiner Bio One, Kremsmünster, Austria) or Matrigel matrix-coated transwell for migration and invasion assays, respectively. Complete medium (900 μL) was added to the lower chamber and incubated for 20 h. After incubation, the migrated or invaded cells were fixed with 100% methanol for 10 min and stained with 0.05% crystal violet for 1 h.

Sphere Assay

Cells (5×10^2) were seeded onto ultra-low attachment 96-well-plates (Corning, New York, NY, USA) and suspended in DMEM-F12 medium containing B-27 supplement, N2 supplement, recombinant human EGF, and recombinant human FGFβ (Gibco). After 7 days, tumorspheres were counted under a microscope.

Cell Viability Assay

CRC cells (3×10^3) were cultured in a 96-well-plate for 24 h and further treated with UPF 648 at concentrations indicated for 72 h. Cell viability was determined by colorimetric assay using 3-(4,5-dimethylthiazol-2-yl)-2,5-diphenyltetrazolium bromide (MTT) assay. Ten microliters of MTT solution (0.5 mg/mL, Sigma-Aldrich, St. Louis, MO, USA) was added to the medium and incubated at 37°C for 3 h. The violet precipitates were dissolved in 100 μL of dimethyl sulfoxide (DMSO), and the absorbance was measured at 570 nm using a UQuant spectrophotometer (BioTek Instruments, Winooski, VT, USA).

OCR and ECAR Analyses

Cells ($3\ 10^4$) were seeded into 24-well-plates for oxygen consumption rate (OCR) and extracellular acidification rate (ECAR) determination using a Seahorse Extracellular Flux XF-24 analyzer (Seahorse Bioscience, North Billerica, MA, USA) according to the manufacturer's instructions. Prior to the assay, the sensor cartridge was hydrated at 37°C in a non-CO_2 incubator overnight. The culture medium was replaced with DMEM (pH 7.4) without sodium bicarbonate. Cells were incubated at 37°C in a non-CO_2 incubator for 1 h. OCR and ECAR were determined before and after the injection of oligomycin (2 μg/mL), FCCP (5 μM), and antimycin A (5 μM). The OCR and ECAR values were analyzed using an XF-24 analyzer and normalized to cell number.

Statistical Analysis

All calculations were performed using SPSS for Windows software, version 22 (SPSS, Chicago, IL, USA). A receiver operating characteristic curve (ROC) analysis was used to select the optimal cutoff values of KMO expression, including proteins (KMO H-score, **Supplementary Figures 2A,B**) and transcripts (KMO RSEM **Supplementary Figures 2C,D**), for defining low vs. high expression of KMO. The KMO expression level as test variable and patient's survival status as state variable were used to calculate coordinates of the ROC curve, sensitivity, and 1-specificity using SPSS software. The Youden index (22), the maximum value of sensitivity+specificity-1, was selected the optimal cutoff values. For survival analysis, overall survival (OS) and disease-free survival (DFS) curves of patients with CRC were plotted using the Kaplan–Meier method and compared using the log-rank test. The association between KMO expression and clinicopathological parameters was analyzed using contingency tables and the chi-square test. Statistical comparisons were performed using non-parametric tests, and statistical significance was defined as a $P < 0.05$.

RESULTS

KMO Is Upregulated in CRC Tumor Tissues and Correlates With Poor Outcome

To investigate the role of KMO in CRC tumorigenesis, we first examined the expression of KMO in tumors, paired polyps, and paired normal tissues by immunohistochemical staining (**Figure 1A**). The results showed that KMO expression in tumor tissues was significantly higher than that in normal tissues (**Figure 1B**). We further analyzed the association between clinicopathological characteristics and KMO expression in CRC patients from the VGHTPE cohort. KMO expression correlated with tumor metastasis but not age, sex, tumor location, pathology, AJCC stage, grade, or lymphovascular invasion (**Table 1**). Moreover, CRC patients with high KMO protein levels in the VGHTPE cohort had shorter survival (**Figure 2A**). To further validate the clinical relevance of KMO, we examined data from the TCGA database and found that CRC patients with higher KMO transcript levels were associated with worse DFS (**Figures 2B,C**). Higher KMO transcripts showed a decreasing trend in 5-year DFS (**Supplementary Figure 3A**). In addition, KMO gene alterations, including copy number variation, mutation, and mRNA dysregulation, correlated with poor OS (**Supplementary Figure 3B**). These results suggest that KMO might serve as a potential biomarker of CRC.

TABLE 1 | Relationship of KMO expression with CRC clinicopathological parameters.

Characteristics	KMO expression		*P*-value
	Low ($n = 99$)	High ($n = 143$)	
Age			
≤60	35 (35.4)	42 (29.4)	0.330
>60	64 (64.6)	101 (70.6)	
Gender			
Female	32 (32.3)	52 (36.4)	0.583
Male	67 (67.7)	91 (63.6)	
Location			
Left	55 (55.6)	87 (60.8)	0.428
Right	44 (44.4)	56 (39.2)	
Pathology			
Adenocarcinoma	92 (92.9)	139 (97.2)	0.194
Carcinoma	0 (0.0)	1 (0.7)	
Mucinous adenocarcinoma	6 (6.1)	3 (2.1)	
Signet ring cell carcinoma	1 (1.0)	0 (0.0)	
AJCC			
I	6 (6.1)	11 (7.7)	0.107
II	34 (34.3)	33 (23.1)	
III	32 (32.3)	41 (28.7)	
IV	27 (27.3)	58 (40.6)	
High grade			
No	90 (90.9)	125 (87.4)	0.495
Yes	7 (7.1)	14 (9.8)	
NA	2 (2.0)	4 (2.8)	
Metastasis			
No (AJCC I–III)	72 (72.7)	85 (59.4)	0.040
Yes (AJCC IV)	27 (27.3)	58 (40.6)	
Lymphovascular invasion			
No	76 (76.8)	98 (68.5)	0.115
Yes	17 (17.2)	38 (26.6)	
NA	6 (6.0)	7 (4.9)	
MSI status			
MSS	90 (90.9)	136 (95.1)	0.292
MSI-H	9 (9.1)	7 (4.9)	

The cutoff value of the H-score of KMO was selected as 184.5.
AJCC, American Joint Commission on Cancer; CRC, colorectal cancer; KMO, kynurenine 3-monooxygenase; MSI, microsatellite instable; MSS, microsatellite stable; MSI-H, microsatellite instable-high; NA, not available.

Knockdown KMO Represses Sphere Formation, Migration, and Invasion Abilities of CRC Cells

We found that KMO was expressed in human CRC cell lines including SW480, Caco-2, HT-29, HCT-116, HCT-15, and Lovo cells (**Figure 3A**). To elucidate the function of KMO in CRC carcinogenesis, CRC cells were transfected with plasmids containing siRNA against KMO or control vector. Immunoblotting data showed that the expression of stemness markers, including CD44 and Nanog, was decreased in KMO-knockdown cells (**Figure 3B**). Sphere formation was significantly suppressed by KMO knockdown (**Figure 3C**). In addition, cell migration and invasion were also repressed in KMO-knockdown cells relative to control cells (**Figures 3D,E**). These data suggest that KMO promotes cancer progression in human CRC cells.

KMO Inhibition Suppresses Cell Motility and Sphere Formation in CRC Cells

KMO is an outer mitochondrial membrane enzyme that controls kynurenine catabolism. KMO inhibitors, which suppress KMO

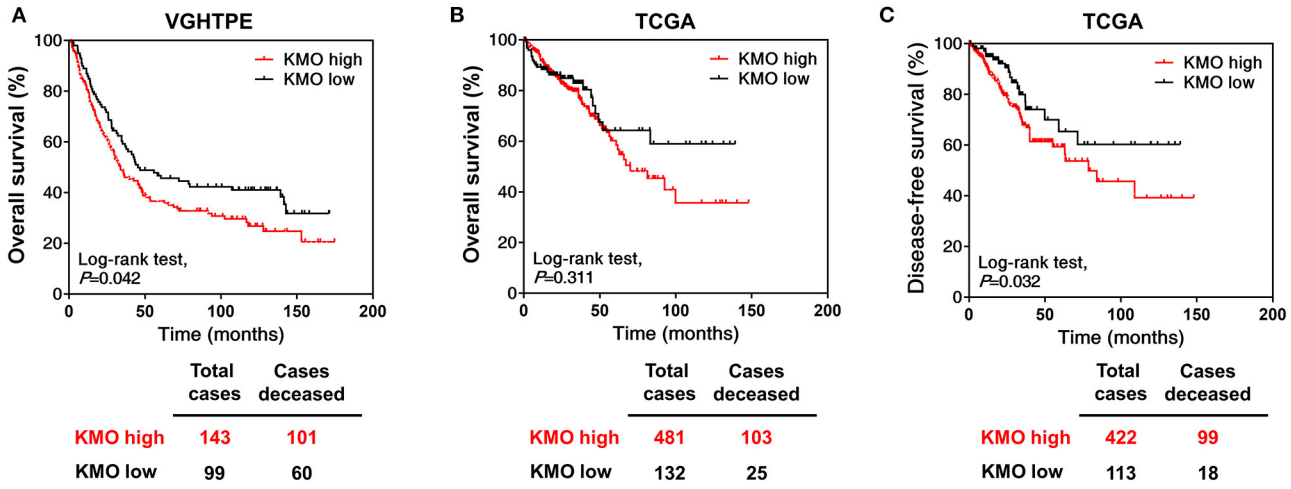

FIGURE 2 | High KMO expression is associated with poor overall survival. **(A)** Overall survival of CRC patients from VGHTPE was plotted against time in month for the protein levels of KMO. **(B,C)** The level 3 data of mRNA RSEM from patients with CRC were selected from the TCGA and Broad GDAC Firehose data portal. Overall **(B)** and disease-free survival **(C)** curves were plotted for CRC patients with high or low transcript expressions of KMO.

activity (16), were used to address the role of KMO activity in CRC progression. Inhibition of KMO with UPF 648 did not affect the OCR or basal ECAR of CRC cells (**Supplementary Figure 4**). UPF 648 exerted differential effects on the viability of CRC cells (**Figure 4A**). Nevertheless, the number of spheres, cell migration, and invasion were diminished by UPF 648 treatment in SW480, HT-29, and Caco-2 cells (**Figures 4B–D**). Likewise, sphere number and cell motility were reduced by the other well-explored KMO inhibitor, Ro 61–8048 (**Supplementary Figures 5A–C**). Taken together, these findings suggest the clinical significance and oncogenic role of KMO in CRC.

DISCUSSION

CRC still has a poor prognosis due to the high frequency of metastasis, recurrence, and drug resistance. As a result, identifying the prognostic factors and developing novel therapeutic strategies for CRC treatment is important. Inflammation is one of the hallmarks of cancer, and pro-inflammatory conditions enhance CRC progression and metastasis (23). KMO is upregulated by pro-inflammatory cytokines (24, 25). In the current study, we observed dysregulation of KMO in CRC. KMO expression was higher in CRC tumor tissues than in healthy tissues and polyps (**Figure 1**). In addition, high levels of KMO in patients with CRC correlated with worse survival rates (**Figure 2**).

Cancer stem cells (CSCs) are defined as tumor-initiating cells with the ability to self-renew and differentiate. Increasing evidence suggests that CSCs participate in tumor growth, metastasis, and recurrence (26). Targeting CSC is considered an effective anti-tumor strategy, including in CRC (27). CD44 is a surface marker of colorectal CSCs (28). CD44 knockdown suppresses clonal formation and tumorigenesis of CRC *in vivo* (29). The transcription factor Nanog regulates pluripotent genes and EMT (30, 31). It has been reported that high expression of Nanog is associated with poor prognosis and lymph node metastasis in CRC (32). Data revealed that knockdown of KMO decreased the number of CRC spheres with a reduction in CSC markers, including Nanog and CD44. Migration and invasion abilities were also reduced by KMO knockdown (**Figure 3**). Although our finding suggests a possible link of KMO to cancer stemness, consolidative supporting evidence is required. Further research is needed to validate the role of KMO in CRC stemness and to elucidate the underlying mechanisms of KMO in the regulation of expressions of CSC markers in CRC.

Miscellaneous KMO inhibitors have been developed and investigated for neurodegenerative disorders (33), for instance, a KMO tight-binding inhibitor, UPF 648, which is able to cross the blood–brain barrier in targeted therapies against neurodegenerative diseases (34). UPF648 treatment significantly reduces 3-HK levels in the brain and exerts neuroprotection (35). Ro 61–8048 and mNBA, both KMO inhibitors, exert neuroprotective effects by reducing 3-HK and quinolinic acid levels (36). Our results manifested that inhibition of KMO activity represses cell migration, invasion, and tumor sphere formation (**Figure 4**, **Supplementary Figure 4**). Notably, we observed that KMO inhibition showed different effects on cell viability and sphere formation. Previous studies indicate that inhibition of druggable genes shows diverse phenotypic outcomes between 2D monolayer culture and 3D sphere formation assays. The microenvironment affects phenotypic responses, suggesting that multiplexed assays render comprehensive information on anticancer target screening (37). Our results highlight the feasibility of KMO inhibitors in CRC treatment.

Recently, immunomodulation has increasingly played a key role in treating metastatic CRC. The tumor microenvironment comprises host stromal cells, tumor cells, and immune cells,

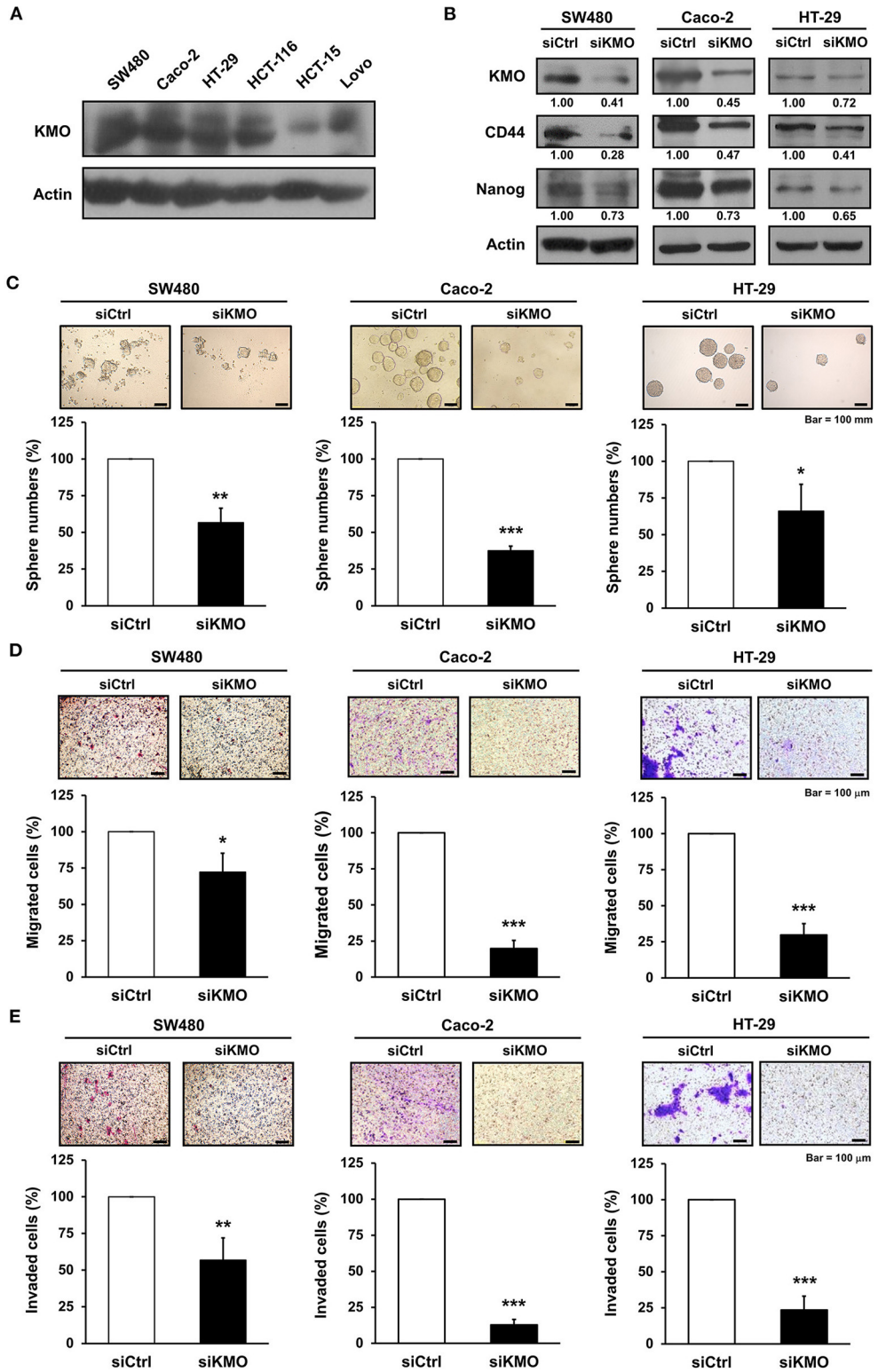

FIGURE 3 | Knockdown of KMO suppresses stemness properties and motility of CRC cells. **(A)** Whole-cell extracts of SW480, Caco-2, HT-29, HCT-116, HCT-15, and Lovo cells were analyzed by western blot analysis using anti-KMO and anti-β-actin antibodies. **(B–E)** Whole-cell extracts of SW480, Caco-2, and HT-29 cells transduced with virus containing KMO siRNA (siKMO) or control (siCtrl) were harvested for western blot analysis using anti-KMO, anti-CD44, anti-Nanog, and anti-β-actin antibodies **(B)**, sphere **(C)**, transwell migration **(D)**, and invasion assays **(E)**. Means ± SD of three independent experiments performed in triplicate are shown [100 magnification times for **(D,E)**]. Student's *t*-test, $^{*}P < 0.05$; $^{**}P < 0.01$; $^{***}P < 0.001$.

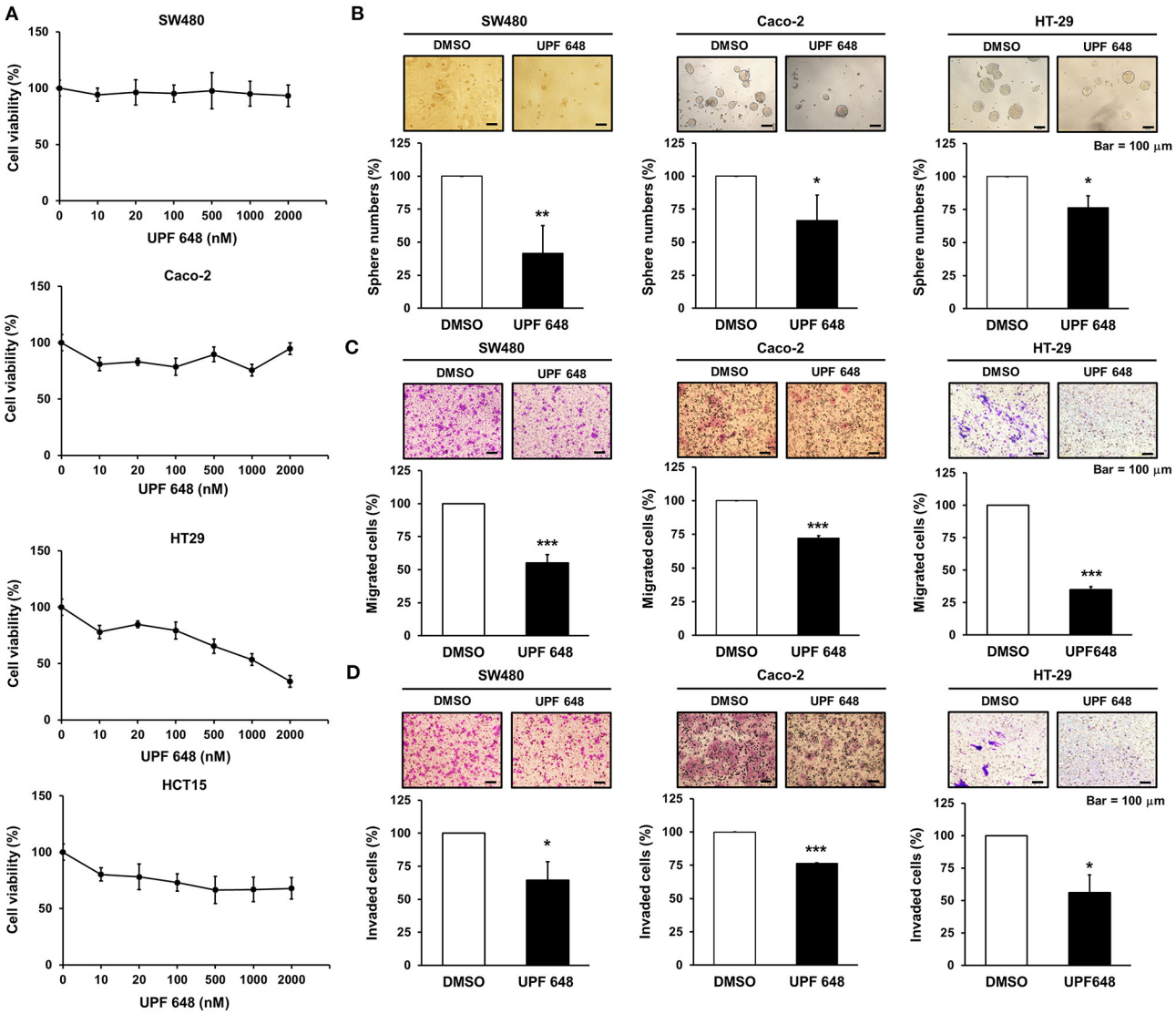

FIGURE 4 | KMO inhibitor reduces the abilities of sphere formation, migration, and invasion in CRC cells. **(A)** SW480, Caco-2, HT-29, and HCT-15 cells were treated with indicated doses of UPF 648 for 72 h and examined by MTT assay. **(B–D)** SW480, Caco-2, and HT-29 cells treated with UPF 648 (1 μM) or DMSO were seeded for sphere **(B)**, transwell migration **(C)**, and invasion assays **(D)**. Means ± SD of three independent experiments performed in triplicate are shown [100 magnification times for **(C,D)**]. Student's *t*-test, $^{*}P < 0.05$; $^{**}P < 0.01$; $^{***}P < 0.001$.

including macrophages and leukocytes. Growing evidence suggests that the tumor microenvironment plays a crucial role in tumor progression and may serve as a therapeutic target (38). Targeting amino acid-metabolizing enzymes, which are involved in the regulation of immunosuppression, is a potential strategy for cancer treatment. It is well-known that L-tryptophan metabolism via the kynurenine pathway is involved in immune regulation. In the kynurenine pathway, IDO is the main rate-limiting enzyme and KMO is the downstream enzyme of IDO. In addition, IDO1 enhances T regulatory cell differentiation and further leads to immunosuppressive myeloid-derived suppressor cell recruitment (39, 40). IDO may serve as a predictive marker of distant metastasis in the early stages of CRC (41). High expression of IDO promotes tryptophan catabolite production, leading to immune escape and defeat of T cell invasion and contributing to CRC progression (42). On the other hand, previous studies indicated that IDO inhibitor 1-L-MT suppressed colitis-associated CRC through cell cycle arrest in an adaptive immunity modulation-independent manner (43). KMO is broadly expressed in various cell types, including immune cells such as macrophages, monocytes, and microglia (44). Nevertheless, the biological function of KMO, the downstream enzyme of IDO, on immunomodulation in CRC is still unclear. The interaction between KMO, IDO, and immunomodulation remains an unmet need.

Our study has some limitations; first, the interpretation of immunohistochemical staining and H-score determination may

have interpersonal variations and future machine learning-based digital pathology should help to reduce the errors and variations. Secondly, despite that the current study showed that KMO inhibition by inhibitors possessed some anticancer effects on CRC cells, our study did not examine the effects of KMO inhibition on 3-HK production and the subsequent possible biological impact on CRC cells. The mechanisms of the anticancer effects of KMO inhibition in CRC cells require further investigation.

In summary, our results demonstrated that KMO is upregulated in CRC tissues and linked to worse survival. Inhibition of KMO reduces CRC progression *in vitro*. Our study suggests that KMO may act as an oncogene and reveals the therapeutic potential of targeting KMO enzymatic activity in CRC.

DATA AVAILABILITY STATEMENT

The original contributions presented in the study are included in the article/**Supplementary Material**, further inquiries can be directed to the corresponding author/s.

ETHICS STATEMENT

The studies involving human participants were reviewed and approved by Institutional Review Board of Taipei Veterans General Hospital. The medical residual samples were acquired from the residual sample bank of Taipei Veterans General Hospital. VGHIRB waived the requirement for the use of an informed consent form.

AUTHOR CONTRIBUTIONS

C-YL and H-WT: conceptualization, supervision, and validation. T-TH, J-LC, and P-YC: data curation. C-HL, J-LC, Y-HL, and Y-YC: investigation. H-CL, S-HY, J-KJ, W-SC, and YC: methodology. C-YL, T-TH, J-LC, C-HL, and H-WT: writing—original draft. All authors had substantial contributions to the conception or design of the work, read the final manuscript, and agreed with the accuracy integrity of all parts of the work.

FUNDING

We thank the grants from the Taiwan Clinical Oncology Research Foundation, the Ministry of Science and Technology, Taiwan (MOST 106-2314-B-075-062; 109-2314-B-075-081-MY3), Yen Tjing Ling Medical Foundation (CI-108-19), and Taipei Veterans General Hospital (V109C-151; V110C-189).

ACKNOWLEDGMENTS

The authors would like to acknowledge the support by the Biobank of Taipei Veterans General Hospital.

SUPPLEMENTARY MATERIAL

The Supplementary Material for this article can be found online at: https://www.frontiersin.org/articles/10.3389/fonc.2021.620361/full#supplementary-material

REFERENCES

1. Kuo CN, Liao YM, Kuo LN, Tsai HJ, Chang WC, Yen Y. Cancers in Taiwan: practical insight from epidemiology, treatments, biomarkers, and cost. *J Formos Med Assoc.* (2019) 119:1731–41. doi: 10.1016/j.jfma.2019.08.023
2. Phipps AI, Limburg PJ, Baron JA, Burnett-Hartman AN, Weisenberger DJ, Laird PW, et al. Association between molecular subtypes of colorectal cancer and patient survival. *Gastroenterology.* (2015) 148:77–87.e2. doi: 10.1053/j.gastro.2014.09.038
3. Nguyen HT, Duong HQ. The molecular characteristics of colorectal cancer: implications for diagnosis and therapy. *Oncol Lett.* (2018) 16:9–18. doi: 10.3892/ol.2018.8679
4. Kamal Y, Schmit SL, Frost HR, Amos CI. The tumor microenvironment of colorectal cancer metastases: opportunities in cancer immunotherapy. *Immunotherapy.* (2020) 12:1083–100. doi: 10.2217/imt-2020-0026
5. Xie YH, Chen YX, Fang JY. Comprehensive review of targeted therapy for colorectal cancer. *Signal Transduct Target Ther.* (2020) 5:22. doi: 10.1038/s41392-020-0116-z
6. Cheng J, Li W, Kang B, Zhou Y, Song J, Dan S, et al. Tryptophan derivatives regulate the transcription of Oct4 in stem-like cancer cells. *Nat Commun.* (2015) 6:7209. doi: 10.1038/ncomms8209
7. Ling W, Zhang J, Yuan Z, Ren G, Zhang L, Chen X, et al. Mesenchymal stem cells use IDO to regulate immunity in tumor microenvironment. *Cancer Res.* (2014) 74:1576–87. doi: 10.1158/0008-5472.CAN-13-1656
8. Opitz CA, Somarribas Patterson LF, Mohapatra SR, Dewi DL, Sadik A, Platten M, et al. The therapeutic potential of targeting tryptophan catabolism in cancer. *Br J Cancer.* (2020) 122:30–44. doi: 10.1038/s41416-019-0664-6
9. Prendergast GC, Smith C, Thomas S, Mandik-Nayak L, Laury-Kleintop L, Metz R, et al. Indoleamine 2,3-dioxygenase pathways of pathogenic inflammation and immune escape in cancer. *Cancer Immunol Immunother.* (2014) 63:721–35. doi: 10.1007/s00262-014-1549-4
10. Boros FA, Vecsei L. Immunomodulatory effects of genetic alterations affecting the kynurenine pathway. *Front Immunol.* (2019) 10:2570. doi: 10.3389/fimmu.2019.02570
11. Bishnupuri KS, Alvarado DM, Khouri AN, Shabsovich M, Chen B, Dieckgraefe BK, et al. IDO1 and kynurenine pathway metabolites activate pi3k-akt signaling in the neoplastic colon epithelium to promote cancer cell proliferation and inhibit apoptosis. *Cancer Res.* (2019) 79:1138–50. doi: 10.1158/0008-5472.CAN-18-0668
12. Gylling B, Myte R, Schneede J, Hallmans G, Haggstrom J, Johansson I, et al. Vitamin B-6 and colorectal cancer risk: a prospective population-based study using 3 distinct plasma markers of vitamin B-6 status. *Am J Clin Nutr.* (2017) 105:897–904. doi: 10.3945/ajcn.116.139337
13. Mole DJ, Webster SP, Uings I, Zheng X, Binnie M, Wilson K, et al. Kynurenine-3-monooxygenase inhibition prevents multiple organ failure in rodent models of acute pancreatitis. *Nat Med.* (2016) 22:202–9. doi: 10.1038/nm.4020
14. Zadori D, Veres G, Szalardy L, Klivenyi P, Fulop F, Toldi J, et al. Inhibitors of the kynurenine pathway as neurotherapeutics: a patent review (2012-2015). *Expert Opin Ther Pat.* (2016) 26:815–32. doi: 10.1080/13543776.2016.1189531
15. Jin H, Zhang Y, You H, Tao X, Wang C, Jin G, et al. Prognostic significance of kynurenine 3-monooxygenase and effects on proliferation, migration, and invasion of human hepatocellular carcinoma. *Sci Rep.* (2015) 5:10466. doi: 10.1038/srep10466

16. Huang TT, Tseng LM, Chen JL, Chu PY, Lee CH, Huang CT, et al. Kynurenine 3-monooxygenase upregulates pluripotent genes through beta-catenin and promotes triple-negative breast cancer progression. *EBioMedicine.* (2020) 54:102717. doi: 10.1016/j.ebiom.2020.102717
17. Detre S, Saclani Jotti G, Dowsett M. A "quickscore" method for immunohistochemical semiquantitation: validation for oestrogen receptor in breast carcinomas. *J Clin Pathol.* (1995) 48:876–8. doi: 10.1136/jcp.48.9.876
18. Gao J, Aksoy BA, Dogrusoz U, Dresdner G, Gross B, Sumer SO, et al. Integrative analysis of complex cancer genomics and clinical profiles using the cBioPortal. *Sci Signal.* (2013) 6:pl1. doi: 10.1126/scisignal.2004088
19. Cerami E, Gao J, Dogrusoz U, Gross BE, Sumer SO, Aksoy BA, et al. The cBio cancer genomics portal: an open platform for exploring multidimensional cancer genomics data. *Cancer Discov.* (2012) 2:401–4. doi: 10.1158/2159-8290.CD-12-0095
20. Liu CY, Huang TT, Chen YT, Chen JL, Chu PY, Huang CT, et al. Targeting SET to restore PP2A activity disrupts an oncogenic CIP2A-feedforward loop and impairs triple negative breast cancer progression. *EBioMedicine.* (2019) 40:263–75. doi: 10.1016/j.ebiom.2018.12.032
21. Liu CY, Chu PY, Huang CT, Chen JL, Yang HP, Wang WL, et al. Varlitinib downregulates HER/ERK signaling and induces apoptosis in triple negative breast cancer cells. *Cancers.* (2019) 11:105. doi: 10.3390/cancers11010105
22. Hajian-Tilaki K. Receiver operating characteristic (ROC) curve analysis for medical diagnostic test evaluation. *Caspian J Intern Med.* (2013) 4:627–35.
23. Lasry A, Zinger A, Ben-Neriah Y. Inflammatory networks underlying colorectal cancer. *Nat Immunol.* (2016) 17:230–40. doi: 10.1038/ni.3384
24. Zunszain PA, Anacker C, Cattaneo A, Choudhury S, Musaelyan K, Myint AM, et al. Interleukin-1beta: a new regulator of the kynurenine pathway affecting human hippocampal neurogenesis. *Neuropsychopharmacology.* (2012) 37:939–49. doi: 10.1038/npp.2011.277
25. Parrott JM, O'Connor JC. Kynurenine 3-Monooxygenase: an influential mediator of neuropathology. *Front Psychiatry.* (2015) 6:116. doi: 10.3389/fpsyt.2015.00116
26. Prager BC, Xie Q, Bao S, Rich JN. Cancer stem cells: the architects of the tumor ecosystem. *Cell Stem Cell.* (2019) 24:41–53. doi: 10.1016/j.stem.2018.12.009
27. Szarynska M, Olejniczak A, Kobiela J, Spychalski P, Kmiec Z. Therapeutic strategies against cancer stem cells in human colorectal cancer. *Oncol Lett.* (2017) 14:7653–68. doi: 10.3892/ol.2017.7261
28. Wang C, Xie J, Guo J, Manning HC, Gore JC, Guo N. Evaluation of CD44 and CD133 as cancer stem cell markers for colorectal cancer. *Oncol Rep.* (2012) 28:1301–8. doi: 10.3892/or.2012.1951
29. Du L, Wang H, He L, Zhang J, Ni B, Wang X, et al. CD44 is of functional importance for colorectal cancer stem cells. *Clin Cancer Res.* (2008) 14:6751–60. doi: 10.1158/1078-0432.CCR-08-1034
30. Zhang J, Espinoza LA, Kinders RJ, Lawrence SM, Pfister TD, Zhou M, et al. NANOG modulates stemness in human colorectal cancer. *Oncogene.* (2013) 32:4397–405. doi: 10.1038/onc.2012.461
31. Pan Q, Meng L, Ye J, Wei X, Shang Y, Tian Y, et al. Transcriptional repression of miR-200 family members by Nanog in colon cancer cells induces epithelial-mesenchymal transition (EMT). *Cancer Lett.* (2017) 392:26–38. doi: 10.1016/j.canlet.2017.01.039
32. Meng HM, Zheng P, Wang XY, Liu C, Sui HM, Wu SJ, et al. Over-expression of Nanog predicts tumor progression and poor prognosis in colorectal cancer. *Cancer Biol Ther.* (2010) 9:295–302. doi: 10.4161/cbt.9.4.10666
33. Smith JR, Jamie JF, Guillemin GJ. Kynurenine-3-monooxygenase: a review of structure, mechanism, and inhibitors. *Drug Discov Today.* (2016) 21:315–24. doi: 10.1016/j.drudis.2015.11.001
34. Amaral M, Levy C, Heyes DJ, Lafite P, Outeiro TF, Giorgini F, et al. Structural basis of kynurenine 3-monooxygenase inhibition. *Nature.* (2013) 496:382–5. doi: 10.1038/nature12039
35. Ceresoli-Borroni G, Guidetti P, Amori L, Pellicciari R, Schwarcz R. Perinatal kynurenine 3-hydroxylase inhibition in rodents: pathophysiological implications. *J Neurosci Res.* (2007) 85:845–54. doi: 10.1002/jnr.21183
36. Carpenedo R, Meli E, Peruginelli F, Pellegrini-Giampietro DE, Moroni F. Kynurenine 3-mono-oxygenase inhibitors attenuate post-ischemic neuronal death in organotypic hippocampal slice cultures. *J Neurochem.* (2002) 82:1465–71. doi: 10.1046/j.1471-4159.2002.01090.x
37. Jeong E, Park C, Moon SU, Cho J, Song M, Ryoo S, et al. Dissecting phenotypic responses of the druggable targetome in cancers. *Sci Rep.* (2019) 9:12513. doi: 10.1038/s41598-019-48989-2
38. Chanmee T, Ontong P, Konno K, Itano N. Tumor-associated macrophages as major players in the tumor microenvironment. *Cancers.* (2014) 6:1670–90. doi: 10.3390/cancers6031670
39. Holmgaard RB, Zamarin D, Li Y, Gasmi B, Munn DH, Allison JP, et al. Tumor-expressed IDO recruits and activates MDSCs in a treg-dependent manner. *Cell Rep.* (2015) 13:412–24. doi: 10.1016/j.celrep.2015.08.077
40. Baban B, Chandler PR, Sharma MD, Pihkala J, Koni PA, Munn DH, et al. IDO activates regulatory T cells and blocks their conversion into Th17-like T cells. *J Immunol.* (2009) 183:2475–83. doi: 10.4049/jimmunol.0900986
41. Ogawa M, Watanabe M, Hasegawa T, Ichihara K, Yoshida K, Yanaga K. Expression of CXCR-4 and IDO in human colorectal cancer: an immunohistochemical approach. *Mol Clin Oncol.* (2017) 6:701–4. doi: 10.3892/mco.2017.1207
42. Brandacher G, Perathoner A, Ladurner R, Schneeberger S, Obrist P, Winkler C, et al. Prognostic value of indoleamine 2,3-dioxygenase expression in colorectal cancer: effect on tumor-infiltrating T cells. *Clin Cancer Res.* (2006) 12:1144–51. doi: 10.1158/1078-0432.CCR-05-1966
43. Liu X, Zhou W, Zhang X, Ding Y, Du Q, Hu R. 1-L-MT, an IDO inhibitor, prevented colitis-associated cancer by inducing CDC20 inhibition-mediated mitotic death of colon cancer cells. *Int J Cancer.* (2018) 143:1516–29. doi: 10.1002/ijc.31417
44. Fujigaki H, Yamamoto Y, Saito K. L-Tryptophan-kynurenine pathway enzymes are therapeutic target for neuropsychiatric diseases: focus on cell type differences. *Neuropharmacology.* (2017) 112 (Pt. B):264–74. doi: 10.1016/j.neuropharm.2016.01.011

Conflict of Interest: The authors declare that the research was conducted in the absence of any commercial or financial relationships that could be construed as a potential conflict of interest.

frontiers in Oncology

ORIGINAL RESEARCH
published: 29 April 2021
doi: 10.3389/fonc.2021.635537

The Clinicopathological Characteristics of Alpha-Fetoprotein-Producing Adenocarcinoma of the Gastrointestinal Tract—A Single-Center Retrospective Study

Xiang-Xing Kong[1,2†], Xin-Lin Li[1,2,3†], Yu Tian[4†], Qian-Cheng Ye[4], Xiao-Ming Xu[2,5], Yue Liu[1,2], Qi Yang[2,5], Li-Na Zhang[1,2], Yan-Xia Mei[1,2], Ji-Hang Wen[1,2], Qian Xiao[1,2], Jing-Song Li[4,6], Ke-Feng Ding[1,2] and Jun Li[1,2]*

[1] Department of Colorectal Surgery and Oncology, Key Laboratory of Cancer Prevention and Intervention, Ministry of Education, The Second Affiliated Hospital, Zhejiang University School of Medicine, Hangzhou, China, [2] Zhejiang University Cancer Center, Hangzhou, China, [3] Department of Breast Surgery, Hwa Mei Hospital, University of Chinese Academy of Sciences, Ningbo, China, [4] Engineering Research Center of EMR and Intelligent Expert System, Ministry of Education, College of Biomedical Engineering and Instrument Science, Zhejiang University, Hangzhou, China, [5] Department of Pathology, Key Laboratory of Cancer Prevention and Intervention, Ministry of Education, The Second Affiliated Hospital, Zhejiang University School of Medicine, Hangzhou, China, [6] Research Center for Healthcare Data Science, Zhejiang Lab, Hangzhou, China

OPEN ACCESS

Edited by:
Kenneth K.W. To, The Chinese University of Hong Kong, China

Reviewed by:
Gopi Sundaram, Central Food Technological Research Institute (CSIR), India
Stefan Urbanski, University of Calgary, Canada

***Correspondence:**
Jun Li
2307016@zju.edu.cn

[†] These authors have contributed equally to this work

Specialty section:
This article was submitted to Gastrointestinal Cancers, a section of the journal Frontiers in Oncology

Received: *30 November 2020*
Accepted: *17 February 2021*
Published: *29 April 2021*

Citation:
Kong X-X, Li X-L, Tian Y, Ye Q-C, Xu X-M, Liu Y, Yang Q, Zhang L-N, Mei Y-X, Wen J-H, Xiao Q, Li J-S, Ding K-F and Li J (2021) The Clinicopathological Characteristics of Alpha-Fetoprotein-Producing Adenocarcinoma of the Gastrointestinal Tract—A Single-Center Retrospective Study. Front. Oncol. 11:635537. doi: 10.3389/fonc.2021.635537

Alpha-fetoprotein (AFP)-producing adenocarcinoma from the gastrointestinal tract (APA-GI) is a rare type of highly malignant tumor with a poor prognosis. It may originate from any site along the GI tract with similar clinicopathological characteristics. As limited research had ever described the characteristics of APA-GI, the present article intends to systemically investigate the clinicopathological characteristics of APA-GI from a single center's retrospective study to deepen the understanding of the disease. A total of 177 patients pathologically diagnosed with APA-GI between 2010 and 2017 at the Second Affiliated Hospital of Zhejiang University, School of Medicine, were included. Also, clinical data of 419 gastric cancers and 609 colorectal cancers from The Cancer Genome Atlas database were also extracted. Clinical information of patients from Second Affiliated Hospital of Zhejiang University, School of Medicine, was collected, and a median follow-up of 14.5 months was performed to investigate clinical characteristics of APA-GI. For the pathological characteristics of APA-GI, hematoxylin–eosin sections were reviewed, and immunohistochemistry of AFP was performed. The results showed that the primary tumor could develop through the whole GI tract, including the esophagus (0.6%), stomach (83.1%), duodenum (1.1%), ileum (0.6%), appendix (0.6%), colon (5.1%), and rectum (7.9%). Hepatoid adenocarcinoma is the main pathological feature of APA-GI. AFP expression level in tumor tissue was not strictly associated with serum AFP or hepatoid differentiation. The prognosis of APA-GI was worse than that of common adenocarcinoma of the GI tract and liver metastasis, and high AFP levels suggest poor prognosis in patients with APA-GI. Therefore, the present study was the first

research to systemically explore the clinicopathological characteristics of APA-GI. APA-GI occurs through the whole GI tract with a significantly worse prognosis than common adenocarcinoma of GI. APA-GI should be regarded as one kind of disease for its similar clinicopathological characteristics within patients.

Keywords: AFP-producing, gastrointestinal, adenocarcinoma, clinical characteristic, pathological characteristic

INTRODUCTION

Alpha-fetoprotein (AFP) is a glycoprotein produced by the fetal liver, yolk sac, and fetal gastrointestinal cells. Its content in adult serum is extremely low, and its abnormal increase is mainly found in hepatocellular carcinoma and yolk sac-derived tumors (1). However, abnormally elevated serum AFP is also reported in some kinds of adenocarcinoma, which are called AFP-producing adenocarcinoma (APA) (2). APA is a rare type of highly malignant tumor with a fairly poor prognosis (3, 4). It can originate from a variety of organs and mainly occurs in the digestive tract. The majority of APAs are developed in the stomach, accounting for 1.3–15% of all gastric cancers (GC) and <1% of all colorectal cancers (CRCs) (5, 6). However, much less is known about the clinicopathological characteristics of APA.

The serum AFP in APA patients is increased (>20ng/ml) and markers representing embryonic stem cells and hepatocellular carcinoma in tumor tissues, such as AFP protein, glypican-3, Sal-like protein-4, and/or hepatocyte antigen-1, are positive (7, 8). APA originated from the gastrointestinal tract (APA-GI) was reported to have some common clinical characteristics, such as early multi-organ metastasis, multidrug resistance, rapidly worsen after diagnosis, and much inferior prognosis than common adenocarcinoma of the gastrointestinal tract (CA-GI) (5, 6, 9–11). Although the previous studies of APA-GI usually only included APA-GC or APA-CRC (3, 12), we found APA-GI could also originate from the whole GI tract, including the esophagus, small intestinal, and appendix.

Therefore, we believe that APA-GI is a separate class of disease that showed similar clinicopathological characteristics within different origins. As the research on APA-GI is limited, how to accurately differentiate it from CA-GI and get accurate treatment to improve the prognosis is still in challenge (2, 13). The present article intends to systemically investigate the clinical and pathological characteristics of APA-GI from a single center's retrospective study to deepen the understanding of the disease.

PATIENTS AND METHODS

Patients From the Second Affiliated Hospital of Zhejiang University, School of Medicine

Patients pathologically diagnosed with APA-GI between 2010 and 2017 at the Second Affiliated Hospital of Zhejiang University, School of Medicine (SAHZU) were included in the study. Also, the exclusion criteria were the following: (1) pregnancy status; (2) synchronously diagnosed with acute or chronic hepatitis, liver cirrhosis, hepatocellular carcinoma, teratoma, and germinoma, or (3) cancer history other than GI adenocarcinoma. APA-GI was defined as follows: (1) pathologically confirmed primary gastrointestinal adenocarcinoma and (2) serum AFP>20 ng/ml during the whole course. Two pathologists reviewed all hematoxylin–eosin (HE) sections to exclude the yolk sac tumor-like area or neuroendocrine component.

Patients From the Cancer Genome Atlas

A total of 419 GC patients and 609 CRC patients from The Cancer Genome Atlas (TCGA) database (URL: http://cancergenome.nih.gov) were included. All these patients have pathologically confirmed adenocarcinoma.

Data Collection and Follow-Up

For patients from SAHZU, clinical characteristics were all collected from the hospital information system, which included age, sex, primary tumor location, tumor size, pathological type, differentiated level, tumor–node–metastasis (TNM) staging, metastasis status, operation method, operation time, post operation pathology, serum AFP level, and treatment strategy. The last follow-up date was January 1, 2019. The major approach for follow-up was telephone calls or outpatient visits.

For patients from TCGA, we extracted patients' sex, pathology, TNM staging, survival time, survival status, and *via* R.

Immunohistochemistry

Immunohistochemistry (IHC) staining was performed according to the standard protocol. Freshly cut 4-μm paraffin-embedded sections were incubated overnight at 62°C and then de-paraffinized by xylene and dehydrated with ethanol. Antigen retrieval was performed using a pressure cooker in citrate antigen retrieval solution (pH 8.0) for 15 min, then incubated with 3% peroxide for 10 min and blocked by nonspecific staining blocking reagent (Dako, Glostrup, Denmark). Staining was performed with AFP polyclonal antibody (ab169552, Abcam). Briefly, 150 μl of rabbit polyclonal anti-AFP antibody at 100× dilution was incubated for 120 min, washed, subsequently incubated with horseradish peroxidase and anti-rabbit antibody-conjugated polymer for 30 min, washed, and finally incubated with 3,3'diaminobenzidine substrate for signal development. Sections were at last counterstained with hematoxylin.

Two pathologists independently reviewed the IHC sections. The staining intensity was scored as 0 (negative), 1 (weak), 2 (moderate), or 3 (strong), whereas the staining extent was scored as 0 (<5 %), 1 (5–25 %), 2 (26–50 %), 3 (51–75 %), and 4 (>75 %) according to the positive staining area proportion. Scores for staining intensity and extent were then multiplied to generate the immunoreactivity score (IRS) for each case. Therefore, IRSs 0–1, 2–3, 4–8, and 9–12 were referred to negative, week positive,

moderately positive, and strongly positive, respectively. IRS < 4 was termed as AFP low expression, whereas IRS ≥ 4 was termed as AFP high expression.

Statistical Analysis

The chi-squared test and Fisher's exact analysis were performed to compare the clinical and pathological characteristics between groups. Non-Gaussian-distributed data were presented as medians and interquartile ranges and evaluated by the Kruskal–Wallis test. Survival data were presented by Kaplan–Meier survival curves and compared using the log-rank test. With the Cox proportional hazards model, univariate and multivariate survival analyses were conducted to identify independently significant variables. Multivariate analyses were all based on factors <0.5, which were tested by univariate analyses. A *P*-value of 0.05 or less indicated statistical significance. Statistical and graphical analyses were performed with SPSS 23.0 and GraphPad Prism 7 software.

RESULTS

Clinical Characteristics of Alpha-Fetoprotein-Producing Adenocarcinoma From the Gastrointestinal Tract

A total of 177 APA-GI patients were finally included. The median age was 63 years old (interquartile range, 53.5–71.0 years old), and males accounted for 69.5%. The primary tumor could develop through the whole gastrointestinal tract, including the esophagus (0.6%), stomach (83.1%), duodenum (1.1%), ileum (0.6%), appendix (0.6%), colon (5.1%), and rectum (7.9%). Meanwhile, it could also synchronously develop in two organs, such as the stomach and rectum (0.6%) and colon and rectum (0.6%). The pathological type of APA-GI included adenocarcinoma with high-, media-, and low-differentiated, signet-ring cell carcinoma and mucinous adenocarcinoma. Among 71 non-metastasis patients, 18.3% received operation, whereas 77.5% received a combination of treatments based on surgery. Within all APA-GI patients, 58.2% of patients present metastasis at the initial diagnosis, whereas 145 (81.9%) of patients finally developed metastasis. The liver was the most common site of APA-GI metastasis with a rate of 53.1%. Among gastric and colorectal APAs, 71 (40.1%) and 11 (47.8%) of patients were initially diagnosed with liver metastasis, respectively (**Table 1**).

Increased serum AFP characterizes APA-GI. We found the AFP-high group (AFP-H group, AFP $\geq$ 200 ng/ml) had more stage IV ($P = 0.009$) and liver metastases ($P < 0.001$) when compared with the AFP-low group (AFP-L group, AFP $<$ 200 ng/ml). Additionally, the AFP-H group was characterized by larger tumor size ($P = 0.047$), a higher proportion of adenocarcinoma ($P = 0.022$), and hepatoid adenocarcinoma (HA) ($P = 0.006$) (**Table 2**).

TABLE 1 | Baseline Characteristics of APA-GI.

Characteristic	Total
Age(y), median(IQR)	63.0 (53.5-71.0)
Sex, Male/Female (Male%)	123/54 (69.5)
Primary site, *n* (%)	
Stomach	147 (83.1)
Colon	9 (5.1)
Rectum	14 (7.9)
Appendix	1 (0.6)
Duodenum	2 (1.1)
Ileum	1 (0.6)
Esophagus	1 (0.6)
Stomach and rectum	1 (0.6)
Colon and rectum	1 (0.6)
Tumor size(cm), median(IQR)	4.5 (3.1-5.5)
Pathological type, *n* (%) Adenocarcinoma	147 (83.1)
Signet ring cell carcinoma	20 (11.3)
Mucinous adenocarcinoma	10 (5.6)
Differentiation, *n* (%)	
Highly differentiated	3 (1.7)
Moderately differentiated	43 (24.3)
Poorly differentiated	109 (61.6)
Default	22 (12.4)
pT, *n* (%)	
1	8 (8.2)
2	12 (12.4)
3	12 (12.4)
4	58 (59.8)
Default	7 (7.2)
pN, *n* (%)	
0	20 (20.6)
1	17 (17.5)
2-3	50 (51.5)
Default	10 (10.3)
TNM staging, *n* (%)	
I	8 (4.5)
II	17 (9.6)
III	46 (26.0)
IV	103 (58.2)
Default	3 (1.7)
Metastatic site#, *n* (%)	
Liver	94 (53.1)
Lymph node	71 (40.1)
Lung	19 (10.7)
Peritoneal cavity	16 (9.0)
Bone	15 (8.5)
Adrenal gland	7 (4.0)
Pelvic cavity	4 (2.3)
Spleen	4 (2.3)
Pancreas	4 (2.3)
Ovary and fallopian tube	4 (2.3)
Brain	3 (1.7)

(Continued)

TABLE 1 | Continued

Characteristic	Total
Lymphatic or/and blood vessel invasion	
Yes	39 (40.2)
No	38 (39.2)
Default	20 (20.6)
Nerve invasion	
Yes	26 (26.8)
No	54 (55.7)
Default	17 (17.5)
Hepatoid Adenocarcinoma*	
Yes	34 (34%)
No	66 (66%)
Treatments	
Chemotherapy	46 (26.0)
Surgery	17 (9.6)
Comprehensive treatment	90 (50.8)
Other(Symptomatic treatment ?Chinese herbology)	24 (13.5)

*#, For patients with multiple metastases, all the metastatic foci of different parts were included separately; *, Only 100 patients receiving second pathological diagnosis were included.*

Hepatoid Adenocarcinoma Is the Main Pathological Feature of Alpha-Fetoprotein-Producing Adenocarcinoma From the Gastrointestinal Tract

Two pathologists reviewed the 100 HE sections available. Thirty-four sections were reported (32 surgical samples and 2 endoscopic samples) containing HA regions. However, only three of these were first diagnosed as HA. Similar to primary hepatocellular carcinoma, HA consists of hepatoid cells with abundant blood sinuses. Cancer cells from HA often present with round nuclei, hyper-chromatin, prominent nucleoli, and clear cytoplasm. HA is also usually nested or banded and can be easily confused with normal adenocarcinoma (**Figure 1**).

We further compared the clinical characteristics between HA and non-HA within APA-GI patients. Seventy-three patients who received the operation were included. Compared with the non-HA group (41 cases), the HA group (32 cases) had more male patients ($P = 0.002$) and a higher proportion of low-differentiation ($P = 0.007$) (**Table 3**). However, the 5-year survival was insignificant between these two groups (non-HA and HA groups: 46.9 vs. 18.5%, respectively, $P = 0.0953$, **Supplementary Figure 1**).

Alpha-Fetoprotein-Producing Was Not Strictly Expressed in Alpha-Fetoprotein-Producing Adenocarcinoma From the Gastrointestinal Tract Patients' Tumor Tissue

IHC was performed in 99 tumor specimens to explore the AFP expression in APA-GI patients. IRS was then evaluated by two

TABLE 2 | Comparison of clinical baseline characteristics of APA-GI patients with different serum AFP levels.

Characteristic	AFP-L	AFP-H	*P* value
Age(y), median(IQR)	63.0 (52.0-72.0)	63.0 (57.0-69.0)	0.814
Sex, Male/Female (Male%)	73/35 (67.6)	50/19 (72.5)	0.492
Primary site, *n* (%)			0.596
Stomach	88 (81.5)	59 (85.5)	
Large intestine	17 (15.7)	7 (10.1)	
Small intestine	1 (0.9)	2 (2.9)	
Esophagus	1 (0.9)	0 (0)	
Multiple primary sites	1 (0.9)	1 (1.4)	
Tumor size(cm), median(IQR)	4.0 (3.0-5.0)	5.0 (4.0-6.0)	0.047
Pathological type, *n* (%)			0.022
Adenocarcinoma	83 (76.9)	64 (92.8)	
Signet ring cell carcinoma	17 (15.7)	3 (4.3)	
Mucinous adenocarcinoma	8 (7.4)	2 (2.9)	
Differentiation, *n* (%)			0.473
Highly differentiated	1 (0.9)	2 (2.9)	
Moderately differentiated	27 (25.0)	16 (23.2)	
Poorly differentiated	64 (59.3)	45 (65.2)	
Default	16 (14.8)	6 (8.7)	
pT, *n* (%)			0.524
1	7 (10.6)	1 (3.2)	
2	10 (15.2)	2 (6.5)	
3	8 (12.1)	4 (12.9)	
4	37 (56.1)	22 (71.0)	
Default	4 (6.1)	2 (6.5)	
pN, *n* (%)			0.643
0	12 (18.2)	8 (25.8)	
1	13 (19.7)	4 (12.9)	
2-3	33 (50.0)	17 (54.8)	
Default	8 (12.1)	2 (6.5)	
TNM staging, *n* (%)			0.009
I-III	51 (47.2)	20 (29.0)	
IV	54 (50.0)	49 (71.0)	
Default	3 (2.8)	0 (0.0)	
Liver metastasis			<0.001
Yes	41 (38.0)	53 (76.8)	
No	67 (62.0)	16 (23.2)	
Extrahepatic metastasis			0.962
Yes	63 (58.3)	40 (58.0)	
No	45 (41.7)	29 (42.1)	
Lymphatic or/and blood vessel invasion			0.509
Yes	24 (36.4)	15 (48.4)	
No	28 (42.4)	10 (32.3)	
Default	14 (21.2)	6 (19.4)	
Nerve invasion			0.126
Yes	14 (21.2)	12 (38.7)	
No	38 (57.6)	16 (51.6)	
Default	14 (21.2)	3 (9.7)	
Hepatoid Adenocarcinoma[#]			0.006
Yes	16 (32.7)	16 (66.7)	
No	33 (67.3)	8 (33.3)	

#, Considering the lack of pathological sample obtained from endoscopy, 73 surgical patients out of 100 patients receiving second pathological diagnosis were included.

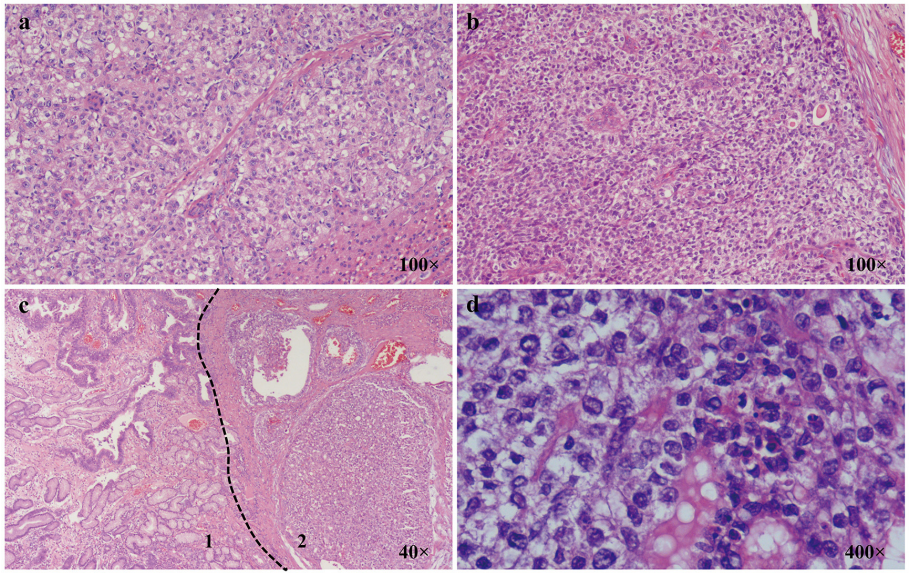

FIGURE 1 | Characteristics of AFP-GI under a light microscope. **(a)** Classic primary hepatic carcinoma (100×); **(b)** Classic hepatoid adenocarcinoma (100×); **(c)** 1. Zone of adenocarcinoma with moderately differentiation; 2. Zone of adenocarcinoma with hepatoid differentiation (40×); **(d)** Zone of adenocarcinoma with hepatoid differentiation is composed of cells with round nuclei, coarse chromatin, obvious nucleoli, and clear cytoplasm (400×).

pathologists independently (**Supplementary Figure 2**). There were 15 AFP high expression patients, and the other 84 patients were classified as AFP low expression. AFP was positive in 36.4% of APA-GI patients, and it was also positive in 43.3% of patients with elevated serum AFP before surgery. Interestingly, AFP was only partly expressed in HA with a positive rate of 73.5%. Among the 36 patients with positive IHC AFP, 5.6% had normal levels of AFP before surgery. Therefore, the AFP expression level in tumor tissue was not strictly associated with serum AFP or hepatoid differentiation. Additionally, for 73 patients who received the operation, 35 patients had neither positive AFP IHC nor HA (AFP-/HA-), whereas the others performed at least one characteristic. However, the 5-year survival between these two groups was similar (44.54 vs. 24.26%, $P = 0.342$, **Supplementary Figure 3**).

Prognosis of Alpha-Fetoprotein-Producing Adenocarcinoma From the Gastrointestinal Tract Was Worse Than That of Common Adenocarcinoma of the Gastrointestinal Tract

To investigate the prognosis of APA-GI, a median follow-up of 14.5 months was performed. There were only 31 (17.5%) who survived, whereas 129 (72.9%) died and 17 (9.6%) lost follow-up among the patients included. The 1-, 3-, and 5-year overall survival rates were 50.6, 28.5, and 17.7%, respectively.

To further compare the prognosis between APA-GI and CA, we extracted the follow-up information of CA-GC and CA-CRC from TCGA. For this reason, only 154 APA-GC and APA-CRC patients of 177 APA-GI patients from our center were analyzed. There was no significant difference in the 5-year survival between stages I–III APA-GC and CA-GC (28.8 vs. 41.9%, respectively, $P = 0.357$). However, the prognosis of APA-GC in stage IV was significantly worse than that of CA-GC (4.4 vs. 32.1%, $P < 0.001$). The 5-year survival of patients with APA-CRC was similar to CA-CRC (5-year survival: stages I–III APA-CRC and CA-CRC, 71.32 vs. 70%, respectively, $P = 0.132$; stage IV APA-CRC and CA-CRC, 13.89 vs. 26.73%, respectively, $P = 0.091$). After combining CRC and GC, survival analysis of APA-GI from our center showed significantly worse 5-year survival than that of CA-GI from TCGA (stages I–III, 32.8 vs. 59.4%, respectively, $P < 0.001$; stage IV, 6.3 vs. 30.1%, respectively, $P < 0.001$; stages I–IV, 17.7 vs. 55.9%, respectively, $P < 0.001$) (**Figure 2**).

Liver Metastasis and High Alpha-Fetoprotein-Producing Levels Suggest Poor Prognosis in Patients With Alpha-Fetoprotein-Producing Adenocarcinoma From the Gastrointestinal Tract

Liver metastasis was found to be an independent risk factor for total survival in APA-GI patients after multivariate Cox regression analysis (hazard ratio 3.59, 95% confidence interval 1.28–10.02, $P = 0.015$) (**Table 4**). To investigate the impact of liver metastasis-free survival, we further conducted Cox multivariate regression analysis on the data, including the level of AFP. We found that AFP $\geq$ 200 ng/ml was an independent risk factor for the liver metastasis of APA-GI (hazard ratio 4.55, 95% confidence interval 1.39–14.87, $P = 0.012$) (**Table 5**).

Kaplan–Meier curve that showed the prognosis of the AFP-H group was significantly worse than that of the AFP-L group.

TABLE 3 | Comparison of clinical baseline characteristics between APA-GI patients with HA and non-HA.

Characteristic	non-HA	HA	*P*-value
Age(y), median(IQR)	61.0 (50.0–70.5)	63.0 (58.0–71.8)	0.247
Sex, Male/Female (Male%)	22/19 (53.7)	28/4 (87.5)	0.002
Primary site, *n* (%)			0.321
Stomach	33 (80.5)	27 (84.4)	
Large intestine	7 (17.1)	3 (9.4)	
Small intestine	1 (2.4)	0 (0.0)	
Esophagus	0 (0.0)	1 (3.1)	
Multiple primary sites	0 (0.0)	1 (3.1)	
Tumor size(cm), median(IQR)	4.5 (3.5–5.3)	5.0 (3.0–6.0)	0.668
Differentiation, *n* (%)			0.007
Highly differentiated	0 (0.0)	0 (0.0)	
Moderately differentiated	17 (41.5)	5 (15.6)	
Poorly differentiated	21 (51.2)	27 (84.4)	
Default	3 (7.3)	0 (0.0)	
pT, *n* (%)			0.913
1	3 (7.3)	2 (6.3)	
2	6 (14.6)	4 (12.5)	
3	5 (12.2)	6 (18.8)	
4	27 (65.9)	20 (62.5)	
pN, *n* (%)			0.825
0	8 (19.5)	7 (21.9)	
1	6 (14.6)	7 (21.9)	
2-3	25 (61.0)	17 (53.1)	
Default	2 (4.9)	1 (3.1)	
TNM staging, *n* (%)			0.514
I-III	31 (75.6)	22 (68.8)	
IV	10 (24.4)	10 (31.3)	
Liver metastasis			0.084
Yes	9 (22.0)	13 (40.6)	
No	32 (78.0)	19 (59.4)	
Extrahepatic metastasis			0.756
Yes	22 (53.7)	16 (50.0)	
No	19 (46.3)	16 (50.0)	
Lymphatic or/and blood vessel invasion			0.269
Yes	19 (46.3)	19 (59.4)	
No	22 (53.7)	13 (40.6)	
Nerve invasion			0.486
Yes	11 (26.8)	11 (34.4)	
No	30 (73.2)	21 (65.6)	

HA, hepatic adenocarcinoma; non-HA, non-hepatic adenocarcinoma.

The 5-year survival of AFP $\geq$ 200 ng/ml was 7.5%, whereas it increased to 26.0% in the APA-GI patients with AFP $<$ 200 ng/ml ($P = 0.002$). The proportion of stage IV patients in the AFP-H and AFP-L groups were 71 and 50%, respectively. The prognosis of stages I–III patients with an AFP $\geq$ 200 ng/ml was worse than that of AFP $<$ 200 ng/ml (5-year survival: 11.3 vs. 44.4%, respectively, $P = 0.030$), whereas there was no statistical difference in the prognosis of stage IV patients (5-year survival: 3.5 vs. 5.6%, respectively, $P = 0.421$) (**Figure 3**).

DISCUSSION

APA is a rare kind of malignant tumor, which could originate from various organs, such as the lung, ovary, kidney, esophagus, stomach, small intestine, colorectal, and appendix (3, 10, 14–18). The present study focused on the clinicopathological features of APA-GI *via* a retrospective analysis. Data from SAHZU showed APA-GI was more likely to occur in middle-aged and older adults, and it could originate from the whole GI tract, especially in the stomach. The rate of tumor metastasis is high, and most patients were initially diagnosed with liver metastasis. The positive rate of AFP in APA-GI tumor tissue was 36.4%, and it was partly expressed in hepatoid differentiated tissue. The prognosis of APA-GI was significantly worse than CA-GI, and patients with AFP $\geq$ 200 ng/ml were even worse in APA-GI. Liver metastasis was an independent risk factor for the overall survival of APA-GI, and patients with AFP $\geq$ 200 ng/ml were more like to develop liver metastasis. Ren et al. had also previously investigated the clinicopathological features and prognosis of APA-CRC, especially the tumor location and survival, which was with our research. Additionally, they divided APA-CRC patients into three histologic types: the common adenocarcinoma type, mucinous adenocarcinoma type, and hepatoid type (3). However, the present research still had some progress. We provided a sufficient sample size with 177 APA-GIs to reach statistically significant conclusions. We included not only APA-CRC but also other GI sites' APA to obtain a full landscape of APA-GI. In addition, we also described several risk factors of liver metastasis and prognosis.

Most APA-GIs were low differentiation. The tumor cells were distributed in clusters or bands, and the stroma was rich in blood sinuses. HA was the main pathological feature of APA-GI. However, among 100 patients included, only three were reported HA in the original pathological diagnosis, whereas there were actually 34 HA patients after reviewing all HE sections. The main reasons for missed diagnosis of APA-GI may be as follows. First, HA is often intermixed within CA components, making the former difficult to recognize, and it leads to the missed diagnosis of APA-GI. Secondly, HA is not necessary to report in routine pathological diagnosis, making pathologists pay insufficient attention. Although HA is the major pathologic type of APA-GI, only 30% of HA cases have been reported within APA-GI in our center. Therefore, the serum AFP index is still essential for the diagnosis of APA-GI. The current diagnostic criteria for HA proposed by the World Health Organization relies on pathological morphology without the need for IHC evidence (World Health Organization Classification of Tumours, 5th Edition, Volume 1. Digestive System Tumours. Lyon: IARC Press, 2019) (19). Therefore, the present study asked two pathologists to independently review HE sections to confirm hepatoid differentiation without additional Hepa-1 and glypican-3 IHC. Additionally, the survival was similar between APA-GI with and without hepatoid differentiation, but both were worse than that of CA-GI. Therefore, using only hepatoid differentiation in the diagnosis of APA-GI will lead to missed diagnosis and inadequate understanding of prognosis. In previous studies, elevated serum AFP levels, positive AFP IHC,

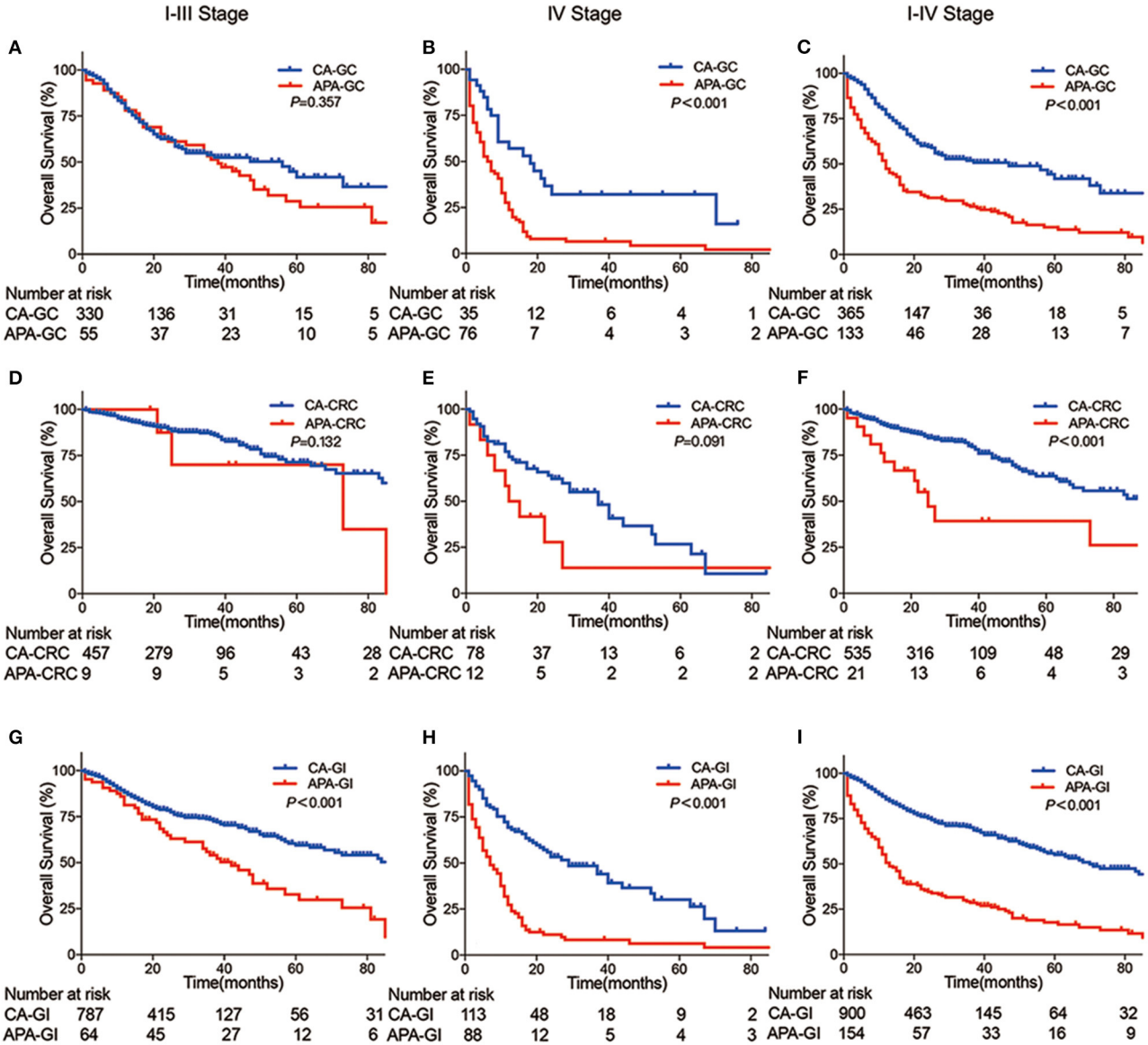

FIGURE 2 | Kaplan–Meier curve between APA-GI and CA-GI. **(A–C)** Survival differences between APA-GC and CA-GC; **(D–F)** survival differences between APA-CRC and CA-CRC; **(G–I)** survival differences between APA-GI and CA-GI; Column 1 shows survival comparison between stages I–III patients. Column 2 shows survival comparison between stage IV patients. Column 3 shows survival comparison between stages I–IV patients. APA-GI patients were composed of 154 APA-GC and APA-CRC from the SAHZU database, whereas CA-GI patients were all extracted from TCGA database. Notably, two APA-GC patients were unable to perform accurate staging due to the lack of medical imaging data. Therefore, they can only be classified as stages I–IV.

or HA detection was used as diagnostic criteria for APA-GI, but there is no standard criteria or consensus until now (6, 20–22). In our study, neither HA nor positive AFP IHC was the sufficient condition of APA-GI diagnosis, as only 52% of patients existed either HA or positive AFP IHC. For these patients, their prognoses were similar to that of APA-GI patients with only elevated serum AFP. Therefore, we suggested APA-GI should be regarded as one kind of disease, and its diagnosis depends on both serum AFP level and pathology. Also, pathologists should pay more attention to hepatoid differentiation, and there should be more molecular pathology research to construct the diagnostic criteria of APA-GI.

High metastasis rate and liver metastasis are the main characteristics of APA-GI at initial diagnosis. Many studies have found that 12–25% of patients with digestive tract adenocarcinoma have metastases after initial diagnosis (23, 24). Nearly 40–50% of patients have metastases during the whole course of the disease (24, 25). Among them, 4–14% gastric

TABLE 4 | Regression analysis for prognostic risk factors of APA-GI.

Variable	Single factor		Multiple factors	
	HR(95%CI)	*P*–value	HR(95%CI)	*P*-value
Age, y		0.078		0.913
<60	1		1	
≥60	1.40 (0.96–2.05)		1.05 (0.42–2.62)	
Sex		0.075		0.551
Male	1		1	
Female	0.70 (0.47–1.04)		1.38 (0.48–3.94)	
AFP, ng/ml		0.005		0.877
<200	1		1	
≥200	1.67 (1.17–2.38)		0.93 (0.38–2.27)	
Primary site		0.241		
Stomach	1			
Large intestine	0.57 (0.32–1.02)			
Small intestine	0.66 (0.16–2.66)			
Esophagus	1.04 (0.14–7.45)			
Multiple primary sites	0.26 (0.04–1.86)			
Tumor size, cm		0.028		0.59
<5	1		1	
≥5	1.99 (1.08–3.65)		0.79 (0.34–1.83)	
Pathological type		0.660		
Adenocarcinoma	1			
Signet ring cell carcinoma	0.78 (0.44–1.37)			
Mucinous adenocarcinoma	0.88 (0.45–1.75)			
Differentiation		0.926		
Highly differentiated	1			
Moderately differentiated	0.90 (0.21–3.79)			
Poorly differentiated	0.84 (0.20–3.42)			
pT		0.056		0.96
1	1		1	
2	1.60 (0.32–7.98)		1.52 (0.15–15.72)	
3	2.68 (0.49–14.73)		1.95 (0.18–21.38)	
4	3.98 (0.96–16.50)		1.60 (0.18–14.01)	
pN		0.028		0.071
0	1		1	
1	2.54 (0.99–6.57)		2.80 (0.79–9.90)	
2+3	2.68 (1.29–5.56)		3.05 (1.16–8.06)	
TNM staging		<0.001		0.486
I-III	1		1	
IV	3.99 (2.69–5.90)		1.39 (0.55-3.53)	
Extrahepatic metastasis		0.031		0.127
No	1		1	
Yes	1.50 (1.04–2.16)		1.95 (0.83–4.60)	
Hepatic metastasis		<0.001		0.015
No	1		1	
Yes	2.79 (1.91–4.06)		3.59 (1.28–10.02)	
Lymphatic or/and blood vessel invasion		0.009		0.140
No	1		1	
Yes	2.30 (1.24–4.29)		2.04 (0.79–5.27)	
Nerve invasion		0.064		0.884
No	1		1	
Yes	1.76 (0.97–3.21)		0.92 (0.29–2.92)	
Hepatoid Adenocarcinoma [#]		0.102		0.228
No	1			
Yes	1.68 (0.90–3.12)			
AFP IHC		0.375		0.288
Low expression	1			
High expression	1.35 (0.70–2.62)			

#, 73 surgical patients out of 100 patients receiving second pathological diagnosis were included.

TABLE 5 | Regression analysis for prognostic risk factors of APA-GI liver metastasis.

Variable	Single factor		Multiple factors	
	HR(95%CI)	*P*-value	HR(95%CI0)	*P*-value
Age, y		0.023		0.193
<60	1		1	
≥60	1.72 (1.08–2.74)		2.13 (0.68–6.65)	
Sex		0.021		0.123
Male	1		1	
Female	0.55 (0.33–0.91)		0.30 (0.07–1.38)	
Primary site		0.906		
Stomach	1			
Large intestine	0.89 (0.47–1.67)			
Other	0.86 (0.27–2.72)			
Tumor size, cm		0.010		0.231
<5	1		1	
≥5	3.47 (1.35–8.89)		1.96 (0.65–5.90)	
Pathological type		0.101		
Adenocarcinoma	1			
Signet ring cell carcinoma	0.50 (0.23–1.09)			
Mucinous adenocarcinoma	0.45 (0.14–1.44)			
Differentiation		0.741		
Highly differentiated	1			
Moderately differentiated	1.34 (0.18–9.94)			
Poorly differentiated	1.10 (0.15–8.00)			
pT		0.113		
1+2+3	1			
4	1.26 (0.95–1.68)			
pN		0.603		
0	1			
1	1.65 (0.56–4.85)			
2+3	1.10 (0.45–2.73)			
AFP, ng/ml		<0.001		0.012
<200	1		1	
≥200	2.24 (1.48–3.39)		4.55 (1.39–14.87)	
Lymphatic or/and blood vessel invasion		0.013		0.354
No	1		1	
Yes	3.31 (1.29–8.49)		1.69 (0.56–5.14)	
Nerve invasion		0.277		
No	1			
Yes	1.6 (0.69–3.73)			
Hepatoid Adenocarcinoma[#]		0.029		0.615
No	1		1	
Yes	2.60 (1.10–6.12)		0.75 (0.35–2.27)	
AFP IHC		0.626		
Low expression	1			
High expression	1.22 (0.54–2.77)			

#, 73 surgical patients out of 100 patients receiving second pathological diagnosis were included.

adenocarcinomas and 25% colorectal adenocarcinomas were initially diagnosed with liver metastasis, and approximately 50% of the patients with digestive adenocarcinoma eventually developed liver metastasis (26, 27). Our study found that in APA-GI, up to 58.2% of patients metastasized after the initial diagnosis, and the final metastasis rate reached 81.9%. Among

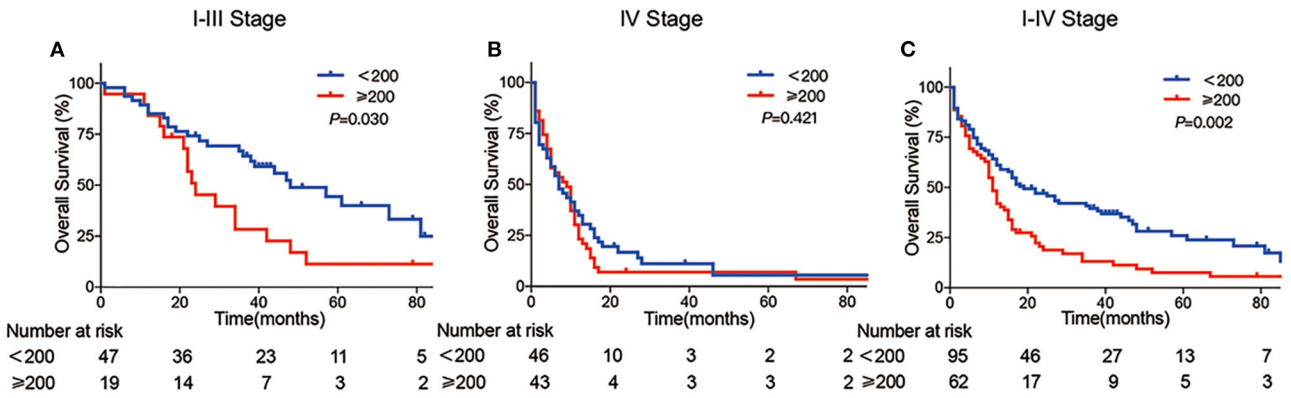

FIGURE 3 | Kaplan–Meier curve of APA-GI compared by AFP level. Comparison of survival between APA-GI patients with AFP ≥ 200 ng/ml and AFP < 200 ng/ml: **(A)** compare between stages I–III patients; **(B)** compare between stage IV patients; **(C)** compare between stages I–IV patients. Notably, two patients were unable to perform accurate staging due to the lack of medical imaging data. Therefore, they can only be classified as stages I–IV. IRS 0–1, 2–3, 4–8, and 9–12 was referred to negative, week positive, moderate positive and strong positive, respectively.

APA-GI, patients with liver metastasis at initial diagnosis were significantly more than those with CA-GI. Additionally, we performed a subgroup analysis by serum AFP with a bound of 200 ng/ml. Consistent with previous studies, the AFP-H group was characterized by a higher rate of stage IV and liver metastasis, a larger tumor size, and a higher proportion of HA (5, 28, 29).

The prognosis of APA-GI was significantly worse than that of CA-GI. However, we did not observe a difference between stages I–III gastric and CRC patients, which may be related to 95.5% of stages I–III patients who underwent surgery. Early diagnosis of APA-GI and radical surgery may be an important treatment to improve prognosis. When APA-GI progressed to stage IV, the 5-year survival was only 6.3%. We hypothesized that stage IV APA-GI patients were less sensitive to 5-Fu-based chemotherapy, similar to the 8.15% response rate of primary liver cancer to chemotherapy (30). Because of selection bias and recall bias in retrospective studies, the results of multivariate analyses varied among previous reports. Shoji and Feng et al. found that liver metastasis was the only independent prognostic factor for APA-GI (6, 31), whereas in other studies, TNM staging, serum AFP level, patient age, peritoneal seeding, lymph node metastasis, vascular invasion, Lauren classification, and AFP IHC results all became independent prognostic factors for APA-GI (29, 32). Our study showed that patients with high AFP levels had a poor prognosis, whereas Cox regression analysis showed that liver metastasis was the only independent risk factor for APA-GI. We speculated that it might be due to the strong influence of liver metastasis on prognosis, thus masking the influence of high AFP level on prognosis. There were still several limitations in the present research. AFP has been reported not only in APA but also in yolk-sac tumors or some neuroendocrine tumors (1, 33, 34). We asked two pathologists to recheck all HE sections and did not found any yolk sac tumor-like area or neuroendocrine component. However, for the other 77 patients without HE sections, we were unable to clarify whether AFP was produced only by APA. Whether APA-GI is homogenous or heterogenous could not be concluded yet. Wang et al. had investigated the molecular features of HA of the stomach but showed limited homogenous (13). Besides, HA is theoretically not exactly the same as APA-GI. In future studies, we need more data from multiple centers to further study the clinicopathological characteristics of APA-GI, and basic research should be encouraged to investigate the pathogenesis of APA-GI.

CONCLUSION

The present study was the first research to systemically explored clinicopathological characteristics of APA-GI. APA-GI occurs through the whole GI tract with a significantly worse prognosis than CA-GI. APA-GI should be regarded as one kind of disease for its similar clinicopathological characteristics within patients.

DATA AVAILABILITY STATEMENT

The raw data supporting the conclusions of this article will be made available by the authors, without undue reservation.

AUTHOR CONTRIBUTIONS

X-XK, X-LL, and X-MX wrote the first draft of the manuscript. All authors commented on previous versions of the manuscript. All authors contributed to the study's conception and design. All authors performed material preparation, data collection, and analysis. All authors commented on previous versions of the manuscript. All authors read and approved the final manuscript.

FUNDING

This work was supported by the Key Technology Research and Development Program of Zhejiang Province (2017C03017), the National Key R&D Program of China (2017YFC0908200), and the National Natural Science Foundation of China (81672916, 11932017, and 82072360).

ACKNOWLEDGMENTS

We gratefully thank Hai-Ting Xie, Zhan-Huai Wang, Shao-Jun Yu, Ye-Ting Hu, Dong Xu, and Li-Feng Sun for helping perform the operations.

SUPPLEMENTARY MATERIAL

The Supplementary Material for this article can be found online at: https://www.frontiersin.org/articles/10.3389/fonc.2021.635537/full#supplementary-material

Supplementary Figure 1 | Kaplan–Meier curve of HA positive and HA negative within APA-GI Comparison of survival between HA positive and HA negative within 73 APA-GI patients who received operation.

Supplementary Figure 2 | Typical immunohistochemical staining images of APA-GI a, Negative; b, Weakly positive; c, Moderately positive; d, Strongly positive.

Supplementary Figure 3 | Kaplan–Meier curve of AFP-/HA- between the other patients within APA-GI. Comparison of survival between AFP-/HA- and the other patients within 73 APA-GI patients who received operation.

REFERENCES

1. El-Bahrawy M. Alpha-fetoprotein-producing non-germ cell tumours of the female genital tract. *Eur J Cancer.* (2010) 46:1317–22. doi: 10.1016/j.ejca.2010.01.028
2. Yamamura N, Fugo K, Kishimoto T. Forkhead box protein A2, a pioneer factor for hepatogenesis, is involved in the expression of hepatic phenotype of alpha-fetoprotein-producing adenocarcinoma. *Pathol Res Pract.* (2017) 213:1082–8. doi: 10.1016/j.prp.2017.07.024
3. Ren F, Weng W, Zhang Q, Tan C, Xu M, Zhang M, et al. Clinicopathological features and prognosis of AFP-producing colorectal cancer: a single-center analysis of 20 cases. *Cancer Manag Res.* (2019) 11:4557–67. doi: 10.2147/CMAR.S196919
4. Wang D, Li C, Xu Y, Xing Y, Qu L, Guo Y, et al. Clinicopathological characteristics and prognosis of alpha-fetoprotein positive gastric cancer in Chinese patients. *Int J Clin Exp Pathol.* (2015) 8:6345–55.
5. Wang YK, Zhang XT. [AFP-producing gastric cancer and hepatoid gastric cancer]. *Zhonghua Zhong Liu Za Zhi.* (2017) 39:801–7. doi: 10.3760/cma.j.issn.0253-3766.2017.11.001
6. Feng Y, Li Y, Dai W, Mo S, Li Q, Cai S. Clinicopathologic features and prognostic factors in alpha-fetoprotein-producing colorectal cancer: analysis of 78 cases. *Cell Physiol Biochem.* (2018) 51:2052–64. doi: 10.1159/000495824
7. Inagawa S, Shimazaki J, Hori M, Yoshimi F, Adachi S, Kawamoto T, et al. Hepatoid adenocarcinoma of the stomach. *Gastric Cancer.* (2001) 4:43–52. doi: 10.1007/s101200100016
8. Supriatna Y, Kishimoto T, Uno T, Nagai Y, Ishikura H. Evidence for hepatocellular differentiation in alpha-fetoprotein-negative gastric adenocarcinoma with hepatoid morphology: a study with in situ hybridisation for albumin mRNA. *Pathology.* (2005) 37:211–5. doi: 10.1080/00313020500099221
9. Tamai Y, Kobayashi K, Haruki Y, Yada T, Urade S, Harada T, et al. [A case of alpha-fetoprotein-producing fetal gut-like small intestinal cancer]. *Nihon Shokakibyo Gakkai Zasshi.* (2013) 110:833–8. doi: 10.11405/nisshoshi.110.833
10. Gushima R, Narita R, Shono T, Naoe H, Yao T, Sasaki Y. Esophageal adenocarcinoma with enteroblastic differentiation arising in ectopic gastric mucosa in the cervical esophagus: a case report and literature review. *J Gastrointestin Liver Dis.* (2017) 26:193–7. doi: 10.15403/jgld.2014.1121.262.gus
11. Takahashi N, Aoyama F, Hiyoshi M, Kataoka H, Sawaguchi A. Establishment and biological characterization of a novel cell line derived from hepatoid adenocarcinoma originated at the ampulla of vater. *Int J Oncol.* (2014) 44:1139–45. doi: 10.3892/ijo.2014.2282
12. Ooi A, Nakanishi I, Sakamoto N, Tsukada Y, Takahashi Y, Minamoto T, et al. Alpha-fetoprotein (AFP)-producing gastric carcinoma. Is it hepatoid differentiation? *Cancer.* (1990) 65:1741–7. doi: 10.1002/1097-0142(19900415)65:8<1741::AID-CNCR2820650814>3.0.CO;2-3
13. Wang Y, Sun L, Li Z, Gao J, Ge S, Zhang C, et al. Hepatoid adenocarcinoma of the stomach: a unique subgroup with distinct clinicopathological and molecular features. *Gastric Cancer.* (2019) 122:183–192. doi: 10.1007/s10120-019-00965-5
14. Liu M, Liu B, Zhou Y, Quan X, Liu B, Dong L. AFP-producing lung squamous carcinoma. *QJM.* (2016) 109:813–4. doi: 10.1093/qjmed/hcw179
15. Acosta AM, Pins MR. Hepatoid carcinoma of the ovary: clinical, histopathologic, and immunophenotypic features. *Arch Pathol Lab Med.* (2019) 143:883–9. doi: 10.5858/arpa.2017-0485-RS
16. Blandamura S, Vendraminelli R, Aversa S, Fedrigo M. Collecting duct carcinoma of kidney producing alpha-fetoprotein. *Eur J Surg Oncol.* (2005) 31:1039–41. doi: 10.1016/j.ejso.2005.07.001
17. Sun W, Liu B, Chen J, Gong P, Wu X, Liu C, et al. Novel characteristics of alpha-fetoprotein (AFP)-producing gastric cancer. *Oncotarget.* (2017) 8. 101944–51. doi: 10.18632/oncotarget.22109
18. Takashima H, Kimura H, Nakamura H, Myojo S, Okuyama Y, Sugeta N, et al. [A case of AFP producing endocrine cell carcinoma of the duodenum]. *Nihon Shokakibyo Gakkai Zasshi.* (2002) 99:798–802. doi: 10.11405/nisshoshi1964.99.798
19. Nagtegaal ID, Odze RD, Klimstra D, Paradis V, Rugge M, Schirmacher P, et al. The 2019 WHO classification of tumours of the digestive system. *Histopathology.* (2020) 76:182–188. doi: 10.1111/his.13975
20. Wang YK, Shen L, Jiao X, Zhang XT. Predictive and prognostic value of serum AFP level and its dynamic changes in advanced gastric cancer patients with elevated serum AFP. *World J Gastroenterol.* (2018) 24:266–73. doi: 10.3748/wjg.v24.i2.266
21. Shimakata T, Kamoshida S, Kawamura J, Ogane N, Kameda Y, Yanagita E, et al. Immunohistochemical expression profiles of solute carrier transporters in alpha-fetoprotein-producing gastric cancer. *Histopathology.* (2016) 69:812–21. doi: 10.1111/his.13004
22. Li Z, Hou X, Chen J, Sun H, Mi Y, Sui Y, et al. Efficacy and safety of SOX chemotherapy with or without surgery in AFP-producing advanced gastric cancer. *Oncol Lett.* (2017) 14:579–86. doi: 10.3892/ol.2017.6240
23. He X, Wu W, Lin Z, Ding Y, Si J, Sun LM. Validation of the american joint committee on cancer (AJCC) 8th edition stage system for gastric cancer patients: a population-based analysis. *Gastric Cancer.* (2018) 21:391–400. doi: 10.1007/s10120-017-0770-1
24. Van Cutsem E, Nordlinger B, Cervantes A, Group EGW. Advanced colorectal cancer: ESMO clinical practice guidelines for treatment. *Ann Oncol.* (2010) 21(Suppl. 5):v93–7. doi: 10.1093/annonc/mdq222
25. Bernards N, Creemers GJ, Nieuwenhuijzen GA, Bosscha K, Pruijt JF, Lemmens VE. No improvement in median survival for patients with metastatic gastric cancer despite increased use of chemotherapy. *Ann Oncol.* (2013) 24:3056–60. doi: 10.1093/annonc/mdt401
26. Song JC, Ding XL, Zhang Y, Zhang X, Sun XH. Prospective and prognostic factors for hepatic metastasis of gastric carcinoma: a retrospective analysis. *J Cancer Res Ther.* (2019) 15:298–304. doi: 10.4103/jcrt.JCRT
27. Nordlinger B, Sorbye H, Glimelius B, Poston GJ, Schlag PM, Rougier P, et al. Perioperative chemotherapy with FOLFOX4 and surgery versus surgery alone for resectable liver metastases from colorectal cancer (EORTC

intergroup trial 40983): a randomised controlled trial. *Lancet.* (2008) 371:1007–16. doi: 10.1016/S0140-6736(08)60455-9
28. Liu X, Cheng Y, Sheng W, Lu H, Xu Y, Long Z, et al. Clinicopathologic features and prognostic factors in alpha-fetoprotein-producing gastric cancers: analysis of 104 cases. *J Surg Oncol.* (2010) 102:249–55. doi: 10.1002/jso.21624
29. Lin HJ, Hsieh YH, Fang WL, Huang KH, Li AF. Clinical manifestations in patients with alpha-fetoprotein-producing gastric cancer. *Curr Oncol.* (2014) 21:e394–9. doi: 10.3747/co.21.1768
30. Qin S, Bai Y, Lim HY, Thongprasert S, Chao Y, Fan J, et al. Randomized, multicenter, open-label study of oxaliplatin plus fluorouracil/leucovorin versus doxorubicin as palliative chemotherapy in patients with advanced hepatocellular carcinoma from Asia. *J Clin Oncol.* (2013) 31:3501–8. doi: 10.1200/JCO.2012.44.5643
31. Hirajima S, Komatsu S, Ichikawa D, Kubota T, Okamoto K, Shiozaki A, et al. Otsuji, Liver metastasis is the only independent prognostic factor in AFP-producing gastric cancer. *World J Gastroenterol.* (2013) 19:6055–61. doi: 10.3748/wjg.v19.i36.6055
32. Yang J, Wang R, Zhang W, Zhuang W, Wang M, Tang C. Clinicopathological and prognostic characteristics of hepatoid adenocarcinoma of the stomach. *Gastroenterol Res Pract 2014.* (2014) 2014:140587. doi: 10.1155/2014/140587
33. Wang CY, Lin JC, Li YF, Yang CW. Alpha-fetoprotein producing pancreatic neuroendocrine tumour. *QJM.* (2020) 113:565–6. doi: 10.1093/qjmed/hcaa018
34. Zhu X, Yong H, Zhang L, Huang Y, Zheng J, Liu C, et al. Pure alpha-fetoprotein-producing neuroendocrine carcinoma of the pancreas: a case report. *BMC Gastroenterol.* (2015) 15:16. doi: 10.1186/s12876-015-0246-x

Conflict of Interest: The authors declare that the research was conducted in the absence of any commercial or financial relationships that could be construed as a potential conflict of interest.

frontiers in Oncology

ORIGINAL RESEARCH
published: 05 May 2021
doi: 10.3389/fonc.2021.628346

Plasma-Derived Exosomal ALIX as a Novel Biomarker for Diagnosis and Classification of Pancreatic Cancer

Jie Yang[1†], Yixuan Zhang[1†], Xin Gao[2†], Yue Yuan[1], Jing Zhao[1], Siqi Zhou[1], Hui Wang[1], Lei Wang[1], Guifang Xu[1], Xihan Li[1], Pin Wang[1], Xiaoping Zou[1], Dongming Zhu[2], Ying Lv[1*] and Shu Zhang[1*]*

[1] Department of Gastroenterology, Nanjing University Medical School Affiliated Nanjing Drum Tower Hospital, Nanjing, China, [2] Department of General Surgery and Pancreatic Disease Research Center, The First Affiliated Hospital of Soochow University, Suzhou, China

OPEN ACCESS

Edited by:
Kenneth K. W. To,
The Chinese University of Hong Kong, China

Reviewed by:
Gopi Sundaram,
Central Food Technological Research Institute (CSIR), India
Yuan-Jia Chen,
Peking Union Medical College Hospital (CAMS), China

***Correspondence:**
Shu Zhang
zhangsgastro@nju.edu.cn
Ying Lv
lvying@njglyy.com
Dongming Zhu
sd310@126.com

[†]These authors have contributed equally to this work

Specialty section:
This article was submitted to Gastrointestinal Cancers, a section of the journal Frontiers in Oncology

Received: 11 November 2020
Accepted: 30 March 2021
Published: 05 May 2021

Citation:
Yang J, Zhang Y, Gao X, Yuan Y, Zhao J, Zhou S, Wang H, Wang L, Xu G, Li X, Wang P, Zou X, Zhu D, Lv Y and Zhang S (2021) Plasma-Derived Exosomal ALIX as a Novel Biomarker for Diagnosis and Classification of Pancreatic Cancer. Front. Oncol. 11:628346. doi: 10.3389/fonc.2021.628346

Background: Pancreatic cancer (PC) has a dismal prognosis due to its insidious early symptoms and poor early detection rate. Exosomes can be released by various cell types and tend to be a potential novel biomarker for PC detection. In this study, we explored the proteomic profiles of plasma exosomes collected from patients with PC at different stages and other pancreatic diseases.

Methods: Plasma samples were collected from six groups of patients, including PC at stage I/II, PC at stage III/IV, well-differentiated pancreatic neuroendocrine tumor (P-NET), pancreatic cystic lesions (PCLs), chronic pancreatitis (CP), and healthy controls (HCs). Plasma-derived exosomes were isolated by ultracentrifugation and identified routinely. Isobaric tags for relative and absolute quantification (iTRAQ) based proteomic analysis along with bioinformatic analysis were performed to elucidate the biological functions of proteins. The expression of exosomal ALIX was further confirmed by enzyme-linked immunosorbent assay in a larger cohort of patients. Furthermore, receiver operating characteristic curve analysis was applied to evaluate the potential of ALIX as a novel diagnostic biomarker.

Results: The proteomic profile revealed a total of 623 proteins expressed among the six groups, and 16 proteins with differential degrees of abundance were found in PC *vs.* other pancreatic diseases (including P-NET, PCLs, and CP). Based on the results of proteomic and bioinformatic analyses, exosomal ALIX was subsequently selected as a novel biomarker for PC detection and validated in another clinical cohort. We noticed that ALIX expression was elevated in PC patients compared with patients with other pancreatic diseases or HC, and it was also closely associated with TNM stage and distant metastasis. Interestingly, the combination of exosomal ALIX and serum CA199 has greater values in differentiating both early *vs.* late PC (AUC value 0.872) and PC *vs.* other pancreatic diseases (AUC value 0.910) than either ALIX or CA199 alone.

Conclusion: In summary, our study demonstrated that based on proteomic profiling, proteins isolated from the plasma-derived exosomes may function as ideal non-invasive

biomarkers for the clinical diagnosis of PC. Importantly, exosomal ALIX combined with CA199 has great potentials in detection of PC, especially in distinguishing PC patients at early stages from advanced stages.

Keywords: exosomes, pancreatic cancer, proteomic profile, ALIX, diagnostic biomarker

INTRODUCTION

As a kind of highly heterogenous malignancy, pancreatic cancer (PC) still faces great challenges in the early diagnosis and treatment options. The most recent data estimated by the American Cancer Society show that the incidence rates and death rates continue to increase for the cancer of pancreas (1). Due to the insidious early symptoms and rapid progression, more than 80% of PC patients are diagnosed at an advanced stage when the disease has been disseminated (1, 2). Nowadays, PC is commonly diagnosed by the combination of classical serum biomarkers (*e.g.* carbohydrate antigen 19-9, CA199), imaging examinations, and endoscopic biopsy. However, all these techniques are either invasive or unspecific. Yachida et al. (3) suggested that PC would take several years to develop from initial mutations to metastatic cancer, highlighting the significance of finding effective methods for early stage detection. Hence, it is very critical for us to develop new sensitive and non-invasive tools for PC diagnosis, and thus increase the early detection rate and overall survival rate for PC patients.

Recently liquid biopsy has been identified as a safer, faster, and non-invasive test compared with tissue biopsy (4, 5). Among various types of liquid biopsies, exosomes are one type of extracellular vesicles of 30–150 nm in diameter, originate from multi-vesicular endosomes, and are initially thought to be cellular debris (6, 7). Now exosomes are recognized and identified to be encompassed by a lipid bilayer membrane, containing specific proteins, nucleic acids, and lipids. They are secreted by diverse cell types and can be detected in most body fluids, so they can reflect the cell type of origin, mediate intercellular communication, and even shape the microenvironment of tumors (6–8). On account of this, exosome biomolecules have great potentials as non-invasive biomarkers for the diagnosis of PC at early stages, or therapeutic targets for the treatment of PC (9–11).

In the present study, we explored the proteomic profiles of exosomes in plasma samples collected from patients with PC (stage I/II and stage III/IV) and other pancreatic diseases, including chronic pancreatitis (CP), pancreatic cystic lesions (PCLs), and well-differentiated pancreatic neuroendocrine tumors (P-NETs). We aim to elucidate some specific exosomal proteins useful in the detection of PC.

MATERIALS AND METHODS

Patients and Plasma Samples

This study included a total of 134 samples collected from patients with pancreatic diseases or healthy controls (HCs) who were admitted to the Nanjing Drum Tower Hospital Affiliated to Nanjing University Medical School and the First Affiliated Hospital of Soochow University between July 2018 and December 2019. Patients considered eligible for this study were those with suspected pancreatic masses and with operation indications. Endoscopic ultrasound-guided fine-needle aspiration (EUS-FNA) and/or surgical resections were performed for initial diagnosis. Plasma samples were all collected prior to EUS-FNA operations or surgical resections. All of them had not received any antitumor therapy before. Classification of PC was determined according to the 8th edition of the American Joint Committee on Cancer (AJCC) Classification. In the discovery stage, plasma samples were selected from 30 subjects with PC (stage I/II and stage III/IV), well-differentiated P-NETs, PCLs, CP and HC (five cases in each group) from Nanjing Drum Tower Hospital. We pooled the samples from the same group into one representative sample with the purpose of increasing the efficiency of analysis and reducing the individual variations. In the validation cohort, in order to determine the diagnostic performance of candidate protein biomarkers, we enrolled another 104 subjects (18 patients with PC at stage I/II, 44 with PC at stage III/IV, 11 with PCLs, eight with well-differentiated P-NET, 13 with CP, and 10 with HC, respectively) from two hospitals. Plasma samples were prepared from EDTA-treated peripheral blood, centrifuged at 2,000×g and 10,000×g for 10 min (4°C) to remove dead cells and cell debris and stored at −80°C until subsequent analysis. The study was approved by the Ethics Committee of the Nanjing Drum Tower Hospital and the First Affiliated Hospital of Soochow University, and informed consent was obtained from all patients before the examinations.

Exosomes Isolation

Exosomes were isolated by ultracentrifugation in accordance with the guidelines proposed by the International Society for Extracellular Vesicles (ISEV) (12). To isolate exosomes, the plasma was thawed on ice and centrifuged at 10,000×g for 30 min and then filtered through a 0.22-um filter (MilliPore, USA). The supernatant was then ultracentrifuged at 110,000×g for 70 min. The pallet was washed in phosphate-buffered saline (PBS) and centrifuged again at 110,000×g for 70 min. The PBS was removed completely, and subsequently 60 μl ice-cold PBS was used to resuspend the exosomal pellet. All centrifugation steps were performed at 4°C.

Exosome Identification

General characterizations of exosomes were performed to demonstrate the purity of our exosome preparation. For images of exosomes at high resolution, about 5 μl of prepared

exosomal suspension (the purified concentrated exosomes were mixed with an equal volume of 2% paraformaldehyde) was applied to the formvar-carbon coated grids, and the membranes were placed in a dry environment for 20 min. Then the grids were transferred to a 50 µl drop of 1% glutaraldehyde for 5 min and washed eight times with distilled waters. Samples were contrasted and embedded on ice with uranyl-oxalate for 5 min and methyl cellulose-uranyl acetate for 10 min, respectively. The excess fluid was blotted gently, and the grids were air dried for 10 min. The images were captured under the transmission electron microscopy (TEM, HT7800, Hitachi, Japan). Besides, the size distribution of exosomes was analyzed by high resolution flow cytometry using a Flow NanoAnalyzer Instrument (N30E, NanoFCM, China). The exosomal protein markers were validated by western blot analysis. We used the BCA protein assay kit (Thermo Fisher Scientific, USA) to quantify total protein concentration of exosomes according to the manufacturer's protocol. The protein samples were denatured at 95°C for 10 min. Approximately 30 µg of protein was separated by 10% SDS-PAGE, subjected to the electrophoresis, and transferred to PVDF membranes. The membranes were then blocked with 5% skim milk for 2 h, incubated with anti-CD63 (Abcam, UK), anti-Tsg101 (Santa Cruz, TX), and anti-β-actin (Abcam, UK) overnight. Then protein bands were washed with tris-buffered saline with tween 20 (TBST) buffer three times and probed with secondary antibodies for 120 min.

Exosomal Protein Lysis

Frozen exosomes were suspended on ice and 8 M urea was added. Then the samples were sonicated in ice for 2 min and incubated in ice for 30 min. We homogenized samples for 10 s every 5 min. The samples were clarified by centrifugation at 12,000×g at 4°C for 20 min. Protein was quantified with BCA protein assay kit (Thermo Fisher Scientific, USA). Approximately 30 µg of total protein was separated by 10% SDS-PAGE gel. Then separation gel was stained by CBB according to Candiano's protocol. The stained gel was scanned by Image Scanner (GE Healthcare, USA) at the resolution of 300 dpi.

Protein Digestion

A 200 ug portion of protein from each sample was reduced and alkylated in 50 mM tris-(2-carboxyethyl) phosphine (TCEP) at 56°C for 1 h and 200 mM methyl methanethiosulfonate (MMTS) at room temperature for 1 h. The chilled acetone was then added in the protein mixtures for precipitation overnight. The solutions were centrifuged at 30,000×g for 30 min at 4°C and dissolved in 0.5 M tetraethyl-ammonium bromide (TEAB) and sonicated in ice. Subsequently, trypsin was added to the samples at a 1:20 (w/w) ratio, and the solutions were incubated for digestion at 37°C for 16 h. Finally, the collections of digested peptides were centrifuged at 12,000 rpm for 20 min.

iTRAQ-Labeling Proteomic Analysis

For iTRAQ-labeling, the lyophilized samples were resuspended in 100 µl TEAB (200 mM) and then labeled by 8-plex iTRAQ reagent (SCIEX, USA) according to the instructions in the kit (PC at stage III/IV with 113 and 114 tags, PC at stage I/II with 115 tag, P-NET with 116 tag, HC with 117 tag, PCLs with 118 tag, CP with 119 tag). The labeled peptides were finally dried for further analysis.

Peptide Fractionation

The high pH reversed-phase liquid chromatography with a C-18 column was used to fractionate the labeled peptides. Briefly, mobile phases B (98% acetonitrile in 5 mM Ammonium formate) was used for gradient elution. The solvent gradient was set as follows: 0–25% B, 5–35 min; 25–45% B, 35–45 min. The peptides were separated at a fluent flow rate of 300 nl/min and finally lyophilized for mass spectrometry.

Liquid Chromatography Coupled to Tandem Mass Spectrometry

LC-MS/MS analysis was performed on a Nanoeasy system (Thermo Fisher Scientific, USA) with a 25 cm-long column (75 µm × 25 cm, 2 µm, 100 Å, C18 packing material, Thermo Fisher Scientific, USA) connected to a Q Exactive hybrid quadrupole-Orbitrap mass spectrometer (Thermo Fisher Scientific, USA). The fractions were dissolved in loading buffer (2% acetonitrile with 0.1% FA) before analysis. Mobile phase B consisted of 98% acetonitrile and 0.1% formic acid. The elution gradient was set from 5 to 40%. Full MS scans were acquired in the mass range of 300–1200 m/z with a mass resolution of 70,000, and the AGC target value was set at 1e6. The ten most intense peaks in MS were fragmented with higher-energy collisional dissociation (HCD) with collision energy of 35. MS/MS spectra were obtained with a resolution of 17,500 with an AGC target of 1e5 and a max injection time of 22 ms. The Fusion dynamic exclusion was set for 60 s and run under positive mode.

Database Search

The Proteome Discovery software (v.2.3) was used for protein identification and quantitation. All the raw data were searched against the Swiss-Prot human database (20,238 entries), with MS tolerance set at 20 ppm and MS/MS tolerance set at 0.1 Da. A global false discovery rate (FDR) was set to 0.01, and protein groups considered for quantification required at least two peptides.

Bioinformatic Analysis

We obtained the information of identified proteins from the UniProt protein sequence database. Both Gene Ontology (GO) analysis and Kyoto Encyclopedia of Genes and Genomes (KEGG) pathway analysis were conducted for the function and pathway analysis of proteins by DAVID (https://david.ncifcrf.gov/) online tool. The STRING database was introduced for protein–protein interaction (PPI) network analysis (http://string-db.org).

ELISA Procedures

The absolute expression levels of exosomal ALIX were tested using a commercial enzyme-linked immunosorbent assay (ELISA) kit (SenBeiJia Biotechnology Co., Ltd., China) based

on the recommended manufacturer's protocol. Firstly, the solubilized exosome samples were diluted five times with sample diluent, then 50 µl of the sample or standards was added to the appropriate wells in order. After the whole reaction, the optical density of each well was determined immediately using a microplate reader set to 450 nm. The concentration of exosomal ALIX was calculated in comparison with a protein standard curve.

Statistical Analysis

All data were analyzed using the GraphPad Prism 6.0 statistical software (La Jolla, CA, USA) and SPSS 20.0 software (Chicago, IL, USA). The Mann–Whitney U test or Student's t test was conducted to investigate the protein expression difference in all subjects. The expression levels of the selected biomarker candidate obtained by ELISA assays were compared using one-way ANOVA. The diagnostic value was evaluated by receiver operating characteristic (ROC) curve analysis. Differences were considered significant when P <0.05.

RESULTS

Isolation and Characterization of Plasma-Derived Exosomes

The study workflow was shown in **Figure 1**. Firstly, the plasma-derived exosomes were isolated separately by ultracentrifugation. As shown in **Figure 2**, the structure of exosomes revealed as a cup-shaped, membrane-enclosed vesicles, with a 30–150 nm size range characterized by TEM and flow cytometry (**Figures 2A, B**). The expression of exosomal biomarkers (CD63, Tsg101) was determined by western blotting using samples from six different groups of patients, which was shown in **Figure 2C**. And no significant difference in CD63 or Tsg101 intensity was observed among all groups of patients. Besides, exosomal biomarkers CD9, CD63, CD81, and Tsg101 were also all observed in the list of proteins identified through proteomic profiling (**Table S1**). In summary, these results absolutely confirmed the purity of plasma-derived exosomes used in this study.

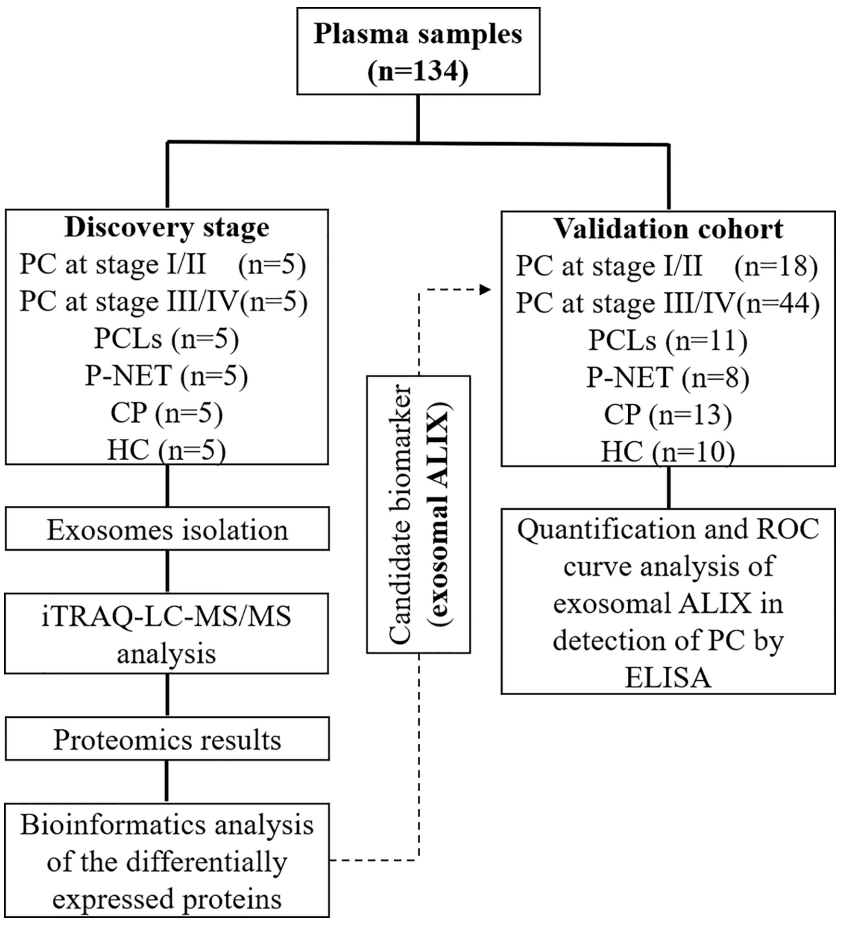

FIGURE 1 | Schematic workflow of the study.

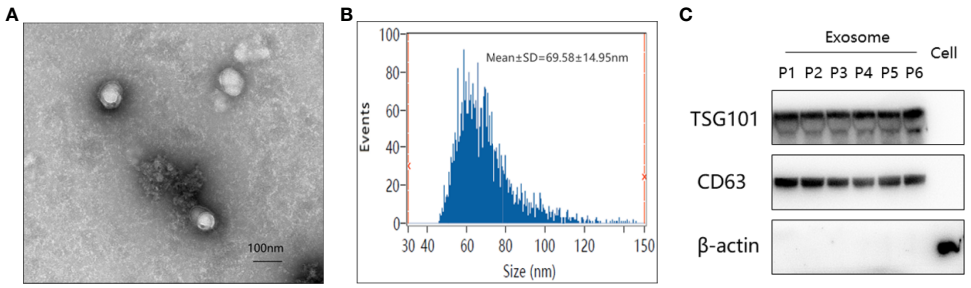

FIGURE 2 | Verification of plasma-derived exosomes from pancreatic cancer patients. **(A)** Transmission electron micrograph of isolated exosomes. Scale bar = 100 nm. **(B)** Size distribution measurements of isolated exosomes by flow cytometry. **(C)** Western blot analysis of exosome-enriched proteins (Tsg101 and CD63) and a control marker (*β*-actin) in isolated exosomal proteins from six different groups of patients and the total protein from PANC-1 cells. (P1–6 represented patients from PC at stage I/II, PC at stage III/IV, well-differentiated P-NET, PCLs, CP, and HC, respectively).

Proteomic Profiles of Plasma Exosomes

In the discovery stage, exosomal proteins were derived from all six groups and detected for iTRAQ-LC-MS/MS proteomic profiling analysis. A total of 623 proteins were identified (**Table S1**), and 366 of them overlapped with the exosome database that was compiled in Vesiclepedia (**Figure 3A**). Moreover, based on the criteria for differentially expressed proteins (fold change >1.20 or fold change <0.83 with a relative quantification *P* value <0.05), 52 up-, 43 down- and six up-, 14 down-regulated proteins in exosomes were discovered from PC stage I/II and stage III/IV patients compared with healthy groups. Besides, 73, 105, and 248 proteins were found to be differentially expressed in exosomes from P-NET, PCLs, and CP groups *versus* HC group (**Figure 3B**). In addition, 22 proteins showed significant differential expression between stage I/II and stage III/IV PC patients. Apart from this, exosomes from P-NET, PCLs, and CP groups had differential expression of 33, 57, and 332 proteins in comparison with PC, respectively (**Figure 3C**). When we compared the identified proteins between PC and other pancreatic diseases groups, we noticed an overlap of 16 proteins, which were presented in **Table 1**.

Identification of Differentially Expressed Proteins in Plasma-Derived Exosomes

Bioinformatic analysis was performed to reveal the functional characterization of the differentially expressed proteins. GO annotations indicated that protein binding, cell part, and cellular process were the most enriched terms in the molecular function (MF), cellular component (CC), and biological process (BP) (**Figure 4A**). KEGG pathway analysis showed that many reported signaling pathways associated with tumorigenesis and metastasis in PC, including transcriptional mis-regulation in cancer, endocytosis, and NF-kappa B signaling pathway were all included in the top 20 enriched pathways (**Figure 4B**). Moreover, an intensity heatmap was also utilized to depict the proteins that were significantly differentially expressed among the six groups and identified in the Uniprot and Vesiclepedia database (150 proteins in total) (**Figure 4C**).

Among all differentially expressed proteins, there were a total of 16 proteins that overlapped between PC and other pancreatic diseases groups. Four proteins were significantly higher in PC compared with other pancreatic diseases, including PDCD6IP (also known as ALIX), GPRC5B, SDCBP, and IST1 (**Figure 5A**).

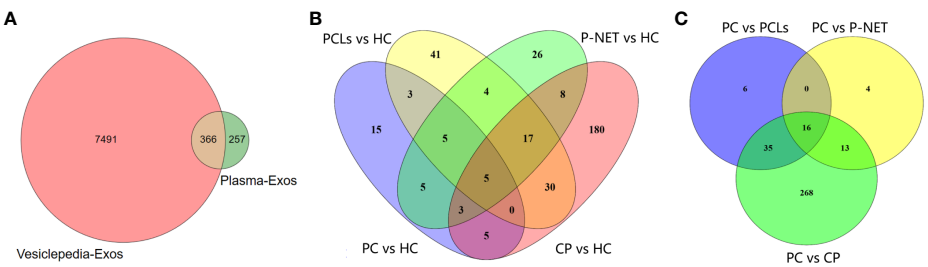

FIGURE 3 | Differential proteomic analysis of plasma-derived exosomes from patients with PC, other pancreatic diseases and healthy individuals. **(A)** The Venn diagram depicted the overlap of proteins identified in present study with those published in the Vesiclepedia database. **(B)** The overlap between differentially expressed proteins in exosomes from PC, P-NET, PCLs, and CP groups *versus* HC group. **(C)** The overlap of identified proteins differentially expressed between PC and other pancreatic diseases.

TABLE 1 | An overlap of 16 differentially expressed proteins between the exosomes of PC and other pancreatic diseases.

Uniprot accession	Gene symbol	Protein name	Protein abundances ratio *(PC/other pancreatic diseases)*
P01024	C3	Complement C3	1.179
A0A075B7D0	IGHV1OR15-1	Immunoglobulin heavy variable 1/OR15-1	0.6249
Q8WUM4	PDCD6IP	Programmed cell death 6-interacting protein	1.8389
Q9NZH0	GPRC5B	G-protein coupled receptor family C group 5 member B	1.7719
G5EA09	SDCBP	Syndecan binding protein (Syntenin), isoform CRA_a	1.5119
P53990	IST1	IST1 homolog	1.5269
P02538	KRT6A	Keratin, type II cytoskeletal 6A	0.2459
P04259	KRT6B	Keratin, type II cytoskeletal 6B	0.2339
P68871	HBB	Hemoglobin subunit beta	0.655
P69905	HBA1	Hemoglobin subunit alpha	0.621
P02533	KRT14	Keratin, type I cytoskeletal 14	0.315
P08779	KRT16	Keratin, type I cytoskeletal 16	0.441
Q04695	KRT17	Keratin, type I cytoskeletal 17	0.270
P01762	IGHV3-11	Immunoglobulin heavy variable 3-11	0.971
P35443	THBS4	Thrombospondin-4	1.045
A0A140TA62	N/A	IF rod domain-containing protein	0.699

PC, pancreatic cancer.

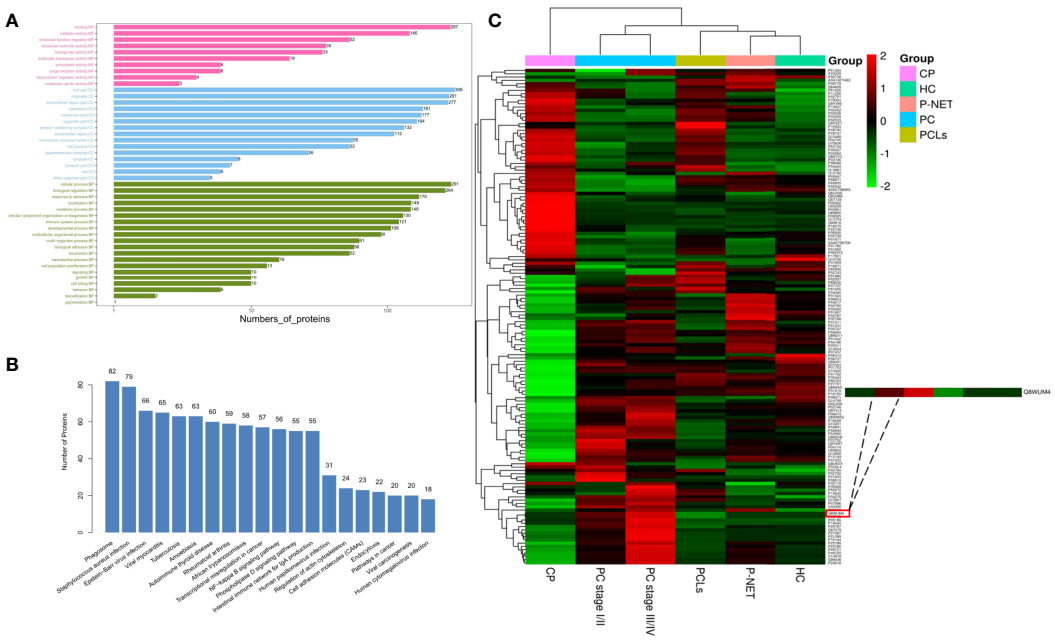

FIGURE 4 | Biological function and quantitative evaluation of plasma-derived exosomal proteins. **(A)** Gene ontology (GO) classification of whole identified exosomal proteins. The enriched terms in the biological process, cellular component, and molecular functions were listed. **(B)** Kyoto Encyclopedia of Genes and Genomes (KEGG) pathway analysis of whole identified exosomal proteins. The top 20 enriched pathways in exosomes were listed. **(C)** Hierarchical clustering heat maps of 150 important proteins, which were identified by t-test. The expression of each protein was illustrated in red and green to indicate high and low expression, respectively.

To reveal the relationships of the 16 proteins, we reconstructed the interaction networks using the STRING protein–protein interaction (PPI) database. The STRING PPI analysis yielded a highly clustered network containing 14 nodes with 16 edges (clustering coefficient: 0.738, enrichment p-value < 0.001). As shown in **Figure 5B**, among the four upregulated proteins in PC group, three were interacted with each other (ALIX, SDCBP and IST1), and the fold change of ALIX expression in PC *vs.* other pancreatic diseases was higher compared with both SDCBP and IST1 (**Table 1**). Based on the above results, we subsequently selected exosomal ALIX as the candidate biomarker for further analysis.

Validation of Exosomal ALIX as a Novel Biomarker for Pancreatic Cancer

Late diagnosis and lack of effective treatments are the main reasons for poor prognosis of PC. Hence, we focused on investigating the diagnostic utility of exosomal ALIX as a novel

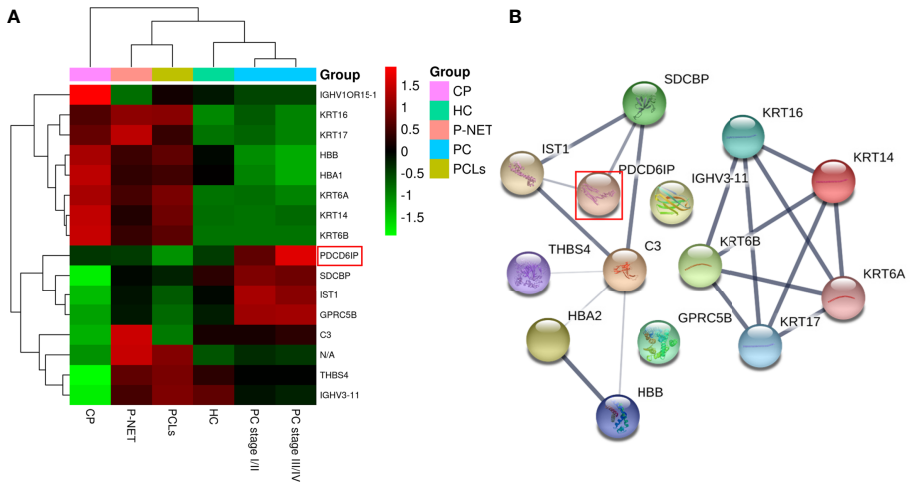

FIGURE 5 | Hierarchical clustering analysis and protein–protein interaction network (PPI) analysis of the 16 overlapped exosomal proteins. **(A)** Heatmap of the 16 proteins differentially expressed between the exosomes of PC and other pancreatic diseases. **(B)** The STRING PPI network of 16 differentially expressed proteins. It yielded a highly clustered network containing 14 nodes with 16 edges (clustering coefficient: 0.738, enrichment p-value < 0.001).

biomarker for PC with plasma samples from patients with PC, other pancreatic diseases, and healthy controls. The expression level of exosomal ALIX was evaluated by ELISA, and ROC curve analysis was performed to assess the diagnostic value of ALIX. A total of 104 individuals were enrolled in this clinical cohort, including 62 patients with PC (stage I/II, n = 18; stage III/IV, n = 44), 11 patients with PCLs, eight patients with well-differentiated P-NET, 13 patients with CP, and 10 healthy subjects. At the same time, the general clinicopathological features were observed and summarized. We noticed that the exosomal ALIX expression was significantly higher in advanced PC than early PC (**Figure 6A**). Moreover, ALIX expression was significantly elevated in all PC patients compared with patients with other pancreatic diseases in total or HC (**Figure 6B**). Interestingly, we also found that the expression of exosomal ALIX in PC patients was higher compared with other pancreatic diseases, including PCLs (P = 0.0037), CP (P = 0.0043) and P-NET (P = 0.1132) separately, though there was no statistically significant difference between

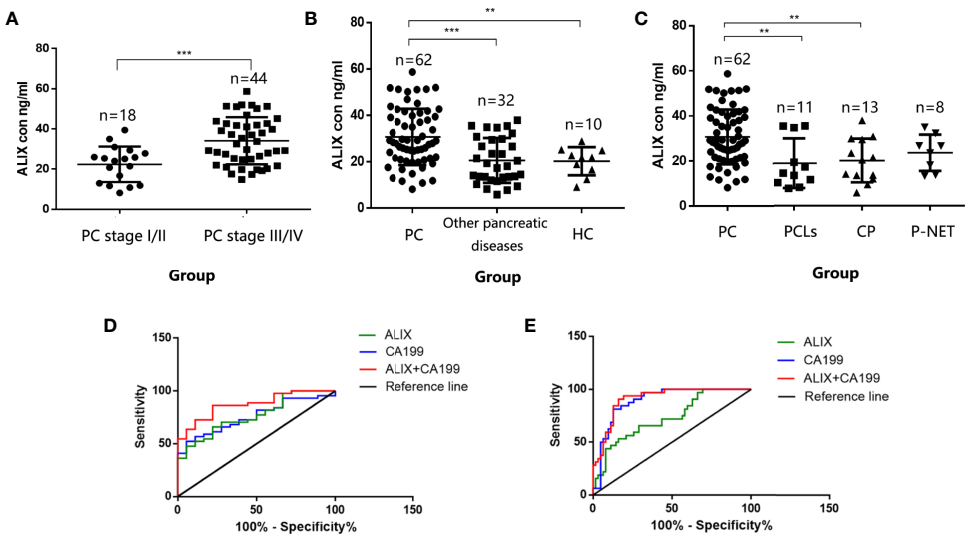

FIGURE 6 | Validation of exosomal ALIX as a novel biomarker for pancreatic cancer diagnosis and classification. **(A)** Scatter dot plots of protein concentrations of exosomal ALIX in patients with PC at different stages analyzed by ELISA. **(B)** Scatter dot plots of protein concentrations of exosomal ALIX in patients with PC, other pancreatic diseases, and healthy controls. **(C)** Scatter dot plots of protein concentrations of exosomal ALIX in patients with PC compared with all other types of pancreatic diseases. **(D)** ROC curve analysis of exosomal ALIX and serum CA199 for discrimination between PC patients at stage I/II and stage III/IV. **(E)** ROC curve analysis of exosomal ALIX and serum CA199 in differentiating PC *vs.* other pancreatic diseases. $^{**}P < 0.01$; $^{***}P < 0.001$.

PC and P-NET (**Figure 6C**). Next, we analyzed the correlations between clinical characteristics and exosomal ALIX expression level in PC patients by univariate analysis, and the results showed that ALIX expression was significantly associated with TNM stage (I/II *vs.* III/IV) and distant metastasis ($P < 0.05$) (**Table 2**). Then, we explored the value of exosomal ALIX alone or in combination with serum CA199 in differential diagnosis of pancreatic diseases (**Table 3**). For one thing, ALIX presented an acceptable diagnostic efficacy with an AUC value of 0.730 between PC and other pancreatic diseases, which was a liter lower than CA199 (0.891). For another, when differentiating PC patients at stage I/II from stage III/IV, ALIX had a slightly higher AUC value (0.768) than CA199 (0.756). We further combined exosomal ALIX with CA199 to estimate their diagnostic performance in differentiating PC *vs.* other pancreatic diseases, as well as early *vs.* late PC. Consequently, the combination of these two markers for the diagnosis of PC *versus* other pancreatic diseases yielded a promising AUC of 0.910, with a sensitivity of 90.6% and specificity of 83.9% at the cut-off point (**Table 3**, **Figure 6E**). They also improved the diagnostic efficacy between patients at stage I/II and stage III/IV with the AUC value of 0.872, which was significantly higher than CA199 alone (**Table 3**, **Figure 6D**). Therefore, we suggested that exosomal ALIX had the capability to detect PC, and the combination of ALIX and CA199 can further improve the diagnostic value, especially in distinguishing early and late PC.

TABLE 2 | Relationship between exosomal ALIX expression and clinicopathological parameters in PC groups.

	Total (n = 62)	ALIX expression		*P* value
		Low	High	
Sex				0.309
Male	30	13	17	
Female	32	18	14	
Age (years)				0.611
<65	30	16	14	
≥65	32	15	17	
Smoking status				0.520
Smoker	12	7	5	
Non-smoker	50	24	26	
Drinking status				0.354
Drinker	5	4	1	
Non-drinker	57	27	30	
Obstructive jaundice				0.562
Positive	16	7	9	
Negative	46	24	22	
Diabetes				0.576
Positive	18	8	10	
Negative	44	23	21	
TNM				0.011*
I/II	18	14	4	
III/IV	44	17	27	
Metastasis				0.007*
Positive	21	5	16	
Negative	41	26	15	

*PC, pancreatic cancer; TNM, T, extent of the primary tumor; N, lymph node involvement; M, metastatic disease. *P < 0.05.*

DISCUSSION

Due to the lack of an effective diagnostic method, the majority of PC patients are still diagnosed at an advanced stage and succumb to death within 12 months of diagnosis (1, 2, 13). Thus, it is urgent for us to seek more valuable biomarkers for early detection of PC. The present study investigated the differentially expressed exosomal proteins extracted from the plasma of patients with PC, other pancreatic diseases, and HC. The approach of iTRAQ-based proteomic analysis was used in the study, and a total of 623 proteins were identified. Bioinformatic analysis also indicated that the differentially expressed proteins were mainly located in the extracellular region and membrane parts and presented with a variety of extracellular functions in the processes of tumor progression and metastasis. Among the 16 differentially expressed proteins overlapped between PC and other pancreatic diseases, we selected exosomal ALIX as the candidate biomarker for further investigation. We found that ALIX protein expression, especially combined with serum CA199, had great potentials in differentiating PC patients at stage I/II from stage III/IV, as well as distinguishing PC from other pancreatic diseases.

Nowadays, PC still remains one of the deadliest cancer types worldwide, and the prominent problem is that no reliable markers are recommended for routine screening because of insufficient sensitivity and specificity. Therefore, exploring a precise and non-invasive biomarker is very critical for the early detection of PC. In recent years, extracellular vesicles (EVs), a heterogeneous group of cell-derived membranous structures, have gotten more and more attention (6–8). Exosomes belong to the group of EVs and can mediate as a functional mediator

TABLE 3 | Diagnostic performance of exosomal ALIX and serum CA199 in distinguishing PC *vs.* patients with other pancreatic diseases and PC patients at different stages.

	Biomarker	AUC value	95%CI	*P* value	Sensitivity	Specificity
PC *vs.*	ALIX	0.730	0.624–0.836	0.0003	53.1%	83.9%
other pancreatic diseases	CA199	0.891	0.825–0.956	<0.0001	81.3%	87.1%
	ALIX+CA199	0.910	0.853–0.968	<0.0001	90.6%	83.9%
PC stage I/II	ALIX	0.768	0.647–0.889	0.001	65.9%	77.8%
vs.	CA199	0.756	0.638–0.875	0.002	52.3%	94.4%
PC stage III/IV	ALIX+CA199	0.872	0.785–0.960	<0.0001	86.4%	77.8%

PC, pancreatic cancer.

(12, 14). Up to now, numerous studies have reported that exosomes are qualified as tumor specific biomarkers (9–11, 15–18). For one thing, as a bridge of communication, exosomes can assist the information exchange among cells in the form of lipids, nucleic acid species, and proteins, so the cargo of exosomes can reflect the real origin of them. For another, the lipid bilayer membrane can prevent exosomes from being degraded and keep information stable. More importantly, exosomes are released by various types of cells and can be simply isolated from different kinds of body fluids, such as blood, urine, saliva, and breast milk. Additionally, Jody et al. (19) compared the identified plasma-derived EVs against those found in unfractionated peripheral plasma and found that 41% proteins had not been previously identified in the latter group, indicating that some useful proteomic signatures may be missed by conventional profiling of total plasma. Based on the special characteristics of exosomes mentioned above, we presume that the plasma-derived exosomes can be an important noninvasive biomarker for early detection of PC.

As we all know, a great number of studies have been performed over the years on the diagnostic value of exosomes as a non-invasive biomarker for PC. Melo et al. (9) identified that $GPC1^+$ circulating exosomes (crExos) could serve as a potential diagnostic and screening tool to detect early stages of PC to facilitate possible curative surgical therapy. Though several follow-up studies queried the effect of $GPC1^+$crExos in the diagnosis of PC (16, 20, 21), the diagnostic value of exosomes still cannot be denied. In 2018, utilizing *in vitro* cellular assays, Jin et al. (22) found that exosomal ZIP4 can significantly promote PC growth, thus confirming the efficacy of ZIP4 as a novel diagnostic biomarker for PC. However, no clinical data have been published to verify the diagnostic value of exosomal ZIP4. Yu et al. (11) provided the first genome-wide analysis of extracellular vesicle long RNAs (exLRs) in plasma from PC patients, demonstrating the feasibility of identifying cancer biomarkers based on exLR profiling. These studies can fully confirm the value of exosomes as an ideal non-invasive biomarker for tumor detection. Unfortunately, no exosomal protein markers have been widely accepted for early detection of PC. Increasing researches have utilized proteomic analysis to discover new biomarkers recently, and iTRAQ is one of the most widely used techniques in the field of quantitative proteomics (23–26), which possesses the advantages of high throughout, high stability, and maximum protein coverage. Koichiro et al. (27) conducted a proteomic analysis using iTRAQ to explore proteins associated with lymph node metastasis in patients with colorectal cancer and identified 60 differentially expressed proteins. An et al. (28) performed the proteomic analysis in the serum-derived exosomal proteins and detected approximately 800 exosomal proteins in each incurably PC patients. In this work, we systemically studied the plasma-derived exosomal proteins and their biological functions in patients with pancreatic diseases and healthy individuals. Exosomes were purified by ultracentrifugation, and iTRAQ labeling couple LC-MS technique was used to evaluate the qualities of exosomal proteins. Out of the total 623 identified proteins, 366 proteins overlapped in the Vesiclepedia protein list. Different from previous studies, broader and larger groups of patients were enrolled in present study, including PC, well-differentiated P-NET, PCLs, CP, and healthy controls. These results are more authentic, providing a basic foundation for our further studies. 16 proteins with differential degrees of abundance were found in exosomes of PC *versus* other pancreatic diseases. Some of them were upregulated in patients with other pancreatic diseases, such as HBB, HBA1, and KRT16 proteins, while some were upregulated only in PC groups (*i.e.* ALIX, GPRC5B, SDCBP, and IST1), highlighting their potential diagnostic value. Moreover, 22 proteins were significantly differentially expressed between PC patients with stage I/II and stage III/IV. GO annotations indicated that protein binding in MF, cell part in CC and cellular process in BP were the most enriched terms. KEGG pathway analysis showed that many reported signaling pathways associated with tumorigenesis and metastasis in PC were all included in the top 20 enriched pathways.

Generally, exosomes are secreted upon fusion of endosomal multivesicular bodies (MVBs) with the plasma membrane, and the endosomal sorting complex required for transport (ESCRT) associated protein ALIX (also referred to as PDCD6IP, protein accession: Q8WUM4) plays an important role in the mechanisms involved in their biogenesis (29). Previous studies have identified that ALIX is a cytoplasmic protein, involved in endocytosis, membrane repair and the pathway of selected sorting by ESCRT-complexes (30, 31). Moreover, several researches have described that ALIX participates in programmed cell death, and its overexpression may block apoptosis (30, 32). As a general marker of exosomes, ALIX has scarcely been reported as a tumor marker, and the relationship between exosomes and protein degree of abundance has not been validated. Diederick et al. (33) compared exosomes from non-cancerous prostate cell lines to exosomes from prostate cancer (PCa) cell lines and finally identified ALIX as being enriched in PCa exosomes. What's more, Monypenny et al. (34) confirmed that the ESCRT-related protein ALIX could regulate tumor-mediated immunosuppression by controlling EGFR activity and PD-L1 presentation. In our study, according to the proteomic results, we noticed that exosomal ALIX was significantly highly expressed in PC patients, especially in those at the advanced stage. Bioinformatic analysis also revealed that ALIX was related to protein binding, apoptotic process, and the pathway of endocytosis, indicating ALIX as a potentially diagnostic marker for PC. Hence, we performed ELISA experiments and demonstrated that ALIX expression was obviously higher in PC than in patients with other pancreatic diseases or healthy controls and was closely associated with TNM stage and distant metastasis. Besides, ALIX expression was significantly enhanced in late PC compared with early PC. Interestingly, combination of exosomal ALIX and serum CA199 has greater values in distinguishing both early *vs.* late PC and PC *vs.* patients with other pancreatic diseases than either ALIX or CA199 alone.

Certain limitations should be considered in the current study. Firstly, the sample size for candidate biomarker validation was not big enough, so we need to conduct a larger and multicenter trial to elucidate the diagnostic value of exosomal ALIX in the next phase. Secondly, we only selected an upregulated protein as the novel biomarker, ignoring the diagnostic value of proteins downregulated in PC groups. What's more, although previous studies have confirmed that exosomes can be purified well

enough by ultracentrifugation, we still cannot rule out the possibility that some information of proteins was lost in the process of exosome isolation.

CONCLUSION

In conclusion, we provided a systematic approach for screening exosome-derived biomarkers for PC detection. Our study revealed that based on the proteomic profiling, plasma-derived exosomal proteins may function as ideal non-invasive biomarkers for early detection of PC. Importantly, exosomal ALIX combined with CA199 has great potentials in detection of PC, especially in distinguishing PC patients at early stages from advanced stages. And the function and molecular mechanisms of exosomal ALIX in PC progression need to be further investigated.

DATA AVAILABILITY STATEMENT

The raw data supporting the conclusions of this article will be made available by the authors, without undue reservation.

ETHICS STATEMENT

The studies involving human participants were reviewed and approved by the Ethics Committee of the Nanjing Drum Tower Hospital and the First Affiliated Hospital of Soochow University. The participants provided their written informed consent to participate in this study.

AUTHOR CONTRIBUTIONS

JY and XG wrote the manuscript. JY, YZ, and YY performed the experiments. JY, SiZ, LW, and PW performed the statistics analysis. YY, JZ, and HW collected the samples and implemented the data acquisition. GX, XL, and ShZ revised the manuscript. YL, ShZ, and DZ contributed to the conception, design, and supervision of the study. All authors contributed to the article and approved the submitted version.

FUNDING

This work was supported by the National Natural Science Foundation of China (81802396), Natural Science Foundation of Jiangsu Province (SBK2019022491 & BK20180117), General Project of Nanjing Medical Science and Technology Development Project (YKK17077), Nanjing Science and Technology Development Plan Project (201715023), Nanjing Medical Science and Technology Development Key Project (ZKX18022), and the Nanjing Science and Technology Project (201911038).

SUPPLEMENTARY MATERIAL

The Supplementary Material for this article can be found online at: https://www.frontiersin.org/articles/10.3389/fonc.2021.628346/full#supplementary-material

Supplementary Table 1 | A list of total proteins identified in the plasma-derived exosomes.

REFERENCES

1. Siegel RL, Miller KD, Jemal A. Cancer Statistics, 2019. *CA Cancer J Clin* (2019) 69(1):7–34. doi: 10.3322/caac.21551
2. Ryan DP, Hong TS, Bardeesy N. Pancreatic Adenocarcinoma. *N Engl J Med* (2014) 371(11):1039–49. doi: 10.1056/NEJMra1404198
3. Yachida S, Jones S, Bozic I, Antal T, Leary R, Fu B, et al. Distant Metastasis Occurs Late During the Genetic Evolution of Pancreatic Cancer. *Nature* (2010) 467(7319):1114–7. doi: 10.1038/nature09515
4. Jacobson RA, Munding E, Hayden DM, Levy M, Kuzel TM, Pappas SG, et al. Evolving Clinical Utility of Liquid Biopsy in Gastrointestinal Cancers. *Cancers* (2019) 11(8):1164. doi: 10.3390/cancers11081164
5. Buscail E, Alix-Panabières C, Quincy P, Cauvin T, Chauvet A, Degrandi O, et al. High Clinical Value of Liquid Biopsy to Detect Circulating Tumor Cells and Tumor Exosomes in Pancreatic Ductal Adenocarcinoma Patients Eligible for Up-Front Surgery. *Cancers* (2019) 11(11):1656. doi: 10.3390/cancers11111656
6. Colombo M, Raposo G, Thery C. Biogenesis, Secretion, and Intercellular Interactions of Exosomes and Other Extracellular Vesicles. *Annu Rev Cell Dev Biol* (2014) 30:255–89. doi: 10.1146/annurev-cellbio-101512-122326
7. Becker A, Thakur BK, Weiss JM, Kim HS, Peinado H, Lyden D. Extracellular Vesicles in Cancer: Cell-to-Cell Mediators of Metastasis. *Cancer Cell* (2016) 30(6):836–48. doi: 10.1016/j.ccell.2016.10.009
8. van Niel G, D'Angelo G, Raposo G. Shedding Light on the Cell Biology of Extracellular Vesicles. *Nat Rev Mol Cell Bio* (2018) 19(4):213–28. doi: 10.1038/nrm.2017.125
9. Melo SA, Luecke LB, Kahlert C, Fernandez AF, Gammon ST, Kaye J, et al. Glypican-1 Identifies Cancer Exosomes and Detects Early Pancreatic Cancer. *Nature* (2015) 523(7559):177–82. doi: 10.1038/nature14581
10. Arbelaiz A, Azkargorta M, Krawczyk M, Santos-Laso A, Lapitz A, Perugorria MJ, et al. Serum Extracellular Vesicles Contain Protein Biomarkers for Primary Sclerosing Cholangitis and Cholangiocarcinoma. *Hepatology* (2017) 66(4):1125–43. doi: 10.1002/hep.29291
11. Yu S, Li Y, Liao Z, Wang Z, Wang Z, Li Y, et al. Plasma Extracellular Vesicle Long RNA Profiling Identifies a Diagnostic Signature for the Detection of Pancreatic Ductal Adenocarcinoma. *Gut* (2020) 69(3):540–50. doi: 10.1136/gutjnl-2019-318860
12. Théry C, Witwer KW, Aikawa E, Alcaraz MJ, Anderson JD, Andriantsitohaina R, et al. Minimal Information for Studies of Extracellular Vesicles 2018 (MISEV2018): A Position Statement of the International Society for Extracellular Vesicles and Update of the MISEV2014 Guidelines. *J Extracell Vesicles* (2018) 7(1):1535750. doi: 10.1080/20013078.2018.1535750
13. Hidalgo M. Pancreatic Cancer. *N Engl J Med* (2010) 362:1605–720. doi: 10.1056/NEJMra0901557
14. Shah R, Patel T, Freedman JE. Circulating Extracellular Vesicles in Human Disease. *N Engl J Med* (2018) 379(10):958–66. doi: 10.1056/NEJMra1704286
15. Severino V, Dumonceau J, Delhaye M, Moll S, Annessi-Ramseyer I, Robin X, et al. Extracellular Vesicles in Bile as Markers of Malignant Biliary Stenoses. *Gastroenterology* (2017) 153(2):495–504. doi: 10.1053/j.gastro.2017.04.043
16. Lai X, Wang M, McElyea SD, Sherman S, House M, Korc M. A microRNA Signature in Circulating Exosomes is Superior to Exosomal Glypican-1 Levels for Diagnosing Pancreatic Cancer. *Cancer Lett* (2017) 393:86–93. doi: 10.1016/j.canlet.2017.02.019
17. Aghebati Maleki A, Nami S, Baghbanzadeh A, Karzar BH, Noorolyai S, Fotouhi A, et al. Implications of Exosomes as Diagnostic and Therapeutic Strategies in Cancer. *J Cell Physiol* (2019) 234(12):21694–706. doi: 10.1002/jcp.28875

18. Armstrong EA, Beal EW, Chakedis J, Paredes AZ, Moris D, Pawlik TM, et al. Exosomes in Pancreatic Cancer: From Early Detection to Treatment. *J Gastrointest Surg* (2018) 22(4):737–50. doi: 10.1007/s11605-018-3693-1
19. Vykoukal J, Sun N, Aguilar-Bonavides C, Katayama H, Tanaka I, Fahrmann JF, et al. Plasma-Derived Extracellular Vesicle Proteins as a Source of Biomarkers for Lung Adenocarcinoma. *Oncotarget* (2017) 8 (56):95466–80. doi: 10.18632/oncotarget.20748
20. Castillo J, Bernard V, San Lucas FA, Allenson K, Capello M, Kim DU, et al. Surfaceome Profiling Enables Isolation of Cancer-Specific Exosomal Cargo in Liquid Biopsies From Pancreatic Cancer Patients. *Ann Oncol* (2018) 29 (1):223–9. doi: 10.1093/annonc/mdx542
21. Frampton AE, Prado MM, Lopez-Jimenez E, Fajardo-Puerta AB, Jawad Z, Lawton P, et al. Glypican-1 is Enriched in Circulating-Exosomes in Pancreatic Cancer and Correlates With Tumor Burden. *Oncotarget* (2018) 9(27):19006–13. doi: 10.18632/oncotarget.24873
22. Jin H, Liu P, Wu Y, Meng X, Wu M, Han J, et al. Exosomal Zinc Transporter ZIP4 Promotes Cancer Growth and is a Novel Diagnostic Biomarker for Pancreatic Cancer. *Cancer Sci* (2018) 109(9):2946–56. doi: 10.1111/cas.13737
23. Unwin RD. Quantification of Proteins by Itraq. *Methods Mol Biol* (2010) 658:205–15. doi: 10.1007/978-1-60761-780-8_12
24. Liu X, Zheng W, Wang W, Shen H, Liu L, Lou W, et al. A New Panel of Pancreatic Cancer Biomarkers Discovered Using a Mass Spectrometry-Based Pipeline. *Brit J Cancer* (2017) 117(12):1846–54. doi: 10.1038/bjc.2017.365
25. Swiatly A, Horala A, Matysiak J, Hajduk J, Nowak-Markwitz E, Kokot Z. Understanding Ovarian Cancer: Itraq-Based Proteomics for Biomarker Discovery. *Int J Mol Sci* (2018) 19(8):2240. doi: 10.3390/ijms19082240
26. Song X, Bandow J, Sherman J, Baker JD, Brown PW, McDowell MT, et al. Itraq Experimental Design for Plasma Biomarker Discovery. *J Proteome Res* (2008) 7(7):2952–8. doi: 10.1021/pr800072x
27. Mori K, Toiyama Y, Otake K, Fujikawa H, Saigusa S, Hiro J, et al. Proteomics Analysis of Differential Protein Expression Identifies Heat Shock Protein 47 as a Predictive Marker for Lymph Node Metastasis in Patients With Colorectal Cancer. *Int J Cancer* (2017) 140(6):1425–35. doi: 10.1002/ijc.30557
28. An M, Lohse I, Tan Z, Zhu J, Wu J, Kurapati H, et al. Quantitative Proteomic Analysis of Serum Exosomes From Patients With Locally Advanced Pancreatic Cancer Undergoing Chemoradiotherapy. *J Proteome Res* (2017) 16(4):1763–72. doi: 10.1021/acs.jproteome.7b00024
29. Colombo M, Moita C, van Niel G, Kowal J, Vigneron J, Benaroch P, et al. Analysis of ESCRT Functions in Exosome Biogenesis, Composition and Secretion Highlights the Heterogeneity of Extracellular Vesicles. *J Cell Sci* (2013) 126(24):5553–65. doi: 10.1242/jcs.128868
30. Odorizzi G. The Multiple Personalities of Alix. *J Cell Sci* (2006) 119(15):3025–32. doi: 10.1242/jcs.03072
31. Colombo M, Moita C, van Niel G, Kowal J, Vigneron J, Benaroch P, et al. Analysis of ESCRT Functions in Exosome Biogenesis, Composition and Secretion Highlights the Heterogeneity of Extracellular Vesicles. *J Cell Sci* (2013) 126(24):5553–65. doi: 10.1242/jcs.128868
32. Wu Y, Pan S, Che S, He G, Nelman-Gonzalez M, Weil MM, et al. Overexpression of Hp95 Induces G1 Phase Arrest in Confluent HeLa Cells. *Different (London)* (2001) 67(4):139–53. doi: 10.1046/j.1432-0436.2001.670406.x
33. Duijvesz D, Burnum-Johnson KE, Gritsenko MA, Hoogland AM, Vredenbregt-van DBM, Willemsen R, et al. Proteomic Profiling of Exosomes Leads to the Identification of Novel Biomarkers for Prostate Cancer. *PloS One* (2013) 8(12):e82589. doi: 10.1371/journal.pone.0082589
34. Monypenny J, Milewicz H, Flores-Borja F, Weitsman G, Cheung A, Chowdhury R, et al. Alix Regulates Tumor-Mediated Immunosuppression by Controlling Egfr Activity and PD-L1 Presentation. *Cell Rep* (2018) 24 (3):630–41. doi: 10.1016/j.celrep.2018.06.066

Conflict of Interest: The authors declare that the research was conducted in the absence of any commercial or financial relationships that could be construed as a potential conflict of interest.

frontiers in Oncology

ORIGINAL RESEARCH
published: 11 May 2021
doi: 10.3389/fonc.2021.654076

A Novel Ferroptosis Related Gene Signature for Prognosis Prediction in Patients With Colon Cancer

Jianhua Nie[1†], Dan Shan[1†], Shun Li[1†], Shuyuan Zhang[1†], Xiaolin Zi[1], Fan Xing[2], Jiaqi Shi[1], Caiqi Liu[1], Tianjiao Wang[3], Xiaoyuan Sun[1], Qian Zhang[1], Meng Zhou[1], Shengnan Luo[1], Hongxue Meng[4], Yanqiao Zhang[1] and Tongsen Zheng[1,5,6*]*

[1] Department of Gastrointestinal Medical Oncology, Harbin Medical University Cancer Hospital, Harbin, China, [2] Department of Radiation Oncology, The Second Affiliated Hospital of Harbin Medical University, Harbin, China, [3] The Seventh Department of the Internal Medicine, Harbin Medical University Cancer Hospital, Harbin, China, [4] Department of Pathology, Harbin Medical University Cancer Hospital, Harbin, China, [5] Department of Phase 1 Trials Center, Harbin Medical University Cancer Hospital, Harbin, China, [6] Key Laboratory of Molecular Oncology, Heilongjiang Cancer Institute, Harbin, China

Purpose: Colon cancer (CC) is a serious disease burden. The prognosis of patients with CC is different, so looking for effective biomarkers to predict prognosis is vitally important. Ferroptosis is a promising therapeutic and diagnosis strategy in CC. However, the role of ferroptosis in prognosis of CC has not been studied. The aim of the study is to build a prognosis model related ferroptosis, and provide clues for further therapy of CC.

Methods: The RNA-seq data were from TCGA (training group) and GEO (testing group). The R language and Perl language were used to process and analyze data. LASSO regression analysis was used to build the prognosis model. ssGSEA was used to compare the immune status between two groups. Immunohistochemistry was used to detect expression of AKR1C1 and CARS1 in colon cancer tissues and adjacent tissues.

Results: The prognosis model consisted of five ferroptosis related genes (AKR1C1, ALOX12, FDFT1, ATP5MC3, and CARS1). The area under curve (AUC) at 1-, 2-, and 3-year were 0.668, 0.678, and 0.686, respectively. The high- and low-risk patients had significant survival probability and could be clearly distinguished by the PCA and t-SNE analysis. The multivariate cox regression analysis also showed the riskscore is an independent prognosis factor. Importantly, we found that the immune status between high- and low-risk patients were different obviously, such as $CD8^+$T cells. And STING, a new promising immune target, was also correlated to our signature genes statistically significantly.

Conclusion: Our ferroptosis prognosis signature could predict survival of CC patients to a certain degree. And the crosstalk between ferroptosis and immune, especially STING need further studies.

Keywords: ferroptosis, prognosis, colon cancer, STING, immune status

OPEN ACCESS

Edited by:
Kenneth K. W. To, The Chinese University of Hong Kong, China

Reviewed by:
Manoj Kumar Kashyap, Amity University Gurgaon, India
Weiyu Chen, Stanford University, United States

***Correspondence:**
Tongsen Zheng
zhengtongsen@hrbmu.edu.cn; zhengtongsen@126.com
Yanqiao Zhang
yanqiaozhang@ems.hrbmu.edu.cn

†These authors have contributed equally to this work

Specialty section:
This article was submitted to Gastrointestinal Cancers, a section of the journal Frontiers in Oncology

Received: *15 January 2021*
Accepted: *08 April 2021*
Published: *11 May 2021*

Citation:
Nie J, Shan D, Li S, Zhang S, Zi X, Xing F, Shi J, Liu C, Wang T, Sun X, Zhang Q, Zhou M, Luo S, Meng H, Zhang Y and Zheng T (2021) A Novel Ferroptosis Related Gene Signature for Prognosis Prediction in Patients With Colon Cancer. Front. Oncol. 11:654076. doi: 10.3389/fonc.2021.654076

INTRODUCTION

According to the latest cancer epidemiology, the global incidence of colorectal cancer ranked the third (10.2%), and mortality of which ranked the second (9.2%) in both sexes combined (1, 2), leading to a huge health and economic burden. The diagnosis and treatment of colon cancer (CC) has made a progress in the advance of clinical treatments, such as immunotherapy and targeted therapy (3, 4). However, current clinical management is still far from achieving satisfying outcomes. And the prognosis of patients with CC diversifies individually. Although there are some prognostic factors, such as stage and carcinoembryonic antigen (CEA), they can't predict patients' prognosis accurately. We still need to search for more accurate biomarkers to predict prognosis of patients with CC, guiding clinical management as well as sparking great potential for discovering novel therapeutic targets. Therefore, there is an urgent need to find new biomarkers for CC patients.

Ferroptosis is a new recognized way of non-apoptosis regulated cell death, characterized by the iron-dependent accumulation of lipid hydroperoxides, holding great promise for fighting against cancers (5). We have already reviewed the role of ferroptosis in digestive system neoplasms in the previous paper (5), which highlighted the essential role of ferroptosis played in hepatocellular carcinoma and other digestive system neoplasms such as gastric cancer, pancreatic cancer, and CC.

A few of studies devoting to investigating the role of ferroptosis in CC proved the central role of ferroptosis in the therapy and prevention for CC. For example, triterpene saponin ardisiacrispin B and epunctanone exerted cytotoxic effects partly *via* ferroptosis in resistant HCT116 p53−/− colon adenocarcinoma cells (6, 7). By inducing ferroptosis and apoptosis, electroporation increased the sensitivity of CC cells to camptothecin analog SN38 (8). Omega-3 polyunsaturated fatty acids (n-3 PUFA) and highly fermentable fiber may induce ferroptosis to reduce the risk of colorectal cancer (9). *Betula etnensis* Raf. (Birch Etna) promoted ferroptosis mediated by heme oxygenase-1(HO-1) hyper-expression in CC (10). Bromelain exerted cytotoxic effects in Kras-mutant colorectal cancer cells *via* downregulating acyl-CoA synthetase long-chain family member 4 (ACSL4) to induce ferroptosis (11). It can be seen that induction of ferroptosis is a promising strategy in diagnosis, treatment, and prevention of CC. However, the prognosis role of ferroptosis in CC has not been assessed.

Ferroptosis is recognized as a form of immunogenic cell death (ICD), in other words, innate and adaptive immune response could be triggered by such dying cells (12). Recently, a research showed that $CD8^+$ T cells regulated tumor ferroptosis during cancer immunotherapy. This is the first time that researchers have confirmed the direct crosstalk between immune system and ferroptosis (13). Immunotherapy and induction of ferroptosis are both considered to be of great significance in clinical management of colon cancer, studying the crosstalk between immunotherapy and ferroptosis thereby can be quite meaningful for developing novel treatment and overcoming resistance to immunotherapy. Stimulator of interferon genes (STING) is a new immune target in cancer therapy (14). A study showed that GPX4, a key regulatory molecule in ferroptosis, facilitated STING activation by maintaining redox homeostasis of lipids, indicating that ferroptosis was related to STING pathway. However, the direct crosstalk between STING and ferroptosis has not been studied yet.

Our study aimed to investigate the role of ferroptosis in the prognosis of CC and look for valuable targets related to ferroptosis for further experimental and clinical research, to better ameliorate clinical management of colon cancer. We also tried to provide clues for the relationship between ferroptosis and immune system, especially STING.

MATERIALS AND METHODS

Colon Adenocarcinoma Datasets and Ferroptosis Related Genes

The RNA-seq transcriptome data and clinical data of patients with colon adenocarcinoma (COAD) were downloaded from the Cancer Genome Atlas (TCGA) database (https://portal.gdc.cancer.gov/) and Gene Expression Omnibus (GEO) database (https://www.ncbi.nlm.nih.gov/geo). We downloaded RNA-seq data of COAD cohort from TCGA as Fragments Per Kilobase of transcript per Million mapped reads (FPKM) as the training group. The RNA-seq data of GSE39582 from GEO was used as the testing group. The ferroptosis related genes were referred from previous studies (15), and the authors collected them from previous important and authoritative literatures related to ferroptosis (16–19).

Construction of Ferroptosis Related Prognosis Model in CC

We used R language to analyze data in the present study (https://www.R-project.org/). The differentially expressed genes (DEG) related ferroptosis between normal tissues and tumor tissues were filtered by "limma" package using wilcox Test [false discovery rate (FDR) <0.05] in the TCGA cohort. Then we used the "survival" package to conduct univariate cox regression analysis ($p < 0.05$) to filter survival-related ferroptosis genes. The intersecting genes between DEG and survival-related ferroptosis genes were used in further analysis. The Least absolute shrinkage and selection operator (LASSO) cox regression analysis (20) was used to build the ferroptosis related prognosis model in CC using "glmnet" and "survival" packages. On the basis of the results of LASSO regression analysis, riskscore of each patient was calculated by the expression levels of genes and the corresponding coefficient in prognosis model using the following formula: $\text{Riskscore} = \text{Exp}_{\text{gene 1}} * \text{Coef}_{\text{gene 1}} + \ldots\ldots \text{Exp}_{\text{gene n}} * \text{Coef}_{\text{gene n}}$, with Coef indicating the coefficient and Exp indicating the expression level of genes. Then all patients were divided into high-risk groups (whose riskscores are above median values) and low-risk groups (whose riskscores were below median values) based on the riskscore.

The Verification of Ferroptosis Related Prognosis Model in CC

Receiver operating characteristic (ROC) was used to evaluate the accuracy of our model using the "survival," "survminer," and "timeROC" packages. The Kaplan-Meier curve was used to compare the survival probability difference between high-risk groups and low-risk groups using the log-rank test with "survival" and "survminer" packages. Principal component analysis (PCA) and t-distributed stochastic neighbor embedding (t-SNE) analysis were used to visualize the data in two dimensions with the "Rtsne" and "ggplot2" packages. The univariate and multivariate Cox regression analysis were used to determine the independent prognosis factors using the "survival" packages. A nomogram was used to predict survival probability of CC patients with the R package "rms."

The Function Analysis of Ferroptosis Related Prognosis Model in CC

Gene ontology (GO) and Kyoto Encyclopedia of Genes and Genomes (KEGG) were conducted to discover the potential function of genes between high- and low-risk groups. Single-sample gene set enrichment analysis (ssGSEA) was used to evaluate the infiltration levels of immune cell types and immune function between the high- and low-risk groups in the R packages of "gsva" (21). The correlation between ferroptosis genes and STING related genes in CC was evaluated using Pearson's correlation coefficient.

Protein-Protein Interactions (PPI) Network and Correlation Plot

The possible predicted pathways between ferroptosis related molecules and STING related molecules were indicated by the correlation plot and PPI network from the perspective of RNA and protein levels, respectively. We built the PPI network by online STRING database (https://string-db.org/). When inputing multiple proteins by names in the search bar, then PPI network was built automatically. We built the correlation plot through "igraph" and "reshape2" packages.

The Human Protein Atlas (HPA)

The human protein atlas (HPA) (22, 23) is a free database which consists of multiple protein expression images in normal tissues and cancer tissues. The immunohistochemistry images of the corresponding genes in the prognosis model were searched in the HPA database to verified the bioinformatics analysis results in our study.

Immunohistochemistry

To verify the results of this study, we collected 54 paired tumor tissues and adjacent tissues from our hospital to carry out immunohistochemistry. Immunohistochemistry was performed as described previously (24, 25) using anti-AKR1C1(ab192785, Abcam) and anti-CARS1(ab126714, Abcam) antibodies. In brief, colon cancer tissues and adjacent tissues sections were deparaffinized in xylene and rehydrated with ethanol. Heat mediated antigen retrieval was performed in 10 mM citrate buffer at pH 6.0. After blocking with normal goat serum, slides were incubated with primary antibodies against AKR1C1 and CARS1 overnight (4°C). Tissue sections were then stained with biotinylated secondary antibody (Vector lab) for 1 h at room temperature, followed by the Vectastain Elite ABC reagent (Vector lab) for 30 min. The peroxidase reaction was developed with diaminobenzidine (DAB kit; Vector lab) and the slides were counterstained with hematoxylin (Sigma).

The positive expression of AKR1C1 and CARS1 were mainly located in the cytoplasm. Positive cells accounted for a percentage score standard: 0 = no positive cells; 1 = 1–25% positive cells; 2 = 26–50% positive cells; 3 = 51–75% positive cells; 4 = more than 75% positive cells.

RESULTS

Establishment of Ferroptosis Related Prognosis Signature in Colon Cancer

The RNA-seq data and clinical data in patients with CC were from two public databases, TCGA and GEO. The ferroptosis related differentially expressed genes between normal population (n = 41) and colon cancer population (n = 473) from TCGA were showed in **Figure 1A**. The prognosis related genes *via* univariate Cox analysis were presented in **Figure 1B**, which implicated AKR1C1, ALOX12, CARS1, and HSPB1 were risk genes for the prognosis of colon cancer patients. However, ATP5MC3 and FDFT1 were protective genes for colon cancer patients. The intersecting genes between differentially expressed ferroptosis related genes and survival related genes were AKR1C1, ALOX12, CARS1, FDFT1, and ATP5MC3 (**Figure 1C**). Next, we built a ferroptosis related gene signature using the above five genes with the method of LASSO regression analysis (**Figures 1D, E**). The riskscore was calculated for each CC patients as the following formula:

0.281948648331575 *the expression levels of AKR1C1 + 0.655 775537737114 *the expression levels of ALOX12 + 0.84534 9664371856 *the expression levels of CARS1 + (−0.32730537 9054264) *the expression level of FDFT1 +(−0.076964324 6539205)*the expression levels of ATP5MC3. To sum up, we have built a ferroptosis related prognosis model to predict prognosis of colon cancer patients, which needed further verification.

Verification of Accuracy of Five Ferroptosis Related Gene Signature in Colon Cancer

To verify the accuracy of our model, Kaplan-Meier survival curves, ROC curves, PCA, and t-SNE were plotted in TCGA cohort and GEO cohort respectively. All patients were divided into high-risk groups and low-risk groups based on the respective median values from TCGA (**Figure 2A**) and GEO database (**Figure 2B**). **Figures 2C, D** showed the survival time trends of all the patients with the increasing of riskscore. The red dots represent the dead patients, and the blue dots represent the patients still be alive. We found that the higher the riskscore was, the more dead people were, proving that our model could predict prognosis of CC patients to a certain degree. In addition, we used a chi-square test to compare the

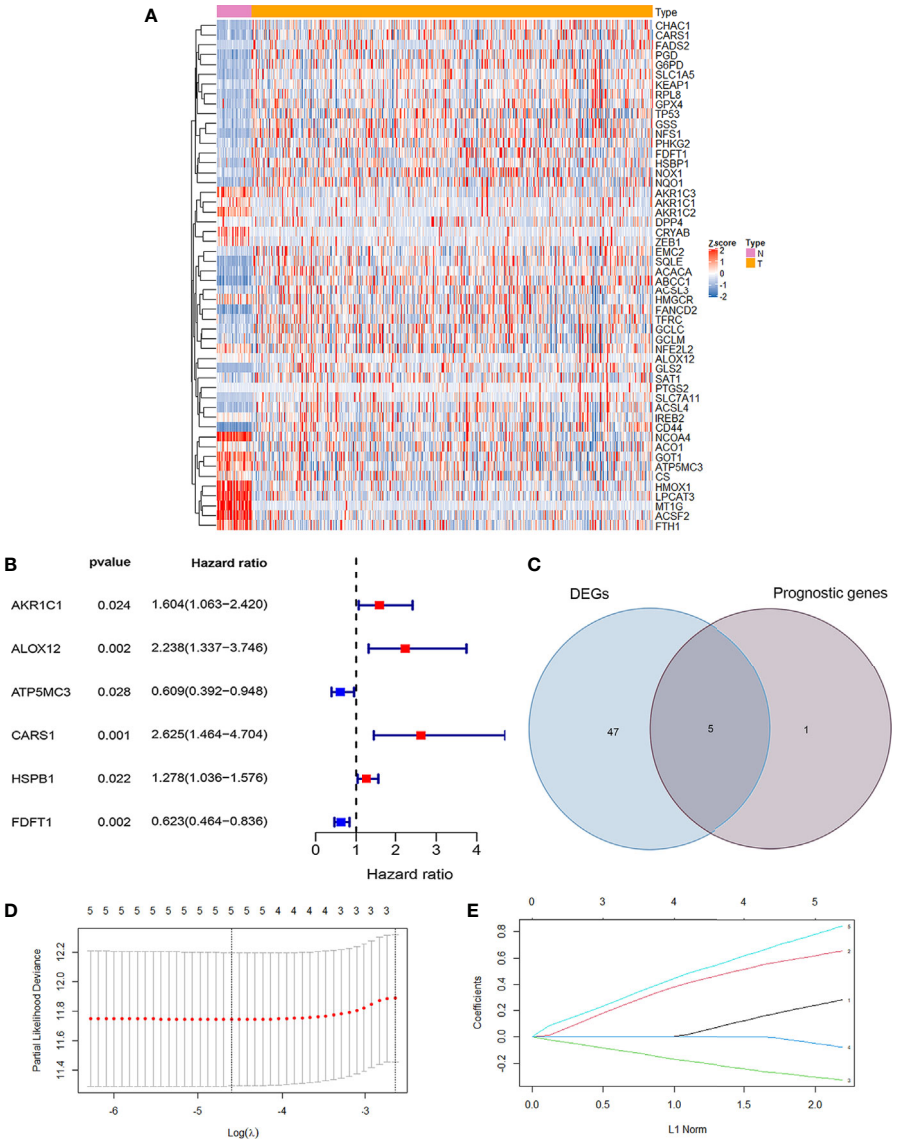

FIGURE 1 | Development of ferroptosis related gene signature in colon cancer. **(A)** The heatmap showed the differentially expressed genes (DEG) related ferroptosis between normal population and colon cancer population from TCGA (P <0.05). **(B)** The forest map showed six prognosis related genes in colon cancer by univariate cox regression analysis (P <0.05). **(C)** The Venn diagram showed the intersecting genes between DEG and survival related genes. **(D)** Partial likelihood deviance against log (λ) is plotted. The first vertical dashed line representatives the λ value with minimum error. **(E)** The LASSO coefficient profiles of ferroptosis-related gene in colon cancer.

number of dead and surviving patients between the high- and low-risk groups in two cohorts. The results indicated that there were more dead patients in the high-risk groups (P <0.01) (**Supplementary Figure 1**). The Kaplan-Meier survival curves showed that the high-risk groups were less likely to survive than the low-risk group in TCGA cohort (p <0.001) and GEO cohort (P <0.05) (**Figures 2E, F**).

ROC curves showed the AUC scores in the 1, 2, and 3 years were 0.668, 0.678, and 0.686, respectively in TCGA cohort (**Figure 3A**). In the GEO cohort, AUC scores in the 1, 2, and 3 years were 0.546, 0.558, and 0.578, respectively (**Figure 3B**). PCA and t-SNE analysis were also applied to test the accuracy of our prognosis model. The PCA plot and t-SNE plot indicated that patients in the high-risk and low-risk group were in two directions in the TCGA and GEO cohort (**Figures 3C–F**). Overall, our five ferroptosis related genes signature can distinguish the prognosis of colon cancer patients to some extent.

What's more, to further confirm the accuracy of the model, we did Kaplan-Meier survival analysis, univariate Cox regression analysis, and LASSO regression analysis towards three typical DEGs (CD44, GCLC, and MT1G). The results implicated that CD44, GCLC, and MT1G were not correlated to prognosis of patients (P>0.05). The Partial likelihood deviance and LASSO

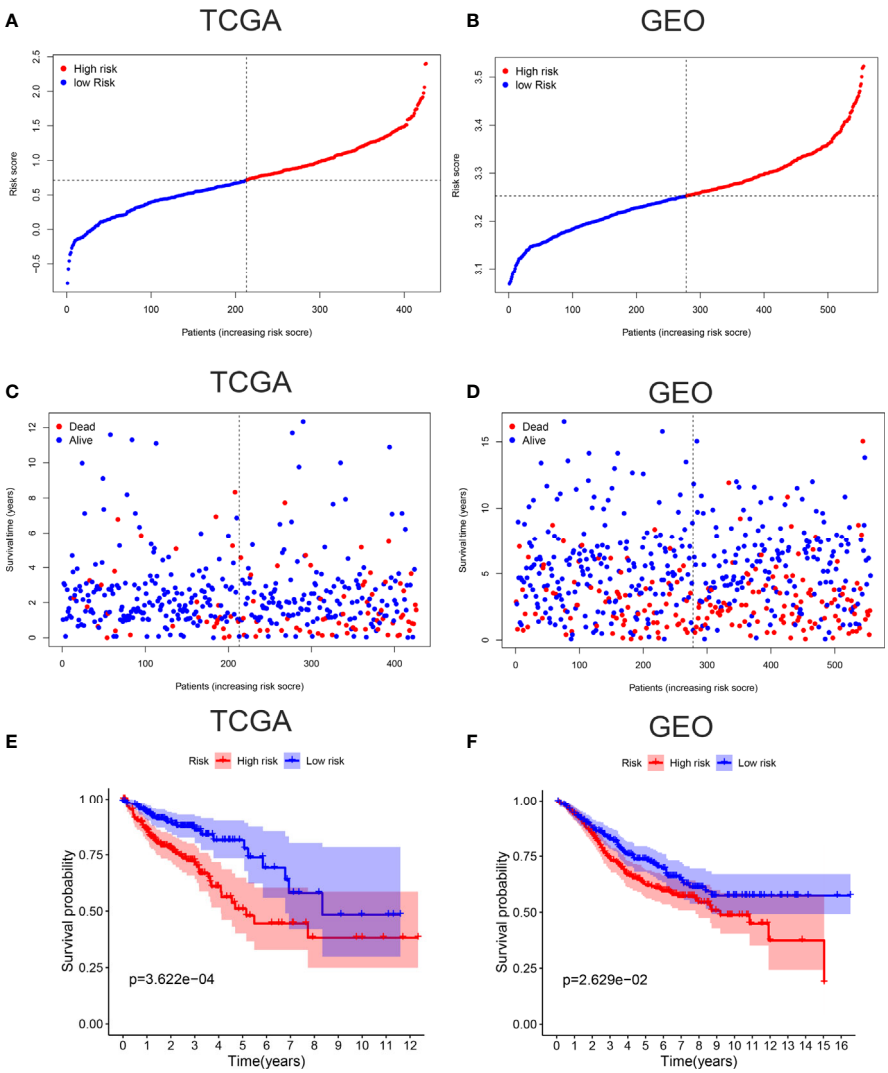

FIGURE 2 | Verification of accuracy of ferroptosis related gene signature in colon cancer. **(A)** The patients from TCGA cohort are divided into high-risk group and low-risk group based on the riskscore median values. **(B)** The patients from GEO cohort are divided into high-risk group and low-risk group based on its own riskscore median values. **(C)** The distribution of survival time in the high-risk group and low-risk group in the TCGA cohort. **(D)** The distribution of survival time in the high-risk group and low-risk group in the GEO cohort. **(E)** Kaplan-Meier curves showed the survival differences between high-risk group and low-risk group using the log-rank test in the TCGA cohort. **(F)** Kaplan-Meier curves showed the survival differences between high-risk group and low-risk group using the log-rank test in the GEO cohort.

coefficient profiles showed CD44, GCLC, and MT1G were not suitable as the model genes (**Supplementary Figure 2**).

Riskscore and Other Clinical Pathology Characters Synergistically Predicted the Survival Probability of Colon Cancer Patients

Univariate and multivariate Cox regression analysis were applied to test whether riskscore is an independent prognostic factor for overall survival (OS). Age, stage, and riskscore were statistically significant associated with the prognosis of colon cancer in TCGA cohort through univariate cox regression analyses, especially riskscore (HR = 2.858, 95% CI = 1.883–4.337, P<0.001) (**Figure 4A**). **Figure 4B** showed that age, stage, and riskscore were independent prognostic factor using multivariate cox regression analyses for OS in the TCGA cohort (HR = 2.102, 95% CI = 1.377–3.208, P<0.001). The univariate and multivariate cox regression analyses of GEO cohort were presented in **Supplementary Figure 3** (P<0.05). We know that single character is not good enough to predict the prognosis of CC patients, so we try to use the multi-characters to better predict their prognosis. Nomogram is a powerful tool to predict prognosis, which may be helpful for the doctors and patients. The system includes four indexes: age, gender, stage, and riskscore. For a specific colon cancer patient, his/her age,

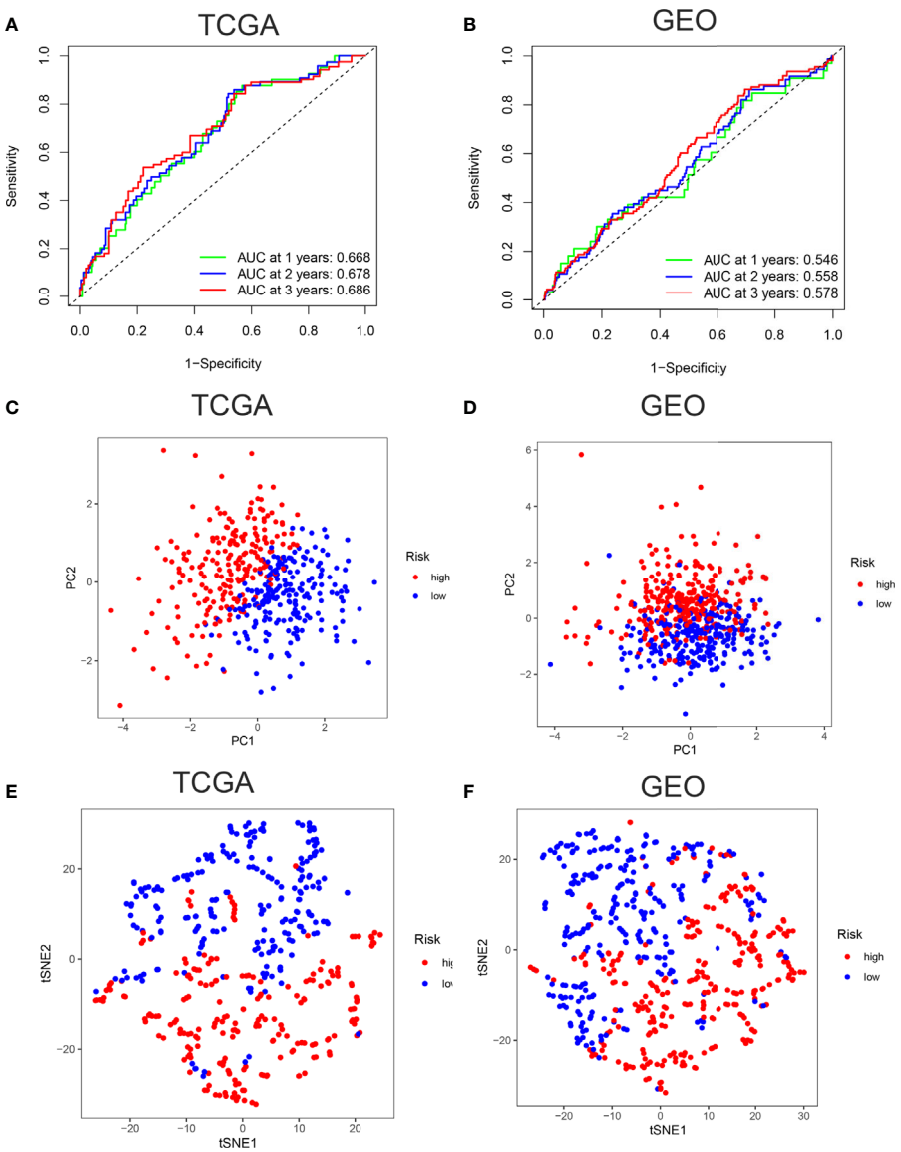

FIGURE 3 | Verification of accuracy of ferroptosis related gene signature in colon cancer. **(A)** The AUC score at 1, 2, 3 years in the TCGA cohort. **(B)** The AUC score at 1, 2, 3 years in the GEO cohort. **(C)** The PCA plot in the TCGA cohort. **(D)** The PCA plot in the GEO cohort. **(E)** The t-SNE plot in the TCGA cohort. **(F)** The t-SNE plot in the GEO cohort.

gender, stage, and riskscore have different scores, then the sum of four points is used to predict the 1-, 3-, and 5-year survival probability (**Figure 4C**). In short, riskscore was an independent prognostic factor and synergistically predicted the survival probability of CC patients.

The Immune Status Difference Between High-Risk and Low-Risk Colon Cancer Patients

According to the riskscore for each patient, we preformed GO and KEGG enrichment analysis between high-risk and low-risk groups. The GO result showed the differences between two groups mainly focus on fatty acid transport, positive regulation of leukocyte chemotaxis, protein maturation, mast cell granule and immunoglobulin complex (**Figure 5A**), which gave us a hint that the differences between two groups were related to immune response, so we further carried out the ssGSEA to compare immune cells and immune function differences between two groups. KEGG results were showed in **Supplementary Figure 4**. **Figure 5B** showed immature dendritic cells (iDCs) were distinct between high- and low-risk groups ($P < 0.01$). In addition, $CD8^+$T cells, DCs, mast cells, Th1 cells, and Th2 cells were different in two groups ($P < 0.05$). Immune related functions such

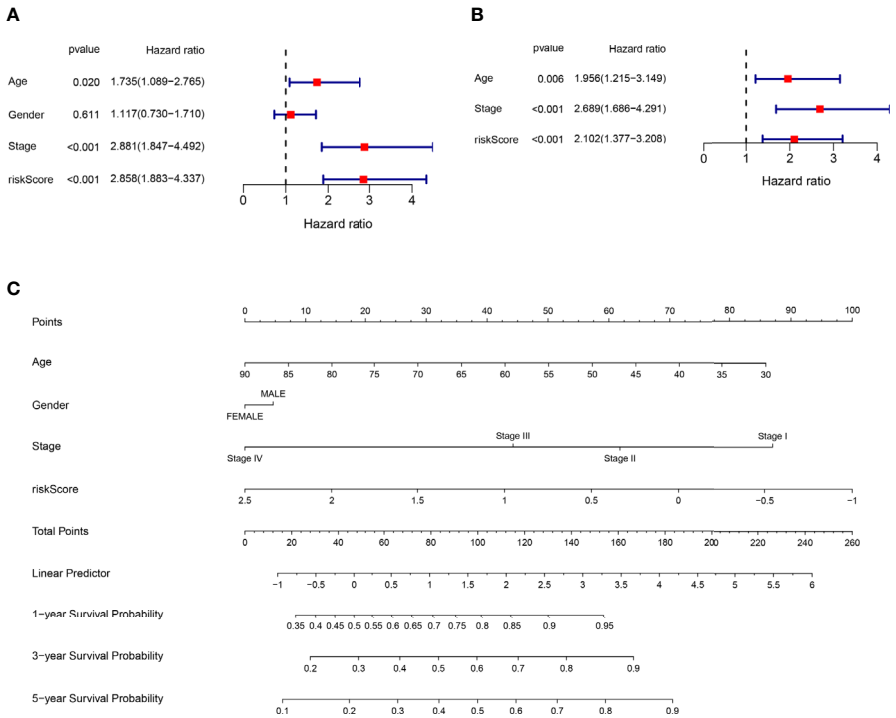

FIGURE 4 | Riskscore and other clinical pathology characters synergistically predicted the survival probability of colon cancer patients. **(A)** Univariate cox regression analysis of age, gender, stage, and riskscore in the TCGA cohort. Riskscore is significantly associated with the survival of colon cancer patients. **(B)** Multivariate cox regression analysis of age, stage, and riskscore in the TCGA cohort. Riskscore is an independent prognostic factor for the survival of colon cancer patients. **(C)** Nomogram for the prediction of 1-, 3-, and 5-year survival probability in patients with colon cancer.

as APC co stimulation, APC co inhibition, CCR, checkpoint, T cell co stimulation, T cell co inhibition, and so on, were also different in two groups (**Figure 5C**). In summary, the immune status in high-risk and low-risk groups were totally different, which can be further elucidated to boost tumor immunotherapy in colon cancer. We used the Pearson's correlation coefficient to grasp the relationship between STING and ferroptosis as showed in **Figure 5D**. The predicted pathways between STING related genes and our model genes based on the TCGA data were showed in **Figure 5E**. **Figure 5F** presented the possible protein-protein interactions between STING and ferroptosis at the protein level.

Experimental Support for the Five Gene Prognostic Signature in Colon Cancer

In the HPA database, we found that the expression of AKR1C1, ALOX12, and CARS1 in colon cancer tissue is higher than normal tissue (**Figures 6A–C**) and the expression of FDFT1 in colon cancer tissue is lower than normal tissue by immunohistochemistry (**Figure 6D**), which is consistent with our results. We also performed immunohistochemistry against AKR1C1 and CARS1 in the colon cancer tissues and adjacent tissues. The representative images of immunohistochemistry were indicated in **Figures 7A**, **B**. **Figure 7C** showed the expression of AKR1C1 and CARS1 were higher in tumor tissues (****, P<0.0001).

DISCUSSION

Our study built a ferroptosis related genes prognosis model in CC, which aimed to predict survival probability of patients with CC and provide clues for further studying the role of ferroptosis in colon cancer. The model consisted of five genes, AKR1C1, ALOX12, CARS1, FDFT1, and ATP5MC3.

Based on the DEG and prognosis related genes in CC, we selected five genes to conduct LASSO regression analysis. And all the five genes were included in the terminal model with corresponding coefficients, then we calculated the riskscore of each CC patients according to the previously mentioned formula. The Kaplan-Meier curves indicated the statistically significant survival probability between the high-risk and low-risk groups in TCGA and GEO cohort, which preliminary proofed the validity of the model to predict the risk in CC. What's more, the AUC at 1, 2 and 3 years were 0.668, 0.678, and 0.686 respectively in TCGA cohort, which further illustrated the accuracy of the model. However, the AUC in GEO cohort was not optimal, which might attribute to the

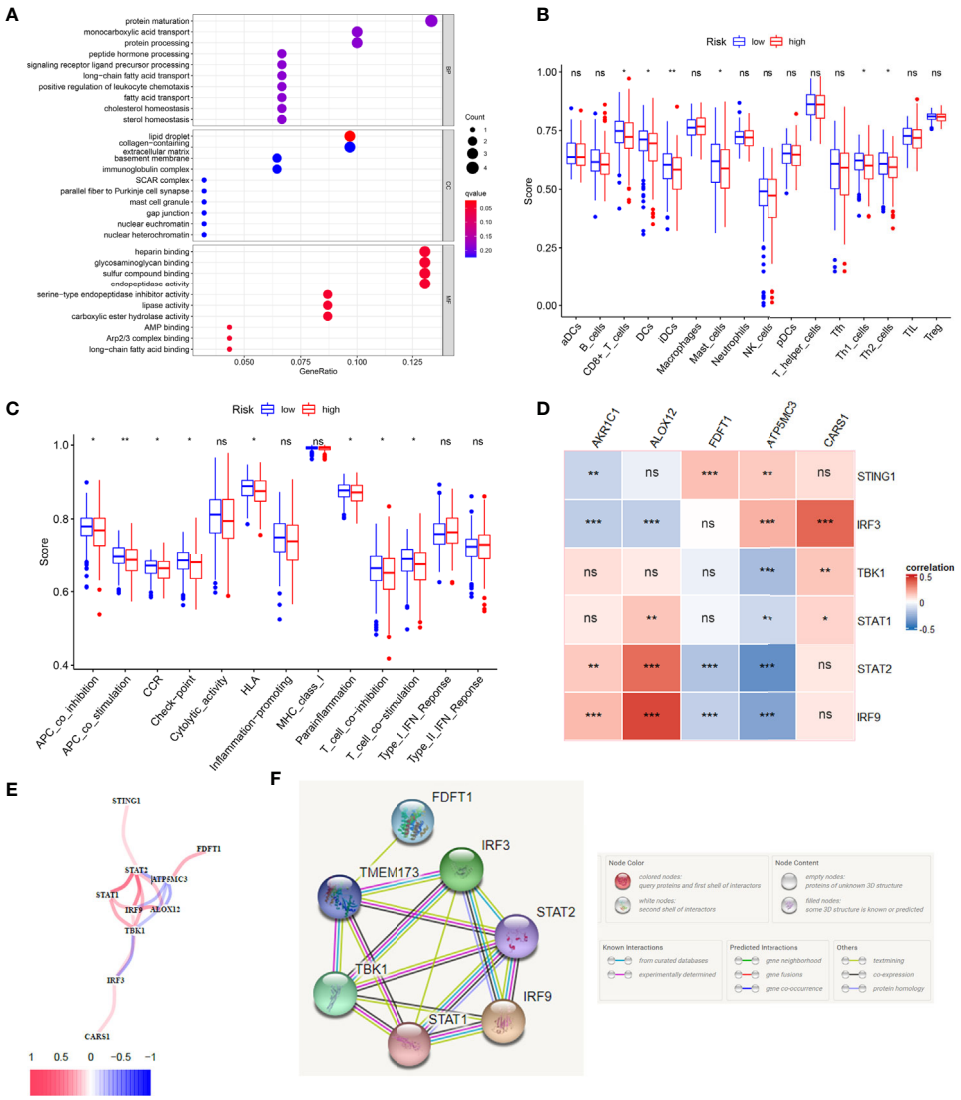

FIGURE 5 | The immune status difference between high risk and low risk in colon cancer patients. **(A)** The GO enrichment analysis between high-risk and low-risk groups in colon cancer. **(B)** The immune cell between high-risk and low-risk groups in colon cancer; *P <0.05; **P <0.01; ***P <0.001. **(C)** The immune related function between high-risk and low-risk groups in colon cancer; *P <0.05; **P <0.01; ***P <0.001. **(D)** The correlation between STING related genes and ferroptosis related genes in CC using the Pearson coefficient; *P <0.05; **P <0.01; ***P <0.001; ns, no significance. **(E)** The predicted gene interactions between STING related genes and ferroptosis related genes based on the RNA-seq data of TCGA cohort in CC. **(F)** The protein-protein interactions (PPI) network of above genes.

heterogeneity of patients and needs other larger population to test the model. PCA and t-SNE analysis demonstrated that the patients in high- and low-risk groups were in two dimensions respectively, indicating that the model could accurately distinguish high- and low-risk patients. Furthermore, the riskscore was an independent prognostic factor in CC. The nomogram combined the known risk factors and riskscore to predict the survival probability at 1, 3, and 5 years of CC, whose prognosis efficacy was prior to the single factor. Immunohistochemistry images of the four genes from HPA database were consistent with the bioinformatics results. We also collected 54 pairs of the tumor issues and adjacent tissues to perform IHC. Results showed the expression of AKR1C1 and CARS1 were different in tumor tissues and adjacent tissues. In summary, our model is a good signature to help to predict the prognosis of CC patients.

Aldo-keto reductases (AKRs) play vital roles in the reductive metabolism (26). The overexpression of AKR1C1 involved in the resistance of cis-diamminedichloroplatinum (CDDP) in colon cancers (27). In melanoma, upregulated AKR1C1 resulted in ferroptotic cell death resistance (28), which perhaps could explain the CDDP resistance in colon cancer and pointed out a possible strategy to overcome CDDP resistance in CC. Besides, AKR1C1 inhibitors could be a therapy medicine to sensitive

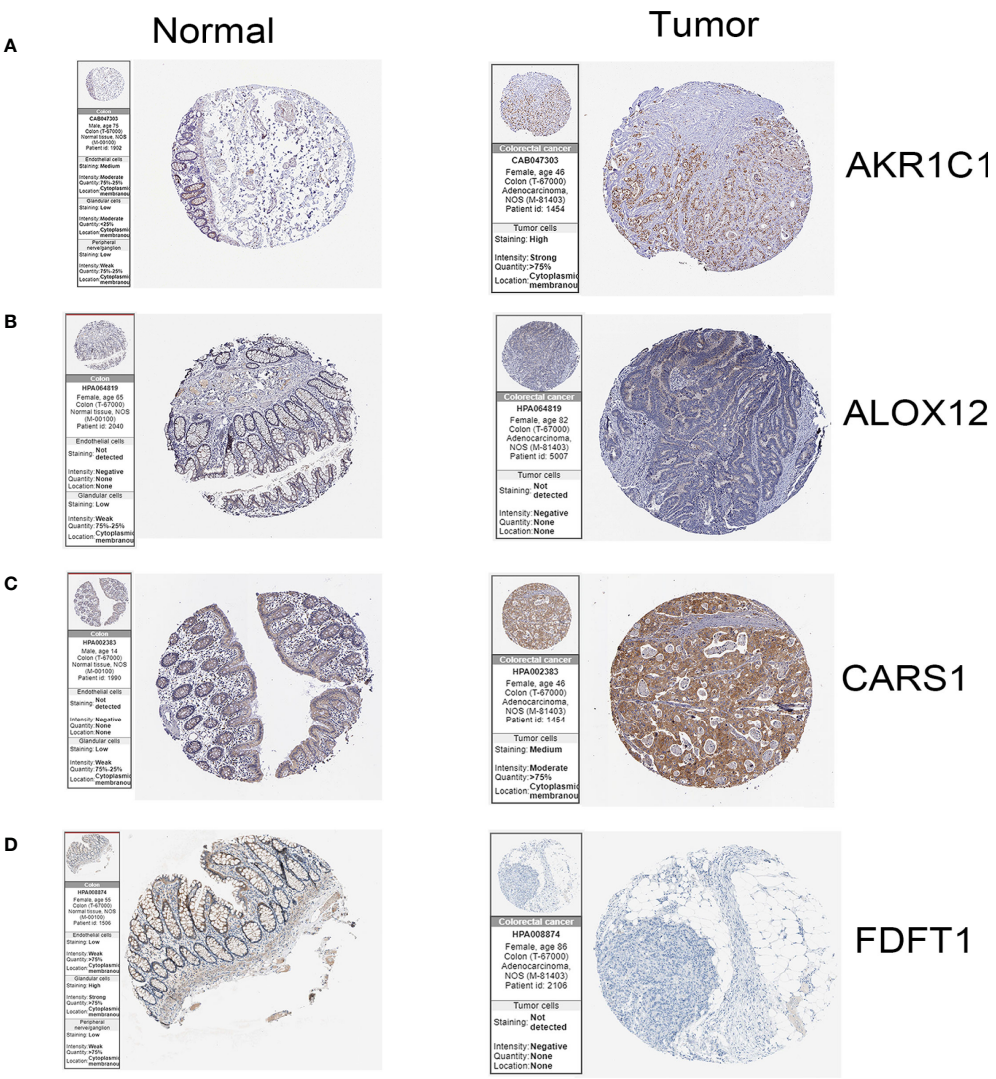

FIGURE 6 | The immunohistochemistry images of related genes from HPA database in normal and cancer tissues.**(A)** The expression levels of AKR1C1 in normal tissues and colon cancer tissue. **(B)** The expression levels of ALOX12 in normal tissues and colon cancer tissue. **(C)** The expression levels of CARS1 in normal tissues and colon cancer tissue. **(D)** The expression levels of FDFT1 in normal tissues and colon cancer tissue.

ferroptosis in colon cancer. Genetic variability in arachidonate lipoxygenase (ALOXs), such as the polymorphisms of ALOX12, may influence risk of colorectal cancer (29). ALOX12 inactivation eliminated p53-mediated ferroptosis in Eμ-Myc lymphoma models (30). Thus, ALOX12 can be a possible target to regulate risk of colon cancer. A study showed that downregulation of FDFT1 was correlated with malignant progression and poor prognosis in colorectal cancer. Somatic variants revealed FDFT1 that frequently mutated only in the liver metastatic patients and targeting FDFT1 could be a feasible strategy in colon cancer, especially in the colorectal liver metastatic patients (31). To sum up, the genes in our model played important roles in colon cancer and were worthy for further studies.

To clarify the function of our model deeply, we conducted GO and KEGG enrichment analysis. It was worth noting that differential genes between high- and low-risk groups were related to immune response, which was consistent with the above phenomenon regarding to the crosstalk between immune and ferroptosis. Then we conducted the ssGSEA to compare the immune cells and immune related function in two groups. According to the results, the innate and adaptive related cells and process were statistically significant in two groups, such as $CD8^+$T cells, iDC, and APC co stimulation, which perhaps presented that targeting ferroptosis could change the immune status in colon cancer or boost the immunotherapy in colon cancer. Our previous study showed that STING is a master regulator in the cancer-

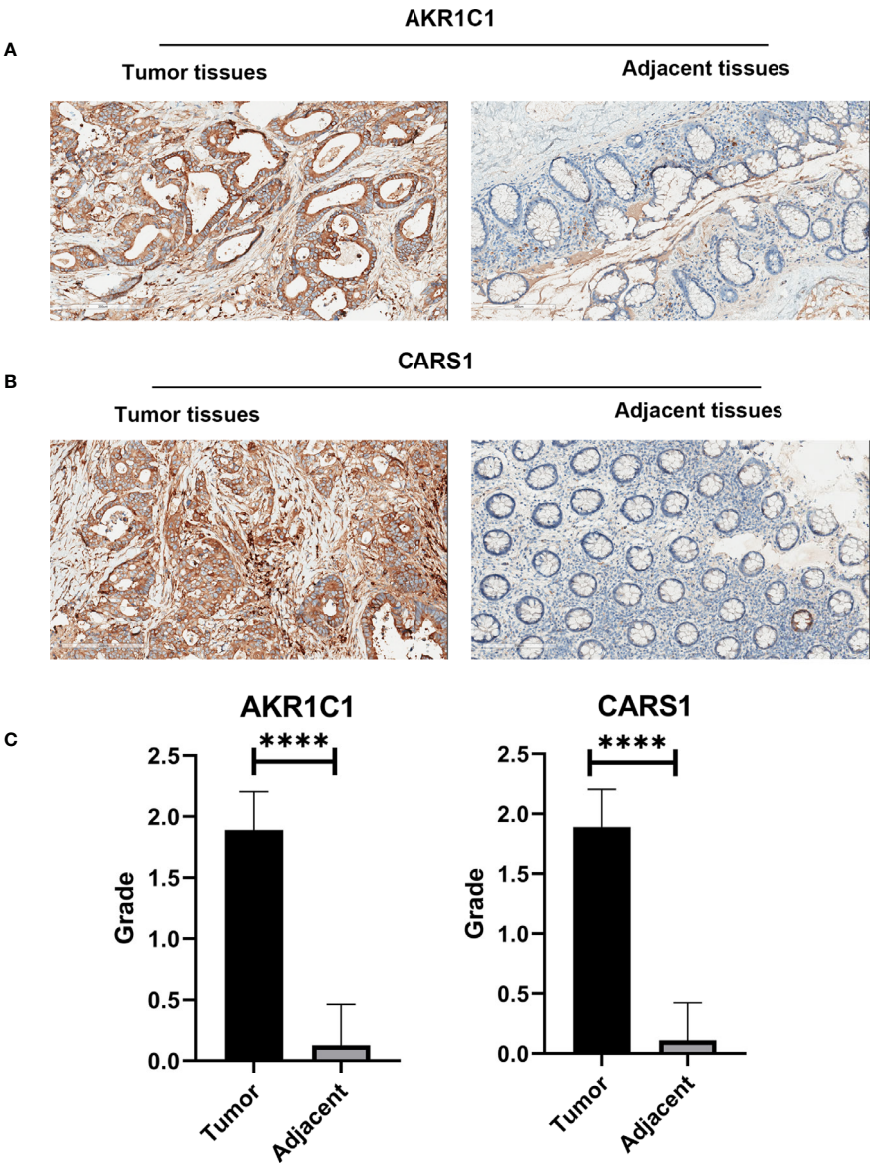

FIGURE 7 | The immunohistochemistry images from wet lab. **(A)** The representative images of AKR1C1 in the tumor tissues and adjacent tissues. **(B)** The representative images of CARS1 in the tumor tissues and adjacent tissues. **(C)** The statistical results of expression of AKR1C1 and CARS1 in the tumor tissues and adjacent tissues; ****P <0.0001.

immunity cycle (14). In this study, we studied the relationship between STING and ferroptosis in CC. We found that the STING related genes were interrelated with ferroptosis in the levels of genes and proteins. However, the exact crosstalk and mechanism of above bioinformatics prediction need verification with well-designed experiments.

In conclusion, we built a prognosis model based on ferroptosis related genes in colon cancer with good prognosis efficacy. We also provide clues to further explore the function of the model genes and crosstalk between immune and ferroptosis to improve immunotherapy for colon cancer.

DATA AVAILABILITY STATEMENT

The original contributions presented in the study are included in the article/**Supplementary Material**. Further inquiries can be directed to the corresponding authors.

ETHICS STATEMENT

All patients in this study have provided written informed consent for the use of their specimens and information for future investigations according to guidelines of the ethics committee.

AUTHOR CONTRIBUTIONS

TZ, YZ, and JN offered main direction and significant guidance of this manuscript. JN, DS, SL, SZ, XZ, FX, JS, CL, TW, XS, MZ, QZ, and SNL analyzed data and illustrated the figures for the manuscript. HM performed the immunohistochemistry. JN, SL, and SZ wrote the paper with input from all authors. All authors contributed to the article and approved the submitted version.

FUNDING

This work was supported by 'Tou Yan' Action of Heilongjiang province, the National Youth Talent Support Program of China (W03070060), the National Natural Science Foundation of China (No. 81872435, No. 81672930 and No. U20A20377 to TZ), and the Excellent Youth Foundation of Heilongjiang Province (No. JQ2019H003). The funders had no role in study design, data collection and analysis, decision to publish, or preparation of the manuscript.

ACKNOWLEDGMENTS

We sincerely thank Jiayi Gao and Xinxin Liang for their technical assistance in the work.

SUPPLEMENTARY MATERIAL

The Supplementary Material for this article can be found online at: https://www.frontiersin.org/articles/10.3389/fonc.2021.654076/full#supplementary-material

Supplementary Figure 1 | The comparison of the number of dead and alive patients between the high- and low-risk groups in two cohorts. Two bar charts indicated that the numbers of dead and alive patients were statistical different in the high and low risk groups in the TCGA (P<0.001) and GEO cohorts (P<0.01). This figure is related to **Figures 2C, D**.

Supplementary Figure 2 | The survival plot, forest map and Lasso results of CD44, GCLC and MT1G in colon cancer. **(A–C)** The expression of CD44, GCLC and MT1G were not related to survival in colon cancer. **(D)** The forest map showed CD44, GCLC and MT1G were not prognostic factors in colon cancer. **(E, F)** The partial likelihood deviance and LASSO coefficient profiles of CD44, GCLC and MT1G were showed. Results showed CD44, GCLC and MT1G should not be included in the model, although they were significant DEGs.

Supplementary Figure 3 | The riskscore was an independent prognostic factor for colon cancer patients in the GEO cohort. **(A)** Univariate cox regression analysis of age, gender, stage and riskscore in the GEO cohort. Riskscore is significantly associated with the survival of colon cancer patients (P<0.01). **(B)** Multivariate cox regression analysis of age, stage and riskscore in the GEO cohort. Riskscore is an independent prognostic factor for the survival of colon cancer patients (P<0.01).

Supplementary Figure 4 | The KEGG enrichment analysis in colon cancer. The KEGG enrichment analysis between high-risk and low-risk groups in colon cancer.

REFERENCES

1. Bray F, Ferlay J, Soerjomataram I, Siegel RL, Torre LA, Jemal A. Global Cancer Statistics 2018: GLOBOCAN Estimates of Incidence and Mortality Worldwide for 36 Cancers in 185 Countries. *CA: Cancer J Clin* (2018) 68 (6):394–424. doi: 10.3322/caac.21492
2. Bray F, Ferlay J, Soerjomataram I, Siegel RL, Torre LA, Jemal A. Erratum: Global Cancer Statistics 2018: GLOBOCAN Estimates of Incidence and Mortality Worldwide for 36 Cancers in 185 Countries. *CA: Cancer J Clin* (2020) 70(4):313. doi: 10.3322/caac.21609.
3. Lizardo DY, Kuang C, Hao S, Yu J, Huang Y, Zhang L. Immunotherapy Efficacy on Mismatch Repair-Deficient Colorectal Cancer: From Bench to Bedside. *Biochim Biophys Acta Rev Cancer* (2020) 1874(2):188447. doi: 10.1016/j.bbcan.2020.188447
4. Dekker E, Tanis PJ, Vleugels JLA, Kasi PM, Wallace MB. Colorectal Cancer. *Lancet (London England)* (2019) 394(10207):1467–80. doi: 10.1016/s0140-6736(19)32319-0
5. Nie J, Lin B, Zhou M, Wu L, Zheng T. Role of Ferroptosis in Hepatocellular Carcinoma. *J Cancer Res Clin Oncol* (2018) 144(12):2329–37. doi: 10.1007/s00432-018-2740-3
6. Mbaveng AT, Ndontsa BL, Kuete V, Nguekeu YMM, Çelik İ, Mbouangouere R, et al. A Naturally Occuring Triterpene Saponin Ardisiacrispin B Displayed Cytotoxic Effects in Multi-Factorial Drug Resistant Cancer Cells Via Ferroptotic and Apoptotic Cell Death. *Phytomedicine* (2018) 43:78–85. doi: 10.1016/j.ejmech.2018.08.036
7. Mbaveng AT, Fotso GW, Ngnintedo D, Kuete V, Ngadjui BT, Keumedjio F, et al. Cytotoxicity of Epunctanone and Four Other Phytochemicals Isolated From the Medicinal Plants Garcinia Epunctata and Ptycholobium Contortum Towards Multi-Factorial Drug Resistant Cancer Cells. *Phytomedicine* (2018) 48:112–9. doi: 10.1016/j.phymed.2018.03.035
8. Nikolova B, Semkova S, Tsoneva I, Stoyanova E, Lefterov P, Lazarova D, et al. Redox-Related Molecular Mechanism of Sensitizing Colon Cancer Cells to Camptothecin Analog Sn38. *Anatomical Rec (Hoboken NJ 2007)* (2020) 40 (9):5159–70. doi: 10.1002/ar.24378
9. Chapkin RS, Navarro SL, Hullar MAJ, Lampe JW. Diet and Gut Microbes Act Coordinately to Enhance Programmed Cell Death and Reduce Colorectal Cancer Risk. *Digest Dis Sci* (2020) 65(3):840–51. doi: 10.1016/j.phymed.2017.12.016
10. Malfa GA, Tomasello B, Acquaviva R, Genovese C, La Mantia A, Cammarata FP, et al. Betula etnensis Raf. (Betulaceae) Extract Induced HO-1 Expression and Ferroptosis Cell Death in Human Colon Cancer Cells. *Int J Mol Sci* (2019) 20(11):2723. doi: 10.3390/ijms20112723
11. Park S, Oh J, Kim M, Jin EJ. Bromelain Effectively Suppresses Kras-mutant Colorectal Cancer by Stimulating Ferroptosis. *Anim Cells Syst* (2018) 22 (5):334–40. doi: 10.1053/j.gastro.2017.07.036
12. Galluzzi L, Vitale I, Warren S, Adjemian S, Agostinis P, Martinez AB, et al. Consensus Guidelines for the Definition, Detection and Interpretation of Immunogenic Cell Death. *J Immunother Cancer* (2020) 8(1):e000337. doi: 10.1136/jitc-2019-000337
13. Wang W, Green M, Choi JE, Gijón M, Kennedy PD, Johnson JK, et al. Cd8(+) T Cells Regulate Tumour Ferroptosis During Cancer Immunotherapy. *Nature* (2019) 569(7755):270–4. doi: 10.1038/s41586-019-1170-y
14. Zhu Y, An X, Zhang X, Qiao Y, Zheng T, Li X. STING: A Master Regulator in the Cancer-Immunity Cycle. *Mol Cancer* (2019) 18(1):152. doi: 10.1186/s12943-019-1087-y
15. Liang JY, Wang DS, Lin HC, Chen XX, Yang H, Zheng Y, et al. A Novel Ferroptosis-Related Gene Signature for Overall Survival Prediction in Patients With Hepatocellular Carcinoma. *Int J Biol Sci* (2020) 16(13):2430–41. doi: 10.7150/ijbs.45050
16. Stockwell BR, Friedmann Angeli JP, Bayir H, Bush AI, Conrad M, Dixon SJ, et al. Ferroptosis: A Regulated Cell Death Nexus Linking Metabolism, Redox Biology, and Disease. *Cell* (2017) 171(2):273–85. doi: 10.1016/j.cell.2017.09.021
17. Hassannia B, Vandenabeele P, Vanden Berghe T. Targeting Ferroptosis to Iron Out Cancer. *Cancer Cell* (2019) 35(6):830–49. doi: 10.1016/j.ccell.2019.04.002
18. Bersuker K, Hendricks JM, Li Z, Magtanong L, Ford B, Tang PH, et al. The CoQ Oxidoreductase FSP1 Acts Parallel to GPX4 to Inhibit Ferroptosis. *Nature* (2019) 575(7784):688–92. doi: 10.1038/s41586-019-1705-2

19. Doll S, Freitas FP, Shah R, Aldrovandi M, da Silva MC, Ingold I, et al. FSP1 is a Glutathione-Independent Ferroptosis Suppressor. *Nature* (2019) 575 (7784):693–8. doi: 10.1038/s41586-019-1707-0
20. Tibshirani R. The Lasso Method for Variable Selection in the Cox Model. *Stat Med* (1997) 16(4):385–95. doi: 10.1002/(sici)1097-0258(19970228)16:4<385::aid-sim380>3.0.co;2-3
21. Hänzelmann S, Castelo R, Guinney J. GSVA: Gene Set Variation Analysis for Microarray and RNA-seq Data. *BMC Bioinf* (2013) 14:7. doi: 10.1186/1471-2105-14-7
22. Uhlen M, Zhang C, Lee S, Sjöstedt E, Fagerberg L, Bidkhori G, et al. A Pathology Atlas of the Human Cancer Transcriptome. *Science* (2017) 357 (6352):eaan2507. doi: 10.1126/science.aan2507
23. Uhlén M, Fagerberg L, Hallström BM, Lindskog C, Oksvold P, Mardinoglu A, et al. Proteomics. Tissue-based Map of the Human Proteome. *Sci (New York NY)* (2015) 347(6220):1260419. doi: 10.1126/science.1260419
24. Liu C, Liu R, Wang B, Lian J, Yao Y, Sun H, et al. Blocking IL-17A Enhances Tumor Response to anti-PD-1 Immunotherapy in Microsatellite Stable Colorectal Cancer. *J Immunother Cancer* (2021) 9(1):e001895. doi: 10.1136/jitc2020-001895
25. Liu R, Li Y, Tian L, Shi H, Wang J, Liang Y, et al. Gankyrin Drives Metabolic Reprogramming to Promote Tumorigenesis, Metastasis and Drug Resistance Through Activating β-Catenin/c-Myc Signaling in Human Hepatocellular Carcinoma. *Cancer Lett* (2019) 443:34–46. doi: 10.1016/j.canlet.2018.11.030
26. Ebert B, Kisiela M, Wsól V, Maser E. Proteasome Inhibitors MG-132 and Bortezomib Induce AKR1C1, Akr1c3, AKR1B1, and AKR1B10 in Human Colon Cancer Cell Lines SW-480 and HT-29. *Chem-Biol Interact* (2011) 191 (1-3):239–49. doi: 10.1016/j.cbi.2010.12.026
27. Matsunaga T, Hojo A, Yamane Y, Endo S, El-Kabbani O, Hara A. Pathophysiological Roles of Aldo-Keto Reductases (AKR1C1 and AKR1C3) in Development of Cisplatin Resistance in Human Colon Cancers. *Chem-Biol Interact* (2013) 202(1-3):234–42. doi: 10.1016/j.cbi.2012.09.024
28. Gagliardi M, Cotella D, Santoro C, Corà D, Barlev NA, Piacentini M, et al. Aldo-Keto Reductases Protect Metastatic Melanoma From ER Stress Independent Ferroptosis. *Cell Death Dis* (2019) 10(12):902. doi: 10.1038/s41419-019-2143-7
29. Kleinstein SE, Heath L, Makar KW, Poole EM, Seufert BL, Slattery ML, et al. Genetic Variation in the Lipoxygenase Pathway and Risk of Colorectal Neoplasia. *Genes Chromosomes Cancer* (2013) 52(5):437–49. doi: 10.1002/gcc.22042
30. Chu B, Kon N, Chen D, Li T, Liu T, Jiang L, et al. ALOX12 is Required for p53-mediated Tumour Suppression Through a Distinct Ferroptosis Pathway. *Nat Cell Biol* (2019) 21(5):579–91. doi: 10.1038/s41556-019-0305-6
31. Ma YS, Wu ZJ, Zhang HW, Cai B, Huang T, Long HD, et al. Dual Regulatory Mechanisms of Expression and Mutation Involving Metabolism-Related Genes FDFT1 and UQCR5 During CLM. *Mol Ther Oncolytics* (2019) 14:172–8. doi: 10.1016/j.omto.2019.04.008

Conflict of Interest: The authors declare that the research was conducted in the absence of any commercial or financial relationships that could be construed as a potential conflict of interest.

frontiers in Oncology

ORIGINAL RESEARCH
published: 25 May 2021
doi: 10.3389/fonc.2021.610264

The Prognostic Value of New Index (LANR) Composed of Pre-operative Lymphocytes, Albumin, and Neutrophils in Patients With Resectable Colorectal Cancer

Xinjun Liang[1,2,3†], *Shuang Yao*[1,2,3†], *Ping Lu*[1,2,3], *Yifei Ma*[2,3,4], *Hongli Xu*[1,2,3], *Zhucheng Yin*[1,2,3], *Junjie Hu*[2,3,4], *Yanyan Liu*[5*] and *Shaozhong Wei*[2,3,4*]

[1] Department of Medical Oncology, Tongji Medical College, Hubei Cancer Hospital, Huazhong University of Science and Technology, Wuhan, China, [2] Colorectal Cancer Clinical Research Center of Hubei Province, Wuhan, China, [3] Colorectal Cancer Clinical Research Center of Wuhan, Wuhan, China, [4] Department of Gastrointestinal Surgery, Tongji Medical College, Hubei Cancer Hospital, Huazhong University of Science and Technology, Wuhan, China, [5] Division of Nephrology, Tongji Medical College, Tongji Hospital, Huazhong University of Science and Technology, Wuhan, China

OPEN ACCESS

Edited by:
Jaw-Yuan Wang,
Kaohsiung Medical University Hospital, Taiwan

Reviewed by:
Feng Fan Chiang,
Taichung Veterans General Hospital, Taiwan
Wan-Hsiang Hu,
Kaohsiung Chang Gung Memorial Hospital, Taiwan

***Correspondence:**
Shaozhong Wei
weishaozhong@163.com
Yanyan Liu
liuyy1919@163.com

[†]These authors have contributed equally to this work

Specialty section:
This article was submitted to Gastrointestinal Cancers, a section of the journal Frontiers in Oncology

Received: 25 September 2020
Accepted: 08 February 2021
Published: 25 May 2021

Citation:
Liang X, Yao S, Lu P, Ma Y, Xu H, Yin Z, Hu J, Liu Y and Wei S (2021) The Prognostic Value of New Index (LANR) Composed of Pre-operative Lymphocytes, Albumin, and Neutrophils in Patients With Resectable Colorectal Cancer. Front. Oncol. 11:610264. doi: 10.3389/fonc.2021.610264

Background: Inflammatory factors and nutritional status are critical to the prognosis of colorectal cancer patients. This study aimed to investigate the prognostic value of the combination of preoperative lymphocytes, albumin, and neutrophils (LANR) in patients with resectable colorectal cancer.

Methods: A total of 753 patients with pathologically diagnosed primary colorectal cancer were included in the study. The value of LANR was defined as follows: LANR, lymphocyte × albumin/neutrophil. The ROC curve, subgroup analysis and Cox proportional hazard regression analysis were used to assess the prognostic value of LANR in overall survival and progression-free survival.

Results: The median age of the patients was 60 years (range 52–67 years). In overall survival, the area under the curve of LANR was 0.6276, and the HR (95% CI) was 0.551 (0.393–0.772). And in progression-free survival, the area under the curve of LANR was 0.5963, and the HR (95% CI) was 0.697 (0.550–0.884). The results indicate that preoperative LANR may be a reliable predictor of overall and progression-free survival in resectable colorectal cancer patients.

Conclusions: LANR is an important prognostic indicator for patients with resectable colorectal cancer, and it can also provide a reference for clinicians and patients to choose a treatment plan.

Keywords: lymphocytes, albumin, neutrophils, colorectal cancer, prognosis

INTRODUCTION

Colorectal cancer (CRC) is an important public health problem. In 2018, there were more than 1.8 million new cases of colorectal cancer and 881,000 deaths worldwide, accounting for about one-tenth of global cancer incidence and deaths. And the incidence of colorectal cancer ranks third and the mortality rate ranks second (1). From a clinical perspective, surgery

has been established as the main treatment for colorectal cancer (2). Although advances in medical treatment have gradually improved the survival of patients (3). In fact, even after surgery, the prognosis of colorectal cancer is far from satisfactory (4, 5). Therefore, finding more effective biomarkers to predict the prognosis of colorectal cancer becomes particularly important.

With the continuous development of tumor prognosis research, more and more evidence indicates the role of inflammatory factors and nutritional status in cancer prognosis (6–8). Systemic inflammatory factors, such as lymphocytes (9), monocytes (10) and neutrophils (11), and blood biochemical indicators related to nutritional status, such as C-reactive protein levels (CRP) (12) and albumin levels (ALB) (13), are valuable prognostic indicators for cancers including colorectal cancer. In addition, studies have shown that the integration of these biochemical indicators such as the modified Glasgow Prognosis Score (mGPS) (14), C-reactive protein to albumin ratio (CAR) (15, 16), and neutrophil to lymphocyte ratio (NLR) (17) can effectively improve the accuracy of cancer prognosis prediction.

However, the prognostic significance of the combination of lymphocyte, albumin, and neutrophil (LANR) in colorectal cancer has not been well-investigated to date. Therefore, in this study, we retrospectively analyzed the preoperative blood biochemical indicators of 753 colorectal cancer patients, and systematically evaluated the survival prognostic value of LANR.

MATERIALS AND METHODS

Patient Cohort

We retrospectively collected 829 patients with pathologically diagnosed primary colorectal cancer at Hubei Cancer Hospital from January 2013 to December 2016. The exclusion criteria were as follows: (1) having history of malignant tumors; (2) having incomplete clinical data; (3) having concurrent malignant tumors other than colorectal cancer; or (4) having other diseases with serious impacts on prognosis, such as ischemic heart disease and stroke. Based on the exclusion criteria, we eventually included 753 patients with colorectal cancer in our study (**Supplementary Figure 1**). Tumor stage was determined based on the Eighth Edition of the American Joint Committee on Cancer (AJCC) Cancer Staging Manual (18). The study was supported by the Ethics Committee and Institutional Review Board of Hubei Cancer Hospital. And all patients provided informed consent.

Data Collection

We collected the clinicopathological information and preoperative blood biochemical indicators of patients with colorectal cancer through electronic and paper medical records from the hospital. Such as gender, age, tumor size, vascular tumor thrombus, nerve invasion, circumferential margin, radiotherapy, chemotherapy, tumor location, TNM stage, differentiation, ALB, lymphocyte, and neutrophil. Based on previous studies (19–22), we found that ALB, lymphocyte, and neutrophil were key biochemical indicators related to tumor prognosis. And we also used these three indicators to construct a new prognostic marker-LANR, which was defined as Lymphocyte × Albumin/Neutrophil. The study follow-up until August 2019. The overall survival (OS) was set as the first outcome and progression-free survival (PFS) as the secondary outcome. The PFS was defined as the time from the date of tumor resection to the date of cancer recurrence, metastasis, death, or the end of follow-up whichever came first, and the OS was calculated as the time from the date of tumor resection to the date of death or the end of follow-up.

Statistical Analysis

The continuous variables were expressed as mean ± standard deviation ($\overline{X} \pm$ SD) or median (interquartile range), and the categorical variables were presented by the number of cases (percentage). Student's *t*-test or Wilcoxon test was used to compare differences between groups of continuous variables. Chi-square or Fisher's exact tests were used to evaluate categorical variables. By using the inflection point as the cut-offs, the receiver operating characteristic (ROC) curve was used to convert continuous variables (albumin, neutrophils, lymphocytes, and LANR) into dichotomous variables. Kaplan–Meier survival curves and log-rank test were used to compare the survival difference between groups classified by dichotomized biochemical indicators. Cox proportional hazard regression model was used for univariate and multivariate regression analysis. Statistically significant variables ($P < 0.05$) in univariate analysis were included in multivariate analysis. Subgroup analysis were performed to show the prognostic association between patients with different characteristics and the new index, and the results were shown in the forest plots (23). Statistical analyses were performed using SAS 9.4 (SAS Institute Inc, Cary, North Carolina, USA) and R 3.5.1 (R Foundation for Statistical Computing, Vienna, Austria). All analyses were two-sided, and $P < 0.05$ were considered statistically significant.

Data Availability Statement

The datasets used and/or analyzed during the current study are available from the corresponding author on reasonable request.

RESULTS

Patient Characteristics

A total of 753 patients with colorectal cancer were included in this study. The demographic and clinicopathological characteristics are shown in **Table 1**. There were 280 females (37.18%) and 473 males (62.82%). The median age of the patients was 60 years (range 52–67 years). There were 84 patients (11.16%) in stage I, 253 (33.60%) in stage II, 274 (36.39%) in stage III, and 142 (18.86%) in stage IV. Of these patients, 452 (60.03%) had rectal tumors, and 301 (39.97%) had colon tumors. A total of 292 (38.78%) patients progressed and 145 patients (19.26%) died. The study's median progression-free survival was 63.47 months, and the median follow-up time was 37.03 months.

Prognostic Value of LANR in Overall Survival

The areas under the ROC curves and inflection points of albumin, neutrophils, lymphocyte counts, and LANR for OS

TABLE 1 | Baseline clinicopathological characteristics of colorectal cancer patients.

		Disease progression		P^*	Death		P^*
		Without (n = 461) (%)	With (n = 292) (%)		No (N = 608) (%)	Yes (N = 145) (%)	
Age (yr)[a]		60 (51–67)	60.5 (53–67)	0.873	59 (51–67)	63 (55–68)	0.004
Sex	Male	283 (61.39)	190 (65.07)	0.316	377 (62.01)	96 (66.21)	0.39
	Female	178 (38.61)	102 (34.93)		231 (37.99)	49 (33.79)	
Tumor location	Colon	179 (38.83)	122 (41.78)	0.446	237 (38.98)	64 (44.14)	0.259
	Rectum	282 (61.17)	170 (58.22)		371 (61.02)	81 (55.86)	
TNM stage	I	73 (15.84)	11 (3.77)	<0.001	81 (13.32)	3 (2.07)	<0.001
	II	195 (42.30)	58 (19.86)		238 (39.14)	15 (10.34)	
	III	164 (35.57)	110 (37.67)		216 (35.53)	58 (40.00)	
	IV	29 (6.29)	113 (38.70)		73 (12.01)	69 (47.59)	
Tumor size (cm)	$d < 2$	12 (2.60)	2 (0.68)	0.160	12 (1.97)	2 (1.38)	0.832
	$2 \leq d < 5$	315 (68.33)	201 (68.84)		418 (68.75)	98 (67.59)	
	$d \geq 5$	134 (29.07)	89 (30.48)		178 (29.28)	45 (31.03)	
Differentiation	Low	45 (9.76)	58 (19.86)	<0.001	72 (11.84)	31 (21.38)	0.004
	Medium	358 (77.66)	214 (73.29)		467 (76.81)	105 (72.41)	
	High	58 (12.58)	20 (6.85)		69 (11.35)	9 (6.21)	
Circumferential margin	No	459 (99.57)	280 (95.89)	<0.001	602 (99.01)	137 (94.48)	0.002
	Yes	2 (0.43)	12 (4.11)		6 (0.99)	8 (5.52)	
Vascular tumor thrombus	No	342 (74.19)	187 (64.04)	0.003	436 (71.71)	93 (64.14)	0.086
	Yes	119 (25.81)	105 (35.96)		172 (28.29)	52 (35.86)	
Nerve invasion	No	375 (81.34)	208 (71.23)	0.002	482 (79.28)	101 (69.66)	0.015
	Yes	86 (18.66)	84 (28.77)		126 (20.72)	44 (30.34)	
Chemotherapy	No	173 (37.53)	57 (19.52)	<0.001	192 (31.58)	38 (26.21)	0.229
	Yes	288 (62.47)	235 (80.48)		416 (68.42)	107 (73.79)	
Radiotherapy	No	444 (96.31)	265 (90.75)	0.002	575 (94.57)	134 (92.41)	0.326
	Yes	17 (3.69)	27 (9.25)		33 (5.43)	11 (7.59)	
ALB (G/L)[a]		42.2 (38.8–45.0)	41.6 (38.0–44.3)	0.032	42.20 (38.95–44.90)	40.44 (37.00–43.40)	<0.001
Lym (10^9/L)[a]		1.47 (1.15–1.83)	1.33 (1.00–1.72)	0.001	1.46 (1.13–1.83)	1.29 (0.94–1.65)	<0.001
Neu (10^9/L)[a]		3.32 (2.65–4.47)	3.89 (2.90–4.98)	0.001	3.48 (2.68–4.60)	3.93 (2.89–5.14)	0.012

Lym, lymphocyte; ALB, albumin; Neu, neutrophils.

**P-values were calculated by the Student's t-test or Wilcoxon test for continuous variables, and the Chi-square test for categorical variables, respectively.*

[a]Age, ALB, Lym, and Neu are continuous variables, the others (Sex, Tumor Location, TNM stage, Tumor size, Differentiation, Circumferential margin, Vascular tumor thrombus, Nerve invasion, Chemotherapy, and Radiotherapy) are categorical variables.

are listed in **Table 2**. According to the ROC curve, we found that the area under the curve of LANR was the best at 0.6276 (**Supplementary Figure 2**). We divided LANR into high-level (n = 418, 55.51%) and low-level (n = 335, 44.49%) groups based on cut-off values (**Supplementary Table 1**), and the Kaplan-Meier survival curve showed that patients with high-level LANR had longer overall survival (**Figure 1**). Univariate analysis revealed that TNM stage, differentiation, circumferential margin, nerve invasion, albumin, neutrophils, lymphocytes, and LANR all showed significant association with OS (all P < 0.05; **Table 2**). Multivariate analysis showed that high levels of albumin, neutrophils, lymphocytes and LANR had 0.681 (95% CI: 0.476–0.974), 1.512 (95% CI: 1.085–2.107), 0.634 (95% CI: 0.445–0.903), and 0.551 (95% CI: 0.393–0.772)-fold risk of death (**Table 2**). LANR presented significant associations with OS among patients in different genders, age (<65 yr), tumor locations (colon), differentiation (medium), and TNM stages (III/IV) (**Supplementary Figure 3**). Combining the area under the curve and the results of multivariate cox regression, we found that LANR is a valuable new prognostic indicator in overall survival.

Prognostic Value of LANR in Progression-Free Survival

The areas under the ROC curves and inflection points of albumin, neutrophils, lymphocyte counts, and LANR for PFS are listed in **Table 3**. According to the ROC curve, we found that the area under the curve of LANR was the best at 0.5963 (**Supplementary Figure 4**). We divided LANR into high-level (n = 367, 48.74%) and low-level (n = 386, 51.26%) groups based on cut-off values (**Supplementary Table 2**), and the Kaplan-Meier survival curve showed that patients with high-level LANR had longer progression-free survival (**Figure 2**). Univariate analysis revealed that TNM stage, differentiation, circumferential margin,

TABLE 2 | Univariate and multivariate Cox regression analysis of overall survival in patients with colorectal cancer.

	AUC	Cut-Point	Univariate		Multivariate*	
			HR (95% CI)	*P*	HR (95% CI)	*P*
ALB (G/L)	0.5968	42.8	0.562 (0.395–0.800)	0.0014	0.681 (0.476–0.974)	0.0355
Neu (10^9/L)	0.5672	4.42	1.706 (1.226–2.373)	0.0015	1.512 (1.085–2.107)	0.0147
Lym (10^9/L)	0.6021	1.50	0.510 (0.359–0.726)	0.0002	0.634 (0.445–0.903)	0.0116
LANR	0.6276	15.3	0.475 (0.341–0.664)	<0.0001	0.551 (0.393–0.772)	0.0005
TNM stage#			6.923 (4.223–11.349)	<0.0001	6.157 (3.745–10.125)	<0.0001
Age			1.488 (1.070–2.068)	0.0181	1.318 (0.944–1.841)	0.1050
Differentiation			0.564 (0.407–0.781)	0.0006	0.641 (0.462–0.889)	0.0077
Circumferential margin			3.968 (1.942–8.109)	0.0002	4.295 (2.077–8.881)	<0.0001
Nerve invasion			1.641 (1.150–2.341)	0.0063	1.625 (1.139–2.318)	0.0074

*HR, Hazard Ratio; CI, Confidence Interval; AUC, Area under the ROC Curve; Lym, lymphocyte; ALB, albumin; Neu, neutrophils; LANR, Lym*Alb/Neu.*
**Multivariate cox regression models included age, TNM stage, differentiation, circumferential margin, nerve invasion, and the clinical indicators for mutual adjustment.*
#*TNM Stage adopted binary classification (I/II vs. III/IV).*
Reference group: TNM (I/II); Differentiation (Low); Circumferential margin (No); Nerve invasion (No).

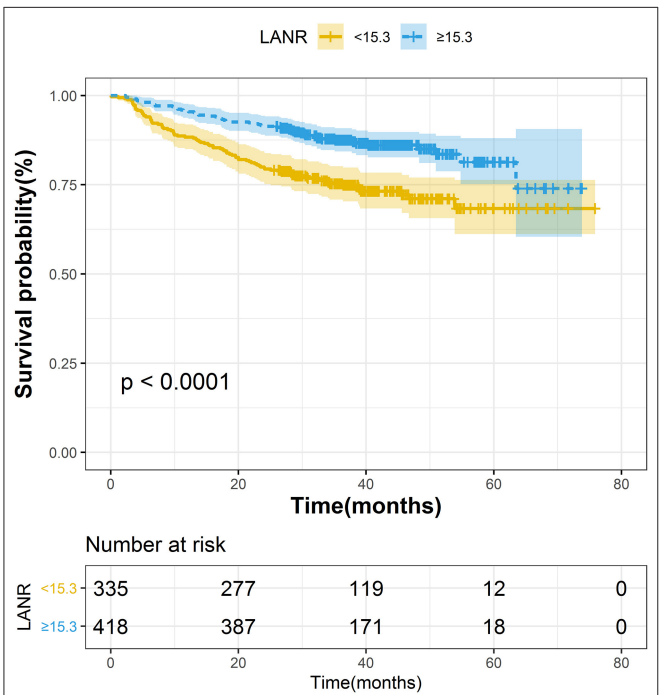

FIGURE 1 | The Kaplan–Meier curves for overall survival of colorectal cancer patients based on LANR.

vascular tumor thrombus, nerve invasion, chemotherapy, radiotherapy, albumin, neutrophils, lymphocytes, and LANR all showed significant association with PFS (all $P < 0.05$; **Table 3**). Multivariate analysis showed that high levels of albumin, neutrophils, lymphocytes, and LANR had 0.800 (95% CI: 0.624–1.026), 1.450 (95% CI: 1.141–1.843), 0.727 (95% CI: 0.570–0.926), and 0.697 (95% CI: 0.550–0.884)-fold risk of disease progression (**Table 3**). LANR presented significant associations with PFS among patients in age (≥65 yr), gender (female), tumor locations (rectum), differentiation (medium), and TNM stages (III/IV) (**Supplementary Figure 5**). Combining the area under the curve and the results of multivariate cox regression, we found that LANR is also a valuable new prognostic indicator in 5-year progression-free survival.

DISCUSSION

In this study, we developed a novel indicator—LANR, which was based on lymphocytes, neutrophils, and albumin, and the results showed that the indicator was significantly correlated with the prognosis of colorectal cancer patients. And to our knowledge, this is the first study to investigate the prognostic value of LANR in colorectal cancer patients.

The development of cancer and its response to treatment are strongly influenced by innate and adaptive immunity, which promote or reduces tumorigenesis and may have opposite effects on the outcome of treatment. At the same time, chronic inflammation promote tumor development, progression, metastatic spread and treatment resistance (24). In addition, studies have shown that systemic inflammation is a marker of poor prognosis present in around 20–40% of colorectal cancer patients (25). Neutrophils are the main circulating granulocytes in humans. They reflect the state of host inflammation and are a hallmark of cancer (26). Neutrophils are involved in different stages of the carcinogenic process, including tumorigenesis, growth, proliferation, or metastatic spread (27, 28). It promotes tumorigenesis by releasing reactive oxygen species (ROS), reactive nitrogen (RNS), or proteases (29), promotes tumor proliferation by weakening the immune system, and also promotes metastatic spread by inhibiting natural killing function and promoting tumor cell extravasation (30). Studies have shown that neutrophils are associated with poor prognosis (31). And the higher the neutrophil level, the higher the risk of progression and death (20, 32). As one of the main cells of human immunity, lymphocytes can produce an immune response to tumor cells, and the decrease of the lymphocytes

TABLE 3 | Univariate and multivariate cox regression analysis of progression-free survival in patients with colorectal cancer.

	AUC	Cut-Point	Univariate		Multivariate*	
			HR (95%CI)	*P*	HR (95%CI)	*P*
ALB (G/L)	0.5462	43.3	0.730 (0.572–0.931)	0.0113	0.800 (0.624–1.026)	0.0789
Neu (10^9/L)	0.5754	3.47	1.680 (1.326–2.130)	<0.0001	1.450 (1.141–1.843)	0.0024
Lym (10^9/L)	0.5720	1.16	0.657 (0.517–0.835)	0.0006	0.727 (0.570–0.926)	0.0099
LANR	0.5963	16.81	0.597 (0.472–0.755)	<0.0001	0.697 (0.550–0.884)	0.0029
TNM stage#			3.568 (2.721–4.678)	<0.0001	3.243 (2.467–4.263)	<0.0001
Differentiation			0.573 (0.455–0.722)	<0.0001	0.623 (0.493–0.788)	<0.0001
Circumferential margin			3.968 (2.222–7.084)	<0.0001	4.545 (2.533–8.156)	<0.0001
Vascular tumor thrombus			1.527 (1.202–1.940)	0.0005	1.449 (1.139–1.843)	0.0025
Nerve invasion			1.642 (1.273–2.117)	0.0001	1.569 (1.216–2.024)	0.0005
Chemotherapy			2.035 (1.523–2.719)	<0.0001	2.015 (1.506–2.696)	<0.0001
Radiotherapy			2.173 (1.460–3.234)	0.0001	1.925 (1.290–2.871)	0.0013

*HR, Hazard Ratio; CI, Confidence Interval; AUC, Area under the ROC Curve; Lym, lymphocyte; ALB, albumin; Neu, neutrophils; LANR, Lym*Alb/Neu.*
**Multivariate cox regression models included age, TNM stage, differentiation, circumferential margin, vascular tumor thrombus, nerve invasion, chemotherapy, radiotherapy, and the clinical indicators for mutual adjustment.*
#*TNM Stage adopted binary classification (I/II vs. III/IV).*
Reference group: TNM (I/II); Differentiation (Low); Circumferential margin (No); Vascular tumor thrombus (No); Nerve invasion (No); Chemotherapy (No); Radiotherapy (No).

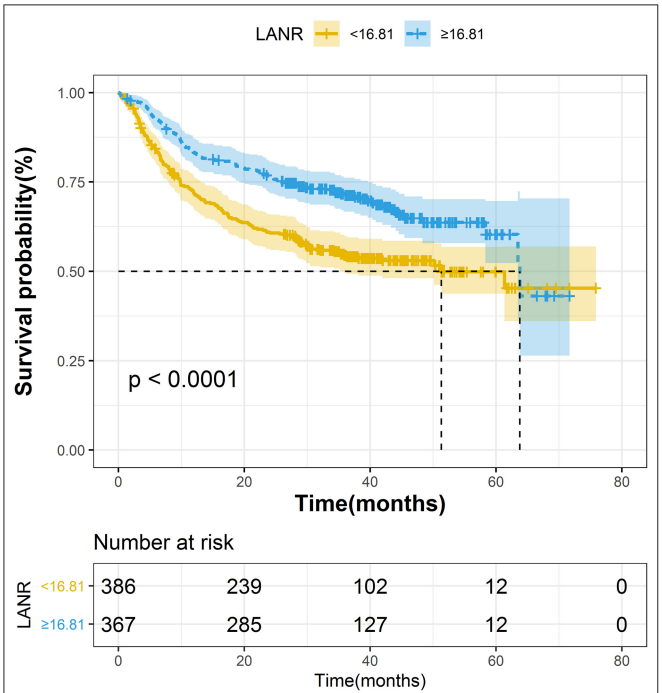

FIGURE 2 | The Kaplan–Meier curves for progression-free survival of colorectal cancer patients based on LANR.

leads to a decrease in the body's ability to inhibit tumors (33). At the same time, lymphocytes participate in cytotoxic cell death and inhibition of tumor cell proliferation and migration (34). As research continues to develop, more and more evidence suggests that lymphocytes play an important role in predicting the prognosis in colorectal cancer (35–37). And high levels of lymphocytes were significantly associated with good tumor behavior and better survival (38). In addition to inflammatory factors, nutritional indicators can also predict complications, recurrence and prognosis in patients with colorectal cancer. Using prognostic nutrition indicators to investigate the nutrition and immune status of patients may be a useful clinical approach (39). Serum albumin is a common indicator of nutritional status (40). Studies have shown that serum albumin levels were significantly related to overall survival (41). And low levels of serum albumin are associated with a poor overall prognosis in patients with colorectal cancer (42, 43). In this study, we combined these valuable indicators to construct a new prognostic indicator that has good prognostic performance for both overall survival (HR: 0.551; 95% CI: 0.393–0.772) and progression-free survival (HR: 0.697; 95% CI: 0.550–0.884). But we also have some limitations. First, the sample size included in the study was relatively small. Second, as a single-center study, the conclusion may be biased. Therefore, a lot of research is needed to further confirm our findings. In this study, we found a new index that is easily available and has good prognostic performance, which will provide a reference for clinicians and patients to choose a treatment method.

DATA AVAILABILITY STATEMENT

The raw data supporting the conclusions of this article will be made available by the authors, without undue reservation.

ETHICS STATEMENT

The study was supported by the Ethics Committee and Institutional Review Board of Hubei Cancer Hospital. And all patients provided informed consent.

AUTHOR CONTRIBUTIONS

SW and YL contributed to the conception and design of the study, reviewed and edited the manuscript, guarantors of this work, who have full access to all the data in the study, and take responsibility for the integrity of the data and the accuracy of the data analysis. XL, SY, PL, YM, HX, ZY, JH, SW, and YL contributed to the acquisition of data, reviewed, and commented on various versions of the manuscript. XL and SY analyzed the data and wrote the first draft of the manuscript. All authors agree to be responsible for all aspects of the work and give final approval for the submission.

FUNDING

This work was supported by the National Key R&D Program of China (Grant No. 2017YFC0908204), the Health commission of Hubei Province scientific research project (Grant Nos. WJ2021Z001 and WJ2019H121), the Natural Science Foundation of Hubei Province (Grant No. 2019ACA135), the applied Basic Research Program of Wuhan Science and Technology Bureau (Grant No. 2020020601012250), the Foundation of Chinese Society of Clinical Oncology (CSCO: Y-QL2019-0351 and Y-HS2019-39).

ACKNOWLEDGMENTS

The authors would like to thank all participants who volunteered to provide data and samples in this study.

SUPPLEMENTARY MATERIAL

The Supplementary Material for this article can be found online at: https://www.frontiersin.org/articles/10.3389/fonc.2021.610264/full#supplementary-material

REFERENCES

1. Bray F, Ferlay J, Soerjomataram I, Siegel RL, Torre LA, Jemal A. Global cancer statistics 2018: GLOBOCAN estimates of incidence and mortality worldwide for 36 cancers in 185 countries. *CA Cancer J Clin.* (2018) 68:394–424. doi: 10.3322/caac.21492
2. Rentsch M, Schiergens T, Khandoga A, Werner J. Surgery for colorectal cancer - trends, developments, and future perspectives. *Visc Med.* (2016) 32:184–91. doi: 10.1159/000446490
3. Zheng C, Jiang F, Lin H, Li S. Clinical characteristics and prognosis of different primary tumor location in colorectal cancer: a population-based cohort study. *Clin Transl Oncol.* (2019) 21:1524–31. doi: 10.1007/s12094-019-02083-1
4. Modest DP, Denecke T, Pratschke J, Ricard I, Lang H, Bemelmans M, et al. Surgical treatment options following chemotherapy plus cetuximab or bevacizumab in metastatic colorectal cancer-central evaluation of FIRE-3. *Eur J Cancer.* (2018) 88:77–86. doi: 10.1016/j.ejca.2017.10.028
5. Peng F, Hu D, Lin X, Liang B, Chen Y, Zhang H, et al. Impact of long-term antihypertensive and antidiabetic medications on the prognosis of post-surgical colorectal cancer: the Fujian prospective investigation of cancer (FIESTA) study. *Aging.* (2018) 10:1166–81. doi: 10.18632/aging.101459
6. Miyamoto Y, Hiyoshi Y, Daitoku N, Okadome K, Sakamoto Y, Yamashita K, et al. Naples prognostic score is a useful prognostic marker in patients with metastatic colorectal cancer. *Dis Colon Rectum.* (2019) 62:1485–93. doi: 10.1097/dcr.0000000000001484
7. Yamamoto M, Saito H, Uejima C, Tanio A, Tada Y, Matsunaga T, et al. Combination of serum albumin and cholinesterase levels as prognostic indicator in patients ith colorectal cancer. *Anticancer Res.* (2019) 39:1085–90. doi: 10.21873/anticanres.13217
8. Hua X, Long ZQ, Huang X, Deng JP, Wen W, He ZY, et al. The preoperative systemic inflammation response index (SIRI) independently predicts survival in postmenopausal women with breast cancer. *Curr Probl Cancer.* (2020) 44:100560. doi: 10.1016/j.currproblcancer.2020.100560
9. Yamamoto M, Saito H, Uejima C, Tanio A, Takaya S, Ashida K, et al. Combined pre- and postoperative lymphocyte count accurately predicts outcomes of patients with colorectal cancer. *Dig Surg.* (2019) 36:487–94. doi: 10.1159/000492340
10. Hu S, Zou Z, Li H, Zou G, Li Z, Xu J, et al. The preoperative peripheral blood monocyte count is associated with liver metastasis and overall survival in colorectal cancer patients. *PLoS ONE.* (2016) 11:e0157486. doi: 10.1371/journal.pone.0157486
11. Zhang H, Liu H, Shen Z, Lin C, Wang X, Qin J, et al. Tumor-infiltrating neutrophils is prognostic and predictive for postoperative adjuvant chemotherapy benefit in patients with gastric cancer. *Ann Surg.* (2018) 267:311–8. doi: 10.1097/sla.0000000000002058
12. Kostner AH, Kersten C, Lowenmark T, Ydsten KA, Peltonen R, Isoniemi H, et al. The prognostic role of systemic inflammation in patients undergoing resection of colorectal liver metastases: C-reactive protein (CRP) is a strong negative prognostic biomarker. *J Surg Oncol.* (2016) 114:895–9. doi: 10.1002/jso.24415
13. Egenvall M, Morner M, Martling A, Gunnarsson U. Prediction of outcome after curative surgery for colorectal cancer: preoperative haemoglobin, C-reactive protein and albumin. *Colorectal Dis.* (2018) 20:26–34. doi: 10.1111/codi.13807
14. Tsuchihashi K, Ito M, Moriwaki T, Fukuoka S, Taniguchi H, Takashima A, et al. Role of predictive value of the modified glasgow prognostic score for later-line chemotherapy in patients with metastatic colorectal cancer. *Clin Colorectal Cancer.* (2018) 17:e687–97. doi: 10.1016/j.clcc.2018.07.004
15. Fan Y, Xiang S, Dai Z, Zou C, Wang X, Gao Z. Prognostic significance of C-reactive protein to albumin ratio in colorectal cancer patients: a meta-analysis. *Int J Colorectal Dis.* (2019) 34:1105–11. doi: 10.1007/s00384-019-03299-x
16. Ishizuka M, Nagata H, Takagi K, Iwasaki Y, Shibuya N, Kubota K. Clinical significance of the C-reactive protein to albumin ratio for survival after surgery for colorectal cancer. *Ann Surg Oncol.* (2016) 23:900–7. doi: 10.1245/s10434-015-4948-7
17. Feliciano EMC, Kroenke CH, Meyerhardt JA, Prado CM, Bradshaw PT, Kwan ML, et al. Association of systemic inflammation and sarcopenia with survival in nonmetastatic colorectal cancer: results from the C SCANS study. *JAMA Oncol.* (2017) 3:e172319. doi: 10.1001/jamaoncol.2017.2319
18. Amin MB, Greene FL, Edge SB, Compton CC, Gershenwald JE, Brookland RK, et al. The eighth edition ajcc cancer staging manual: continuing to build a bridge from a population-based to a more "personalized" approach to cancer staging. *CA Cancer J Clin.* (2017) 67:93–99. doi: 10.3322/caac.21388
19. Wei Y, Xu H, Dai J, Peng J, Wang W, Xia L. Prognostic significance of serum lactic acid, lactate dehydrogenase, and albumin levels in patients with metastatic colorectal cancer. *Biomed Res Int.* (2018) 2018:1804086. doi: 10.1155/2018/1804086
20. Sjoquist KM, Renfro LA, Simes RJ, Tebbutt NC, Clarke S, Seymour MT, et al. Personalizing survival predictions in advanced colorectal cancer: the ARCAD nomogram project. *J Natl Cancer Inst.* (2018) 110:638–48. doi: 10.1093/jnci/djx253
21. Chen JH, Zhai ET, Yuan YJ, Wu KM, Xu JB, Peng JJ, et al. Systemic immune-inflammation index for predicting prognosis of colorectal cancer. *World J Gastroenterol.* (2017) 23:6261–72. doi: 10.3748/wjg.v23.i34.6261
22. Song Y, Yang Y, Gao P, Chen X, Yu D, Xu Y, et al. The preoperative neutrophil to lymphocyte ratio is a superior indicator of prognosis compared with other

inflammatory biomarkers in resectable colorectal cancer. *BMC Cancer.* (2017) 17:744. doi: 10.1186/s12885-017-3752-0
23. Sedgwick P. How to read a forest plot in a meta-analysis. *BMJ.* (2015) 351:h4028. doi: 10.1136/bmj.h4028
24. Shalapour S, Karin M. Immunity, inflammation, and cancer: an eternal fight between good and evil. *J Clin Invest.* (2015) 125:3347–55. doi: 10.1172/jci80007
25. Tuomisto AE, Makinen MJ, Vayrynen JP. Systemic inflammation in colorectal cancer: underlying factors, effects, and prognostic significance. *World J Gastroenterol.* (2019) 25:4383–404. doi: 10.3748/wjg.v25.i31.4383
26. Ocana A, Nieto-Jimenez C, Pandiella A, Templeton AJ. Neutrophils in cancer: prognostic role and therapeutic strategies. *Mol Cancer.* (2017) 16:137. doi: 10.1186/s12943-017-0707-7
27. Swierczak A, Mouchemore KA, Hamilton JA, Anderson RL. Neutrophils: important contributors to tumor progression and metastasis. *Cancer Metastasis Rev.* (2015) 34:735–51. doi: 10.1007/s10555-015-9594-9
28. Coffelt SB, Wellenstein MD, de Visser KE. Neutrophils in cancer: neutral no more. *Nat Rev Cancer.* (2016) 16:431–46. doi: 10.1038/nrc.2016.52
29. Antonio N, Bonnelykke-Behrndtz ML, Ward LC, Collin J, Christensen IJ, Steiniche T, et al. The wound inflammatory response exacerbates growth of pre-neoplastic cells and progression to cancer. *EMBO J.* (2015) 34:2219–36. doi: 10.15252/embj.201490147
30. Spiegel A, Brooks MW, Houshyar S, Reinhardt F, Ardolino M, Fessler E, et al. Neutrophils suppress intraluminal NK Cell-mediated tumor cell clearance and enhance extravasation of disseminated carcinoma cells. *Cancer Discov.* (2016) 6:630–49. doi: 10.1158/2159-8290.cd-15-1157
31. Xiong Y, Wang K. Profiles of immune infiltration in colorectal cancer and their clinical significant: a gene expression-based study. *Cancer Med.* (2018) 7:4496–508. doi: 10.1002/cam4.1745
32. Dimitriou N, Felekouras E, Karavokyros I, Alexandrou A, Pikoulis E, Griniatsos J. Neutrophils to lymphocytes ratio as a useful prognosticator for stage II colorectal cancer patients. *BMC Cancer.* (2018) 18:1202. doi: 10.1186/s12885-018-5042-x
33. Jin LJ, Chen WB, Zhang XY, Bai J, Zhao HC, Wang ZY. Analysis of factors potentially predicting prognosis of colorectal cancer. *World J Gastrointest Oncol.* (2019) 11:1206–17. doi: 10.4251/wjgo.v11.i12.1206
34. Wu Q, Hu T, Zheng E, Deng X, Wang Z. Prognostic role of the lymphocyte-to-monocyte ratio in colorectal cancer: an up-to-date meta-analysis. *Medicine.* (2017) 96:e7051. doi: 10.1097/md.0000000000007051
35. Kong JC, Guerra GR, Pham T, Mitchell C, Lynch AC, Warrier SK, et al. Prognostic impact of tumor-infiltrating lymphocytes in primary and metastatic colorectal cancer: a systematic review and meta-analysis. *Dis Colon Rectum.* (2019) 62:498–508. doi: 10.1097/dcr.0000000000001332
36. Berntsson J, Svensson MC, Leandersson K, Nodin B, Micke P, Larsson AH, et al. The clinical impact of tumour-infiltrating lymphocytes in colorectal cancer differs by anatomical subsite: a cohort study. *Int J Cancer.* (2017) 141:1654–66. doi: 10.1002/ijc.30869
37. Palin RP, Devine AT, Hicks G, Burke D. Association of pretreatment neutrophil-lymphocyte ratio and outcome in emergency colorectal cancer care. *Ann R Coll Surg Engl.* (2018) 100:308–15. doi: 10.1308/rcsann.2017.0232
38. Ko YS, Pyo JS. Clinicopathological significance and prognostic role of tumor-infiltrating lymphocytes in colorectal cancer. *Int J Biol Markers.* (2019) 34:132–8. doi: 10.1177/1724600818817320
39. Tokunaga R, Sakamoto Y, Nakagawa S, Miyamoto Y, Yoshida N, Oki E, et al. Prognostic nutritional index predicts severe complications, recurrence, and poor prognosis in patients with colorectal cancer undergoing primary tumor resection. *Dis Colon Rectum.* (2015) 58:1048–57. doi: 10.1097/dcr.0000000000000458
40. Shibutani M, Maeda K, Nagahara H, Iseki Y, Ikeya T, Hirakawa K. Prognostic significance of the preoperative ratio of C-reactive protein to albumin in Patients with colorectal cancer. *Anticancer Res.* (2016) 36:995–1001
41. Ihara K, Yamaguchi S, Shida Y, Ogata H, Domeki Y, Okamoto K, et al. Poor nutritional status before and during chemotherapy leads to worse prognosis in unresectable advanced or recurrent colorectal cancer. *Int Surg.* (2015). doi: 10.9738/intsurg-d-15-00079.1. [Epub ahead of print].
42. Zhou QP, Li XJ. C-Reactive protein to albumin ratio in colorectal cancer: a meta-analysis of prognostic value. *Dose Response.* (2019) 17:1559325819889814. doi: 10.1177/1559325819889814
43. Montomoli J, Erichsen R, Antonsen S, Nilsson T, Sørensen HT. Impact of preoperative serum albumin on 30-day mortality following surgery for colorectal cancer: a population-based cohort study. *BMJ Open Gastroenterol.* (2015) 2:e000047. doi: 10.1136/bmjgast-2015-000047

Conflict of Interest: The authors declare that the research was conducted in the absence of any commercial or financial relationships that could be construed as a potential conflict of interest.

frontiers in Oncology

ORIGINAL RESEARCH
published: 08 June 2021
doi: 10.3389/fonc.2021.669774

Beta-2-microglobulin Mutations Are Linked to a Distinct Metastatic Pattern and a Favorable Outcome in Microsatellite-Unstable Stage IV Gastrointestinal Cancers

Elena Busch[1†], Aysel Ahadova[2†], Kosima Kosmalla[2], Lena Bohaumilitzky[2], Pauline L. Pfuderer[2], Alexej Ballhausen[2], Johannes Witt[2], Jan-Niklas Wittemann[2], Hendrik Bläker[3], Elke Holinski-Feder[4,5], Dirk Jäger[1,2], Magnus von Knebel Doeberitz[2], Georg Martin Haag[1‡] and Matthias Kloor[2*‡]*

[1] Department of Medical Oncology, National Centre for Tumor Diseases, Heidelberg University Hospital, Heidelberg, Germany, [2] Department of Applied Tumor Biology, Heidelberg University Hospital, Clinical Cooperation Unit Applied Tumor Biology, German Cancer Research Centre (DKFZ), Heidelberg, Germany, [3] Institute of Pathology, University Hospital Leipzig, Leipzig, Germany, [4] Medizinische Klinik und Poliklinik IV, Klinikum der Universität München, Munich, Germany, [5] MGZ – Medical Genetics Centre, Munich, Germany

Immune checkpoint blockade (ICB) shows remarkable clinical effects in patients with metastatic microsatellite-unstable (MSI) cancer. However, markers identifying potential non-responders are missing. We examined the prevalence of *Beta-2-microglobulin* (*B2M)* mutations, a common immune evasion mechanism, in stage IV MSI gastrointestinal cancer and its influence on metastatic pattern and patients' survival under ICB. Twenty-five patients with metastatic, MSI gastrointestinal adenocarcinoma were included. Eighteen patients received ICB with pembrolizumab and one patient with nivolumab/ipilimumab. Sequencing was performed to determine *B2M* mutation status. *B2M* mutations and loss of B2M expression were detected in 6 out of 25 stage IV MSI cancers. *B2M* mutations were strongly associated with exclusively peritoneal/peritoneal and lymph node metastases (p=0.0055). However, no significant differences in therapy response (25% *vs*. 46.6%, p>0.99) and survival (median PFS: 19.5 *vs* 33.0 months, p=0.74; median OS 39 months *vs*. not reached, p>0.99) were observed between *B2M*-mutant and *B2M*-wild type tumor patients. Among metastatic MSI GI cancers, *B2M*-mutant tumors represent a biologically distinct disease with distinct metastatic patterns. To assess ICB response in *B2M*-mutant MSI cancer patients, future studies need to account for the fact that baseline survival of patients with *B2M*-mutant MSI cancer may be longer than of patients with *B2M*-wild type MSI cancer.

Keywords: MSI cancer, metastatic pattern, immune checkpoint blockade, *B2M* mutation, prognosis, therapy response

OPEN ACCESS

Edited by:
Jaw-Yuan Wang, Kaohsiung Medical University Hospital, Taiwan

Reviewed by:
Stefan Kasper-Virchow, Essen University Hospital, Germany
Louise Catherine Connell, Cornell University, United States

***Correspondence:**
Matthias Kloor
matthias.kloor@med.uni-heidelberg.de
Aysel Ahadova
aysel.ahadova@med.uni-heidelberg.de

†These authors share first authorship

‡These authors share senior authorship

Specialty section:
This article was submitted to Gastrointestinal Cancers, a section of the journal Frontiers in Oncology

Received: *19 February 2021*
Accepted: *17 May 2021*
Published: *08 June 2021*

Citation:
Busch E, Ahadova A, Kosmalla K, Bohaumilitzky L, Pfuderer PL, Ballhausen A, Witt J, Wittemann J-N, Bläker H, Holinski-Feder E, Jäger D, von Knebel Doeberitz M, Haag GM and Kloor M (2021) Beta-2-microglobulin Mutations Are Linked to a Distinct Metastatic Pattern and a Favorable Outcome in Microsatellite-Unstable Stage IV Gastrointestinal Cancers. Front. Oncol. 11:669774. doi: 10.3389/fonc.2021.669774

INTRODUCTION

DNA mismatch repair (MMR) deficiency is one of the major mechanisms enabling genomic instability in cancer. MMR-deficient cancers accumulate a high load of somatic mutations, predominantly insertion/deletion mutations at microsatellite sequences (microsatellite instability, MSI). Insertion/deletion mutations of coding microsatellites can cause shifts of the translational reading frame and generation of long *neo*antigen stretches containing *neo*epitopes (1). These *neo*antigens elicit strong immune responses against MSI tumors (2).

However, exhaustion can limit the efficacy of T cell responses upon prolonged antigen exposure without elimination of target cells due to the binding of inhibitory receptors, such as PD-1 (programmed cell death 1), to one of its ligands, most prominently PD-L1 (3). Blockade of these immune checkpoints with re-activation of T cells has therefore had remarkable clinical success particularly in MSI cancer patients (4).

Although immune checkpoint blockade (ICB) can lead to complete responses in a subset of patients, a substantial proportion of MSI cancer patients do not respond to ICB, and predictors of therapy response among MSI cancer patients are lacking.

Besides misdiagnosis of MMR-proficient tumors as MSI (5), non-functionality of tumor cells' antigen presentation machinery, mediated by mutations of the *Beta2-microglobulin* (*B2M*) gene, has been discussed as a key mechanism of resistance towards ICB in some cancer types, such as melanoma (6, 7).

MSI cancers commonly present with *B2M* mutations as a mechanism of immune evasion (8, 9). In contrast to other tumor types including melanoma or non-small cell lung cancer, MSI colorectal cancers display biallelic *B2M* mutations in up to 30% already at the time point of diagnosis (8). An association of *B2M* mutations with improved survival under adjuvant therapy had previously been reported for MSI colorectal cancer patients (10).

We therefore asked whether the response to immunotherapy and the metastatic pattern of stage IV MSI cancers at the time point of diagnosis may differ depending on *B2M* mutation status.

METHODS

Material Collection

Clinical data and tumor material (formalin-fixed, paraffin-embedded (FFPE) tumor specimens) from patients with metastatic MSI GI cancer were collected at the National Center for Tumor Diseases, Heidelberg, Germany. The study was performed in accordance with the Declaration of Helsinki. Written informed consent was obtained from all patients and the study was approved by the Ethics Committee (V5.1 S207/2005).

Molecular Tumor Testing

5 µm FFPE tissue sections were stained using hematoxylin&eosin, histologically analyzed and manually microdissected to obtain DNA. MSI status was determined using a combination of three mononucleotide markers (BAT25, BAT26, CAT25) and three dinucleotide markers (D2S123, D5S346, D17S250) as described previously (11). *B2M* mutation status was determined using targeted sequencing, as previously (12). Briefly, PCR amplification of B2M exons 1 and 2 was performed using primer sequences: Exon 1 For— GGCATTCC TGAAGCTGACA, Exon 1 Rev— AGAGCGGGAGAGGAA GGAC, Exon 2a For—TTTCCCGATATTCCTCAGGTA, Exon 2a Rev— AATTCAGTGTAGTACAAGAG and Exon 2b For— TGTCTTTCA GCAAGGACTGG, Exon 2b Rev— CAAAGTCACATGGTTCACACG. The obtained PCR products (QIAquick PCR Purification Kit) were purified, and the sequencing reaction was performed using the BigDye® Terminator v1.1 Cycle Sequencing Kit (Thermo Fisher Scientific, Wilmington, DE, USA). After dissolving the precipitated products in 12 µl of HiDi Formamide (Thermo Fisher Scientific, Wilmington, DE, USA), sequencing was performed on ABI 3130*xl* Genetic Analyser and analyzed using Sequencing Analysis Software V6.0 (Applied Biosystems). B2M protein expression was analyzed by immunohistochemistry staining using a standard protocol described before (13).

Statistical Analysis

Statistical analyses for categorical data were performed using two-tailed Fisher's exact test. Kaplan-Meier curves for progression-free survival (PFS) and overall survival (OS) were generated using GraphPad Prism (Version 6). Statistical significance was analyzed using log-rank test. A logistic regression model was estimated using the glm (generalized linear model) function within the stats package (14). R: A language and environment for statistical computing. R Foundation for Statistical Computing, Vienna, Austria. URL https://www.R-project.org/). To predict the binary outcome (peritoneal/lymphatic metastasis or non- peritoneal/lymphatic metastasis) we use *B2M* mutation status and the site of the primary tumor (colorectal or gastric cancer, excluded cholangiocellular carcinoma) as predictors.

RESULTS

Patient Characteristics

Primary tumors (19 colorectal, 5 gastric, and 1 cholangiocellular carcinomas) from 25 patients (13 female and 12 male, median age 65 years (range 29 to 78) presenting with a stage IV MSI adenocarcinoma have been analyzed in this study. The clinical and molecular data are summarized in **Table 1**.

Metastatic Patterns According to *B2M* Status

Previously, *B2M* mutations had been shown to be associated with locally restricted disease in MSI GI cancer patients (8, 10). In our study, however, 6 out of 25 (24%) tumors presented with biallelic *B2M* mutations (4 colorectal, 2 gastric cancers, **Table 1**), demonstrating that *B2M* mutations can also occur in stage IV

MSI GI cancers. Immunohistochemical staining revealed loss of B2M protein expression in all *B2M*-mutant tumors, supporting biallelic inactivation and loss of function.

Interestingly, metastatic patterns differed between patients with *B2M*-mutant and *B2M*-wild type tumors. *B2M*-mutant tumor patients predominantly presented with peritoneal metastases, with 2 patients having exclusively peritoneal and 2 patients with peritoneal and lymph node metastases, in contrast to only one patient with a singular hepatic metastasis. On the contrary, only one out of 19 patients with *B2M*-wild type tumors had an exclusively peritoneal/peritoneal and lymph node metastatic pattern (p=0.0055), but 10/19 patients showed extensive hepatic disease (**Table 1**).

As the analyzed patient cohort was heterogeneous with regard to the primary tumor site, which could also influence the observed metastatic pattern, we estimated a logistic regression model using the GLM (generalized linear model) function. Mutant *B2M* status (vs wt *B2M*) increased the log odds of peritoneal/peritoneal and lymphatic metastasis (vs non-peritoneal/peritoneal and lymphatic metastasis) by 3.873 (p=0.00968). The coefficients for primary tumor location (colorectal or gastric cancer) had no significant effect on the metastasis location (log odds -1.283, p value 0.45063).

We also calculated the average marginal effect (AME) for both predictors (*B2M* status and primary site of the tumor). The AME of mutant *B2M* status on metastasis location is 0.6494 (~65%), meaning that on average a *B2M*-mutant tumor has a ~65% higher probability of having a peritoneal/peritoneal and lymphatic metastasis (p = 0.0006). The primary tumor site had no significant AME on the metastatic pattern (p value 0.3952, AME = -0.1063).

Response to ICB Therapy

Nineteen out of 25 patients received ICB therapy with pembrolizumab or nivolumab/ipilimumab (**Table 1**). Therapy response was observed in 8/19 cases (42.1%), with one complete response (CR) and seven patients with partial response (PR, **Figures 1A, B**). Disease stabilization (SD) was observed in seven patients (36.8%), resulting in a disease control rate of 78.9% (**Figure 1A**). With a median follow-up of 29 months (range 1 to 56 months), median PFS was 24 months and median OS was 48 months.

Among *B2M*-wild type cancer patients, 7/15 (46.6%) showed therapy response, and 4/15 (26.6%) had SD (**Figure 1A**). Three patients showed progressive disease (PD, 20%), in one patient the first tumor assessment during ICB therapy is still pending.

Among 4 *B2M*-mutant cancer patients receiving ICB, only one patient (25% as opposed to 46.6% among *B2M*-wild type cancer patients, p>0.99), with initial disease stabilization, showed PR on subsequent imaging as best response, the other three patients had SD. No significant difference in PFS (median PFS: 19.5 *vs* 33.0 months, respectively, p=0.74, **Figure 1C**) or OS (median OS 39 months *vs*. not reached, respectively, p>0.99, **Figure 1D**) was observed between patients with *B2M*-mutant and *B2M*-wild type tumors. Also when using the start of palliative treatment as a reference time point, no significant influence of *B2M* mutation status on OS was observed (**Supplementary Table 1**).

TABLE 1 | Clinical and molecular patient characteristics.

Patient	Age	Gender	Diagnosis	Metastic site	B2M satatus	ICB therapy	Therapy line	Best response
1	29	female	CCC	HEP, PUL	wt	p	3	CR
2	64	male	CRC, sigma	OTH (local recurrence)	wt	p	1	n.a.
3	53	male	CRC, transversum	HEP	wt	p	3	PD
4	68	female	CRC, sigma	PER	wt	p	1	PD
5	65	male	CRC, ascendens	PER, ADR, OTH (spleen), LYM	wt	p	2	PD
6	47	male	CRC, transversum	PUL, HEP, LYM, PER	wt	p	3	PR
7	42	female	CRC, cecum	HEP, PUL, PER	wt	p	3	PR
8	34	female	CRC, transversum	HEP	wt	p	2	PR
9	67	male	CRC, RF	HEP, PER	wt	p	1	PR
10	77	female	CRC, ascendens	LYM, OTH (kidney)	wt	p	2	PR
11	72	female	Crc, rectum	HEP	wt	p	2	PR
12	41	male	CRC, ascendens	HEP, PER, LYM, OTH (muscle)	wt	p	7	SD
13	73	female	CRC, transversum	PUL, HEP, PER	wt	p	2	SD
14	44	female	CRC, cecum	OSS, OTH (ovary)	wt	p	2	SD
15	62	female	CRC, transversum	HEP, LYM, PER	wt	p	2	SD
16	54	female	CRC, cecum	LYM, PER, OTH (ovary, uterus)	wt	(-)	(-)	(-)
17	67	male	gastric cancer	BRA (resected and irradiated)	wt	(-)	(-)	(-)
18	54	male	gastric cancer	ADR (irradiated)	wt	(-)	(-)	(-)
19	78	male	gastric cancer	ADR, LYM (irradiated)	wt	(-)	(-)	(-)
20	36	male	CRC, cecum	PER (resected)	mut	(-)	(-)	(-)
21	71	male	CRC, descendens	PER, LYM	mut	p	1	PR
22	52	male	CRC, LF	PER, LYM, HEP	mut	p	3	SD
23	70	female	gastric cancer	PER, LYM	mut	p	2	SD
24	38	female	gastric cancer	PER, OSS, MAR,ADR	mut	n/i	2	SD
25	69	female	CRC,cecum	PER (resected)	mut	(-)	(-)	(-)

18 out of 19 patients received pembrolizumab (p), one gastric cancer patient (#24) was treated with nivolumab first and, failing to respond, was then escalated to nivolumab/ipilimumab (n/i) combination therapy. CRC, colorectal cancer; CCC, cholangiocellular carcinoma; LF, left flexure; RF, right flexure.

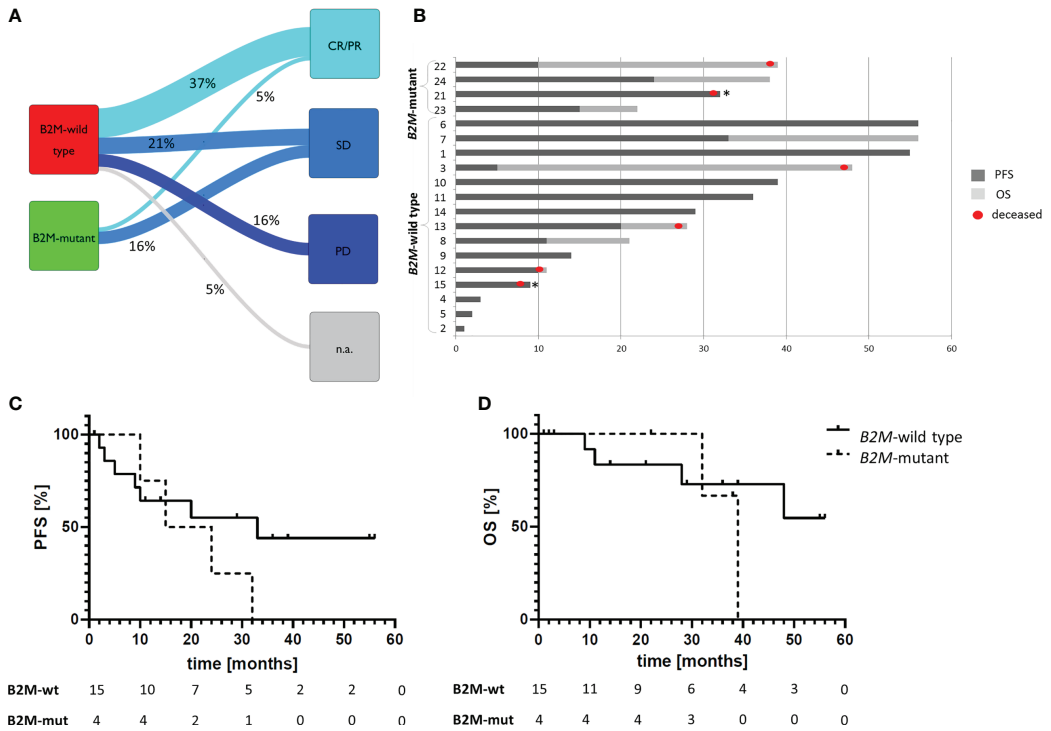

FIGURE 1 | ICB therapy response depending on the tumor *B2M* mutation status**. (A)** Sankey diagram summarizing the therapy responses in 19 MSI GI cancer patients under ICB therapy. **(B)** Swimmer plot describing progression free survival (dark grey) and follow-up duration in 19 patients. Deceased patients are marked with a red dot, death unrelated to tumor disease is marked with an asterisk (*): one patient died because of concurrent cardiovascular disease, one patient died in septic shock, both patients did not show any signs of disease progression at this point. Patients #6-11, and 21 demonstrated PR, and patient #1 demonstrated CR as best response. Numbers refer to Patient IDs in **Table 1**. **(C, D)** Survival curves of patients receiving ICB therapy depending on the *B2M* status of the tumor: progression-free **(C)** and overall survival **(D)**. Despite nominal differences in PFS of *B2M*-mutant (n=4) and *B2M*-wild type (n=15) tumor patients (median PFS: 19.5 *vs* 33.0 months, respectively, p=0.74), the OS did not differ between these two patient groups (median OS 39 months *vs*. not reached, respectively, p>0.99), indicating good prognosis of patients with *B2M*-mutant tumors irrespectively of immune checkpoint blockade therapy. Statistical significance was analyzed using log-rank test.

DISCUSSION

B2M Mutations and Prognosis

B2M mutations have been reported to be associated with prolonged survival for non-metastatic MSI cancer patients (8, 10, 15, 16). To the best of our knowledge, no systematic data exist about the survival of *B2M*-mutant stage IV MSI cancer patients. However, a previous study demonstrated that MSI GI cancer patients presenting with peritoneal metastases had a favorable baseline outcome compared to MSI GI cancer patients displaying a hematogenous metastatic pattern (17), notably without application of ICB therapy. We for the first time show that *B2M* mutation is associated with peritoneal metastasis in stage IV MSI GI cancer. Mutant *B2M* status significantly increased the odds of peritoneal metastasis, whereas the primary tumor site was not related to the metastatic pattern. *B2M* mutation therefore may represent a molecular marker of peritoneal metastasis and favorable baseline prognosis among stage IV MSI GI cancer.

What may be the mechanisms responsible for a favorable clinical course of *B2M*-mutant cancers in the absence of ICB? Previous studies have demonstrated that B2M loss limits the metastatic potential in MSI colorectal cancer (8, 15, 16) and other tumor types, such as uveal melanoma (18). Although the details are not yet fully understood, one hypothesis suggests that the lack of HLA class I antigens as ligands to the NK cell-inhibitory receptors renders *B2M*-mutant cells susceptible to NK cell-mediated elimination (18, 19). In addition, the association of tumor cells with platelets, a process relevant specifically for hematogenous metastases, seems to be disrupted by loss of HLA class I antigens (20). These factors may favor peritoneal metastasis and lower the likelihood of hematogenous spread. The hypothesis of *B2M*-mutant tumor cells being "trapped" in the peritoneum is supported by the metastatic patterns of *B2M*-mutant MSI cancers observed in our study.

Clinical Implications

Our study for the first time provides clinical evidence that the biology and clinical course of metastatic *B2M*-mutant MSI GI cancers is substantially different from *B2M*-wild type MSI GI cancers. Considering that metastatic MSI cancers represent two distinct subgroups depending on *B2M* mutation status, the impact of *B2M* mutation status on response to ICB needs to be reconsidered. In particular, differences in baseline survival and

prognosis need to be accounted for when analyzing the effectiveness of ICB in *B2M*-mutant and *B2M*-wild type GI cancers. The favorable outcome of *B2M*-mutant metastatic MSI cancer patients receiving ICB reported by Middha et al. (21) may be attributable to distinct baseline survival instead of representing actual treatment responses. Our data strongly encourage stratification of patients in clinical ICB studies according to *B2M* mutation status or peritoneal *vs*. hematogenous metastasis.

Previous studies also identified a potential impact of *KRAS*/*NRAS* mutations on ICB response (22). In our cohort, only 4 patients had colorectal cancer with *KRAS*/*NRAS* mutations, three of them (all *B2M*-wt) received ICB therapy and showed PR as best response. One patient had a colorectal cancer harboring both, *B2M* and *KRAS* mutations, but did not receive ICB. No significant correlation between *RAS* or *RAF* mutation status and presence or absence of *B2M* mutations was observed. Thus, although our study has limited power for analyzing the influence of *KRAS*/*NRAS* mutations on response to ICB therapy, no correlation between *BRAF* or *KRAS*/*NRAS* and the prevalence of *B2M* mutations could be observed.

The present study has strengths and limitations. The major strength is linking the previously described difference in baseline survival of stage IV MSI GI cancer patients to the *B2M* mutation status of the tumor and survival under ICB therapy. One limitation is that baseline survival data of *B2M*-mutant cancer patients are not available, as follow-up data were only retrieved for patients receiving ICB treatment. In addition, owing to the rarity of stage IV *B2M*-mutant MSI cancers, sample size of the present study is limited. However, the absence of *B2M* mutation status-dependent survival differences under ICB therapy is also compatible with the hypothesis that a biologically-determined favorable course of *B2M*-mutant tumors with peritoneal metastasis may leave limited room for further improvement under ICB therapy (**Figure 2**).

A study assessing the impact of B2M loss on ICB therapy in animal models demonstrated a major role of CD4-positive T cells in the immune response stimulated by combined anti-CTLA-4 and anti-PD-l therapy against tumors lacking MHC class I-associated antigen expression (23). Interestingly, this study also demonstrated limited effect of anti-PD-1 therapy alone on B2M-deficient tumors in mouse models and did not identify differences in OS or PFS in patients with tumors showing different B2M expression levels. This is in line with our findings showing no significant difference in PFS or OS between 15 *B2M*-wt and 4 *B2M*-mutant tumor patients receiving ICB therapy. Whether the patients with *B2M*-mutant tumors might benefit from combined ICB therapy approaches, remains to be confirmed in future human studies. In our study, only one patient with a *B2M*-mutant tumor and several metastases not restricted to peritoneal or lymphatic sites was treated with a combination of anti-CTLA-4 and anti-PD-l antibodies (ipilimumab and nivolumab) and demonstrated SD as best response.

Our study demonstrates that in stage IV GI MSI cancers peritoneal metastasis is closely associated with *B2M* mutations. The favorable prognosis associated with peritoneal metastasis in MSI cancer patients may mimic response to ICB. Future clinical trials are strongly encouraged to focus on this important clinical question. For that, prospective trials with larger patient cohorts

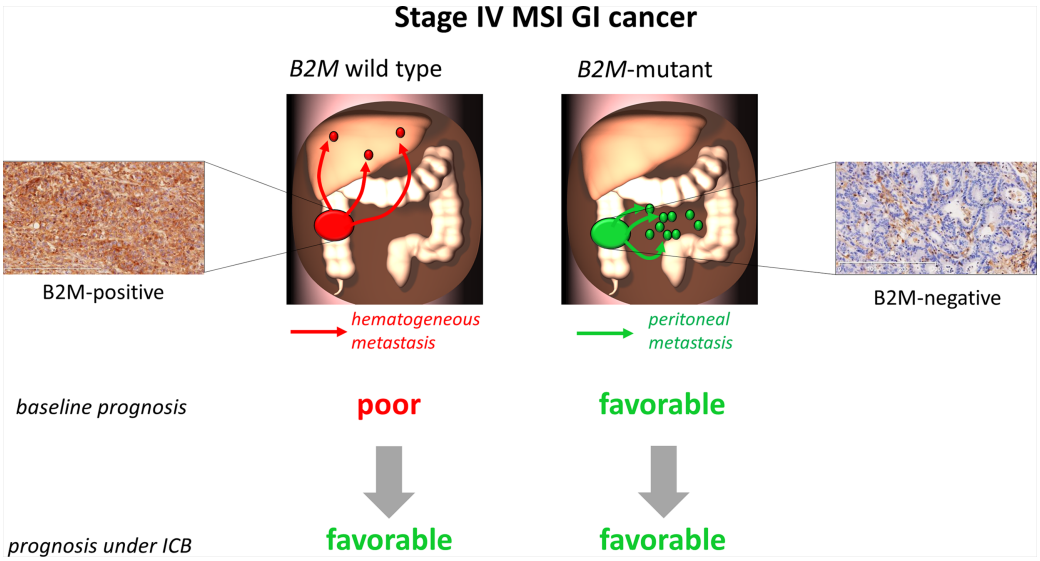

FIGURE 2 | Hypothesis scheme. Patients with *B2M*-wild type MSI tumors and unimpaired B2M expression (left part of the figure) have a comparatively poor prognosis with high risk of hematogenous metastasis, thus these patients may benefit most from immune checkpoint blockade (ICB) therapy. In contrast, patients with *B2M*-mutant MSI tumors and loss of B2M expression (right part of the figure) due to biological characteristics of this tumor type rather present with a favorable prognosis and low risk of hematogenous metastasis. Thus, in these patients ICB therapy may not substantially improve the clinical picture.

recording metastatic patterns and *B2M* mutation status are required, which shall reveal whether the good survival of *B2M*-mutant M1 MSI cancer patients under ICB reflects the biology of the tumor cells, or indicates treatment response. This will ensure more tailored treatment selection for patients with metastasized MSI cancer and reduce treatment-related side effects in patients who may have no benefit from ICB. In addition, functional immunological studies contributing to understanding the mechanistic background of natural or ICB-induced immune response against tumors with impaired MHC class I expression are warranted.

Beyond the specific implications for *B2M*-mutant tumor patients and their response to ICB therapy, our study underlines the importance of better understanding the molecular characteristics of a tumor and their impact on patient's prognosis when assessing the effect of certain therapies on patient's survival.

DATA AVAILABILITY STATEMENT

The original contributions presented in the study are included in the article/**Supplementary Material**, further inquiries can be directed to the corresponding authors.

ETHICS STATEMENT

The studies involving human participants were reviewed and approved by Ethics Committee of Medical Faculty, University Heidelberg. The patients/participants provided their written informed consent to participate in this study.

AUTHOR CONTRIBUTIONS

Conceptualization: EB, AA, GMH, and MK. Data Curation: EB, AA, KK, LB, PP, AB, JW, J-NW, and EHF. Formal Analysis: EB, AA, KK, LB, PP, EB, AB, JW, and J-NW. Funding Acquisition: MK, MKD, AA, and EB. Investigation: EB, AA, GMH, and MK. Methodology: EB, AA, GMH, and MK. Project Administration: GMH, and MK. Supervision: MKD, DJ, HB, EHF, GMH, and MK. Visualization: EB, AA, and MK. Writing – Original Draft: EB, AA, GMH, and MK. Writing – Review & Editing: all authors. All authors contributed to the article and approved the submitted version.

FUNDING

This study was supported by Else Kröner-Fresenius Foundation (grant number 2018_A44, PI: MK), German Cancer Aid (grant number 70113455, Subroject PI: MK) and NCT Elevator Pitch (PIs: AA and EB).

ACKNOWLEDGMENTS

The excellent technical assistance of Nina Nelius, Petra Höfler and Lena Ehret-Maßholder are gratefully acknowledged.

SUPPLEMENTARY MATERIAL

The Supplementary Material for this article can be found online at: https://www.frontiersin.org/articles/10.3389/fonc.2021.669774/full#supplementary-material

REFERENCES

1. Kloor M, von Knebel Doeberitz M. The Immune Biology of Microsatellite-Unstable Cancer. *Trends Cancer* (2016) 2(3):121–33. doi: 10.1016/j.trecan.2016.02.004
2. Dolcetti R, Viel A, Doglioni C, Russo A, Guidoboni M, Capozzi E, et al. High Prevalence of Activated Intraepithelial Cytotoxic T Lymphocytes and Increased Neoplastic Cell Apoptosis in Colorectal Carcinomas With Microsatellite Instability. *Am J Pathol* (1999) 154:1805–13. doi: 10.1016/S0002-9440(10)65436-3
3. Wherry EJ, Kurachi M. Molecular and Cellular Insights Into T Cell Exhaustion. *Nat Rev Immunol* (2015) 15:486–99. doi: 10.1038/nri3862
4. Le DT, Durham JN, Smith KN, Wang H, Bartlett BR, Aulakh LK, et al. Mismatch Repair Deficiency Predicts Response of Solid Tumors to PD-1 Blockade. *Science* (2017) 357:409–13.
5. Cohen R, Hain E, Buhard O, Guilloux A, Bardier A, Kaci R, et al. Association of Primary Resistance to Immune Checkpoint Inhibitors in Metastatic Colorectal Cancer With Misdiagnosis of Microsatellite Instability or Mismatch Repair Deficiency Status. *JAMA Oncol* (2019) 5:551–5. doi: 10.1001/jamaoncol.2018.4942
6. Zaretsky JM, Garcia-Diaz A, Shin DS, Escuin-Ordinas H, Hugo W, Hu-Lieskovan S, et al. Mutations Associated With Acquired Resistance to PD-1 Blockade in Melanoma. *N Engl J Med* (2016) 375:819–29. doi: 10.1056/NEJMoa1604958
7. Sade-Feldman M, Jiao YJ, Chen JH, Rooney MS, Barzily-Rokni M, Eliane JP, et al. Resistance to Checkpoint Blockade Therapy Through Inactivation of Antigen Presentation. *Nat Commun* (2017) 8:1136. doi: 10.1038/s41467-017-01062-w
8. Kloor M, Michel S, Buckowitz B, Ruschoff J, Buttner R, Holinski-Feder E, et al. Beta2-microglobulin Mutations in Microsatellite Unstable Colorectal Tumors. *Int J Cancer* (2007) 121:454–8. doi: 10.1002/ijc.22691
9. Ozcan M, Janikovits J, von Knebel Doeberitz M, Kloor M. Complex Pattern of Immune Evasion in MSI Colorectal Cancer. *Oncoimmunology* (2018) 7:e1445453. doi: 10.1080/2162402X.2018.1445453
10. Tikidzhieva A, Benner A, Michel S, Formentini A, Link KH, Dippold W, et al. Microsatellite Instability and Beta2-Microglobulin Mutations as Prognostic Markers in Colon Cancer: Results of the FOGT-4 Trial. *Br J Cancer* (2012) 106:1239–45. doi: 10.1038/bjc.2012.53
11. Boland CR, Thibodeau SN, Hamilton SR, Sidransky D, Eshleman JR, Burt RW, et al. A National Cancer Institute Workshop on Microsatellite Instability for Cancer Detection and Familial Predisposition: Development of International Criteria for the Determination of Microsatellite Instability in Colorectal Cancer. *Cancer Res* (1998) 58:5248–57.
12. Echterdiek F, Janikovits J, Staffa L, Muller M, Lahrmann B, Fruhschutz M, et al. Low Density of FOXP3-Positive T Cells in Normal Colonic Mucosa Is Related to the Presence of Beta2-Microglobulin Mutations in Lynch Syndrome-Associated Colorectal Cancer. *Oncoimmunology* (2016) 5:e1075692. doi: 10.1080/2162402X.2015.1075692
13. Janikovits J, Muller M, Krzykalla J, Korner S, Echterdiek F, Lahrmann B, et al. High Numbers of PDCD1 (PD-1)-Positive T Cells and B2M Mutations in Microsatellite-Unstable Colorectal Cancer. *Oncoimmunology* (2018) 7:e1390640. doi: 10.1080/2162402X.2017.1390640
14. R Core Team. R: A language and environment for statistical computing. R Foundation for Statistical Computing, Vienna, Austria. (2020). Available at: https://www.R-project.org/.

15. Koelzer VH, Baker K, Kassahn D, Baumhoer D, Zlobec I. Prognostic Impact of Beta-2-microglobulin Expression in Colorectal Cancers Stratified by Mismatch Repair Status. *J Clin Pathol* (2012) 65:996–1002. doi: 10.1136/jclinpath-2012-200742
16. Barrow P, Richman SD, Wallace AJ, Handley K, Hutchins GGA, Kerr D, et al. Confirmation That Somatic Mutations of Beta-2 Microglobulin Correlate With a Lack of Recurrence in a Subset of Stage II Mismatch Repair Deficient Colorectal Cancers From the QUASAR Trial. *Histopathology* (2019) 75:236–46. doi: 10.1111/his.13895
17. Fujiyoshi K, Yamamoto G, Takenoya T, Takahashi A, Arai Y, Yamada M, et al. Metastatic Pattern of Stage IV Colorectal Cancer With High-Frequency Microsatellite Instability as a Prognostic Factor. *Anticancer Res* (2017) 37:239–47. doi: 10.21873/anticanres.11313
18. Jager MJ, Hurks HM, Levitskaya J, Kiessling R. HLA Expression in Uveal Melanoma: There Is No Rule Without Some Exception. *Hum Immunol* (2002) 63:444–51. doi: 10.1016/S0198-8859(02)00389-0
19. Liao NS, Bix M, Zijlstra M, Jaenisch R, Raulet D. MHC Class I Deficiency: Susceptibility to Natural Killer (NK) Cells and Impaired NK Activity. *Science* (1991) 253:199–202. doi: 10.1126/science.1853205
20. Reimers MS, Bastiaannet E, Langley RE, van Eijk R, van Vlierberghe RL, Lemmens VE, et al. Expression of HLA Class I Antigen, Aspirin Use, and Survival After a Diagnosis of Colon Cancer. *JAMA Intern Med* (2014) 174:732–9. doi: 10.1001/jamainternmed.2014.511
21. Middha S, Yaeger R, Shia J, Stadler ZK, King S, Guercio S, et al. Majority of B2M-Mutant and -Deficient Colorectal Carcinomas Achieve Clinical Benefit From Immune Checkpoint Inhibitor Therapy and Are Microsatellite Instability-High. *JCO Precis Oncol* (2019) 3:PO.18.0032. doi: 10.1200/PO.18.00321
22. Andre T, Shiu KK, Kim TW, Jensen BV, Jensen LH, Punt C, et al. Pembrolizumab in Microsatellite-Instability-High Advanced Colorectal Cancer. *N Engl J Med* (2020) 383:2207–18. doi: 10.1056/NEJMoa2017699
23. Germano G, Lu S, Rospo G, Lamba S, Rousseau B, Fanelli S, et al. Cd4 T Cell Dependent Rejection of Beta 2 Microglobulin Null Mismatch Repair Deficient Tumors. *Cancer Discovery* (2021) candisc.0987.2020. doi: 10.1158/2159-8290.CD-20-0987

Conflict of Interest: GMH: Consulting or Advisory Role: Bristol-Myers Squibb, MSD Sharp & Dohme, EsoCap, Lilly; Honoraria: Servier, MSD Sharp & Dohme, Lilly; Research Funding: Nordic Pharma; Taiho Pharmaceutical, MSD Sharp & Dohme; Travel, Accommodations: Bristol-Myers Squibb; Lilly.

The remaining authors declare that the research was conducted in the absence of any commercial or financial relationships that could be construed as a potential conflict of interest.

frontiers in Oncology

ORIGINAL RESEARCH
published: 18 June 2021
doi: 10.3389/fonc.2021.684531

LncRNA HCP5 : A Potential Biomarker for Diagnosing Gastric Cancer

Shiyi Qin[1,2,3†], *Lei Yang*[1,2,3†], *Shan Kong*[1,2,3], *Yanhua Xu*[1,2,3], *Bo Liang*[4*] *and Shaoqing Ju*[1*]

[1] Department of Laboratory Medicine, Affiliated Hospital of Nantong University, Nantong, China, [2] Research Center of Clinical Medicine, Affiliated Hospital of Nantong University, Nantong, China, [3] Medical School of Nantong University, Nantong University, Nantong, China, [4] Department of Medical Ultrasonics, Affiliated Hospital of Nantong University, Nantong, China

OPEN ACCESS

Edited by:
Jaw-Yuan Wang,
Kaohsiung Medical University Hospital, Taiwan

Reviewed by:
Matthew Brendan O'Rourke, University of Technology Sydney, Australia
Peng-Chan Lin, National Cheng Kung University, Taiwan
De-Chuan Chan, Tri-Service General Hospital, Taiwan

***Correspondence:**
Bo Liang
281692191@qq.com
Shaoqing Ju
jsq814@hotmail.com

[†]These authors have contributed equally to this work

Specialty section:
This article was submitted to Gastrointestinal Cancers, a section of the journal Frontiers in Oncology

Received: 23 March 2021
Accepted: 24 May 2021
Published: 18 June 2021

Citation:
Qin S, Yang L, Kong S, Xu Y, Liang B and Ju S (2021) LncRNA HCP5 : A Potential Biomarker for Diagnosing Gastric Cancer. Front. Oncol. 11:684531. doi: 10.3389/fonc.2021.684531

Background: It has been reported that long non-coding RNAs (lncRNAs) can be regarded as a biomarker and had particular clinical significance for early screening and gastric cancer (GC) diagnosis. Therefore, this study aimed to investigate whether serum HCP5 could be a new diagnostic biomarker.

Methods: Filtered out the HCP5 from the GEO database. The specificity of HCP5 was verified by real-time fluorescence quantitative PCR (qRT-PCR), and then the stability of HCP5 was verified by room temperature storage and repeated freeze-thaw experiments. Meanwhile, the accuracy of HCP5 was verified by agarose gel electrophoresis (AGE) and Sanger sequencing. Simultaneously, the expression level of serum HCP5 was detected by qRT-PCR in 98 patients with primary gastric cancer, 21 gastritis patients, 82 healthy donors, and multiple cancer types. Then, the methodology analysis was carried on. Moreover, receiver operating characteristic (ROC) was used to evaluate its diagnostic efficiency.

Results: qRT-PCR method had good repeatability and stability in detecting HCP5. The expression level of HCP5 in the serum of gastric cancer patients was remarkably higher than that of healthy controls, and it could distinguish gastritis patients from healthy donors. Besides, the expression of HCP5 was increased dramatically in MKN-45 and MGC-803. The FISH assay showed that HCP5 was mainly distributed in the cytoplasm of MKN-45 and BGC-823 cells. When HCP5 was combined with existing tumor markers, the diagnostic efficiency of HCP5 was the best, and the combined diagnosis of carcinoembryonic antigen (CEA), carbohydrate antigen199 (CA199), and HCP5 can significantly improve the diagnostic sensitivity. Besides, compared with the expression levels of thyroid cancer (THCA), colorectal cancer (CRC), and breast cancer (BRCA), serum HCP5 in gastric cancer was the most specific. Moreover, the high expression of serum HCP5 was related to differentiation, lymph node metastasis, and nerve invasion. The term of serum HCP5 after the operation was significantly lower than that of patients with primary gastric cancer.

Conclusion: Serum HCP5 can be used as a potential biomarker of non-invasive fluid biopsy, which had a unique value in the early diagnosis, development, and prognosis of gastric cancer.

Keywords: gastric cancer, GC, HCP5, biomarker, diagnosis, gastritis

INTRODUCTION

Gastric cancer (GC) is one of the most common malignant tumors globally, with high mortality and morbidity (1). As shown by data, 50% of gastrointestinal cancer cases have occurred in China, of which gastric cancer accounts for the most significant proportion, and the 5-year overall survival rate is meager, which was reported <35% in 2013-2015 (2). Among several factors, helicobacter pylori infection was the most common one, including other high-risk factors like genetic susceptibility, diet, drinking, smoking, etc. (3). At this stage, gastric cancer treatment mainly relies on surgical techniques, traditional radiotherapy, chemotherapy, and neoadjuvant therapies. However, since GC is rarely diagnosed early, it has usually advanced to most patients' late stages. Furthermore, traditional surgery, radiotherapy, and chemotherapy are often not as effective as early-stage disease, malignant invasion, and metastasis later appeared (4). That means it is urgent to find a screening index with high specificity and sensitivity. Studies have shown that molecular analysis of non-invasive body fluids may help diagnose GC (5). In recent years, more and more literature has demonstrated that long non-coding RNA (lncRNA) played an essential role in the pathogenesis and process of GC (6–8). Hence, lncRNA has become the focus of attention in recent years.

LncRNA is a non-coding RNA with a length of more than 200nt, lacking the potential of coding peptides (9). Increasing evidence has shown that lncRNA can regulate genes by directly binding to genes, participating in translation inhibition, splicing modification, and messenger RNA (mRNA) degradation, and using microRNA (miRNA) as a competitive endogenous RNA (ceRNA) to prevent mRNA degradation and stabilize mRNA (10, 11). It plays a vital role in the regulation of splicing, transcription control, and post-transcriptional processing (12). Moreover, lncRNA may act as tumor suppressor genes and oncogenes, affecting cell proliferation (13), apoptosis (14), differentiation (15), metastasis (16), DNA damage (17), angiogenesis (18), and immune response (19), and so on. Simultaneously, the existing literature has confirmed that lncRNAs also exist in serum, plasma, urine, and exosomes of various cancer types, indicating that they can also be used as classic markers for liquid biopsy. For example, FAM83H-AS1 and lncRNA-ATB were significantly high in serum breast cancer patients, showing the potential ability to monitor breast cancer progression and staging (20). Besides, lncRNA GAS5 resulted in a specific reduction of plasma expression in coronary artery disease (CAD) patients, which could be used as a specific biomarker for diagnosing CAD (21). What's more, the up-regulation of LncRNA XIST transported by serum extracellular vesicles was related to the progression of colorectal cancer (CRC) (22). It was also reported HYMA1, OTX2-AS1 linc00477, and loc100506688 in urine exosomes, which were found in bladder cancer, could potentially serve as biomarkers and therapeutic targets (23). Consequently, lncRNAs could be used as molecular markers for tumor diagnosis and new targets for tumor treatment shortly (24).

Histocompatibility leukocyte antigen complex P5 (HCP5) is a momentous lncRNA located between MHC class I polypeptide related sequence A (MICA) and MHC class I polypeptide related sequence B (MICB) genes in the MHC class I chain-related gene (MHCI) region, involving many autoimmune diseases and malignant tumors (25). Moreover, the abnormal expression of HCP5 is closely related to cell proliferation, migration, invasion, apoptosis, lymphatic metastasis, and drug resistance in various cancers (26–29). Hence, HCP5 is expected to become a biomarker and therapeutic target in multiple cancers (25). Functional tests verified that HCP5 could function as an oncogene in osteosarcoma and was activated by the transcription factor 1 (SP1), convincing that SP1 induced the up-regulation of HCP5, which impacted the development of osteosarcoma (30). Moreover, Wu et al. (31) observed that overexpression of HCP5 could interact with miR-3619-5p, which upregulated peroxisome proliferative activated receptor gamma (PPARG) coactivator 1 alpha (PPARGC1A) through miR-3619-5p/the AMP-activated protein kinase (AMPK)/transcription complex peroxisome proliferator-activated receptor (PPAR) coactivator-1α (PGC1α)/enhancer-binding protein beta (CEBPB) axis, regulating 5-Fluorouracil (5-Fu) and oxaliplatin resistance in gastric cancer. This study surveyed 98 GC patients, 82 healthy donors, 21 gastritis patients, and 56 patients from diverse cancers. A diagnostic model consisting of serum HCP5 and existing indicators carcinoembryonic antigen (CEA) and carbohydrate antigen199 (CA199) was established to improve diagnostic efficacy. Besides, the role of HCP5 in the dynamic monitoring of tumors in GC patients has also been discovered.

METHODS

Serum Samples Collection

From January 2016 to January 2021, Serum samples of 98 GC patients, 21 gastritis patients, 19 thyroid cancer (THCA) patients, 20 colorectal cancer (CRC) patients, 17 breast cancer (BRCA) patients, and 82 healthy donors were collected at the clinical laboratory of Affiliated Hospital of Nantong University (Nantong, China). All serum samples were stored in RNase-free test tubes at -80°C for later use. All samples mentioned above were collected under the ethics of the World Medical Association, and informed consent was obtained for experiments on human subjects.

Besides, this study was approved by the Human Research Ethics Committee of Nantong University Hospital. (Ethics review report number: 2018-L055).

RNA Extraction

According to the serum extraction kit (BioTeke, Wuxi, China), total RNA was extracted from 300μl serum. Then, 900μl lysis buffer was added, mixed by pipetting, vortexed for 1min, and incubated at 15-30°C for 5min. Adding 180μl chloroform in them and let them stand. After then, the serum samples were centrifuged at 12000rpm for 10min in a 4°C low-temperature high-speed centrifuge, followed by colorless water phases and organic phases. The colorless aqueous phase was then absorbed and transferred into a 1.5ml RNase-free tube, added to 700μl 70% ethanol, mixed upside down, and moved to the adsorption column. Centrifuged at 12000rpm for 1min and discarded the liquid. They were then adding 500μl deproteinized liquid, centrifuged at 12000rpm for 1min. After cleaning with 700μl rinsing solution, leaving for 2min and the liquid was transferred to a new 1.5ml RNase-free tube. Then, added 30μl RNase-free water in a warm bath, standing at room temperature for 2min, centrifuged at 12000rpm, and twice in 1min. After centrifugation, put it in the refrigerator at -80°C for later use.

Complementary DNA (cDNA) Synthesis and Real-Time Fluorescence Quantitative Polymerase Chain Reaction (qRT-PCR)

The reverse transcription kit (Thermo Fisher Scientific) was used, adding 4μl 5×Reaction Buffer, 2μl 10mM deoxyribonucleotide triphosphate (dNTPs), 1μl Oligo (dT) Primer, 1μl RNase inhibitor (20U/μl), and 1μl Reverse Transcriptase (200U/μl) to form the reaction system, which was reverse-transcribed into cDNA with the total 11μl RNA solution. Then, we incubated the 20μl total system at 25°C for 5 minutes, 42°C for 60 minutes, 70°C for 5 minutes and stored the synthesized cDNA at -80°C when not in use. After that, qRT-PCR assays were performed on the Roche Lightcycler 480 (Roche, Switzerland), using SYBR Green I mix (Roche) as the fluorescent dyes for a total of 20μl system. The primers used in this article were all synthesized by RiboBio Corporation (Suzhou, China). The primer sequences are as follows: HCP5, 5'-TGAGAGCAGGACAGGAAAA-3' (forward) and 5'-CCAACCAGACCCTAAGTGA-3' (reverse); 18S ribosomal RNA (18S): 5'-CGCTCGCTCC TCTCCTACTT-3' (forward) and 5'-CGGGTTGGTTTTGATCTGATAA-3' (reverse).

The PCR cycling program included that activating the enzyme at 95°C for 10min, denaturation at 95°C for 15s, annealing at 60°C for 30s, then collecting fluorescence information at 80°C for a total of 45 cycles. The $2^{-\Delta\Delta Ct}$ method was used to calculate the relative expression of the target gene. ΔΔCt means the difference between the experimental group and the control group.

Cell Culture

Human gastric epithelial cell (GES-1) and gastric cancer cell line (MKN-45, MGC-803, BGC-823, HGC-27) were purchased from the Cell Bank of the Chinese Academy of Sciences (Shanghai, China). Cells were cultured in RPMI-1640 (Corning, USA) containing 10% fetal bovine serum (FBS) (Gibco, USA) and 1% penicillin-streptomycin in a humid condition of 5% CO_2 at 37°C.

Cell Secretion Assay

The 1, 3, 5, and 7 days cell supernatants of MKN-45, MGC-803, and GES-1 were extracted. Furthermore, the expression level of lncRNA was later detected.

Linear Verification Experiment

To verify the linearity of lncRNA, a healthy donor's serum cDNA was diluted by 10, 10^2, and 10^3 times, respectively.

Stability Verification Experiment

The mixed serum samples were placed at room temperature for 0, 6, 12, 18, and 24 h. Besides, repeated freezing and thawing for 0, 1, 3, 5, and 10 times to verify the stability of lncRNA.

Agarose Gel Electrophoresis (AGE)

50×TAE 1:49 diluted to 1×, configured 2% gels, and waited for use. 1μl the loading buffer and 5μl products were added, then electrophoresed at 110-120V for about 30min. The accuracy of the product was verified by sequencing analysis.

Cell Passage

Firstly, the original culture medium was discarded and washed 1-2 times with phosphate buffer saline (PBS). Secondly, cells in the T25 culture flasks were digested for 1min by adding about 1ml 0.25% trypsin-EDTA (Gibco, USA). Next, adding 2-3ml of the complete medium to culture flasks to stop digestion, rinsed, and suspended until all the cells were flushed down. They were then transferred to 15ml centrifuge tubes and centrifuged at 1000 rpm for 5min. Adding about 3ml complete medium to infiltrate the bottom of T25 culture flasks. While centrifugation was finished, we discarded the supernatant, adding about 4ml complete medium to suspend and evenly 2ml suspension to each bottle, mixed well, and then incubated in the condition with 5% CO_2 at 37°C.

Cell Cryopreservation

The original culture medium was discarded, rinsed 1-2 times with PBS, added approximately 1ml 0.25% trypsin-EDTA to digest cells in the T25 culture bottle for 1min. 2-3ml of complete medium was added to terminate digestion, transferred to a 15ml centrifuge tube and centrifuged for 5min at 1000rpm. Then, the suspension was transferred to the freezer tube and quickly placed in a refrigerator at -80°C for later use.

Fluorescence In Situ Hybridization (FISH)

According to instructions of the manufacturer, the fluorescence *in situ* hybridization kit (RiboBio, Guangzhou, China) was used to repair and penetrate cells. 200μl prehybridization solution was incubated at 37°C for 30min, followed by 20μmol FISH probes/hybridization buffer for overnight incubation at 37°C. Rinsed each well with washing solution I, II, III and PBS in turn. 4',6-Diamidino-2'-phenylindole (DAPI) was then dyed in the dark for 10min, and photos were taken under a fluorescence

microscope. The HCP5 Fish probe was designed and synthesized by RiboBio (RiboBio, Guangzhou, China).

Data Analysis

All statistics were analyzed using SPSS 20.0 software (IBM SPSS Statistics, Chicago, Illinois, USA) and GraphPad Prism V.8.00 software (GraphPad Software, La Jolla, USA). Meanwhile, all data were expressed as the mean ± standard deviation (SD) of values obtained in three independent experiments. According to the actual situation, independent sample t-test, one-way analysis of variance (ANOVA), and $\chi 2$ test were used for statistical analysis. The receiver operating characteristic curve (ROC) and the area under the ROC curve (AUC) were used to evaluate the diagnostic value of HCP5. Besides, bivariate logistic regression was used to analyze the diagnostic value of HCP5, CEA, and CA199. The ROC curve and AUC were obtained through non-parametric analysis. Youden index (Youden index = sensitivity + specificity - 1) was used as the expression value of serum HCP5. The overall survival (OS) was estimated by using the Kaplan-Meier method. All values of $p<0.05$ were considered to reach a statistically significant difference.

RESULTS

The Innovative Detection Method of Serum HCP5

LncRNA, as a classic non-coding RNA, played a vital role in liquid biopsies as a biomarker. The literature confirmed that 18S had good linearity and stability compared with the reference genes glyceraldehyde 3-phosphate dehydrogenase, U6 small nuclear RNA (U6), β-actin (ACTB), and tubulin (TUB) in gastric cancer (32). Therefore, 18S was selected as the endogenous reference gene in this assay. To verify whether HCP5 was suitable for clinical laboratory analysis, we performed a methodological assessment of HCP5 detected by the qRT-PCR method. To verify its linearity, we built a continuous 10-fold dilution of cDNA and diluted the original serum cDNA concentrations 10, 10^2 and 10^3 times. Different concentrations of serum HCP5 were detected by qRT-PCR, and data analysis was performed (**Figure 1A**). At the same time, 18S was analyzed, as shown in **Figure 1B**. It could be seen that R^2 of the standard curve of HCP5 was 0.960, and the regression equation was y=-0.901x+23.57, indicating that qRT-PCR was an effective method for detecting different concentrations of serum HCP5. In addition, we selected the mixture of serums for HCP5 precision determination. The results showed that the inter-and intra-assay coefficients of variation (CV) for HCP5 were 2.99% and 2.11%, respectively (**Table 1**). Secondly, to verify the stability of HCP5 in liquid biopsies, we placed the mixed standard human serum samples at room temperatures of 0, 6, 12, 18, and 24h. Similarly, we performed frozen-thawed cycles for another set of mixed samples 0, 1, 3, 5, and 10 times. All of these samples were stored in RNase-free tubes and kept at -80°C for later use. As shown in **Figures 1C, D**, when environmental conditions changed, the level of serum HCP5 remained significantly unchanged, indicating that HCP5 had good stability. Besides, the smooth unimodal melting curve also indicated the high

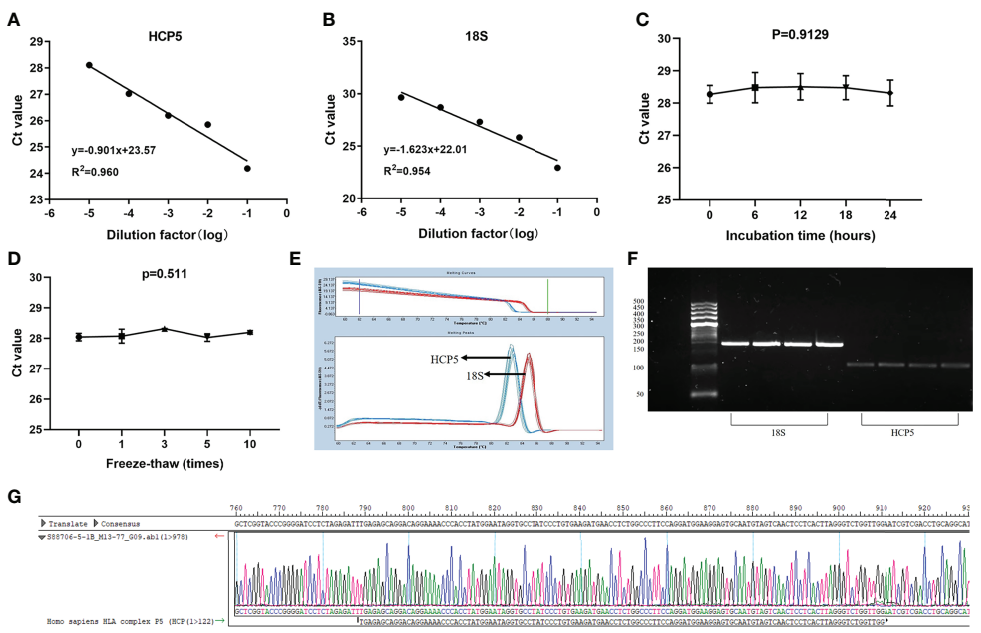

FIGURE 1 | Methodology evaluation of HCP5 in GC serum samples. **(A, B)** Standard curves of serum HCP5 and 18S in a ten-fold serial dilution to show the linearity. **(C, D)** Stability of HCP5 under room temperature incubation time or multiple freeze-thaw cycles. Data were presented as raw Ct value (n=3). **(E)** The specificity of PCR products by the melting curve. **(F)** The validation of PCR products by the agarose gel electrophoresis. **(G)** The product sequence was verified by Sanger sequencing.

TABLE 1 | Intra- and inter-assay reproducibility of HCP5 and 18S rRNA.

	HCP5	18s
inter-assay CV,%	**2.99%**	**3.28%**
intra-assay CV,%	**2.11%**	**2.58%**

specificity of amplified product serum HCP5 (**Figure 1E**). By analyzing the PCR products through AGE, the result showed that the band was 122bp and the accuracy was verified (**Figure 1F**). Sanger sequencing showed that the PCR product sequence was consistent with HCP5, with a sequence size of 122bp, further verifying the accuracy of the PCR method (**Figure 1G**). In this section, from all of these results, we found that the detection of HCP5 by qRT-PCR was susceptible and specific.

The Expression Level and Diagnostic Efficacy of Serum HCP5 in Gastric Cancer

To verify whether HCP5 can be used as an emerging GC diagnostic marker. We detected the expression of serum HCP5 in 98 GC patients and 82 healthy donors by qRT-PCR. The results showed that the expression level of serum HCP5 in GC patients was significantly higher than that in healthy donors (**Figure 2A**). In addition, HCP5 can clearly distinguish patients with gastritis and gastric cancer (**Figure 2B**). Besides, CEA and CA199 are usually widely used for screening and auxiliary diagnosis of GC. As shown in **Figures 2C, D**, the expression levels of serum CEA and CA199 in GC patients were also higher than those in healthy controls. The ROC curves showed that the area under the curve of serum HCP5 detected by qRT-PCR was 0.818 (95% CI:0.757-0.880 P<0.001) (**Figure 2E**). Under this cut-off value, the sensitivity was 80%, and the specificity was 70% (**Table 2**). Moreover, the clinical indicators CEA and CA199 area under the curve were 0.725 (95% CI:0.650-0.799, P<0.001) and 0.687 (95% CI:0.610-0.764, P<0.001), respectively (**Figures 2F, G**). Besides, we also analyzed the expression level of HCP5 and the comprehensive diagnostic analysis between CEA and CA199. As mentioned above, compared with the separate detection, the three combined diagnoses provided the high AUC 0.870 (95% CI:0.819-0.921, P<0.001) in the distinction between gastric cancer and healthy donors (**Figure 2H**). Then, through logistic regression analysis, the diagnostic efficiency of several serum biomarkers was discussed. Besides, compared with single detection, combined detection can better distinguish GC patients from healthy donors, especially when compared with the combined diagnosis model of HCP5, CEA, and CA199, the combination of which can increase sensitivity and specificity, which could reach 81% and 79%, respectively (**Table 2**). The above data showed that the single diagnosis of HCP5 had a significant AUC, and the combined diagnosis of HCP5, CEA, and CA199 can improve the diagnosis efficiency of GC.

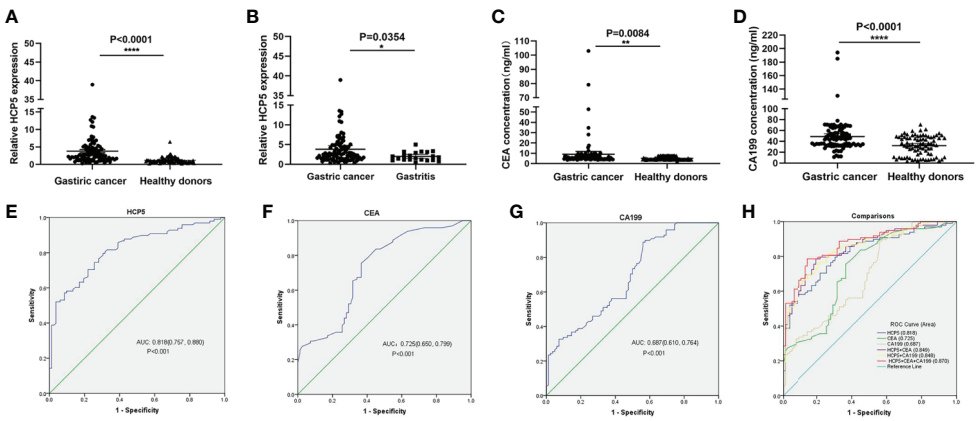

FIGURE 2 | Concentrations of serum HCP5, CEA, and CA199 in GC cases and diagnostic efficacy**. (A)** Detection of serum HCP5 in GC patients (n=98), healthy donors (n=82). **(B)** Detection of serum HCP5 in GC (n=98) and gastritis (n=21) patients. **(C)** The concentrations of serum CEA. **(D)** The concentrations of serum CA199. *P < 0.05, **P < 0.01, ****P < 0.001, NS means no statistically difference. **(E)** The ROC curve of serum HCP5 in GC cases. **(F)** The ROC curve of serum CEA in GC cases. **(G)** The ROC curve of serum CA199 in GC cases. **(H)** The diagnostic efficacy of the combined diagnosis.

TABLE 2 | Combination of serum HCP5, CEA and CA199 levels significantly improves the diagnostic sensitivity between GC patients and healthy donors.

	SEN,%	SPE,%	ACCU,%	PPV,%	NPV,%
HCP5	0.80(78/98)	0.70(57/82)	0.75(135/180)	0.76(78/103)	0.74(57/77)
CEA	0.67(66/98)	0.66(54/82)	0.67(120/180)	0.70(66/94)	0.63(54/86)
CA199	0.56(55/98)	0.59(48/82)	0.57(103/180)	0.62(55/89)	0.53(48/91)
HCP5+CEA	0.79(77/98)	0.80(66/82)	0.79(143/180)	0.83(77/93)	0.76(66/87)
HCP5+CEA+CA199	0.81(79/98)	0.79(65/82)	0.80(144/180)	0.81(79/98)	0.77(65/84)

Origin of HCP5 in GC Samples

To understand the overall expression level of HCP5 in GC, we collected 20 pairs of tissue samples. The result showed that HCP5 was significantly highly expressed in GC tissues (**Figure 3A**). Because of the high expression of HCP5 in serum GC, we assumed whether HCP5 was secreted by GC cells. Then, we detected the expression level of HCP5 in two GC cell lines (MKN-45, MGC-803) and normal control cells GES-1 for 1, 3, 5, and 7 days, respectively (**Figure 3B**). The results showed that compared with normal cell lines, HCP5 increased in MKN-45 and MGC-803 over time, especially in MKN-45. Hence, we speculated that the high expression of HCP5 in peripheral blood might be derived from the secretion of some tumor cells. Furthermore, we detected the subcellular localization of lncRNA HCP5, and the results showed that HCP5 was mainly distributed in the cytoplasm of MKN-45 and BGC-823 cells (**Figure 3C**).

Diagnostic Efficacy of Serum HCP5 in Various Cancer Types and Distinguishing Between Gastritis and Healthy Donors

To verify the specificity of HCP5 expression levels, serum expression levels of 19 thyroid cancer patients, 20 colorectal cancer patients, and 17 breast cancer patients were examined. The results showed that HCP5 expression was not statistically significant not only in thyroid cancer but also in colorectal cancer, and in breast cancer had a little significance (**Figures 4A–C**). At the same time, we detected expression levels of serum HCP5, CEA, and CA199 in 21 patients with gastritis patients and 21 healthy donors, respectively (**Figures 4D–F**). Collectively, the results indicated that serum HCP5 could distinguish gastritis patients from healthy donors. Thus, it can be seen HCP5 can be regarded as a specific biomarker for GC diagnosis.

Correlation Between Serum HCP5 Expression and GC Clinicopathological Parameters

The clinicopathological parameters of 98 patients with GC were summarized in **Table 3**. Based on the cut-off value of serum HCP5, 98 GC patients were divided into the high-value and low-value groups. Chi-square test showed that although we did not find any correlation with serum HCP5 expression in pathological parameters such as gender, age, tumor size, TNM stage, distant metastasis, and CEA. Nevertheless, the high expression of serum HCP5 was correlated with differentiation (P<0.05), lymph node

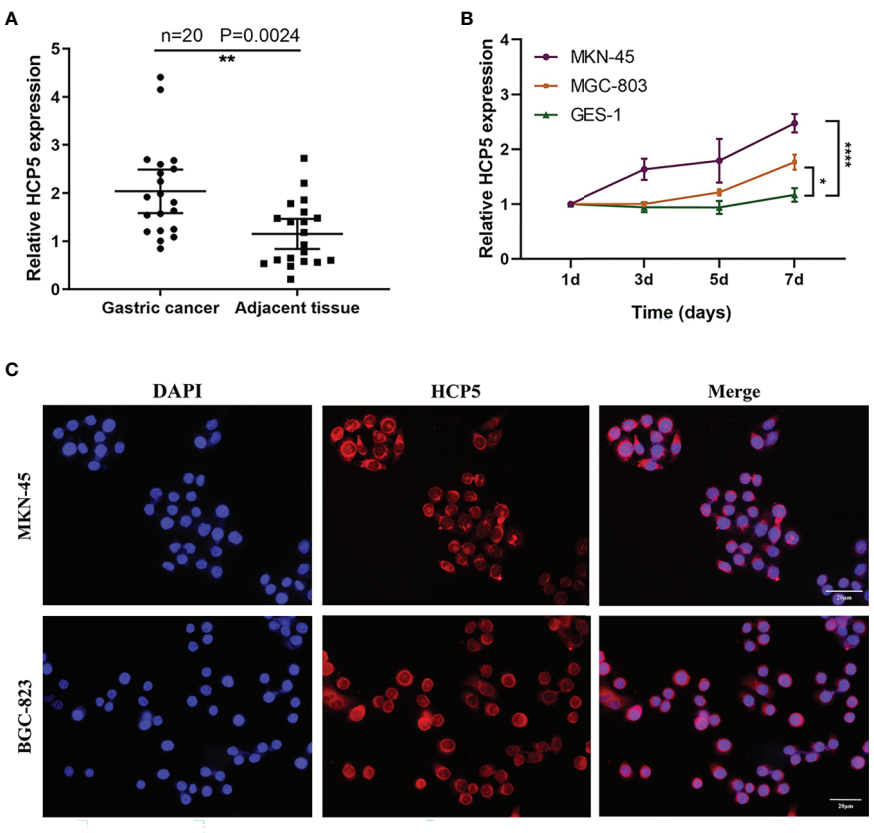

FIGURE 3 | The origin of serum HCP5 in GC cases. **(A)** The expression level of HCP5 in 20 pairs of GC tissues. **(B)** HCP5 was secreted into the culture medium by MKN-45 and MGC-803 cells in a time-dependent manner. *P < 0.05, **P < 0.01, ****P < 0.001. **(C)** The FISH assay of HCP5 in MKN-45 and BGC-823 cells. Scale bars: 20μm.

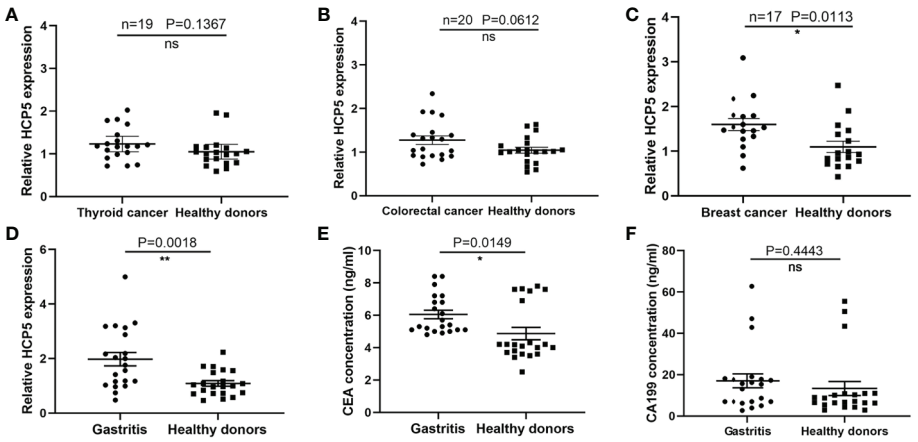

FIGURE 4 | The specificity of serum HCP5 in GC and differentiating from gastritis and healthy donors. **(A)** Detection of serum HCP5 in 19 thyroid cancer patients. **(B)** Detection of serum HCP5 in 20 colorectal cancer patients. **(C)** Detection of serum HCP5 in 17 breast cancer patients. **(D)** The expression levels of HCP5 in gastritis patients (n=21) and healthy donors (n=21). **(E)** The concentrations of CEA in gastritis patients (n=21) and healthy donors (n=21). **(F)** The concentrations of CA199 in gastritis patients (n=21) and healthy donors (n=21). *P < 0.05, **P < 0.01, NS means no statistically difference.

metastasis (P<0.05), and nerve invasion (P<0.05), indicating that serum HCP5 expression was correlated with some GC clinicopathological parameters.

Tumor Dynamic Monitoring of Serum HCP5 in GC Patients

Due to previous reports and our current research, circulating lncRNAs may be secreted by tumor cells, and they would return to an average level after surgery. To verify whether the expression of serum HCP5 was related to tumor dynamic monitoring, we compared serum HCP5 in unpaired samples, including 98 patients with primary gastric cancer, 46 patients with surgical treatment, and 57 patients with tumor recurrence. It was found that the serum HCP5 expression of patients after treatment was significantly lower than that of GC patients and relapsed patients before treatment (**Figure 5A**). Meanwhile, we investigated the differences in serum HCP5 levels in 15 pairs of GC patients before and after surgery. The results showed the expression level of HCP5 after gastrectomy was significantly lower than that of patients with primary GC, which showed that HCP5 could be used for dynamic monitoring (**Figure 5B**). Besides, the survival curve revealed that the overall survival rate of patients with high HCP5 expression was significantly lower than that of patients with low HCP5 expression (P=0.0079) (**Figure 5C**). To sum up, we believed that serum HCP5 could be regarded as a new marker for early diagnosis of GC and tumor dynamic monitoring.

DISCUSSION

Gastric cancer is the common cancer with high mortality and morbidity. Recently, the treatment effect and prediction were still poor and low. Surgical resection was still the primary treatment at present. lncRNA can be divided into sense, antisense, intronic, bidirectional transcripts, intergenic and enhancer RNAs (33). Current studies have shown that lncRNA carried out strict regulation and abnormal expression during the development of different cancers, which can be divided into (1) chromatin regulation; (2) regulation of histone modification; (3) regulation of DNA methylation; (4) interaction with transcription factors; (5) regulation of genomic tissue through enhancer cycle; (6) post-transcriptional regulation (34). For example, kinds of literature have shown that NEAT1 affects chromatin remodeling, increased histone acetylation level, promoted aldehyde dehydrogenase 1 family (ALDH1) and c-Myc expression, and improved drug resistance and tumor dryness 5-FU (35). Zhang et al. (36) found that lnc-LALC bonded to enhancer of zeste homolog 2 (EZH2), recruited DNA methyltransferase (DNMT) to Leucine zipper putative tumor suppressor 1 (LZTS1) promoter, and changed the expression of LZTS1. Another literature reported that in ischemic heart disease, the combination of lncCIRBIL and BCL2-related transcription factor1 (Bclaf1) had a protective effect on I/R damage and was a potential target for treating ischemic heart disease (37). What's more, it also has been convinced that the chromatin cyclization between enhancers E1 and E2 and lncRNA promoter played a co-regulatory role in prostate cancer (38). Furthermore, Wang et al. (39) found that linc00336 can act as an endogenous sponge of miRNA to inhibit lung cancer hypertrophy. Simultaneously, more and more pieces of literature have confirmed that lncRNA can be used as a potential biomarker for tumor screening and prognosis monitoring (20–24). Inspired by this idea, this study was devoted to finding suitable tumor biomarkers.

HCP5, also named P5-1, is located on chromosome 6p21.33. Previous experiments have shown that HCP5 can participate in regulating various tumors, such as HCP5, which was mediated by transforming growth factor β (TGF β) and regulated by recombinant SMAD family member 3 (SMAD3) transcription, could promote the growth and metastasis of lung adenocarcinoma (LUAD) tumors (40). Moreover, HCP5 can encourage the

TABLE 3 | The Correlation between HCP5 expression and clinicopathologic parameters of GC patients.

Characteristics	Total	HCP5		P value
		High expression n = 49	Low expression n = 49	
Gender				0.306
Male	57	31	26	
Female	41	18	23	
Age (years)				0.541
≥60	43	20	23	
<60	55	29	26	
Differentiation				0.026*
Poorly/moderately poorly	53	32	21	
Well/medium-well	45	17	28	
Tumor size (cm)				0.258
≥5	27	11	16	
<5	71	38	33	
TNM stage				0.840
TI-TII	51	26	25	
TIII-TIV	47	23	24	
Lymph node metastasis				0.043*
Positive	50	30	20	
Negative	48	19	29	
Distant metastasis				0.106
Positive	50	29	21	
Negative	48	20	28	
Nerve invasion				0.026*
Positive	51	31	20	
Negative	47	18	29	
CEA (ng/ml)				0.389
≥5.0	66	35	31	
<5.0	32	14	18	

*Statistical analyses were carried out using Pearson χ^2 test. *P < 0.05 was considered significant.*

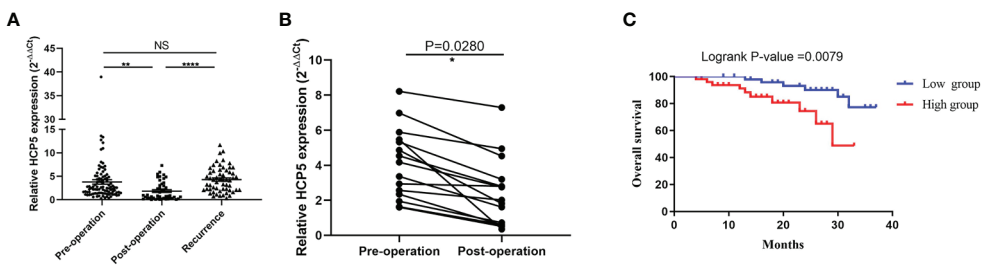

FIGURE 5 | Serum HCP5 in monitoring tumor dynamics in GC patients. **(A)** Detection of serum HCP5 expression in GC pre-operation patients (n=98), post-operation patients (n=46) and recurrence patients (n=57). **(B)** Altered expression of serum HCP5 in 15 paired samples preoperatively and postoperatively. **(C)** The survival curve of patients with GC. *P < 0.05, **P < 0.01, ****P < 0.001, NS means no statistically difference.

development of cervical cancer by inhibiting microRNA-15a regulating metastasis-associated in colon cancer-1 (MACC1) (30). The above studies illustrated that HCP5 was a regulator in the process of tumor development, and it may become a predictor of tumor diagnosis and treatment. At present, real-time fluorescence quantitative PCR (41), microarray (42), and next-generation sequencing (NGS) (43) are often used for quantitative analysis of ncRNA. qRT-PCR was considered a reliable method for detecting non-coding RNA gene expression because of its high sensitivity, speed, and efficiency, as the small sample requirements and ease of interpretation of the results were significant advantages (44). Consequently, in this study, we chose the qRT-PCR method to evaluate serum HCP5 expression, and 18S was selected as the internal reference. The results showed that the expression of HCP5 in GC patients by this method had good linearity, stability, specificity, and repeatability. Besides, large serum samples of gastric cancer detected by qRT-PCR showed that HCP5 could not only significantly distinguish between GC patients and healthy donors, but also could distinguish GC patients from gastritis patients well. The diagnostic efficiency of HCP5 alone was substantially higher than that of CEA and CA199, and the combined diagnosis of HCP5, CEA, and CA199 can improve the diagnostic efficiency of gastric cancer. Then, we detected the expression level of serum HCP5 in thyroid, colorectal, and breast

cancer, found that its expression in the serum GC was the most specific. At the same time, we also detected the expression level of serum HCP5 in gastritis and normal controls. Compared with the typical clinical diagnostic indicators CEA and CA199, the results showed that serum HCP5 could better distinguish gastritis patients from healthy donors. From the above experiments, it can be seen that HCP5 showed a remarkable advantage as a specific biomarker for the diagnosis of GC. Besides, clinicopathological parameters also showed that the high expression of serum HCP5 in GC was notably correlated with differentiation ($P<0.05$), lymph node metastasis ($P<0.05$), and nerve invasion ($P<0.05$), indicating that serum HCP5 expression was correlated with some GC clinicopathological parameters. Moreover, the statistics of 20 pairs of GC tissues showed that HCP5 had a conspicuous trend of high expression. What's more, previous literature reported a pronounced correlation between the expression of circulating biomarkers in blood and cells (45). To verify whether HCP5 was secreted by tumor cells, we also examined the expression of HCP5 in GES-1, MGC-803, and MKN-45. We found that the expression of HCP5 in MGC-803 and MKN-45 was dramatically increased, especially in MKN-45. It was speculated that HCP5 might come from the secretion of tumor cells and was mainly related to tumor metastasis. Meanwhile, the FISH assay showed that HCP5 was mainly present in the cytoplasm of MKN-45 and BGC-823. Besides, by comparing the expression of serum HCP5 in patients with primary gastric cancer, patients undergoing surgery, and patients with postoperative recurrence, we found that serum HCP5 rebounded in patients with tumor recurrence and it had the ability to monitor tumor dynamics. Meanwhile, we also detected the expression level of HCP5 in 15 pairs of GC patients before and after an operation. The results showed that the expression level of HCP5 after gastrectomy was strikingly lower than that in patients with primary GC, which indicated that HCP5 could be a specific biomarker and played an important role in dynamic monitoring. The survival curve showed that the OS rate of patients with high serum HCP5 was significantly lower than that of patients with low expression of serum HCP5. It showed a positive correlation between a high level of HCP5 and poor survival and prognosis of GC.

In short, our study showed that the increase of serum HCP5 could significantly distinguish between patients with primary gastric cancer and healthy controls, and the combined diagnosis of HCP5, CEA, and CA199 had high diagnostic efficiency. At present, gastritis is mainly divided into gastroscopy and laboratory examination, which included gastric juice analysis, pepsinogen test, serum gastrin test, and Helicobacter pylori test. There may be no significant difference in laboratory indexes among different types and locations of Lauren tumors, which had some limitations (46). For Helicobacter pylori testing, studies have shown that bacteria could be eliminated in atrophic gastritis development, so it also had certain limitations (47). Hence, it was indispensable to find other specific serum biomarkers combined with other preventive measures. Compared with the traditional clinical indexes, serum HCP5 can better distinguish gastritis from healthy donors. Thus, it can be concluded that serum HCP5 may be a potential biomarker in dynamic monitoring of gastric cancer and tumor. Nevertheless, there were some limitations in this study. The samples of this study were only limited to one hospital in China. If conditions permit, serum samples from patients in multiple hospitals could be collected for further study. In addition, due to the limited sample size of patients with gastritis, it was necessary to increase further gastritis samples and long-term observation of patients with gastritis to obtain new insights into the potential mechanism of the diagnostic and prognostic value of HCP5.

DATA AVAILABILITY STATEMENT

The original contributions presented in the study are included in the article/**Supplementary Material**. Further inquiries can be directed to the corresponding author.

ETHICS STATEMENT

The studies involving human participants were reviewed and approved by the ethics committee of the Affiliated Hospital of Nantong University (ethical review report number: 2018-L055). The patients/participants provided their written informed consent to participate in this study. Written informed consent was obtained from the individual(s) for the publication of any potentially identifiable images or data included in this article.

AUTHOR CONTRIBUTIONS

SQ designed the experiment, conducted the data analysis, made charts, and wrote the article. LY performed the experiment and conducted the data collection. SK gave some suggestions and carried out the revision of the article. YX gave advice for some charts and participated in the final revision. BL and SJ provided resources and guidance for the paper. All authors contributed to the article and approved the submitted version.

FUNDING

This project was supported by grants from the National Natural Science Foundation of China [grant number: 81871720, 82072363], and Jiangsu Province "science, education, and health" key discipline [grant number: ZDXKB2016011].

SUPPLEMENTARY MATERIAL

The Supplementary Material for this article can be found online at: https://www.frontiersin.org/articles/10.3389/fonc.2021.684531/full#supplementary-material

Supplementary Figure 1 | (A) The ROC curve of the poorly, moderately poorly groups and well, medium-well groups. **(B)** The ROC curve of the lymph node metastasis positive and negative groups. **(C)** The ROC curve of the nerve invasion positive and negative groups.

Supplementary Figure 2 | (A) Serum HCP5 expression of differentiation. **(B)** Serum HCP5 expression of lymph node metastasis. **(C)** Serum HCP5 expression of nerve invasion.

Supplementary Figure 3 | The time-dependent studies on HGC-27, BGC-823, and GES-1 cells.

Supplementary Figure 4 | (A) The ROC curve of the TIII-TIV group. **(B)** The ROC curve of the TI-TII group.

REFERENCES

1. Sung H, Ferlay J, Siegel R, Laversanne M, Soerjomataram I, Jemal A, et al. Global Cancer Statistics 2020: GLOBOCAN Estimates of Incidence and Mortality Worldwide for 36 Cancers in 185 Countries. *CA: Cancer J Clin* (2021) 70:313. doi: 10.3322/caac.21660
2. Zeng H, Chen W, Zheng R, Zhang S, Ji JS, Zou X, et al. Changing Cancer Survival in China During 2003-15: A Pooled Analysis of 17 Population-Based Cancer Registries. *Lancet Glob Health* (2018) 6(5):e555–67. doi: 10.1016/S2214-109X(18)30127-X
3. Cai Z, Liu Q. Understanding the Global Cancer Statistics 2018: Implications for Cancer Control. *Sci China Life Sci* (2019) 87:162–8. doi: 10.1007/s11427-019-9816-1
4. Portuondo J, Tran Cao H, da Costa W, Sada Y, Harris A, Massarweh N. Treatment Approach, Hospital Practice Patterns, and Receipt of Multimodality Therapy as Measures of Quality for Locally Advanced Gastric Cancer. *J Surg Oncol* (2021) 123:1724–35. doi: 10.1002/jso.26460
5. Yamamoto H, Watanabe Y, Sato Y, Maehata T, Itoh F. Non-Invasive Early Molecular Detection of Gastric Cancers. *Cancers* (2020) 12(10):2880. doi: 10.3390/cancers12102880
6. Zhang F, Wang H, Yu J, Yao X, Yang S, Li W, et al. Lncrna CRNDE Attenuates Chemoresistance in Gastric Cancer *Via* SRSF6-Regulated Alternative Splicing of PICALM. *Mol Cancer* (2021) 20(1):6. doi: 10.1186/s12943-020-01299-y
7. Shuai Y, Ma Z, Liu W, Yu T, Yan C, Jiang H, et al. TEAD4 Modulated LncRNA Mnx1-AS1 Contributes to Gastric Cancer Progression Partly Through Suppressing BTG2 and Activating BCL2. *Mol Cancer* (2020) 19 (1):6. doi: 10.1186/s12943-019-1104-1
8. Wang C, Zhu C, Xu J, Wang M, Zhao W, Liu Q, et al. The Lncrna UCA1 Promotes Proliferation, Migration, Immune Escape and Inhibits Apoptosis in Gastric Cancer by Sponging Anti-Tumor MiRNAs. *Mol Cancer* (2019) 18 (1):115. doi: 10.1186/s12943-019-1032-0
9. Hung T, Chang H. Long Noncoding RNA in Genome Regulation: Prospects and Mechanisms. *RNA Biol* (2010) 7(5):582–5. doi: 10.4161/rna.7.5.13216
10. Sun W, Lv J, Duan L, Lin R, Li Y, Li S, et al. Long Noncoding RNA H19 Promotes Vascular Remodeling by Sponging let-7a to Upregulate the Expression of Cyclin D1. *Biochem Biophys Res Commun* (2019) 508 (4):1038–42. doi: 10.1016/j.bbrc.2018.11.185
11. Svitich O, Sobolev V, Gankovskaya L, Zhigalkina P, Zverev V. The Role of Regulatory RNAs (miRNAs) in Asthma. *Allergol Immunopathol* (2018) 46 (2):201–5. doi: 10.1016/j.aller.2017.09.015
12. Mercer T, Dinger M, Mattick J. Long Non-Coding RNAs: Insights Into Functions. *Nat Rev Genet* (2009) 10(3):155–9. doi: 10.1038/nrg2521
13. Kretz M, Webster D, Flockhart R, Lee C, Zehnder A, Lopez-Pajares V, et al. Suppression of Progenitor Differentiation Requires the Long Noncoding RNA Ancr. *Genes Dev* (2012) 26(4):338–43. doi: 10.1101/gad.182121.111
14. Zhang J, Sui S, Wu H, Zhang J, Zhang X, Xu S, et al. The Transcriptional Landscape of lncRNAs Reveals the Oncogenic Function of LINC00511 in ER-Negative Breast Cancer. *Cell Death Dis* (2019) 10(8):599. doi: 10.1038/s41419-019-1835-3
15. Wang P, Xue Y, Han Y, Lin L, Wu C, Xu S, et al. The STAT3-Binding Long Noncoding RNA lnc-DC Controls Human Dendritic Cell Differentiation. *Science (New York NY)* (2014) 344(6181):310–3. doi: 10.1126/science.1251456
16. Zhang H, Liu L, Wang Y, Zhao G, Xie R, Liu C, et al. KLF8 Involves in TGF-Beta-induced EMT and Promotes Invasion and Migration in Gastric Cancer Cells. *J Cancer Res Clin Oncol* (2013) 139(6):1033–42. doi: 10.1007/s00432-012-1363-3
17. Shahabi S, Kumaran V, Castillo J, Cong Z, Nandagopal G, Mullen D, et al. Linc00261 Is An Epigenetically Regulated Tumor Suppressor Essential for Activation of the DNA Damage Response. *Cancer Res* (2019) 79(12):3050–62. doi: 10.1158/0008-5472.Can-18-2034
18. Yu B, Wang S. Angio-Lncrs: LncRNAs That Regulate Angiogenesis and Vascular Disease. *Theranostics* (2018) 8(13):3654–75. doi: 10.7150/thno.26024
19. Wu M, Fu P, Qu L, Liu J, Lin A. Long Noncoding RNAs, New Critical Regulators in Cancer Immunity. *Front Oncol* (2020) 10:550987. doi: 10.3389/fonc.2020.550987
20. El-Ashmawy N, Hussien F, El-Feky O, Hamouda S, Al-Ashmawy G. Serum LncRNA-ATB and FAM83H-AS1 as Diagnostic/Prognostic Non-Invasive Biomarkers for Breast Cancer. *Life Sci* (2020) 259:118193. doi: 10.1016/j.lfs.2020.118193
21. Yin Q, Wu A, Liu M. Plasma Long Non-Coding RNA (LncRNA) GAS5 Is a New Biomarker for Coronary Artery Disease. *Med Sci Monitor Int Med J Exp Clin Res* (2017) 23:6042–8. doi: 10.12659/msm.907118
22. Yu J, Dong W, Liang J. Extracellular Vesicle-Transported Long Non-Coding RNA (LncRNA) X Inactive-Specific Transcript (XIST) in Serum Is a Potential Novel Biomarker for Colorectal Cancer Diagnosis. *Med Sci Monitor Int Med J Exp Clin Res* (2020) 26:e924448. doi: 10.12659/msm.924448
23. Berrondo C, Flax J, Kucherov V, Siebert A, Osinski T, Rosenberg A, et al. Expression of the Long Non-Coding RNA Hotair Correlates With Disease Progression in Bladder Cancer and Is Contained in Bladder Cancer Patient Urinary Exosomes. *PloS One* (2016) 11(1):e0147236. doi: 10.1371/journal.pone.0147236
24. Kopp F, Mendell J. Functional Classification and Experimental Dissection of Long Noncoding RNAs. *Cell* (2018) 172(3):393–407. doi: 10.1016/j.cell.2018.01.011
25. Zou Y, Chen B. Long Non-Coding RNA HCP5 in Cancer. *Clinica Chimica acta; Int J Clin Chem* (2021) 512:33–9. doi: 10.1016/j.cca.2020.11.015
26. Liang L, Xu J, Wang M, Xu G, Zhang N, Wang G, et al. Lncrna HCP5 Promotes Follicular Thyroid Carcinoma Progression *Via* miRNAs Sponge. *Cell Death Dis* (2018) 9(3):372. doi: 10.1038/s41419-018-0382-7
27. Wang L, Luan T, Zhou S, Lin J, Yang Y, Liu W, et al. Lncrna HCP5 Promotes Triple Negative Breast Cancer Progression as a ceRNA to Regulate BIRC3 by Sponging Mir-219a-5p. *Cancer Med* (2019) 8(9):4389–403. doi: 10.1002/cam4.2335
28. Wu J, Chen H, Ye M, Wang B, Zhang Y, Sheng J, et al. Long Noncoding RNA HCP5 Contributes to Cisplatin Resistance in Human Triple-Negative Breast Cancer *Via* Regulation of PTEN Expression. *Biomed Pharmacother = Biomed Pharmacother* (2019) 115:108869. doi: 10.1016/j.biopha.2019.108869
29. Liu Y, Wang J, Dong L, Xia L, Zhu H, Li Z, et al. Long Noncoding Rna HCP5 Regulates Pancreatic Cancer Gemcitabine (Gem) Resistance by Sponging Hsa-Mir-214-3p To Target Hdgf. *OncoTargets Ther* (2019) 12:8207–16. doi: 10.2147/ott.S222703
30. Zhao W, Li L. SP1-Induced Upregulation of Long Non-Coding RNA HCP5 Promotes the Development of Osteosarcoma. *Pathol Res Pract* (2019) 215 (3):439–45. doi: 10.1016/j.prp.2018.12.006
31. Wu H, Liu B, Chen Z, Li G, Zhang Z. MSC-Induced Lncrna HCP5 Drove Fatty Acid Oxidation Through Mir-3619-5p/AMPK/PGC1α/CEBPB Axis to Promote Stemness and Chemo-Resistance of Gastric Cancer. *Cell Death Dis* (2020) 11(4):233. doi: 10.1038/s41419-020-2426-z
32. Grace M, McLeland C, Gagliardi S, Smith J, Jackson W, Blakely W. Development and Assessment of a Quantitative Reverse transcription-PCR Assay for Simultaneous Measurement of Four Amplicons. *Clin Chem* (2003) 49: (9):1467–75. doi: 10.1373/49.9.1467
33. Beermann J, Piccoli M, Viereck J, Thum T. Non-Coding RNAs in Development and Disease: Background, Mechanisms, and Therapeutic Approaches. *Physiol Rev* (2016) 96(4):1297–325. doi: 10.1152/physrev.00041.2015
34. Schmitz S, Grote P, Herrmann B. Mechanisms of Long Noncoding RNA Function in Development and Disease. *Cell Mol Life Sci CMLS* (2016) 73 (13):2491–509. doi: 10.1007/s00018-016-2174-5
35. Zhu Y, Hu H, Yuan Z, Zhang Q, Xiong H, Hu Z, et al. Lncrna NEAT1 Remodels Chromatin to Promote the 5-Fu Resistance by Maintaining Colorectal Cancer Stemness. *Cell Death Dis* (2020) 11(11):962. doi: 10.1038/s41419-020-03164-8
36. Zhang C, Wang L, Jin C, Zhou J, Peng C, Wang Y, et al. Long Non-Coding RNA lnc-LALC Facilitates Colorectal Cancer Liver Metastasis *Via* Epigenetically Silencing LZTS1. *Cell Death Dis* (2021) 12(2):224. doi: 10.1038/s41419-021-03461-w

37. Zhang Y, Zhang X, Cai B, Li Y, Jiang Y, Fu X, et al. The Long Noncoding RNA lncCIRBIL Disrupts the Nuclear Translocation of Bclaf1 Alleviating Cardiac Ischemia-Reperfusion Injury. *Nat Commun* (2021) 12(1):522. doi: 10.1038/s41467-020-20844-3
38. Chen Z, Song X, Li Q, Xie L, Guo T, Su T, et al. Tmprss2androgen Receptor-Activated Enhancers Simultaneously Regulate Oncogene and lncRNA in Prostate Cancer. *Cells* (2019) 8(8):864. doi: 10.3390/cells8080864
39. Wang M, Mao C, Ouyang L, Liu Y, Lai W, Liu N, et al. Long Noncoding RNA LINC00336 Inhibits Ferroptosis in Lung Cancer by Functioning as a Competing Endogenous RNA. *Cell Death Differ* (2019) 26(11):2329–43. doi: 10.1038/s41418-019-0304-y
40. Jiang L, Wang R, Fang L, Ge X, Chen L, Zhou M, et al. HCP5 is a SMAD3-Responsive Long Non-Coding RNA That Promotes Lung Adenocarcinoma Metastasis *Via* miR-203/SNAI Axis. *Theranostics* (2019) 9(9):2460–74. doi: 10.7150/thno.31097
41. Benes V, Castoldi M. Expression Profiling of microRNA Using Real-Time Quantitative PCR, How to Use It and What Is Available. *Methods (San Diego Calif)* (2010) 50(4):244–9. doi: 10.1016/j.ymeth.2010.01.026
42. Qin Y, Hou Y, Liu S, Zhu P, Wan X, Zhao M, et al. A Novel Long Non-Coding RNA Lnc030 Maintains Breast Cancer Stem Cell Stemness by Stabilizing Sqle mRNA and Increasing Cholesterol Synthesis. *Advanced Sci (Weinheim Baden Wurttemberg Germany)* (2021) 8(2):2002232. doi: 10.1002/advs.202002232
43. Sikora M, Marycz K, Smieszek A. Small and Long Non-Coding RNAs as Functional Regulators of Bone Homeostasis, Acting Alone or Cooperatively. *Mol Ther Nucleic Acids* (2020) 21:792–803. doi: 10.1016/j.omtn.2020.07.017
44. Anfossi S, Babayan A, Pantel K, Calin G. Clinical Utility of Circulating non-Coding RNAs - An Update. *Nat Rev Clin Oncol* (2018) 15(9):541–63. doi: 10.1038/s41571-018-0035-x
45. Pritchard C, Kroh E, Wood B, Arroyo J, Dougherty K, Miyaji M, et al. Blood Cell Origin of Circulating microRNAs: A Cautionary Note for Cancer Biomarker Studies. *Cancer Prev Res (Philadelphia Pa)* (2012) 5(3):492–7. doi: 10.1158/1940-6207.Capr-11-0370
46. Bornschein J, Selgrad M, Wex T, Kuester D, Malfertheiner P. Serological Assessment of Gastric Mucosal Atrophy in Gastric Cancer. *BMC Gastroenterol* (2012) 12:10. doi: 10.1186/1471-230x-12-10
47. D'Elios M, Appelmelk B, Amedei A, Bergman M, Del Prete G. Gastric Autoimmunity: The Role of Helicobacter Pylori and Molecular Mimicry. *Trends Mol Med* (2004) 10(7):316–23. doi: 10.1016/j.molmed.2004.06.001

Conflict of Interest: The authors declare that the research was conducted in the absence of any commercial or financial relationships that could be construed as a potential conflict of interest.

GLOSSARY

GC	gastric cancer
lncRNA	long non-coding RNA
mRNA	messenger RNA
miRNA	microRNA
ceRNA	competitive endogenous RNA
CAD	coronary artery disease
CRC	colorectal cancer
HCP5	Histocompatibility leukocyte antigen complex P
MICA	MHC class I polypeptide related sequence A
MICB	MHC class I polypeptide related sequence B
MHCI	MHC class I chain-related gene
SP1	the transcription factor 1
PPARG	peroxisome proliferative activated receptor gamma
PPARGC1A	PPARG coactivator 1 alpha
AMPK	the AMP-activated protein kinase
PPAR	peroxisome proliferator-activated receptor
PGC1α	PPAR coactivator-1α
CEBPB	enhancer-binding protein β
5-Fu	5-Fluorouracil
CEA	carcinoembryonic antigen
CA199	carbohydrate antigen199
THCA	thyroid cancer
BRCA	breast cancer
cDNA	Complementary DNA
qRT-PCR	real-time fluorescence quantitative polymerase chain reaction
dNTPs	deoxyribonucleotide triphosphate
18S	18S ribosomal RNA
FBS	fetal bovine serum
AGE	Agarose Gel Electrophoresis
PBS	phosphate buffer saline
FISH	fluorescence *in situ* hybridization
DAPI	4'’,6-Diamidino-2'-phenylindole
SD	standard deviation
ANOVA	one-way analysis of variance
ROC	receiver operating characteristic curve
AUC	area under the ROC curve
OS	overall survival
U6	U6 small nuclear RNA
ACTB	β-actin
TUB	tubulin
CV	coefficients of variation
STAD	stomach adenocarcinoma
ALDH1	aldehyde dehydrogenase 1 family
EZH2	enhancer of zeste homolog 2
DNMT	DNA methyltransferase
LZTS1	Leucine zipper putative tumor suppressor 1
Bclaf1	BCL2-related transcription factor1
TGF β	transforming growth factor β
SMAD3	recombinant SMAD family member 3
LUAD	Lung adenocarcinoma
MACC1	metastasis-associated in colon cancer-1
NGS	next-generation sequencing

frontiers in Oncology

ORIGINAL RESEARCH
published: 24 June 2021
doi: 10.3389/fonc.2021.614462

Exosomal circRNA in Digestive System Tumors: The Main Player or Coadjuvants?

Haoying Wang[1,2], *Xi Zeng*[1,2], *Ya Zheng*[1,2], *Yuping Wang*[1,2*] *and Yongning Zhou*[1,2*]

[1] Department of Gastroenterology, The First Hospital of Lanzhou University, Lanzhou, China, [2] Key Laboratory for Gastrointestinal Diseases of Gansu Province, Lanzhou University, Lanzhou, China

Exosomes are a type of extracellular microvesicles with a diameter of 40–160 nm. Circular RNA (circRNA) is a type of closed circular RNA molecule that is highly conserved in evolution. Exosomal circRNA plays a vital role in the proliferation, invasion, migration, and drug resistance of digestive system tumors. In this study, we used The Cancer Genome Atlas (TCGA) database, UALCAN, Python crawler, miRTargetLink Human, Database for Annotation, Visualization, and Integrated Discovery (DAVID), micBioinformatic online tool, and Cytoscape software (3.7.1). The results showed that circ-RanGAP1 in gastric cancer, circUHRF1 in hepatocellular carcinoma, and circFMN2 in colorectal cancer regulate the malignant behavior of tumors and affect the expression of their host gene through sponging miR-877-3p, miR-449c-5p, and miR-1182, respectively. Twenty exosomal circRNAs regulate 6,570 target genes through sponging 23 miRNAs. Firstly, 270 of those target genes are regulated by two or more miRNAs, which are highly correlated with 83 tumor-related pathways and six Kyoto Encyclopedia of Genes and Genomes pathways. Secondly, 1,146 target genes were significantly differentially expressed in corresponding digestive system tumors, and functional enrichment analysis revealed that 78 of those were involved in 20 cancer-related pathways. In short, the bioinformatics analysis showed that these exosomal circRNAs are stably expressed in body fluids, and regulate the occurrence and development of gastric cancer, hepatocellular carcinoma, colorectal cancer, and other digestive system tumors through sponging miRNAs. Exosomal circRNAs may be used as biomarkers for the diagnosis of disease and identification of effective therapeutic targets in the future, as well as improve the prognosis of patients with digestive system tumors.

Keywords: exosome, circRNA, digestive system tumors, gastrointestinal tumors, bioinformatics

OPEN ACCESS

Edited by:
Kenneth K. W. To,
The Chinese University of Hong Kong, China

Reviewed by:
Li Zhang,
University of Minnesota Twin Cities, United States
Jingyu Xu,
Zunyi Medical University, China

****Correspondence:***
Yongning Zhou
zhouyn@lzu.edu.cn
Yuping Wang
wangyuping@lzu.edu.cn

Specialty section:
This article was submitted to Gastrointestinal Cancers, a section of the journal Frontiers in Oncology

Received: *06 October 2020*
Accepted: *10 June 2021*
Published: *24 June 2021*

Citation:
Wang H, Zeng X, Zheng Y, Wang Y and Zhou Y (2021) Exosomal circRNA in Digestive System Tumors: The Main Player or Coadjuvants? Front. Oncol. 11:614462. doi: 10.3389/fonc.2021.614462

INTRODUCTION

Five of the top 10 tumors with the highest mortality rate worldwide are tumors of the digestive system, including esophageal, gastric, colorectal, hepatocellular, and pancreatic cancers (1). At the same time, esophageal, hepatocellular, gastric, and colorectal cancers rank among the top 10 tumor diseases with the most severe morbidity (1). Hence, the digestive system tumors pose a serious threat to human health worldwide.

In recent years, a large number of genomics studies have investigated the underlying mechanism of malignant tumors. The most common changes are observed in the tumor and immune microenvironment, post-transcriptional modifications (e.g., DNA methylation), and abnormalities in mesenchymal and tumor stem cells (2–6). However, in recent years, an increasing number of studies have shown that are involved in a variety of tumor biological processes in digestive system tumors (7, 8).

Exosomes are a type of extracellular microbubbles with a diameter of 40–160 nm; they are wrapped by a lipid bilayer membrane and secreted by eukaryotic cells (9). Initially, exosomes were considered wastes of cell metabolism (10). However, with the advancement of biological technology, researches gradually realized that exosomes are involved in a widespread mode of intercellular communication that regulates Alzheimer's disease, diabetes, tumors, and many other diseases (7, 11, 12). Exosomes can promote tumor epithelial–mesenchymal transition, proliferation, invasion, migration, and inhibit tumor cell apoptosis by transporting a variety of proteins, non-coding RNA, metabolites, and lipids (13). In recent years, the potential of exosomes as targets for the diagnosis and treatment of tumors has received extensive research attention, especially with regard to digestive system tumors.

Circular RNA (circRNA) is a type of closed circular RNA molecule, without a 5' cap structure and 3' poly-A tail, that is highly conserved in evolution (14). Similar to exosomes, circRNA was initially considered to be a non-functional mis-splicing body. It was later discovered that it plays an irreplaceable role in a variety of biological processes, particularly tumor progression (15). Numerous studies have shown that circRNA acts on remote tissues and cells by being wrapped by exosomes. It has the ability to regulate various signal pathways, thereby promoting the progression of malignant tumors (16, 17).

In this study, we collected experimentally verified exosomal circRNAs from five types of digestive system tumors (i.e., esophageal, gastric, colorectal, liver, and pancreatic cancers), and investigated the biological functions of these circRNAs and their sponging of miRNAs and target genes. Our results showed that exosomal circRNA participated in a complex competing endogenous RNA network, and regulated the occurrence and development of digestive system tumors. They are expected to be used as important diagnostic and treatment markers for digestive system tumors in the future.

MATERIALS AND METHODS

Search for Exosomal circRNAs

Research literature related to exosomal circRNA and digestive system tumors (published prior to August 2020) was retrieved from the PubMed database. The keywords used are as follows: exosomal, circRNA, circular RNA, hsa_circ, esophageal, gastric, hepatocellular, colorectal, pancreatic, cancer, carcinoma, tumor, and neoplasm. Only studies investigating exosomal circRNA through western blotting, reverse-transcription polymerase chain reaction, and cell phenotyping or animal experiments were included in the present analysis. There were no language or other restrictions. All circRNAs in the literature are derived from the detection of clinical samples.

Expression Levels of the Host Gene of Exosomal circRNA

The UALCAN online tool (http://ualcan.path.uab.edu/index.html) was used to analyze the expression of the host gene of exosomal circRNA (18). The background data of this website are derived from TCGA, which is committed to providing global cancer researchers with extensive and reliable information on the expression of human tumor-related genes, miRNAs and proteins (18). We used Python crawler (https://www.python.org/) to download website data.

Prediction and Enrichment of miRNA Target Genes

The miRTargetLink Human (https://ccb-web.cs.uni-saarland.de/mirtargetlink/) online tool was used to analyze the target genes of miRNA and create a miRNA-mRNA interaction network (19). The miRTargetLink Human offers detailed information on human microRNA-mRNA interactions in the form of interactive interaction networks (19). Therefore, all the predicted target genes and subsequent data analysis in this study are all based on human-derived genes. The Database for Annotation, Visualization, and Integrated Discovery (DAVID) website (https://david.ncifcrf.gov/) was used to perform Kyoto Encyclopedia of Genes and Genomes (KEGG) analysis and Gene Ontology (GO) analysis of miRNA target genes. The micBioinformatic (http://www.bioinformatics.com.cn/) online tool was used to create graphs for the KEGG and GO analyses (20, 21). **S1**–**S7** shows target genes with fold change >2 or <0.05, and $p<0.05$.

Competing Endogenous RNA Network in Digestive System Tumors

The Cytoscape (Version 3.7.1, https://cytoscape.org/) tool was used to construct the circRNA-miRNA-mRNA interaction network.

RESULTS

We retrieved 30 research articles. From the analysis, we identified 32 exosomal circRNAs related to digestive system tumors, including one for esophageal cancer, seven for gastric cancer, 12 for hepatocellular carcinoma, 10 for colorectal cancer, and two for pancreatic cancer (**Table 1**) (22–51). Among these, 26 molecules were upregulated, six molecules were downregulated, and 20 molecules sponged miRNA (**Table 1**). We separately analyzed the host gene and target miRNA of the 32 exosomal circRNAs. Two different strategies were used to analyze the target gene of miRNA. Finally, the circRNA-miRNA-mRNA interaction network was constructed based on the key molecules obtained. **Figure 1** shows the flow diagram of the study.

TABLE 1 | Description of circRNAs in digestive system tumors.

Type of Cancer	CircRNA	Expression	Function	Host gene	Expression	Sponged miRNA	Mechanism	Clinical (Biomarker)	Target Gene	Ref
Esophageal Cancer	hsa_circ_0001946	Down	TS	CDR1	Down*			Diagnostic		(22)
Gastric Cancer	hsa_circ_0000936	Up	Oncogene	SHKBP1	Up	miR-582-3p	CeRNA	Diagnostic, Prognosis	HUR/VEGF, HSP90	(23)
	hsa_circ_0000419	Down	TS	RAB3IP	Up			Diagnostic		(24)
	hsa_circ_0065149	Down	TS	SETD2	Up			Prognosis		(25)
	hsa_circ_0063526	Up	Oncogene	RanGAP1	Up	miR-877-3p	CeRNA	Prognosis	VEGFA	(26)
	hsa_circ_0004771	Up	Oncogene	NRIP1	Up	miR-149-5p	CeRNA	Prognosis	AKT1/mTOR	(27)
	hsa_circ_0010522	Up	Oncogene	RAP1GAP	Down*	miR-133	CeRNA		PRDM16	(28)
	hsa_circ_0130810	Down	TS	KIAA1244	Up			Prognosis		(29)
Hepatocellular Cancer	hsa_circ_0048677	Up	Oncogene	UHRF1	Up	miR-449c-5p	CeRNA	Resistance to anti-PD1	TIM-3	(30)
	hsa_circ_0004001	Up	Oncogene	CLK1	Up			Prognosis		(31)
	hsa_circ_0004123	Up	Oncogene	ETV6	Up			Prognosis		(31)
	hsa_circ_0075792	Up	Oncogene	KDM1B	Up			Prognosis		(31)
	hsa_circ_0017252	Up	Oncogene	AKT3	Down			Prognosis		(32)
	has_circ_0039411	Up	Oncogene	MMP2	Up	miR-136-5p	CeRNA	Prognosis		(33)
	hsa_circ_100338	Up	Oncogene	SNX27	Up			Prognosis	HUVECs	(34)
	hsa_circ_0051443	Down	TS	TRAPPC6A	Up	miR-331-3p	CeRNA	Diagnostic	BAK1	(35)
	has_circ_0025129	Up	Oncogene	TNFRSF1A	Down	miR-34a	CeRNA	Prognosis	USP7	(36)
	circPTGR1[#]	Up	Oncogene	PTGR1	Down*	miR449a	CeRNA	Prognosis	MET	(37)
	hsa_circ_0001946	Up	Oncogene	CDR1	Down	miR-1270	CeRNA	Upregulated AFP	AFP	(38)
	hsa_circ_100284	Up	Oncogene	GCLM	Up	miR-217	CeRNA	Carcinogenesis by arsenite	EZH2	(39)
Colorectal Cancer	hsa_circ_0000677	Up	Oncogene	ABCC1	Up			Prognosis	Wnt/catenin	(40)
	hsa_circ_0010522	Up	Oncogene	RAP1GAP	Down*	miR-133a	CeRNA	Prognosis	GEF-H1/RhoA	(41)
	hsa_circ_0101802	Up	Oncogene	PNN	Up	miR-6833-3p/let-7i-3p/miR-1301-3p	CeRNA	Diagnostic		(42)
	hsa_circ_0005963	Up	Oncogene	TMEM128	Down*	miR-122	CeRNA	Resistance to oxaliplatin	PKM2	(43)
	hsa_circ_0069313	Up	Oncogene	PACRGL	Up	miR-142-3p/miR-506-3p	CeRNA	Prognosis	TGF-β1	(44)
	hsa_circ_0008558	Up	Oncogene	LONP2	Up	miR-17	CeRNA	Prognosis		(45)
	hsa-circ-0004771	Up	Oncogene	NRIP1	Down			Diagnostic		(46)
	hsa_circ_0005100	Up	Oncogene	FMN2	Down	miR-1182		Prognosis	hTERT	(47)
	hsa_circ_0000338	Down	TS	FCHSD2	Down*			FOLFOX-resistance		(48)
	hsa_circ_0067835	Up	Oncogene	IFT80	Up	miR-1236-3p	CeRNA	Prognosis	HOXB7	(49)
Pancreatic Cancer	hsa_circ_0036627	Up	Oncogene	PDE8A	Down	miR-338	CeRNA	Prognosis	MACC1/MET	(50)
	hsa_circ_0087502	Up	Oncogene	IARS	Up*	miR-122	CeRNA	Prognosis	ZO-1, RhoA, RhoA-GTP	(51)

(*) Statistically not significant. [#]: In Ref (37), hsa_circ_0008043, hsa_circ_0003731, and hsa_circ_0088030 were all transcribed from the same gene (prostaglandin reductase 1, PTGR1) and were therefore collectively named circPTGR1; Up, Upregulated; Down, Downregulated; TS, Tumor suppressor; CeRNA, competitive endogenous RNAs; Ref., References.

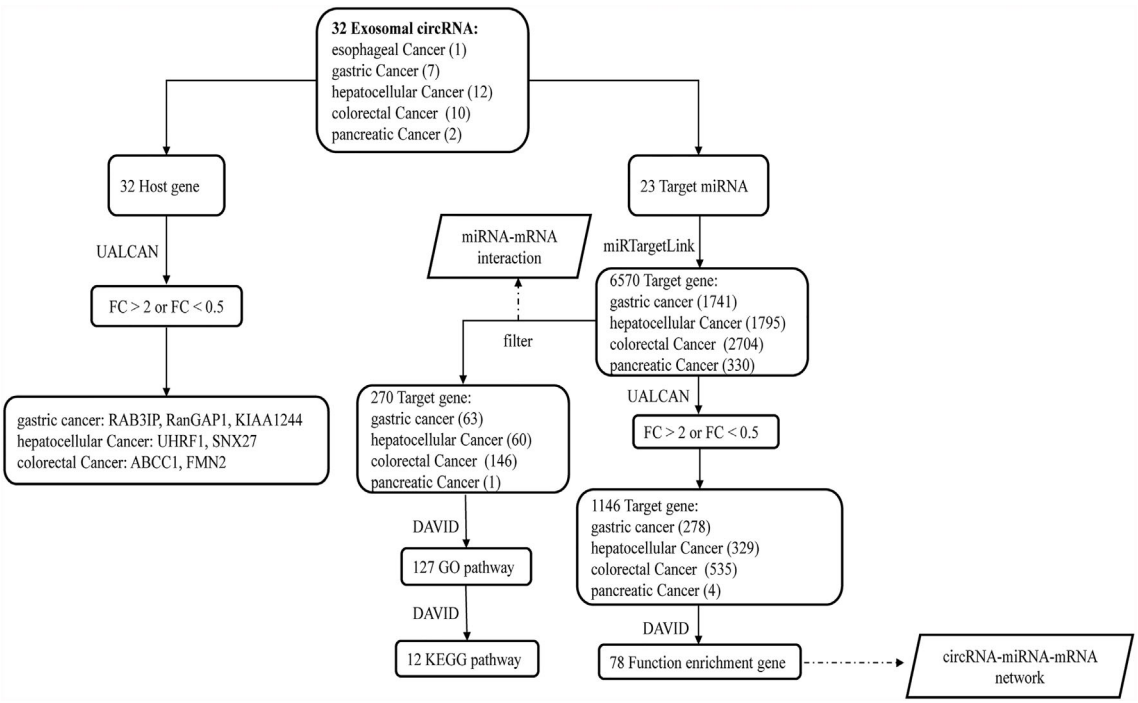

FIGURE 1 | The flow diagram of the study. After obtaining 32 exosomal circRNAs from the literature, we further analyzed their 32 host genes and 23 target miRNAs. Among the 32 host genes, 7 host genes of circRNAs were significantly differentially expressed in the corresponding tumors. Two different methods were used to analyze the downstream target genes and related functions of 23 miRNAs.

Expression of the Host Gene in Digestive System Tumors

TCGA data showed the expression profile of host genes of exosomal circRNAs in corresponding digestive system tumors. Compared with adjacent tissues, we found that the expression of the host gene CDR1 of hsa_circ_0001946 was downregulated in esophageal cancer; however, the difference was not statistically significant (**Table S1**). In gastric cancer, six and one host genes were upregulated and downregulated, respectively. Among them, RAB3A interacting protein (RAB3IP), Ran GTPase-activating protein 1 (RanGAP1), and KIAA1244 exhibited a fold change >2, indicating significantly high expression in gastric cancer (**Table S1**). The expression of Rap1 GTPase activating protein (RAP1GAP) was downregulated in gastric cancer, but the difference was not statistically significant (**Table S1**). In hepatocellular carcinoma, eight and four host genes were upregulated and downregulated, respectively. Among them, ubiquitin-like with PHD and ring finger domains 1 (UHRF1) and sorting nexin 27 (SNX27) with a fold change >2, revealing significantly high expression in hepatocellular carcinoma (**Table S1**). Three of the four downregulated host genes were 0.5 < fold change < 1, while the expression of prostaglandin reduce 1 (PTGR1) was downregulated in hepatocellular carcinoma, but the difference was not statistically significant (**Table S1**). In colorectal cancer, five and five host genes were upregulated and downregulated. Among them, the ATP-binding cassette subfamily C member 1 (ABCC1) and formin 2 (FMN2) showed fold change >2 and <0.5, respectively (**Table S1**). Five downregulated host genes were 0.5 < fold change < 1 or had no significant difference in the expression. In pancreatic cancer, there was no significant difference in the expression of the host genes of the two exosomes circRNAs compared with the adjacent tissues (**Table S1**). In general, in digestive system tumors, some exosomal circRNAs and their host genes exhibited similar expression patterns, whereas others showed opposite expression patterns (**Table 1**).

Sponging of miRNAs and Their Target Genes in Digestive System Tumors

As mentioned earlier, 20 molecules of the 32 exosomal circRNA sponged miRNAs, adsorbing a total of 23 target miRNAs. We used the miRTargetLink Human online tool to predict the target genes of these 23 miRNAs and obtained 6,570 molecules: gastric cancer (1,741 target genes), hepatocellular carcinoma (1,795 target genes), colorectal cancer (2,704 target genes), and pancreatic cancer (330 target genes) (**Table S2**). We used two different methods to analyze these miRNAs and target genes.

Method 1: In the target genes of each type of digestive system tumors, we searched for genes that are regulated by at least two miRNAs, and performed GO and KEGG analyses on those. The results revealed 63, 60, 146, and one target gene in gastric cancer, hepatocellular carcinoma, colorectal cancer, and pancreatic cancer, respectively (**Figure 2** and **Table S3**).

Method 2: The data obtained from the TCGA database showed that, among the 6,570 target genes, only 1,146 target

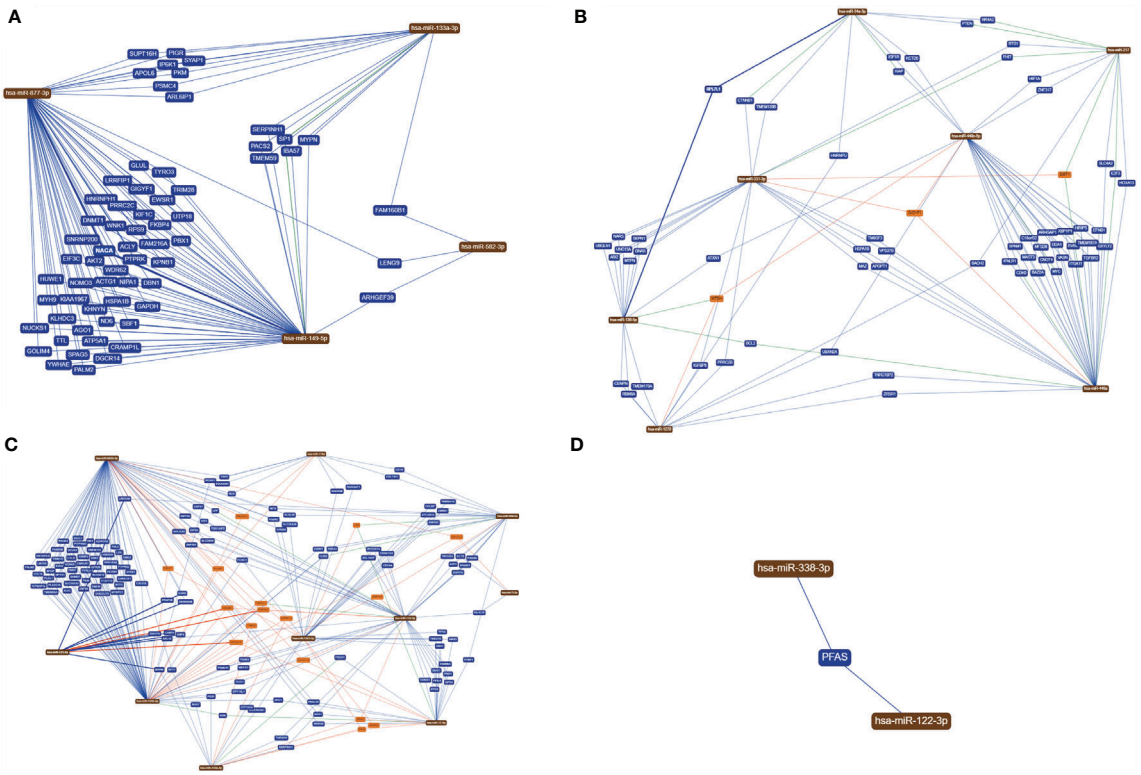

FIGURE 2 | MiRNAs with the same target genes. **(A)** In gastric cancer, 63 target genes are regulated by at least two miRNAs; **(B)** in hepatocellular carcinoma, 60 target genes are regulated by at least two miRNAs; **(C)** in colorectal cancer, 146 target genes are regulated by at least two miRNAs; **(D)** In pancreatic cancer, only one target gene is regulated by two miRNAs at the same time.

genes exhibited significant differential expression of ≥ 2 fold change (761 genes) or ≤ 0.5 fold change (385 genes): gastric cancer (278 genes), hepatocellular carcinoma (329 genes), colorectal cancer (535 genes), and pancreatic cancer (four genes) (**Table S6**). Subsequently, we performed functional enrichment analysis on all 1,146 target genes differentially expressed in digestive system tumors.

Intersection of the target genes obtained by two different methods in digestive system tumors, then we obtained ten, 11, 28 target genes in gastric cancer (NUCKS1, ACLY, SPAG5, EIF3C, TRIM28, TTL, PALM2, DNMT1, WDR62, UTP18), hepatocellular carcinoma (CENPN, SEPN1, UNC13A, FHIT, HSPA1B, TMEM120B, MAZ, NR4A2, E2F3, SLC4A2, BACH2), and colorectal cancer (CPEB3, PVRL4, CCL16, PPAP2B, PITPNM3, SLC25A32, SEMA3E, MYOCD, DCLK3, EVC2, KLF2, PLA2G16, LPP, C1orf115, CMKLR1, EMCN, PALM2, CENPJ, KCNK5, HMGA1, RANGAP1, TMEM41A, CDCA4, HMGB1, PNO1, PANK3, CD1D, RCAN1), respectively, and in pancreatic cancer, there were no same target gene in the intersection (**Figure S1**).

Functional Enrichment of Target Genes

GO and KEGG analyses were performed on the 270 target genes obtained through Method 1. The former showed that these genes were involved in 127 cancer-related functions, and the p-values of 83 cancer-related functions were <0.05 (**Table S4** and **Figure 3**). The latter showed that they were involved in 12 KEGG pathways, and the p-values of six KEGG pathways were <0.05 (**Table S5** and **Figure 4**).

Functional enrichment analysis of the 1,146 differentially expressed target genes identified through Method 2 revealed that 78 genes related to other tumors were involved in 20 cancer-related pathways (e.g., chronic lymphocytic leukemia, glioma, prostate cancer, melanoma, bladder cancer, small cell lung cancer, non-small cell lung cancer, basal cell carcinoma, renal cell carcinoma, thyroid cancer, etc.) (**Table S7** and **Figure 5**).

CircRNA-miRNA-mRNA Network in Digestive System Tumors

Finally, based on the previous analysis, we obtained 16 exosomal circRNAs closely related to digestive system tumors, which regulated 78 target genes through sponging of 18 miRNAs (**Table S7** and **Figure 6**). Both circ-RanGAP1 and its host gene were highly expressed in gastric cancer. Exosomes circ-RanGAP1 regulated 10 target genes (DNA methyltransferase 1 [DNMT1], E2F transcription factor 2 [E2F2], ETS variant transcription factor 4 [ETV4], cytochrome P450 family 19 subfamily A member 1 [CYP19A1], inositol 1,4,5-trisphosphate receptor type 3 [ITPR3], myosin light chain kinase [MYLK], ret proto-oncogene [RET],

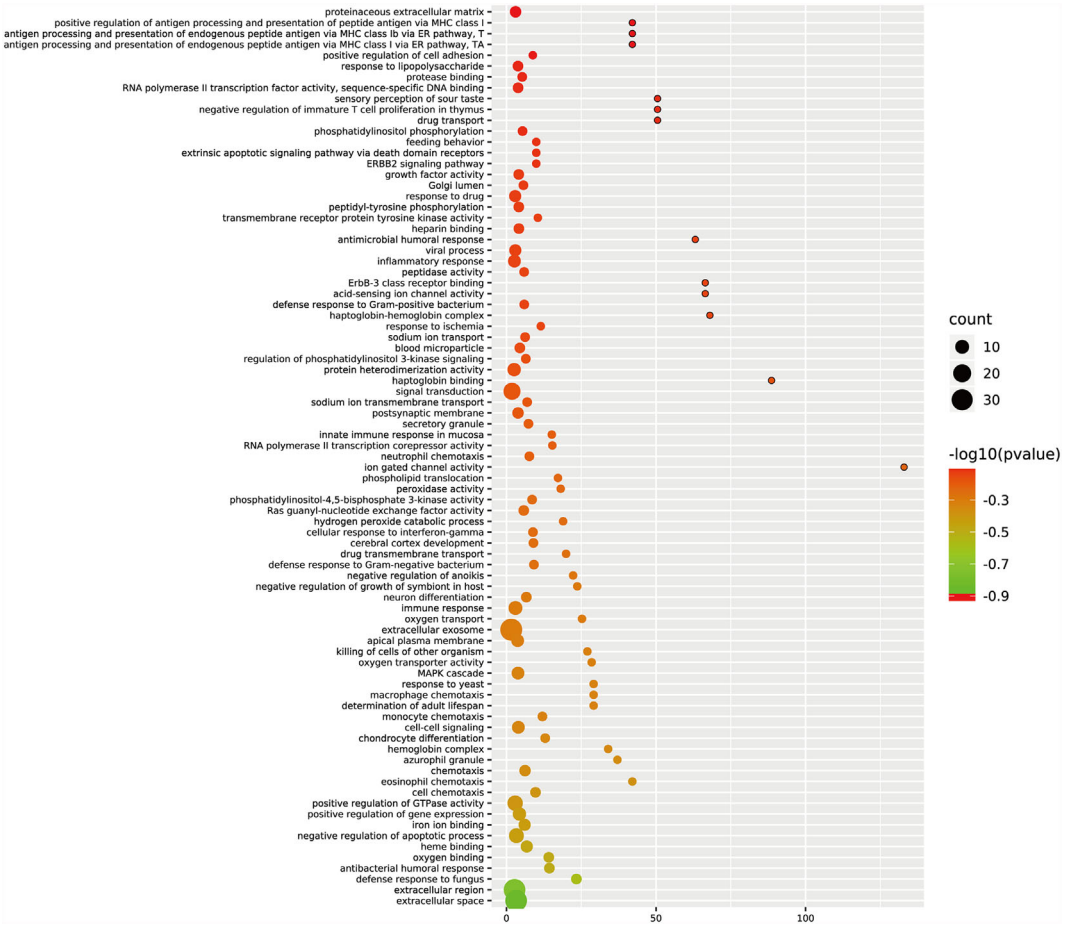

FIGURE 3 | GO analysis of target genes in digestive system tumors. 270 target genes regulated by at least two miRNAs were involved in 83 cancer-related pathways. $P < 0.05$.

scavenger receptor class B member 1 [SCARB1], small nuclear ribonucleoprotein polypeptide F [SNRPF], solute carrier family 6 member 8 [SLC6A8]) through sponging hsa-miR-877-3p to promote the progression of gastric cancer (**Table 2**). Among the 10 target genes, the expression of MYLK, RET and SLC6A8 was down regulated in gastric cancer, while the expression of the other 7 genes was up-regulated in gastric cancer (**Table S6**). Both circUHRF1 and its host gene were highly expressed in hepatocellular carcinoma. The exosomal circUHRF1 regulated the expression of RET by sponging hsa-miR-449c-5p to promote the progression of hepatocellular carcinoma (**Table 2**). In colorectal cancer, circFMN2 was upregulated in, whereas its host gene was downregulated. Exosomes circFMN2 upregulated the expression of seven target genes (CD44, G protein subunit gamma 7 [GNG7], RB transcriptional corepressor 1 [RB1], collagen type I alpha 2 chain [COL1A2], phospholipase C beta 1 [PLCB1], solute carrier family 17 member 7 [SLC17A7], telomerase reverse transcriptase [TERT]) by binding miR-1182, thereby promoting the occurrence and development of colorectal cancer (**Table 2**).

DISCUSSION

Exosomes are extracellular microvesicles with an average diameter of 100 nm and a double-layer liposome membrane (9). The biogenesis of exosomes is similar to endocytosis: the cell membrane is invaded to encapsulate proteins, non-coding RNA, lipids, etc. This forms intraluminal vesicles, and the luminal vesicles gradually form mature multivesicular bodies and are secreted as the exosomes (52). Exosomes secreted by cells can exist in a variety of body fluids (e.g., serum, plasma, saliva, urine, lymph, etc.), and are transported to distant tissue and cells to exert a wide range of regulatory effects (53). The substances in exosomes are diverse. Data (http://www.exocarta.org) have shown that 3,408 types of mRNA, 2,838 kinds of miRNA, 9,769 kinds of proteins, and 1,116 kinds of lipids are present in exosomes (54). CircRNA is another large type of non-coding RNA in exosomes, which is widespread in eukaryotes (55). This special molecule is formed by reverse splicing, which regulates the expression of the target protein by competitively binding miRNA, thereby affecting multiple signal transduction pathways and regulating multiple biological processes (56). It has

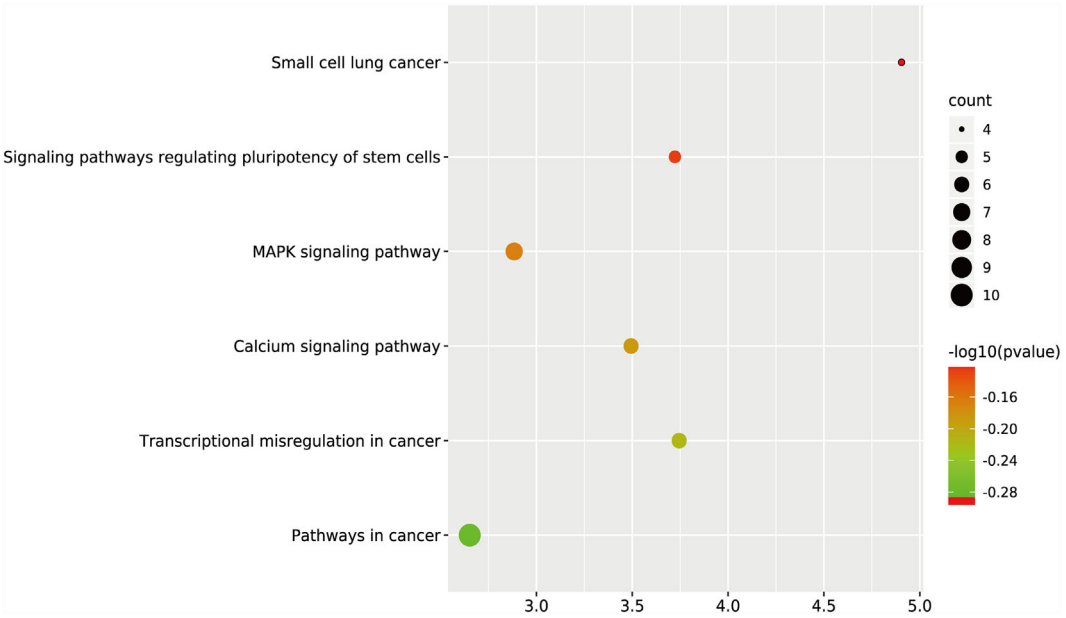

FIGURE 4 | KEGG analysis of target genes in digestive system tumors. 270 target genes regulated by at least two miRNAs were involved in six KEGG pathways. $P < 0.05$.

been demonstrated that various exosomal circRNAs are involved in the regulation of malignant tumor proliferation, migration, invasion, and drug resistance. CircWHSC1 promotes the progression of ovarian cancer by competitively binding miR-1182 and miR-145 (57). CircSMARCA5 affects the malignant behavior of glioma by regulating serine and arginine rich splicing factor 1 (SRSF1)/SRSF3/PTB (57). Our research focused on tumors of the digestive system. We collected 32 exosomal circRNAs that were highly related to them, observed and predicted their sponging of miRNAs and target genes, analyzed the functions of these target genes and possible signal pathways involved in these processes. Moreover, we discussed their potential usefulness as tumor markers, as well as diagnostic and treatment targets.

RAB3IP, RanGAP1, and KIAA1244 are host genes of exosomal circRNA which exhibited more than two-fold differences in gastric cancer (**Table S1**). Although the fold change shown for RanGAP1 was not the highest, its homologous circRNA was the only molecule among the three circRNAs that has been proven to bind miRNA (26). Circ-RanGAP1 regulated vascular endothelial growth factor A (VEGFA) by targeting miR-877-3p, thereby promoting the metastasis and invasion of gastric cancer (26). At the same time, circ-RanGAP1/miR-877-3p may have 10 binding sites, such as DNMT1 in gastric cancer (**Table 2**). These proteins were closely related to multiple signaling pathways, such as cysteine and methionine metabolism, arachidonic acid metabolism, linoleic acid, cell cycle, etc. (**Table S7**). UHRF1 and SNX27 were host genes of exosomal circRNA that showed more than two-fold difference in expression in hepatocellular carcinoma (**Table S1**). Compared with normal liver tissues, the expression of UHRF1 in liver cancer was upregulated by 17.73-fold. Its homologous molecule circUHRF1 induced the depletion of natural killer T cells by targeting miR-449c-5p, thereby participating in the development of drug resistance by liver cancer cells (30). RET was a possible target protein of this process, and may be involved in the regulation of multiple signal pathways, such as peroxisome proliferator activated receptor (PPAR), PI3K-Akt, thyroid hormone, etc. (**Table S7**). ABCC1 and FMN2 were host genes of exosomal circRNA that were differentially expressed by more than two-fold in colorectal cancer (**Table S1**). Their homologous molecule hsa_circ_0000677 promoted the occurrence of colorectal cancer by directly regulating the Wnt signaling pathway, while circFMN2 promoted the proliferation of colorectal cancer by regulating miR-1182/hTERT (40, 47). CircFMN2/miR-1182 may also regulate the progression of colorectal cancer by targeting CD44, GNG7, RB1, COL1A2, PLCB1, SLC17A7, and TERT (**Table 2**). These target genes were widely involved in the regulation of extracellular matrix-receptor interaction, Ras, chemokine, PI3K-Akt, and other signaling pathways (**Table S7**). The function of these target genes in tumors warrants further experimental verification.

Interestingly, we found that circ-RanGAP1 and its host gene in gastric cancer, circUHRF1, as well as its host gene in hepatocellular carcinoma exhibited the same expression pattern. In contrast, circFMN2 and its host gene showed opposite patterns in colorectal cancer. CircRNA can be as a regulatory factor for host gene transcription and expression at both the transcription and post-transcription levels (58). However, currently, there are few studies on the interaction between circRNAs and their host genes, and the detailed mechanism involved in this process warrants further investigation.

We used two methods to screen the target genes, and performed functional enrichment analysis on the two screening results, respectively. The results of the miRNA-mRNA network analysis (**Figure 2**) and their functional enrichment analysis

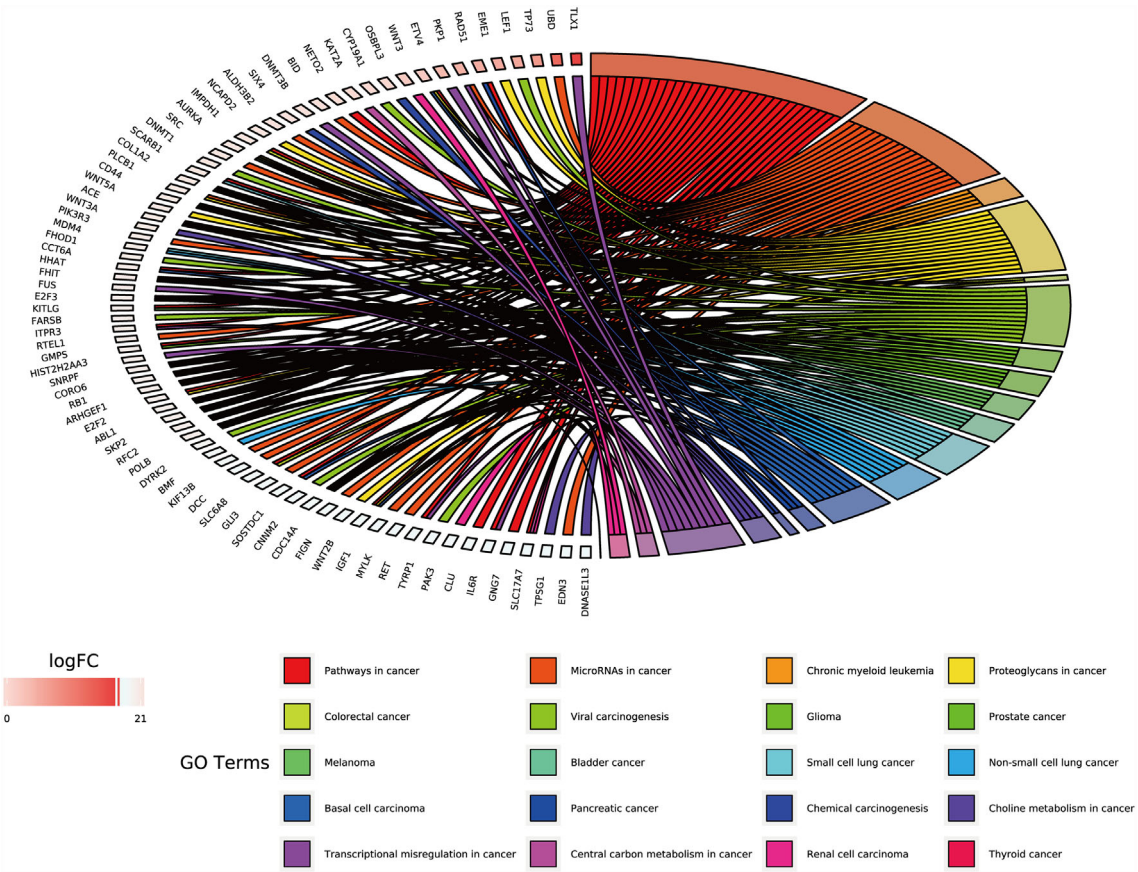

FIGURE 5 | GO chord of target genes in digestive system tumors. 78 target genes differentially expressed in tumors of the digestive system were deeply involved in 20 cancer-related pathways. $P < 0.05$.

(**Figures 3** and **4**) in various digestive system tumors showed that 270 target genes were regulated by at least two miRNAs, which were involved in 83 cancer-related pathways and six KEGG pathways. Among them, the cancer-related functions with the most enriched genes (count ≥10) were extracellular space, extracellular region, extracellular exosome, negative regulation of the apoptotic process, positive regulation of GTPase activity, immune response, and signal transduction. The most enriched genes in the KEGG pathway were also "pathways in cancer". The functional enrichment analysis of 1,146 target genes differentially expressed in tumors of the digestive system showed that 78 target genes were deeply involved in 20 cancer-related pathways (**Figure 5**).

The focus of the two screening methods is different. Method 1 screened the target genes regulated by at least two miRNAs in digestive system tumors. Most of these target genes are genes that play a key role in cell proliferation and metabolism, and they form a complex signal transduction network with a variety of miRNAs to regulate cell behavior. Phosphatase and tensin homologue (PTEN), as inhibitors of the phosphatidylinositol 3-kinase/Akt/mammalian target of rapamycin (PI3K/Akt/mTOR) pathway, is down-regulated by miR–29b and miR–301 in breast cancer, while it is regulated by miR–106b~25 and miR–22 in prostate cancer, which enhances the activity of the PI3K/Akt/mTOR pathway, thereby promoting tumor cell proliferation and inhibiting apoptosis (59). Similar to PTEN, the 270 target genes obtained by method 1 are all negatively regulated by multiple miRNAs, and construct a huge regulatory network in digestive system tumors, affecting the proliferation, invasion, migration, and other malignant phenotype of gastric cancer, hepatocellular carcinoma, and colorectal cancer, and pancreatic cancer. Method 2 screened out 1146 target genes that were significantly differentially expressed in four digestive system tumors. The differential expression of key genes in cancer and adjacent tissues is often the basis for changes in cell function (60). Several researches on the mechanism of tumors explore after discovering differentially expressed genes through microarray or sequencing (60, 61). These two methods only focus on a certain characteristic of the target gene in digestive system tumors, and the two complement each other. **Figure S1** shown the intersection of target genes obtained by two methods in gastric cancer (ten genes), hepatocellular carcinoma (11 genes), colorectal cancer (28 genes), and pancreatic cancer (zero genes). These 49 genes are in four digestive system tumors are significantly differentially expressed, and are

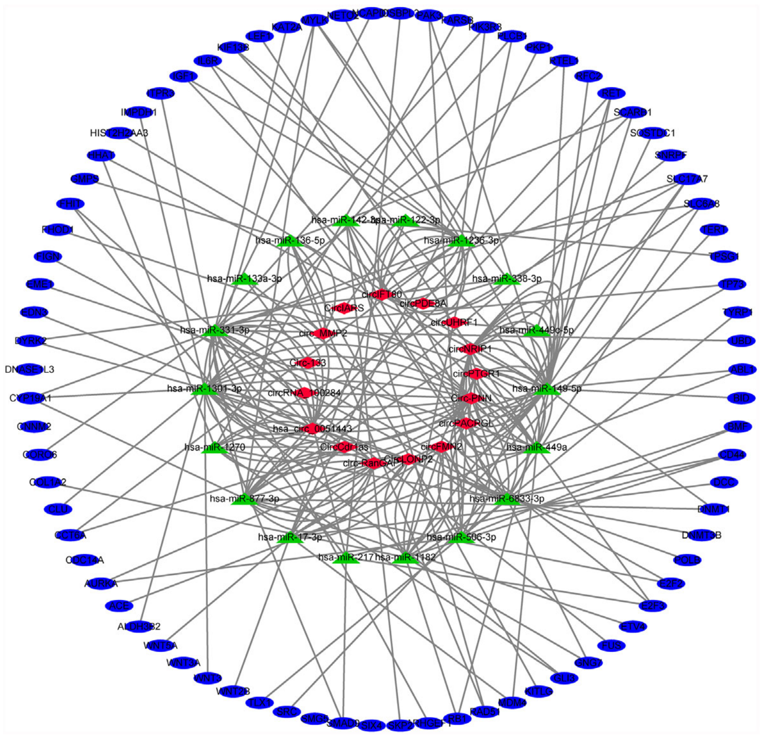

FIGURE 6 | Exosomal circRNA-miRNA-mRNA network in digestive system tumors. 16 exosomal circRNAs closely related to digestive system tumors, which regulated 78 target genes through sponging of 18 miRNAs.

regulated by at least two miRNAs. Therefore, they are more likely to play an irreplaceable role in digestive system tumors.

CircRNA as a miRNA sponge regulates tumor progression through the competing endogenous RNA mechanism. Non-coding RNA in exosomal exerts a wider range of effects to regulate tumors by promoting multiple-signal communication between tumor cells and the tumor microenvironment (including cancer related fibroblasts, tumor stem cells, macrophages, lymphocytes, mesenchymal stem cells etc) (13). Deepak Nagrath et al. found that mir-22, let7a and mir-125b in cancer-related fibroblast-derived exosomes change the energy metabolism of prostate cancer cells by inhibiting oxidative phosphorylation, which may be regulated by circRNA (62). Hong Zhao et al. found that hsa_circ_0000677 in exosomal activates Wnt signal pathway by mediating β-catenin into the nucleus, thereby significantly enhancing the metastatic ability and cell stemness of colorectal cancer (40). It has been reported that miR-503-3p in exosomes derived from bone marrow mesenchymal stem cells can increase the content of cancer stem cells in colorectal cancer, thereby promoting the growth of colorectal cancer (63). In addition to acting as competitive endogenous RNA, recent studies have found that circRNA with internal ribosome entry site (IRES) can bind to ribosomes and encode short peptides and proteins, thus directly regulating the function of tumor cells (64). Last but not least, as transcription factors or protein scaffolds, some circRNA interact directly with proteins to regulate the biological behavior of tumor cells (65).

Exosomes also have a profound impact on immune cells in the tumor microenvironment. The exosomes secreted by tumors can promote the transformation of macrophages into the M2 type, increase the activity of regulatory T cells, and inhibit natural killer cell toxicity, thereby forming immunity inhibition. Simultaneously, some exosomes produced by immune cells inhibit the maturation of antigen-presenting cells and the secretion of anti-tumor factors, and participate in the occurrence and development of tumors (66–68). PengFei Zhang et al. confirmed that circUHRF1 inhibits the activation of natural killer cells and the release of cytokines (IFN-γ and TNF-α) through sponge miR-449c-5p in hepatocellular carcinoma, which induced resistance to anti-PD-1 therapy in patients with hepatocellular carcinoma (30). In gastric cancer, exosomal ciRS-133 promotes white adipose tissue browning by inhibiting miR-133 and activating PRDM16, thereby reducing the oxygen consumption of the gastric cancer microenvironment and promoting tumor growth (28). In short, exosomes non-coding RNA promote the malignant phenotype of tumors through the aforementioned processes, and inhibit the detection and killing tumors by immune cells, thereby participating in the occurrence and development of malignant tumors (**Figure 7**). Exosomes, as intercellular messengers, widely exist in various body fluids and are easy to be extracted, isolated and identified. The differential expression of non-coding RNA between tumor and normal tissues and cells provides an effective marker for clinical diagnosis and treatment of diseases (69). Therefore, exosomal non- coding RNA has great potential in future cancer research. However, in the studies

TABLE 2 | The main competing endogenous RNA pathways in three digestive system tumors.

Type of Cancer	CircRNA	Mode	MiRNA	Target Gene
Gastric cancer	circ-RanGAP1	1	hsa-miR-877-3p	DNMT1, E2F2, ETV4, CYP19A1, ITPR3, MYLK, RET, SCARB1, SNRPF, SLC6A8
Hepatocellular Cancer	circUHRF1	1	hsa-miR-449c-5p	RET
Colorectal Cancer	circFMN2	2	hsa-miR-1182	CD44, GNG7, RB1, COL1A2, PLCB1, SLC17A7, TERT

Mode 1 means the expression pattern of circRNA and its host gene is the same in the tumor. Mode 2 means the expression pattern of circRNA and its host gene is opposite in the tumor.

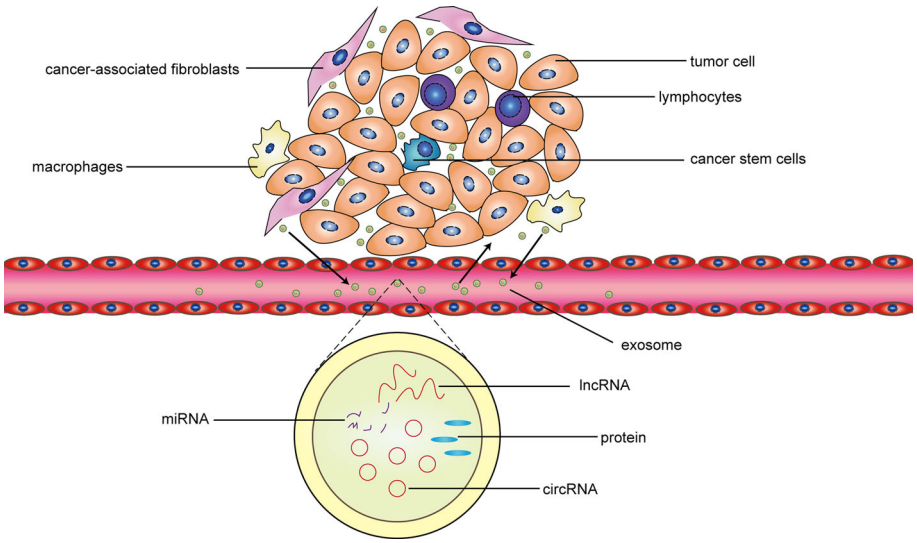

FIGURE 7 | The interaction between exosomes and the tumor microenvironment. In general, cancer-related fibroblasts, cancer stem cells, macrophages and lymphocytes are important components of the tumor microenvironment. The exosomes released by the four types cells promote tumor proliferation, invasion, migration, drug resistance, and other malignant phenotype through the circRNA-miRNA-protein or lncRNA-miRNA-protein mechanism. Simultaneously, these four types cells are regulated by some exosomes released by the tumor cell. In addition, these exosomes not only act on adjacent tissue cells, but also be transported to the distal through blood to take effect.

of exosomal non-coding RNA regulating tumors, we noticed that the research on exosomal miRNA and long non-coding RNA has been abundant, while the related research on exosomal circRNA is extremely limited. The mechanism of exosomal circRNA regulating tumor cells and tumor microenvironment still needs further explore.

Our research and previous literature have shown that exosomal circRNA plays a significant role in the progression of a various digestive system tumors, particularly gastric cancer, hepatocellular carcinoma, and colorectal cancer. Bioinformatics research is helpful for screening molecules and identifying valuable intervention targets. However, this approach is characterized by limitations and certain biases compared with biological experiments. Thus, our results warrant further experimental verification.

CONCLUSION

In general, the expression of exosomal circRNA is stable and easily detectable in body fluids. Circ-RanGAP1 in gastric cancer, circUHRF1 in hepatocellular carcinoma, and circFMN2 in colorectal cancer may be useful as tumor markers, as well as diagnostic and treatment targets. These factors may improve early diagnosis and prognosis of these three gastrointestinal malignancies.

DATA AVAILABILITY STATEMENT

The original contributions presented in the study are included in the article/**Supplementary Material**. Further inquiries can be directed to the corresponding authors.

AUTHOR CONTRIBUTIONS

Conceptualization: HW and XZ. Formal analysis: HW and YZhe. Funding Acquisition: YZho. Writing—original draft: HW. Writing—review and editing: HW and YW. All authors contributed to the article and approved the submitted version.

FUNDING

This research was supported by the National Natural Science Foundation of China (71964021), National Key R&D Program of China (2016YFC1302201 and 2017YFC0908302), the University Scientific Research Project of Gansu Province (2018B-011), the Fundamental Research Funds for the Central Universities (lzujbky-2020-kb16).

ACKNOWLEDGMENTS

Thanks to Min Liu, Qinghong Guo, Quanlin Guan, Rui Ji and Yongning Zhou for funding this research.

SUPPLEMENTARY MATERIAL

The Supplementary Material for this article can be found online at: https://www.frontiersin.org/articles/10.3389/fonc.2021.614462/full#supplementary-material

Supplementary Figure 1 | Venny map for the outcomes of two different gene screening methods in various digestive system tumors. Method 1 searched for target genes that were regulated by at least two miRNAs. Method 2 obtained target genes that significant differential expression of ≥ two-fold change. **(A)** Ten same target genes obtained from method 1 and method 2 in gastric cancer (NUCKS1, ACLY, SPAG5, EIF3C, TRIM28, TTL, PALM2, DNMT1, WDR62, UTP18); **(B)** 11 same target genes obtained from method 1 and method 2 in hepatocellular carcinoma (CENPN, SEPN1, UNC13A, FHIT, HSPA1B, TMEM120B, MAZ, NR4A2, E2F3, SLC4A2, BACH2); **(C)** 28 same target genes obtained from method 1 and method 2 in colorectal cancer (CPEB3, PVRL4, CCL16, PPAP2B, PITPNM3, SLC25A32, SEMA3E, MYOCD, DCLK3, EVC2, KLF2, PLA2G16, LPP, C1orf115, CMKLR1, EMCN, PALM2, CENPJ, KCNK5, HMGA1, RANGAP1, TMEM41A, CDCA4, HMGB1, PNO1, PANK3, CD1D, RCAN1); **(D)** there were no same target gene from method 1 and method 2 in pancreatic cancer.

REFERENCES

1. Bray F, Ferlay J, Soerjomataram I, Siegel RL, Torre LA, Jemal A. Global Cancer Statistics 2018: GLOBOCAN Estimates of Incidence and Mortality Worldwide for 36 Cancers in 185 Countries. *CA Cancer J Clin* (2018) 68 (6):394–424. doi: 10.3322/caac.21492
2. Roma-Rodrigues C, Mendes R, Baptista PV, Fernandes AR. Targeting Tumor Microenvironment for Cancer Therapy. *Int J Mol Sci* (2019) 20(4):840. doi: 10.3390/ijms20040840
3. Yong SB, Chung JY, Song Y, Kim J, Ra S, Kim YH. Non-Viral Nano-Immunotherapeutics Targeting Tumor Microenvironmental Immune Cells. *Biomaterials* (2019) 219:119401. doi: 10.1016/j.biomaterials.2019.119401
4. Adam JB, Vesteinn T, Ilya S, Sheila MR, Michael M, Brady B, et al. Comprehensive Molecular Characterization of Gastric Adenocarcinoma. *Nature* (2014) 513 (7517):202–9. doi: 10.1038/nature13480
5. Li W, Zhang L, Guo B, Deng J, Wu S, Li F, et al. Exosomal FMR1-AS1 Facilitates Maintaining Cancer Stem-Like Cell Dynamic Equilibrium *Via* TLR7/Nfκb/c-Myc Signaling in Female Esophageal Carcinoma. *Mol Cancer* (2019) 18(1):22. doi: 10.1186/s12943-019-0949-7
6. Sharma A. Role of Stem Cell Derived Exosomes in Tumor Biology. *Int J Cancer* (2018) 142(6):1086–92. doi: 10.1002/ijc.31089
7. Fu M, Gu J, Jiang P, Qian H, Xu W, Zhang X. Exosomes in Gastric Cancer: Roles, Mechanisms, and Applications. *Mol Cancer* (2019) 18(1):41. doi: 10.1186/s12943-019-1001-7
8. He M, Qin H, Poon TC, Sze SC, Ding X, Co NN, et al. Hepatocellular Carcinoma-Derived Exosomes Promote Motility of Immortalized Hepatocyte Through Transfer of Oncogenic Proteins and RNAs. *Carcinogenesis* (2015) 36 (9):1008–18. doi: 10.1093/carcin/bgv081
9. Ruivo CF, Adem B, Silva M, Melo SA. The Biology of Cancer Exosomes: Insights and New Perspectives. *Cancer Res* (2017) 77(23):6480–8. doi: 10.1158/0008-5472.CAN-17-0994
10. Ratajczak MZ, Ratajczak J. Extracellular Microvesicles/Exosomes: Discovery, Disbelief, Acceptance, and the Future? *Leukemia* (2020) 34(12):3126–35. doi: 10.1038/s41375-020-01041-z
11. Hamlett ED, Ledreux A, Potter H, Chial HJ, Patterson D, Espinosa JM, et al. Exosomal Biomarkers in Down Syndrome and Alzheimer's Disease. *Free Radic Biol Med* (2018) 114:110–21. doi: 10.1016/j.freeradbiomed.2017.08.028
12. Sun Y, Shi H, Yin S, Ji C, Zhang X, Zhang B, et al. Human Mesenchymal Stem Cell Derived Exosomes Alleviate Type 2 Diabetes Mellitus by Reversing Peripheral Insulin Resistance and Relieving β-Cell Destruction. *ACS Nano* (2018) 12(8):7613–28. doi: 10.1021/acsnano.7b07643
13. Dai J, Su Y, Zhong S, Cong L, Liu B, Yang J, et al. Exosomes: Key Players in Cancer and Potential Therapeutic Strategy. *Signal Transduct Target Ther* (2020) 5(1):145. doi: 10.1038/s41392-020-00261-0
14. Louis C, Desoteux M, Coulouarn C. Exosomal circRNAs: New Players in the Field of Cholangiocarcinoma. *Clin Sci (Lond)* (2019) 133(21):2239–44. doi: 10.1042/CS20190940
15. Liu J, Li D, Luo H, Zhu X. Circular RNAs: The Star Molecules in Cancer. *Mol Aspects Med* (2019) 70:141–52. doi: 10.1016/j.mam.2019.10.006
16. Guan X, Zong ZH, Liu Y, Chen S, Wang LL, Zhao Y. Circpum1 Promotes Tumorigenesis and Progression of Ovarian Cancer by Sponging miR-615-5p and Mir-6753-5p. *Mol Ther Nucleic Acids* (2019) 18:882–92. doi: 10.1016/j.omtn.2019.09.032
17. Chen X, Chen RX, Wei WS, Li YH, Feng ZH, Tan L, et al. Prmt5 Circular RNA Promotes Metastasis of Urothelial Carcinoma of the Bladder Through Sponging miR-30c to Induce Epithelial-Mesenchymal Transition. *Clin Cancer Res* (2018) 24(24):6319–30. doi: 10.1158/1078-0432.CCR-18-1270
18. Chandrashekar DS, Bashel B, Balasubramanya SAH, Creighton CJ, Ponce-Rodriguez I, Chakravarthi B, et al. Ualcan: A Portal for Facilitating Tumor Subgroup Gene Expression and Survival Analyses. *Neoplasia* (2017) 19 (8):649–58. doi: 10.1016/j.neo.2017.05.002
19. Huang HY, Lin YC, Li J, Huang KY, Shrestha S, Hong HC, et al. miRTarBase 2020: Updates to the Experimentally Validated microRNA-Target Interaction Database. *Nucleic Acids Res* (2020) 48(D1):D148–d54. doi: 10.1093/nar/gkz896
20. Huang da W, Sherman BT, Lempicki RA. Systematic and Integrative Analysis of Large Gene Lists Using DAVID Bioinformatics Resources. *Nat Protoc* (2009) 4(1):44–57. doi: 10.1038/nprot.2008.211
21. Huang da W, Sherman BT, Lempicki RA. Bioinformatics Enrichment Tools: Paths Toward the Comprehensive Functional Analysis of Large Gene Lists. *Nucleic Acids Res* (2009) 37(1):1–13. doi: 10.1093/nar/gkn923
22. Fan L, Cao Q, Liu J, Zhang J, Li B. Circular RNA Profiling and its Potential for Esophageal Squamous Cell Cancer Diagnosis and Prognosis. *Mol Cancer* (2019) 18(1):16. doi: 10.1186/s12943-019-1050-y
23. Xie M, Yu T, Jing X, Ma L, Fan Y, Yang F, et al. Exosomal circSHKBP1 Promotes Gastric Cancer Progression *Via* Regulating the miR-582-3p/HUR/VEGF Axis and Suppressing HSP90 Degradation. *Mol Cancer* (2020) 19 (1):112. doi: 10.1186/s12943-020-01208-3
24. Tao X, Shao Y, Lu R, Ye Q, Xiao B, Ye G, et al. Clinical Significance of Hsa_Circ_0000419 in Gastric Cancer Screening and Prognosis Estimation. *Pathol Res Pract* (2020) 216(1):152763. doi: 10.1016/j.prp.2019.152763
25. Shao Y, Tao X, Lu R, Zhang H, Ge J, Xiao B, et al. Hsa_Circ_0065149 Is an Indicator for Early Gastric Cancer Screening and Prognosis Prediction. *Pathol Oncol Res* (2020) 26(3):1475–82. doi: 10.1007/s12253-019-00716-y
26. Lu J, Wang YH, Yoon C, Huang XY, Xu Y, Xie JW, et al. Circular RNA circ-RanGAP1 Regulates VEGFA Expression by Targeting miR-877-3p to Facilitate Gastric Cancer Invasion and Metastasis. *Cancer Lett* (2020) 471:38–48. doi: 10.1016/j.canlet.2019.11.038
27. Zhang X, Wang S, Wang H, Cao J, Huang X, Chen Z, et al. Circular RNA circNRIP1 Acts as a microRNA-149-5p Sponge to Promote Gastric Cancer Progression *Via* the AKT1/mTOR Pathway. *Mol Cancer* (2019) 18(1):20. doi: 10.1186/s12943-018-0935-5
28. Zhang H, Zhu L, Bai M, Liu Y, Zhan Y, Deng T, et al. Exosomal circRNA Derived From Gastric Tumor Promotes White Adipose Browning by Targeting the miR-133/PRDM16 Pathway. *Int J Cancer* (2019) 144(10):2501–15. doi: 10.1002/ijc.31977
29. Tang W, Fu K, Sun H, Rong D, Wang H, Cao H. CircRNA Microarray Profiling Identifies a Novel Circulating Biomarker for Detection of Gastric Cancer. *Mol Cancer* (2018) 17(1):137. doi: 10.1186/s12943-018-0888-8
30. Zhang PF, Gao C, Huang XY, Lu JC, Guo XJ, Shi GM, et al. Cancer Cell-Derived Exosomal circUHRF1 Induces Natural Killer Cell Exhaustion and may Cause Resistance to anti-PD1 Therapy in Hepatocellular Carcinoma. *Mol Cancer* (2020) 19(1):110. doi: 10.1186/s12943-020-01222-5
31. Sun XH, Wang YT, Li GF, Zhang N, Fan L. Serum-Derived Three-circRNA Signature as a Diagnostic Biomarker for Hepatocellular Carcinoma. *Cancer Cell Int* (2020) 20:226. doi: 10.1186/s12935-020-01302-y
32. Luo Y, Liu F, Gui R. High Expression of Circulating Exosomal circAKT3 Is Associated With Higher Recurrence in HCC Patients Undergoing Surgical Treatment. *Surg Oncol* (2020) 33:276–81. doi: 10.1016/j.suronc.2020.04.021

33. Liu D, Kang H, Gao M, Jin L, Zhang F, Chen D, et al. Exosome-Transmitted Circ_MMP2 Promotes Hepatocellular Carcinoma Metastasis by Upregulating MMP2. *Mol Oncol* (2020) 14(6):1365–80. doi: 10.1002/1878-0261.12637
34. Huang XY, Huang ZL, Huang J, Xu B, Huang XY, Xu YH, et al. Exosomal circRNA-100338 Promotes Hepatocellular Carcinoma Metastasis *Via* Enhancing Invasiveness and Angiogenesis. *J Exp Clin Cancer Res* (2020) 39 (1):20. doi: 10.1186/s13046-020-1529-9
35. Chen W, Quan Y, Fan S, Wang H, Liang J, Huang L, et al. Exosome-Transmitted Circular RNA Hsa_Circ_0051443 Suppresses Hepatocellular Carcinoma Progression. *Cancer Lett* (2020) 475:119–28. doi: 10.1016/j.canlet.2020.01.022
36. Zhang H, Deng T, Ge S, Liu Y, Bai M, Zhu K, et al. Exosome circRNA Secreted From Adipocytes Promotes the Growth of Hepatocellular Carcinoma by Targeting Deubiquitination-Related USP7. *Oncogene* (2019) 38(15):2844–59. doi: 10.1038/s41388-018-0619-z
37. Wang G, Liu W, Zou Y, Wang G, Deng Y, Luo J, et al. Three Isoforms of Exosomal circPTGR1 Promote Hepatocellular Carcinoma Metastasis *Via* the miR449a-MET Pathway. *EBioMedicine* (2019) 40:432–45. doi: 10.1016/j.ebiom.2018.12.062
38. Su Y, Lv X, Y in W, Zhou L, Hu Y, Zhou A, et al. circRNA Cdr1as Functions as a Competitive Endogenous RNA to Promote Hepatocellular Carcinoma Progression. *Aging (Albany NY)* (2019) 11(19):8182–203. doi: 10.18632/aging.102312
39. Dai X, Chen C, Yang Q, Xue J, Chen X, Sun B, et al. Exosomal circRNA_100284 From Arsenite-Transformed Cells, *Via* microRNA-217 Regulation of EZH2, Is Involved in the Malignant Transformation of Human Hepatic Cells by Accelerating the Cell Cycle and Promoting Cell Proliferation. *Cell Death Dis* (2018) 9(5):454. doi: 10.1038/s41419-018-0485-1
40. Zhao H, Chen S, Fu Q. Exosomes From CD133(+) Cells Carrying circ-ABCC1 Mediate Cell Stemness and Metastasis in Colorectal Cancer. *J Cell Biochem* (2020) 121(5-6):3286–97. doi: 10.1002/jcb.29600
41. Yang H, Zhang H, Yang Y, Wang X, Deng T, Liu R, et al. Hypoxia Induced Exosomal circRNA Promotes Metastasis of Colorectal Cancer *Via* Targeting GEF-H1/RhoA Axis. *Theranostics* (2020) 10(18):8211–26. doi: 10.7150/thno.44419
42. Xie Y, Li J, Li P, Li N, Zhang Y, Binang H, et al. Rna-Seq Profiling of Serum Exosomal Circular RNAs Reveals Circ-PNN as a Potential Biomarker for Human Colorectal Cancer. *Front Oncol* (2020) 10:982. doi: 10.3389/fonc.2020.00982
43. Wang X, Zhang H, Yang H, Bai M, Ning T, Deng T, et al. Exosome-Delivered circRNA Promotes Glycolysis to Induce Chemoresistance Through the miR-122-PKM2 Axis in Colorectal Cancer. *Mol Oncol* (2020) 14(3):539–55. doi: 10.1002/1878-0261.12629
44. Shang A, Gu C, Wang W, Wang X, Sun J, Zeng B, et al. Exosomal circPACRGL Promotes Progression of Colorectal Cancer *Via* the miR-142-3p/miR-506-3p- Tgf-β1 Axis. *Mol Cancer* (2020) 19(1):117. doi: 10.1186/s12943-020-01235-0
45. Han K, Wang FW, Cao CH, Ling H, Chen JW, Chen RX, et al. CircLONP2 Enhances Colorectal Carcinoma Invasion and Metastasis Through Modulating the Maturation and Exosomal Dissemination of Microrna-17. *Mol Cancer* (2020) 19(1):60. doi: 10.1186/s12943-020-01184-8
46. Pan B, Qin J, Liu X, He B, Wang X, Pan Y, et al. Identification of Serum Exosomal hsa-circ-0004771 as a Novel Diagnostic Biomarker of Colorectal Cancer. *Front Genet* (2019) 10:1096. doi: 10.3389/fgene.2019.01096
47. Li Y, Li C, Xu R, Wang Y, Li D, Zhang B. A Novel circFMN2 Promotes Tumor Proliferation in CRC by Regulating the miR-1182/hTERT Signaling Pathways. *Clin Sci (Lond)* (2019) 133(24):2463–79. doi: 10.1042/CS20190715
48. Hon KW, Ab-Mutalib NS, Abdullah NMA, Jamal R, Abu N. Extracellular Vesicle-derived Circular RNAs Confers Chemoresistance in Colorectal Cancer. *Sci Rep* (2019) 9(1):16497. doi: 10.1038/s41598-019-53063-y
49. Feng W, Gong H, Wang Y, Zhu G, Xue T, Wang Y, et al. Circift80 Functions as a ceRNA of miR-1236-3p to Promote Colorectal Cancer Progression. *Mol Ther Nucleic Acids* (2019) 18:375–87. doi: 10.1016/j.omtn.2019.08.024
50. Li Z, Yanfang W, Li J, Jiang P, Peng T, Chen K, et al. Tumor-Released Exosomal Circular RNA PDE8A Promotes Invasive Growth *Via* the miR-338/MACC1/MET Pathway in Pancreatic Cancer. *Cancer Lett* (2018) 432:237–50. doi: 10.1016/j.canlet.2018.04.035
51. Li J, Li Z, Jiang P, Peng M, Zhang X, Chen K, et al. Circular RNA Iars (circ-IARS) Secreted by Pancreatic Cancer Cells and Located Within Exosomes Regulates Endothelial Monolayer Permeability to Promote Tumor Metastasis. *J Exp Clin Cancer Res* (2018) 37(1):177. doi: 10.1186/s13046-018-0822-3
52. Ibrahim A, Marbán E. Exosomes: Fundamental Biology and Roles in Cardiovascular Physiology. *Annu Rev Physiol* (2016) 78:67–83. doi: 10.1146/annurev-physiol-021115-104929
53. Xu R, Greening DW, Zhu HJ, Takahashi N, Simpson RJ. Extracellular Vesicle Isolation and Characterization: Toward Clinical Application. *J Clin Invest* (2016) 126(4):1152–62. doi: 10.1172/JCI81129
54. Xie F, Zhou X, Fang M, Li H, Su P, Tu Y, et al. Extracellular Vesicles in Cancer Immune Microenvironment and Cancer Immunotherapy. *Adv Sci (Weinh)* (2019) 6(24):1901779. doi: 10.1002/advs.201901779
55. Kristensen LS, Andersen MS, Stagsted LVW, Ebbesen KK, Hansen TB, Kjems J. The Biogenesis, Biology and Characterization of Circular RNAs. *Nat Rev Genet* (2019) 20(11):675–91. doi: 10.1038/s41576-019-0158-7
56. Fanale D, Taverna S, Russo A, Bazan V. Circular RNA in Exosomes. *Adv Exp Med Biol* (2018) 1087:109–17. doi: 10.1007/978-981-13-1426-1_9
57. Zong ZH, Du YP, Guan X, Chen S, Zhao Y. CircWHSC1 Promotes Ovarian Cancer Progression by Regulating MUC1 and hTERT Through Sponging miR-145 and Mir-1182. *J Exp Clin Cancer Res* (2019) 38(1):437. doi: 10.1186/s13046-019-1437-z
58. Yang Q, Du WW, Wu N, Yang W, Awan FM, Fang L, et al. A Circular RNA Promotes Tumorigenesis by Inducing C-Myc Nuclear Translocation. *Cell Death Differ* (2017) 24(9):1609–20. doi: 10.1038/cdd.2017.86
59. Song MS, Salmena L, Pandolfi PP. The Functions and Regulation of the PTEN Tumour Suppressor. *Nat Rev Mol Cell Biol* (2012) 13(5):283–96. doi: 10.1038/nrm3330
60. Favero F, Joshi T, Marquard AM, Birkbak NJ, Krzystanek M, Li Q, et al. Sequenza: Allele-Specific Copy Number and Mutation Profiles From Tumor Sequencing Data. *Ann Oncol* (2015) 26(1):64–70. doi: 10.1093/annonc/mdu479
61. Longo JF, Weber SM, Turner-Ivey BP, Carroll SL. Recent Advances in the Diagnosis and Pathogenesis of Neurofibromatosis Type 1 (NF1)-Associated Peripheral Nervous System Neoplasms. *Adv Anat Pathol* (2018) 25(5):353–68. doi: 10.1097/PAP.0000000000000197
62. Zhao H, Yang L, Baddour J, Achreja A, Bernard V, Moss T, et al. Tumor Microenvironment Derived Exosomes Pleiotropically Modulate Cancer Cell Metabolism. *Elife* (2016) 5:e10250. doi: 10.7554/eLife.10250
63. Seo M, Kim SM, Woo EY, Han KC, Park EJ, Ko S, et al. Stemness-Attenuating miR-503-3p as a Paracrine Factor to Regulate Growth of Cancer Stem Cells. *Stem Cells Int* (2018) 2018:4851949. doi: 10.1155/2018/4851949
64. Jiang T, Xia Y, Lv J, Li B, Li Y, Wang S, et al. A Novel Protein Encoded by circMAPK1 Inhibits Progression of Gastric Cancer by Suppressing Activation of MAPK Signaling. *Mol Cancer* (2021) 20(1):66. doi: 10.1186/s12943-021-01358-y
65. Wang HY, Wang YP, Zeng X, Zheng Y, Guo QH, Ji R, et al. Circular RNA Is a Popular Molecule in Tumors of the Digestive System (Review). *Int J Oncol* (2020) 57(1):21–42. doi: 10.3892/ijo.2020.5054
66. Xie Y, Dang W, Zhang S, Yue W, Yang L, Zhai X, et al. The Role of Exosomal Noncoding RNAs in Cancer. *Mol Cancer* (2019) 18(1):37. doi: 10.1186/s12943-019-0984-4
67. Seo N, Akiyoshi K, Shiku H. Exosome-Mediated Regulation of Tumor Immunology. *Cancer Sci* (2018) 109(10):2998–3004. doi: 10.1111/cas.13735
68. Whiteside TL. Immune Modulation of T-Cell and NK (Natural Killer) Cell Activities by TEXs (Tumour-Derived Exosomes). *Biochem Soc Trans* (2013) 41(1):245–51. doi: 10.1042/BST20120265
69. Wang Y, Liu J, Ma J, Sun T, Zhou Q, Wang W, et al. Exosomal circRNAs: Biogenesis, Effect and Application in Human Diseases. *Mol Cancer* (2019) 18 (1):116. doi: 10.1186/s12943-019-1041-z

Conflict of Interest: The authors declare that the research was conducted in the absence of any commercial or financial relationships that could be construed as a potential conflict of interest.

frontiers in Oncology

ORIGINAL RESEARCH
published: 28 June 2021
doi: 10.3389/fonc.2021.646885

OPEN ACCESS

Edited by:
Jaw-Yuan Wang,
Kaohsiung Medical University Hospital, Taiwan

Reviewed by:
Toru Furukawa,
Tohoku University, Japan
Prashanth Kumar M V,
JSS Academy of Higher Education and Research, India

***Correspondence:**
Susanne Sebens
susanne.sebens@email.uni-kiel.de

†Present address:
Alexander Hendricks,
Department of General Surgery, University Medicine Rostock, Rostock, Germany
Reinhild Geisen,
SYNENTEC GmbH, Elmshorn, Germany
Clemens Schafmayer,
Department of General Surgery, University Medicine Rostock, Rostock, Germany
Sebastian Hinz,
Department of General Surgery, University Medicine Rostock, Rostock, Germany

‡These authors share last authorship

Specialty section:
This article was submitted to Gastrointestinal Cancers, a section of the journal Frontiers in Oncology

Received: 28 December 2020
Accepted: 11 May 2021
Published: 28 June 2021

Citation:
Hendricks A, Dall K, Brandt B, Geisen R, Röder C, Schafmayer C, Becker T, Hinz S and Sebens S (2021) Longitudinal Analysis of Circulating Tumor Cells in Colorectal Cancer Patients by a Cytological and Molecular Approach: Feasibility and Clinical Application. Front. Oncol. 11:646885. doi: 10.3389/fonc.2021.646885

Longitudinal Analysis of Circulating Tumor Cells in Colorectal Cancer Patients by a Cytological and Molecular Approach: Feasibility and Clinical Application

Alexander Hendricks[1†], Katharina Dall[1], Burkhard Brandt[2], Reinhild Geisen[3†], Christian Röder[4], Clemens Schafmayer[1†], Thomas Becker[1], Sebastian Hinz[1†‡] and Susanne Sebens[4‡]*

[1] Department of General, Visceral, Thoracic, Transplantation and Pediatric Surgery, University Hospital Schleswig-Holstein Campus Kiel, Kiel, Germany, [2] Institute of Clinical Chemistry, University Hospital Schleswig-Holstein Campus Kiel, Kiel, Germany, [3] ORGA Labormanagement GmbH, Ochtrup, Germany, [4] Institute for Experimental Cancer Research, Kiel University and University Hospital Schleswig-Holstein Campus, Kiel, Kiel, Germany

Introduction: Liquid biopsies allowing for individualized risk stratification of cancer patients have become of high significance in individualized cancer diagnostics and treatment. The detection of circulating tumor cells (CTC) has proven to be highly relevant in risk prediction, e.g., in colorectal cancer (CRC) patients. In this study, we investigate the clinical relevance of longitudinal CTC detection over a course of follow-up after surgical resection of the tumor and correlate these findings with clinico-pathological characteristics.

Methods: In total, 49 patients with histologically proven colorectal carcinoma were recruited for this prospective study. Blood samples were analyzed for CTC presence by two methods: first by marker-dependent immunofluorescence staining combined with automated microscopy with the NYONE® cell imager and additionally, indirectly, by semi-quantitative Cytokeratin-20 (CK20) RT-qPCR. CTC quantification data were compared and correlated with the clinico-pathological parameters.

Results: Detection of CTC over a post-operative time course was feasible with both applied methods. In patients who were pre-operatively negative for CTCs with the NYONE® method or below the cut-off for relative CK20 mRNA expression after analysis by PCR, a statistically significant rise in the immediate post-operative CTC detection could be demonstrated. Further, in the cohort analyzed by PCR, we detected a lower CTC load in patients who were adjuvantly treated with chemotherapy compared to patients in the follow-up subgroup. This finding was contrary to the same patient subset analyzed with the NYONE® for CTC detection.

Conclusion: Our study investigates the occurrence of CTC in CRC patients after surgical resection of the primary tumor and during postoperative follow-up. The resection of the

tumor has an impact on the CTC quantity and the longitudinal CTC analysis supports the significance of CTC as a prognostic biomarker. Future investigations with an even more extended follow-up period and larger patient cohorts will have to validate our results and may help to define an optimal longitudinal sampling scheme for liquid biopsies in the post-operative monitoring of cancer patients to enable tailored therapy concepts for precision medicine.

Keywords: circulating tumor cells, colorectal cancer, NYONE® cell imager, CK20 RT-qPCR, longitudinal follow-up, liquid biopsies

INTRODUCTION

Despite tremendous efforts in the diagnosis and treatment of colorectal cancer (CRC), it still represents one of the most common causes of cancer-related deaths in Western countries (1). The fact that a proportion of patients is diagnosed with a localized tumor that can be resected in sano (R0) but later develop a tumor recurrence or distant metastases underlines the need for valid prognostic and predictive biomarkers that help to identify high-risk patients. Profound criteria for the stratification of patients at risk who might benefit from an adjuvant treatment have been developed (2, 3), though these almost all rely on histopathological parameters amongst very few other mutational characteristics of the primary tumor.

Consequentially, the concept of individualized diagnostics and therapeutic options has yielded major attention in recent years (4, 5), and biomarkers for either early detection of cancer or proof of minimal residual disease have been identified (6). As a potential tool, circulating tumor cells (CTC) have been identified and their suitability to serve as an additional instrument in risk stratification has been demonstrated manifold (7). These CTC are shed into the peripheral bloodstream not only from the primary but also from metastatic tumor sites and are linked to progressive disease and metastatic formation. In most cases of CRC patients with local disease, tumor resection is considered as a curative approach. The impact of surgery on the CTC count in the bloodstream has been already described, with generally a steep increase in CTC numbers shortly after surgical resection, but also a rapid normalization and often decrease in cell numbers within a short period of time (8). Though, studies on the enumeration of CTC in the long-term longitudinal follow-up of patients with solid tumors after surgery are rare.

CTC are extremely rare in the bloodstream and their valid detection and enumeration amongst multifarious numbers of leukocytes pose a major challenge. Up to date, various enrichment and detection techniques are available (9, 10). Categorically, CTC can be directly detected and enumerated by the means of cytological immunological staining, or indirectly detected by molecular approaches using PCR. The cytological approach for CTC enumeration is mostly marker-dependent, though many techniques employ only single antibodies for visualization of CTC. In this context, the most commonly used target antigens are EpCAM or several cytokeratins, which are highly specific to CTC of epithelial tumors. For the molecular detection of CTC, we previously reported on an RT-qPCR against cytokeratin 20 (CK20), which was already established to determine the prognostic value of the CTC load at the time point of surgery in respectable CRC patients (11, 12). By the introduction of a cut-off value allowing a relative CTC quantification, the negative prognostic significance of the amount of CK20-positive CTC in CRC patients could clearly be demonstrated (13).

In order to further extend these findings and to validate our CTC detection approach, this study aimed at a proof-of-principle study for a longitudinal follow-up of CRC patients after surgical resection with a series of set timepoints for blood draw. Furthermore, both a novel immunofluorescence-based and a molecular detection approach for enumeration and detection of CTC was employed and the results of both methods were compared. For both detection methods, peripheral blood mononuclear cells (PBMC) were enriched by density gradient centrifugation (Ficoll® or CPT Vacutainer) and then applied in either analysis For enumeration by the semi-automated cell-imager (NYONE®, SYNENTEC, Elmshorn, Germany) CTC were immunofluorescently (IF) stained utilizing a set of antibodies against highly specific antigens of CTC in CRC patients, namely, anti-EpCAM, anti-EGFR, anti-pan-Cytokeratin(CK), and anti-Her2, as established in an earlier study (14). Additionally, an established CK20 RT-qPCR assay was applied for relative CTC quantification, as described elsewhere (13). The obtained data were then correlated to clinical characteristics and follow-up records, e.g., local recurrence, adjuvant treatment. Special emphasis was laid on the longitudinal postoperative CTC detection since individual therapeutic decisions are frequently made based on the histopathological characterization of the tumor at the time of primary surgery.

MATERIALS AND METHODS

Patient Recruitment and Serial Sampling

In total, 49 patients with a histologically verified CRC were enrolled in this prospective study in the years 2017 and 2018. All patients were operated on at the Department of General, Visceral, Thoracic, Transplantation and Paediatric Surgery of the University Hospital Schleswig-Holstein (UKSH), Campus Kiel. In case staging diagnostics of a rectal carcinoma revealed a locally progressed tumor burden with either T3/T4 and/or N+ according to the TNM classification (TNM Classification of Malignant Tumors eighth edition), patients were admitted to a neoadjuvant radio-chemotherapy (RCTX). Patients, who were staged UICC (Union internationale contre le cancer) III or IV

after histopathological examination were recommended to be admitted to either adjuvant or palliative chemotherapy (CTX) post-operatively. All decisions were made according to the present guidelines (German S3-Guideline Colorectal Carcinoma, Version 2.1 – January 2019 AWMF-Registration Number: 021/007OL) and the general patients´ constitution in terms of morbidity and endorsement. All patients gave written informed consent to participate in this study. The study was approved by the local ethics committee of the UKSH Campus Kiel and the Medical Faculty, University of Kiel (#A110/99). Classification of the pathological tumor stage was handled by the Department of Pathology, UKSH Campus Kiel, according to the TNM-classification. Clinical data were obtained from the clinical research database of the oncological biobank of the Comprehensive Cancer Center Kiel (BMB-CCC) and data was verified by re-examination of original patient records.

Blood samples from the following time points were analyzed for the presence of CTC: Pre-operatively (t0) and the primary endpoint of the study was reached if a patient reached the last blood draw at 12 months post-operatively (t5). For this, each patient received an individualized follow-up regimen for a visit and blood sample drawing at set time points after the surgical procedure: one month (t1), three months (t2), 6 months (t3), 9 months (t4), and 12 months (t5) (**Figure 1A**). The peripheral blood samples were either taken shortly prior to surgery (t0) from a central venous line or obtained by puncture of the median cubital vein for the blood samples collected at the follow-up time points (t1-t5).

For this study, two different approaches for CTC detection were applied. For the immunofluorescence detection by NYONE®, approximately 8 ml of blood were collected into a Sodium Citrate-Monovette® (Sarstedt, Nümbrecht, Germany). For CTC detection by PCR, approximately 20 ml of blood were drawn into lithium heparin-Monovettes® (Sarstedt). All samples were further processed within 2 hours after blood draw.

Sample Analysis With the Semi-Automated Microscope—NYONE®

The establishment and procedure of CTC enumeration by semi-automated microscopic detection with the cell imager NYONE® (SYNENTEC, Elmshorn, Germany) has been described previously (14). Briefly, the mononuclear cell (MNC) fraction was isolated by Ficoll-cushion centrifugation and resuspended in a fixation buffer (#14190-094, Biolegend, San Diego, CA, USA), incubated for 15 minutes at room temperature (RT), after which the samples were stored at 4°C for up to four days until further analysis.

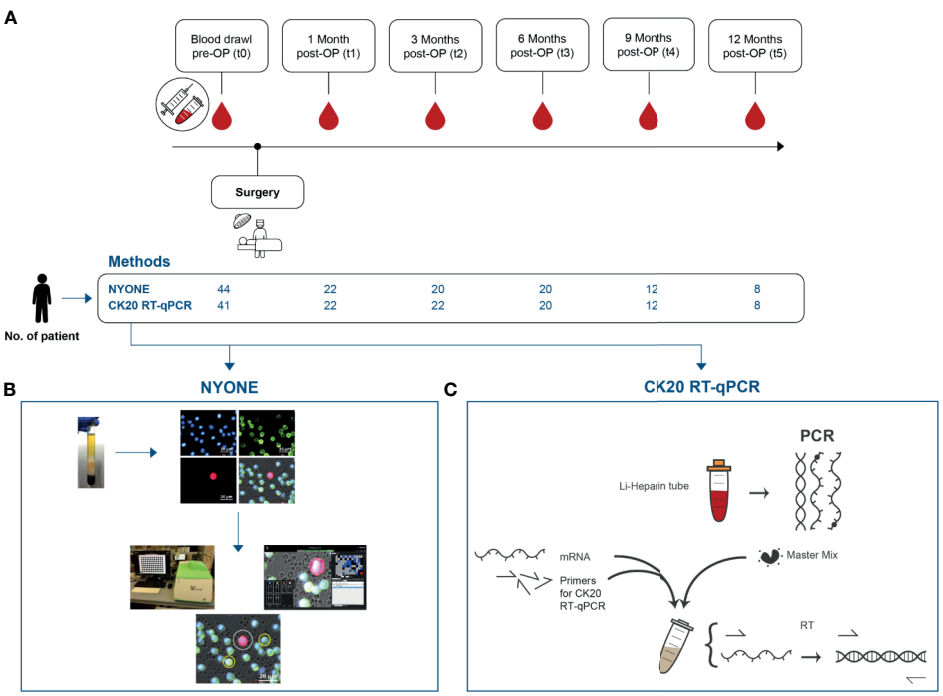

FIGURE 1 | Study outline and synopsis of the employed techniques for CTC detection. **(A)** Blood samples were collected repeatedly over a course of 12 months post-operatively. The first blood sample of each recruited patient was drawn immediately pre-operatively t0. Over the study period, five more samples were collected at set follow-up visits of each patient at 4 weeks (t1), 3 months (t2), 6 months (t3), 9 months (t4), and 12 months (t5). **(B)** NYONE® – After CTC enrichment by Ficoll centrifugation *via* CPT tubes, PBMC were fixed, permeabilized, and stained with anti-CD45-Alexa488 (green to detect leukocytes), anti-EpCAM, anti-EGFR, anti-Her2, and anti-pan-CK antibodies (all Alexa647-coupled, red to detect epithelial cells) and DAPI (blue) for nuclei staining. The enumeration process of CTC was carried out by the cell imager NYONE®. After image analysis, CTC (DAPI positive, negative for Alexa488, and positive for Alexa647) were encircled allowing cytological assessment. **(C)** Semi-quantitative RT-qPCR against CK20 –After Ficoll centrifugation of the blood plasma samples, the enriched fraction of PBMC was isolated and cDNA was obtained after RNA preparation. Then, a TaqMan gene expression assay [KRT20 (CK20)] and TBP as a house-keeping gene were used.

Then, cells were permeabilized in a Perm-/Wash-Buffer (#421002, Biolegend) for 5 minutes at RT and centrifuged at 330xg for 10 minutes. Afterward, cells were incubated with an Fc-blocking buffer (#422301/2, Biolegend) for 15 minutes. Then, cells were incubated for 30 minutes with the following antibodies: anti-CD45-AF488 (#304017; Biolegend), anti-EpCAM-AF647 (#324212; Biolegend), anti-pan-CK-AF647 (#628604; Biolegend), anti-EGFR-AF647 (#sc-120 AF647; SantaCruz, Dallas, TX, USA), and anti-Her2-AF647 (#3244412; Biolegend). Finally, a buffer containing DAPI (1:10,000) (#422801; Biolegend) was added to the cells.

Subsequently, 200 µl of the stained cell suspension was transferred into each a well of two 96-well plates (Sarstedt), which was centrifuged at 330xg for 10 minutes, and afterward placed in the NYONE® cell imager.

For analysis, the plates were scanned only for the detection of Alexa647 fluorescence (Ex 632/22, Em 685/40) as only CTC should be positive in this setting, which was detected by the respective antibody cocktail against epithelial markers EpCAM, pan-cytokeratin, EGFR, HER2. SYNENTEC's proprietary YT®-Software automatically analyzed the images already during scanning and detected positive events (**Figure 1B**). The image processing settings for this analysis were determined previously using blood samples from healthy donors spiked with HT29 tumor cells (14). Each event was then automatically further analyzed in depth by creating a region of interest (ROI) around it. This ROI was scanned in four channels (DAPI: Ex 377/50 Em 452/45, Alexa488: Ex 475/28 Em 530/43, Alexa-647: Ex 632/22 Em 685/40, brightfield: Ex brightfield Em blue). YT®-Software then automatically detected the cells´ nuclei (DAPI, blue fluorescence) and analyzed whether a virtual cytoplasm surrounding the nuclei was fluorescing green (CD45) or red (EpCAM, pan-CK, EGFR, Her2). These events were finally presented separately by the software and the investigator was able to examine the morphology of the potential CTC (**Figure 1B**).

Sample Analysis by Molecular mRNA Detection: Semi-Quantitative CK20 RT-qPCR

The application of a semi-quantitative CK20 RT-qPCR for CTC detection (**Figure 1C**) in CRC patients has been previously established in our work group (13). Briefly, blood samples were processed by ficoll-centrifugation to isolate the MNC fraction. Then, RNA was isolated with RNAPure® reagent (VWR Peqlab, Darmstadt, Germany) and cDNA was obtained by reverse transcription of 3 µg total RNA (Maxima First Strand cDNA Synthesis Kit, Thermo Fisher Scientific, Darmstadt, Germany). The qPCRs were run in a total volume of 20 µl per well of a 96-well plate (Sarstedt) using the TaqMan gene expression assays for CK20 (KRT20, Hs00966063_m1) and for the housekeeping gene TBP (TATA-box binding protein), Hs00427620_m1, as a reference in combination with the TaqMan Fast Advanced Master Mix on a StepOne Plus realtime PCR System (all ThermoFisher Scientific). All samples were run in triplicate. Relative gene expression was calculated as arbitrary expression units [EU] by a simplified ΔC_t method normalizing the CK20 expression against the reference gene TBP expression.

Statistical Analysis

All reported P-values are two-sided and were regarded statistically significant at $P < 0.05$. When a Gaussian distribution of the data was assumed, the parametric data were analyzed by either a repeated measure or ordinary one-way-ANOVA test. Non-parametric data were analyzed by a Mann-Whitney U-test. Statistical calculation and testing were performed with GraphPad Prism 8 (GraphPad Software, San Diego, CA, USA).

RESULTS

Patients Demographics

A synopsis of all patient data relating to the entire cohort but also the subgroups in terms of detection method is given in **Table 1**. In total, blood samples from 49 patients were included in this prospective study (**Figure 1A**). A total of 30 male and 19 female patients were enrolled and the median age at the time of operation and first blood sample collection was 67 years (range: 48–89 years). In total, 32 patients were diagnosed with colon carcinoma and 17 patients with rectal carcinoma. Amongst the colon carcinoma subset, an equal composition between left- and right-sided carcinoma (both 16 cases) was noted. The study cohort was further stratified by a clinico-pathological staging according to the UICC stages I-IV, with the most patients diagnosed with stage III (38.8%). In total, 10 patients (all rectal carcinoma) were treated by neoadjuvant radio-chemotherapy, and 18 patients received adjuvant chemotherapy.

TABLE 1 | Patient demographics and clinical characteristics of the entire study population and further breakdown according to the utilized detection modes.

	Total *N* (%)	NYONE *N* (%)	CK20 *N* (%)
	49 (100)	44 (100)	47 (100)
Gender			
Male	30 (61.2)	26 (59.1)	29 (61.7)
Female	19 (38.8)	18 (40.9)	18 (38.8)
Age			
Median (range)	67 (45-89)	66 (45-89)	67 (45-89)
<65	21 (42.9)	18 (40.9)	21 (44.7)
≥65	28 (57.1)	26 (59.1)	26 (55.3)
Tumor site			
Colon	32 (65.3)	32 (72.7)	30 (63.8)
Right	16 (50.0)	16 (50.0)	15 (50.0)
Left	16 (50.0)	16 (50.0)	15 (50.0)
Rectum	17 (34.7)	12 (27.3)	17 (36.2)
UICC stage			
I	14 (28.6)	12 (27.3)	14 (29.8)
II	9 (18.4)	9 (20.5)	8 (17.0)
III	19 (38.8)	18 (40.9)	18 (38.3)
IV	7 (14.3)	5 (11.4)	7 (14.9)
Neoadj. treatment			
Yes	10 (58.8)	6 (50.0)	10 (58.8)
No	7 (41.2)	6 (50.0)	7 (41.2)
Adjuvant treatment			
Yes	18 (36.7)	14 (31.8)	17 (36.2)
No	31 (63.3)	30 (68.2)	30 (63.8)

The subset of patients who received neoadjuvant treatment solely comprised of patients with rectal carcinoma. UICC, Union internationale contre le cancer.

Altogether, 44 and 47 patients were enrolled for CTC analysis by the cytological semi-automated microscopy (NYONE®, **Figure 1B**) and the indirect molecular approach by CK20 RT-qPCR (**Figure 1C**), respectively. Generally, the distribution of the two subsets of patients according to the demographical and clinical parameters was assimilable. The median age of patients within the NYONE® subgroup was 66 years (range: 45–89 years) and within the PCR group 67 years (range: 45–89 years) at the time of blood draw. In both groups, the majority of patients were male (59.1% – NYONE® and 61.7% – PCR) and were diagnosed with a colon carcinoma (72.7% – NYONE® and 63.8% – PCR). Again, most of the patients were diagnosed with locally advanced tumor burden and staged UICC III (40.9% – NYONE® and 38.3% PCR).

Longitudinal Analysis of CTC Count by IF and the NYONE® Cell-Imager

Altogether, we were able to enroll 44 patients for the longitudinal follow-up. During the time of the study period, the number of patient re-visits declined (**Figure 1A**).

In general, positivity rates during the collection time-course of CTC by the NYONE® technique were low and comparable at the first (pre-operative, t0) time points (**Table 2**), ranging between a mean CTC count of 0.89 and 1.5. At t5, a considerable increase of the mean CTC count could be observed (mean 4.25 CTC; SD: 10.01). However, this might be explained by one patient´s exceedingly high CTC count of 29 IF-positive cells.

Surgical resection of the tumor did not seem to have an effect on the frequency of CTC in the peripheral blood of the patients as the mean count of CTC was 0.89 CTC (range: 0–7 CTC; SD: 1.57) at t0 (prior to surgery) and 1.18 CTC (range: 0–4 CTC; SD: 1.33) at t1 (p not significant). Furthermore, analyzing the following blood samples over the time course, the CTC count of the overall study population did not show any significant alterations from the initial CTC prevalence (all p not significant) (**Table 2** and **Figure 2A**).

Stratifying the study population by means of CTC positivity (n=16 patients) *vs*. negativity (n=28 patients) at t0, a statistically significant increase in the CTC count at t1 was monitored in the subgroup without any pre-operative signs of CTC (mean: 0.00; SD: 0.00 at t0 and mean: 0.93; SD: 1.22 at t1; p=0.023). In all other measurements at later time points of the study, no significant differences compared to the baseline at t0 were observed in this subgroup (all p not significant) (**Figure 2B**). In contrast, in patients who initially had shown evidence of CTC in the peripheral blood, a general decrease in CTC by trend could be monitored (**Figure 2C**).

Next, we further stratified the cohort by adjuvant chemotherapeutic treatment and analyzed patients who received treatment (CTX+) in comparison to patients who were solely admitted to follow-up care (CTX-). We analyzed the patients´ CTC counts accordingly and compared the mean cell counts of CTC at each time point individually. Surprisingly, CTX+ patients showed higher CTC counts almost throughout the entire study period with a statistically significant higher CTC amount at t5 (CTX+: mean 7.75 cells, SD 14.17 *vs*. CTX-: mean 0.75 cells, SD 0.5; p=0.015) (**Table 2** and **Figure 2D**).

We additionally analyzed the development of the cohort during the observation period based on the amount of CTC. Subgroups were defined by the absence of CTC (0 cells per patient sample), intermediate frequency (1–2 cells per patient sample), and high CTC rates (≥3 cells per patient sample). The definition of high CTC frequency as ≥3 cells was based on different studies which proposed this as a clinically significant cut-off determined by the CellSearch® system (15). Interestingly, while the percentage of patients with no cells in the blood declined during the time period of the study, a highly significant increase in patients with both intermediate (1–2 CTC) and high prevalence of CTC (≥3 CTC) was monitored for the duration of the study (p=0.002) (**Figure 2E**). In detail, at t0 approximately 63.3% of the patients were CTC negative while at t5 the percentage declined to 25.0%.

Longitudinal Analysis of the Relative CTC Load by CK20 RT-qPCR

In total, 47 patients were recruited in this study arm. **Table 1** gives an overview of the clinical and pathological data of the

TABLE 2 | CTC quantity partitioned for each technique of CTC detection and outlined for each follow-up timepoint with association of the impact of adjuvant chemotherapy on the CTC quantity over the study period.

	t0	*p*	t1	*p*	t2	*p*	t3	*p*	t4	*p*	t5	p
NyOne												
CTC positive patients: fraction (%)	16/44 (36.4)		12/22 (54.5)		12/22 (54.5)		9/20 (45.0)		7/12 (58.3)		6/8 (75.0)	
CTC count per patient: mean (SD)	0.89 (1.57)		1.18 (1.33)		1.50 (2.61)		1.00 (1.69)		1.33 (1.67)		4.25 (10.01)	
CTC count according to adjuvant chemotherapy												
CTX+: mean (SD)	1.50 (2.28)	ns	2.60 (1.34)	ns	2.25 (3.28)	ns	0.86 (0.90)	ns	0.83 (0.98)	ns	7.75 (14.17)	**0.015**
CTX-: mean (SD)	0.60 (1.04)		0.76 (1.03)		1.07 (2.16)		1.08 (2.02)		1.83 (2.14)		0.75 (0.50)	
CK20 RT-qPCR												
CTC positive patients: fraction (%)	33/41 (80.5)		19/22 (86.4)		17/22 (77.3)		16/20 (80.0)		7/12 (58.3)		8/8 (100.0)	
CTC count per patient: mean (SD)	3.11 (3.81)		3.55 (6.17)		3.08 (3.19)		2.41 (1.62)		1.61 (1.95)		4.16 (5.66)	
Patients ≥ cut-off: fraction (%)	15/41 (36.6)		8/22 (36.4)		11/22 (50.0)		10/20 (50.0)		2/12 (16.7)		3/8 (37.5)	
CTC count according to adjuvant chemotherapy												
CTX+: mean (SD)	2.43 (2.42)	ns	2.00 (1.85)	ns	3.21 (3.98)	ns	1.74 (1.45)	ns	1.21 (1.49)	ns	1.86 (0.55)	ns
CTX-: mean (SD)	3.40 (4.26)		4.14 (7.13)		3.00 (2.81)		2.76 (1.64)		2.01 (2.41)		6.45 (7.77)	

All p values in bold are regarded as statistically significant. UICC, Union internationale contre le cancer; SD, standard deviation; CTC, Circulating tumor cells; CTX, chemotherapy; ns, not significant.

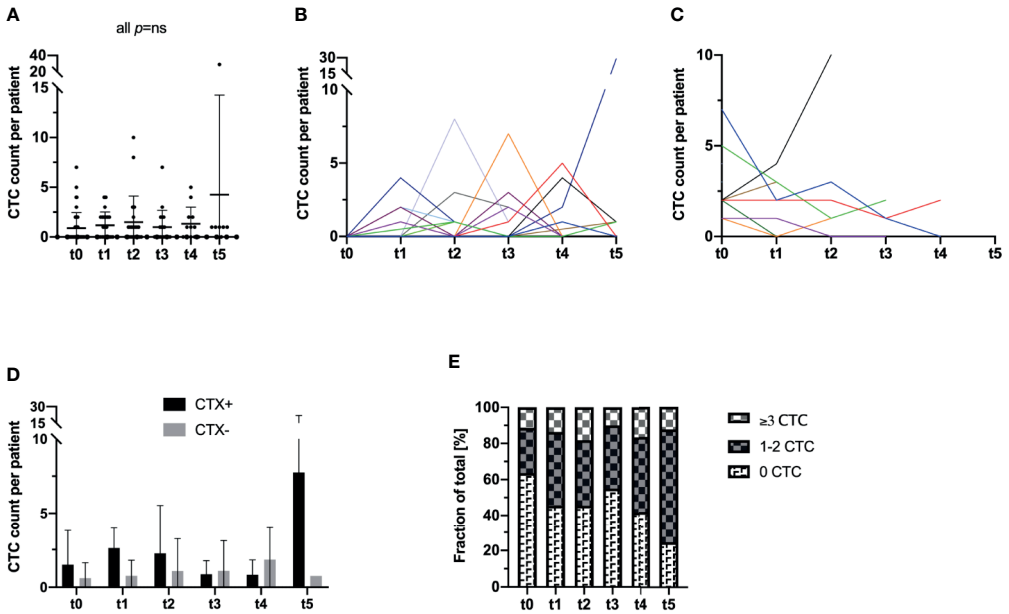

FIGURE 2 | Longitudinal analysis of blood samples of 44 CRC patients for the incidence and enumeration of CTC by a semi-automated microscopical approach with NYONE®. **(A)** In the study cohort as a whole, no statistically significant deviations in terms of an in- or decrease of the CTC count compared to t0 could be observed. The bar represents the mean count of CTC. **(B, C)** The individual patient with its longitudinal CTC quantification data is displayed by each line (each color represents one patient). **(B)** All patients that pre-operatively (t0) had no detectable CTC were analyzed in this subset. At t1, there was a statistically significant (p=0.023) increase in the CTC quantity. Throughout the further visits, no significant deviation from the initial CTC quantity (t0) was observed. **(C)** All patients with detectable CTC at t0 were sub-grouped for this analysis. There was no statistical significance for deviations over the study period from the initial CTC count. **(D)** Patients were stratified and subdivided according to their necessity of adjuvant chemotherapeutic treatment (CTX+). Patients that did not require adjuvant treatment were grouped in the follow-up subset (CTX-). **(E)** Patients were stratified and grouped according to the patients´ individual quantity of CTC: No CTC, 1-2 CTC (intermediate), ≥3 CTC (high). Analyzing the data as fractions of a whole, throughout the study a significant increase of patients with intermediate or high CTC counts was monitored.

patients. Blood samples that were collected at the time of operation and further samples that allowed for longitudinal CTC analysis were available from 41 patients.

In terms of tumor stages, the present patient cohort is representative, and the sensitivity rate of our applied CK20 RT-qPCR (80.42% positive for CTC, **Table 2**) is comparable to our previously reported data (13).

In line with the findings obtained with the NYONE® cell imager, no statistically significant short-term effect on the CTC/CK20-positivity load by the surgical procedure could be observed (mean: 3.11 [EU], SD: 3.81 at t0, and mean: 3.55 [EU], SD: 6.17 at t1; p not significant). Like the cytological analysis with the NYONE® cell-imager, the RT-qPCR analysis did also not reveal any significant alteration of the relative CTC/CK20-positivity throughout the study period compared to the pre-operative CTC signal at t0 (all p not significant) (**Table 2** and **Figure 3A**).

Next, we further stratified patients by applying a clinically and prognostically relevant cut-off for relative CTC positivity by CK20 RT-qPCR, which was established in a previous study (13). Patients were divided into two subgroups pre-operatively exhibiting either a high CTC positivity (≥2.77 [EU]; CTC-high) or a low CTC positivity (<2.77 [EU]; CTC-low). Patients who were pre-operatively (t0) in the CTC-low group, post-operatively (t1) showed a statistically significant increase in CTC numbers measured by CK20 RT-qPCR (mean: 1.17 [EU], SD: 0.85 at t0 *vs.* 4.36 [EU], SD: 7.94 at t1; p=0.047) (**Figures 3B, D**) which then declined again until t4 (mean: 0.78 [EU], SD: 0.99). Interestingly, a statistically significant increase in the relative CTC/CK20-positivity could be monitored from 9 to 12 months after surgery (t4 to t5; mean: 0.78 EU, SD: 0.99 at t4 *vs.* mean: 2.44 EU, SD: 0.77 at t5; p=0.018).

In contrast, in patients with a pre-operative high CTC-positivity, the surgical procedure and hence tumor burden reduction significantly reduced the CTC load during the first month (mean: 6.49 EU, SD: 4.56 at t0 *vs.* 2.68 EU, SD: 1.51 at t1; p<0.001). However, analyses at later time points throughout the study then revealed a slight increase of CTC compared to the post-operative CTC load at t1 (**Figures 3C, E**).

Interestingly, comparing the data obtained at t1 of both patient subsets, no difference emerged in the relative quantity of CTC between the groups (mean: 2.68 [EU], SD: 1.51 at t1 CTC high and mean: 4.36 [EU], SD: 7.94 at t1 CTC low; p=ns). Patients with pre-operative high CTC counts dropped post-operatively to a comparable level of patients with pre-operative low CTC counts who exhibited a post-operative increase in relative CTC loads.

Next, we subdivided the patients examined by CK20 RT-qPCR according to their status of adjuvant chemotherapy analogs to the cohort of patients in the NYONE® subset.

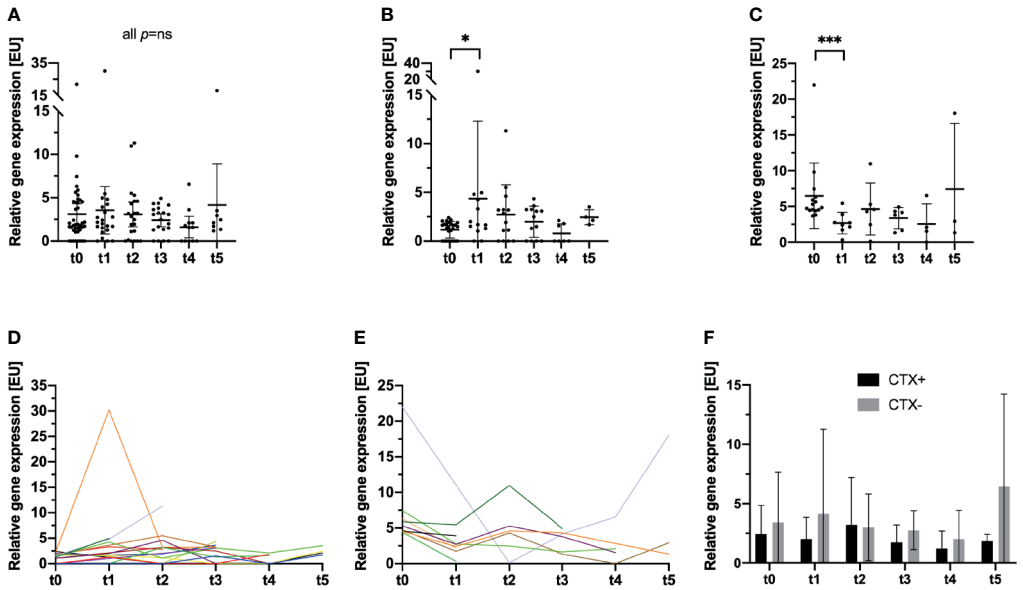

FIGURE 3 | Longitudinal analysis of blood samples of 47 CRC patients for the incidence and relative enumeration of CTC by a semi-quantitative CK20 RT-qPCR. Results are expressed by expression units [EU]. The bar represents the mean relative CTC count expressed by [EU]. **(A)** The entire study cohort is analyzed, and no statistically significant deviations of the relative CTC count compared to t0 were monitored. **(B–E)** The previously reported clinically significant cut-off value for CTC detection by CK20 PCR in CRC patients (13) was applied and the cohort stratified for further analysis. **(B, D)** In patients, who were below the cut-off at t0, a significant increase in CTC at t1 was monitored (p=0.047). No further differences were monitored at later visits compared to t0. Each color represents an individual patient. **(C, E)** For patients who were above the cut-off at t0, a significant decrease in the relative CTC quantity was recorded (p<0.001). No further significant deviations were monitored at later visits. **(F)** Patients were stratified and subdivided according to their necessity of adjuvant chemotherapeutic treatment (CTX+). Patients that did not require adjuvant treatment were grouped in the follow-up subset (CTX-). *p≤0.05; ***p≤0.001.

Contrary to the obtained data of the NYONE® subgroup analysis, CTX seemed to have an effect on the CTC enumeration. Patients in the CTX+ cohort showed lower relative CTC counts by trend at almost all re-visits. Only at t2 was there a slightly higher CTC count in patients of the CTX- subgroup (CTX+: mean 3.21 [EU], SD 3.98 *vs.* CTX-: mean 3.00 [EU], SD 2.81; p=ns) (**Table 2** and **Figure 3F**)

Evaluation of Individual Longitudinal Patient Courses

After having analyzed the overall cohort, we next focused on patients´ individual CTC courses detected by the two enumeration methods and linking the obtained results to the clinical follow-up data.

Figure 4A exemplarily displays the context and interplay of CTC enumeration and adjuvant treatment after surgery. This patient was diagnosed with an adenocarcinoma of the descending colon, but with locally progressed tumor burden and nodal positive stage III disease. In line with the guidelines (German S3-Guideline Colorectal Carcinoma, Version 2.1 – January 2019 AWMF-Registration Number: 021/007OL) the patient was admitted to adjuvant chemotherapy after surgical resection. Fitting to the advanced tumor burden, the patient showed exceptionally high numbers of CTC pre-operatively (t0) (NYONE®: 7 cells, PCR: 7.44 [EU]) in comparison to the general average of the cohort. Around 1 month (t1) after surgery and shortly before initiation of chemotherapy, the CTC count had dropped significantly (NYONE®: 2 cells, PCR: 2.77 [EU]) and remained below the cut-off values of both detection methods during the entire course of adjuvant chemotherapy (t1 up to t3) and the end of the observation period (t5). However, even though CTC enumeration from t3 until t5 was below the cut-off value, the PCR-based approach revealed a slight increase in the CTC enumeration starting at t4, at which the cytological approach further indicated a decline in the CTC load. Tumor markers CEA and CA19.9 were monitored at t0 and were not elevated at that time. Follow-up diagnostics were performed within the investigation period and did not show any signs of macroscopical tumor relapse. Since the patient dropped out of the study after t5, we could not further elaborate whether the CTC increase determined indirectly by CK20 RT-qPCR was indicative of a reactivation of a minimal residual disease (MRD) and clinical relapse.

Figure 4B exemplarily displays the disease course of a patient diagnosed with a stage II adenocarcinoma of the descending colon and provides an example of the potential of CTC as biomarkers for add-on recurrence diagnostics. According to the general guidelines (German S3-Guideline Colorectal Carcinoma, Version 2.1 – January 2019 AWMF-Registration Number: 021/007OL), adjuvant chemotherapy was not given, and the patient was only admitted to oncological follow-up. Pre-operatively (t0), no CTC could be detected with the NYONE® cell imager and the relative enumeration by CK20 RT-qPCR also revealed a measurement below the cut-off value. At t2 (3 months later), CTC detection by both the NYONE® and PCR was still

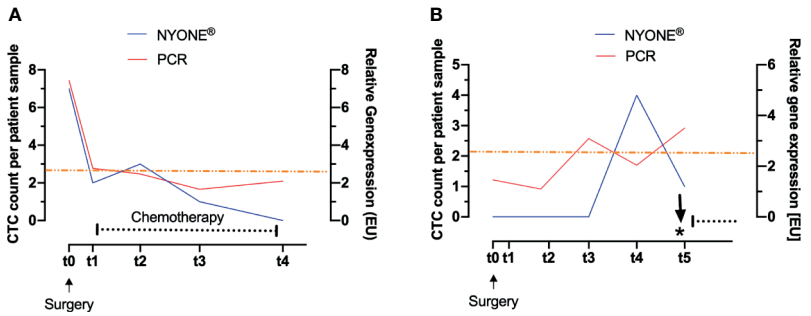

FIGURE 4 | Evaluation of CTC load during individual longitudinal patient courses. CTC were enumerated by two altering methods: cytologically after IF-staining by detection with the NYONE® (blue line) and molecularly by analysis of CK20-gene expression by RT-qPCR (red line). The asterisk indicates the time point of diagnosis of the local recurrence of carcinoma. The black dotted line indicates the interval of chemotherapy. The orange line represents the clinically significant cut-off value of CTC detected by CK20 RT-qPCR. **(A)** CRC patient with stage III carcinoma of the descending colon. After the operation, the CTC load dropped markedly and under the adjuvant therapy, no significant rise in CTC was observed. **(B)** CRC patient with stage II carcinoma of the descending colon. A total of 24 weeks after the operation, a clear rise of CTC in both detection methods was monitored, with the PCR-based approach being even earlier Clinically no significant follow-up event was recorded. Thirteen months after t0 a local recurrence of the carcinoma was diagnosed.

negative, and the PCR-based analysis even revealed a slight decrease of the CTC count (1.46 [EU] at t0 and 1.10 [EU] at t2). At t3 (6 months later), a relevant increase of the relative CTC enumeration above the cut-off value could be monitored by CK20 RT-qPCR (3.09 [EU]), while the NYONE® analysis still did not reveal any CTC positivity. At t4 (9 months after surgery), a significant increase in the CTC count could also be detected by the microscopical enumeration approach (0 cells at t0-t3 and 4 cells at t4). The last measurement at t5 (12 months after surgery) revealed a continuous increase in the relative quantification of CTC by CK20 RT-qPCR (3.50 [EU]), but surprisingly a declining cytological detection by the NYONE® (4 cells at t4 and 1 cell at t5). Interestingly, 13 months after initial surgery, a local recurrence of the primary adenocarcinoma was detected. Important to note that the tumor markers CEA and CA19.9 were below the cut-off levels at all times. In summary, these findings suggest that we were able to monitor a significant increase in CTC by both techniques being indicative of a reactivation of an MRD prior to its detection by the imaging diagnostics conducted according to the standard guidelines of follow-up (German S3-Guideline Colorectal Carcinoma, Version 2.1 – January 2019 AWMF-Registration Number: 021/007OL).

DISCUSSION

The benefit of CTC diagnostics as a biomarker for assessing the disease prognosis in cancer patients is evident (6, 9). However, the majority of studies firstly focus on patients with systemic stage IV disease and, secondly, conclude the patients' prognosis by CTC-analysis from a single pre- or post-operative blood sample only. Accordingly, CTC numbers or CTC associated parameters were determined only once and correlated with the clinical follow-up (16–21). Only very few studies have analyzed the prognostic potential of longitudinal CTC quantification over a period of time (22, 23).

In this prospective pilot study, we longitudinally monitored a cohort of CRC patients of miscellaneous tumor stages, who underwent surgical resection of the tumor and postoperatively were either admitted to oncological follow-up or adjuvant chemotherapy treatment. All patients enrolled were recontacted for serial blood samples, partially on the occasion of routine follow-up examination over a course of 12 months post-operatively. CTC enumeration was carried out by two differing techniques, (i) cytologically, by IF staining and microscopical detection by the semi-automated cell imager (NYONE®), and (ii) molecularly, by a semi-quantitative RT-qPCR detecting CK20 mRNA as an epithelial cell marker. CTC enumeration data obtained by either method was correlated with clinical characteristics and follow-up data.

Firstly, contrary to our expectations, surgery did not have any statistically significant effect on the quantity of CTC detected by the cytological approach utilizing the cell imager NYONE® regarding the overall complied cohort of our study population. Generally, and described by Galizia et al. (24), one could expect the resection of the tumor to have a significant negative impact on the incidence of CTC postoperatively in the overall cohort. Despite this, we were able to demonstrate a significant short-term increase in CTC quantity post-operatively but only in patients who were pre-operatively negative for CTC in the cytological method or below the cut-off in the PCR-based analysis. During the surgical procedure and mechanical manipulation of the tumor, an excess of CTC may be released into the bloodstream (25–27). Owing to a short half-life of CTC, their numbers are significantly reduced but still elevated 3 months after surgery compared to the preoperative status. Interestingly, in patients who pre-operatively showed evidence for CTC in the NYONE® or were above the cut-off for the CK20 RT-qPCR method, CTC levels post-operatively dropped significantly. Concluding, the removal and physical manipulation of the tumor in this subset of patients did surprisingly lead to a significant decrease in CTC numbers in the short term. In a large single-center study comprising 403 patients with breast cancer, van Dalum et al. analyzed CTC with the CellSearch® system over a long follow-up period (median 5.7 years). In their study, they did not observe any relevant impact of the surgical

procedure on CTC frequency. Enumeration levels were fairly constant over the study period (28). Then again, CTC are often thought to be directly linked to the primary tumor. Hence, once the tumor is resected, the general opinion would be that CTC numbers are decreasing and due to CTC clearance ultimately disappear from peripheral blood samples. Our data suggest that CTC remain detectable even in the mid and long-term after the surgical procedure. Notable in this context is the exceedingly high CTC count of 29 IF positive cells in one patient twelve months post-operatively. Interestingly, this was a patient who was diagnosed with a colon cancer of the descending colon with a singular hepatic metastasis who underwent synchronous resection of the primary tumor and the metastasis. Then, the patient received an adjuvant chemotherapy and CTC counts remained low throughout the study period. The blood draw at t5 was during the routine visit of oncological follow-up. Unfortunately, the patient then dropped out for further analysis.

Presumably, these CTC are shed into the bloodstream and are derived from disseminated tumor cells (DTC) that rest in a dormant-like stage in the bone marrow or lymph nodes. When suitable triggers are active, they initiate local recurrence or macro-metastasis.

In a xenograft mouse model and co-culture experimental set-up, Möhrmann et al. demonstrated the importance of DTC and their potential to act as a source for tumor relapse (29). In a study of breast cancer patients, Meng et al. showed that in 13 of 36 patients, where follow-up data were available, CTC were detectable up to 22 years after treatment. As they concluded slowly replicating or dormant DTC to be the cause of this (30), it is reasonable to assume that the origin of CTC detectable in our patients after surgical removal of the tumor are DTC or derivatives of these.

Furthermore, our data further underscore the potential of CTC as prognostic biomarkers in CRC, which has been already shown in previous studies (11–13). By applying our CK20 RT-qPCR on blood samples over the post-operative course of the disease, we were able to detect a relative rise in CTC ahead of clinical symptoms or positive radiological imaging in a patient with stage II colon carcinoma who was diagnosed with local tumor recurrence thirteen months after tumor resection (**Figure 4A**). In other malignancies, for instance, in leukemia patients, the concept of molecular minimal residual disease (MRD) monitoring is well established (31). PCR methods for detection of genes or genetic aberrations for MRD monitoring have been standardized by the Europe Against Cancer (EAC) consortium and are widely instituted (32). In terms of colorectal cancer as a common solid tumor entity, concepts comparable to the MRD monitoring in leukemia are still lacking. The follow-up is mainly conducted by clinical examinations and imaging diagnostics according to the general guidelines (German S3-Guideline Colorectal Carcinoma, Version 2.1 – January 2019 AWMF-Registration Number: 021/007OL). In this study, we demonstrate an example where disease monitoring by CK20 RT-qPCR based CTC detection is feasible and plausible. Even though no clinical recommendation can be drawn based on our data yet, attention should be given to the unambiguous case report of the stage II colon cancer patient reported on above.

In our study, we were able to identify patients with unusual CTC courses. The initial blood draw, revisit and correlation of the data with clinical follow-up characteristics of some patients allowed for individual insights into the prognostic potential and relevance of CTC. Again, the vast majority of studies focus on the overall potential of CTC as a biomarker in cancer patients. Larger patient cohorts are recruited, and the relevance of CTC enumeration is correlated to clinical follow-up data. Though, for further analysis of the principles of changes over time in the CTC quantity, further in-depth analysis possibly also investigating the biology of these individual CTC are desirable.

Future investigations on the prognostic potential of CTC in the follow-up analysis of CRC patients should aim at a multi-marker approach. As a widely employed and well-esteemed technique for CTC detection, CellSearch® (Menarini Silicon Biosystems) is up to date the only method approved by the FDA (Food and Drug Administration) and therefore commercially available for clinical application. Here, CTC are enriched and enumerated by an immunological antibody-based method, which has been described in detail elsewhere (33). The CellSearch® technique utilizes antibodies targeting two antigens: EpCAM and EGFR. The clinical significance had been documented firstly by Cohen et al. in a large prospective study, though patients enrolled were all diagnosed with stage IV disease (15). It is the general opinion that a high tumor burden with distant metastasis (stage IV disease) correlates with high numbers of CTC, hence the detection of CTC by those two markers as applied by CellSearch® is presumably more likely leading to significant numbers of CTC. Only very few studies were conducted analyzing non-metastatic CRC patients and the incidence of CTC by CellSearch® detection. A possible explanation could be the concise enumeration rates of CTC detected by CellSearch®. As presented by Thorsteinson et al. in their study analyzing the prognostic relevance of CTC detection by CellSearch® in non-metastatic patients, the detection rate of CTC is poor (34), though the samples size in terms of the number of patients recruited was quite small. Another investigation by Gazzaniga et al., in which high-risk non-metastatic CRC patients were enrolled, led to similar results of low CTC numbers detected and a lack of correlation with clinical characteristics or efficacy as a prognostic marker (35). Perchance, the sensitivity of the CellSearch® system is limited due to only two markers being applied, and hence the rate of undetected CTC is high.

Therefore, to overcome this potential pitfall, we intended to establish a strategy employing a multi-marker approach extending the utilized range of markers EpCAM and EGFR by two further broadly established epithelial markers: pan-CK and HER2. However, despite broadening the range of applied markers for detection, the rate of CTC was also low in our study. A possible explanation for this could be the process of Epithelial-Mesenchymal-Transition (EMT). CTC that have undergone this process may have lost or downregulated such epithelial antigens (36, 37). Consequently, these CTC were missed by IF staining for our markers and thus not detected. Few studies have been published analyzing appropriate mesenchymal marker antigens for CTC detection in CRC patients. Yokobori et al. for example, have identified the actin-

bundling protein Plastin 3 by microarray analysis of a cohort of CRC patients and demonstrated its negative prognostic value in a large patient cohort (38). In future efforts, the significance and potential of mesenchymal antigens have to be further validated. An approach for evading the issue of epithelial- and mesenchymal-specific detection of CTC could be the label-free isolation and enumeration. In general, CTC are thought to be significantly larger (>8 μm) than leucocytes, allowing for the concept of isolation by size of epithelial tumor cells (ISET) (39, 40). One way of conducting CTC enumeration by ISET is the filtration of blood samples through a porous membrane, allowing leucocytes to pass and CTC to be effectively retained on the membrane as it has been exemplarily demonstrated with the ScreenCell® isolation devices (ScreenCell®, Sarcelles, France). Staining of these CTC then allows for cytological analysis and enumeration. The feasibility and prognostic value have been demonstrated (18, 41, 42).

In summary, our study enlightens the kinetics of CTC in CRC patients after resection of the primary tumor and provides data concerning the CTC quantity over a long-term follow-up. This study not only supports the significance of CTC as a prognostic biomarker but also provides a more in-depth longitudinal analysis of CTC over the course of the disease. Furthermore, these data suggest that by using CK20 RT-qPCR for CTC detection and enumeration approach (e.g., during long-term follow-up), a molecular MRD monitoring might be feasible in CRC patients allowing earlier detection and therapy decision making in relapse situations. However, future investigations with an even more extended follow-up and larger patient cohorts will have to validate our results and may help to define an optimal longitudinal sampling scheme for liquid biopsies in the post-operative monitoring of cancer patients to enable tailored therapy concepts for precision medicine.

DATA AVAILABILITY STATEMENT

The original contributions presented in the study are included in the article/supplementary material. Further inquiries can be directed to the corresponding author.

ETHICS STATEMENT

The studies involving human participants were reviewed and approved by ethics committee of the UKSH Campus Kiel and the Medical Faculty, University of Kiel. The patients/participants provided their written informed consent to participate in this study.

AUTHOR CONTRIBUTIONS

Conceptualization: AH, BB, RG, CR., SH, and SS. Data curation: AH, BB, and RG. Formal analysis: AH, KD, BB, and SS. Investigation: AH. Methodology: KD, BB, and RG. Project administration: SH and SS. Resources: BB, CR, CS, TB, SH, and SS. Software: BB and RG. Supervision: SH and SS. Validation: BB. Visualization: AH. Writing—original draft: AH and SS. Writing—review and editing: AH, KD, BB, RG, CR, CS, TB, SH, and SS. All authors contributed to the article and approved the submitted version.

ACKNOWLEDGMENTS

We thank Bianca Zinke, Liane Carstensen, Julia Wilking, and Jannik Kerber for their excellent technical and methodological support. We thank the biobank of Comprehensive Cancer Center North (BMB-CCC) for providing blood samples and clinical data for this study. The BMB-CCC is a member of the PopGen 2.0 Biobanking Network (P2N) Kiel and was funded by the German Federal Ministry of Education and Research (BMBF grant 01EY1103). We thank ORGA Labormanagement GmbH for the possibility to use their NYONE® for purposes of conducting this study. We thank SYNENTEC GmbH (especially Stefan Hummel) for the development of templates and image processing algorithms allowing the detection and visualization of positive cells.

REFERENCES

1. Siegel RL, Miller KD, Fedewa SA, Ahnen DJ, Meester RGS, Barzi A, et al. Colorectal Cancer Statistics, 2017. *CA Cancer J Clin* (2017) 67:177–93. doi: 10.3322/caac.21395
2. O'Connell MJ, Campbell ME, Goldberg RM, Grothey A, Seitz J-F, Benedetti JK, et al. Survival Following Recurrence in Stage II and III Colon Cancer: Findings From the ACCENT Data Set. *J Clin Oncol* (2008) 26:2336–41. doi: 10.1200/JCO.2007.15.8261
3. You YN, Rustin RB, Sullivan JD. Oncotype DX(®) Colon Cancer Assay for Prediction of Recurrence Risk in Patients With Stage II and III Colon Cancer: A Review of the Evidence. *Surg Oncol* (2015) 24:61–6. doi: 10.1016/j.suronc.2015.02.001
4. Le Tourneau C, Delord J-P, Gonçalves A, Gavoille C, Dubot C, Isambert N, et al. Molecularly Targeted Therapy Based on Tumour Molecular Profiling *Versus* Conventional Therapy for Advanced Cancer (SHIVA): A Multicentre, Open-Label, Proof-of-Concept, Randomised, Controlled Phase 2 Trial. *Lancet Oncol* (2015) 16:1324–34. doi: 10.1016/S1470-2045(15)00188-6
5. Sicklick JK, Kato S, Okamura R, Schwaederle M, Hahn ME, Williams CB, et al. Molecular Profiling of Cancer Patients Enables Personalized Combination Therapy: The I-PREDICT Study. *Nat Med* (2019) 25:744–50. doi: 10.1038/s41591-019-0407-5
6. Pantel K, Alix-Panabières C. Liquid Biopsy and Minimal Residual Disease - Latest Advances and Implications for Cure. *Nat Rev Clin Oncol* (2019) 16:409–24. doi: 10.1038/s41571-019-0187-3
7. Ignatiadis M, Lee M, Jeffrey SS. Circulating Tumor Cells and Circulating Tumor DNA: Challenges and Opportunities on the Path to Clinical Utility. *Clin Cancer Res* (2015) 21:4786–800. doi: 10.1158/1078-0432.CCR-14-1190
8. Kaifi JT, Li G, Clawson G, Kimchi ET, Staveley-O'Carroll KF. Perioperative Circulating Tumor Cell Detection: Current Perspectives. *Cancer Biol Ther* (2016) 17:859–69. doi: 10.1080/15384047.2016.1167296
9. Krebs MG, Metcalf RL, Carter L, Brady G, Blackhall FH, Dive C. Molecular Analysis of Circulating Tumour Cells-Biology and Biomarkers. *Nat Rev Clin Oncol* (2014) 11:129–44. doi: 10.1038/nrclinonc.2013.253
10. Alix-Panabières C, Pantel K. Technologies for Detection of Circulating Tumor Cells: Facts and Vision. *Lab Chip* (2014) 14:57–62. doi: 10.1039/c3lc50644d

11. Hinz S, Röder C, Tepel J, Hendricks A, Schafmayer C, Becker T, et al. Cytokeratin 20 Positive Circulating Tumor Cells Are a Marker for Response After Neoadjuvant Chemoradiation But Not for Prognosis in Patients With Rectal Cancer. *BMC Cancer* (2015) 15:953. doi: 10.1186/s12885-015-1989-z
12. Hinz S, Hendricks A, Wittig A, Schafmayer C, Tepel J, Kalthoff H, et al. Detection of Circulating Tumor Cells With CK20 RT-PCR Is an Independent Negative Prognostic Marker in Colon Cancer Patients - a Prospective Study. *BMC Cancer* (2017) 17:53. doi: 10.1186/s12885-016-3035-1
13. Hendricks A, Eggebrecht G-L, Bernsmeier A, Geisen R, Dall K, Trauzold A, et al. Identifying Patients With an Unfavorable Prognosis in Early Stages of Colorectal Carcinoma. *Oncotarget* (2018) 9:27423–34. doi: 10.18632/oncotarget.25384
14. Hendricks A, Brandt B, Geisen R, Dall K, Röder C, Schafmayer C, et al. Isolation and Enumeration of CTC in Colorectal Cancer Patients: Introduction of a Novel Cell Imaging Approach and Comparison to Cellular and Molecular Detection Techniques. *Cancers (Basel)* (2020) 12. doi: 10.3390/cancers12092643
15. Cohen SJ, Punt CJA, Iannotti N, Saidman BH, Sabbath KD, Gabrail NY, et al. Relationship of Circulating Tumor Cells to Tumor Response, Progression-Free Survival, and Overall Survival in Patients With Metastatic Colorectal Cancer. *J Clin Oncol* (2008) 26:3213–21. doi: 10.1200/JCO.2007.15.8923
16. Gorges TM, Stein A, Quidde J, Hauch S, Röck K, Riethdorf S, et al. Improved Detection of Circulating Tumor Cells in Metastatic Colorectal Cancer by the Combination of the CellSearch® System and the Adnatest®. *PLoS One* (2016) 11:e0155126. doi: 10.1371/journal.pone.0155126
17. Kidess-Sigal E, Liu HE, Triboulet MM, Che J, Ramani VC, Visser BC, et al. Enumeration and Targeted Analysis of KRAS, BRAF and PIK3CA Mutations in CTCs Captured by a Label-Free Platform: Comparison to ctDNA and Tissue in Metastatic Colorectal Cancer. *Oncotarget* (2016) 7:85349–64. doi: 10.18632/oncotarget.13350
18. Nicolazzo C, Raimondi C, Gradilone A, Emiliani A, Zeuner A, Francescangeli F, et al. Circulating Tumor Cells in Right- and Left-Sided Colorectal Cancer. *Cancers (Basel)* (2019) 11. doi: 10.3390/cancers11081042
19. Huang M-Y, Tsai H-L, Huang J-J, Wang J-Y. Clinical Implications and Future Perspectives of Circulating Tumor Cells and Biomarkers in Clinical Outcomes of Colorectal Cancer. *Transl Oncol* (2016) 4:340–7. doi: 10.1016/j.tranon.2016.06.006
20. Lu CY, Uen YH, Tsai HL, Chuang SC, Hou MF, Wu DC, et al. Molecular Detection of Persistent Postoperative Circulating Tumour Cells in Stages II and III Colon Cancer Patients Via Multiple Blood Sampling: Prognostic Significance of Detection for Early Relapse. *Br J Cancer* (2011) 104(7):1178–84. doi: 10.1038/bjc.2011.40
21. Wang JY, Lin S-R, Wu D-C, Lu C-Y, Yu F-J, Hsieh J-S, et al. Multiple Molecular Markers as Predictors of Colorectal Cancer in Patients With Normal Perioperative Serum Carcinoembryonic Antigen Levels. *Clin Cancer Res* (2007) 13(8):2406–13. doi: 10.1158/1078-0432.CCR-06-2054
22. Tan K, Leong SM, Kee Z, Caramat PV, Teo J, Blanco MVM, et al. Longitudinal Monitoring Reveals Dynamic Changes in Circulating Tumor Cells (CTCs) and CTC-associated miRNAs in Response to Chemotherapy in Metastatic Colorectal Cancer Patients. *Cancer Lett* (2018) 423:1–8. doi: 10.1016/j.canlet.2018.02.039
23. Musella V, Pietrantonio F, Di Buduo E, Iacovelli R, Martinetti A, Sottotetti E, et al. Circulating Tumor Cells as a Longitudinal Biomarker in Patients With Advanced Chemorefractory, RAS-BRAF Wild-Type Colorectal Cancer Receiving Cetuximab or Panitumumab. *Int J Cancer* (2015) 137:1467–74. doi: 10.1002/ijc.29493
24. Galizia G, Gemei M, Orditura M, Romano C, Zamboli A, Castellano P, et al. Postoperative Detection of Circulating Tumor Cells Predicts Tumor Recurrence in Colorectal Cancer Patients. *J Gastrointest Surg* (2013) 17:1809–18. doi: 10.1007/s11605-013-2258-6
25. Martin OA, Anderson RL, Narayan K, MacManus MP. Does the Mobilization of Circulating Tumour Cells During Cancer Therapy Cause Metastasis? *Nat Rev Clin Oncol* (2017) 14:32–44. doi: 10.1038/nrclinonc.2016.128
26. Wind J, Tuynman JB, Tibbe AGJ, Swennenhuis JF, Richel DJ, van Berge Henegouwen MI, et al. Circulating Tumour Cells During Laparoscopic and Open Surgery for Primary Colonic Cancer in Portal and Peripheral Blood. *Eur J Surg Oncol* (2009) 35:942–50. doi: 10.1016/j.ejso.2008.12.003
27. Pantel K, Brakenhoff RH, Brandt B. Detection, Clinical Relevance and Specific Biological Properties of Disseminating Tumour Cells. *Nat Rev Cancer* (2008) 8:329–40. doi: 10.1038/nrc2375
28. van Dalum G, van der Stam GJ, Tibbe AGJ, Franken B, Mastboom WJB, Vermes I, et al. Circulating Tumor Cells Before and During Follow-Up After Breast Cancer Surgery. *Int J Oncol* (2015) 46:407–13. doi: 10.3892/ijo.2014.2694
29. Möhrmann L, Zowada MK, Strakerjahn H, Siegl C, Kopp-Schneider A, Krunic D, et al. A Perivascular Niche in the Bone Marrow Hosts Quiescent and Proliferating Tumorigenic Colorectal Cancer Cells. *Int J Cancer* (2020) 147:519–31. doi: 10.1002/ijc.32933
30. Meng S, Tripathy D, Frenkel EP, Shete S, Naftalis EZ, Huth JF, et al. Circulating Tumor Cells in Patients With Breast Cancer Dormancy. *Clin Cancer Res* (2004) 10:8152–62. doi: 10.1158/1078-0432.CCR-04-1110
31. Voso MT, Ottone T, Lavorgna S, Venditti A, Maurillo L, Lo-Coco F, et al. MRD in AML: The Role of New Techniques. *Front Oncol* (2019) 9:655. doi: 10.3389/fonc.2019.00655
32. Gabert J, Beillard E, van der Velden VHJ, Bi W, Grimwade D, Pallisgaard N, et al. Standardization and Quality Control Studies of "Real-Time" Quantitative Reverse Transcriptase Polymerase Chain Reaction of Fusion Gene Transcripts for Residual Disease Detection in Leukemia - a Europe Against Cancer Program. *Leukemia* (2003) 17:2318–57. doi: 10.1038/sj.leu.2403135
33. Allard WJ, Matera J, Miller MC, Repollet M, Connelly MC, Rao C, et al. Tumor Cells Circulate in the Peripheral Blood of All Major Carcinomas But Not in Healthy Subjects or Patients With Nonmalignant Diseases. *Clin Cancer Res* (2004) 10:6897–904. doi: 10.1158/1078-0432.CCR-04-0378
34. Thorsteinsson M, Söletormos G, Jess P. Low Number of Detectable Circulating Tumor Cells in non-Metastatic Colon Cancer. *Anticancer Res* (2011) 31:613–7.
35. Gazzaniga P, Gianni W, Raimondi C, Gradilone A, Lo Russo G, Longo F, et al. Circulating Tumor Cells in High-Risk Nonmetastatic Colorectal Cancer. *Tumour Biol* (2013) 34:2507–9. doi: 10.1007/s13277-013-0752-9
36. Yu M, Bardia A, Wittner BS, Stott SL, Smas ME, Ting DT, et al. Circulating Breast Tumor Cells Exhibit Dynamic Changes in Epithelial and Mesenchymal Composition. *Science* (2013) 339:580–4. doi: 10.1126/science.1228522
37. Kalluri R, Weinberg RA. The Basics of Epithelial-Mesenchymal Transition. *J Clin Invest* (2009) 119:1420–8. doi: 10.1172/JCI39104
38. Yokobori T, Iinuma H, Shimamura T, Imoto S, Sugimachi K, Ishii H, et al. Plastin3 is a Novel Marker for Circulating Tumor Cells Undergoing the Epithelial-Mesenchymal Transition and Is Associated With Colorectal Cancer Prognosis. *Cancer Res* (2013) 73:2059–69. doi: 10.1158/0008-5472.CAN-12-0326
39. Farace F, Massard C, Vimond N, Drusch F, Jacques N, Billiot F, et al. A Direct Comparison of CellSearch and ISET for Circulating Tumour-Cell Detection in Patients With Metastatic Carcinomas. *Br J Cancer* (2011) 105:847–53. doi: 10.1038/bjc.2011.294
40. Desitter I, Guerrouahen BS, Benali-Furet N, Wechsler J, Jänne PA, Kuang Y, et al. A New Device for Rapid Isolation by Size and Characterization of Rare Circulating Tumor Cells. *Anticancer Res* (2011) 31:427–41.
41. Kuvendjiska J, Bronsert P, Martini V, Lang S, Pitman MB, Hoeppner J, et al. Non-Metastatic Esophageal Adenocarcinoma: Circulating Tumor Cells in the Course of Multimodal Tumor Treatment. *Cancers (Basel)* (2019) 11. doi: 10.3390/cancers11030397
42. Rizzo MI, Ralli M, Nicolazzo C, Gradilone A, Carletti R, Di Gioia C, et al. Detection of Circulating Tumor Cells in Patients With Laryngeal Cancer Using ScreenCell: Comparative Pre- and Post-Operative Analysis and Association With Prognosis. *Oncol Lett* (2020) 19:4183–8. doi: 10.3892/ol.2020.11528

Conflict of Interest: At the time of the study, RG was working for ORGA Labormanagement GmbH, which provided a CTC test using NYONE®. She is now working for SYNENTEC GmbH, which produces and distributes the NYONE® imaging system.

The remaining authors declare that the research was conducted in the absence of any commercial or financial relationships that could be construed as a potential conflict of interest.

frontiers in Oncology

REVIEW
published: 29 June 2021
doi: 10.3389/fonc.2021.684871

Comprehensive Roles and Future Perspectives of Exosomes in Peritoneal Metastasis of Gastric Cancer

Xiangliu Chen[1], *Haiyong Wang*[1], *Yingying Huang*[1], *Yanyan Chen*[1], *Chuanzhi Chen*[1], *Wei Zhuo*[2] *and Lisong Teng*[1]*

[1] Department of Surgical Oncology, The First Affiliated Hospital, School of Medicine, Zhejiang University, Hangzhou, China, [2] Department of Cell Biology, School of Medicine, Zhejiang University, Hangzhou, China

Gastric cancer (GC) is one of the most prevalent digestive malignancies. A great number of patients at first visit or post curative resections are diagnosed with widespread metastasis within the peritoneal cavity. Overwhelming evidence has demonstrated that exosomes, a variety of biologically functional extracellular vesicles comprising active factors, mediate the progression and metastasis of GC. Although the regulatory mechanisms of exosomes remain fairly elusive, they are responsible for intercellular communication between tumor cells and normal stroma, cancer-related fibroblasts, immune cells within the primary tumor and metastatic niche. In this review, we provide new insight into the molecular signatures of GC-associated exosomes in reprogramming the tumor microenvironment and the subsequent promotion of peritoneal metastasis—including infiltration of the gastric wall, implantation of tumor cells onto the pre-metastatic peritoneum, and remodeling of the pre-metastatic niche. Based on this review, we hope to draw a more general conclusion for the functions of exosomes in the progression and peritoneal metastasis of GC and highlight the future perspective on strategies targeting exosomes in prognostic biomarkers and therapy for peritoneal metastasis.

Keywords: gastric cancer, exosomes, peritoneal metastasis, microenvironment, pre-metastatic niche

OPEN ACCESS

Edited by:
Jaw-Yuan Wang, Kaohsiung Medical University Hospital, Taiwan

Reviewed by:
Theresa L. Whiteside, University of Pittsburgh, United States
Long-sen Chang, National Sun Yat-sen University, Taiwan

***Correspondence:**
Lisong Teng
lsteng@zju.edu.cn

Specialty section:
This article was submitted to Gastrointestinal Cancers, a section of the journal Frontiers in Oncology

Received: *24 March 2021*
Accepted: *07 June 2021*
Published: *29 June 2021*

Citation:
Chen X, Wang H, Huang Y, Chen Y, Chen C, Zhuo W and Teng L (2021) Comprehensive Roles and Future Perspectives of Exosomes in Peritoneal Metastasis of Gastric Cancer. Front. Oncol. 11:684871. doi: 10.3389/fonc.2021.684871

INTRODUCTION

Gastric cancer (GC) is the fifth most lethal malignancies worldwide and the third dominating cause of cancer-related death, responsible for 7% of cancer cases and 9% of the deaths (1), especially in East Asia, such as Japan, Korea, and China (2). Generally, peritoneal dissemination (PD) is the most common distant metastasis mode for GC and the most important factor leading to shortened survival of patients (3). Without treatment, a 5-year survival rate of GC patients with peritoneal metastases (PM) is 2% with the median survival time of 3–5 months (4). Despite radical operation of gastric cancer, around 50% of GC patients with advanced disease develop peritoneal metastasis (5). Nowadays, the combinations of platinum agents with addition of taxane, fluoproyrimidine, or

anthracyclines are usually regarded as the standard regimens for advanced or recurrent GC, including peritoneal metastases, but the efficacy of these systemic chemotherapy drugs for patients with PD is still limited (6).

Exosomes are membrane vesicles generated from the multivesicular endosomes with size ranging from 30 to 100 nm in diameter (7). Exosomes are released by all kinds of malignant and normal cells and are distributed in various bodily fluids such as plasma, urine, saliva, and malignant effusions (8). Exosomes display significant roles in intercellular communications to local and remote cells and organs, by selectively transferring its cargo (protein, lipids, DNA, RNA, and membrane) (9, 10). Notably, extensive studies have validated that exosomes contribute to different aspects of GC progression and PM by promoting primary tumor cells growth, invasion, and remodeling the peritoneal microenvironment to make it suitable for metastatic niches (11, 12). Exosomes participate in pluripotent cell functions in PM, inducing cancer-associated fibroblasts (CAFs), epithelial–mesenchymal transition (EMT) of cancer cells, mesothelial-to-mesenchymal transition (MMT) of peritoneal cells, angiogenesis, and immune suppression, changing the environment in both local and pre-metastatic stroma (13, 14).

In this review, it is stated that exosomes secreted by GC cells and other stroma cells have internal and external effects on GC growth, invasion, and PM, as summarized in **Figure 1** and **Table 1**. We have systematically clarified the roles of exosomes in all conceivable steps of PM, in which cancer cells spread from primary to peritoneum and finally form metastatic lesions. Since the characteristics of exosomes are dependent on their donor cells and the conditions of their formation, clarifying complete property practices of exosomes is conducive to their applications. The most thorough understanding of the content of the exosomes and underlying mechanisms on PM will be promising in aiding the novel discovery of potential diagnostic molecules and targets for treatment of GC.

TUMOR-DERIVED EXOSOMES ASSIST GASTRIC TUMOR CELLS IN DETACHING FROM THE PRIMARY TUMOR SITES

The PM cascade of GC is composed of a series of sequential events that GC cells have to accomplish, including metastatic spread of primary tumor mass, formation of pre-metastatic niches and final planting of metastatic sites (13). These exosomes, either tumor-derived exosomes or stromal cell-derived exosomes, are mobile elements participating in the first process—the spread of GC cells out of serosa, recruitment and activation of fibroblasts, induction of angiogenesis, and EMT promotion.

Tumor-Derived Exosomes Are Involved in Converting Stroma Cells to CAFs

Cancer-associated fibroblasts (CAFs) are the major part of cellular constituents of the cancer stroma and are indicative of the myofibroblast phenotype and strong contractility, which result in the remodeling and hardening of the extracellular matrix (ECM) and provide an appropriate microenvironment for cancer cell mobility and metastasis (52). Apart from the soluble factors, exosomes play an essential role in connection between cancer cells and CAFs. In a study, researchers found an extremely high level of miR-27a in exosomes secreted from patients' sera and cell lines of GC, which may contribute to the transition of stroma fibroblasts into CAFs by targeting a downstream target cysteine and glycine-rich protein 2 (CSRP2). Similarly, over-expression of miR-27a CAFs could increase the proliferation, motility, and invasion abilities of GC cells *in-vitro* and *in-vivo* (15). This indicates that GC-derived exosomes alone are competent in the induction of functional changes from normal fibroblasts to pathogenic CAFs. Similar studies have verified the potential of GC exosomes in converting normal stroma to CAFs. Stroma cells such as normal pericytes and mesenchymal stem cells could be induced into CAFs by GC exosome-mediated BMP

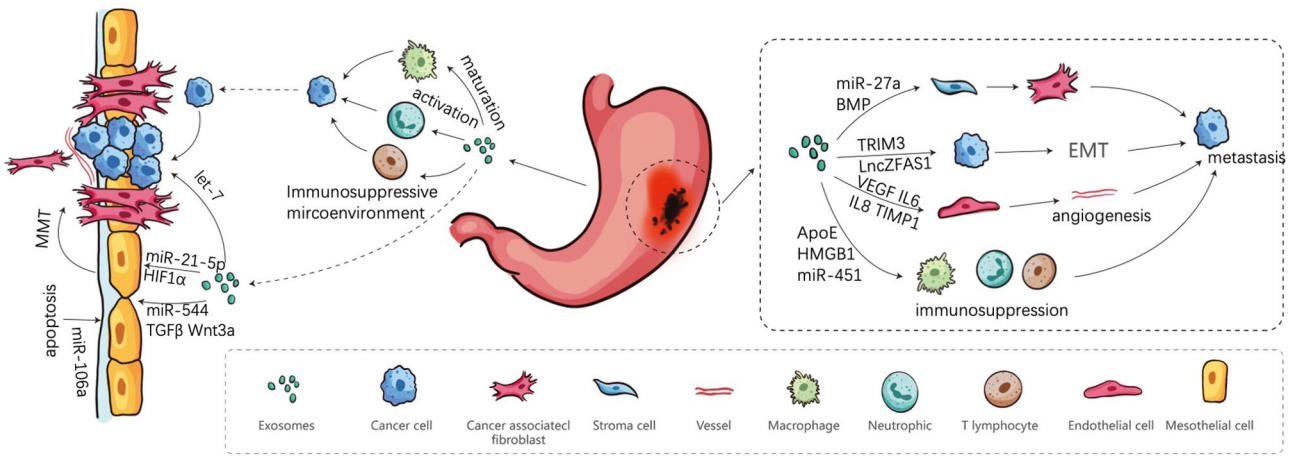

FIGURE 1 | Involvement of exosomes in peritoneal metastasis Cascade. Firstly, cancer cells are shed from the primary sites, and secondly transported in the peritoneal cavity. Finally, cancer cells adhere to the MCs and implant in peritoneum.

TABLE 1 | Function of exosomes in progression and peritoneal metastasis.

Exosomal cargo	Donor cells	Recipient cells	Role/Mechanism	Ref.
miR-27a	Gastric cancer	Stroma fibroblasts	Tumorigenesis and metastasis/CSRP2	(15)
BMP	Gastric cancer	Pericytes	Metastasis/PI3K and MEK pathway	(16)
TGF-β	Gastric cancer	MSCs	Metastasis/Smad	(17)
TRIM3/ ZFAS1	Gastric cancer	Gastric cancer	Growth and metastasis/EMT	(18, 19)
circNRIP1	Serum	Gastric cancer	metastasis/miR-149-5p-AKT-mTOR	(20)
\	Gastric cancer	PMCs	MMT/ERK pathway	(21)
miR-21-5p	Gastric cancer	PMCs	MMT/TGF-β pathway	(22)
miR-106a	Gastric cancer	PMCs	Apoptosis/SMAD7	(23)
Wnt3a	Gastric cancer	PMCs	Tumor invasion	(24)
VEGF,TIMP-1,IL6,IL8,FGF	Gastric cancer	Endothelial cell	Angiogenesis	(25, 26)
miR-130a	Gastric cancer	Endothelial cell	Angiogenesis/c-MYB	(27)
miR-135b/155	Gastric cancer	Endothelial cell	Angiogenesis/FOXO1/3	(28, 29)
MET	Gastric cancer	macrophage	Proinflammatory environment/ NF-κB /IL-1β	(30, 31)
\	Gastric cancer	PD1+TAMs	Immunosuppression/IL10	(32)
\	Gastric cancer	MSCs	Inflammatory environment/ NF-κB	(33)
miR-107	Gastric cancer	MDSCs	Immunosuppression/DICER1,PTEN	(34)
miR-451	Gastric cancer	Th17	Angiogenesis/mTOR	(35)
HMGB1	Gastric cancer	neutrophils	Migration/ NF-κB	(36)
\	Gastric cancer	CD8+Tcell	Immunosuppression/cytokine	(37)
\	CAF	Gastric cancer	Invasion/MMP2	(38)
\	Gastric cancer	PMCs	Adhesion/fibronectin,laminin gamma10	(39)
CD44H,CD44v6	Gastric cancer	Gastric cancer	Growth,angiogenesis	(40)
Let-7 miRNA	AZ-P7a	Gastric cancer	,Tumorigenesisi, PM	(41)
TGF-β,Wnt3,HIFα,Src	Gastric cancer	Stromal cell	MMT	(42)
miR-139	CAF	Gastric cancer	Growth and metastasis/MMP11	(43)
ApoE	TAMs	Gastric cancer	Migration/PI3K-AKT	(44)
IL6,IL8,ICAM1,GRO	Omentum	Gastric cancer	Progression/metastasis	(45–48)
miR-544-5p	PLF	PMCs	MMT/PLZF	(49)
\	MA	PMCs/GC	Metastasis/ MMT, EMT	(50, 51)

transfer (PI3K/AKT and MEK/ERK pathway) and TGF-β transfer (TGF-β/Smad pathway) respectively (16, 17).

As of now, these studies have confirmed that tumor-derived exosome are able to induce the change from normal stroma to cancerous stroma, which is essential for cancer progression of cancer cells and secondary metastatic growth. Exosomes derived from GC could deliver functional elements to induce CAF formation by activating AKT, ERK, and TGF-β/Smad signaling pathway, which are consistent with the studies of other cancers (53, 54).

Tumor-Derived Exosomes Induce EMT Process of GC

EMT allows epithelial cancer cells to lose epithelial-like traits and acquire a mesenchymal phenotype of the migratory and invasive characteristics for morphogenesis, which is an essential part of GC dissemination and metastasis (55, 56). Tumor-derived exosomes carry proteins and non-coding RNAs (lncRNA, miRNA, and circRNA) that directly enhance the invasive and migratory capabilities of GC cell (57). For example, exosomal Tripartite motif-containing 3 (TRIM3) and long non-coding RNA ZFAS1 of GC cells can promote growth and metastasis of cancer cells through mediating stem factors and EMT markers *in-vitro* and *in-vivo* (18, 19). Zhang et al. detected higher circNRIP1expression in GC tissues *via* RNA-seq analysis and transmission of circNRIP1 by exosomal communication between GC cells relative to normal tissues. Additionally, circNRIP1 is able to thicken the proliferation, migration, invasion and the expression of EMT markers in GC cells *via* sponging of the miR-149-5p/AKT/mTOR pathway. Formidably, exosomal circNRIP1 functions as a promoter of peritoneal metastasis in BABL/c nude mice (20). To some extent, exosomes derived from GC cells can transmit functional elements participating in the process of EMT on themselves, which is inevitable for onset of metastasis.

ROLES OF EXOSOMES IN PRE-METASTATIC NICHE FORMATION OF GASTRIC CANCER

Post exfoliation from the serosa of the stomach into the abdominal cavity, GC cells survive by creating a favorable microenvironment for subsequent metastases in secondary organs. The "seeds and soil" hypothesis has been instrumental to our understanding of PM, which depends on the characteristics of cancer cells (seeds) and target organs (soil) (58). For example, pancreatic ductal adenocarcinoma patients who developed liver metastasis produce tumor-derived exosomes carrying high macrophage migration inhibitory factor (MIF), which could induce liver pre-metastatic niche formation and subsequently enlarge liver metastatic burden (59). In the progression of PM, exosomes play multifaceted roles in affecting pre-metastatic microenvironment through inducing mesothelial-to-mesenchymal transition (MMT) of peritoneal mesothelial cells (PMCs), supporting the pro-angiogenic function of endothelial cells and immune evasion of tumor cells (57).

Tumor-Derived Exosomes Contribute to Breach the Barriers for Tumor Invasion Within the Pre-Metastatic Niche

Intraperitoneal metastasis of GC is formed by reciprocal interaction between exfoliated cancer cells and peritoneal cells, especially PMCs (60). In particular, MMT of PMCs could present the peritoneum more willing for cancer cells' attachment and invasion and contributes to pre-metastatic niche forming by promoting its vascularization (61). Accumulated studies demonstrate that tumor-associated exosomes can disrupt mesothelial barrier to facilitate peritoneal metastasis.

Deng et al. found that exosomes derived from GC cell lines could damage the mesothelial barrier and elicit PMCs to undergo MMT and effect apoptosis *in-vivo* and *in-vitro*. They also observed that at the molecular mechanism, ERK pathway plays a crucial part in MMT of PMCs, but not apoptosis. Also evident is the exosomal mediated increased expression of MMT-related protein, including Vimentin, Fibronectin, and Collagen-I through ERK1/2 activation (21). However, the element in exosomes responsible for the MMT of PMCs remains to be fully identified and explained. Recently, a study revealed that this process could be induced by GC-derived exosomal miR-21-5p targeting SMAD7 to activate TGF-β/smad pathway and to effect the increase of invasion and attachment of PMCs (22). Subsequently, Zhu at al. also identified that GC-derived exosomes enriching miR-106a destroy the mesothelial barrier by breaking the PMCs' balance of apoptosis and proliferation through targeting SMAD7 (23).

The progression of peritoneal metastasis of GC is dependent on the breaching of barriers of the peritoneum. Intriguingly, PMCs undergoing MMT process acquire high migratory and invasive abilities which help them invade the submesothelial space and induce formation of fibrosis and angiogenesis; so it is a crucial component of premetastatic niche (62). In this regard, there is still a diverting study as to the exact function of PMCs during the first phase of primary cancer progression. Tanaka et al. detected that PMCs could cover the gastric wall and infiltrate into submucosal to create a suitable niche for tumor invasion. Meanwhile, GC cells also release exosomes involving Wnt3a, thus promoting PMC infiltration. PMCs in turn boost cancer cells' invasion out of the stomach and the formation of peritoneal metastatic lesions (24). Tumor-associated exosomes would facilitate the initiation of the invasion-metastasis cascades by taking part in the clearance of physiological peritoneum barriers which restrain metastasis of tumor cells.

Tumor-Derived Exosomes Participate in Angiogenesis

To ensure adequate nutrition and oxygen supply, endothelial cells begin neoangiogenesis in the primary tumor mass and pre-metastatic microenvironment. GC cells and endothelial cells can interact with each other through exosomes, which can partially induce the angiogenesis of the later to regulate the peritoneal metastasis of GC (63). Tumor cells release exosomes loaded with pro-angiogenic factors such as VEGF, TIMP-1, IL-6, IL-8, and FGF and carry paracrine signaling elements and miRNAs to drive genetic expression towards angiogenesis (25, 26). MiRNAs (miR-130a, miR-135b, miR-155) wrapped in tumor-derived exosomes have been found to promote GC angiogenesis and metastasis through c-MYB, forkhead box O1 (FOXO1), and FOXO3 respectively (27–29). Notably, these miRNAs have promotional effect on viability and migration of human umbilical vein endothelial cells. Tumor-derived exosomes, as well as exosomes secreted from stromal cells, release factors to recruit and activate endothelial progenitor cells to enhance angiogenic response (25). In pre-metastatic niche, exosomes released by normal stromal cells have a role in microenvironment homeostasis, but tumor-derived exosomes are actively involved in the formation of pre-metastatic niche. Nevertheless, we still do not know whether exosomes derived from other several tumor-associated stromal cells play the same role in PM of GC as other types of cancers.

Tumor-Derived Exosomes Mediate Immunosuppression Within the Pre-Metastatic Niche

It is important for tumor cells to escape immunological elimination and establish an immunosuppressive microenvironment in the primary tumor sites and pre-metastatic niche (64). GC-derived exosomes exist in neoplastic lesions or biologic fluids of cancer patients possessing immunosuppressive molecules that mediate immune cell dysfunction and transform the suitable microenvironment for isolated tumor cells survival and metastasis, including suppression for immune cell activation and induction of immunosuppressing cells (65). Wu et al. found that exosomes derived from GC can stimulate the activation of NF-κB pathway in macrophages to promote GC progression through regulating proinflammatory microenvironment (30). However, the question of which substance from exosomes promotes the activation of macrophages has not been analyzed clearly. Recently, exosomal mesenchymal–epithelial transition factor (MET) was found to be higher in *H. pylori*-infected GC cells and educated the macrophages toward pro-tumorigenesis *in-vivo* and *in-vitro* (31). GC-derived exosomes could effectively elicit monocytes to differentiate into PD1+ tumor-associated macrophages (TAMs) with M2 surface profile and functional characteristics. These cells then secrete a great number of IL-10 to destroy the antitumor cells (CD8+ T cells) and thereby create a favorable immune microenvironment for GC angiogenesis and metastasis (32). Furthermore, mesenchymal stem cells (MSCs) are an important component of tumor immunomodulation. Shen et al. revealed that GC-derived exosomes affect the biological functions of MSCs through NF-κB pathway to activate immune cells, maintain inflammatory conditions, and stimulate tumor metastasis (33). For example, MSCs can facilitate macrophage phagocytosis and the activation of CD4/CD69 (the early activation of T cell markers) double-positive T cells. In addition, exosomes transferring miRNA-107 from tumor expand and activate myeloid-derived suppression cells to promote immunosuppression in the tumor microenvironment and help GC cells' growth and survival by targeting DICER1 and PTEN gene (34). Exosomes which comprise of miR-451 from GC targets mTOR to enhance differentiation of T-helper 17 (Th17) cells which infiltrate

into GC sites to promote angiogenesis and support cancer progression (35). Exosome-mediated transfer of high mobility group box-1 (HMGB1) from GC cells activates neutrophils by NF-κB pathway, which promotes tumor cell's migration (36). Recently, a study demonstrated that exosomes derived from GC can regulate CD8+ T cell gene expression and cytokine secretion patterns to establish an immunosuppressive microenvironment for metastatic niche formation (37).

In brief, these findings point out that exosomes play an important role in remodeling a robust pre-metastatic niche, which allows for immune evasion of tumor cells, especially GC-derived exosomes. Those exosomes delivering to immune cells can educate macrophages and neutrophils into protumor phenotype, impair CD8+ T cells' activation, induce MSCs for tumor immunomodulation, and increase Th17 differentiation within primary tumor sites and pre-metastatic niche. With a better understanding of the roles of exosomes in immune regulation, it may provide novel and efficient antitumor therapies in PM of GC.

EXOSOME-EDUCATED CELLS IN THE PRE-METASTATIC NICHE PROMOTE METASTASIS

GC-derived exosomes could facilitate exfoliative tumor cells' invasion, settlement, colonization, and metastasis within the pre-metastatic mass while inhibiting the host anti-tumor immune response. Following the successful formation of the pre-metastatic microenvironment, activated PMCs, CAFs and TAMs can then support peritoneal implantation of GC through their own exosome secretion (24, 32, 38). Experimental evidence has shown that PMCs internalizing GC-derived exosomes could up-regulate expression of adhesion molecules (fibronectin and laminin gamma 1) and significantly promote adhesion with exfoliated GC cells, while the same is not true for internalization of mesothelial cell-derived exosomes (39). Cluster of differentiation 44 (CD44), an adhesive molecule, is important for attachment of tumor cells to the peritoneum (66). Simultaneously, CD44 also serves a similar role in attachment between tumor cells and exosomes. Malgorzata et al. discovered that exosomes isolated from GC cell lines expressed CD44H and CD44v6 involved in interaction with GC cells to support GC growth and angiogenesis (40). The study manifests that exosomes act as macro-messengers in delivering molecular cargo and signals to enhance their own carcinogenicity *via* autocrine tumor loops. In another study, researchers disclosed that AZ-P7a cells, a high peritoneal-metastatic potential gastric cancer line, secrete exosomes containing abundant let-7 miRNA family as compared to other metastatic cancer lines. And let-7 miRNAs were released into the extracellular matrix to maintain their tumorigenesis and PM (41). This study indicated that exosomes secreted by secondary metastatic lesions rather than primary cancer mass are more inclined to promote proliferation and invasion. Recently, TAMs play a distinctly supportive function to promote GC cells' invasion, in which TAMs transfer tumor-derived extracellular vesicles containing RNA and proteins (TGF-β, activated Src, Wnt3, and HIF1α) to peritoneal stromal cells and elicit a pro-tumor microenvironment, such as induction of MMT of PMCs (42).

Overall, previous data demonstrate that tumor-derived exosomes may not only assist tumor cells' attachment to mesothelial cells, but also further facilitate tumor metastasis and progression. There are many factors that promote PM occurrence of GC, but the role of tumor-derived exosomes in this process remains to be further investigated. Additionally, exosomes carry various known and unknown factors which may play functional and non-functional roles in those recipient cells, so the characteristics and contents of exosomes should be continuously clarified.

ROLES OF EXOSOMES DERIVED FROM OTHER SOURCES IN THE PROCESSES OF PM

The occurrence and development of PM induced by exosomes are complex and dynamic. Not only tumor derived exosomes are actively involved in PM of GC as described above, non-tumor derived exosomes with potential pro-oncogenic functions are also involved in promoting tumor metastases.

Exosomes Secreted by Tumor-Reprogrammed Normal Cells Play Supporting Roles in PM

CAFs induced by cancer cells can secrete functional exosomes to accelerate cancer progression and metastases. Recent evidence showed that CD9-positive exosomes from CAFs may promote the migration and invasive ability of cancer cells through MMP2 activation in scirrhous-type gastric cancer (38). Additionally, CAF-derived exosomes can also deliver miR-139 to suppress the progression and metastasis of GC by down-regulating MMP11, which can facilitate cancer cells' migration (43). Aside from this effect, CAFs also increase basement membrane permeability for cancer cells' invasion by stretching and pulling it to seal gaps (67). As for exosomes derived from immune cells, TAMs with M2 phenotype transfer apolipoprotein E (ApoE) by exosomes to trigger the activation of PI3K–Akt signaling pathway in GC cells and subsequently aggregate tumor cells' migration (44). In addition, one such study demonstrated that omental tissue-derived exosomes of gastric cancer patients shuttle higher levels of interleukin-6 (IL-6), interleukin-8 (IL-8), intercellular adhesion molecule-1 (ICAM-1), growth related oncogene (GRO), basic fibroblast growth factor (bFGF), adiponectin, and C-C Motif Chemokine Ligand (CCL4) (45), which had been studied as GC-related cytokines facilitating gastric cancer proliferation, angiogenesis, invasion, immunomodulation, and peritoneal metastasis (46–48). These studies demonstrated that tumor-derived exosomes benefit from the production of tumor-reprogrammed stromal cells, which simultaneously secrete functional non-tumor-derived exosomes capable of promoting cancer progression and metastases.

Roles of MA-Derived Exosomes in PM

The abdominal cavity is a huge physiological cavity, and peritoneal fluid is rich in various functional factors. The GC patients' peritoneal fluids could contain numerous exosomes derived from tumor cells and tumor-associated cells, with capabilities to boost the development of PM. Exosomes derived from peritoneal fluid of GC patients with PM carried higher miR-544-5p, suppressing the promyelocytic leukemia zinc finger (PLZF) expression in peritoneum cells, in which suppression induces MMT of peritoneum and results in increased invasion potential of abdominal free tumor cells (49). Similarly, gastric malignant ascites (MAs)-derived exosomes also participate in the development of peritoneal metastasis. Experimental evidence has shown that MA-derived exosomes enhance the level of fibroblast activation protein (FAP), alpha-smooth muscle actin (α-SMA), and fibronectin, which are CAF specific markers. Functionally, PMCs cause MMT by exosomal effected increase of the capacities of proliferation and formation of peritoneum fibrosis through TGF-β1 *in-vitro* and *in-vivo* mouse models (50). Moreover, Hu et al. demonstrated that MA-derived exosomes facilitate GC cells' invasion by the up-regulation of EMT signaling and peritoneal metastasis in GC cells' intraperitoneal metastatic xenograft mouse model (51). Therefore, exosomes secreted from various tumor-associated cells can participate in the formation of pro-oncogenic abdominal microenvironment and contribute to the progression of PM in GC patients. The peritoneal fluid-derived exosomes of GC patients are different in molecular, genetic, and functional heterogeneity, so it is necessary to further explore the division of labor of different cells derived exosomes in these stages of PM.

EXOSOMES AS PRE-METASTATIC NICHE BIOMARKERS AND THERAPEUTIC APPLICATIONS

Exosomes possess several apparent advantages as biomarkers of predicting the occurrence and development of PM, as they are exceedingly stable, ample, and tumor-specific. Therefore, they are promising biomarkers within the blood and ascites that deserve abundant investigation in this deadly cancer. In addition, exosomes are extremely potent intercellular communicators and are expected to bring great breakthrough in therapies for various diseases, including PM of GC.

Exosomal miRNAs as Biomarkers of PM

Given that exosomes are widely present in various body fluids (blood, urine, ascites) and contain many inclusions (DNA, RNA, protein), exosomes are suggested to be optimal candidates for relatively non-invasive method of diagnosis of diseases and evaluation of therapy efficacy (68). Increasing pieces of evidence have shown that exosomes have a great potential to act as biomarkers for PM of GC. Thus, highly sensitive and specific molecular markers are necessary to predict and assess tumor burden in the peritoneal cavity. Furthermore, liquid biopsy is a common strategy, in which circulating tumor cells and cell-shed exosomes could be detected from body fluids, including ascites and plasma (69). Fortunately, a team performed a high throughput sequencing of ascite-derived exosomes among eight paired GC patients with peritoneal dissemination before and after intraperitoneal chemotherapy, of which three had non-malignant disease. They detected an increase in MA-derived exosomes associated with five miRNAs (miR-760, miR-6821-5p, miR-4745-5p, miR-200a-5p, miR-4741, and miR-320) in the malignant disease group as compared to those individuals with non-malignant diseases (51). Interestingly, some identified miRNAs in exosomes could be down-regulated or up-regulated in those GC patients who were after their peritoneal chemotherapy. Tokihisa et al. analyzed the miRNA microarrays among six MA samples and 24 peritoneal lavage fluid (PLF) samples and demonstrated that exosomal miR-21 and miR-1225-5p were significantly up-regulated in those MA and PLF of serosa-invasive GC and associated with serosal invasion. What is more, the two candidate miRNAs may potentially act as biomarkers of peritoneal recurrence following curative GC resection (70). More recently, there was a miRNA expression profile analysis of peritoneal lavage fluid derived exosomes among patients with PM and patients without PM (71). They identified that the expression of miR-21-5p, miR-92a-3p, miR-233-3p, and miR-342-3p was significantly higher in former samples and positively associated with pathological serosal exposure and the extent of peritoneal cancer throughout the peritoneal cavity. In contrast, exosomal miR-29 family was down-regulated in PM (+) patients, and the expression of miR-29b-3 was negatively correlated with worse peritoneal recurrence-free survival and overall survival. This result shows that the role of miR-21 is similar to previous ones. Similarly, Ohzawa et al. revealed that down-regulated miR-29s are a strong risk factor of peritoneal recurrence and worse overall survival. This indicates that the expression of miR-29s in MA or PLF could be a reliable biomarker to assess the probability of peritoneal recurrence in patients undergoing curative surgery (72).

Thus, the clinical utility of liquid biopsy in the detection of exosomal biomarkers can potentially be an important diagnostic and prognostic tool for the assessment of PM in GC (69). Owing to individual differences, the tremendous heterogeneity exists in exosomes of GC patients, and it remains unknown whether exosomal biomarkers from body fluids present adequate sensitivity and specificity to assess the authentic situation of PM's occurrence and recurrence. This requires sufficient samples of GC patients and multi-center research to screen for more sensitive and specific exosomal markers.

Exosomes as Therapeutic Applications Targeting PM of GC

As yet, systemic chemotherapy is considered the standard treatment for PM of gastric cancer, but the survival outcomes of patients are still poor (73). Nevertheless, effective methods for treatment of PM are extremely needed. At present, therapeutic exosome-based strategies are an emerging treatment and currently focus on exploration of the targeting moieties of exosomes to primary cancer cells and metastatic tumor (74). Exosomes could become a new avenue for transporting anti-cancer molecules and drugs in the treatment of cancer because of

their low immunogenicity, high biocompatibility, high efficacy of delivery and biodegradable characteristic (75). One of the first demonstrations for this potent capability of exosomes came from a study in which exosomes were engineered to target the recipient cells with high Her2 expression by displaying anti-Her2 single chain variable fragment on the exosome surface (76). Similarly, modified exosomes loaded with anticancer agent paclitaxel and doxorubicin specifically interact with αv integrin-positive breast cancer and pulmonary metastases with overexpressed sigma receptor respectively, exhibiting high anticancer efficacy (77, 78). One research group synthesized engineered exosome-thermosensitive liposomes hybrid NPs, which efficiently penetrated into peritoneal metastasis nodules and released payloads to inhibit tumor development in cancer line-derived xenografts and patient-derived tumor xenografts (79). The study provides evidence to support the feasibility of therapeutic exosome-based approach in improving drug delivery and treatment of metastatic peritoneal carcinoma.

For instance, exosome-mediated delivery of miRNA (miR-374a-5p, miR-214) inhibition could possibly antagonize the effect on growth, migration, and chemoresistance of GC cells to retrieve drug effectiveness (80, 81). Zhang et al. revealed that hepatocyte growth factor (HGF) siRNA packed in exosomes could inhibit proliferation and migration of cancer cells and vascular cells through activation of MAPK, PIK3, and Stat3, as well as up-regulating VEGF expression (82). To date, there are few studies that have focused on exosomes for targeting peritoneal metastasis of GC. TRIM3-overexpression of exosomes can decrease the size and number of metastatic tumor nodes in PM models (82). Additionally, silencing of exosomal miR-21-5p could block MMT of peritoneum through attenuating TGFβ/SMAD pathway (22). This targeted technology has potential for suppression of metastatic niche progression and is an efficient area of future chemotherapeutic study.

Tumor-derived exosomes preparing the pre-metastatic niche must undergo homing to remote organs and other sites. Exosome proteomics have demonstrated that specific expression patterns of integrin largely contribute to this process. Exosomal integrins $\alpha6\beta4$ and $\alpha6\beta1$ were related with lung metastasis, and exosomal integrin $\alpha v\beta5$ was associated with liver metastasis. Nevertheless, targeting these integrins could restrain exosomes' uptake, as well as respective metastasis (83). The study serves as an inspiring proof of the concept that using specific exosomal integrin blockers can efficiently battle metastasis. Various malignancies exhibit unique exosome profiles and have distinct propensity to metastasize to specific sites (84). Additionally, there was a direct proof verifying that tumor-derived exosomes transmit signals over long ranges to metastatic niches *in-vivo* (85). Therefore, further elucidating the homing pattern of tumor-derived exosomes which bind to peritoneal cells could surface information on novel tumor biomarkers and is a promising therapeutic strategy in avoiding the occurrence of PM. Given the immaturity of exosome biology and strenuous preliminary work of clinical transformation, more effort is needed in the attempt to accelerate its development and maturation

CONCLUSION AND PERSPECTIVES

GC-derived exosomes partially promote occurrence of PM *via* stromal cell remodeling, angiogenesis, immunosuppression, and oncogenic reprogramming. In addition, tumor-reprogrammed stromal cells also secret exosomes absorbed by tumor cells to the malignant phenotype of GC cells. Ever since exosomes have become the new focus of scientific research, significant progress has been made in revealing the contribution of exosomes in conditioning the GC cells for subsequent metastatic processes. Exosomes, acting as correspondents between cells, present substantial effects on shaping the tumor microenvironment, especially pre-metastatic niches. Although exosomes are involved in all steps of PM, more explorations about underlying mechanisms are still lacking. Fortunately, emerging technologies (liquid biopsy and exosomes media) may help early diagnosis of PM by screening exosome miRNAs and exosome-based treatment by transferring anti-tumor drugs and restricting exosomes homing in PM.

AUTHOR CONTRIBUTIONS

Conceptualization, LT. Investigation, XC. Writing—original draft preparation, XC. Writing—review and editing, XC, HW, CC, and YH. Supervision, WZ. Project administration, HW. Funding acquisition, LT. All authors contributed to the article and approved the submitted version.

FUNDING

This study was supported by the project of the Regional Diagnosis and Treatment Center of the Health Planning Committee (No. JBZX-201903).

ACKNOWLEDGMENTS

The authors are grateful to Mrs. Yichen Wu for providing help in draft editing.

REFERENCES

1. Bray F, Ferlay J, Soerjomataram I, Siegel RL, Torre LA, Jemal A. Global Cancer Statistics 2018: GLOBOCAN Estimates of Incidence and Mortality Worldwide for 36 Cancers in 185 Countries. *CA Cancer J Clin* (2018) 68 (6):394–424. doi: 10.3322/caac.21492
2. Tan P, Yeoh KG. Genetics and Molecular Pathogenesis of Gastric Adenocarcinoma. *Gastroenterology* (2015) 149(5):1153–62 e3. doi: 10.1053/j.gastro.2015.05.059
3. Nashimoto A, Akazawa K, Isobe Y, Miyashiro I, Katai H, Kodera Y, et al. Gastric Cancer Treated in 2002 in Japan: 2009 Annual Report of the JGCA Nationwide Registry. *Gastric Cancer* (2013) 16(1):1–27. doi: 10.1007/s10120-012-0163-4
4. Thomassen I, van Gestel YR, van Ramshorst B, Luyer MD, Bosscha K, Nienhuijs SW, et al. Peritoneal Carcinomatosis of Gastric Origin: A Population-Based Study on Incidence, Survival and Risk Factors. *Int J Cancer* (2014) 134(3):622–8. doi: 10.1002/ijc.28373
5. Coccolini F. Peritoneal Carcinomatosis. *World J Gastroenterol* (2013) 19 (41):6979–94. doi: 10.3748/wjg.v19.i41.6979
6. Kitayama J, Ishigami H, Yamaguchi H, Sakuma Y, Horie H, Hosoya Y, et al. Treatment of Patients With Peritoneal Metastases From Gastric Cancer. *Ann Gastroenterol Surg* (2018) 2(2):116–23. doi: 10.1002/ags3.12060

7. Tschuschke M, Kocherova I, Bryja A, Mozdziak P, Angelova Volponi A, Janowicz K, et al. Inclusion Biogenesis, Methods of Isolation and Clinical Application of Human Cellular Exosomes. *J Clin Med* (2020) 9(2):436. doi: 10.3390/jcm9020436
8. Vlassov AV, Magdaleno S, Setterquist R, Conrad R. Exosomes: Current Knowledge of Their Composition, Biological Functions, and Diagnostic and Therapeutic Potentials. *Biochim Biophys Acta* (2012) 1820(7):940–8. doi: 10.1016/j.bbagen.2012.03.017
9. Feng W, Dean DC, Hornicek FJ, Shi H, Duan Z. Exosomes Promote Pre-Metastatic Niche Formation in Ovarian Cancer. *Mol Cancer* (2019) 18(1):124. doi: 10.1186/s12943-019-1049-4
10. Ruivo CF, Adem B, Silva M, Melo SA. The Biology of Cancer Exosomes: Insights and New Perspectives. *Cancer Res* (2017) 77(23):6480–8. doi: 10.1158/0008-5472.CAN-17-0994
11. Yan Y, Fu G, Ye Y, Ming L. Exosomes Participate in the Carcinogenesis and the Malignant Behavior of Gastric Cancer. *Scandinavian J Gastroenterol* (2017) 52(5):499–504. doi: 10.1080/00365521.2016.1278458
12. Psaila B, Lyden D. The Metastatic Niche: Adapting the Foreign Soil. *Nat Rev Cancer* (2009) 9(4):285–93. doi: 10.1038/nrc2621
13. Lobb RJ, Lima LG, Möller A. Exosomes: Key Mediators of Metastasis and Pre-Metastatic Niche Formation. *Semin Cell Dev Biol* (2017) 67:3–10. doi: 10.1016/j.semcdb.2017.01.004
14. Guo Y, Ji X, Liu J, Fan D, Zhou Q, Chen C, et al. Effects of Exosomes on Pre-Metastatic Niche Formation in Tumors. *Mol Cancer* (2019) 18(1):39. doi: 10.1186/s12943-019-0995-1
15. Wang J, Guan X, Zhang Y, Ge S, Zhang L, Li H, et al. Exosomal Mir-27a Derived From Gastric Cancer Cells Regulates the Transformation of Fibroblasts Into Cancer-Associated Fibroblasts. *Cell Physiol Biochem* (2018) 49(3):869–83. doi: 10.1159/000493218
16. Ning X, Zhang H, Wang C, Song X. Exosomes Released by Gastric Cancer Cells Induce Transition of Pericytes Into Cancer-Associated Fibroblasts. *Med Sci Monitor* (2018) 24:2350–9. doi: 10.12659/MSM.906641
17. Gu J, Qian H, Shen L, Zhang X, Zhu W, Huang L, et al. Gastric Cancer Exosomes Trigger Differentiation of Umbilical Cord Derived Mesenchymal Stem Cells to Carcinoma-Associated Fibroblasts Through TGF-β/Smad Pathway. *PloS One* (2012) 7(12):e52465. doi: 10.1371/journal.pone.0052465
18. Fu H, Yang H, Zhang X, Wang B, Mao J, Li X, et al. Exosomal TRIM3 is a Novel Marker and Therapy Target for Gastric Cancer. *J Exp Clin Cancer Res* (2018) 37(1):162. doi: 10.1186/s13046-018-0825-0
19. Pan L, Liang W, Fu M, Huang ZH, Li X, Zhang W, et al. Exosomes-Mediated Transfer of Long Noncoding RNA ZFAS1 Promotes Gastric Cancer Progression. *J Cancer Res Clin Oncol* (2017) 143(6):991–1004. doi: 10.1007/s00432-017-2361-2
20. Zhang X, Wang S, Wang H, Cao J, Huang X, Chen Z, et al. Circular RNA circNRIP1 Acts as a microRNA-149-5p Sponge to Promote Gastric Cancer Progression Via the AKT1/mTOR Pathway. *Mol Cancer* (2019) 18(1):20. doi: 10.1186/s12943-018-0935-5
21. Deng G, Qu J, Zhang Y, Che X, Cheng Y, Fan Y, et al. Gastric Cancer-Derived Exosomes Promote Peritoneal Metastasis by Destroying the Mesothelial Barrier. *FEBS Lett* (2017) 591(14):2167–79. doi: 10.1002/1873-3468.12722
22. Li Q, Li B, Li Q, Wei S, He Z, Huang X, et al. Exosomal miR-21-5p Derived From Gastric Cancer Promotes Peritoneal Metastasis Via Mesothelial-to-Mesenchymal Transition. *Cell Death Dis* (2018) 9(9):854. doi: 10.1038/s41419-018-0928-8
23. Zhu M, Zhang N, He S, Lu X. Exosomal miR-106a Derived From Gastric Cancer Promotes Peritoneal Metastasis Via Direct Regulation of Smad7. *Cell Cycle* (2020) 19(10):1200–21. doi: 10.1080/15384101.2020.1749467
24. Tanaka M, Kuriyama S, Itoh G, Maeda D, Goto A, Tamiya Y, et al. Mesothelial Cells Create a Novel Tissue Niche That Facilitates Gastric Cancer Invasion. *Cancer Res* (2017) 77(3):684–95. doi: 10.1158/0008-5472.CAN-16-0964
25. Skog J, Würdinger T, van Rijn S, Meijer DH, Gainche L, Curry WT, et al. Glioblastoma Microvesicles Transport RNA and Proteins That Promote Tumour Growth and Provide Diagnostic Biomarkers. *Nat Cell Biol* (2008) 10(12):1470–6. doi: 10.1038/ncb1800
26. Zhang Z, Dombroski JA, King MR. Engineering of Exosomes to Target Cancer Metastasis. *Cell Mol Bioeng* (2020) 13(1):1–16. doi: 10.1007/s12195-019-00607-x
27. Bai M, Li J, Yang H, Zhang H, Zhou Z, Deng T, et al. Mir-135b Delivered by Gastric Tumor Exosomes Inhibits FOXO1 Expression in Endothelial Cells and Promotes Angiogenesis. *Mol Ther* (2019) 27(10):1772–83. doi: 10.1016/j.ymthe.2019.06.018
28. Zhou Z, Zhang H, Deng T, Ning T, Liu R, Liu D, et al. Exosomes Carrying Microrna-155 Target Forkhead Box O3 of Endothelial Cells and Promote Angiogenesis in Gastric Cancer. *Mol Ther Oncolytics* (2019) 15:223–33. doi: 10.1016/j.omto.2019.10.006
29. Yang H, Zhang H, Ge S, Ning T, Bai M, Li J, et al. Exosome-Derived Mir-130a Activates Angiogenesis in Gastric Cancer by Targeting C-MYB in Vascular Endothelial Cells. *Mol Ther* (2018) 26(10):2466–75. doi: 10.1016/j.ymthe.2018.07.023
30. Wu L, Zhang X, Zhang B, Shi H, Yuan X, Sun Y, et al. Exosomes Derived From Gastric Cancer Cells Activate NF-kappaB Pathway in Macrophages to Promote Cancer Progression. *Tumour Biol* (2016) 37(9):12169–80. doi: 10.1007/s13277-016-5071-5
31. Che Y, Geng B, Xu Y, Miao X, Chen L, Mu X, et al. Helicobacter Pylori-Induced Exosomal MET Educates Tumour-Associated Macrophages to Promote Gastric Cancer Progression. *J Cell Mol Med* (2018) 22(11):5708–19. doi: 10.1111/jcmm.13847
32. Wang F, Li B, Wei Y, Zhao Y, Wang L, Zhang P, et al. Tumor-Derived Exosomes Induce PD1(+) Macrophage Population in Human Gastric Cancer That Promotes Disease Progression. *Oncogenesis* (2018) 7(5):41. doi: 10.1038/s41389-018-0049-3
33. Shen Y, Xue C, Li X, Ba L, Gu J, Sun Z, et al. Effects of Gastric Cancer Cell-Derived Exosomes on the Immune Regulation of Mesenchymal Stem Cells by the NF-kB Signaling Pathway. *Stem Cells Dev* (2019) 28(7):464–76. doi: 10.1089/scd.2018.0125
34. Ren W, Zhang X, Li W, Feng Q, Feng H, Tong Y, et al. Exosomal miRNA-107 Induces Myeloid-Derived Suppressor Cell Expansion in Gastric Cancer. *Cancer Manag Res* (2019) 11:4023–40. doi: 10.2147/CMAR.S198886
35. Liu F, Bu Z, Zhao F, Xiao D. Increased T-helper 17 Cell Differentiation Mediated by Exosome-Mediated microRNA-451 Redistribution in Gastric Cancer Infiltrated T Cells. *Cancer Sci* (2018) 109(1):65–73. doi: 10.1111/cas.13429
36. Zhang X, Shi H, Yuan X, Jiang P, Qian H, Xu W. Tumor-Derived Exosomes Induce N2 Polarization of Neutrophils to Promote Gastric Cancer Cell Migration. *Mol Cancer* (2018) 17(1):146. doi: 10.1186/s12943-018-0898-6
37. Liu J, Wu S, Zheng X, Zheng P, Fu Y, Wu C, et al. Immune Suppressed Tumor Microenvironment by Exosomes Derived From Gastric Cancer Cells Via Modulating Immune Functions. *Sci Rep* (2020) 10(1):14749. doi: 10.1038/s41598-020-71573-y
38. Miki Y, Yashiro M, Okuno T, Kitayama K, Masuda G, Hirakawa K, et al. CD9-Positive Exosomes From Cancer-Associated Fibroblasts Stimulate the Migration Ability of Scirrhous-Type Gastric Cancer Cells. *Br J Cancer* (2018) 118(6):867–77. doi: 10.1038/bjc.2017.487
39. Arita T, Ichikawa D, Konishi H, Komatsu S, Shiozaki A, Ogino S, et al. Tumor Exosome-Mediated Promotion of Adhesion to Mesothelial Cells in Gastric Cancer Cells. *Oncotarget* (2016) 7(35):56855–63. doi: 10.18632/oncotarget.10869
40. Stec M, Szatanek R, Baj-Krzyworzeka M, Baran J, Zembala M, Barbasz J, et al. Interactions of Tumour-Derived Micro(Nano)Vesicles With Human Gastric Cancer Cells. *J Transl Med* (2015) 13:376. doi: 10.1186/s12967-015-0737-0
41. Wölfl S, Ohshima K, Inoue K, Fujiwara A, Hatakeyama K, Kanto K, et al. Let-7 MicroRNA Family Is Selectively Secreted Into the Extracellular Environment Via Exosomes in a Metastatic Gastric Cancer Cell Line. *PloS One* (2010) 5(10):e13247. doi: 10.1371/journal.pone.0013247
42. Umakoshi M, Takahashi S, Itoh G, Kuriyama S, Sasaki Y, Yanagihara K, et al. Macrophage-Mediated Transfer of Cancer-Derived Components to Stromal Cells Contributes to Establishment of a Pro-Tumor Microenvironment. *Oncogene* (2019) 38(12):2162–76. doi: 10.1038/s41388-018-0564-x
43. Xu G, Zhang B, Ye J, Cao S, Shi J, Zhao Y, et al. Exosomal miRNA-139 in Cancer-Associated Fibroblasts Inhibits Gastric Cancer Progression by Repressing MMP11 Expression. *Int J Biol Sci* (2019) 15(11):2320–9. doi: 10.7150/ijbs.33750
44. Zheng P, Luo Q, Wang W, Li J, Wang T, Wang P, et al. Tumor-Associated Macrophages-Derived Exosomes Promote the Migration of Gastric Cancer Cells by Transfer of Functional Apolipoprotein E. *Cell Death Dis* (2018) 9(4):434. doi: 10.1038/s41419-018-0465-5
45. Kersy O, Loewenstein S, Lubezky N, Sher O, Simon NB, Klausner JM, et al. Omental Tissue-Mediated Tumorigenesis of Gastric Cancer Peritoneal Metastases. *Front Oncol* (2019) 9:1267. doi: 10.3389/fonc.2019.01267

46. Yin Y, Si X, Gao Y, Gao L, Wang J. The Nuclear Factor-Kappab Correlates With Increased Expression of Interleukin-6 and Promotes Progression of Gastric Carcinoma. *Oncol Rep* (2013) 29(1):34–8. doi: 10.3892/or.2012.2089
47. Li W, Zhou Y, Yang J, Zhang X, Zhang H, Zhang T, et al. Gastric Cancer-Derived Mesenchymal Stem Cells Prompt Gastric Cancer Progression Through Secretion of Interleukin-8. *J Exp Clin Cancer Res* (2015) 34(1):52. doi: 10.1186/s13046-015-0172-3
48. Kimura R, Yoneshige A, Hagiyama M, Otani T, Inoue T, Shiraishi N, et al. Expression of Cell Adhesion Molecule 1 in Gastric Neck and Base Glandular Cells: Possible Involvement in Peritoneal Dissemination of Signet Ring Cells. *Life Sci* (2018) 213:206–13. doi: 10.1016/j.lfs.2018.10.017
49. Kong W, Liu X, Yin G, Zheng S, Zhu A, Yu P, et al. Extracellular Vesicle Derived miR-544 Downregulates Expression of Tumor Suppressor Promyelocytic Leukemia Zinc Finger Resulting in Increased Peritoneal Metastasis in Gastric Cancer. *Aging (Albany NY)* (2020) 12(23):24009–22. doi: 10.18632/aging.104082
50. Wei M, Yang T, Chen X, Wu Y, Deng X, He W, et al. Malignant Ascites-Derived Exosomes Promote Proliferation and Induce Carcinoma-Associated Fibroblasts Transition in Peritoneal Mesothelial Cells. *Oncotarget* (2017) 8 (26):42262–71. doi: 10.18632/oncotarget.15040
51. Hu Y, Qi C, Liu X, Zhang C, Gao J, Wu Y, et al. Malignant Ascites-Derived Exosomes Promote Peritoneal Tumor Cell Dissemination and Reveal a Distinct miRNA Signature in Advanced Gastric Cancer. *Cancer Lett* (2019) 457:142–50. doi: 10.1016/j.canlet.2019.04.034
52. Yamaguchi H, Sakai R. Direct Interaction Between Carcinoma Cells and Cancer Associated Fibroblasts for the Regulation of Cancer Invasion. *Cancers* (2015) 7(4):2054–62. doi: 10.3390/cancers7040876
53. Hawinkels LJ, Paauwe M, Verspaget HW, Wiercinska E, van der Zon JM, van der Ploeg K, et al. Interaction With Colon Cancer Cells Hyperactivates TGF-β Signaling in Cancer-Associated Fibroblasts. *Oncogene* (2014) 33(1):97–107. doi: 10.1038/onc.2012.536
54. Wang L, Yang D, Tian J, Gao A, Shen Y, Ren X, et al. Tumor Necrosis Factor Receptor 2/AKT and ERK Signaling Pathways Contribute to the Switch From Fibroblasts to CAFs by Progranulin in Microenvironment of Colorectal Cancer. *Oncotarget* (2017) 8(16):26323–33. doi: 10.18632/oncotarget.15461
55. Paolillo M, Schinelli S. Extracellular Matrix Alterations in Metastatic Processes. *Int J Mol Sci* (2019) 20(19):4947. doi: 10.3390/ijms20194947
56. Liao T-T, Yang M-H. Hybrid Epithelial/Mesenchymal State in Cancer Metastasis: Clinical Significance and Regulatory Mechanisms. *Cells* (2020) 9 (3):632. doi: 10.3390/cells9030623
57. Li K, Chen Y, Li A, Tan C, Liu X. Exosomes Play Roles in Sequential Processes of Tumor Metastasis. *Int J Cancer* (2019) 144(7):1486–95. doi: 10.1002/ijc.31774
58. Paget S. The Distribution of Secondary Growths in Cancer of the Breast. *1889 Cancer Metastasis Rev* (1989) 8(2):98–101. doi: 10.1016/S0140-6736(00)49915-0
59. Costa-Silva B, Aiello NM, Ocean AJ, Singh S, Zhang H, Thakur BK, et al. Pancreatic Cancer Exosomes Initiate Pre-Metastatic Niche Formation in the Liver. *Nat Cell Biol* (2015) 17(6):816–26. doi: 10.1038/ncb3169
60. Mikuła-Pietrasik J, Uruski P, Tykarski A, Książek K. The Peritoneal "Soil" for a Cancerous "Seed": A Comprehensive Review of the Pathogenesis of Intraperitoneal Cancer Metastases. *Cell Mol Life Sci* (2018) 75(3):509–25. doi: 10.1007/s00018-017-2663-1
61. Sandoval P, Jiménez-Heffernan JA, Rynne-Vidal Á, Pérez-Lozano ML, Gilsanz Á, Ruiz-Carpio V, et al. Carcinoma-Associated Fibroblasts Derive From Mesothelial Cells Via Mesothelial-to-Mesenchymal Transition in Peritoneal Metastasis. *J Pathol* (2013) 231(4):517–31. doi: 10.1002/path.4281
62. Loureiro J, Aguilera A, Selgas R, Sandoval P, Albar-Vizcaíno P, Pérez-Lozano ML, et al. Blocking TGF-β1 Protects the Peritoneal Membrane From Dialysate-Induced Damage. *J Am Soc Nephrol* (2011) 22(9):1682–95. doi: 10.1681/ASN.2010111197
63. Gowda R, Robertson BM, Iyer S, Barry J, Dinavahi SS, Robertson GP. The Role of Exosomes in Metastasis and Progression of Melanoma. *Cancer Treat Rev* (2020) 85:101975. doi: 10.1016/j.ctrv.2020.101975
64. Liu Y, Cao X. Characteristics and Significance of the Pre-metastatic Niche. *Cancer Cell* (2016) 30(5):668–81. doi: 10.1016/j.ccell.2016.09.011
65. Huang T, Song C, Zheng L, Xia L, Li Y, Zhou Y. The Roles of Extracellular Vesicles in Gastric Cancer Development, Microenvironment, Anti-Cancer Drug Resistance, and Therapy. *Mol Cancer* (2019) 18(1):62. doi: 10.1186/s12943-019-0967-5
66. Jayne DG. The Molecular Biology of Peritoneal Carcinomatosis From Gastrointestinal Cancer. *Ann Acad Med Singap* (2003) 32(2):219–25.
67. Glentis A, Oertle P, Mariani P, Chikina A, El Marjou F, Attieh Y, et al. Cancer-Associated Fibroblasts Induce Metalloprotease-Independent Cancer Cell Invasion of the Basement Membrane. *Nat Commun* (2017) 8(1):924. doi: 10.1038/s41467-017-00985-8
68. Simpson RJ, Lim JW, Moritz RL, Mathivanan S. Exosomes: Proteomic Insights and Diagnostic Potential. *Expert Rev Proteomics* (2009) 6(3):267–83. doi: 10.1586/epr.09.17
69. Mathai RA, Vidya RVS, Reddy BS, Thomas L, Udupa K, Kolesar J, et al. Potential Utility of Liquid Biopsy as a Diagnostic and Prognostic Tool for the Assessment of Solid Tumors: Implications in the Precision Oncology. *J Clin Med* (2019) 8(3):373. doi: 10.3390/jcm8030373
70. Tokuhisa M, Ichikawa Y, Kosaka N, Ochiya T, Yashiro M, Hirakawa K, et al. Exosomal miRNAs From Peritoneum Lavage Fluid as Potential Prognostic Biomarkers of Peritoneal Metastasis in Gastric Cancer. *PloS One* (2015) 10(7): e0130472. doi: 10.1371/journal.pone.0130472
71. Ohzawa H, Kumagai Y, Yamaguchi H, Miyato H, Sakuma Y, Horie H, et al. Exosomal microRNA in Peritoneal Fluid as a Biomarker of Peritoneal Metastases From Gastric Cancer. *Ann Gastroenterol Surg* (2019) 4(1):84–93. doi: 10.1002/ags3.12296
72. Ohzawa H, Saito A, Kumagai Y, Kimura Y, Yamaguchi H, Hosoya Y, et al. Reduced Expression of Exosomal miR29s in Peritoneal Fluid is a Useful Predictor of Peritoneal Recurrence After Curative Resection of Gastric Cancer With Serosal Involvement. *Oncol Rep* (2020) 43(4):1081–8. doi: 10.3892/or.2020.7505
73. Smyth EC, Verheij M, Allum W, Cunningham D, Cervantes A, Arnold D. Gastric Cancer: ESMO Clinical Practice Guidelines for Diagnosis, Treatment and Follow-Up. *Ann Oncol* (2016) 27(suppl 5):v38–49. doi: 10.1093/annonc/mdw350
74. Wu M, Wang G, Hu W, Yao Y, Yu XF. Emerging Roles and Therapeutic Value of Exosomes in Cancer Metastasis. *Mol Cancer* (2019) 18(1):53. doi: 10.1186/s12943-019-0964-8
75. Wortzel I, Dror S, Kenific CM, Lyden D. Exosome-Mediated Metastasis: Communication From a Distance. *Dev Cell* (2019) 49(3):347–60. doi: 10.1016/j.devcel.2019.04.011
76. Longatti A, Schindler C, Collinson A, Jenkinson L, Matthews C, Fitzpatrick L, et al. High Affinity Single-Chain Variable Fragments are Specific and Versatile Targeting Motifs for Extracellular Vesicles. *Nanoscale* (2018) 10(29):14230–44. doi: 10.1039/C8NR03970D
77. Tian Y, Li S, Song J, Ji T, Zhu M, Anderson GJ, et al. A Doxorubicin Delivery Platform Using Engineered Natural Membrane Vesicle Exosomes for Targeted Tumor Therapy. *Biomaterials* (2014) 35(7):2383–90. doi: 10.1016/j.biomaterials.2013.11.083
78. Kim MS, Haney MJ, Zhao Y, Yuan D, Deygen I, Klyachko NL, et al. Engineering Macrophage-Derived Exosomes for Targeted Paclitaxel Delivery to Pulmonary Metastases: In Vitro and In Vivo Evaluations. *Nanomedicine* (2018) 14(1):195–204. doi: 10.1016/j.nano.2017.09.011
79. Lv Q, Cheng L, Lu Y, Zhang X, Wang Y, Deng J, et al. Thermosensitive Exosome-Liposome Hybrid Nanoparticle-Mediated Chemoimmunotherapy for Improved Treatment of Metastatic Peritoneal Cancer. *Adv Sci (Weinh)* (2020) 7(18):2000515. doi: 10.1002/advs.202000515
80. Wang X, Zhang H, Bai M, Ning T, Ge S, Deng T, et al. Exosomes Serve as Nanoparticles to Deliver Anti-miR-214 to Reverse Chemoresistance to Cisplatin in Gastric Cancer. *Mol Ther* (2018) 26(3):774–83. doi: 10.1016/j.ymthe.2018.01.001
81. Ji R, Zhang X, Gu H, Ma J, Wen X, Zhou J, et al. Mir-374a-5p: A New Target for Diagnosis and Drug Resistance Therapy in Gastric Cancer. *Mol Ther Nucleic Acids* (2019) 18:320–31. doi: 10.1016/j.omtn.2019.07.025
82. Zhang H, Wang Y, Bai M, Wang J, Zhu K, Liu R, et al. Exosomes Serve as Nanoparticles to Suppress Tumor Growth and Angiogenesis in Gastric Cancer by Delivering Hepatocyte Growth Factor Sirna. *Cancer Sci* (2018) 109(3):629–41. doi: 10.1111/cas.13488
83. Hoshino A, Costa-Silva B, Shen TL, Rodrigues G, Hashimoto A, Tesic Mark M, et al. Tumour Exosome Integrins Determine Organotropic Metastasis. *Nature* (2015) 527(7578):329–35. doi: 10.1038/nature15756
84. Ge Y, Mu W, Ba Q, Li J, Jiang Y, Xia Q, et al. Hepatocellular Carcinoma-Derived Exosomes in Organotropic Metastasis, Recurrence and Early Diagnosis Application. *Cancer Lett* (2020) 477:41–8. doi: 10.1016/j.canlet.2020.02.003

85. Zomer A, Maynard C, Verweij FJ, Kamermans A, Schäfer R, Beerling E, et al. In Vivo Imaging Reveals Extracellular Vesicle-Mediated Phenocopying of Metastatic Behavior. *Cell* (2015) 161(5):1046–57. doi: 10.1016/j.cell.2015.04.042

Conflict of Interest: The authors declare that the research was conducted in the absence of any commercial or financial relationships that could be construed as a potential conflict of interest.

frontiers in Oncology

MINI REVIEW
published: 30 June 2021
doi: 10.3389/fonc.2021.655479

CDK10 in Gastrointestinal Cancers: Dual Roles as a Tumor Suppressor and Oncogene

Zainab A. Bazzi[1,2] *and Isabella T. Tai*[1,2]*

[1] Division of Gastroenterology, Department of Medicine, University of British Columbia, Vancouver, BC, Canada,
[2] Canada's Michael Smith Genome Sciences Centre, British Columbia (BC) Cancer, Vancouver, BC, Canada

Cyclin-dependent kinase 10 (CDK10) is a CDC2-related serine/threonine kinase involved in cellular processes including cell proliferation, transcription regulation and cell cycle regulation. CDK10 has been identified as both a candidate tumor suppressor in hepatocellular carcinoma, biliary tract cancers and gastric cancer, and a candidate oncogene in colorectal cancer (CRC). CDK10 has been shown to be specifically involved in modulating cancer cell proliferation, motility and chemosensitivity. Specifically, in CRC, it may represent a viable biomarker and target for chemoresistance. The development of therapeutics targeting CDK10 has been hindered by lack a specific small molecule inhibitor for CDK10 kinase activity, due to a lack of a high throughput screening assay. Recently, a novel CDK10 kinase activity assay has been developed, which will aid in the development of small molecule inhibitors targeting CDK10 activity. Discovery of a small molecular inhibitor for CDK10 would facilitate further exploration of its biological functions and affirm its candidacy as a therapeutic target, specifically for CRC.

Keywords: colorectal cancer, cyclin-dependent kinases, gastrointestinal cancers, hepatocellular carcinoma, gastric cancer, biliary tract cancer, CDK10

OPEN ACCESS

Edited by:
Jaw-Yuan Wang, Kaohsiung Medical University Hospital, Taiwan

Reviewed by:
Pei-Jung Lu, National Cheng Kung University, Taiwan
Peng-Chan Lin, National Cheng Kung University, Taiwan
Long-sen Chang, National Sun Yat-sen University, Taiwan

***Correspondence:**
Isabella T. Tai
itai@bcgsc.ca

Specialty section:
This article was submitted to Gastrointestinal Cancers, a section of the journal Frontiers in Oncology

Received: *18 January 2021*
Accepted: *16 June 2021*
Published: *30 June 2021*

Citation:
Bazzi ZA and Tai IT (2021) CDK10 in Gastrointestinal Cancers: Dual Roles as a Tumor Suppressor and Oncogene. Front. Oncol. 11:655479. doi: 10.3389/fonc.2021.655479

INTRODUCTION

Cyclin-dependent kinases (CDKs) are a family of serine/threonine protein kinases that play a critical role in regulating cellular processes, including cell division and cell death (1). Currently, more than 20 members of the CDK family have been identified by their characteristic ATP-binding pocket, PSTAIRE-like cyclin-binding domain and activating T-loop motif (1, 2). CDKs become active when non-covalently bound to their cyclin partner, *via* association with the PSTAIRE-like cyclin binding domain. The interaction of a CDK to its cyclin partner forms a heterodimer, in which the CDK acts as the catalytic subunit and the cyclin functions as the regulatory subunit. Cyclins are responsible for regulation of a CDK's kinase activity and substrate specificity. CDKs, their cyclin interacting partners, and functions are summarized in **Table 1**.

CDKs are generally categorized into two groups, based on their functions (1): cell cycle regulators; and (2) transcription regulators. CDKs involved in cell cycle regulation include CDK1, CDK2, CDK4 and CDK6. These CDKs are regulated through oscillation of expression throughout the cell cycle (55). CDK1 triggers the G2/M phase transition, while CDK2, CDK4 and

TABLE 1 | CDKs in gastrointestinal cancers.

Name	Putative Functions	Expression in Tumors vs. Normal Tissue					References
		CRC	Gastric Cancer	Liver Cancer ¥	Pancreatic Cancer	Other	
CDK1	Regulates the G2/M-phase transition	↑	↑	↑	↑		(3–6)
CDK2	Promotes cell cycle G1/S-phase transition	↑	NS*	NS*	NS*		(7)
CDK3	Involved in G0/G1 transition *via* phosphorylation of pRb.	↑	↓*	↓*	↓*		(8, 9)
CDK4	Regulates the G1/S-phase cell cycle transition *via* phosphorylation of Rb	↑	↑	↑	↑		(10–13)
CDK5	No known cell cycle functions Shown to be involved in brain development and neuronal differentiation	↑	↓	↑	↑		(14–18)
CDK6	Regulates the G1/S-phase cell cycle transition *via* phosphorylation of Rb	↑	↑	NS*	NS*	↑esophageal	(19–21)
CDK7	Activates CDK1, CDK2, CDK4 and CDK6 *via* phosphorylation of specific threonine sites; Forms complex with TFIIH to regulate RNA polymerase II transcription	NS*	↑	↑*	↑		(22, 23)
CDK8	Regulates gene expression *via* phosphorylation of RNA polymerase II	↑	↑	↑	↑		(24–27)
CDK9	Facilitates transcriptional elongation *via* phosphorylation of RNA polymerase II	↑	↑	NS*	↑		(28–30)
CDK10	Phosphorylation of ETS2 resulting in ETS2 degradation	↑	↓	↓	N/A		(31–33)
CDK11	Involved in regulation of pre-mRNA splicing	NS*	NS*	↑*	↑*	↑esophageal	(34, 35)
CDK12	Regulates gene expression *via* phosphorylation of RNA polymerase II	NS*	↓↑	NS*	NS*		(36, 37)
CDK13	Involved in transcription regulation and pre-mRNA splicing	↑	↓*	↑	NS*		(38)
CDK14	Activator of Wnt signaling pathway	↑	↑	↑	↑	↑esophageal	(39–43)
CDK15	Inhibits TRAIL-induced apoptosis *via* phosphorylation of survivin	↑*	↓*	NS*	NS*		(44)
CDK16	Promotes skeletal myogenesis and spermatogenesis	NS*	NS*	↑	NS*		(45–47)
CDK17	Involved in neuronal differentiation	↑*	NS*	NS*	NS*		(48)
CDK18	Prevents accumulation of DNA damage and genomic instability	↓*	↑	↓*	↓*		(49, 50)
CDK19	Involved in transcriptional regulation of RNA polymerase II	↓*	↑	NS*	NS*		(44, 51)
CDK20	Promotes transition from G1 to S phase *via* phosphorylation of CDK2	↑	NS*	↑	↓*		(52, 53)

*¥ includes hepatocellular and cholangiocarcinoma; ↑ increase in tumor vs. normal tissue; ↓ decrease in tumor vs. normal tissue; NS not significant; * based on Human Protein Atlas (54).*

CDK6 are regulators of the G1/S phase transition (56). CDKs involved in transcription regulation include CDK7, CDK8, CDK9, CDK10 and CDK11. Expression of CDKs involved in transcription regulation do not oscillate and are instead regulated by protein-protein interactions (56). They regulate transcription through phosphorylation of RNA polymerase II and through pre-mRNA splicing regulation.

CDKs often are dysregulated in malignancies, as shown in **Table 1**, causing dysregulation to cell cycle and transcription, leading to abnormal cell proliferation and inhibition of cell death (56). Genetic aberrations of CDKs and cyclins in tumor cells result in continuous cell proliferation or unscheduled cell cycle progression (56). Given their dysregulation in cancer, and their roles in mediating cell cycle progression, CDKs have been considered viable therapeutic targets for cancers, including gastrointestinal cancers.

Cyclin-dependent kinase 10 (CDK10) is a Cdc2-related kinase that was discovered based on its homology to the Cdc2 PSTA1RE amino acid domain (57). CDK10 plays a pivotal role in the regulation of fundamental cellular processes, including cell proliferation, transcription regulation and cell cycle regulation. Initial reports have indicated that CDK10 may act as a tumor suppressor in breast cancer. CDK10 is significantly downregulated in breast cancer compared to normal breast tissue (58). Additionally, CDK10 expression was inversely correlated with tumor stage and lymph node metastasis (58). Importantly, CDK10 expression was associated with better overall survival and may be a predictor of prognosis in breast cancer (58). Additional studies have demonstrated tumor suppressive and oncogenic roles for CDK10 in other malignancies. Specifically, CDK10 has been identified as a candidate tumor suppressor in hepatobiliary cancers, gastric cancer, glioma and nasopharyngeal carcinoma (31, 32, 59–61). Additionally, CDK10 has been shown to promote tumorigenesis in colorectal cancer (CRC) (62). Herein, we present a review of CDK10: its interacting partners, its role in gastrointestinal malignancies and its viability as a therapeutic target.

Molecular Genetics of CDK10

CDK10 was discovered in 1994 based on its homology to the Cdc2 PSTA1RE amino acid domain. PCR-based cloning was used to amplify cDNA encoding a novel human Cdc2-related kinase, which was called PISSLRE, and later termed CDK10 (57). Amino acid analysis revealed 38-45% identity with other CDKs (57). The chromosomal location of the gene encoding CDK10 was determined to be 16q24.3. The gene *CDK10* (as designed by HUGO) consists of thirteen exons, distributed over approximately 15,000 kilobases of genomic DNA.

A putative method of regulation of CDK10 is through alternative splicing of pre-mRNA transcripts. Several *CDK10* alternatively spliced isoforms have been identified. These alternatively spliced transcripts differ in exon 11 and in their 5' and 3' untranslated regions (UTRs). Of the differentially spliced transcripts identified, two produce functional proteins: the full-length transcript, which encodes for a 360 amino acid protein and a second transcript that encodes a truncated 272 amino acid variant, as shown in **Figure 1**. The latter protein is missing the ATP-binding domain and is therefore enzymatically inactive. Additionally, the shorter isoform does not interact with ETS2 and only weakly interacts with Cyclin M (33). It is therefore thought that alternative splicing is an important method of regulating CDK10 kinase activity.

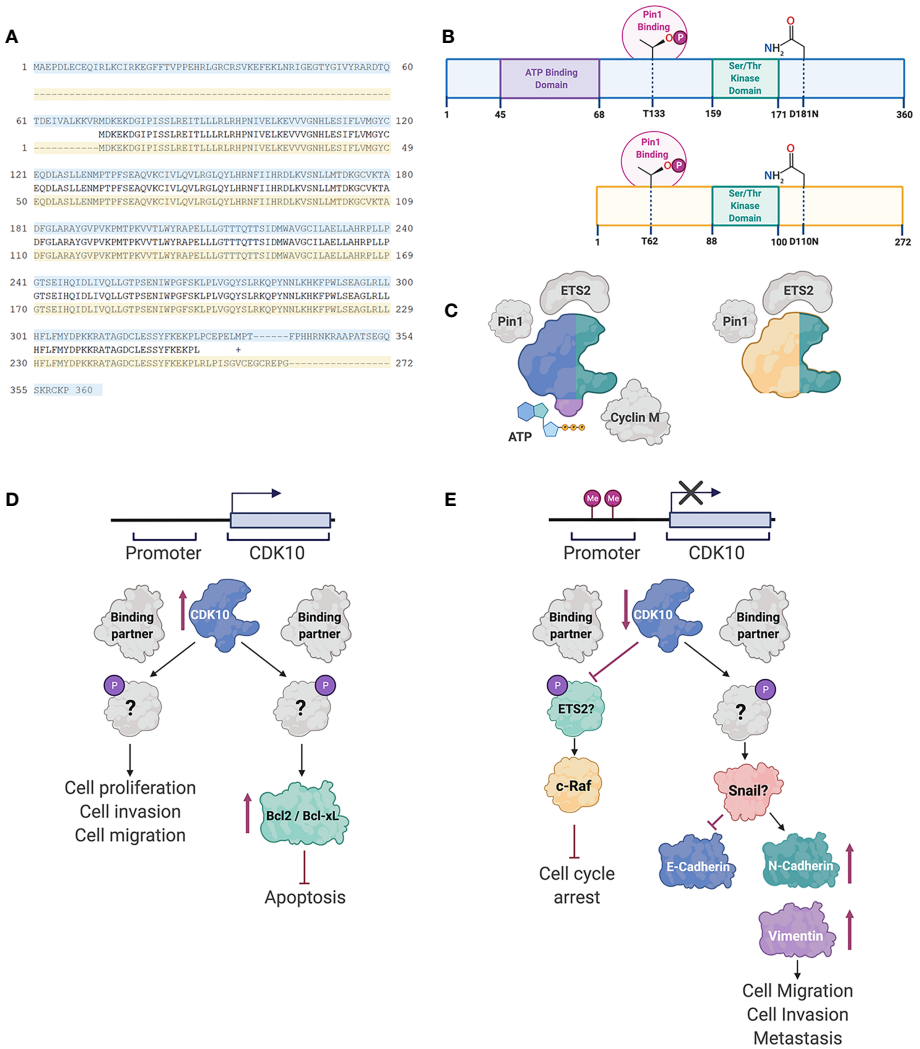

FIGURE 1 | CDK10 isoforms and interacting partners. **(A)** Protein sequence alignment of the full length CDK10 isoform (blue) and the splice variant (yellow). **(B)** Schematics of the full length CDK10 isoform and splice isoform, showing the ATP binding domain, the Ser/Thr kinase domain and Thr133, which is involved in Pin1 binding. **(C)** Models of CDK10 full-length protein and splice isoform with putative binding partners. Figures were created using BioRender. **(D)** Proposed CDK10 oncogenic signaling pathways. **(E)** Proposed CDK10 tumor suppressive signaling pathways. "?" denotes not yet shown in gastrointestinal and hepatobiliary cancers (60, 62–64).

Interacting Partners of CDK10

Binding of a CDK to its partner cyclin is generally required for its activation and subsequent kinase function. CDK10 stood alone as the last CDK lacking identification of a cyclin partner. Recently, cyclin M was identified as a CDK10 binding partner by yeast two-hybrid screening and immunoprecipitation (33). The binding of CDK10 to cyclin M is independent of the kinase domain, however, the interaction of CDK10 with cyclin M was shown to regulate the kinase activity of CDK10, in STAR syndrome, (**Figure 1**) (33). This interaction, however, has not been shown in cancers involving the GI tract or hepatobiliary system.

Using a yeast interaction trap, CDK10 was shown to bind to transcription factor ETS2, both *in vitro* and *in vivo*, using human embryonic kidney 293 cells (**Figure 1**) (65). This interaction occurs *via* the N-terminus of ETS2, and mutation of the kinase domain of CDK10 (resulting in CDK10DN variant) did not impact the binding of ETS2 to CDK10. CDK10 has been shown to regulate transactivation of ETS2. Mass spectrometric analysis revealed ETS2 as a substrate for CDK10/cyclin M phosphorylation (33) and it has been reported that phosphorylation of ETS2 by CDK10/Cyclin M results in inhibition of ETS2 transactivation.

Subcellular localization of CDK10 and Cyclin M at the base of the primary cilia, and specific co-localization with centrosomal proteins, suggests a role for CDK10/Cyclin M in ciliogenesis (33). Knockdown of CDK10/Cyclin M significantly decreases stress fiber formation and ciliogenesis in human telomerase reverse transcriptase retinal pigmented epithelial (hTERT RPE-1) cells (33). Using an *in vitro* kinase assay, known core centrosomal proteins and regulators of ciliogenesis and actin dynamics were screened as candidate substrates for CDK10/Cyclin M.

This method was used to identify protein kinase C-like 2 (PKN2) as an interacting partner and substrate for CDK10/Cyclin M, both *in vitro* and *in vivo* (33). CDK10/Cyclin M was shown to phosphorylate residues T121 and T124 of PKN2 and furthermore, to repress ciliogenesis in a RhoA-dependent manner. Cyclin M, however, has yet to be shown to be a CDK10 binding partner in gastrointestinal and hepatobiliary cancers.

Pin1 interaction with CDK10 has been documented in ER-positive breast cancer cells (**Figure 1**) (63). Pin1 is known to interact with Ser/Thr-Pro motifs, where the serine or threonine preceding the proline is phosphorylated. CDK10 does not contain any Ser-Pro motifs, however, does contain three Thr-Pro motifs. Mutagenesis of the three Thr-Pro motifs in CDK10 revealed Thr133 as an important residue for Pin1/CDK10 binding. Furthermore, treatment of CDK10 with a phosphatase demonstrated that Pin1 interacts with CDK10 in a phosphorylation-dependent manner. Consequently, interaction of Pin1 with CDK10 results in ubiquitination of CDK10 and subsequent degradation.

There is also evidence of CDK10 interaction with additional binding partners in non-human cell types. Specifically, CDK10 was shown to interact with Hsc70, Hsp90 and EcRB1 in *Helicoverpa armigera* (66). The interaction between CDK10 and Hsc70 and Hsp90 was augmented upon CDK10 phosphorylation. CDK10 forms a complex with Hsc70 and Hsp90, which sequentially binds with EcRB1 to facilitate the interaction between EcRB1 and EcRE to regulate 20E-mediated gene expression (66). Further studies are warranted to assess these as candidate binding partners for CDK10 in humans, and specifically, cancers involving the gastrointestinal tract and hepatobiliary system.

CDK10 AS A TUMOR SUPPRESSOR IN GASTROINTESTINAL AND HEPATOBILIARY CANCERS

Hepatobiliary Cancer

CDK10 has been identified as a candidate tumor suppressor in hepatobiliary cancers, including hepatocellular carcinoma (HCC) and biliary tract cancers (BTC) (31, 32, 64, 67). Examination of HCC tumor tissue revealed decreased expression of *CDK10* mRNA and CDK10 protein compared to adjacent normal liver tissue (31). Immunohistological staining of CDK10 showed weak or no staining in HCC tissue samples. Significantly, CDK10 abundance was found to be inversely correlated to tumor size and tumor stage in HCC. In BTC, downregulation of *CDK10* gene expression and CDK10 protein was observed in cancer tissue and cell lines, and was adversely associated with tumor stage, and lymph node invasion (64). Specifically, CDK10 was significantly downregulated in intrahepatic cholangiocarcinoma and gallbladder cancer, compared to normal tissue.

Several studies have characterized the effects of CDK10 on proliferation of hepatobiliary cancers *in vitro* (31, 64). Zhong et al. found that ectopic expression of *CDK10* in the HCC cell line SMMC-7721 resulted in inhibition of cell proliferation (31). Similarly, in BTC, ectopic expression of *CDK10* decreased cell proliferation, and downregulation of *CDK10* expression significantly increased cell proliferation (64). Furthermore, cell cycle analysis of HCC cells following CDK10 overexpression revealed a significant increase in the G_0-G_1 phase population of cells, and a decrease in the S phase population (31). Consistently, BTC cells overexpressing CDK10 had a significant increase in the population of cells in G_1 phase, and a significant decrease in the population of cells in G_2/M phase (64).

Studies have also assessed the impact of CDK10 expression on cell invasion and migration (31, 64). In HCC, ectopic expression of *CDK10* significantly delayed wound healing (31). Yu et al. also reported a significant decrease in BTC cell migration upon CDK10 overexpression (64). Consistently, they also reported a significant increase in BTC cell migration following downregulation of CDK10 (64). These studies, however, did not examine the mechanism by which CDK10 inhibits cancer cell invasion and migration. In glioma, CDK10 was shown to regulate cell motility through inhibition of epithelial to mesenchymal transition (EMT) (60). *CDK10* knockdown decreased E-cadherin and increased vimentin and N-cadherin expression. Conversely, overexpression of CDK10 increased E-cadherin and decreased vimentin and N-cadherin expression. CDK10 was shown to regulate expression of the EMT transcription factor, Snail, and the effects of CDK10 on EMT in glioma were partially reversed by manipulation of Snail expression (60). Importantly, Snail is a known regulator of EMT in hepatobiliary cancersCDK10 may regulate cell motility of hepatobiliary cancer cells through inhibition of EMT *via* Snail downregulation.

Therapeutic resistance is a major hindrance on treatment of gastrointestinal cancers. There is significant evident identifying CDK10 as an important modulator of tamoxifen sensitivity in breast cancer, suggesting a potential role for CDK10 in chemosensitivity in other cancers (63, 68). In patients with ER-positive breast cancer, low CDK10 expression was associated with shorter overall survival and clinical resistance to tamoxifen (68). This study used gene silencing to identify CDK10 as a modulator of tamoxifen resistance in breast cancer through regulation of p42/p44 MAPK pathway (68). In BTC, Yu et al. found that knockdown of *CDK10* significantly decreased sensitivity to 5-fluorouracil (64). Furthermore, overexpression of *CDK10* increased BTC cell sensitivity to 5-fluorouracil, adriamycin/epirubicin, cisplatin and hydroxylcamptothecin *in vitro* (64). Similar to endocrine resistance in breast cancer, cell cycle arrest at G_1 phase was observed in 5-fluorouracil-treated cells overexpressing CDK10 (64, 68). In HCC, overexpression of CDK10 increased chemosensitivity to cisplatin and epirubicin in SMMC-7721 cells but not HepG2 cells (31). Furthermore, overexpression of CDK10 increased gall bladder cancer sensitivity to gemcitabine (69). Anticipating a mechanism similar to endocrine therapy resistance in breast cancer, CDK10 expression was shown to downregulate c-Raf levels in BTC (64, 69). Furthermore, in gall bladder cancer, knockdown of c-Raf resulted in a significant increase in gemcitabine sensitivity in cells overexpressing CDK10 (69). Downregulation of CDK10 increased ETS2-mediated transcription of c-Raf, resulting in activation of the MAPK pathway. Additionally, Khanal et al. investigated the

association between CDK10 and Pin1 expression in tamoxifen-resistant breast cancer cells (63). This study observed a significant inverse correlation between Pin1 and CDK10 expression in tamoxifen-resistant breast cancer. Khanal et al. also found that overexpression of CDK10 increased breast cancer cell sensitivity to tamoxifen treatment, and decreased Pin1-mediated c-Raf phosphorylation (63). However, further research is warranted to delineate the mechanism by which CDK10 regulates c-Raf levels in gastrointestinal cancers and how that results in cell cycle arrest.

Gastric Cancer

In addition to hepatobiliary cancers, CDK10 has been identified as a candidate tumor suppressor in gastric cancer. Independent studies found decreased expression of CDK10 in gastric cancer compared to normal gastric tissue (32, 67). Consistently, these studies found a significant correlation between loss of CDK10 expression and advanced tumor stage, lymph node invasion and distant metastasis, in patients with gastric cancer. Furthermore, these studies also identified loss of CDK10 expression as an unfavorable prognostic marker in gastric cancer. However, Fukui et al. found that CDK10 was upregulated in peritoneal and liver metastases in human gastric cancer cell lines established following injection into nude mice (70).

Studies have also assessed the effect of CDK10 on cell proliferation and cell motility in gastric cancers. Ectopic expression of *CDK10* decreased cell proliferation, while downregulation of *CDK10* expression significantly increased cell proliferation (32). Treatment of gastric cancer cells with quercetin, a flavonol shown to induce apoptosis, significantly decreased expression of *CDK10* (71). Additionally, in gastric cancer, overexpression of CDK10 decreased cell invasion, while knockdown of CDK10 promoted cell invasion (32).

Mechanisms of CDK10 Downregulation in Gastrointestinal Cancers

As previously mentioned, CDK10 expression is downregulated in hepatobiliary cancers and gastric cancers (31, 32, 64). Mechanisms of CDK10 downregulation have not been examined in gastrointestinal cancers. Chromosomal deletions at the q24 region of chromosome 16 are associated with human cancers, including gastric cancer and HCC (72, 73). Furthermore, aberrant methylation of chromosome 16 is a mechanism of gene expression dysregulation in chronic hepatitis, liver cirrhosis and HCC (74, 75). Promoter hypermethylation was found to be a mechanism of CDK10 suppression in breast cancer and nasopharyngeal carcinoma (61, 68). Therefore, suppression of CDK10 may result from loss of heterozygosity and hypermethylation at the q24 region of chromosome 16. Further research is warranted to assess loss of heterozygosity and promoter hypermethylation as potential mechanisms of CDK10 downregulation in gastrointestinal cancers.

CDK10 IN COLORECTAL CANCER

A meta-analysis of CRC gene expression profiling studies identified *CDK10* as a gene consistently upregulated in CRC (76). Consistent with this meta-analysis, Weiswald et al. found overexpression of CDK10 in CRC tissue and CRC cell lines, compared to matched normal tissue and normal colon cells, respectively (62). This observation is similar to other studies that found upregulation of *CDK10* in prostate cancer and seminomas (77, 78). Furthermore, increased expression of CDK10 was found to be correlated with lymph node positive tumors in CRC (79).

Weiswald et al. also found that CRC growth and survival were significantly affected by manipulation of *CDK10* gene expression. Specifically, CDK10 knockdown decreased cell survival and promoted apoptosis in CRC cell lines. Similarly, overexpression of CDK10 increased cell proliferation and inhibited apoptosis *in vitro*, in a Bcl-2/Bcl-$_{XL}$-dependent manner. Consistently, suppression of CDK10 in patient-derived xenograft CRC tumors inhibited tumor growth and decreased expression of Bcl-2 *in vivo*. Interestingly, CDK10 expression did not affect cell cycle progression in CRC, indicating that the impact of CDK10 on cell proliferation and apoptosis is independent of cell cycle regulation.

Furthermore, Weiswald et al. evaluated the effects of CDK10 on chemotherapy resistance. CRC cell lines overexpressing CDK10 were significantly less responsive to 5-fluorouracil compared to controls (62). Additionally, compared to CDK10WT, cell lines expressing CDK10DN were more sensitive to 5-fluorouracil, indicating kinase involvement in CDK10-mediated chemoresistance in CRC. Indeed, CDK10 expression may be a viable biomarker for chemotherapy resistance and should be assessed as a potential biomarker for CRC recurrence. Importantly, while this study suggests a kinase-dependent role for CDK10, an interacting partner to CDK10 has yet to be identified and implicated in CRC.

The role of CDK10 in CRC cell invasion and migration is yet to be determined. However, Zehra et al. demonstrated upregulation of CDK10 and ETS2 in a corneal epithelial wound healing model (80). This study infers a potential role for CDK10 in cancer metastasis, as inhibition of CDK10 resulted in a significant delay in corneal epithelial cell migration.

CDK10 AS A THERAPEUTIC TARGET FOR GASTROINTESTINAL CANCERS

Research has been dedicated to the development of candidate CDK small molecule inhibitors, however, the majority of CDK inhibitors lack specificity and clinical trials have had disappointing outcomes. Several strategies have been employed in drug discovery to develop effective CDK inhibitors, including reversible ATP-competitive and non-competitive inhibition, reversible and irreversible allosteric inhibition, antibodies, and CDK-targeted degradation. Non-specific pan-CDK inhibitors exhibit low anti-cancer activity and high toxicity. Due to their non-specificity, these inhibitors block several cell processes, including cell proliferation, transcription, and translation. Given the tumor suppressive nature of CDK10 in breast cancer, HCC, BTC and gastric cancer, targeting CDK10 *via* pan-CDK inhibitors may have limited the therapeutic response.

The development of therapeutics targeting CDK10 has been hindered by lack of a CDK10 activity assay, and lack of a specific small molecule inhibitor to identify novel therapies. Discovery of a small molecule inhibitor for CDK10 would facilitate further

exploration of its biological functions and affirm its candidacy as a therapeutic target, specifically for CRC. Recently, Robert et al. described a novel CDK10/Cyclin M *in vitro* activity assay (81). This luminescence-based assay uses a synthetic peptide phosphorylation substrate for the CDK10/Cyclin M complex.

Flavopiridol is the most extensively studied pan-CDK inhibitor. It has been shown to inhibit CDK1, CDK2, CDK4, CDK6, CDK9 and CDK10. While flavopiridol can inhibit CDK10, the IC50 for flavopiridol inhibition against CDK10/Cyclin M is less potent than flavopiridol inhibition of other CDKs (81). *In vitro* studies in gastrointestinal cells demonstrated that flavopiridol was effective in inducing apoptosis through blockage of cell cycle progression at G_1 (82, 83). However, clinical trials in patients with gastrointestinal cancers did not result in favorable outcomes (84, 85) and reported significant toxicity among patients.

Additional CDK inhibitors such as dinaciclib, SDS-032, AZD4573, AT7519 and riviciclib were all tested on CDK10/Cyclin M, however none of these potently inhibited CDK10 kinase activity (81). Ibrahim et al. synthesized novel flavopiridol analogs and assessed their inhibitory activity on CDK2, CDK5 and CDK9 (86). This series of inhibitors was more potent towards CDK9 than the other CDKs examined in the study. Given the close relation between CDK9 and CDK10, these inhibitors may exhibit inhibitory activity towards CDK10 (2).

The development of therapeutics targeting CDK10 should account for the tissue-specific biological activity of CDK10. Given that CDK10 acts as a tumor suppressor in some gastrointestinal and hepatobiliary cancers, future drug development should focus on inhibiting other CDKs, while maintaining activity of CDK10. In these cancers, CDK10 expression levels may be indicative of chemoresistance. The promotion of tumorigenesis by CDK10 in CRC suggests its inhibition is a promising therapeutic strategy. Given that the kinase domain has been implicated CDK10-mediated inhibition of apoptosis in CRC, inhibition of CDK10 kinase activity may be an effective therapeutic approach. The development of a CDK10-specific inhibitor may be a viable therapeutic target for the treatment of CRC.

CONCLUSION

CDK10 has been implicated as both a tumor suppressor and an oncogene in gastrointestinal and hepatobiliary cancers. CDK10 is involved in cell proliferation, cell motility, and plays an important role in chemosensitivity and chemoresistance. Further studies are warranted to understand the tissue-specific functions of CDK10 and the mechanisms that influence its oncogenic and tumor suppressive potential in gastrointestinal cancer. Implications of CDK10 as an oncogene in CRC make inhibition of CDK10 a viable therapeutic strategy. The development of therapeutics targeting CDK10 has been hindered by lack of a high throughput CDK10 activity screening assay. Detection of CDK10 kinase activity will allow for identification of small molecule inhibitors of CDK10. This will aid in further understanding the role of CDK10 in disease progression, and the development of therapeutics for the treatment of gastrointestinal cancers.

AUTHOR CONTRIBUTIONS

ZB: drafting and editing the manuscript. IT: editing and critically reading manuscript. All authors contributed to the article and approved the submitted version.

FUNDING

This study was supported by the Canadian Institutes of Health Research (CIHR) (Grant #MOP-82881) and CIHR New Investigator salary award to IT (MSH-95344).

ACKNOWLEDGMENTS

Figures were created using biorender.com.

REFERENCES

1. Lim S, Kaldis P. Cdks, Cyclins and CKIs: Roles Beyond Cell Cycle Regulation. *Development* (2013) 140:3079–93. doi: 10.1242/dev.091744
2. Cao L, Chen F, Yang X, Xu W, Xie J, Yu L. Phylogenetic Analysis of CDK and Cyclin Proteins in Premetazoan Lineages. *BMC Evol Biol* (2014) 14:10. doi: 10.1186/1471-2148-14-10
3. Piao J, Zhu L, Sun J, Li N, Dong B, Yang Y, et al. High Expression of CDK1 and BUB1 Predicts Poor Prognosis of Pancreatic Ductal Adenocarcinoma. *Gene* (2019) 701:15–22. doi: 10.1016/j.gene.2019.02.081
4. Gan W, Zhao H, Li T, Liu K, Huang J. CDK1 Interacts With iASPP to Regulate Colorectal Cancer Cell Proliferation Through p53 Pathway. *Oncotarget* (2017) 8:71618–29. doi: 10.18632/oncotarget.17794
5. Shi Q, Ni X, Lei M, Xia Q, Dong Y, Zhang Q, et al. Phosphorylation of Islet-1 Serine 269 by CDK1 Increases its Transcriptional Activity and Promotes Cell Proliferation in Gastric Cancer. *Mol Med* (2021) 27:47. doi: 10.1186/s10020-021-00302-6
6. Yang W-X, Pan Y-Y, You C-G. Cdk1, CCNB1, Cdc20, BUB1, Mad2l1, MCM3, Bub1b, MCM2, and RFC4 may Be Potential Therapeutic Targets for Hepatocellular Carcinoma Using Integrated Bioinformatic Analysis. *BioMed Res Int* (2019) 2019:1245072. doi: 10.1155/2019/1245072
7. Li J-Q, Miki H, Ohmori M, Wu F, Funamoto Y. Expression of Cyclin E and Cyclin-Dependent Kinase 2 Correlates With Metastasis and Prognosis in Colorectal Carcinoma. *Hum Pathol* (2001) 32:945–53. doi: 10.1053/hupa.2001.27116
8. Ren S, Rollins BJ. Cyclin C/Cdk3 Promotes Rb-Dependent G0 Exit. *Cell* (2004) 117:239–51. doi: 10.1016/S0092-8674(04)00300-9
9. Lu J, Zhang ZL, Huang D, Tang N, Li Y, Peng Z, et al. Cdk3-promoted Epithelial-Mesenchymal Transition Through Activating AP-1 is Involved in Colorectal Cancer Metastasis. *Oncotarget* (2016) 7:7012–28. doi: 10.18632/oncotarget.6875
10. Lu JW, Lin YM, Chang JG, Yeh KT, Chen RM, Tsai JJ, et al. Clinical Implications of Deregulated CDK4 and Cyclin D1 Expression in Patients With Human Hepatocellular Carcinoma. *Med Oncol* (2013) 30:379. doi: 10.1007/s12032-012-0379-5
11. Lindberg D, Hessman O, Åkerström G, Westin G. Cyclin-Dependent Kinase 4 (Cdk4) Expression in Pancreatic Endocrine Tumors. *Neuroendocrinology* (2007) 86:112–8. doi: 10.1159/000106762
12. Wang S, Wang X, Gao Y, Peng Y, Dong N, Xie Q, et al. RN181 is a Tumor Suppressor in Gastric Cancer by Regulation of the ERK/MAPK-cyclin D1/CDK4 Pathway. *J Pathol* (2019) 248:204–16. doi: 10.1002/path.5246
13. Ikeda K, Monden T, Tsujie M, Izawa H, Yamamoto H, Ohnishi T, et al. [Cyclin D, CDK4 and p16 Expression in Colorectal Cancer]. *Nihon Rinsho* (1996) 54:1054–9.

14. Zhuang K, Zhang J, Xiong M, Wang X, Luo X, Han L, et al. CDK5 Functions as a Tumor Promoter in Human Colorectal Cancer Via Modulating the ERK5–AP-1 Axis. *Cell Death Dis* (2016) 7:e2415–5. doi: 10.1038/cddis.2016.333
15. Ohshima T, Ward JM, Huh CG, Longenecker G, Veeranna, Pant HC, et al. Targeted Disruption of the Cyclin-Dependent Kinase 5 Gene Results in Abnormal Corticogenesis, Neuronal Pathology and Perinatal Death. *Proc Natl Acad Sci* (1996) 93:11173–8. doi: 10.1073/pnas.93.20.11173
16. Zhang R, Lin P, Yang H, He Y, Dang Y-W, Feng Z-B, et al. Clinical Role and Biological Function of CDK5 in Hepatocellular Carcinoma: A Study Based on Immunohistochemistry, RNA-seq and *In Vitro* Investigation. *Oncotarget* (2017) 8:108333–54. doi: 10.18632/oncotarget.22659
17. Eggers JP, Grandgenett PM, Collisson EC, Lewallen ME, Tremayne J, Singh PK, et al. Cyclin-Dependent Kinase 5 Is Amplified and Overexpressed in Pancreatic Cancer and Activated by Mutant K-Ras. *Clin Cancer Res* (2011) 17:6140–50. doi: 10.1158/1078-0432.CCR-10-2288
18. Cao L, Zhou J, Zhang J, Wu S, Yang X, Zhao X, et al. Cyclin-Dependent Kinase 5 Decreases in Gastric Cancer and Its Nuclear Accumulation Suppresses Gastric Tumorigenesis. *Clin Cancer Res* (2015) 21:1419–28. doi: 10.1158/1078-0432.CCR-14-1950
19. Feng L, Xie Y, Zhang H, Wu Y. miR-107 Targets Cyclin-Dependent Kinase 6 Expression, Induces Cell Cycle G1 Arrest and Inhibits Invasion in Gastric Cancer Cells. *Med Oncol* (2012) 29:856–63. doi: 10.1007/s12032-011-9823-1
20. Tadano T, Kakuta Y, Hamada S, Shimodaira Y, Kuroha M, Kawakami Y, et al. MicroRNA-320 Family is Downregulated in Colorectal Adenoma and Affects Tumor Proliferation by Targeting CDK6. *World J gastrointestinal Oncol* (2016) 8:532–42. doi: 10.4251/wjgo.v8.i7.532
21. Baba Y, Watanabe M, Murata A, Shigaki H, Miyake K, Ishimoto T, et al. : LINE-1 Hypomethylation, DNA Copy Number Alterations, and CDK6 Amplification in Esophageal Squamous Cell Carcinoma. *Clin Cancer Res* (2014) 20:1114–24. doi: 10.1158/1078-0432.CCR-13-1645
22. Lu P, Geng J, Zhang L, Wang Y, Niu N, Fang Y, et al. THZ1 Reveals CDK7-dependent Transcriptional Addictions in Pancreatic Cancer. *Oncogene* (2019) 38:3932–45. doi: 10.1038/s41388-019-0701-1
23. Wang Q, Li M, Zhang X, Huang H, Huang J, Ke J, et al. Upregulation of CDK7 in Gastric Cancer Cell Promotes Tumor Cell Proliferation and Predicts Poor Prognosis. *Exp Mol Pathol* (2016) 100:514–21. doi: 10.1016/j.yexmp.2016.05.001
24. Xu W, Wang Z, Zhang W, Qian K, Li H, Kong D, et al. Mutated K-ras Activates CDK8 to Stimulate the Epithelial-to-Mesenchymal Transition in Pancreatic Cancer in Part Via the Wnt/β-Catenin Signaling Pathway. *Cancer Lett* (2015) 356:613–27. doi: 10.1016/j.canlet.2014.10.008
25. Seo JO, Han SI, Lim SC. Role of CDK8 and Beta-Catenin in Colorectal Adenocarcinoma. *Oncol Rep* (2010) 24:285–91. doi: 10.3892/or_00000858
26. Kim M-Y, Han SI, Lim S-C. Roles of Cyclin-Dependent Kinase 8 and β-Catenin in the Oncogenesis and Progression of Gastric Adenocarcinoma. *Int J Oncol* (2011) 38:1375–83. doi: 10.3892/ijo.2011.948
27. Han SI, Lim S-C. Expression and Prognostic Significance of CDK8 and β-Catenin in Hepatocellular Carcinoma. *In Vivo (Athens Greece)* (2020) 34:1387–94. doi: 10.21873/invivo.11918
28. Kretz AL, Schaum M, Richter J, Kitzig EF, Engler CC, Leithäuser F, et al. CDK9 is a Prognostic Marker and Therapeutic Target in Pancreatic Cancer. *Tumor Biol* (2017) 39:1010428317694304. doi: 10.1177/1010428317694304
29. Lu Y, Tang L, Zhang Q, Zhang Z, Wei W. MicroRNA-613 Inhibits the Progression of Gastric Cancer by Targeting CDK9. *Artif Cells Nanomed Biotechnol* (2018) 46:980–4. doi: 10.1080/21691401.2017.1351983
30. Wang J, Liu J, Tian F, Zhan Y, Kong D. Cyclin-Dependent Kinase 9 Expression and its Association With CD8(+) T Cell Infiltration in Microsatellite-Stable Colorectal Cancer. *Oncol Lett* (2019) 18:6046–56. doi: 10.3892/ol.2019.10970
31. Zhong XY, Xu XX, Yu JH, Jiang GX, Yu Y, Tai S, et al. Clinical and Biological Significance of Cdk10 in Hepatocellular Carcinoma. *Gene* (2012) 498:68–74. doi: 10.1016/j.gene.2012.01.022
32. You Y, Bai F, Ye Z, Zhang N, Yao L, Tang Y, et al. Downregulated CDK10 Expression in Gastric Cancer: Association With Tumor Progression and Poor Prognosis. *Mol Med Rep* (2018) 17:6812–8. doi: 10.3892/mmr.2018.8662
33. Guen VJ, Gamble C, Flajolet M, Unger S, Thollet A, Ferandin Y, et al. CDK10/Cyclin M is a Protein Kinase That Controls ETS2 Degradation and is Deficient in STAR Syndrome. *Proc Natl Acad Sci USA* (2013) 110:19525–30. doi: 10.1073/pnas.1306814110
34. Hu D, Mayeda A, Trembley JH, Lahti JM, Kidd VJ. CDK11 Complexes Promote pre-mRNA Splicing. *J Biol Chem* (2003) 278:8623–9. doi: 10.1074/jbc.M210057200
35. Du Y, Yan D, Yuan Y, Xu J, Wang S, Yang Z, et al. Cdk11(p110) Plays a Critical Role in the Tumorigenicity of Esophageal Squamous Cell Carcinoma Cells and is a Potential Drug Target. *Cell Cycle (Georgetown Tex)* (2019) 18:452–66. doi: 10.1080/15384101.2019.1577665
36. Liu M, Fan H, Li T, Sihong L, Qiao S, Bi J. Low Expression of CDK12 in Gastric Cancer is Correlated With Advanced Stage and Poor Outcome. *Pathol - Res Pract* (2020) 216:152962. doi: 10.1016/j.prp.2020.152962
37. Ji J, Zhou C, Wu J, Cai Q, Shi M, Zhang H, et al. Expression Pattern of CDK12 Protein in Gastric Cancer and its Positive Correlation With CD8(+) Cell Density and CCL12 Expression. *Int J Med Sci* (2019) 16:1142–8. doi: 10.7150/ijms.34541
38. Kim H-E, Kim D-G, Lee KJ, Son JG, Song M-Y, Park Y-M, et al. Frequent Amplification of CENPF, GMNN and CDK13 Genes in Hepatocellular Carcinomas. *PloS One* (2012) 7:e43223. doi: 10.1371/journal.pone.0043223
39. Chen L, Wang Y, Jiang W, Ni R, Wang Y, Ni S. CDK14 Involvement in Proliferation Migration and Invasion of Esophageal Cancer. *Ann Trans Med* (2019) 7:681–1. doi: 10.21037/atm.2019.11.105
40. Sun Y, Zhu Q, Yang W, Shan Y, Yu Z, Zhang Q, et al. Lncrna H19/miR-194/PFTK1 Axis Modulates the Cell Proliferation and Migration of Pancreatic Cancer. *J Cell Biochem* (2019) 120:3874–86. doi: 10.1002/jcb.27669
41. Yang L, Zhu J, Huang H, Yang Q, Cai J, Wang Q, et al. Pftk1 Promotes Gastric Cancer Progression by Regulating Proliferation, Migration and Invasion. *PloS One* (2015) 10:e0140451. doi: 10.1371/journal.pone.0140451
42. Pang EY, Bai AH, To KF, Sy SM, Wong NL, Lai PB, et al. Identification of PFTAIRE Protein Kinase 1, a Novel Cell Division Cycle-2 Related Gene, in the Motile Phenotype of Hepatocellular Carcinoma Cells. *Hepatology* (2007) 46:436–45. doi: 10.1002/hep.21691
43. Mao Y, Jia Y, Zhu H, Wang W, Jin Q, Huang F, et al. High Expression of PFTK1 in Cancer Cells Predicts Poor Prognosis in Colorectal Cancer. *Mol Med Rep* (2017) 16:224–30. doi: 10.3892/mmr.2017.6560
44. Park MH, Kim SY, Kim YJ, Chung Y-H. ALS2CR7 (CDK15) Attenuates TRAIL Induced Apoptosis by Inducing Phosphorylation of Survivin Thr34. *Biochem Biophys Res Commun* (2014) 450:129–34. doi: 10.1016/j.bbrc.2014.05.070
45. Mikolcevic P, Sigl R, Rauch V, Hess MW, Pfaller K, Barisic M, et al. Cyclin-Dependent Kinase 16/PCTAIRE Kinase 1 is Activated by Cyclin Y and is Essential for Spermatogenesis. *Mol Cell Biol* (2012) 32:868–79. doi: 10.1128/MCB.06261-11
46. Shimizu K, Uematsu A, Imai Y, Sawasaki T. Pctaire1/Cdk16 Promotes Skeletal Myogenesis by Inducing Myoblast Migration and Fusion. *FEBS Lett* (2014) 588:3030–7. doi: 10.1016/j.febslet.2014.05.060
47. Liu Q, Wang C, Jiang Z, Li S, Li F, Tan H-B, et al. circRNA 001306 Enhances Hepatocellular Carcinoma Growth by Up-Regulating CDK16 Expression Via Sponging Mir-584-5p. *J Cell Mol Med* (2020) 24:14306–15. doi: 10.1111/jcmm.16047
48. Kerr N, Pintzas A, Holmes F, Hobson SA, Pope R, Wallace M, et al. The Expression of ELK Transcription Factors in Adult DRG: Novel Isoforms, Antisense Transcripts and Upregulation by Nerve Damage. *Mol Cell Neurosci* (2010) 44:165–77. doi: 10.1016/j.mcn.2010.03.005
49. Barone G, Staples CJ, Ganesh A, Patterson KW, Bryne DP, Myers KN, et al. Human CDK18 Promotes Replication Stress Signaling and Genome Stability. *Nucleic Acids Res* (2016) 44:8772–85. doi: 10.1093/nar/gkw615
50. Li P, Ge D, Li P, Hu F, Chu J, Chen X, et al. CXXC Finger Protein 4 Inhibits the CDK18-ERK1/2 Axis to Suppress the Immune Escape of Gastric Cancer Cells With Involvement of ELK1/MIR100HG Pathway. *J Cell Mol Med* (2020) 24:10151–65. doi: 10.1111/jcmm.15625
51. Zhao JQ, Li XN, Fu LP, Zhang N, Cai JH. ISOC1 Promotes the Proliferation of Gastric Cancer Cells by Positively Regulating CDK19. *Eur Rev Med Pharmacol Sci* (2020) 24:11602–9. doi: 10.26355/eurrev_202011_23803
52. Feng H, Yu Z, Tian Y, Lee YY, Li MS, Go MY, et al. A CCRK-EZH2 Epigenetic Circuitry Drives Hepatocarcinogenesis and Associates With Tumor Recurrence and Poor Survival of Patients. *J Hepatol* (2015) 62:1100–11. doi: 10.1016/j.jhep.2014.11.040

53. An X, Ng SS, Xie D, Zeng YX, Sze J, Wang J, et al. Functional Characterisation of Cell Cycle-Related Kinase (CCRK) in Colorectal Cancer Carcinogenesis. *Eur J Cancer* (2010) 46:1752–61. doi: 10.1016/j.ejca.2010.04.007
54. Uhlén M, Björling E, Agaton C, Szigyarto CA-K, Amini B, Andersen E, et al. : A Human Protein Atlas for Normal and Cancer Tissues Based on Antibody Proteomics. *Mol Cell Proteomics* (2005) 4:1920–32. doi: 10.1074/mcp.M500279-MCP200
55. Simmons Kovacs LA, Mayhew MB, Orlando DA, Jin Y, Li Q, Huang C, et al. Cyclin-Dependent Kinases are Regulators and Effectors of Oscillations Driven by a Transcription Factor Network. *Mol Cell* (2012) 45:669–79. doi: 10.1016/j.molcel.2011.12.033
56. Malumbres M, Barbacid M. Cell Cycle, CDKs and Cancer: A Changing Paradigm. *Nat Rev Cancer* (2009) 9:153–66. doi: 10.1038/nrc2602
57. Graña X, Claudio PP, De Luca A, Sang N, Giordano A. PISSLRE, a Human Novel CDC2-related Protein Kinase. *Oncogene* (1994) 9:2097–103.
58. You Y, Li H, Qin X, Zhang Y, Song W, Ran Y, et al. Decreased CDK10 Expression Correlates With Lymph Node Metastasis and Predicts Poor Outcome in Breast Cancer Patients - A Short Report. *Cell Oncol (Dordr)* (2015) 38:485–91. doi: 10.1007/s13402-015-0246-4
59. Crawford J, Ianzano L, Savino M, Whitmore S, Cleton-Jansen AM, Settasatian C, et al. The PISSLRE Gene: Structure, Exon Skipping, and Exclusion as Tumor Suppressor in Breast Cancer. *Genomics* (1999) 56:90–7. doi: 10.1006/geno.1998.5676
60. Li H, You Y, Liu J. Cyclin−Dependent Kinase 10 Prevents Glioma Metastasis Via Modulation of Snail Expression. *Mol Med Rep* (2018) 18:1165–70. doi: 10.3892/mmr.2018.9059
61. You Y, Yang W, Wang Z, Zhu H, Li H, Lin C, et al. Promoter Hypermethylation Contributes to the Frequent Suppression of the CDK10 Gene in Human Nasopharyngeal Carcinomas. *Cell Oncol (Dordr)* (2013) 36:323–31. doi: 10.1007/s13402-013-0137-5
62. Weiswald L-B, Hasan MR, Wong JCT, Pasiliao CC, Rahman M, Ren J, et al. Inactivation of the Kinase Domain of CDK10 Prevents Tumor Growth in a Preclinical Model of Colorectal Cancer, and is Accompanied by Downregulation of Bcl-2. *Mol Cancer Ther* (2017) 16(10):2292–303. doi: 10.1158/1535-7163.MCT-16-0666
63. Khanal P, Yun HJ, Lim SC, Ahn SG, Yoon HE, Kang KW, et al. Proyl Isomerase Pin1 Facilitates Ubiquitin-Mediated Degradation of Cyclin-Dependent Kinase 10 to Induce Tamoxifen Resistance in Breast Cancer Cells. *Oncogene* (2012) 31:3845–56. doi: 10.1038/onc.2011.548
64. Yu JH, Zhong XY, Zhang WG, Wang ZD, Dong Q, Tai S, et al. CDK10 Functions as a Tumor Suppressor Gene and Regulates Survivability of Biliary Tract Cancer Cells. *Oncol Rep* (2012) 27:1266–76. doi: 10.3892/or.2011.1617
65. Kasten M, Giordano A. Cdk10, a Cdc2-related Kinase, Associates With the Ets2 Transcription Factor and Modulates its Transactivation Activity. *Oncogene* (2001) 20:1832–8. doi: 10.1038/sj.onc.1204295
66. Liu W, Cai M-J, Wang J-X, Zhao X-F. In a Nongenomic Action, Steroid Hormone 20-Hydroxyecdysone Induces Phosphorylation of Cyclin-Dependent Kinase 10 to Promote Gene Transcription. *Endocrinology* (2014) 155:1738–50. doi: 10.1210/en.2013-2020
67. Zhao BW, Chen S, Li YF, Xiang J, Zhou ZW, Peng JS, et al. Low Expression of CDK10 Correlates With Adverse Prognosis in Gastric Carcinoma. *J Cancer* (2017) 8:2907–14. doi: 10.7150/jca.20142
68. Iorns E, Turner NC, Elliott R, Syed N, Garrone O, Gasco M, et al. Identification of CDK10 as an Important Determinant of Resistance to Endocrine Therapy for Breast Cancer. *Cancer Cell* (2008) 13:91–104. doi: 10.1016/j.ccr.2008.01.001
69. Yu J, Zhang W, Lu B, Qian H, Tang H, Zhu Z, et al. miR-433 Accelerates Acquired Chemoresistance of Gallbladder Cancer Cells by Targeting Cyclin M. *Oncol Lett* (2018) 15:3305–12. doi: 10.3892/ol.2017.7708
70. Fukui R, Nishimori H, Hata F, Yasoshima T, Ohno K, Nomura H, et al. Et Al: Metastases-related Genes in the Classification of Liver and Peritoneal Metastasis in Human Gastric Cancer. *J Surg Res* (2005) 129:94–100. doi: 10.1016/j.jss.2005.04.030
71. Shang HS, Lu HF, Lee CH, Chiang HS, Chu YL, Chen A, et al. Quercetin Induced Cell Apoptosis and Altered Gene Expression in AGS Human Gastric Cancer Cells. *Environ Toxicol* (2018) 33:1168–81. doi: 10.1002/tox.22623
72. Mori Y, Matsunaga M, Abe T, Fukushige S, Miura K, Sunamura M, et al. Chromosome Band 16q24 is Frequently Deleted in Human Gastric Cancer. *Br J Cancer* (1999) 80:556–62. doi: 10.1038/sj.bjc.6690391
73. Riou P, Saffroy R, Comoy J, Gross-Goupil M, Thiery JP, Emile JF, et al. Investigation in Liver Tissues and Cell Lines of the Transcription of 13 Genes Mapping to the 16q24 Region That are Frequently Deleted in Hepatocellular Carcinoma. *Clin Cancer Res* (2002) 8:3178–86.
74. Kanai Y, Ushijima S, Tsuda H, Sakamoto M, Sugimura T, Hirohashi S. Aberrant DNA Methylation on Chromosome 16 is an Early Event in Hepatocarcinogenesis. *Japanese J Cancer Res Gann* (1996) 87:1210–7. doi: 10.1111/j.1349-7006.1996.tb03135.x
75. Kanai Y, Ushijima S, Tsuda H, Sakamoto M, Hirohashi S. Aberrant DNA Methylation Precedes Loss of Heterozygosity on Chromosome 16 in Chronic Hepatitis and Liver Cirrhosis. *Cancer Lett* (2000) 148:73–80. doi: 10.1016/S0304-3835(99)00316-X
76. Chan SK, Griffith OL, Tai IT, Jones SJ. Meta-Analysis of Colorectal Cancer Gene Expression Profiling Studies Identifies Consistently Reported Candidate Biomarkers. *Cancer Epidemiol Biomarkers Prev* (2008) 17:543–52. doi: 10.1158/1055-9965.EPI-07-2615
77. Magee JA, Araki T, Patil S, Ehrig T, True L, Humphrey PA, et al. Expression Profiling Reveals Hepsin Overexpression in Prostate Cancer. *Cancer Res* (2001) 61:5692–6.
78. Leman ES, Magheli A, Yong KM, Netto G, Hinz S, Getzenberg RH. Identification of Nuclear Structural Protein Alterations Associated With Seminomas. *J Cell Biochem* (2009) 108:1274–9. doi: 10.1002/jcb.22357
79. Han SW, Ahn JY, Lee S, Noh YS, Jung HC, Lee MH, et al. Gene Expression Network Analysis of Lymph Node Involvement in Colon Cancer Identifies AHSA2, CDK10, and CWC22 as Possible Prognostic Markers. *Sci Rep* (2020) 10:7170. doi: 10.1038/s41598-020-63806-x
80. Zehra M, Mushtaq S, Ghulam Musharraf S, Ghani R, Ahmed N. Association of Cyclin Dependent Kinase 10 and Transcription Factor 2 During Human Corneal Epithelial Wound Healing *In Vitro* Model. *Sci Rep* (2019) 9:11802. doi: 10.1038/s41598-019-48092-6
81. Robert T, Johnson JL, Guichaoua R, Yaron TM, Bach S, Cantley LC, et al. Development of a CDK10/CycM *In Vitro* Kinase Screening Assay and Identification of First Small-Molecule Inhibitors. *Front Chem* (2020) 8:147. doi: 10.3389/fchem.2020.00147
82. Jung C, Motwani M, Kortmansky J, Sirotnak FM, She Y, Gonen M, et al. The Cyclin-Dependent Kinase Inhibitor Flavopiridol Potentiates Gamma-Irradiation-Induced Apoptosis in Colon and Gastric Cancer Cells. *Clin Cancer Res* (2003) 9:6052–61.
83. Miyashita K, Shiraki K, Fuke H, Inoue T, Yamanaka Y, Yamaguchi Y, et al. The Cyclin-Dependent Kinase Inhibitor Flavopiridol Sensitizes Human Hepatocellular Carcinoma Cells to TRAIL-induced Apoptosis. *Int J Mol Med* (2006) 18:249–56. doi: 10.3892/ijmm.18.2.249
84. Ang C, O'Reilly EM, Carvajal RD, Capanu M, Gonen M, Doyle L, et al. A Nonrandomized, Phase II Study of Sequential Irinotecan and Flavopiridol in Patients With Advanced Hepatocellular Carcinoma. *Gastrointestinal Cancer Res GCR* (2012) 5:185–9.
85. Aklilu M, Kindler HL, Donehower RC, Mani S, Vokes EE. Phase II Study of Flavopiridol in Patients With Advanced Colorectal Cancer. *Ann Oncol* (2003) 14:1270–3. doi: 10.1093/annonc/mdg343
86. Ibrahim N, Bonnet P, Brion J-D, Peyrat J-F, Bignon J, Levaique H, et al. Identification of a New Series of Flavopiridol-Like Structures as Kinase Inhibitors With High Cytotoxic Potency. *Eur J Med Chem* (2020) 199:112355. doi: 10.1016/j.ejmech.2020.112355

Conflict of Interest: The authors declare that the research was conducted in the absence of any commercial or financial relationships that could be construed as a potential conflict of interest.

frontiers in Oncology

ORIGINAL RESEARCH
published: 19 July 2021
doi: 10.3389/fonc.2021.654439

Biliary Neuroendocrine Neoplasms: Analysis of Prognostic Factors and Development and Validation of a Nomogram

*Shengnan Zhou[1], Shitao Jiang[2], Weijie Chen[1], Haixin Yin[1], Liangbo Dong[1], Hao Zhao[1], Shaoqi Han[1] and Xiaodong He[1]**

[1] General Surgery Department, Peking Union Medical College Hospital, China Academy of Medical Science & Peking Union Medical College, Beijing, China, [2] Liver Surgery Department, Peking Union Medical College Hospital, China Academy of Medical Science & Peking Union Medical College, Beijing, China

OPEN ACCESS

Edited by:
Jaw-Yuan Wang, Kaohsiung Medical University Hospital, Taiwan

Reviewed by:
Ravindra Deshpande, Wake Forest School of Medicine, United States
Wen-Tsan Chang, Kaohsiung Medical University Hospital, Taiwan

***Correspondence:**
Xiaodong He
hxdpumch@163.com

Specialty section:
This article was submitted to Gastrointestinal Cancers, a section of the journal Frontiers in Oncology

Received: *29 January 2021*
Accepted: *05 July 2021*
Published: *19 July 2021*

Citation:
Zhou S, Jiang S, Chen W, Yin H, Dong L, Zhao H, Han S and He X (2021) Biliary Neuroendocrine Neoplasms: Analysis of Prognostic Factors and Development and Validation of a Nomogram. Front. Oncol. 11:654439. doi: 10.3389/fonc.2021.654439

Background: For this study, we explored the prognostic profiles of biliary neuroendocrine neoplasms (NENs) patients and identified factors related to prognosis. Further, we developed and validated an effective nomogram to predict the overall survival (OS) of individual patients with biliary NENs.

Methods: We included a total of 446 biliary NENs patients from the SEER database. We used Kaplan-Meier curves to determine survival time. We employed univariate and multivariate Cox analyses to estimate hazard ratios to identify prognostic factors. We constructed a predictive nomogram based on the results of the multivariate analyses. In addition, we included 28 biliary NENs cases from our center as an external validation cohort.

Results: The median survival time of biliary NENs from the SEER database was 31 months, and the value of gallbladder NENs (23 months) was significantly shorter than that of the bile duct (45 months) and ampulla of Vater (33.5 months, p=0.023). Multivariate Cox analyses indicated that age, tumor size, pathological classification, SEER stage, and surgery were independent variables associated with survival. The constructed prognostic nomogram demonstrated good calibration and discrimination C-index values of 0.783 and 0.795 in the training and validation dataset, respectively.

Conclusion: Age, tumor size, pathological classification, SEER stage, and surgery were predictors for the survival of biliary NENs. We developed a nomogram that could determine the 3-year and 5-year OS rates. Through validation of our central database, the novel nomogram is a useful tool for clinicians in estimating individual survival among biliary NENs patients.

Keywords: biliary neuroendocrine neoplasms, nomogram, prognostic factors, survival rate, SEER database

INTRODUCTION

Neuroendocrine neoplasms represent a group of highly heterogeneous diseases (depending on the primary site) and originate from peptidergic neurons and neuroendocrine cells (1). Gastroenteropancreatic neuroendocrine neoplasms (GEP-NENs) account for approximately 55% of all NENs. However, according to the European Neuroendocrine Tumour Society (ENETS) (2), biliary NENs are relatively rare because the mucosa lacks neuroendocrine cells and likely originates from either multipotent stem cells or neuroendocrine cells in intestinal or gastric metaplasia of the epithelium.

Given the rarity of biliary NENs, the clinicopathological characteristics and prognosis of these patients remain unclear. To date, the literature on biliary NENs is relatively sparse, and most studies are case reports (3, 4). Recently, some retrospective studies (5) with small samples have provided prognostic factors. For example, neuroendocrine carcinoma (NEC), classified by pathology, has been linked to poor prognosis in Korean patients with biliary NENs (6). Our research team also reviewed 28 biliary NENs patients in our center and found that the recurrence of the disease correlated with poor prognosis (7). Since the number of cases in each center was too small to conduct a subgroup analysis of biliary NENs, specifically focusing on the primary site of tumors (8), some studies have been performed according to national databases. For example, Cen et al. (9) selected 248 gallbladder neuroendocrine neoplasms (GB-NENs) patients from the Surveillance, Epidemiology, and End Results (SEER) database; they suggested that age, marital status, tumor size, and SEER stage are prognostic factors. However, none of these risk factors can answer the question—asked by both patients and clinicians—about survival rates, especially in regard to individual survival time. As it happens, nomogram as the graphic depictions of a statistical model that can be used to predict outcomes, and the selective advantage of the nomogram is able to provide a visual interface to aid in calculating the predicted probability that a patient will achieve a particular clinical endpoint and communication with patients.

In the present study, we sought to analyze and compare the prognostic features of biliary NENs based on a relatively large number of cases collected from the SEER database and to develop an elaborate nomogram to predict 3-year and 5-year overall survival (OS) rates based on significant prognostic factors. Further, we carried out external validation for this prediction model using our hospital database.

MATERIALS AND METHODS

Patients

We obtained the data in this study from two sources. The first was from the SEER database. We used the SEER 18 Registries provided by the SEER*Stat Database (version 8.3.8), which consists of information on the neuroendocrine neoplasms of biliary patients (such as demographics, tumor site and morphology, tumor stage, mortality, and therapy). We derived the frequency and case distribution data from the SEER 18 Databases. The other data source was comprised of biliary NENs patients who were diagnosed with NENs and received treatment at Peking Union Medical College Hospital from 1991 to 2017. And histological assessment of tumor tissues and immunohistochemical tests were performed at the Pathology Department of Peking Union Medical College Hospital to confirm pathology and histological classification. Since SEER data are publicly available and all patient data are de-identified, institutional review board approval and informed consent were not required for this study. The included patients from our center provided oral consent and approved by the Institutional Review Board of Peking Union Medical College Hospital (S-K597). This study was performed in accordance with the 1964 Helsinki Declaration and its later amendments ethical standards.

We identified all patients with a diagnosis of neuroendocrine carcinoma, carcinoid, small cell carcinoma, large cell neuroendocrine carcinoma, and mixed adenoneuroendocrine carcinoma (MANEC) of the gallbladder, bile duct, and ampulla of Vater (AoV) using the SEER codes generated from the International Classification of Diseases for Oncology (third edition, ICD-O-3) published by the World Health Organization (WHO). The corresponding ICD-O-3 codes were 8246/3, 8240/3, 8041/3, 8013/3 and 8244/3, respectively. For the primary site of the disease, we used the topographical codes 'C23.9, C22.1, C24.0, C24.9 and C24.1'. In addition, all included cases had a positive pathological diagnosis. We excluded patients for whom demographic or survival information was not available. **Figure 1** outlines the strategy we used to distinguish the selected cases from the SEER database.

Data Extraction

We extracted demographic information (age, sex, race), clinicopathological characteristics (morphology/pathological classification, primary site, tumor size, SEER stage), survival time, and therapy information (surgery) from the chosen cases. We performed the pathological classification of NENs according to the 2010 ENETS/WHO criteria (10): neuroendocrine tumor (G1, G2) and neuroendocrine carcinoma (G3, small cell, large cell).

Survival Analysis

We estimated overall survival time using the Kaplan-Meier method and long-rank test. Overall survival (OS) was defined as the period from the date of diagnosis to the date of death from various causes. Patients alive at the date of the last contact were censored. We used the univariate Cox proportional hazards model to screen out significant prognostic variables (p value<0.1) for further multivariate Cox analysis and to establish their covariate-adjusted effects on survival time. We designed all significant variables in the multivariate Cox regression (p value<0.05) and previously defined 'variables of interest' (site of primary tumor) as prognostic factors in the performance of nomogram construction. We carefully chose variables for inclusion to ensure parsimony of the final model.

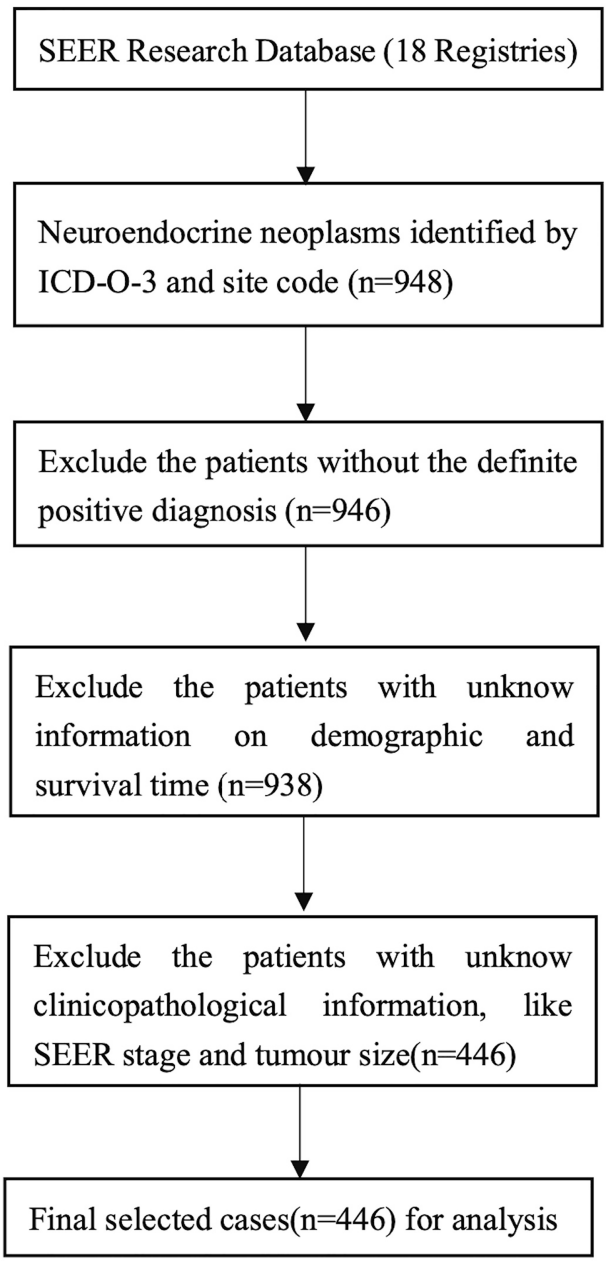

FIGURE 1 | Flowchart displaying the selection procedure of NENs of biliary system cases in the SEER database.

Nomogram Construction and Validation

For nomogram construction and external validation, we used the SEER database as the training set, and harnessed our hospital patient data set as the external validation cohort. We selected the prognostic variables for survival time *via* univariate and multivariate Cox analyses. Based on the predictive model using the identified prognostic factors, we built a nomogram to determine the 3- and 5-year OS rates. The performance of the nomogram validation included its discrimination and calibration curves through the external validation set from our hospital. We evaluated discrimination by employing a concordance index (C-index), which quantifies the probability that of two random patients, the patient who relapses first has a higher probability of the event of interest. A higher C-index indicates better discrimination. We generated a calibration plot by comparing the mean predicted survival rate with the mean actual survival rate, established through Kaplan–Meier analysis. We performed all analyses using SPSS version 25 (IBM, Armonk, NY) and R version 4.0.3. We considered $p<0.05$ to be statistically significant.

RESULTS

Clinical Characteristics

We selected a total of 446 biliary NENs cases diagnosed between 2000 and 2017 from the SEER database. **Table 1** displays the general demographic and clinicopathological features of patients chosen from the SEER database. The majority of primary sites of biliary NENs were the gallbladder (46.4%) and AoV (41.7%). In GB-NENs, the proportion of females (65.7%) was greater than

TABLE 1 | Characteristics of the included patients in SEER database.

	Gallbladder N=207 (%)	Bile duct N=53 (%)	Ampulla of Vater N=186 (%)	Total N=446 (%)
Age				
<65 years	100 (48.3)	33 (62.3)	95 (51.1)	228 (51.1)
≥65 years	107 (51.7)	20 (37.7)	91 (48.9)	218 (48.9)
Gender				
Male	71 (34.3)	36 (67.9)	101 (54.3)	208 (46.6)
Female	136 (65.7)	17 (32.1)	85 (45.7)	238 (53.4)
Race				
White	156 (75.4)	39 (73.6)	142 (76.3)	337 (75.6)
Black	34 (16.4)	6 (11.3)	27 (14.5)	67 (15.0)
Asian/American Indian	17 (8.2)	8 (15.1)	17 (9.1)	42 (9.4)
SEER stage				
Localized	97 (46.9)	20 (37.7)	57 (30.6)	174 (39.0)
Regional	39 (18.8)	28 (52.8)	103 (55.4)	170 (38.1)
Distant	71 (34.3)	5 (9.4)	26 (14.0)	102 (22.9)
Classification				
NET	67 (32.4)	18 (34)	90 (48.4)	175 (39.2)
NEC	131 (63.3)	35 (66)	93 (30.0)	259 (58.1)
MANEC	9 (4.3)	0 (0)	3 (1.6)	12 (2.7)
Surgery				
No surgery	45 (21.7)	12 (22.6)	28 (15.1)	85 (19.1)
Partial excision	37 (17.9)	20 (37.7)	51 (27.4)	108 (24.2)
Total excision	106 (51.2)	8 (15.1)	36 (19.4)	150 (33.6)
Radical surgery	19 (9.2)	13 (24.5)	71 (38.2)	103 (23.1)
Tumor size				
≤2 cm	90 (43.5)	32 (60.4)	114 (61.3)	236 (52.9)
2–5 cm	62 (30.3)	12 (22.6)	68 (36.2)	142 (31.8)
≥5 cm	55 (26.6)	9 (17.0)	4 (2.2)	68 (15.2)

No surgery, no surgery of primary site or autopsy only; Partial excision, simple or partial surgical removal of primary site; Total excision, total surgical removal of primary site; Radical surgery, partial or total removal of the primary site with a resection in continuity (partial or total removal) with other organs.

that of males, which was opposite to the NENs of the bile duct and AoV. Among the 446 NENs cases, according to the 2010 ENETS/WHO classifications, NEC (58.1%) accounted for a higher share than neuroendocrine tumors (NETs) (39.2%) and MANECs (29.7%). Regarding the SEER stage, the probability of metastasis to other organs was 22.9%. An increased number of patients exhibited a tumor size of less than 2 cm (52.9%). Most patients (80.9%) underwent operation therapy; among these operations, we classified them into three categories: partial excision, total excision, and radical surgery. More than half of the operations involved complete excision of the lesion. In addition, 28 patients from Peking Union Medical College Hospital were investigated; our colleagues have reported on their characteristics (7).

Figure 2 depicts the Kaplan-Meier curves based on age, race, sex, classification, SEER stage, tumor size, primary site, and surgical options. The median OS of all included patients was 31 months. Patients younger than 65 years (43.5 months) and NETs (62 months) had longer median survival times than patients older than 65 years (19 months), neuroendocrine carcinomas (NECs) (18 months), and MANECs (12 months). With the increased severity of the SEER stage, the median survival time of patients gradually decreased (localized: regional: distant = 57: 29.5: 8.5 months). Further, patients with a smaller tumor size had better survival outcomes; the median survival time of patients with a size less than 2 cm was 55.5 months. All differences were statistically significant ($p<0.001$) through the long-rank test. We also found that patients with a primary site in the bile duct (median survival time: 45 months) had a significantly better outcome than patients with a primary site in the gallbladder (23 months) and AoV (33.5 months; $p=0.023$). Among the patients who underwent surgery, we discovered that whether the excision was partial or total had a beneficial effect on survival time. However, we did not detect increased survival time in radical surgery compared with patients who only had tumor excision.

Table 2 presents the results of univariate and multivariate Cox analyses of biliary NENs patients from the SEER database. We regarded being older than 65, the classifications of NECs and MANECs, regional and distant stage, and the tumor size greater than 2 cm to be significant risk factors for decreased survival time. In addition, we associated the excision of primary tumors with prolonged survival time.

Nomogram Construction and Validation

In addition to the primary site ($p=0.476$ and 0.459)—which we previously defined as 'variables of interest'—we recognized the following variables as prognostic factors for survival time in multivariate Cox regression analysis: age, pathological classification, stage, surgery, and tumor size. Therefore, we included all of the above variables to develop the nomogram for survival time. The nomogram can be used to predict the probability of a patient's survival rate at 3 or 5 years (**Figure 3**). The nomogram is a graphic depiction of the model, the figure legends describe how to use the nomograms. The concordance index (C-index) of this Cox model was 0.783 (95% CI: 0.754-0.812). We performed external verification of the nomogram. The outcomes of external verification indicated that the C-index of the nomogram was 0.795 (95% CI: 0.632-0.958). **Figure 4** portrays the calibration plots for the external cross-validation at 3 years and 5 years. The x-axis represents the survival rate predicted by the nomogram, whereas the y-axis denotes the actual survival rate obtained using the Kaplan–Meier method. The findings demonstrate that the predicted 3-year and 5-year OS rates closely correspond to the actual survival rates.

DISCUSSION

In our study, by reviewing the clinicopathological characteristics of biliary NENs patients and exploring the prognosis and related risk factors, we developed a nomogram for the prediction of 3-year and 5-year survival rates for these patients, and performed nomogram validation using the data from our center. By using the Kaplan–Meier method and univariate and multivariate Cox analysis, we found that being older than 65 years, advanced SEER stage, increased tumor size, and pathological classification of NECs was statistically and significantly related to decreased survival time. Moreover, biliary NENs patients who underwent surgery had a better survival outcome. The developed nomogram model we used helps to easily ascertain clinical and pathological risk factors to predict the OS time for patients and physicians.

Previous studies, including case reports and literature reviews, have studied the survival time and risk factors for the prognosis of NENs with different classifications at various biliary system sites. Ayabe et al. (11) illustrated that the median OS of 300 GB-NENs, selected from NCDB Participant User Files (PUFs), was 25 months, which is similar to our result (23 months) of 207 GB-NENs. However, Karim et al. (12) reviewed the prognosis of gallbladder-NENs (GB-NENs), and discovered the median survival time to be only 9.8 months among 278 patients with GB-NENs from the SEER database, which was far below our finding. This is probably because our studies contain a certain number of well-differentiated NENs cases, which are associated with better outcomes (13, 14). Therefore, we performed subgroup analysis in these 207 cases according to pathological classification. The median survival times for NECs and MANECs were 11 months and 9 months, respectively, which is also supported by the results of Acosta et al. (15). Therefore, the pathological classification underscores this survival difference, and once again confirms that the ENETS/WHO classification is a vital prognostic factor (16). Based on this, we continued to implement subgroup analysis of NENs in the bile duct and ampulla. **Table 3** outlines the results. As the bile duct is the extremely rare primary site of NENs, with an incidence of extrahepatic bile duct NENs of 0.32% (17) among digestive system NENs, studies that focus on a statistical analysis of patient survival are usually unable to proceed, and most are case reports. However, one study (18) reported that the median survival of extrahepatic cholangiocarcinoma with neuroendocrine differentiation fluctuates between 21 and 27 months. Similar to our outcomes, the median survival of bile duct NECs was 28 months. With regard to the AoV, Randle et al. (19) indicated that the median

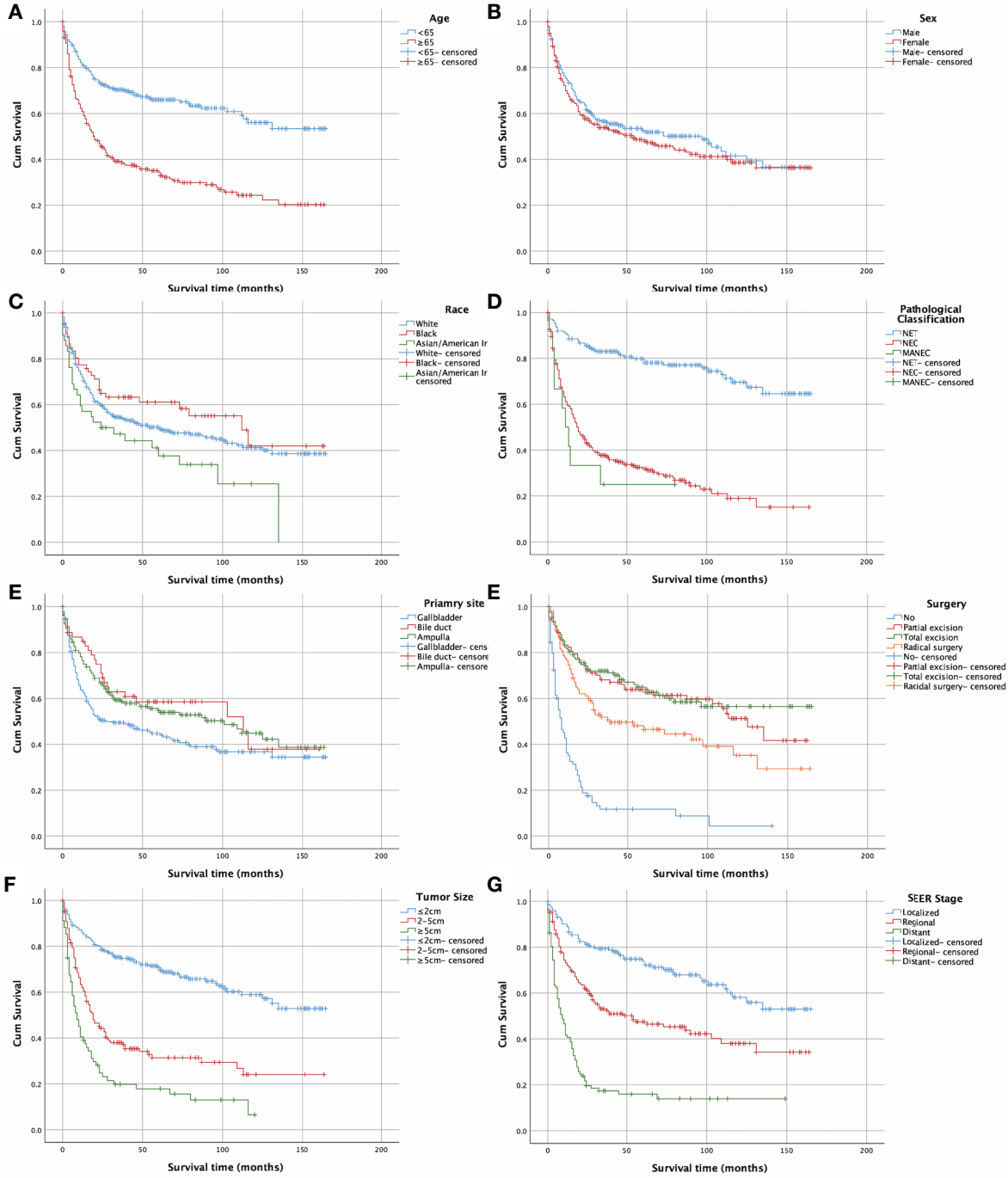

FIGURE 2 | Kaplan–Meier curves of OS according to **(A)** age, **(B)** sex, **(C)** race, **(D)** pathological classification, **(E)** primary site, **(F)**surgery, **(G)** tumour size, and **(H)** SEER stage.

survival of ampullary NENs was 98 months and far higher than our results (33.5 months). This difference may be due to the bias in the inclusion of patients. Hence, it is not objective to discuss the prognosis of NENs patients while ignoring the pathological classification and primary site.

In addition to the pathological classification related to the prognosis of the biliary system, other clinical or pathological characteristics obtained in the course of diagnosis and treatment can be used to evaluate individual outcomes. For example, patients with metastasis—regardless of regional lymph nodes

TABLE 2 | Univariate and multivariate Cox analysis of survival time in patients selected from SEER database.

Variables	Univariate analysis		Multivariate analysis	
	HR (95%)	p	HR (95%)	p
Sex				
Male	1		–	
Female	1.119 (0.864-1.449)	0.309	–	–
Age				
<65 years	1		1	
≥65 years	2.596 (1.981-3.402)	**<0.001**	2.216 (1.677-2.930)	**<0.001**
Race				
White	1		–	
Black	0.794 (0.536-1.177)	0.251	0.867 (0.579-1.302)	0.495
Asian/American Indian	1.493 (1.002-2.226)	**0.049**	1.272 (0.844-1.917)	0.250
Classification				
NET	1		1	
NEC	4.892 (3.480-6.876)	**<0.001**	2.585 (1.748-3.822)	**<0.001**
MANEC	6.522 (3.156-13.481)	**<0.001**	2.925 (1.351-6.336)	**0.006**
Primary site				
Gallbladder	1		1	
Biliary tract	0.652 (0.824-1.518)	**0.056**	0.836 (0.510-1.369)	0.476
Ampulla	0.714 (0.542-0.941)	**0.017**	0.873 (0.611-1.249)	0.459
SEER Stage				
Localized	1		1	
Regional	2.133 (1.527-2.978)	**<0.001**	1.343 (0.917-1.968)	0.130
Distant	5.908 (4.178-8.355)	**<0.001**	2.006 (1.338-3.006)	**<0.001**
Surgery				
No surgery	1		1	
Partial excision	0.204 (0.140 -0.298)	**<0.001**	0.474 (0.315-0.715)	**<0.001**
Total excision	0.185 (0.129-0.265)	**<0.001**	0.398 (0.263-0.601)	**<0.001**
Radical surgery	0.320 (0.225-0.454)	**<0.001**	0.556 (0.370-0.836)	**0.005**
Tumor size				
≤2 cm	1		1	
2-5 cm	2.933 (2.171-3.963)	**<0.001**	1.578 (1.131-2.201)	**0.007**
≥5 cm	5.136 (3.633-7.260)	**<0.001**	1.879 (1.204-2.931)	**0.005**

The bold p value in the column of univariate analysis means that the variable was selected in the next multivariate analysis, and the bold p value in the column of multivariate analysis means that the variable was included in the construction of the nomogram.

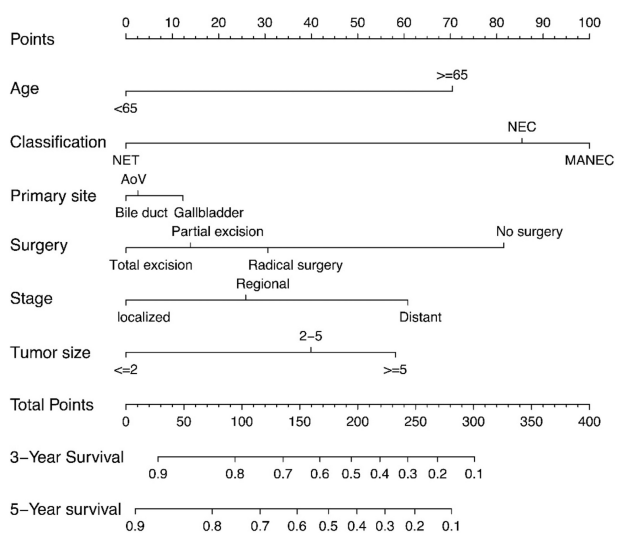

FIGURE 3 | Nomograms predicting 3-year and 5-year rates of OS. Summarizing the scores of each variables together and the total points projected on the bottom scales indicate the probabilities of 3- and 5-year overall survival.

(20) or adjacent and distant organs—without resection of primary tumors (21) are more likely to have shorter survival times. Tumor size may also be a usable prognostic factor, but remains controversial. Kurita et al. (22) revealed that small, localized (≤ 2 cm) pancreatic neuroendocrine neoplasms have a better outcome. When the primary site was converted to the biliary system (7), tumor size was no longer a specific independent prognostic factor associated with survival time, perhaps because the diameter of the bile duct was too small to have enough space for tumor intraluminal growth. For tumor sizes of less than 1 cm, the possibility of distant metastasis is 67%, higher than that of sizes ranging between 1 and 2 cm (27.6%) and over 2 cm (28.6%) (23), so it is not recommended to predict prognosis by tumor size. However, our findings of the univariate and multivariable Cox regression analyses signal that tumor size is an independent prognostic factor. Perhaps the larger sample size and several primary sites contained could account for the differences between our results and those of prior research. Interestingly, the median survival of NENs patients who underwent radical surgery was lower than that of patients who received partial and total tumor excision. This is likely because among the 103 patients who had radical surgery, the proportion of NECs and MANECs was 66.1%, and the share of NECs and

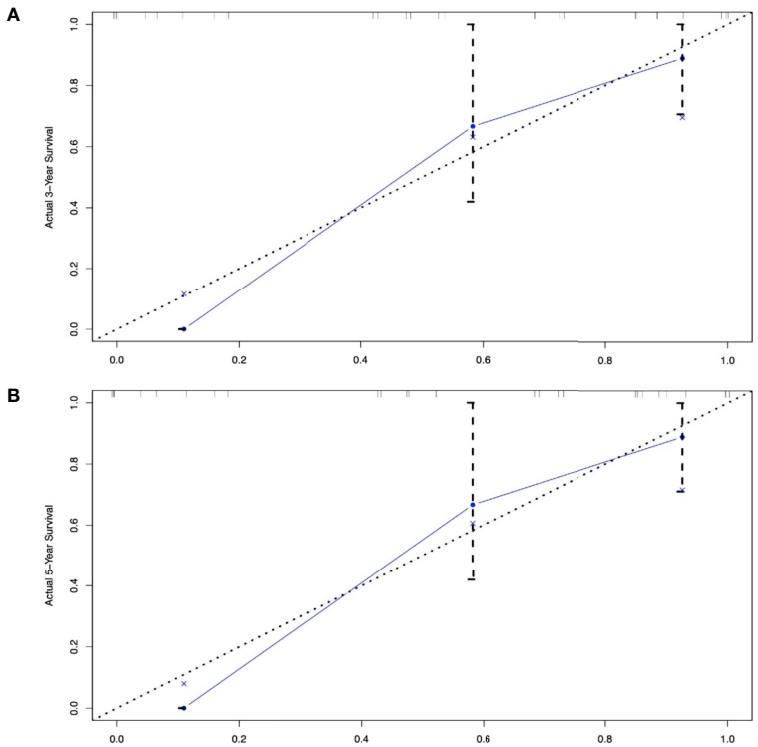

FIGURE 4 | External calibration plot: **(A)** 3-year and **(B)** 5-year OS nomogram calibration curves.

MANECs (46.9%) was lower in patients who received partial excision and total excision. One study (9) with similar results to ours showed that the combination of gallbladder surgery and lymphadenectomy had no effect on survival outcomes.

Although the multivariable Cox analysis in our research identified prognostic factors—age, SEER stage, surgery, tumor size, and pathological classification—these variables could not provide an accurate and discriminatory prediction for biliary system NENs, especially the survival rates that have been a concern for clinicians, patients, and their families. Thus, a prognostic prediction model is needed to answer these questions. For NENs, the TNM staging system (24) and ENETS/WHO classifications (25) have a certain predictive value; the former focuses on the tumor's invasive nature, while the latter emphasizes the pathological classification. It is with great regret that confusion will likely arise from these parallel systems. The nomogram rose in response to the proper time and conditions based on these systems, including effective variables to enhance predictive ability. Regarding the nomogram in NENs, preceding studies have demonstrated its predictive value in the OS of gastric neuroendocrine neoplasms (26), the pancreas (27, 28), the small intestine (29, 30), the rectum (31), and the digestive system (32). These outcomes all signal that a specific, clinically applicable nomogram can accurately estimate the prognosis of patients with NENs. However, there is no prognostic model for biliary NENs. Our study filled this gap by creating a nomogram model to establish the OS rate of biliary NENs based on a large database. This nomogram has a predictive value with a C-index of 0.795 (95% CI: 0.632-0.958). In addition, the calibration plots of external validation, using our central database, demonstrated that the predicted 3- and 5-year OS rates closely corresponded with the actual survival rates, and verified that the nomogram exhibited excellent predictive ability. We applied the nomogram in an external validation dataset and showed that the nomogram had a good predictive value (the C-index for calibration is 0.852; 95% CI: 0.777-0.927). Hence, the nomogram can be employed to assess individual clinical outcomes more objectively.

Our study also has limitations. A major constraint is that our nomogram was created using just six clinicopathological factors, lacking other additional variables such as Ki-67 (33, 34), and the high Ki-67 index is associated with portal venous tumor invasion which is a prognostic factor for patients with pancreatic NENs

TABLE 3 | Median survival time (months) of different classification.

Items	Gallbladder	Bile duct	Ampulla
NET	79	78	50.5
NEC	11	28	24
MANEC	9	–	33
All	23	45	33.5

(35). Besides, lactate dehydrogenase (LDH) has been found to increase in patients with NEC (36). However, these variables are not available in the SEER database and it's necessary to incorporate LDH level and Ki-67 into analysis in further investigation. Another obstacle is that the sample size of the validation cohort was small, and only one center was included. Although the verification results and power analysis (Power = 0.8689) were good, the value of the C-index may change after adding samples or centers. Future studies could include validation cohorts from different centers to control for selection bias to some extent. Besides, in terms of treatment of NENs, we only considered the effects of surgery on prognosis, ignoring neoadjuvant or adjuvant therapy (37), as well as other medical therapies, like somatostatin analogues, peptide receptor radionuclide therapy (38) and target therapies. The last limitation is that we regard the AoV as part of the biliary system, but from an anatomical angle, the AoV is the junction between the bile duct and the pancreatic duct. The SEER database did not provide anatomical information on AoV. With the accumulation of cases, subgroup analysis could be performed in future studies according to the primary location of the disease.

CONCLUSION

In conclusion, age, tumor size, pathological classification, surgery, and SEER stage are predictors for the survival of biliary NENs patients. We established and externally validated an unprecedented nomogram to determine the prognoses of patients with biliary NENs. Because our nomogram included only six common clinicopathological variables, it can be used as a potentially objective clinical tool for physicians to predict the prognosis of these patients around the world.

DATA AVAILABILITY STATEMENT

The raw data supporting the conclusions of this article will be made available by the authors, without undue reservation.

ETHICS STATEMENT

The studies involving human participants were reviewed and approved by Institutional Review Board of Peking Union Medical College Hospital. Written informed consent for participation was not required for this study in accordance with the national legislation and the institutional requirements.

AUTHOR CONTRIBUTIONS

SZ participated in the design of this study and wrote the manuscript. XH conceived the original idea, supervised the overall direction and planning of the project. SZ, SJ, HY, LD, WC, SH, and HZ contributed to the acquisition of the data, analysis, and interpretation of the data. All authors contributed to the article and approved the submitted version.

FUNDING

This study was funded by CAMS Innovation Fund for Medical Sciences (CIFMS, 2017-I2M-4-003), and Program Focus Health of Liver and Gallbladder in Elder (ZYJ201912).

ACKNOWLEDGMENTS

We gratefully acknowledge the help of SJ for his constant encouragement and guidance. Without his consistent and illuminating instruction, this thesis could not have reached its present form.

SUPPLEMENTARY MATERIAL

The Supplementary Material for this article can be found online at: https://www.frontiersin.org/articles/10.3389/fonc.2021.654439/full#supplementary-material

REFERENCES

1. Mafficini A, Scarpa A. Genetics and Epigenetics of Gastroenteropancreatic Neuroendocrine Neoplasms. *Endocr Rev* (2019) 40(2):506–36. doi: 10.1210/er.2018-00160
2. O'Toole D, Kianmanesh R, Caplin M. ENETS 2016 Consensus Guidelines for the Management of Patients With Digestive Neuroendocrine Tumors: An Update. *Neuroendocrinology* (2016) 103(2):117–8. doi: 10.1159/000443169
3. Hosoda K, Kobayashi A, Shimizu A, Kitagawa N, Ito T, Yamada A, et al. Neuroendocrine Tumor of the Common Bile Duct. *Surgery* (2016) 160 (2):525–6. doi: 10.1016/j.surg.2016.01.001
4. Skalicky A, Vistejnova L, Dubova M, Malkus T, Skalicky T, Troup O. Mixed Neuroendocrine-Non-Neuroendocrine Carcinoma of Gallbladder: Case Report. *World J Surg Oncol* (2019) 17(1):55. doi: 10.1186/s12957-019-1598-4
5. Kim J, Lee WJ, Lee SH, Lee KB, Ryu JK, Kim YT, et al. Clinical Features of 20 Patients With Curatively Resected Biliary Neuroendocrine Tumours. *Dig Liver Dis* (2011) 43(12):965–70. doi: 10.1016/j.dld.2011.07.010
6. Lee KJ, Cho JH, Lee SH, Lee KH, Park BK, Lee JK, et al. Clinicopathological Characteristics of Biliary Neuroendocrine Neoplasms: A Multicenter Study. *Scand J Gastroenterol* (2017) 52(4):437–41. doi: 10.1080/00365521.2016.1261938
7. Zheng Z, Chen C, Li B, Liu H, Zhou L, Zhang H, et al. Biliary Neuroendocrine Neoplasms: Clinical Profiles, Management, and Analysis of Prognostic Factors. *Front Oncol* (2019) 9:38. doi: 10.3389/fonc.2019.00038
8. Yao JC, Hassan M, Phan A, Dagohoy C, Leary C, Mares JE, et al. One Hundred Years After "Carcinoid": Epidemiology of and Prognostic Factors for Neuroendocrine Tumors in 35,825 Cases in the United States. *J Clin Oncol* (2008) 26(18):3063–72. doi: 10.1200/JCO.2007.15.4377
9. Cen D, Liu H, Wan Z, Lin Z, Wang Y, Xu J, et al. Clinicopathological Features and Survival for Gallbladder NEN: A Population-Based Study. *Endocr Connect* (2019) 8(9):1273–81. doi: 10.1530/EC-19-0124
10. Klimstra DS, Modlin IR, Coppola D, Lloyd RV, Suster S. The Pathologic Classification of Neuroendocrine Tumors: A Review of Nomenclature, Grading, and Staging Systems. *Pancreas* (2010) 39(6):707–12. doi: 10.1097/MPA.0b013e3181ec124e

11. Ayabe RI, Wach M, Ruff S, Martin S, Diggs L, Wiemken T, et al. Primary Gallbladder Neuroendocrine Tumors: Insights Into a Rare Histology Using a Large National Database. *Ann Surg Oncol* (2019) 26(11):3577–85. doi: 10.1245/s10434-019-07440-6
12. Eltawil KM, Gustafsson BI, Kidd M, Modlin IM. Neuroendocrine Tumors of the Gallbladder: An Evaluation and Reassessment of Management Strategy. *J Clin Gastroenterol* (2010) 44(10):687–95. doi: 10.1097/MCG.0b013e3181d7a6d4
13. Hofland J, Kaltsas G, de Herder WW. Advances in the Diagnosis and Management of Well-Differentiated Neuroendocrine Neoplasms. *Endocr Rev* (2020) 41(2):371–403. doi: 10.1210/endrev/bnz004
14. Rindi G, Wiedenmann B. Neuroendocrine Neoplasia of the Gastrointestinal Tract Revisited: Towards Precision Medicine. *Nat Rev Endocrinol* (2020) 16 (10):590–607. doi: 10.1038/s41574-020-0391-3
15. Acosta AM, Wiley EL. Primary Biliary Mixed Adenoneuroendocrine Carcinoma (MANEC): A Short Review. *Arch Pathol Lab Med* (2016) 140 (10):1157–62. doi: 10.5858/arpa.2015-0102-RS
16. O'Toole D, Kianmanesh R, Caplin M. ENETS 2016 Consensus Guidelines for the Management of Patients With Digestive Neuroendocrine Tumors: An Update. *Neuroendocrinology* (2016) 103(2):117–8. doi: 10.1159/000443169
17. Modlin IM, Lye KD, Kidd M. A 5-Decade Analysis of 13,715 Carcinoid Tumors. *Cancer* (2003) 97(4):934–59. doi: 10.1002/cncr.11105
18. Hong SM, Kim MJ, Pi DY, Jo D, Yu E, Ro JY. Neuroendocrine Differentiation in Extrahepatic Bile Duct Carcinomas and its Prognostic Significance. *Hum Pathol* (2005) 36(7):732–40. doi: 10.1016/j.humpath.2005.05.002
19. Randle RW, Ahmed S, Newman NA, Clark CJ. Clinical Outcomes for Neuroendocrine Tumors of the Duodenum and Ampulla of Vater: A Population-Based Study. *J Gastrointest Surg* (2014) 18(2):354–62. doi: 10. 1007/s11605-013-2365-4
20. Yan S, Wang Y, Chen X, Zhang Y, Huang Z, Zhao J, et al. Clinical Analysis of 15 Cases of Gallbladder Neuroendocrine Carcinoma and Comparison With Gallbladder Adenocarcinoma Using a Propensity Score Matching. *Cancer Manag Res* (2020) 12:1437–46. doi: 10.2147/CMAR.S227501
21. Oh TG, Chung MJ, Park JY, Bang SM, Park SW, Chung JB, et al. Prognostic Factors and Characteristics of Pancreatic Neuroendocrine Tumors: Single Center Experience. *Yonsei Med J* (2012) 53(5):944–51. doi: 10.3349/ymj.2012.53.5.944
22. Kurita Y, Hara K, Kuwahara T, Mizuno N, Okuno N, Haba S, et al. Comparison of Prognosis Between Observation and Surgical Resection Groups With Small Sporadic Non-Functional Pancreatic Neuroendocrine Neoplasms Without Distant Metastasis. *J Gastroenterol* (2020) 55(5):543–52. doi: 10.1007/s00535-019-01655-w
23. Michalopoulos N, Papavramidis TS, Karayannopoulou G, Pliakos I, Papavramidis ST, Kanellos I. Neuroendocrine Tumors of Extrahepatic Biliary Tract. *Pathol Oncol Res* (2014) 20(4):765–75. doi: 10.1007/s12253-014-9808-4
24. Yang M, Zhang Y, Zeng L, Ke NW, Tan CL, Tian BL, et al. Prognostic Validity of the American Joint Committee on Cancer Eighth Edition Tnm Staging System for Surgically Treated and Well-Differentiated Pancreatic Neuroendocrine Tumors: A Comprehensive Analysis of 254 Consecutive Patients From a Large Chinese Institution. *Pancreas* (2019) 48(5):613–21. doi: 10.1097/MPA.0000000000001305
25. Kloppel G, Rindi G, Perren A, Komminoth P, Klimstra DS. The ENETS and AJCC/UICC TNM Classifications of the Neuroendocrine Tumors of the Gastrointestinal Tract and the Pancreas: A Statement. *Virchows Arch* (2010) 456(6):595–7. doi: 10.1007/s00428-010-0924-6
26. Zhang S, Tong YX, Zhang XH, Zhang YJ, Xu XS, Xiao AT, et al. A Novel and Validated Nomogram to Predict Overall Survival for Gastric Neuroendocrine Neoplasms. *J Cancer* (2019) 10(24):5944–54. doi: 10.7150/jca.35785
27. Liang W, Yang P, Huang R, Xu L, Wang J, Liu W, et al. A Combined Nomogram Model to Preoperatively Predict Histologic Grade in Pancreatic Neuroendocrine Tumors. *Clin Cancer Res* (2019) 25(2):584–94. doi: 10.1158/1078-0432.CCR-18-1305
28. Ellison TA, Wolfgang CL, Shi C, Cameron JL, Murakami P, Mun LJ, et al. A Single Institution's 26-Year Experience With Nonfunctional Pancreatic Neuroendocrine Tumors: A Validation of Current Staging Systems and a New Prognostic Nomogram. *Ann Surg* (2014) 259(2):204–12. doi: 10.1097/SLA.0b013e31828f3174
29. Modlin IM, Gustafsson BI, Pavel M, Svejda B, Lawrence B, Kidd M. A Nomogram to Assess Small-Intestinal Neuroendocrine Tumor ('Carcinoid') Survival. *Neuroendocrinology* (2010) 92(3):143–57. doi: 10.1159/000319784
30. Levy S, van Veenendaal LM, Korse CM, Breekveldt ECH, Verbeek WHM, Vriens MR, et al. Survival in Patients With Neuroendocrine Tumours of the Small Intestine: Nomogram Validation and Predictors of Survival. *J Clin Med* (2020) 9(8):2502. doi: 10.3390/jcm9082502
31. Feng X, Wei G, Wang W, Zhang Y, Zeng Y, Chen M, et al. Nomogram for Individually Predicting Overall Survival in Rectal Neuroendocrine Tumours. *BMC Cancer* (2020) 20(1):865. doi: 10.1186/s12885-020-07328-9
32. Lin Z, Wang H, Zhang Y, Li G, Pi G, Yu X, et al. Development and Validation of a Prognostic Nomogram to Guide Decision-Making for High-Grade Digestive Neuroendocrine Neoplasms. *Oncologist* (2020) 25(4):e659–e67. doi: 10.1634/theoncologist.2019-0566
33. Pulvirenti A, Javed AA, Landoni L, Jamieson NB, Chou JF, Miotto M, et al. Multi-Institutional Development and External Validation of a Nomogram to Predict Recurrence After Curative Resection of Pancreatic Neuroendocrine Tumors. *Ann Surg* (2019). doi: 10.1097/sla.0000000000003579
34. Centonze G, Lagano V, Sabella G, Mangogna A, Garzone G, Filugelli M, et al. Myeloid and T-Cell Microenvironment Immune Features Identify Two Prognostic Sub-Groups in High-Grade Gastroenteropancreatic Neuroendocrine Neoplasms. *J Clin Med* (2021) 10(8):1741. doi: 10.3390/jcm10081741
35. Kato T, Kudo A, Kinowaki Y, Ishikawa Y, Watanabe S, Akahoshi K, et al. A Novel Classification of Portal Venous Tumor Invasion to Predict Residual Tumor Status After Surgery in Patients With Pancreatic Neuroendocrine Neoplasms. *J Cancer Res Clin Oncol* (2021). doi: 10.1007/s00432-021-03660-0
36. Shiba S, Morizane C, Hiraoka N, Sasaki M, Koga F, Sakamoto Y, et al. Pancreatic Neuroendocrine Tumors: A Single-Center 20-Year Experience With 100 Patients. *Pancreatology* (2016) 16(1):99–105. doi: 10.1016/j.pan.2015.11.001
37. Jeong H, Shin J, Jeong JH, Kim KP, Hong SM, Kim YI, et al. Capecitabine Plus Temozolomide in Patients With Grade 3 Unresectable or Metastatic Gastroenteropancreatic Neuroendocrine Neoplasms With Ki-67 Index <55%: Single-Arm Phase II Study. *ESMO Open* (2021) 6(3):100119. doi: 10.1016/j.esmoop.2021.100119
38. Basu S, Parghane RV, Kamaldeep, Chakrabarty S. Peptide Receptor Radionuclide Therapy of Neuroendocrine Tumors. *Semin Nucl Med* (2020) 50(5):447–64. doi: 10.1053/j.semnuclmed.2020.05.004

Conflict of Interest: The authors declare that the research was conducted in the absence of any commercial or financial relationships that could be construed as a potential conflict of interest.

frontiers in Oncology

ORIGINAL RESEARCH
published: 27 July 2021
doi: 10.3389/fonc.2021.670396

Mucin-1 Protein Is a Prognostic Marker for Pancreatic Ductal Adenocarcinoma: Results From the CONKO-001 Study

Jana Käthe Striefler[1], Hanno Riess[1], Philipp Lohneis[2], Sven Bischoff[1], Annika Kurreck[1], Dominik Paul Modest[1], Marcus Bahra[3], Helmut Oettle[4], Marianne Sinn[5], Henrik Bläker[6], Carsten Denkert[7], Sebastian Stintzing[1], Bruno Valentin Sinn[8†] and Uwe Pelzer[1†]*

[1] Department of Hematology, Oncology, and Tumor Immunology, Charité–Universitätsmedizin Berlin, Corporate Member of Freie Universität Berlin, Humboldt-Universität zu Berlin, and Berlin Institute of Health, Berlin, Germany, [2] Faculty of Medicine and University Hospital Cologne, Institute of Pathology, University of Cologne, Cologne, Germany, [3] Department of Surgery, Charité – Universitätsmedizin Berlin, Corporate Member of Freie Universität Berlin, Humboldt-Universität zu Berlin, and Berlin Institute of Health, Berlin, Germany, [4] Dayclinic for Oncology and Hematology, Outpatient Department of Medical Oncology, Friedrichshafen, Germany, [5] University Medical Center Hamburg-Eppendorf, Oncology, Hematology and Bone Marrow Transplantation with the Section Pneumology (II Medical Clinic and Polyclinic), Hamburg, Germany, [6] Institute of Pathology, Leipzig University Medicine, Leipzig, Germany, [7] Institute of Pathology, University Clinic of Gießen and Marburg, Marburg, Germany, [8] Institute of Pathology, Charité–Universitätsmedizin Berlin, Corporate Member of Freie Universität Berlin, Humboldt-Universität zu Berlin, and Berlin Institute of Health, Berlin, Germany

OPEN ACCESS

Edited by:
Jaw-Yuan Wang, Kaohsiung Medical University Hospital, Taiwan

Reviewed by:
Stefan Kasper-Virchow, Essen University Hospital, Germany
Nelson J. Dusetti, Institut National de la Santé et de la Recherche Médicale (INSERM), France

***Correspondence:**
Jana Käthe Striefler
jana.striefler@charite.de

[†]These authors have contributed equally to this work

Specialty section:
This article was submitted to Gastrointestinal Cancers, a section of the journal Frontiers in Oncology

Received: *21 February 2021*
Accepted: *24 June 2021*
Published: *27 July 2021*

Citation:
Striefler JK, Riess H, Lohneis P, Bischoff S, Kurreck A, Modest DP, Bahra M, Oettle H, Sinn M, Bläker H, Denkert C, Stintzing S, Sinn BV and Pelzer U (2021) Mucin-1 Protein Is a Prognostic Marker for Pancreatic Ductal Adenocarcinoma: Results From the CONKO-001 Study. Front. Oncol. 11:670396. doi: 10.3389/fonc.2021.670396

Background: The Mucin-family protein, MUC1, impacts on carcinogenesis and tumor invasion. We evaluated the impact of MUC1 expression on outcome in a cohort of 158 patients with resected pancreatic ductal adenocarcinomas (PDAC) in the CONKO-001 study (adjuvant gemcitabine [gem] *vs*. observation [obs]).

Methods: The percentage of MUC1-positive tumor cells by immunohistochemistry (IHC) and the staining intensity were evaluated by two observers blinded to outcome. The numeric values of both parameters were multiplied, resulting in an immunoreactivity score (IRS) ranging from 0 to 12. The level of MUC1 expression was defined as follows: IRS 0–4 (low) *vs* IRS >4 (high). Outcomes in terms of disease-free (DFS) and overall survival (OS) were evaluated by Kaplan–Meier method, log-rank tests and Cox regressions.

Results: In total, tumors of 158 study patients were eligible for immunohistochemistry of MUC1. High cytoplasmic MUC1 expression was associated with impaired DFS and OS in the overall study population (hazard ratio (HR) for DFS: 0.49, 95% CI 0.31 to 0.78, p = .003; HR for OS: 0.46, 95% CI 0.29 to 0.73, p = .001). In the study arms, prognostic effects of MUC1 were also evident in the observation group (HR for DFS: 0.55; 95% CI 0.29 to 1.04, p = .062; HR for OS: 0.34, 95% CI 0.17 to 0.67, p = .001) and trending in the gem group (HR for DFS: 0.48, 95% CI 0.24 to 0.95, p = .041; HR for OS: 0.56, 95% CI 0.28 to1.11, p = .093).

Conclusion: Our data suggest that MUC1 expression is a powerful prognostic marker in patients with PDAC after curatively intended resection.

Keywords: pancreatic cancer, gemcitabine, MUC1, prognostic marker, CONKO 001 trial, adjuvant therapy

HIGHLIGHTS

- MUC1 is widely used as tumor marker especially in breast, ovarian, lung and pancreatic cancer.
- Low MUC1 expression is significantly associated with favorable prognosis in patients with pancreatic cancer after curatively intended resection.
- Prognostic impact of MUC1 is irrespective of active treatment *vs*. observation in the setting of the CONKO 001 trial.
- MUC1 expression might help to guide adjuvant treatment strategies and improve the outcome of patients at high risk of relapse and death.

INTRODUCTION

Pancreatic Cancer

Adjuvant chemotherapy is standard of care (SOC) in patients with PDAC after R0/R1 resection of the primary tumor with curative intent. Several regimens have been developed, of those gemcitabine monotherapy remains the standard for patients that are unfit for intensive combinations treatment (1–4).

Role of Mucin-1

The transmembrane mucin glycoprotein Mucin-1 (MUC1), also known as CA 15-3, is a member of the mucin family of proteins expressed at the apical surface of epithelial cells. In cancer cells MUC1 accumulates within the mitochondria and the nucleus. The cytoplasmic tail of MUC1 serves as an adaptor protein connecting kinases and other cell signaling proteins, leading to increased cell proliferation, changes in adhesive state of the cell, invasion into the extracellular matrix and deregulation of apoptosis. MUC1 positive carcinomas are associated with a hyperactivation of critical signaling pathways such as mitogen-activated protein kinase (MAPK), phosphatidylinositol 3-kinase (PI3K/Akt) and wingless type (Wnt) pathway (5).

MUC1 as CA 15-3 is widely used as tumor marker especially in breast, ovarian, lung and pancreatic cancer. In breast cancer, MUC1 was shown to provide predictive information for therapy response and also for survival (6). Previous investigations of human tissue specimens suggested a crucial prognostic role for MUC1 in pancreatic adenocarcinoma (7).

Furthermore, as recently shown in murine pancreatic cancer cell lines MUC1 is a potential therapeutic target (8) with small molecules in early clinical development, stimulating the characterization of a potential target population in pancreatic cancer (9).

To the best of our knowledge, no data from prospective clinical trials evaluating the expression and prognostic role of MUC1 in pancreatic cancer patients are available, yet. The aim of our analysis was to evaluate the impact on outcome of MUC1 in the CONKO-001 trial allowing for assessment of effects with and without adjuvant therapy.

Study Population

CONKO-001 was a phase III trial, where 368 patients with pancreatic adenocarcinoma were randomized to an adjuvant treatment with gemcitabine or to observation only after a curatively intended resection.

We aimed to demonstrate that low MUC1 expression is a valuable prognostic factor in pancreatic cancer patients. As this analysis is unplanned and exploratory, the results should be interpreted as such.

METHODS

The Reporting Recommendations for Tumor Marker Prognostic Studies (REMARK) criteria were followed for reporting this study.

Study

Baseline data of CONKO-001: The prospective randomized phase III CONKO-001 trial investigated the role of an adjuvant treatment with gemcitabine as compared to observation. A total of 368 patients with completely resected pancreatic cancer (R0 and R1 resection) were recruited between July 1998 and December 2004. Gemcitabine (1,000 mg/m^2) was given for 6 months in an outpatient setting. Follow-ups were scheduled in eight weekly intervals. Please refer to the existing primary publications of the trial for details (10, 11). The study was approved by the institutional review committee (trial registration isrctn.org Identifier: *ISRCTN34802808*).

Patients

In total, 354 out of 368 patients were included into the survival analysis (gem: n = 179, obs: n = 175). Archival tumor tissue was available from 165 cases.

MUC1

Immunohistochemical staining for Mucin-1 was carried out on tissue microarrays (TMAs) according to standard procedures (1:200; clone MA695; Leica Biosystems Newcastle, Ltd, Newcastle Upon Tyne, UK). To reduce effects of intratumoral heterogeneity, three representative 1-mm-tissue cores (0.785 mm^2) were selected for the construction of tissue microarrays using a manual tissue microarrayer (Beecher Instruments, Sun Prairie, Wisconsin, USA). The stained slides were digitalized (Mirax Scan, Zeiss, Jena, Germany) and evaluated by virtual microscopy using the VMScope Silde Explorer (VMScope, Berlin, Germany) by two observers who were blinded to clinical outcome (MS, BVS). The percentage of positive tumor

Abbreviations: CONSORT, Consolidated Standards of Reporting Trials; DFS, disease-free survival; e.g., exempli gratia; gem, gemcitabine; HR, hazard ratio; IRS, immunoreactivity score; MAPK, mitogen-activated protein kinase; mFOLFIRINOX, modified FOLFIRINOX regime (fluorouracil, leucovorin, irinotecan, oxaliplatin); MUC1, Mucin-1; OS, overall survival; obs, observation; PDAC, pancreatic ductal adenocarcinoma; PI3K/Akt, phosphatidylinositol 3-kinase; REMARK, Reporting Recommendations for Tumor Marker Prognostic Studies; SOC, standard of care; TMA, tissue microarray; Wnt, wingless type; 95% CI, 95% confidence interval.

cells (0% = 0, 1–10% = 1, 11–50% = 2, 51–80% = 3, 81–100% = 4) and the staining intensity (negative = 0, weak = 1, moderate = 2, strong = 3) were evaluated [see **Figure 1**: *Representative TMAs (**A**) MUC1 negative, (**B**) MUC1 low, and (**C**) MUC1 high*]. For quantification of the expression level we used the well-established immunoreactivity score (IRS) ranging from 0 to 12, who is calculated by multiplication of the numeric values of both parameters.

Statistical Considerations

For exploratory statistical analysis, two groups with low or high MUC1 expression were defined based on data distribution (IRS 0–4 *vs.* IRS >4). For determination of the cut-off separating most precisely survival differences an publicly accessible online tool was used (https://molpathoheidelberg.shinyapps.io/CutoffFinder_v1/), for more detailed information please refer to (12). Kaplan–Meier analyses for disease-free survival (DFS) and overall survival (OS) were performed according to MUC1 expression. In multivariable Cox regressions standard clinical and biomarker characteristics (age, sex, treatment arm, T stage, nodal status, grading, resection margin, and Karnofsky index) were investigated.

Disease-free survival (DFS) was defined as time from study entry to local or distant disease relapse, overall survival (OS) as time from study entry to death of any cause. The relation of MUC1 expression with clinical and pathological tumour characteristics was evaluated using χ^2-tests. The Kaplan–Meier method with log-rank tests was used for univariable survival analyses. Cox regressions were used for multivariable survival models. In general, P-values <0.05 (calculated 2-sided) were considered significant.

RESULTS

MUC1 Analyzed Subpopulation

In total, 368 patients were enrolled in the CONKO 001 trial. N = 186 were randomized to the gemcitabine (gem) group and n = 182 to the observation (obs) group. Of those, in n = 165 cases tumor tissue was available for analysis of MUC1 expression. Of these 165 cases, seven samples (gem n = 5, obs n = 2) were excluded from the analysis due to poor quality (see **Figure 2**: *CONSORT diagram MUC1 in CONKO 001*), resulting in 88 cases of the gemcitabine-group and 70 cases of the observational group

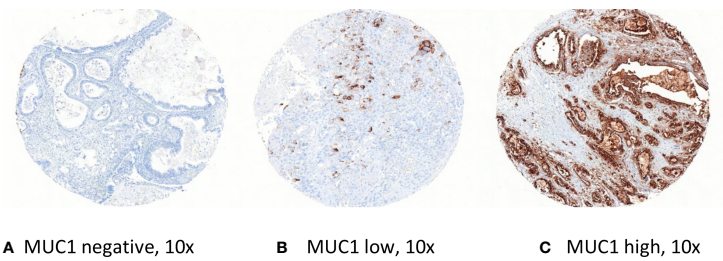

FIGURE 1 | Representative TMAs **(A)** MUC1 negative, **(B)** MUC1 low, and **(C)** MUC1 high.

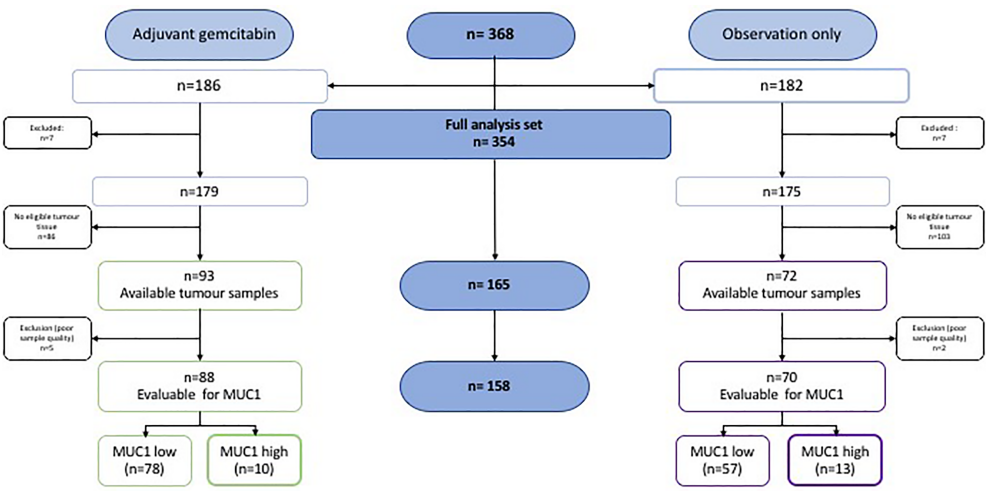

FIGURE 2 | CONSORT diagram MUC1 in CONKO 001.

TABLE 1 | Shown are the relevant clinical and histopathological features of the studied subgroups in which MUC1 expression level was analyzed.

Clinical and histopathological features	Overall study population (n = 354)			MUC1 analyzed subpopulation (n = 158)	
	Overall	Gemcitabine n = 179	Observation n = 175	Gemcitabine n = 88	Observation n = 70
Age					
median (range), y	62 (34–82)	62 (34–82)	62 (36–81)	63 (37–80)	60 (36–81)
<65 years	219 (62)	115 (61)	104 (59)	51	48
≥65 years	135 (38)	64 (36)	71 (41)	37	22
Karnofsky performance status scale					
median (range), %	80 (50–100)	80 (60–100)	80 (50–100)	90 (60–100)	80 (50–100)
>80%	230 (65)	129 (72)	101 (58)	63 (72)	46 (66)
≤80%	124 (35)	50 (28)	74 (42)	25 (28)	24 (34)
Gender, (%)					
male	203 (57)	105 (59)	98 (56)	54 (61)	40 (57)
female	151 (43)	74 (41)	77 (44)	34 (39)	30 (43)
T stage, (%)					
T1–2	49 (14)	25 (14)	24 (14)	9 (10)	7 (10)
T3–4	305 (86)	154 (86)	151 (86)	79 (90)	63 (90)
Nodal status, (%)		5	4		
N–	100 (28)	2 (29)	8 (27)	18 (20)	16 (23)
N+	254 (72)	127 (71)	127 (73)	70 (80)	54 (77)
Grading, (%)					
G1–2	218 (63)	113 (64)	105 (61)	53 (61)	37 (54)
G3	130 (37)	63 (36)	67 (39)	34 (39)	32 (46)
Resection margin, (%)					
R0	293 (83)	145 (81)	148 (85)	73 (83)	55 (79)
R1	61 (17)	34 (19)	27 (15)	15 (17)	15 (21)

Grading was not available in all cases. T1–2, T1–2 stage; T3–4; T3–4 stage; N–, nodal negative stage; N+ nodal positive stage; R0, R0 resection stage; R1, R1 resection stage.

in the analyzed population. The patients′ and the tumor characteristics were well balanced across both groups and did not differ from the overall CONKO 001 study population. Please refer to **Table 1**: *Baseline patients and tumor characteristics*.

Archival Tissue Samples and Staining Results

As described above, sufficient quality of immunohistochemical staining of MUC1 expression was achieved in 158 of 165 tumor samples (gem: n = 88, obs: n = 70). In the gem arm, n = 78 samples were evaluated as low, and n = 10 as high MUC1 expression, respectively. In those patients randomized to observation only, n = 57 were assessed as low, and n = 13 as high MUC1 expression. Cytoplasmic staining was the most frequently observed pattern (please refer to **Figure 2**: *CONSORT diagram MUC1 in CONKO 001*).

Clinical and Histopathological Characteristics of the MUC1 Subpopulation

Patients with low *vs.* high MUC1 expression were found in similar frequencies in both arms of the trial (MUC1 low: gem n = 78, 58%, obs n = 57, 42% *vs.* MUC1 high: gem n = 10, 43% obs n = 13, 57%). The only baseline characteristic that appeared to be associated with MUC1 expression was age. The frequency of patients under the age of 65 was clearly higher in the MUC1 low group (MUC1 low: n = 90, 67% *vs.* MUC1 high: n = 9, 39%; p = .018). No relevant differences in other clinical and histopathological features were found in the MUC1 low *vs.* high cohort (please refer to **Table 2**:

TABLE 2 | Association of MUC1 expression level and selected patient characteristics.

MUC1 analyzed subpopulation, n = (%)			
Clinical and histopathological features	**MUC1 low n = 135 (85)**	**MUC1 high n = 23 (15)**	**p =**
Age			.018
median (range), y	61 (36–79)	67 (37–81)	
<65 years	90 (67)	9 (39)	
≥65 years	45 (33)	14 (61)	
Karnofsky performance status scale			.999
median (range), %	80 (50–100)	80 (70–100)	
>80%	93 (69)	16 (70)	
≤80%	42 (31)	7 (30)	
Gender, (%)			.649
male	79 (59)	15 (65)	
female	56 (41)	8 (35)	
T stage, (%)			.471
T1–2	15 (11)	1 (4)	
T3–4	120 (89)	22 (96)	
Nodal status, (%)			.586
N–	28 (21)	6 (26)	
N+	107 (79)	17 (74)	
Grading, (%)			.171
G1–2	80 (60)	10 (43)	
G3	53 (40)	13 (57)	
Resection margin, (%)			.152
R0	112 (83)	16 (70)	
R1	23 (17)	7 (30)	
Treatment arm, (%)			.257
Gemcitabin	78 (58)	10 (43)	
Observation	57 (42)	13 (57)	

Grading was not available in all cases. T1–2, T1–2 stage; T3–4; T3–4 stage; N–, nodal negative stage; N+ nodal positive stage; R0, R0 resection stage; R1, R1 resection stage.

Association of MUC1 expression level and selected patient characteristics).

Survival

In the overall study population, low cytoplasmic MUC1 expression was associated with favorable DFS and OS (hazard ratio (HR) for DFS: 0.5, 95% CI 0.31 to 0.78, p = .003; HR for OS: 0.46, 95% CI 0.29 to 0.74, p = .001) see **Figures 3A, B**: *Survival analyses in subgroups for MUC1 low vs. high*.

Referring to the MUC1 low subpopulation, disease free survival was significantly improved in patients treated with gemcitabine compared to those of the observation only group (HR for DFS: 0.58; 95% CI 0.40 to 0.85, p = .004). By contrast, there was no relevant difference in overall survival observed (HR for OS: 0.51, 95% CI 0.21 to 1.23, p = .131), see **Figures 3C, D**: *Survival analyses in subgroups for MUC1 low vs. high*.

In the observation group, we found favorable prognostic effects of low MUC1 expression (HR for DFS: 0.55; 95% CI 0.29 to 1.04, p = .062; HR for OS: 0.35, 95% CI 0.18 to 0.68, p = .001) as well as a strong trend for improved survival in the gemcitabine group (HR for DFS: 0.48; 95% CI 0.24 to 0.96, p = .041; HR for OS: 0.56, 95% CI 0.28 to 1.11, p = .093), see **Figures 3E–H**: *Survival analyses in subgroups for gemcitabine vs. observation.*

Multivariable Analysis

In multivariable Cox regressions including standard clinical and biomarker characteristics, only treatment arm was independently predictive for DFS (HR 0.49 [95% CI: 0.29–0.83]; $p = .008$), whereas MUC1 (HR 0.47 [95% CI: 0.22–0.99]; $p = .05$) and grading (HR 0.61 [95% CI: 0.37–1.00]; $p = .05$) were strongly trending to predict OS, respectively, see also **Figure 4** for detailed exploratory analyses: *Survival analyses in subgroups for (**A, B**) disease free survival and (**C, D**) overall survival.*

DISCUSSION

In the presented analysis we explored the prognostic impact of MUC1 expression in pancreatic cancer patients in the context of a controlled randomized trial with a highly characterized population with mature outcome data. This cohort allows for rather valid data generation also acknowledging the retrospective and hypothesis-generating character of the article.

In the CONKO 001 trial, low MUC1 expression level appeared more frequent in patients under the age of 65 years. The reason thereof is not fully understood although this observation corresponds to pre-existing data (6, 13).

The remaining clinical and histopathological features did not significantly differ between the MUC1 low and MUC1 high cohort, respectively. Concurrently, in other solid cancer types MUC1 expression level does not correlate with specific clinicopathological parameters. As an exception, in several studies of breast cancer, MUC1 positivity was found to correlate with adverse metastases stages, nodal status and histological grading as well as hormone insensitivity (12–14). By contrast, the expression level of MUC1 in colon cancer and gastric cancer apparently did not correlate with any clinicopathological parameter but still is an independent marker of prognosis (15, 16).

Accordingly, low MUC1 expression levels were clearly associated with favorable outcome of patients. The positive prognostic effect was slightly higher in patients treated with gemcitabine in regard to DFS only. In contrast, significance could not be demonstrated for all subsets, likely due to limited sample size. Thus, this finding appeared evident irrespective of study arm and endpoint (DFS, OS) in the overall study population. Importantly, exploratory subgroup analyses did not identify specific patients in which the prognostic effect was more or less pronounced, indicating that MUC1 could be a relatively general biomarker of prognosis.

No relevant interaction of treatment efficacy (with gemcitabine) and MUC1 expression for OS was observed, suggesting that MUC1 is not predictive of gemcitabine efficacy. Interestingly, this is somehow contrasted by (preclinical) reports that suggest an association of gemcitabine efficacy with high MUC1 expression. An association of MUC1 upregulation and gemcitabine resistance in pancreatic tumor cells was described in several preclinical investigations (5, 17, 18).

However, gemcitabine monotherapy is no longer the undisputed standard of care in the adjuvant setting of PDAC for patients with a sufficient performance status for a combination therapy. Therefore, the impact of MUC1 expression level might be different if intensified cytostatic regimes are administered. However, our data are able to confirm the pure prognostic effect of MUC1 expression due to the comparison of adjuvant chemotherapy to observation. Certainly, the prognostic role of MUC1 in the context of resectable pancreatic cancer needs to be validated by other study groups. For instance, it is unclear to which extent our findings can be generalized to cohorts using more intensive adjuvant regimens such as mFOLFIRINOX, and gemcitabine plus capecitabine (1, 2).

Furthermore, it might be concluded that the poor outcome of patients with high MUC1 expression could be improved with the mentioned more active treatment regimens. Potentially, MUC1 high expressing PDAC defines a high-risk subgroup in the adjuvant setting. Therefore, intensive treatment approaches with active surveillance should be evaluated prospectively in this subgroup.

Additionally, the specific localization and expression level of MUC1 in PDAC differing from healthy pancreatic tissue, enables multiple immunotherapeutic strategies. Interestingly, several antibodies targeting MUC1 are currently in development (19), as well as vaccine formulations that may increase mucin-specific cytotoxic T-lymphocytes (20). Finally, also in the context of CAR T cells, MUC1-specific T-cells (TAB004) are already tested in a phase I clinical trial in patients with advanced solid tumors [NCT04137900].

Several limitations of this analysis should be considered in the interpretation of the data: The biomaterial was collected not before completion of the trial. Thus, of the initial 354 patients

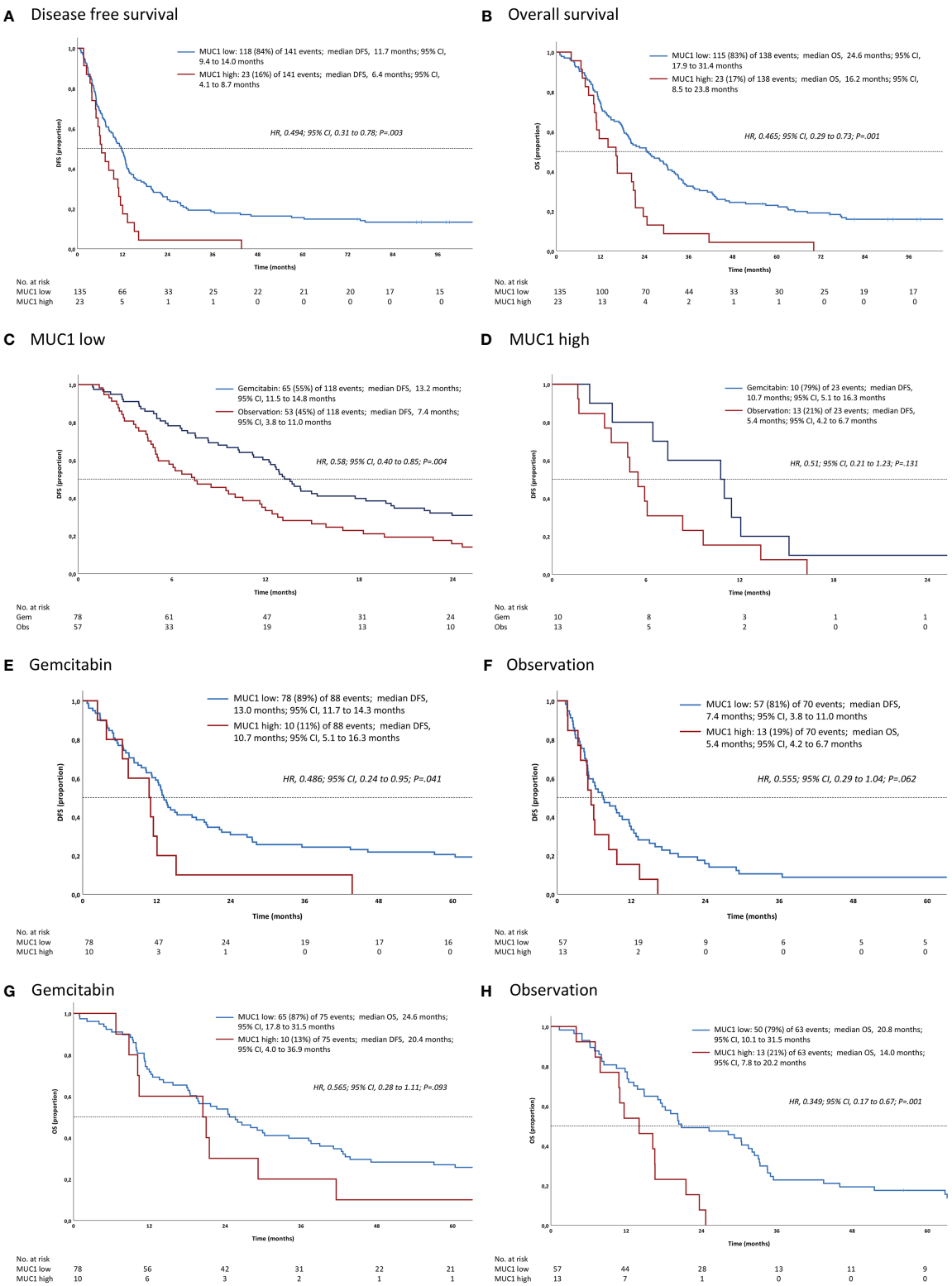

Kaplan-Meier estimates of the MUC1 analyzed subpopulation for (A, C-D) disease-free survival and (B) overall survival of the overall MUC1 cohort, and the gemcitabine arm (E) and (G) as well as observation only arm (F) and (H). Hazard ratios (HR) derived from univariable Cox regression testing. *P* values derived from log-rank test. Gem, gemcitabine; Obs, observation; MUC 1 low, MUC1 immunoreactivity score, IRS, 0-4; MUC1 high, IRS 5-10.

FIGURE 3 | Survival analyses in subgroups for **(A–D)** MUC1 low *vs*. high, and gemcitabine *vs*. observation **(E–H)**.

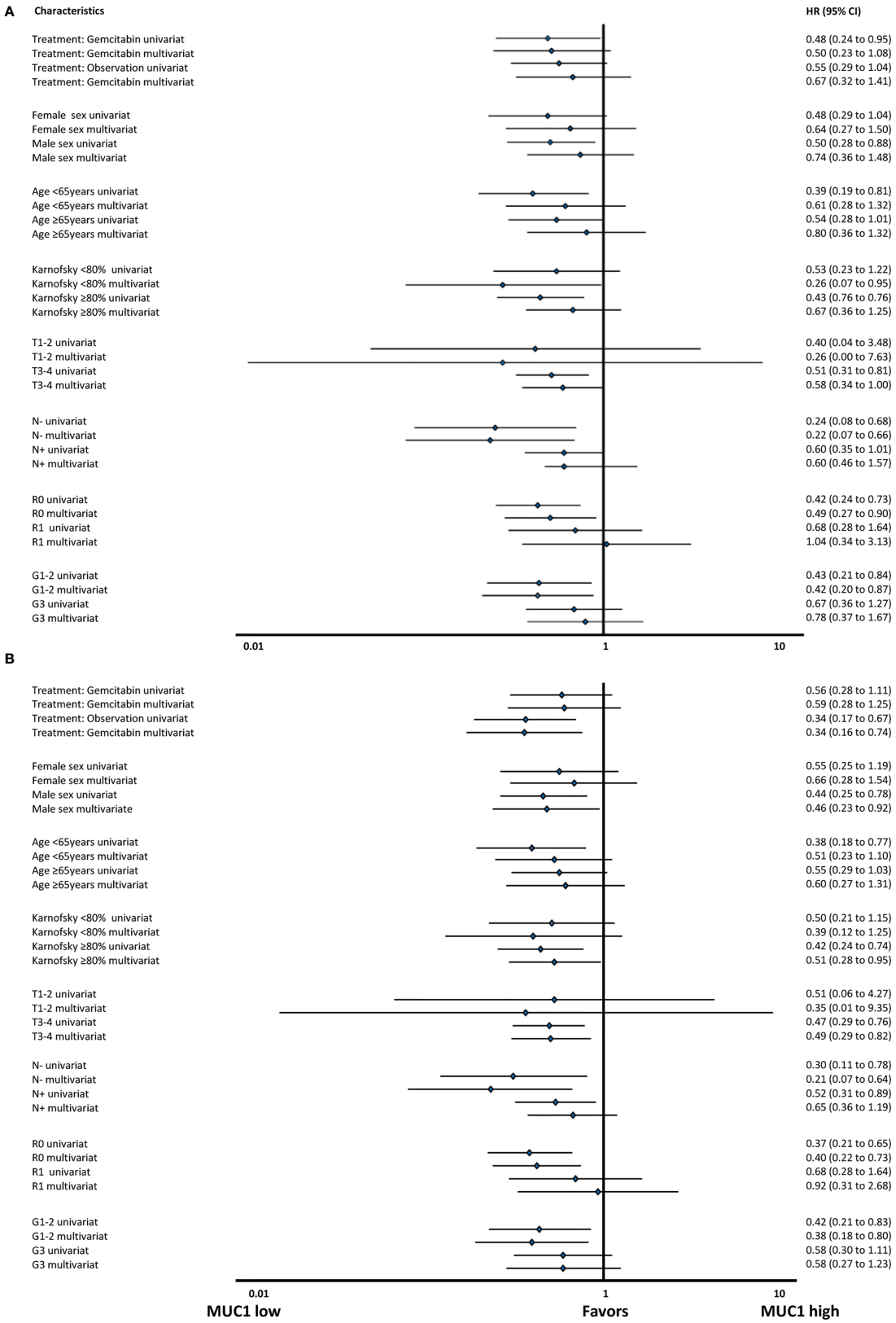

FIGURE 4 | Survival analyses in subgroups for **(A)** disease free survival and **(B)** overall survival.

included in the CONKO 001 survival analysis, there was archival tumor tissue in only n = 165 cases available. The number was further reduced due to poor quality to n = 158 (45%) samples of whom the tissue microarray were constructed. However, the clinical and histopathological features of the here presented subset are comparable to the overall intention to treat population. A further limitation might be inherent in the tissue microarray approach which is limited in its ability to assess tissue and tumour heterogeneity. Therefore, we examined tissue microarray cores in triplicate to overcome sample bias. Due to the shortage of tissue samples, comparison of MUC1 with various other potential biomarkers relating to their respective prognostic role was not realizable. Referring to the classification of MUC1 expression level by the IRS, there exists no well-established standard. Thus, the here presented cut off might serve as a reference for subsequent analyses in resectable pancreatic cancer. For this analysis, we assumed a good correlation of the immunohistochemical staining with the MUC1 expression on the transcriptional level which as it was shown for other solid cancer types e.g. breast cancer (6). The limited quantity of available biomaterial made it impossible to analyze the respective gene expression in our cohort and thus represents a potential bias of our study. Comparison with transcriptomic signatures might further clarify the prognostic value of MUC1 in pancreatic cancer (21–25). However, to the best of our knowledge, there exists no such gene expression score for resectable pancreatic cancer yet. In addition, none of the previously published transcriptomic signatures is sufficient as sole basis for therapeutic decision making. Thus, an evaluation of gene expression patterns is urgently needed to be implemented prospectively into adjuvant trials. Correlation of our data, and MUC1 expression level respectively, with transcriptomic signatures might contribute to the development of reproducible prognostic scores. Naturally, stratification of study arms and MUC1 expression heavily limits the sample size in subgroups, resulting in small numbers that may generate hypothesis but do not allow definite conclusions.

CONCLUSION

Low MUC1 expression is significantly associated with favorable DFS and OS in patients with pancreatic cancer after curatively intended resection. This finding appeared to be irrespective of active treatment *vs*. observation in the setting of the CONKO 001 trial. No conclusions of a potential predictive value can be drawn. Future studies should clarify if the negative prognostic impact of high MUC1 expression can be generalized and to which extent more intensive adjuvant treatment strategies such as the widely used mFOLFIRINOX improve the outcome of patients at high risk of relapse and death.

DATA AVAILABILITY STATEMENT

The raw data supporting the conclusions of this article will be made available by the authors, without undue reservation.

AUTHOR CONTRIBUTIONS

JS had full access to all of the data in the study and takes responsibility for the integrity of the data and the accuracy of the data analysis. Concept and design: JS, MS, BS, and UP. Acquisition, analysis or interpretation of data: JS, UP, and BS. Drafting of the manuscript: JS. Critical revision of the manuscript for important intellectual content: BS, DM, and UP. Statistical analysis: JS, SB, DM, and UP. Administrative, technical, or material support: JS, HO, MB, HB, CD, SS, UP, and BS. All authors contributed to the article and approved the submitted version.

ACKNOWLEDGMENTS

The CONKO-001 study was supported in part by a grant from Lilly Deutschland, Bad Homburg, Germany. CONKO-001 was an investigator-initiated-trial; Lilly Deutschland had no part in the design and conduct of the trial or in the collection, analysis and interpretation of the data. No funding was necessary for the present study.

SUPPLEMENTARY MATERIAL

The Supplementary Material for this article can be found online at: https://www.frontiersin.org/articles/10.3389/fonc.2021.670396/full#supplementary-material

REFERENCES

1. Conroy T, Hammel P, Hebbar M, Abdelghani MB, Wei AC, Raoul J-L, et al. FOLFIRINOX or Gemcitabine as Adjuvant Therapy for Pancreatic Cancer. *N Engl J Med* (2018) 379(25):2395–406. doi: 10.1056/NEJMoa1809775
2. Neoptolemos JP, Palmer DH, Ghaneh P, Psarelli EE, Valle JW, Halloran CM, et al. Comparison of Adjuvant Gemcitabine and Capecitabine With Gemcitabine Monotherapy in Patients With Resected Pancreatic Cancer (ESPAC-4): A Multicentre, Open-Label, Randomised, Phase 3 Trial. *Lancet* (2017) 389(10073):1011–24. doi: 10.1016/S0140-6736(16)32409-6
3. Uesaka K, Boku N, Fukutomi A, Okamura Y, Konishi M, Uesaka K, et al. Adjuvant Chemotherapy of S-1 Versus Gemcitabine for Resected Pancreatic Cancer: A Phase 3, Open-Label, Randomised, Non-Inferiority Trial (JASPAC 01). *Lancet (Lond Engl* (2016) 388(10041):248–57. doi: 10.1016/S0140-6736(16)30583-9
4. Tempero MA, Reni M, Riess H, Pelzer U, O'Reilly EM, Winter JM, et al. APACT: Phase III, Multicenter, International, Open-Label, Randomized Trial of Adjuvant Nab-Paclitaxel Plus Gemcitabine (Nab-P/G) *vs* Gemcitabine (G) for Surgically Resected Pancreatic Adenocarcinoma. *J Clin Oncol* (2019) 37 (15_suppl):4000–0. doi: 10.1200/JCO.2019.37.15_suppl.4000
5. Nath S, Daneshvar K, Roy LD, Grover P, Kidiyoor A, Mosley L, et al. MUC1 Induces Drug Resistance in Pancreatic Cancer Cells via Upregulation of Multidrug Resistance Genes. *Oncogenesis* (2013) 2(6):e51. doi: 10.1038/oncsis.2013.16
6. Sinn BV, von Minckwitz G, Denkert C, Eidtmann H, Darb-Esfahani S, Tesch H, et al. Evaluation of Mucin-1 Protein and mRNA Expression as Prognostic and

Predictive Markers After Neoadjuvant Chemotherapy for Breast Cancer. *Ann Oncol* (2013) 24(9):2316–24. doi: 10.1093/annonc/mdt162
7. Hinoda Y, Ikematsu Y, Horinochi M, Sato S, Yamamoto K, Nakano T, et al. Increased Expression of MUC1 in Advanced Pancreatic Cancer. *J Gastroenterol* (2003) 38(12):1162–6. doi: 10.1007/s00535-003-1224-6
8. Dréau D, Moore LJ, Wu M, Roy LD, Dillion L, Porter T, et al. Combining the Specific Anti-MUC1 Antibody TAB004 and Lip-MSA-IL-2 Limits Pancreatic Cancer Progression in Immune Competent Murine Models of Pancreatic Ductal Adenocarcinom. *Front Oncol* (2019) 9:330. doi: 10.3389/fonc.2019.00330
9. *ADC Franchise: Daiichi Sankyo Europe Gmb*. Available at: https://www.daiichi-sankyo.eu/oncology/adc-franchise (Accessed December 01, 2019).
10. Oettle H, Neuhaus P, Hochhaus A, Hartmann JT, Gellert K, Ridwelski K, et al. Adjuvant Chemotherapy With Gemcitabine and Long-Term Outcomes Among Patients With Resected Pancreatic Cancer: The CONKO-001 Randomized Trial. *JAMA* (2013) 310(14):1473–81. doi: 10.1001/jama.2013.279201
11. Oettle H, Post S, Neuhaus P, Gellert K, Langrehr J, Ridwelski K, et al. Adjuvant Chemotherapy With Gemcitabine vs Observation in Patients Undergoing Curative-Intent Resection of Pancreatic Cancer: A Randomized Controlled Trial. *JAMA* (2007) 297(3):267. doi: 10.1001/jama.297.3.267
12. Budczies J, Klauschen F, Sinn BV, Győrffy B, Schmitt WD, Darb-Esfahani S, et al. Cutoff Finder: A Comprehensive and Straightforward Web Application Enabling Rapid Biomarker Cutoff Optimization. *PLoS One* (2012) 7(12):e51862, 2012. doi: 10.1371/journal.pone.0051862
13. Jing X, Liang H, Hao C, Yang X, Cui X. Overexpression of MUC1 Predicts Poor Prognosis in Patients With Breast Cancer. *Oncol Rep* (2019) 41(2):801–10. doi: 10.3892/or.2018.6887
14. Do S-I, Kim K, Kim D-H, Chae SW, Park YL, Park CH, et al. Associations Between the Expression of Mucins (MUC1, MUC2, MUC5AC, and MUC6) and Clinicopathologic Parameters of Human Breast Ductal Carcinoma. *J Breast Cancer* (2013) 16(2):152–8. doi: 10.4048/jbc.2013.16.2.152
15. Wang R-Q, Fang D-C. Alterations of MUC1 and MUC3 Expression in Gastric Carcinoma: Relevance to Patient Clinicopathological Features. *J Clin Pathol* (2003) 56(5):378–84. doi: 10.1136/jcp.56.5.378
16. Duncan TJ, Watson NFS, Al-Attar AH, Scholefield JH, Durrant LG. The Role of MUC1 and MUC3 in the Biology and Prognosis of Colorectal Cancer. *World J Surg Oncol* (2007) 5:31. doi: 10.1186/1477-7819-5-31
17. Shukla SK, Purohit V, Mehla K, Gunda V, Chaika NV, Vernucci E, et al. MUC1 and HIF-1alpha Signaling Crosstalk Induces Anabolic Glucose Metabolism to Impart Gemcitabine Resistance to Pancreatic Cancer. *Cancer Cell* (2017) 32(1):71–87.e7. doi: 10.1016/j.ccell.2017.06.004
18. Tsai L-H, Hsu K-W, Chiang C-M, Yang H-J, Liu Y-H, Yang S-F, et al. Targeting Interleukin-17 Receptor B Enhances Gemcitabine Sensitivity Through Downregulation of Mucins in Pancreatic Cancer. *Sci Rep* (2020) 10(1):1–10. doi: 10.1038/s41598-020-73659-z
19. Fan X-N, Karsten U, Goletz S, Cao Y. Reactivity of a Humanized Antibody (Hpankomab) Towards a Tumor-Related MUC1 Epitope (TA-MUC1) With Various Human Carcinomas. *Pathol Res Pract* (2010) 206(8):585–9. doi: 10.1016/j.prp.2010.03.006
20. Kaur S, Kumar S, Momi N, Sasson AR, Batra SK. Mucins in Pancreatic Cancer and its Microenvironment. *Nat Rev Gastroenterol Hepatol* (2013) 10(10):607–20. doi: 10.1038/nrgastro.2013.120
21. Bailey P, Chang DK, Nones K, Johns AL, Patch A-M, Gingras M-C, et al. Genomic Analyses Identify Molecular Subtypes of Pancreatic Cancer. *Nature* (2016) 531(7592):47–52. doi: 10.1038/nature16965
22. Moffitt RA, Marayati R, Flate EL, Volmar KE, Loeza SGH, Hoadley KA, et al. Virtual Microdissection Identifies Distinct Tumor- and Stroma-Specific Subtypes of Pancreatic Ductal Adenocarcinoma. *Nat Genet* (2015) 47(10):1168–78. doi: 10.1038/ng.3398
23. Collisson EA, Sadanandam A, Olson P, Gibb WJ, Truitt M, Gu S, et al. Subtypes of Pancreatic Ductal Adenocarcinoma and Their Differing Responses to Therapy. *Nat Med* (2011) 17(4):500–3. doi: 10.1038/nm.2344
24. Nicolle R, Blum Y, Duconseil P, Vanbrugghe C, Brandone N, Poizat F, et al. Establishment of a Pancreatic Adenocarcinoma Molecular Gradient (PAMG) That Predicts the Clinical Outcome of Pancreatic Cancer. *EBioMedicine* (2020) 57:102858. doi: 10.1016/j.ebiom.2020.102858
25. Rashid NU, Peng XL, Jin C, Moffitt RA, Volmar KE, Belt BA, et al. Purity Independent Subtyping of Tumors (PurIST), A Clinically Robust, Single-Sample Classifier for Tumor Subtyping in Pancreatic Cancer. *Clin Cancer Res* (2020) 26(1):82–92. doi: 10.1158/1078-0432.CCR-19-1467

Conflict of Interest: The authors declare that the research was conducted in the absence of any commercial or financial relationships that could be construed as a potential conflict of interest.

frontiers in Oncology

ORIGINAL RESEARCH
published: 14 September 2021
doi: 10.3389/fonc.2021.650026

Fecal Microbiota and Gut Microbe-Derived Extracellular Vesicles in Colorectal Cancer

Jihye Park[1†], Nam-Eun Kim[2†], Hyuk Yoon[3], Cheol Min Shin[3], Nayoung Kim[3], Dong Ho Lee[3], Jae Yong Park[4], Chang Hwan Choi[4], Jae Gyu Kim[4], Yoon-Keun Kim[5], Tae-Seop Shin[5], Jinho Yang[5] and Young Soo Park[3]*

[1] Department of Internal Medicine, Yonsei University College of Medicine, Seoul, South Korea, [2] Department of Public Health Sciences, Graduate School of Public Health, Seoul National University, Seoul, South Korea, [3] Department of Internal Medicine, Seoul National University Bundang Hospital, Seongnam, South Korea, [4] Department of Internal Medicine, Chung-Ang University College of Medicine, Seoul, South Korea, [5] R&D Center, Institute of MD Healthcare Inc., Seoul, South Korea

The human microbiota comprises trillions of microbes, and the relationship between cancer and microbiota is very complex. The impact of fecal microbiota alterations on colorectal cancer (CRC) pathogenesis is emerging. This study analyzed changes in the microbial composition in CRC subjects with both fecal microbiota and gut microbe-derived extracellular vesicles (EVs). From August 2017 to August 2018, 70 CRC patients and 158 control subjects were enrolled in the study. Metagenomic profiling of fecal microbiota and gut microbe-derived EVs in stool was performed using 16S ribosomal DNA sequencing. Relative abundance, evenness, and diversity in both the gut microbiota and gut microbe-derived EVs were analyzed. Additionally, microbial composition changes according to the stage and location of CRC were analyzed. Microbial composition was significantly changed in CRC subjects compared to control subjects, with evenness and diversity significantly lower in the fecal microbiota of CRC subjects. Gut microbe-derived EVs of stool demonstrated significant differences in the microbial composition, evenness, and diversity in CRC subjects compared to the control subjects. Additionally, microbial composition, evenness, and diversity significantly changed in late CRC subjects compared to early CRC subjects with both fecal microbiota and gut microbe-derived EVs. *Alistipes*-derived EVs could be novel biomarkers for diagnosing CRC and predicting CRC stages. *Ruminococcus* 2-derived EVs significantly decreased in distal CRC subjects than in proximal CRC subjects. Gut microbe-derived EVs in CRC had a distinct microbial composition compared to the controls. Profiling of microbe-derived EVs may offer a novel biomarker for detecting and predicting CRC prognosis.

Keywords: microbiome, metagenome, gut microbe-derived extracellular vesicles, colorectal cancer, cancer stage

OPEN ACCESS

Edited by:
Jaw-Yuan Wang, Kaohsiung Medical University Hospital, Taiwan

Reviewed by:
Maria Principia Scavo, National Institute of Gastroenterology S. de Bellis Research Hospital (IRCCS), Italy
Chung-Yen Lin, Academia Sinica, Taiwan
Ling-Hui Li, Academia Sinica, Taiwan

***Correspondence:**
Young Soo Park
dkree@snubh.org

[†]These authors have contributed equally to this work

Specialty section:
This article was submitted to Gastrointestinal Cancers, a section of the journal Frontiers in Oncology

Received: *06 January 2021*
Accepted: *09 August 2021*
Published: *14 September 2021*

Citation:
Park J, Kim N-E, Yoon H, Shin CM, Kim N, Lee DH, Park JY, Choi CH, Kim JG, Kim Y-K, Shin T-S, Yang J and Park YS (2021) Fecal Microbiota and Gut Microbe-Derived Extracellular Vesicles in Colorectal Cancer. Front. Oncol. 11:650026. doi: 10.3389/fonc.2021.650026

INTRODUCTION

Colorectal cancer (CRC) has become a global health problem because of the increasing incidence of CRC in young adults (1, 2). Western dietary patterns and obesity have been strongly linked to CRC development (3, 4). Various studies have suggested that the pathogenesis of CRC is influenced not only by genetic factors but also by gut microbial composition altered due to ingested food or environmental factors. Gut microbiota induce oxidative stress and DNA damage in response to chronic inflammation, cell proliferation, and the production of metabolites such as butyrate (5). In animal studies, *Fusobacterium nucleatum* is associated with CRC pathogenesis by expressing a bacterial cell surface adhesion component, which can bind to host E-cadherin (6, 7). Enterotoxigenic *Bacteroides fragilis* is enriched in human CRC, resulting in cell morphology changes, E-cadherin cleavage stimulation, and colonic barrier function reduction (8).

Efforts to develop microbe-based cancer therapy have attracted more than 100 years from Coley's toxin in patients with bone cancer (9). Immunotherapy, including anti-programmed death receptor-1 (PD-1) inhibitors and anti-cytotoxic T-lymphocyte associated protein 4 (CTLA-4), provides a therapeutic response by modulating the gut microbiota (10, 11). Several approaches, including probiotics such as VSL#3 and LGG, could alter the gut microbiota composition (12, 13). Probiotics may regulate the immune system and inhibit the progression of CRC. Dietary changes by eliminating animal fat and a high-fiber diet may ultimately be a considered cancer therapy in some studies (14, 15). Nevertheless, the human microbiota comprises trillions of microbes, and the relationship between cancer and microbiota is very complex. Due to the heterogeneity of the microbiota, there are many limitations to finding therapeutic agents targeting specific microbiota.

Gut microbes, including gram-negative bacteria and some gram-positive bacteria, can produce extracellular vesicles (EVs), also called nanovesicles, and are upregulated during cell activation and growth during cancer development (16). Excess EVs can be released into the circulation, including plasma, saliva, gastric juice, and intestinal luminal liquid. There are many approaches for studying EV-associated RNA, membrane lipids, and proteomic composition of EVs (17, 18). EV-based early diagnostic biomarkers in patients with gastrointestinal cancer are challenging areas (19). Kanwar et al. developed a microfluidic device for circulating exosome characterization in patients with pancreatic cancer patients (20). Choi et al. found some proteins in colorectal cancer-derived EVs by proteomic analysis (21, 22). However, to the best of our knowledge, there have been very few reports on the development of CRC biomarkers by 16S ribosomal DNA sequencing metagenomic profiling with EV samples isolated from stool samples (23).

This study hypothesized that microbe-derived EVs interact with the gut microbiota and are associated with CRC development. Microbial composition changes in CRC subjects were analyzed and compared with control subjects of microbiota with both stool samples and microbe-derived EV samples. Additionally, differences in microbial composition were analyzed according to the stage and location of CRC.

Abbreviations: CRC, colorectal cancer; EV, extracellular vesicle; PD-1, programmed death receptor-1; CTLA-4, cytotoxic T-lymphocyte associated protein 4; out, operational taxonomic unit; PCoA, principal coordinate analysis; ROC, receiver operating characteristic; RF, random forest; AUC, area under the curve; IBD, inflammatory bowel disease.

MATERIALS AND METHODS

Patients and Sampling

Between August 2017 and August 2018, 158 stool samples were collected from control subjects, and 70 stool samples were collected from colorectal cancer patients who visited the CRC clinic at Seoul National University Bundang Hospital (Seongnam, Republic of Korea) and Chung-Ang University College of Medicine (Seoul, Republic of Korea) before undergoing any treatment. The exclusion criteria were as follows: (i) patients who had been diagnosed with gastric cancer, colorectal cancer, or other malignant diseases in the past and had undergone surgery and chemotherapy; (ii) patients who had been diagnosed with gastric dysplasia or gastric adenoma; (iii) pregnant women; (iv) patients who had been taking antibiotics or probiotics within last three months; and (v) patients who declined to participate in the study. For the enrolled patients, extensive medical data were collected every time they visited our clinic using electronic medical records. Fecal samples were self-sampled and stored at -20°C, transported to the laboratory, and frozen at -70°C. Control stool samples were selected from a previously collected cohort of healthy patients above 40 years of age who had abdominal symptoms but were not diagnosed with irritable bowel syndrome. There was no overlap of participants in the control group between previous studies. This study was approved by the Institutional Review Board of Seoul National University Bundang Hospital (IRB No: B-1708/412–301). Written informed consent for the use of medical records was obtained from all the participants. 23 CRC patients (only fecal microbiota samples) overlap with those in previous reports (24). 31 CRC patients (both fecal microbiota and gut microbe-derived EV samples) overlap with those in previous reports (23).

Extracellular Vesicles (EV) Isolation and DNA Extraction

Human stool samples were filtered through a cell strainer after being diluted in 10 mL of PBS for 24 h. The samples were centrifuged at 10,000 × g for 10 min at 4°C to separate EVs from stool samples. After centrifugation, stool sample pellets contained bacterial cells, and the supernatant of stool samples contained EVs. Bacteria and foreign particles were thoroughly eliminated from the stool sample supernatant by sterilizing the supernatant through a 0.22-μm filter. To extract DNA from bacterial cells and bacterial EVs, bacteria and EVs were boiled for 40 min at 100°C. To eliminate the remaining floating particles and waste, the supernatant was collected after 30 min of centrifugation at 13,000 rpm at 4°C. DNA was extracted using a DNeasy PowerSoil Kit (QIAGEN, Germany) according to the instructions of the manufacturer. DNA extracted from bacterial

cells and EVs in each sample was quantified using a QIAxpert system (QIAGEN, Germany).

Bacterial Metagenomic Analysis Using Extracellular Vesicles (EV) DNA

Bacterial genomic DNA was amplified with 16S_V3_F (5′-TCGTCGGCAGCGTCAGATGTGTATAAGAGACAGCCTACGGGNGGCWGCAG-3′) and 16S_V4_R (5′-GTCTCGTGGGCTCGGAGATGTGTATAAGAGACAGGACTACHVGGGTATCTAATCC-3′) primers, specific for the V3-V4 hypervariable regions of the 16S rRNA gene. Libraries were prepared using PCR products according to the MiSeq System guide (Illumina, USA) and quantified using the QIAxpert (QIAGEN, Germany). Each amplicon was quantified, set equimolar ratio, pooled, and sequenced on a MiSeq platform (Illumina, USA) according to the recommendations of the manufacturer.

Analysis of Bacterial Composition in the Microbiota

Paired-end reads that matched the adapter sequences were trimmed using Cutadapt version 1.1.6, with a minimum overlap of 11, a maximum error rate of 15%, and a minimum length of 10 (25). The resulting FASTQ files containing paired-end reads were merged with CASPER version 0.8.2, with a mismatch ratio of 0.27, and then quality-filtered using the Phred (Q) score-based criteria described by Bokulich (26, 27). Any reads shorter than 350 bp or longer than 550 bp after merging were discarded. A reference-based chimera detection step was conducted with VSEARCH version 2.3.0 against the SILVA gold database (28, 29) to identify the chimeric sequences. Sequence reads were clustered into operational taxonomic units (OTUs) using VSEARCH with an open clustering algorithm under a 97% sequence similarity threshold. The representative sequences of the OTUs were finally classified using the SILVA 132 database with UCLUST (*parallel_assign_taxonomy_uclust.py* script in QIIME version 1.9.1) under default parameters (30). The original contributions presented in the study are publicly available in NCBI. Raw reads of the fecal microbiota and microbe-derived EVs for colorectal cancer patients were deposited into the NCBI SRA database, respectively (Accession Numbers: SRR15182562–SRR15182631; SRR15182632–SRR15182701). Raw reads of the fecal microbiota and microbe-derived EVs for control patients from three datasets were deposited into the NCBI SRA database respectively (dataset 1: SRR15056567–SRR15056766; SRR15056787–SRR15056992; dataset 2: SRR15244175-SRR15244358; SRR15245161-SRR15245345; dataset 3: SRR15204197-SRR15221118; SRR15243500-SRR15243683) (**Supplementary Data**).

Statistical Analyses

Group comparisons for diversity metrics were conducted and graphed using R (version 3.6.3). α-Diversity (observed OTUs, Shannon index, and phylogenetic diversity) was compared by the decimal log-transformed relative abundance fecal microbiota between groups using the Wilcoxon rank-sum test (R package 'microbiome version 1.9.19'). Group distances for β-diversity (weighted UniFrac metric and unweighted UniFrac metric) were generated with permutational analysis of variance (PERMANOVA) using 1000 Monte Carlo permutations (R package 'phyloseq version 1.30.0' and 'vegan version 2.5.6') and visualized with principal coordinate analysis (PCoA) plots. Receiver operating characteristic (ROC) curves of the random forest (RF) model were obtained using age, sex, and taxa for predicting CRC. The RF method was used with the RandomForestClassifier function of the sklearn package in Python (version 2.7.17), and a 10-fold cross-validation was applied to the training set. For ROC curves and the area under the curve (AUC), the pROC package in R was utilized. Discriminate taxa (>0.1% abundance) between the groups were identified using Welch's t-test. Adjusted p-values controlling the false discovery rate (FDR) were reported where appropriate.

RESULTS

Fecal Microbiota Composition in Colorectal Cancer (CRC) Patients and Control Subjects

16S rRNA filtered gene sequences (**Supplementary Table 1**) were obtained from 228 stool samples (70 CRC subjects and 158 control subjects). The overall composition of the gut microbiota was altered in CRC subjects compared to that in the controls. Gut microbiota composition profiles were compared at the phylum, family, and genus levels (**Figures 1A–C**). CRC subjects showed a significant enrichment of Bacteroidetes phylum and depletion of Actinobacteria phylum ($p < 0.001$, **Table 1**). Within the phylum Bacteroidetes, relative enrichment was prominent for the family *Bacteroidaceae*, including genus *Bacteroides* (**Table 1**). Within Actinobacteria, relative depletion was prominent for the *Bifidobacterium* (*Bifidobacterium* genus) family in CRC subjects. Although there was no overall difference at the phylum level, several compositional changes were found at the family and genus levels. The relative abundance of the family *Clostridiaceae* 1 (genus *Clostridium sensu stricto* 1), *Family XIII* (genus *Family XIII* AD3011 group), and *Erysipelotrichaceae* (genus *Erysipelotrichaceae* UCG-003) was lower in the CRC group than in the control group (**Table 1**). *Ruminococcus* I, *Ruminococcaceae* UCG-013 (family *Ruminococcaceae*), *Blautia [Eubacterium] hallii* group, and *Lachnospiraceae* NC2004 group (family *Lachnospiraceae*) were also significantly depleted in the CRC group (**Table 1**).

Gut microbial community structure, assessed by richness and diversity, demonstrated a significantly lower richness and diversity in CRC subjects than in control subjects (**Figures 1D** and **2A, B**). A combined ROC analysis using clinical data and fecal microbiota revealed an AUC of 0.923 (**Figure 3**).

Gut Microbe-Derived Extracellular Vesicles Composition in Colorectal Cancer (CRC) Patients and Control Subjects

We compared microbiota with gut microbe-derived EVs between CRC subjects and control subjects at the phylum, family, and genus levels (**Figures 4A–C**). CRC subjects showed a significant enrichment

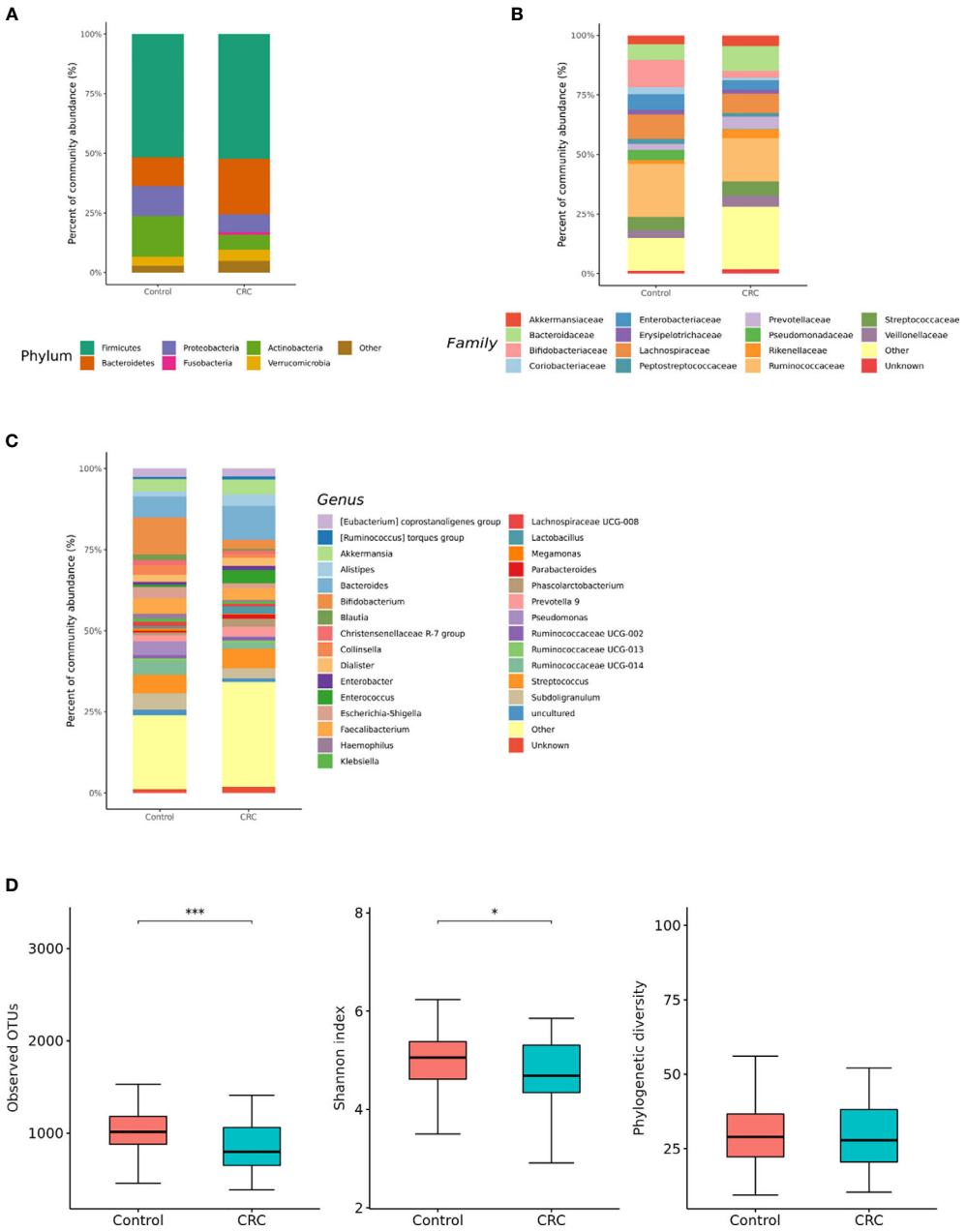

FIGURE 1 | Relative abundance plots of the gut microbiota of control (n = 158) subjects and CRC subjects (n = 70) **(A)** at the phylum, **(B)** family, and **(C)** genus levels. **(D)** Boxplots of alpha diversity indices comparing CRC with control in the gut microbiota. ***$p < 0.005$ and *$p < 0.05$. CRC; colorectal cancer, OTU; operational taxonomic unit.

of Firmicutes ($p = 0.008$) and depletion of the Verrucomicrobia phylum ($p = 0.002$, **Table 2**). Within the Firmicutes phylum, the relative abundances of *Clostridiaceae* 1 (genus *Clostridium sensu stricto* 1), *Erysipelotrichaceae* (genus *Turicibacter*), *Peptostreptococcaceae* (genus *Romboutsia* and *Terrisporobacter*), *Veillonellaceae* (genus *Dialister*), *Staphylococcaceae* (genus *Staphylococcus*), and *Acidaminococcaceae* (genus *Phascolarctobacterium*) was lower in the control group (**Table 2**). Relative enrichment was prominent for the family *Erysipelotrichaceae* (genus *Catenibacterium, Erysipelotrichaceae* UCG-003), *Ruminococcaceae* (genus *Faecalibacterium, Ruminococcus 2*), *Lachnospiraceae* [genus *Blautia, (Eubacterium) hallii* group, *(Ruminococcus) torque* group, *Oribacterium, Dorea*] (**Table 2**). Within the Verrucomicrobia phylum, the *Akkermansiaceae* (genus *Akkermansia*) family was significantly lower in the CRC group than in the control group (**Table 2**). Within the Actinobacteria phylum, a significant enrichment of the family *Coriobacteriaceae* (genus *Collinsella*) was prominent (**Table 2**).

TABLE 1 | Taxa showing a significant different in the abundance between CRC with control in the gut microbiota.

Taxon	t-statistic	Unadjusted *p*-value	Adjusted *p*-value	Reference
Phylum Firmicutes				
Family *Clostridiaceae 1*	-4.17	<0.001	**0.002**	(31)
Genus *Clostridium sensu stricto 1*	-4.17	<0.001	**0.004**	
Family *Family XIII*	-3.73	<0.001	**0.004**	(32)
Genus *Family XIII AD 3011 group*	-3.73	<0.001	**0.008**	
Family *Erysipelotrichaceae*	-3.50	<0.001	**0.016**	(31)
Genus *Erysipelotrichaceae UCG-003*	-3.50	0.001	**0.042**	
Genus *Turicibacter*	-2.89	0.004	0.129	(31)
Family *Ruminococcaceae*				(31, 33)
Genus *Ruminococcus 1*	-5.81	<0.001	**0.004**	(34, 35)
Genus *Ruminococcaceae UCG-013*	-3.78	<0.001	**0.004**	
Genus *Butyricicoccus*	-2.68	0.009	0.224	(36)
Genus *Subdoligranulum*	-2.59	0.012	0.286	
Family *Lachnospiraceae*				(31, 34)
Genus *Blautia*	-4.27	<0.001	**0.009**	(35)
Genus *[Eubacterium] hallii group*	-3.82	<0.001	**0.003**	(37)
Genus *Lachnospiraceae NC2004 group*	-3.45	<0.001	**0.003**	
Genus *[Eubacterium] ventriosum*	-3.08	0.004	0.117	(37)
Genus *[Ruminococcus] torques group*	-2.15	0.037	0.553	
Family *Peptostreptococcaceae*	-2.80	0.008	0.128	(31, 33)
Genus *Romboutsia*	-3.15	0.002	0.071	
Genus *Terrisporobacter*	-2.43	0.020	0.393	
Family *Christensenellaceae*	-2.76	0.007	0.124	(31)
Genus *Christensenellaceae R-7 group*	-2.76	0.007	0.207	
Family *Leuconostocaceae*	-2.77	0.008	0.124	(38)
Genus *Weissella*	-2.77	0.008	0.209	
Family *Lactobacillaceae*	-2.37	0.022	0.234	(31)
Genus *Lactobacillus*	-2.37	0.022	0.405	
Phylum Bacteriodetes	6.55	<0.001	**<0.001**	
Family *Bacteroidaceae*	5.26	<0.001	**0.002**	
Genus *Bacteroides*	5.26	<0.001	**0.004**	(34, 39)
Family *Marinifilaceae*	2.69	0.009	0.128	
Genus *Odoribacter*	2.69	0.009	0.227	(31, 33, 34, 39)
Family *Rikenellaceae*	2.47	0.015	0.185	(31)
Genus *Alistipes*	2.47	0.015	0.325	(33, 34)
Family *Tannerellaceae*	2.03	0.046	0.390	
Genus *Parabacteroides*	2.03	0.046	0.613	(34)
Phylum Actinobacteria	-5.82	<0.001	**<0.001**	
Family *Bifidobacteriaceae*	-5.93	<0.001	**0.002**	(31)
Genus *Bifidobacterium*	-5.93	<0.001	**0.004**	(34, 35)
Family *Eggerthellaceae*	-2.52	0.014	0.185	
Genus *Eggerthella*	-2.52	0.014	0.321	(33)
Family *Actinomycetaceae*	-2.36	0.021	0.234	
Genus *Actinomyces*	-2.36	0.021	0.405	(31)

The change of column (log2 fold) represents the multiplicative change in taxa abundance from CRC to control.
Negative numbers represent a trend of decreasing abundance in CRC group compared with control group.
The data ($p < 0.05$) was provied as bold values.

The gut microbe-derived extracellular vesicle composition and gut microbial community structure, assessed by richness and diversity, demonstrated a significant difference in richness and diversity between the CRC and control subjects (**Figures 2C, D**, **4D**). A combined ROC analysis using clinical data and gut microbe-derived EVs revealed an AUC of 0.963 (**Figure 3**).

Differences in the Microbial Composition According to the Colorectal Cancer (CRC) Stage

We analyzed the differences in the microbial composition according to the CRC stage. Out of the 70 patients with CRC, 62 patients were in stages I, II, or III, defined as early CRC, and 8 patients were in stage IV, defined as late CRC. In fecal microbiota, late CRC subjects tended to have an enrichment of Bacteroidetes and depletion of Actinobacteria compared with early CRC subjects (**Figures 5A–C**). In fecal microbiota, within Bacteroidetes, relative enrichment was prominent for the family *Marinifilaceae* (genus *Odoribacter*) and *Rikenellaceae* (genus *Alistipes*) in late CRC subjects than in early CRC subjects before adjustment (**Supplementary Table 2**). *Odoribacter* and *Alistipes* genera were significantly increased in CRC subjects compared to control subjects (**Table 1**). Microbial composition changes in control and CRC subjects and those of early and late CRC subjects were similar. Relative depletion was prominent for

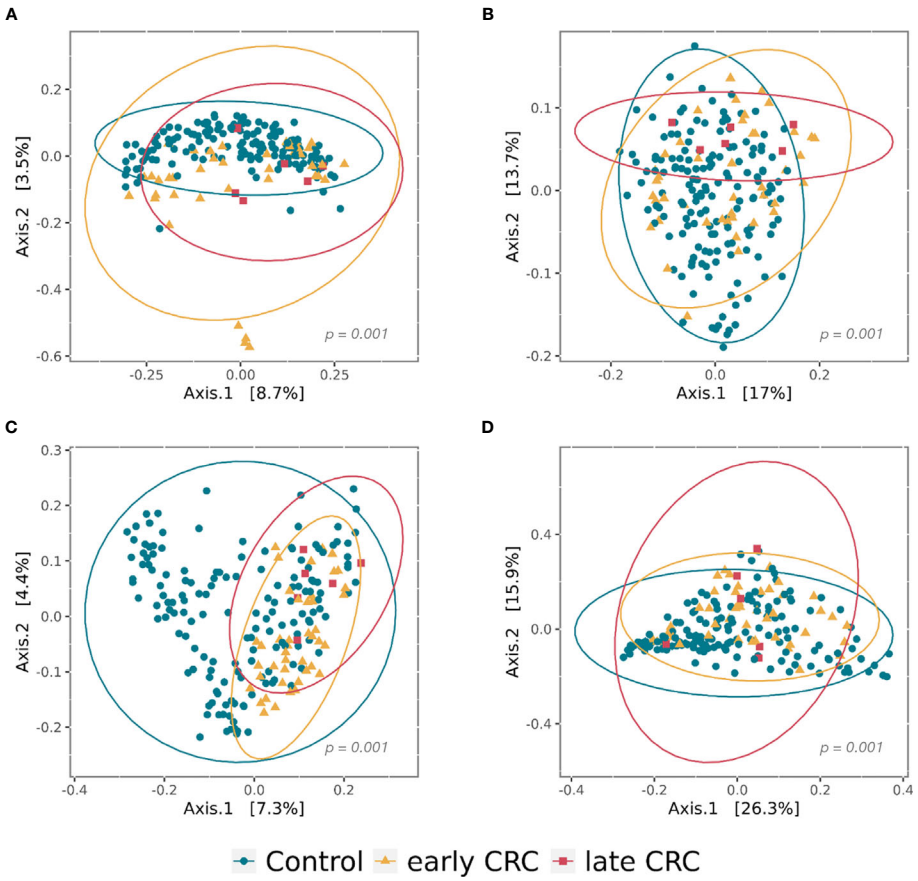

FIGURE 2 | Principal coordinate analysis (PCoA) plots of beta diversity analysis of control, early CRC, and late CRC patients in the gut microbiota **(A–B)** and the gut microbe-derived extracellular vesicles **(C–D)**. Between-sample dissimilarities were measured by unweighted UniFrac distances **(A, C)** and weighted UniFrac distances **(B, D)**. Permutational multivariate analysis of variance (PERMANOVA) was performed to analyze statistical significance (p = 0.001).

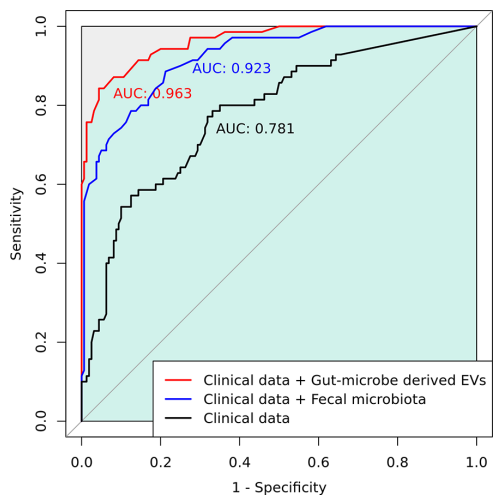

FIGURE 3 | A combined receiver operating characteristic (ROC) analysis using clinical data and gut microbe-derived EVs.

the family *Prevotellaceae* (genus *Prevotella 9*) in late CRC subjects. Within Firmicutes, relative depletion was prominent for the family *Ruminococcaceae* (genus *Butyricicoccus*) in late CRC subjects (**Supplementary Table 2**). *Butyricicoccus* was significantly decreased in CRC subjects compared to control subjects (**Table 1**).

In the microbiota with gut microbe-derived EVs, relative enrichment was prominent for the family *Rikenellaceae* (genus *Alistipes*) in late CRC subjects compared to early CRC subjects before adjustment (**Figures 6A–C** and **Supplementary** Table 3). Within Firmicutes, relative enrichment was prominent for the family *Acidaminococcaceae* (genus *Phascolarctobacterium*), and relative depletion was prominent for the family *Lactobacillaceae* (genus *Lactobacillus*) in late CRC subjects compared to early CRC subjects before adjustment (**Supplementary Table 3**).

CRC fecal microbiota and CRC gut microbe-derived EV composition and gut microbial community structure, assessed by richness and diversity, demonstrated a significantly different richness and diversity in late CRC subjects than in early CRC subjects. (**Figures 2A, B**, **5D** and **6D**).

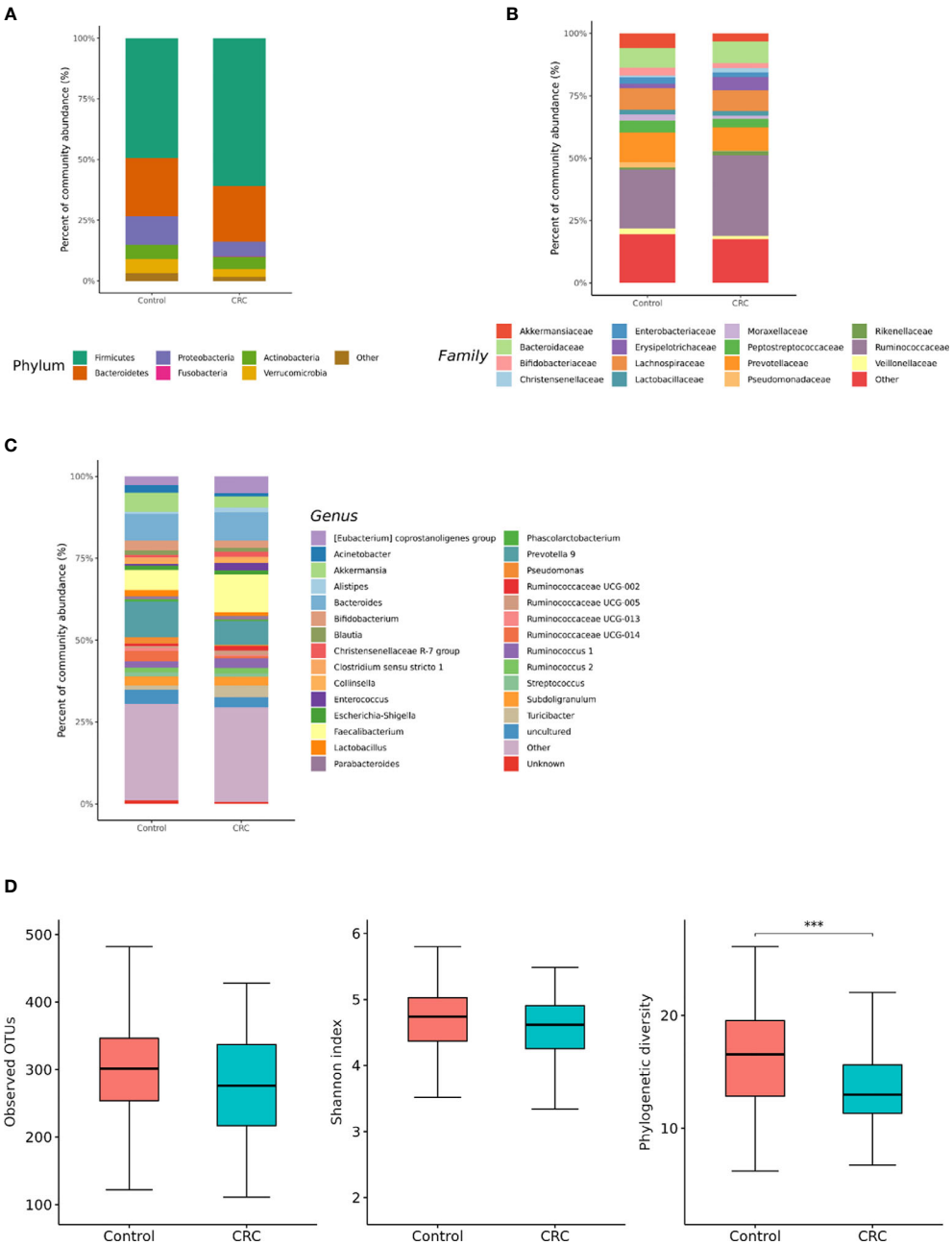

FIGURE 4 | Relative abundance plots of gut microbe-derived extracellular vesicles of control (n = 158) subjects and CRC subjects (n = 70) **(A)** at the phylum, **(B)** family, and **(C)** genus levels. **(D)** Boxplots of alpha diversity indices comparing CRC with control in gut microbe-derived extracellular vesicles. ***$p < 0.005$. CRC; colorectal cancer, OTU; operational taxonomic unit.

Differences in the Microbial Composition According to the Colorectal Cancer (CRC) Location

We also analyzed the differences in the microbial composition according to the CRC location. Of the 70 patients with CRC, 20 had proximal CRC and 50 had distal CRC. There were no significant differences in gut microbial composition changes between the proximal and distal CRC subjects (**Figures 7A–C**). In microbiota with gut microbe-derived EVs, within the Firmicutes phylum, relative depletion was prominent for family *Ruminococcaceae* (genus *Ruminococcus* 2) in the distal CRC subjects compared to proximal CRC subjects (**Figures 8A–C** and **Supplementary Table 4**). Alpha diversity was not different between distal CRC and proximal CRC in both fecal microbiota and gut

TABLE 2 | Taxa showing a significant different in the abundance between CRC with control in the gut microbe-derived extracellular vesicles.

Taxon	t-statistic	Unadjusted *p*-value	Adjusted *p*-value
Phylum Firmicutes	3.16	0.002	**0.008**
Family *Clostridiaceae 1*	-3.36	0.001	**0.019**
Genus *Clostridium sensu stricto 1*	-3.36	0.001	**0.003**
Family *Erysipelotrichaceae*	3.28	0.001	**0.019**
Genus *Catenibacterium*	7.51	<0.001	**0.004**
Genus *Erysipelotrichaceae UCG-003*	4.41	<0.001	**0.004**
Genus *Turicibacter*	-2.00	0.043	0.541
Family *Ruminococcaceae*	4.22	<0.001	**0.002**
Genus *Faecalibacterium*	3.41	<0.001	**0.020**
Genus *Ruminococcus 1*	2.96	0.004	0.089
Genus *Ruminococcus 2*	2.23	0.028	**0.028**
Family *Lachnospiraceae*			
Genus *Blautia*	3.78	<0.001	**0.012**
Genus *[Eubacterium] hallii group*	5.04	<0.001	**0.004**
Genus *[Ruminococcus] torques group*	4.85	<0.001	**0.004**
Genus *Oribacterium*	3.79	<0.001	**0.012**
Genus *Dorea*	3.91	0.004	**0.018**
Genus *Lachnospiraceae UCG-008*	2.52	0.012	0.230
Family *Peptostreptococcaceae*	-3.25	0.003	**0.033**
Genus *Romboutsia*	-4.35	<0.001	**0.001**
Genus *Terrisporobacter*	-3.56	<0.001	**0.003**
Genus *Intestinibacter*	-3.07	0.004	0.092
Family *Veillonellaceae*	-6.10	<0.001	**0.002**
Genus *Dialister*	-6.10	<0.001	**0.004**
Family *Staphylococcaceae*	-4.61	<0.001	**0.002**
Genus *Staphylococcus*	-4.61	<0.001	**0.004**
Family *Acidaminococcaceae*	-3.28	0.001	**0.018**
Phylum Proteobacteria			
Family *Moraxellaceae*			
Genus *Enhydrobacter*	-2.15	0.034	0.476
Phylum Actinobacteria			
Family *Coriobacteriaceae*	4.78	<0.001	**0.004**
Genus *Collinsella*	4.78	<0.001	**0.007**
Phylum Verrucomicrobia	-3.77	<0.001	**0.002**
Family *Akkermansiaceae*	-3.77	<0.001	**0.004**
Genus *Akkermansia*	-3.77	<0.001	**0.012**

The change of column (log2 fold) represents the multiplicative change in taxa abundance from CRC to control.
Negative numbers represent a trend of decreasing abundance in CRC group compared with control group.
The data ($p < 0.05$) was provied as bold values.

microbe-derived EVs (**Figures 7D** and **8D**). Microbial community structure was assessed by evenness with both stool and microbe-derived EVs, but distal CRC subjects did not differ from proximal CRC subjects.

DISCUSSION

The human gut microbiota comprises trillions of microbes, and 20% of human malignancies are caused by dysbiosis (40). In the past decade, metagenomic sequencing has broadened our understanding of microbial composition. The gut microbiota plays an important role in CRC initiation by chronic inflammation, which affects the intestinal epithelial cells. Fecal and mucosal microbial changes in CRC patients have been studied; however, no consistent patterns among these studies have been observed (6, 41–43).

This study analyzed stool profiling to identify the changes in microbial composition in CRC patients in South Korea. CRC subjects showed a significant enrichment of Bacteroidetes phylum and depletion of Actinobacteria phylum. At the genus level, the relative abundances of *Bacteroides*, *Odoribacter*, *Alistipes*, and *Parabacteroides* were higher in the CRC patients than in the healthy controls. The top five genera dominant in CRC patients were *Bifidobacterium*, *Ruminococcus* 1, *Blautia*, *Clostridium sensu stricto* 1, and *the Eubacterium hallii* group. In previous studies, patients with CRC had higher proportions of pathogenic bacteria, including *Bacteroides*, *Odoribacter*, and *Alistipes*, and fewer *Bifidobacterium*, *Ruminococcus*, and *Blautia*, similar to our results (34, 44). Putrefactive bacteria such as *Alistipes* and *Bacteroides* can produce short-chain fatty acids and promote chronic intestinal inflammation (45). The decrease in *Bifidobacterium*, *Ruminococcus*, and *Blautia*, which act as potential probiotics and function as antibacterial agents, could enhance CRC development (35). Additionally, we found that the richness and diversity of the fecal microbiota of patients with CRC were significantly lower than those of the healthy controls. Dongmei et al. also suggested that alpha diversity was significantly higher in the control subjects than in the CRC subjects (46). The difference in fecal microbial composition between the CRC and control subjects suggests that fecal microbiota could be a possible diagnostic biomarker in the future.

To discover a new effective biomarker of CRC stages, we also analyzed the different genera between early and late CRC subjects. We found that *the Odoribacter* and *Alistipes* genera were significantly increased not only in late CRC subjects compared to early CRC subjects but also in CRC subjects compared to control subjects. *Odoribacter* and *Alistipes* genera could be novel biomarkers for diagnosing CRC and predicting CRC stages. Genus *Alistipes* is an emerging gut bacteria related to inflammation, cancer, and mental health, as per a recent review (45). *Alistipes* evokes colitis and proximal colon cancers in IL10-/- mice (47). In addition, *Butyricicoccus* was significantly decreased in CRC subjects compared to control subjects. *Butyricicoccus* is a gut butyrate-producing bacterium that improves the clinical outcome of CRC by administration of *Butyricicoccus pullicaecorum*, as demonstrated in a previous mouse model (48). This result suggests that *Butyricicoccus* might be a novel pharmacological agent to prevent CRC pathogenesis.

To the best of our knowledge, there are few studies on the composition of gut microbe-derived EVs in CRC patients compared with controls (23). In principal coordinate analysis, the microbial community structure of the CRC gut microbe-derived EVs was different from that of the control subjects. This study showed that the composition of gut microbe-derived EVs differed significantly from that of fecal microbiota. These results indicate that gut microbe-derived EVs might be a better novel biomarker than fecal microbiota. Gut microbe-derived EVs

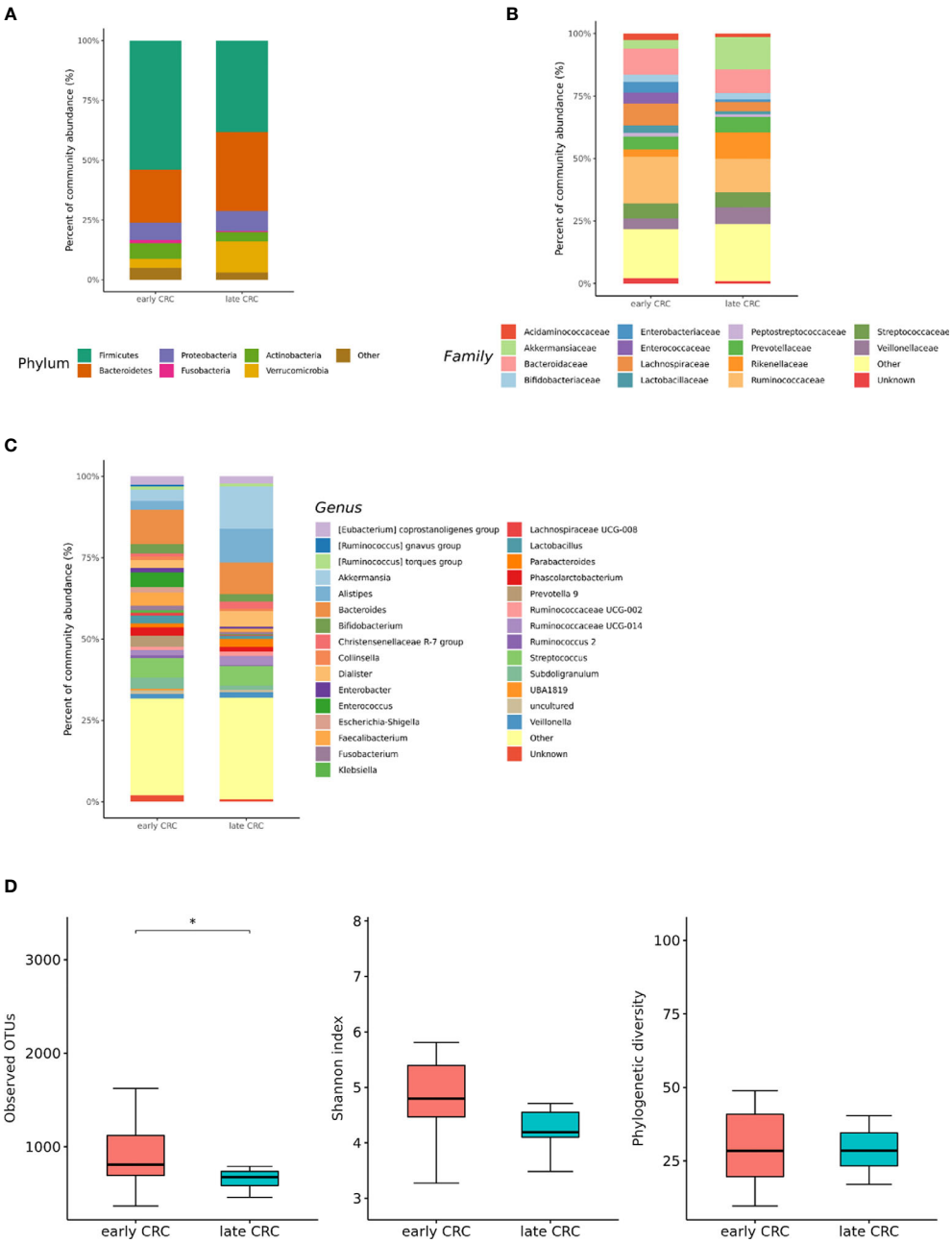

FIGURE 5 | Relative abundance plots of the gut microbiota of early CRC (n = 62) and late CRC (n=8) **(A)** at the phylum, **(B)** family, and **(C)** genus levels. **(D)** Boxplots of alpha diversity indices comparing late CRC with early CRC in the gut microbiota. *$p < 0.05$. CRC; colorectal cancer, OTU; operational taxonomic unit.

could play an important role in transferring proteins and nucleic acids from cells to other cells as nanocarriers (49). Tumors and other cells secrete EVs, and tumor-derived EVs can stimulate tumor progression, invasion, angiogenesis, and metastasis (50). Gut microbe-derived EVs in CRC patients may play a pivotal role in tumorigenesis. Several studies have examined EVs in CRC patients and animal models of IBD (51, 52). In the present study, *Clostridium sensu stricto* 1, *Turicibacter*, *Romboutsia*, *Terrisporobacter*, *Dialister*, *Staphylococcus*, *Phascolarctobacterium*, and *Akkermansia*-derived EVs could be effective therapeutic candidates for CRC treatment. Additionally, *Catenibacterium*, *Erysipelotrichaceae* UCG-003, *Faecalibacterium*, *Ruminococcus* 2, *Blautia [Eubacterium] hallii* group, *Ruminococcus torques* group, *Oribacterium*, *Dorea*, and *Collinsella-derived* EVs could be novel biomarkers for CRC diagnosis. Although it is difficult to determine whether the differentially relative abundance of microbe-derived

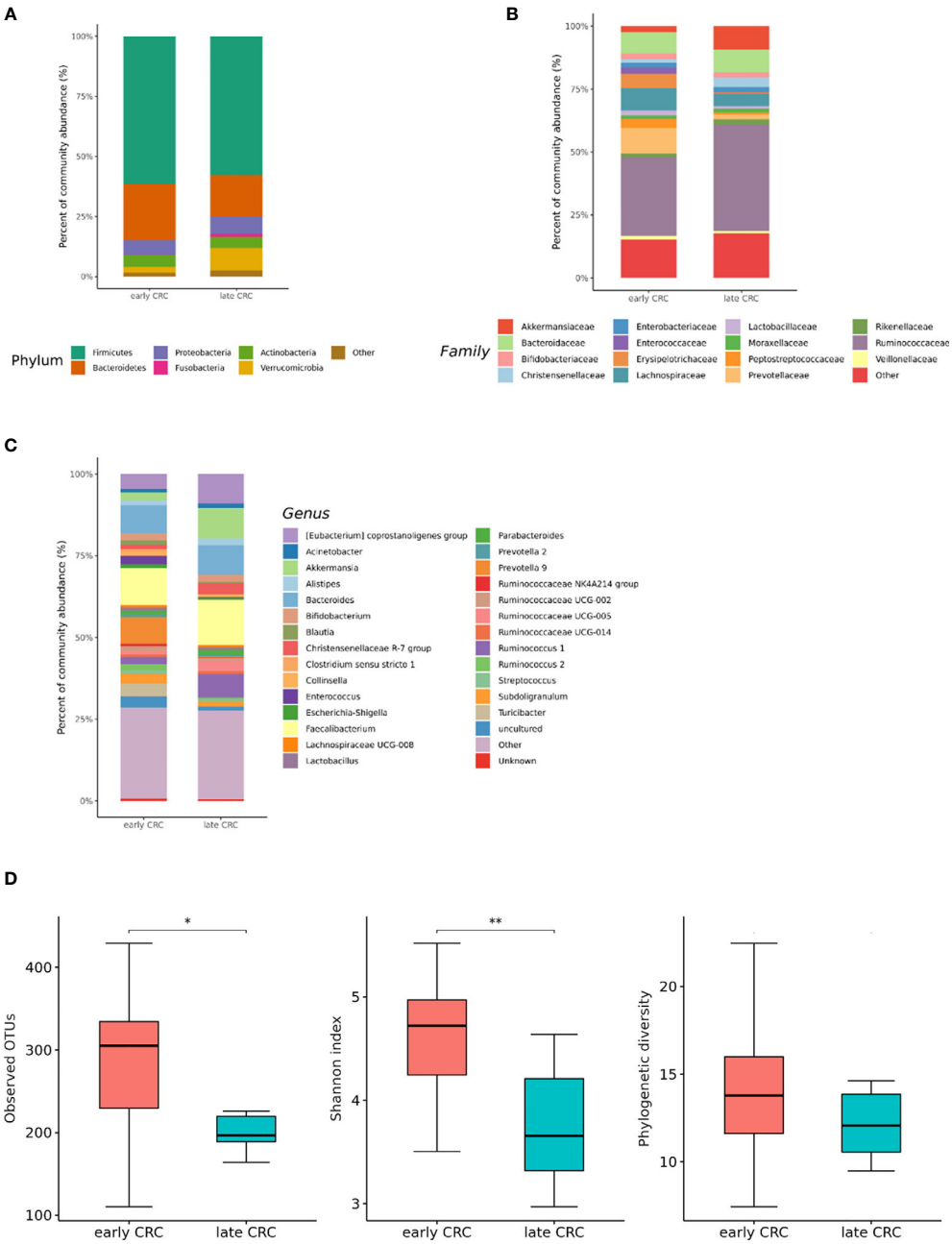

FIGURE 6 | Relative abundance plots of gut microbe-derived extracellular vesicles of early CRC (n = 62) and late CRC (n=8) **(A)** at the phylum, **(B)** family, and **(C)** genus levels. **(D)** Boxplots of alpha diversity indices comparing late CRC with early CRC in gut microbe-derived extracellular vesicles. $^{**}p < 0.01$ and $^{*}p < 0.05$. CRC; colorectal cancer, OTU; operational taxonomic unit.

EVs between CRC patients and healthy controls, the development of targeted analysis of cancer-derived EVs with specimens for the diagnosis and treatment monitoring in clinical settings has gained attention and challenges in recent years (53). We performed ROC analysis and established a prediction model for CRC diagnosis using gut-derived EVs compared to fecal microbiota. The microbiota enhanced the performance for predicting CRC diagnosis compared to the model with only clinical data. Among the microbiota data, gut-derived EVs outperformed fecal microbiota.

According to the CRC stage, *Alistipes*-derived EVs were significantly increased not only in late CRC subjects compared to early CRC subjects but also in CRC subjects compared to control subjects. *Alistipe*-derived EVs could be novel

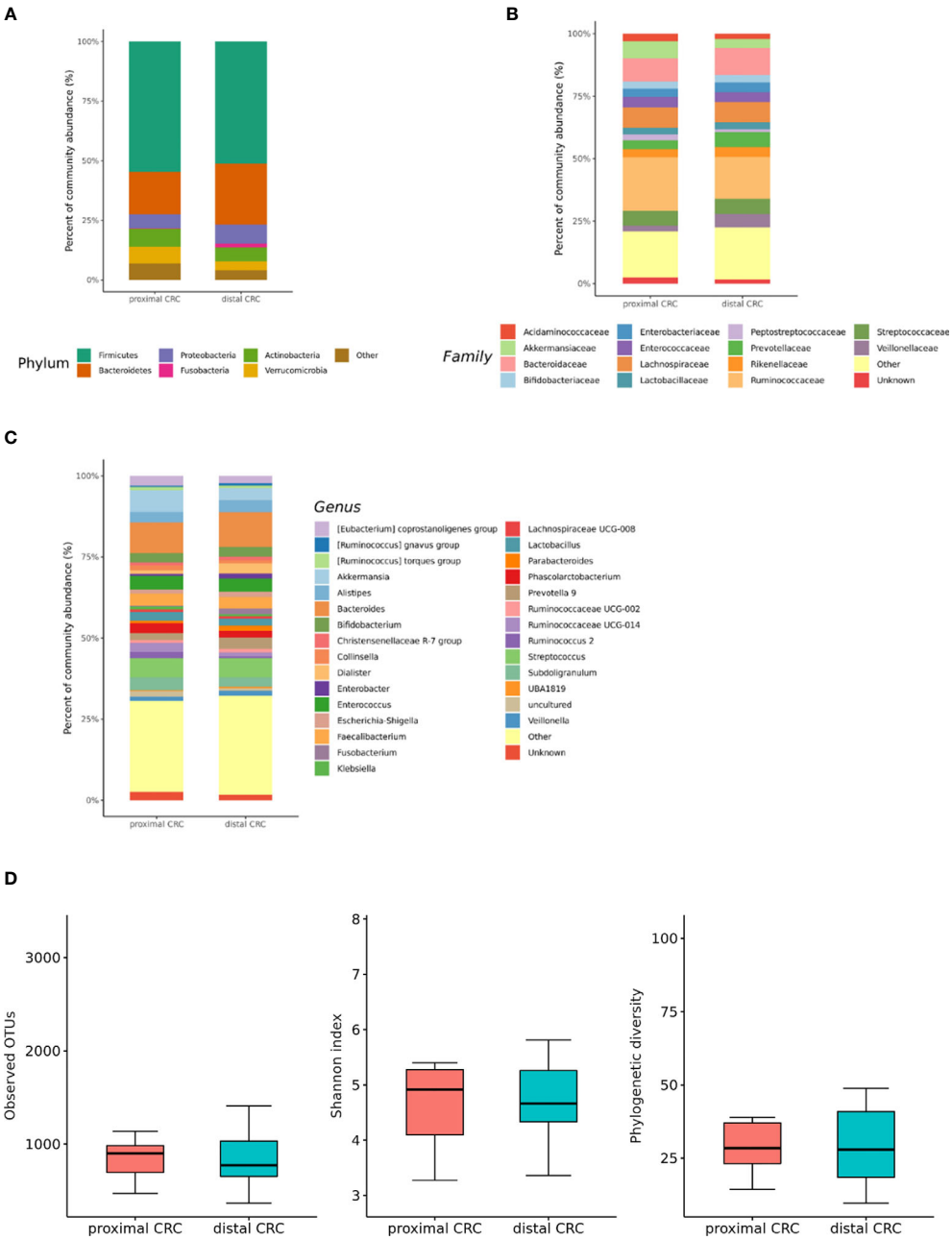

FIGURE 7 | Relative abundance plots of the gut microbiota of proximal CRC (n = 20) versus distal CRC (n = 50) **(A)** at the phylum, **(B)** family, and **(C)** genus levels. **(D)** Boxplots of alpha diversity indices comparing distal CRC with proximal CRC in the gut microbiota. CRC; colorectal cancer, OTU; operational taxonomic unit.

biomarkers for diagnosing CRC and predicting CRC stages. *Phascolarctobacterium*-derived EVs were significantly increased, and *Lactobacillacea*-derived EVs were significantly decreased in late CRC subjects compared to early CRC subjects. Gut microbe-derived EVs in CRC patients could play an important role in the development and growth of CRC.

Studies have identified metagenomic biomarkers for CRC formation (54). We analyzed the differences in the microbial composition according to the CRC location. In the microbiota with gut microbe-derived EVs, *Ruminococcus* 2 was lower in the distal CRC subjects than in the proximal CRC subjects. The microenvironment could affect the pathogenesis of CRC development, and enrichment of *Ruminococcus* 2 could be associated specifically with proximal CRC development. However, the difference according to the CRC stage was more significant than that according to the CRC location.

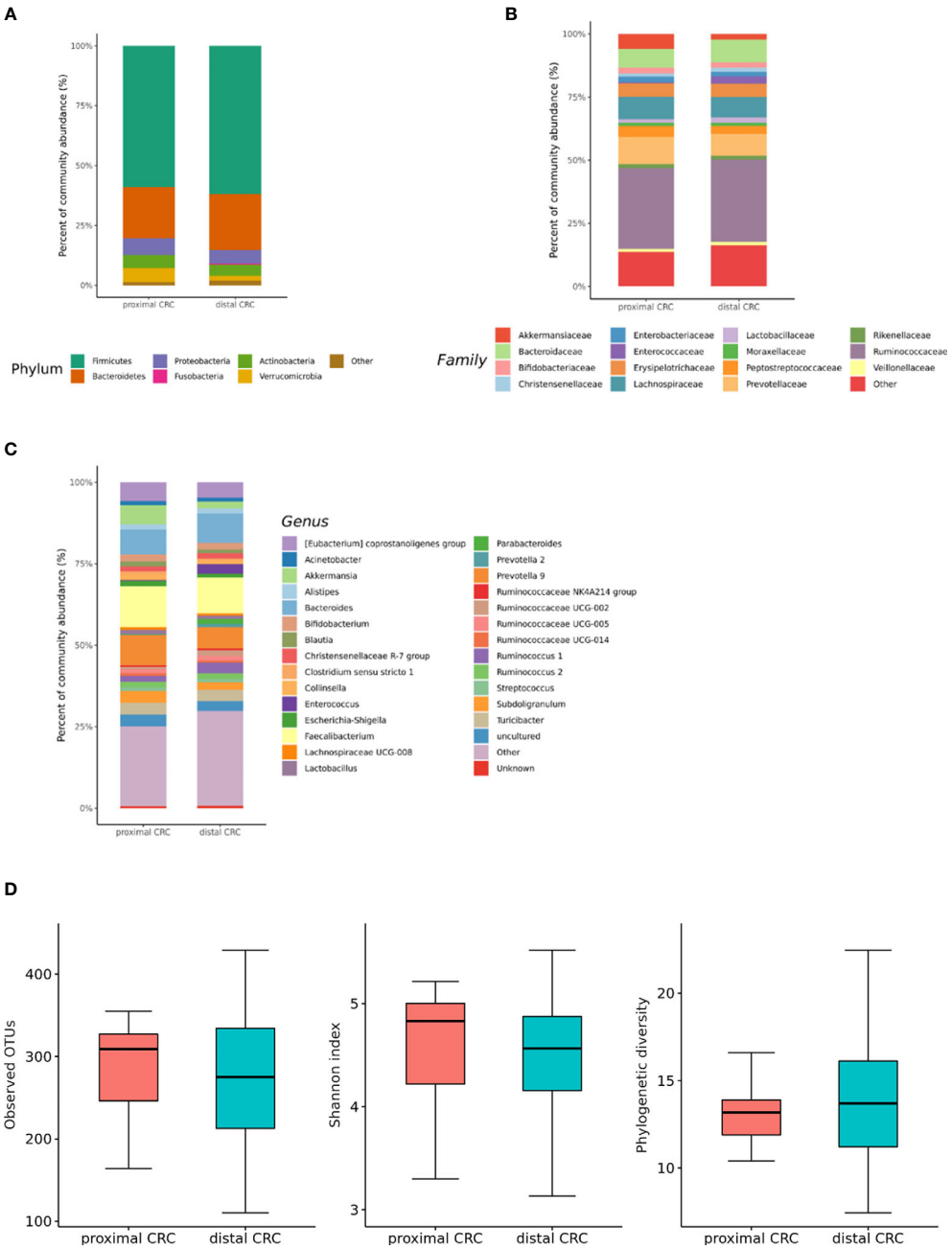

FIGURE 8 | Relative abundance plots of gut microbe-derived extracellular vesicles of proximal CRC (n = 20) versus distal CRC (n = 50) **(A)** at the phylum, **(B)** family, and **(C)** genus levels. **(D)** Boxplots of alpha diversity indices comparing distal CRC with proximal CRC in gut microbe-derived extracellular vesicles. CRC; colorectal cancer, OTU; operational taxonomic unit.

Our study has several limitations. First, although our research team has approved the EV isolation method in previous studies, ultracentrifugation with a relatively low number of turns could influence our results. Second, future studies for dynamic light scattering (DLS) or transmission electron microscopy (TEM) images to trace the size of vesicles are warranted. Third, we discovered candidate microbe-derived EVs for CRC prediction, but we did not validate them. Further study for validation with PCR on the target taxa will be warranted to quantify the microbe-derived EVs for CRC prediction.

In summary, this is a report on the metagenomic analysis of gut microbe-derived EVs in CRC patients. Profiling of microbe-derived EVs may offer a novel biomarker for detecting and predicting the prognosis of CRC.

DATA AVAILABILITY STATEMENT

The datasets presented in this study can be found in online repositories. The names of the repository/repositories and accession number(s) can be found below: https://www.ncbi.nlm.nih.gov/, SRR15182562–SRR15182631, https://www.ncbi.nlm.nih.gov/, SRR15182632–SRR15182701, https://www.ncbi.nlm.nih.gov/, SRR15056567–SRR15056766, https://www.ncbi.nlm.nih.gov/, SRR15056787–SRR15056992, https://www.ncbi.nlm.nih.gov/, SRR15244175-SRR15244358, https://www.ncbi.nlm.nih.gov/, SRR15245161-SRR15245345, https://www.ncbi.nlm.nih.gov/, SRR15204197-SRR15221118, https://www.ncbi.nlm.nih.gov/, SRR15243500-SRR15243683.

ETHICS STATEMENT

The studies involving human participants were reviewed and approved by Institutional Review Board of Seoul National University Bundang Hospital (IRB No: B-1708/412–301). The patients/participants provided their written informed consent to participate in this study.

AUTHOR CONTRIBUTIONS

Guarantor of the article: YP. Development of study concept and design: JP, HY, CS, and YP. Study supervision: HY, CS, YP, NK, and DL. Acquisition, analysis, and interpretation of data: N-EK, JP, HY, CS, JYP, CC, JK, YP, NK, DL, Y-KK, T-SS, and JY. Statistical analysis: N-EK. Drafting of the manuscript: JP. Critical revision of the manuscript for important intellectual content: HY, CS, and YP. All authors contributed to the article and approved the submitted version.

FUNDING

This research was supported by the Bio & Medical Technology Development Program of the National Research Foundation (NRF), funded by the Ministry of Science and ICT (2017M3A9F3047495).

SUPPLEMENTARY MATERIAL

The Supplementary Material for this article can be found online at: https://www.frontiersin.org/articles/10.3389/fonc.2021.650026/full#supplementary-material

REFERENCES

1. Siegel RL, Torre LA, Soerjomataram I, Hayes RB, Bray F, Weber TK, et al. Global Patterns and Trends in Colorectal Cancer Incidence in Young Adults. *Gut* (2019) 68:2179–85. doi: 10.1136/gutjnl-2019-319511
2. Vuik FE, Nieuwenburg SA, Bardou M, Lansdorp-Vogelaar I, Dinis-Ribeiro M, Bento MJ, et al. Increasing Incidence of Colorectal Cancer in Young Adults in Europe Over the Last 25 Years. *Gut* (2019) 68(10):1820–6. doi: 10.1136/gutjnl-2018-317592
3. Mehta RS, Song M, Nishihara R, Drew DA, Wu K, Qian ZR, et al. Dietary Patterns and Risk of Colorectal Cancer: Analysis by Tumor Location and Molecular Subtypes. *Gastroenterology* (2017) 152(8):1944–53.e1. doi: 10.1053/j.gastro.2017.02.015
4. Bardou M, Barkun AN, Martel M. Obesity and Colorectal Cancer. *Gut* (2013) 62(6):933–47. doi: 10.1136/gutjnl-2013-304701
5. Abreu MT, Peek RM Jr. Gastrointestinal Malignancy and the Microbiome. *Gastroenterology* (2014) 146(6):1534–46.e3. doi: 10.1053/j.gastro.2014.01.001
6. Kostic AD, Gevers D, Pedamallu CS, Michaud M, Duke F, Earl AM, et al. Genomic Analysis Identifies Association of Fusobacterium With Colorectal Carcinoma. *Genome Res* (2012) 22(2):292–8. doi: 10.1101/gr.126573.111
7. Rubinstein MR, Wang X, Liu W, Hao Y, Cai G, Han YW. Fusobacterium Nucleatum Promotes Colorectal Carcinogenesis by Modulating E-Cadherin/Beta-Catenin Signaling *via* Its Fada Adhesin. *Cell Host Microbe* (2013) 14(2):195–206. doi: 10.1016/j.chom.2013.07.012
8. Sears CL. Enterotoxigenic Bacteroides Fragilis: A Rogue Among Symbiotes. *Clin Microbiol Rev* (2009) 22(2):349–69. doi: 10.1128/CMR.00053-08
9. Mellmann A, Harmsen D, Cummings CA, Zentz EB, Leopold SR, Rico A, et al. Prospective Genomic Characterization of the German Enterohemorrhagic Escherichia Coli O104:H4 Outbreak by Rapid Next Generation Sequencing Technology. *PloS One* (2011) 6(7):e22751. doi: 10.1371/journal.pone.0022751
10. Derosa L, Hellmann MD, Spaziano M, Halpenny D, Fidelle M, Rizvi H, et al. Negative Association of Antibiotics on Clinical Activity of Immune Checkpoint Inhibitors in Patients With Advanced Renal Cell and Non-Small-Cell Lung Cancer. *Ann Oncol* (2018) 29(6):1437–44. doi: 10.1093/annonc/mdy103
11. McQuade JL, Daniel CR, Helmink BA, Wargo JA. Modulating the Microbiome to Improve Therapeutic Response in Cancer. *Lancet Oncol* (2019) 20(2):e77–91. doi: 10.1016/S1470-2045(18)30952-5
12. Hibberd AA, Lyra A, Ouwehand AC, Rolny P, Lindegren H, Cedgard L, et al. Intestinal Microbiota Is Altered in Patients With Colon Cancer and Modified by Probiotic Intervention. *BMJ Open Gastroenterol* (2017) 4(1):e000145. doi: 10.1136/bmjgast-2017-000145
13. Osterlund P, Ruotsalainen T, Korpela R, Saxelin M, Ollus A, Valta P, et al. Lactobacillus Supplementation for Diarrhoea Related to Chemotherapy of Colorectal Cancer: A Randomised Study. *Br J Cancer* (2007) 97(8):1028–34. doi: 10.1038/sj.bjc.6603990
14. Cotillard A, Kennedy SP, Kong LC, Prifti E, Pons N, Le Chatelier E, et al. Dietary Intervention Impact on Gut Microbial Gene Richness. *Nature* (2013) 500(7464):585–8. doi: 10.1038/nature12480
15. Wu GD, Chen J, Hoffmann C, Bittinger K, Chen YY, Keilbaugh SA, et al. Linking Long-Term Dietary Patterns With Gut Microbial Enterotypes. *Science* (2011) 334(6052):105–8. doi: 10.1126/science.1208344
16. Lee EY, Bang JY, Park GW, Choi DS, Kang JS, Kim HJ, et al. Global Proteomic Profiling of Native Outer Membrane Vesicles Derived From Escherichia Coli. *Proteomics* (2007) 7(17):3143–53. doi: 10.1002/pmic.200700196
17. Yoo JY, Rho M, You YA, Kwon EJ, Kim MH, Kym S, et al. 16S Rrna Gene-Based Metagenomic Analysis Reveals Differences in Bacteria-Derived Extracellular Vesicles in the Urine of Pregnant and Non-Pregnant Women. *Exp Mol Med* (2016) 48:e208. doi: 10.1038/emm.2015.110
18. Choi JH, Moon CM, Shin TS, Kim EK, McDowell A, Jo MK, et al. Lactobacillus Paracasei-Derived Extracellular Vesicles Attenuate the Intestinal Inflammatory Response by Augmenting the Endoplasmic Reticulum Stress Pathway. *Exp Mol Med* (2020) 52(3):423–37. doi: 10.1038/s12276-019-0359-3
19. Barteneva NS, Baiken Y, Fasler-Kan E, Alibek K, Wang S, Maltsev N, et al. Extracellular Vesicles in Gastrointestinal Cancer in Conjunction With Microbiota: On the Border of Kingdoms. *Biochim Biophys Acta Rev Cancer* (2017) 1868(2):372–93. doi: 10.1016/j.bbcan.2017.06.005
20. Kanwar SS, Dunlay CJ, Simeone DM, Nagrath S. Microfluidic Device (Exochip) for On-Chip Isolation, Quantification and Characterization of Circulating Exosomes. *Lab Chip* (2014) 14(11):1891–900. doi: 10.1039/c4lc00136b

21. Choi DS, Park JO, Jang SC, Yoon YJ, Jung JW, Choi DY, et al. Proteomic Analysis of Microvesicles Derived From Human Colorectal Cancer Ascites. *Proteomics* (2011) 11(13):2745–51. doi: 10.1002/pmic.201100022
22. Choi DS, Yang JS, Choi EJ, Jang SC, Park S, Kim OY, et al. The Protein Interaction Network of Extracellular Vesicles Derived From Human Colorectal Cancer Cells. *J Proteome Res* (2012) 11(2):1144–51. doi: 10.1021/pr200842h
23. Kim DJ, Yang J, Seo H, Lee WH, Ho Lee D, Kym S, et al. Colorectal Cancer Diagnostic Model Utilizing Metagenomic and Metabolomic Data of Stool Microbial Extracellular Vesicles. *Sci Rep* (2020) 10(1):2860. doi: 10.1038/s41598-020-59529-8
24. Yang J, McDowell A, Kim EK, Seo H, Lee WH, Moon CM, et al. Development of a Colorectal Cancer Diagnostic Model and Dietary Risk Assessment Through Gut Microbiome Analysis. *Exp Mol Med* (2019) 51(10):1–15. doi: 10.1038/s12276-019-0313-4
25. Martin M. Cutadapt Removes Adapter Sequences From High-Throughput Sequencing Reads. *EMBnet. J* (2011) 17(1):10–2. doi: 10.14806/ej.17.1.200
26. Kwon S, Lee B, Yoon S. CASPER: Context-Aware Scheme for Paired-End Reads From High-Throughput Amplicon Sequencing. In: *BMC Bioinformatics*. BioMed Central (2014).
27. Bokulich NA, Subramanian S, Faith JJ, Gevers D, Gordon JI, Knight R, et al. Quality-Filtering Vastly Improves Diversity Estimates From Illumina Amplicon Sequencing. *Nat Methods* (2013) 10(1):57. doi: 10.1038/nmeth.2276
28. Rognes T, Flouri T, Nichols B, Quince C, Mahé F. VSEARCH: A Versatile Open Source Tool for Metagenomics. *PeerJ* (2016) 4:e2584. doi: 10.7717/peerj.2584
29. Quast C, Pruesse E, Yilmaz P, Gerken J, Schweer T, Yarza P, et al. The SILVA Ribosomal RNA Gene Database Project: Improved Data Processing and Web-Based Tools. *Nucleic Acids Res* (2012) 41(D1):D590–6. doi: 10.1093/nar/gks1219
30. Caporaso JG, Kuczynski J, Stombaugh J, Bittinger K, Bushman FD, Costello EK, et al. QIIME Allows Analysis of High-Throughput Community Sequencing Data. *Nat Methods* (2010) 7(5):335–6. doi: 10.1038/nmeth.f.303
31. Hibberd AA, Lyra A, Ouwehand AC, Rolny P, Lindegren H, Cedgard L, et al. Intestinal Microbiota Is Altered in Patients With Colon Cancer and Modified by Probiotic Intervention. *BMJ Open Gastroenterol* (2017) 4(1):e000145. doi: 10.1136/bmjgast-2017-000145
32. Rajilic-Stojanovic M, de Vos WM. The First 1000 Cultured Species of the Human Gastrointestinal Microbiota. *FEMS Microbiol Rev* (2014) 38(5):996–1047. doi: 10.1111/1574-6976.12075
33. Sheng Q, Du H, Cheng X, Cheng X, Tang Y, Pan L, et al. Characteristics of Fecal Gut Microbiota in Patients With Colorectal Cancer at Different Stages and Different Sites. *Oncol Lett* (2019) 18(5):4834–44. doi: 10.3892/ol.2019.10841
34. Feng Q, Liang S, Jia H, Stadlmayr A, Tang L, Lan Z, et al. Gut Microbiome Development Along the Colorectal Adenoma-Carcinoma Sequence. *Nat Commun* (2015) 6:6528. doi: 10.1038/ncomms7528
35. Liu X, Mao B, Gu J, Wu J, Cui S, Wang G, et al. Blautia-A New Functional Genus With Potential Probiotic Properties? *Gut Microbes* (2021) 13(1):1–21. doi: 10.1080/19490976.2021.1875796
36. Chang SC, Shen MH, Liu CY, Pu CM, Hu JM, Huang CJ. A Gut Butyrate-Producing Bacterium Butyricicoccus Pullicaecorum Regulates Short-Chain Fatty Acid Transporter and Receptor to Reduce the Progression of 1,2-Dimethylhydrazine-Associated Colorectal Cancer. *Oncol Lett* (2020) 20 (6):327. doi: 10.3892/ol.2020.12190
37. Ai D, Pan H, Li X, Gao Y, Liu G, Xia LC. Identifying Gut Microbiota Associated With Colorectal Cancer Using a Zero-Inflated Lognormal Model. *Front Microbiol* (2019) 10:826. doi: 10.3389/fmicb.2019.00826
38. Jacqueline C, Brazier L, Faugere D, Renaud F, Thomas F, Roche B. Can Intestinal Microbiota Be Associated With Non-Intestinal Cancers? *Sci Rep* (2017) 7(1):12722. doi: 10.1038/s41598-017-11644-9
39. Yamamoto M, Matsumoto S. Gut Microbiota and Colorectal Cancer. *Genes Environ* (2016) 38:11. doi: 10.1186/s41021-016-0038-8
40. de Martel C, Ferlay J, Franceschi S, Vignat J, Bray F, Forman D, et al. Global Burden of Cancers Attributable to Infections in 2008: A Review and Synthetic Analysis. *Lancet Oncol* (2012) 13(6):607–15. doi: 10.1016/S1470-2045(12)70137-7
41. Shen XJ, Rawls JF, Randall T, Burcal L, Mpande CN, Jenkins N, et al. Molecular Characterization of Mucosal Adherent Bacteria and Associations With Colorectal Adenomas. *Gut Microbes* (2010) 1(3):138–47. doi: 10.4161/gmic.1.3.12360
42. Marchesi JR, Dutilh BE, Hall N, Peters WH, Roelofs R, Boleij A, et al. Towards the Human Colorectal Cancer Microbiome. *PloS One* (2011) 6(5):e20447. doi: 10.1371/journal.pone.0020447
43. Yeo EJ. Hypoxia and Aging. *Exp Mol Med* (2019) 51(6):1–15. doi: 10.1038/s12276-019-0233-3
44. Yamamoto M, Matsumoto S. Gut Microbiota and Colorectal Cancer. *Genes Environ* (2016) 38:11. doi: 10.1186/s41021-016-0038-8
45. Parker BJ, Wearsch PA, Veloo ACM, Rodriguez-Palacios A. The Genus Alistipes: Gut Bacteria With Emerging Implications to Inflammation, Cancer, and Mental Health. *Front Immunol* (2020) 11:906. doi: 10.3389/fimmu.2020.00906
46. Ai D, Pan H, Li X, Gao Y, Liu G, Xia LC. Identifying Gut Microbiota Associated With Colorectal Cancer Using a Zero-Inflated Lognormal Model. *Front Microbiol* (2019) 10:826. doi: 10.3389/fmicb.2019.00826
47. Moschen AR, Gerner RR, Wang J, Klepsch V, Adolph TE, Reider SJ, et al. Lipocalin 2 Protects From Inflammation and Tumorigenesis Associated With Gut Microbiota Alterations. *Cell Host Microbe* (2016) 19(4):455–69. doi: 10.1016/j.chom.2016.03.007
48. Eeckhaut V, Wang J, Van Parys A, Haesebrouck F, Joossens M, Falony G, et al. The Probiotic Butyricicoccus Pullicaecorum Reduces Feed Conversion and Protects From Potentially Harmful Intestinal Microorganisms and Necrotic Enteritis in Broilers. *Front Microbiol* (2016) 7:1416. doi: 10.3389/fmicb.2016.01416
49. Tran TH, Mattheolabakis G, Aldawsari H, Amiji M. Exosomes as Nanocarriers for Immunotherapy of Cancer and Inflammatory Diseases. *Clin Immunol* (2015) 160(1):46–58. doi: 10.1016/j.clim.2015.03.021
50. Rak J. Microparticles in Cancer. *Semin Thromb Hemost* (2010) 36(8):888–906. doi: 10.1055/s-0030-1267043
51. Dai S, Wei D, Wu Z, Zhou X, Wei X, Huang H, et al. Phase I Clinical Trial of Autologous Ascites-Derived Exosomes Combined With GM-CSF for Colorectal Cancer. *Mol Ther* (2008) 16(4):782–90. doi: 10.1038/mt.2008.1
52. Kang CS, Ban M, Choi EJ, Moon HG, Jeon JS, Kim DK, et al. Extracellular Vesicles Derived From Gut Microbiota, Especially Akkermansia Muciniphila, Protect the Progression of Dextran Sulfate Sodium-Induced Colitis. *PloS One* (2013) 8(10):e76520. doi: 10.1371/journal.pone.0076520
53. Mathew M, Zade M, Mezghani N, Patel R, Wang Y, Momen-Heravi F. Extracellular Vesicles as Biomarkers in Cancer Immunotherapy. *Cancers (Basel)* (2020) 12(10):2825. doi: 10.3390/cancers12102825
54. Gao Z, Guo B, Gao R, Zhu Q, Qin H. Microbiota Disbiosis is Associated With Colorectal Cancer. *Front Microbiol* (2015) 6:20. doi: 10.3389/fmicb.2015.00020

Conflict of Interest: Authors Y-KK, T-SS and JY were employed by Institute of MD Healthcare Inc.

The remaining authors declare that the research was conducted in the absence of any commercial or financial relationships that could be construed as a potential conflict of interest.

Publisher's Note: All claims expressed in this article are solely those of the authors and do not necessarily represent those of their affiliated organizations, or those of the publisher, the editors and the reviewers. Any product that may be evaluated in this article, or claim that may be made by its manufacturer, is not guaranteed or endorsed by the publisher.

Advantages of publishing in Frontiers

OPEN ACCESS
Articles are free to read for greatest visibility and readership

FAST PUBLICATION
Around 90 days from submission to decision

HIGH QUALITY PEER-REVIEW
Rigorous, collaborative, and constructive peer-review

TRANSPARENT PEER-REVIEW
Editors and reviewers acknowledged by name on published articles

Frontiers
Avenue du Tribunal-Fédéral 34
1005 Lausanne | Switzerland

Visit us: www.frontiersin.org
Contact us: frontiersin.org/about/contact

REPRODUCIBILITY OF RESEARCH
Support open data and methods to enhance research reproducibility

DIGITAL PUBLISHING
Articles designed for optimal readership across devices

FOLLOW US
@frontiersin

IMPACT METRICS
Advanced article metrics track visibility across digital media

EXTENSIVE PROMOTION
Marketing and promotion of impactful research

LOOP RESEARCH NETWORK
Our network increases your article's readership